frontiers | Research Topics

Solutions to High-Quality Development: Theories and Practices in Ecological Aspects

Edited by
Jinyan Zhan, Shiliang Liu, Hongbo Su and Fan Zhang

Published in
Frontiers in Environmental Science
Frontiers in Ecology and Evolution

ISSN 1664-8714
ISBN 978-2-83250-911-1
DOI 10.3389/978-2-83250-911-1

About Frontiers

Frontiers is more than just an open access publisher of scholarly articles: it is a pioneering approach to the world of academia, radically improving the way scholarly research is managed. The grand vision of Frontiers is a world where all people have an equal opportunity to seek, share and generate knowledge. Frontiers provides immediate and permanent online open access to all its publications, but this alone is not enough to realize our grand goals.

Frontiers journal series

The Frontiers journal series is a multi-tier and interdisciplinary set of open-access, online journals, promising a paradigm shift from the current review, selection and dissemination processes in academic publishing. All Frontiers journals are driven by researchers for researchers; therefore, they constitute a service to the scholarly community. At the same time, the *Frontiers journal series* operates on a revolutionary invention, the tiered publishing system, initially addressing specific communities of scholars, and gradually climbing up to broader public understanding, thus serving the interests of the lay society, too.

Dedication to quality

Each Frontiers article is a landmark of the highest quality, thanks to genuinely collaborative interactions between authors and review editors, who include some of the world's best academicians. Research must be certified by peers before entering a stream of knowledge that may eventually reach the public - and shape society; therefore, Frontiers only applies the most rigorous and unbiased reviews. Frontiers revolutionizes research publishing by freely delivering the most outstanding research, evaluated with no bias from both the academic and social point of view. By applying the most advanced information technologies, Frontiers is catapulting scholarly publishing into a new generation.

What are Frontiers Research Topics?

Frontiers Research Topics are very popular trademarks of the *Frontiers journals series*: they are collections of at least ten articles, all centered on a particular subject. With their unique mix of varied contributions from Original Research to Review Articles, Frontiers Research Topics unify the most influential researchers, the latest key findings and historical advances in a hot research area.

Find out more on how to host your own Frontiers Research Topic or contribute to one as an author by contacting the Frontiers editorial office: frontiersin.org/about/contact

Solutions to High-Quality Development: Theories and Practices in Ecological Aspects

Topic editors

Jinyan Zhan — Beijing Normal University, China
Shiliang Liu — Beijing Normal University, China
Hongbo Su — Florida Atlantic University, United States
Fan Zhang — Institute of Geographic Sciences and Natural Resources Research, Chinese Academy of Sciences (CAS), China

Citation

Zhan, J., Liu, S., Su, H., Zhang, F., eds. (2022). *Solutions to high-quality development: theories and practices in ecological aspects*. Lausanne: Frontiers Media SA. doi: 10.3389/978-2-83250-911-1

Table of contents

frontiers | Frontiers in Environmental Science

TYPE Editorial
PUBLISHED 17 November 2022
DOI 10.3389/fenvs.2022.1028676

OPEN ACCESS

EDITED AND REVIEWED BY
Jay E. Diffendorfer,
United States Geological Survey (USGS), United States

*CORRESPONDENCE
Jinyan Zhan,
zhanjy@bnu.edu.cn

SPECIALTY SECTION
This article was submitted to Conservation and Restoration Ecology, a section of the journal Frontiers in Environmental Science

RECEIVED 26 August 2022
ACCEPTED 02 November 2022
PUBLISHED 17 November 2022

CITATION
Zhan J, Liu S, Su H and Zhang F (2022), Editorial: Solutions to high-quality development: Theories and practices in ecological aspects.
Front. Environ. Sci. 10:1028676.
doi: 10.3389/fenvs.2022.1028676

Editorial: Solutions to high-quality development: Theories and practices in ecological aspects

Jinyan Zhan[1]*, Shiliang Liu[1], Hongbo Su[2] and Fan Zhang[3]

[1]School of Environment, Beijing Normal University, Beijing, China, [2]Department of Civil, Environmental and Geomatics Engineering, Florida Atlantic University, Boca Raton, FL, United States, [3]Institute of Geographic Sciences and Natural Resources Research, Chinese Academy of Sciences, Beijing, China

KEYWORDS

high-quality development, sustainable development, ecosystem service, human well-being, ecological restoration, remote sensing, carbon emission and carbon reduction, urban ecological transformation

Editorial on the Research Topic
Solutions to high-quality development: Theories and practices in ecological aspects

High-quality development (HQD) first appeared in the report of the 19th National Congress of the Communist Party of China in 2017. The report stated that China's economy had shifted from a stage of high growth to a stage of HQD. It initially referred to the development of the economy. As scholars and the government continue to enrich its connotation, the current meaning of high-quality development includes six main aspects: 1) people-centered, 2) stable macroeconomic growth, 3) fostering competitive enterprises, 4) innovation-driven, 5) marketization, legalization and internationalization, and 6) green development with ecological priority. With the introduction of the Sustainable Development Goals (SDGs) by the United Nations, the concept of sustainable development has become well known around the world (United Nations, 2015). Although HQD and sustainable development share certain similarities, they do have some distinct differences. Sustainable development focuses on addressing the environmental, economic and social aspects of the development process, whereas high-quality development puts more emphasis on development itself, showing a greater ambition for environmental improvement, economic growth and social progress. Therefore, HQD can be described as an initiative focusing on improving the quality and efficiency of development and enhancing human well-being on the basis of sustainable development (Liu et al., 2022). Smart growth is also a concept similar to HQD, however, it emphasizes more on the improvement of land use efficiency in a city or community for environmental protection, economic development, human well-being, *etc.* (US Environmental Protection Agency, 2022; Smart Growth Online, 2022). HQD is a new concept to guide China's economic and social development, and corresponding

experience from China may also benefit countries in other regions. It is inextricably linked to the implementation of international initiatives and conventions such as the Paris Agreement, the Convention on Biological Diversity and the achievements of the SDGs (Sachs et al., 2019; Huang, 2022).

Global issues such as climate change, biodiversity loss, and ecosystem services reduction have led to great challenges in human development (Cardinale et al., 2012; Wheeler and von Braun, 2013; Liu W. et al., 2022). To achieve HQD, in terms of the ecological aspects, it is necessary to alleviate natural resource conflicts, transform the development modes, solve prominent environmental problems and maintain regional ecological security (Kerr et al., 2007; Huang, 2022). This Research Topic (RT) "*Solutions to High-Quality Development: Theories and Practices in Ecological Aspects*" is a collection of 20 articles, including two theoretical studies and 18 empirical studies. It is intended to encourage scholars to disseminate the most recent theories and practices of HQD in ecological and environmental aspects, and to provide some references for the exploration of possible solutions to achieve the goal of HQD.

The need to optimize resource utilization derives not only from the urgency to resolve the outstanding contradiction between conservation and development, but also the demand to promote a harmonious coexistence between humans and nature. Three articles set out to explore such optimization. The article by Deng et al. focused on China's rural revitalization strategy and constructed a framework system to improve the efficiency of resource utilization, refine the effect of urban–rural integration, and optimize the efficiency of industrial development to increase farmers' income. Faced with challenges such as limited space for growing quantity of cultivated land, difficulties in improving cropland quality, insufficient supply of labor resources, uneven distribution of water resources and low utilization efficiency of agricultural water resources, China's rural areas needs to shift from single to multiple resources to improve resource utilization efficiency, and the urban-rural integration effect needs to move from extensive to lean, while optimizing the efficiency of industrial concentration from management to integrated services. To address water resource management issues, Wang et al. assessed historical virtual water flows and future agricultural water demand in various sectors in Zhangye City in West China, supporting the development of climate change adaptation strategies. The study by Zhao et al. accounted for the ecological water demand of indicator species in the main stream of the Yellow River and provided policy implications for regional water management.

Promoting industrial development and upgrading industrial structure and production efficiency is a necessary path to HQD. A total of four articles focused on this scientific aspect. Zhang et al. assessed the total Gross Ecosystem Product (GEP) of Chinese cropland ecosystems in the last 2 decades. The study found that the GEP of cropland ecosystems in most Chinese provinces, except developed provinces such as Beijing and Shanghai, showed an increasing trend. Meanwhile, the study by Li et al. found that international trade contributed to the slow growth in China's agricultural carbon emissions performance over the last 15 years, emphasizing that good ecological and environmental condition are the greatest development advantage of rural areas and that sustainable rural development needs to be promoted in terms of agricultural emission reduction, tourism and service industry development. The article from Wang et al. reported that the overall trend of agricultural eco-efficiency in China increased from 2001 to 2019, and it was mostly the eastern provinces that were of higher agro-ecological efficiency. He et al. also analyzed the spatial and temporal patterns of ecological benefits of grass-based livestock husbandry and the influencing factors in the context of rural revitalization strategies and proposed relevant development suggestions with the goal of revitalizing grass-based livestock husbandry.

The key to effective ecosystems management is to monitoring changes in ecosystem quality and corresponding drivers. In this RT, a total of eight empirical research articles focused on the changes and their drivers in a variety of ecosystemss, including grasslands, mountains, plateaus, and urban areas. Li et al. assessed changes in grassland ecosystem services and influencing factors in Hulunbuir and found that soil potassium content was the most influential factor on grassland ecosystem services, while economic and social factors were less influential. In the paper by Jin et al., a framework combining water quantity and ecological risk was constructed to analyze the spatial and temporal variability of water services and ecological risk in the Ziwuling Mountains of China. Also focusing on water-related ecosystem services, the paper by Wang et al. assessed future water production and soil conservation services in the Changbai Mountains, and analyzed the mechanisms by which both services are driven under climate change and Land Use/Cover Change. Madrigal-Martínez et al. calculated land use change and loss of ecosystem service values under glacial retreat and highlighted the urgency of ecosystem restoration and management at the watershed level. Understanding the spatial flow of ecosystem services can be of aid in diminishing the imbalance between supply and demand of ecosystem services, which is a difficult and important focus of current ecosystem service research. Meanwhile, Wang et al. used a network model to simulate the spatial flow of carbon sequestration services on the Qinghai-Tibetan Plateau and investigated the driving role of human activity in changes of carbon sequestration services. Yang et al. reported the changes in vegetation status along the Qinghai-Tibet Plateau highway and clarified the driving mechanisms of climate and distance on ES indicators, which are beneficial for supporting regional ecological restoration along the Qinghai-Tibet Plateau

highway. Derived from ecological security, land ecological security focuses on the sustainable use of land resources on the basis of denoting a state of harmony between people and nature (Liu et al.). In the article by Liu et al., a study in Jinan City, Shandong Province, assessed the historical changes in land ecological security status and its influencing factors. The study found that urban expansion has the greatest impact on the differentiated pattern of land ecological security, and urban development should pay attention to the protection of areas with high levels of land ecological security. At the urban community level, a study by Wang et al. in Beijing analyzed the carbon emissions and influencing factors of household consumption through a household survey, which provides a reference for community management and carbon reduction.

Territorial spatial planning is a spatial blueprint for HQD. Three articles in this RT are related to territorial spatial planning, covering coastal zones and land areas. The study by Guo et al. constructed a system of indicators for coastal spatial management, which provides a basis for the management of coastal spatial planning and facilitates the construction of coastal spaces for HQD. Identifying priority areas for ecosystem restoration can increase the provisioning of multiple ecosystem services and save economic costs. Facing the challenges of landscape fragmentation and habitat loss due to urbanization, Zhai and Huang identified potential ecological networks in urban agglomerations with priority areas for restoration and conservation, providing spatial guidance for the implementation of ecological conservation and restoration projects. Huang et al. took Guizhou Province, China as an example and revealed the importance of considering the influence of spatial structure characteristics of the landscape on ecological restoration effects in the process of ecological restoration.

Two additional papers in the RT were an empirical study on the improvement of the surface net radiation estimation algorithm and an investigation of plant growth mechanisms. Liu et al. improved the algorithm for estimating surface net radiation in mountainous environments with complex topography and verified the accuracy of the algorithm in the Haihe River basin. Yu et al. reported that arbuscular mycorrhizal fungi (AMF) can promote the growth of parasitized plants and activate the plant defense response to insect feeding.

Overall, the 20 articles in this RT brought together the latest practical experiences and scientific findings to support HQD. They cover key scientific issues related to regional HQD such as optimization of resource utilization, industrial upgrading and development, monitoring and attribution analysis of ecological and environmental changes, and formulation of territorial spatial planning. They also provided science-based suggestions for regional development. Development is the eternal theme of human society. We hope that this RT can trigger more extensive thinking and discussion on the theories and practices of HQD in the academic community, to synergize economic development and environmental protection, and ultimately help human society achieve HQD.

Author contributions

JZ, SL, HS, and FZ devised the concept for the editorial. JZ drafted the manuscript. SL, HS, and FZ provided editorial comments and revisions. JZ finalized the manuscript and submitted.

Funding

JZ acknowledged the support she received while working on this publication from the Second Scientific Expedition to the Qinghai-Tibet Plateau (2019QZKK0405) and the State Key Program of National Natural Science Foundation of China (72033005).

Acknowledgments

We would like to thank the reviewers who volunteered their time and efforts in contributing to this Research Topic.

Conflict of interest

The authors declare that the research was conducted in the absence of any commercial or financial relationships that could be construed as a potential conflict of interest.

Publisher's note

References

Cardinale, B. J., Duffy, J. E., Gonzalez, A., Hooper, D. U., Perrings, C., Venail, P., et al. (2012). Biodiversity loss and its impact on humanity. *Nature* 486 (7401), 59–67. doi:10.1038/nature11148

US Environmental Protection Agency (2022). Smart Growth. Available at: https://www.epa.gov/smartgrowth (Accessed on October 6, 2022).

Huang, R. (2022). The road to China's sustainable development. *Sustain. Horizons* 1, 100004.

Kerr, J. T., Kharouba, H. M., and Currie, D. J. (2007). The macroecological contribution to global change solutions. *Science* 316 (5831), 1581–1584. doi:10.1126/science.1133267

Liu, W., Zhan, J., Zhao, F., Wang, C., Zhang, F., Teng, Y., et al. (2022b). Spatio-temporal variations of ecosystem services and their drivers in the pearl river delta, China. *J. Clean. Prod.* 337, 130466. doi:10.1016/j.jclepro.2022.130466

Sachs, J. D., Schmidt-Traub, G., Mazzucato, M., Messner, D., Nakicenovic, N., and Rockström, J. (2019). Six transformations to achieve the sustainable development goals. *Nat. Sustain.* 2 (9), 805–814. doi:10.1038/s41893-019-0352-9

Smart Growth Online (2022). Available at: http://smartgrowth.org/ (Accessed on October 6, 2022).

United Nations (2015). *Transforming our world: The 2030 agenda for sustainable development*. Available at: https://sustainabledevelopment.un.org/post2015/transformingourworld/publication (Accessed October 05, 2022).

Wheeler, T., and von Braun, J. (2013). Climate change impacts on global food security. *Science* 341 (6145), 508–513. doi:10.1126/science.1239402

frontiers in Ecology and Evolution

ORIGINAL RESEARCH
published: 02 February 2022
doi: 10.3389/fevo.2022.828979

Linking MSPA and Circuit Theory to Identify the Spatial Range of Ecological Networks and Its Priority Areas for Conservation and Restoration in Urban Agglomeration

Tianlin Zhai[1] *and Longyang Huang*[2]*

[1] College of Resources and Environmental Sciences, Henan Agricultural University, Zhengzhou, China, [2] School of Resource and Environmental Sciences, Wuhan University, Wuhan, China

OPEN ACCESS

Edited by:
Fan Zhang,
Institute of Geographic Sciences and Natural Resources Research, Chinese Academy of Sciences (CAS), China

Reviewed by:
Shuyao Wu,
Shandong University, China
Dan Roesiemphrey Hu,
Research Center for Eco-Environmental Sciences, Chinese Academy of Sciences (CAS), China
Gui Jin,
China University of Geosciences Wuhan, China

***Correspondence:**
Longyang Huang
hly@whu.edu.cn

Specialty section:
This article was submitted to Conservation and Restoration Ecology, a section of the journal Frontiers in Ecology and Evolution

Received: *04 December 2021*
Accepted: *10 January 2022*
Published: *02 February 2022*

Citation:
Zhai T and Huang L (2022) Linking MSPA and Circuit Theory to Identify the Spatial Range of Ecological Networks and Its Priority Areas for Conservation and Restoration in Urban Agglomeration. Front. Ecol. Evol. 10:828979. doi: 10.3389/fevo.2022.828979

Rapid urbanization has led to the continuous degradation of natural ecological space within large urban agglomerations, triggering landscape fragmentation and habitat loss, which poses a great threat to regional ecological sustainability. Ecological networks (ENs) are a comprehensive control scheme to protect regional ecological sustainability. However, in the current research about ENs, most studies can only determine the orientation of ecological corridors but not their specific spatial range. This leads to the fact that ENs can only be abstract concepts composed of points and lines, and cannot be implemented into concrete spatial planning. In this study, taking the Shandong Peninsula urban agglomeration as an example, ecological sources were identified by morphological spatial pattern analysis (MSPA) and habitat quality assessment, ecological resistance surfaces were constructed based on habitat risk assessment (HRA). And circuit theory was used to simulate the ecosystem processes in heterogeneous landscapes via by calculating the cumulative current value and cumulative current recovery value, to identify the spatial range and key areas of ecological corridors. The results showed that the ENs includes 6,263.73 km^2 of ecological sources, 12,136.61 km^2 of ecological corridors, 283.61 km^2 of pinch points and 347.51 km^2 of barriers. Specifically, ecological sources were distributed in a spatial pattern of five groups, and ecological corridors were short and dense within groups, long in distance and narrow in width between groups. The pinch points and barriers mainly exist in the ecological corridors connecting the inner and outer parts of the central city and in the inter-group corridors. In order to ensure the connectivity and effectiveness of ENs, it is necessary to focus on the pinch points and barriers and include them in the priority areas for protection and restoration. Based on MSPA and circuit theory, this study provides a new method for determining the spatial range of ENs and the specific locations of priority areas, and provides a feasible solution for the concrete implementation of ENs to achieve effective ecological protection and restoration.

Keywords: ecological networks, MSPA, habitat risk, circuit theory, spatial range of ecological corridors, pinch points, barriers, Shandong Peninsula urban agglomerations

INTRODUCTION

In recent decades, with the acceleration of global environmental change and urbanization, land cover and related surface processes have undergone significant changes (Deng et al., 2009; Kong et al., 2017). Especially in large urban agglomeration, with the continuous expansion of construction land, the land use pattern had undergone great changes in quantity, quality and spatial layout (Peng et al., 2017; Salvati et al., 2018). It was mainly embodied in the transformation from the original natural ecosystem with ecological land as the carrier to the socio-economic system with construction land as the carrier (Rebelo et al., 2011). In the process of system transformation, on the one hand, with the decrease of natural ecological space, a series of ecological functions such as regional biodiversity, carbon storage, climate regulation and water conservation were destroyed (Pei et al., 2015; Mcdonald et al., 2018; Wang et al., 2019; Jin et al., 2020). On the other hand, with the continuous expansion of urban space, the population have been concentrated in urban areas, which lead to the continuous increase of pollutant emissions and accelerated consumption of natural resources (Elansky et al., 2018; Wang et al., 2019), destroying the ecological environment and threatening the safety of the entire ecosystem (Hammad and Tumeizi, 2012; Masum et al., 2017).

Researchers have proposed the concept of ecological networks (ENs) aimed at avoiding threats to the basic structure and function of ecosystems from the uncontrolled expansion of urban construction. ENs is essentially a spatial regulation scheme that coordinates natural ecosystems with socio-economic systems (Liang et al., 2018; D'Aloia et al., 2019; De Montis et al., 2019). It identifies the most important areas by comparing the importance of different landscape patches to ecological processes and ecological functions, and constructs a network system that can maintain the integrity of regional ecosystems and the continuity of ecological processes (Isaac et al., 2018; Cunha and Magalhães, 2019; Huang X. et al., 2021; Tang et al., 2021). Thus, it avoids the occupation and disturbance of these areas by urban expansion and ultimately ensures the ecological sustainability of regional development (Huang X. et al., 2021). Similar concepts include ecological infrastructure (EI) (Marchant, 2014; Sigwela et al., 2017), green infrastructure (GI) (Weber et al., 2006; Liquete et al., 2015; Coppola et al., 2019; Afionis et al., 2020), ecological security pattern (ESP) (Peng et al., 2018a, 2019; Huang et al., 2019; Wang and Pan, 2019).

After decades of development, ENs construction has formed a basic research paradigm of "identifying ecological sources, constructing ecological resistance surfaces, and extracting ecological corridors" (Weber et al., 2006; Peng et al., 2018b; Huang L. et al., 2021; Huang X. et al., 2021). Various techniques within the framework are also evolving. Among them, ecological sources are habitat patches that are important to regional ecosystems or have radiating functions. They are the basis for building ENs, which are generally identified by quantitative evaluation of ecological importance. Ecological functional importance is generally determined by calculating the ecosystem services that ecological patches can provide, such as biodiversity, climate regulation and pollution prevention (Huang et al., 2019; Peng et al., 2019; Dai et al., 2021). Landscape connectivity, ecological sensitivity and environmental suitability are also important indicators in the ecological importance evaluation system (Pierik et al., 2016; Su et al., 2016; Zhang et al., 2016). In addition, morphological spatial pattern analysis (MSPA) is gradually becoming a key technical method for ecological sources identification because of its emphasis on structural connectivity to increase the scientific nature of ecological source selection (Xiao et al., 2020; Huang X. et al., 2021). Ecological resistance surface is another core element in the ENs construction. It is generally obtained by assigning values to land use types. Since direct assignment is too subjective and ignores the internal differences under the same land use type, it hides the influence of human activities on the ecological resistance coefficient (Huang et al., 2019; Li et al., 2020). Therefore, indicators such as nighttime light intensity, impervious area, and surface moisture index, which can reflect the landscape heterogeneity of the study area, are gradually used for the correction of the resistance surface (Peng et al., 2018b, 2019; Huang L. et al., 2021). In the ecological corridor extraction, the minimum cumulative resistance model (MCR) is the traditional method which can determine the direction and optimal route of biological flow, but cannot clarify the spatial extent and key nodes of ecological corridors (Huang et al., 2019; Dai et al., 2021). The application of circuit theory effectively bridges this gap by simulating the direction of bio-flow through the random walk of electric current and determining the key locations in the corridor according to the magnitude of current intensity (Peng et al., 2018b; Yang et al., 2021; Yu et al., 2021) (**Figure 1**).

In recent years, research on ENs has gradually begun to focus on the identification of the spatial range of ENs, where the core research problem is the determination of the width of ecological corridors. Once the width of the ecological corridor is determined, it will make ENs no longer abstract networks composed of points and lines, but landscape entities with relatively defined spatial range. This will provide the theoretical and methodological foundation for promoting ecological conservation and restoration implementation planning and further research within the spatial range of ENs (Huang L. et al., 2021). Peng et al. (2018a) identified the width of ecological corridors in Yunnan Province based on the threshold of cummulated resistance. Dong et al. (2020) integrated spatial continuous wavelet transform and kernel density analysis to determine the spatial range of ecological corridors in Beijing. Huang L. et al. (2021) determined the width of ecological corridors in Shanghai according to different cumulative resistance thresholds and the change trends of risk indexes. These studies, based on the edge effect of ecological corridors, determined the width of ecological corridors according to the change trend of indicators reflecting the landscape heterogeneity on both sides inside and outside the corridor, which were the useful attempt in the study of determining the width of ecological corridors and promotes the study of the identification of the spatial range of ENs. However, these methods suffer from strong subjectivity in the selection of indicators and large spatial gradients, making the accuracy and spatial precision of ecological corridor widths doubtful. In general, the current research on

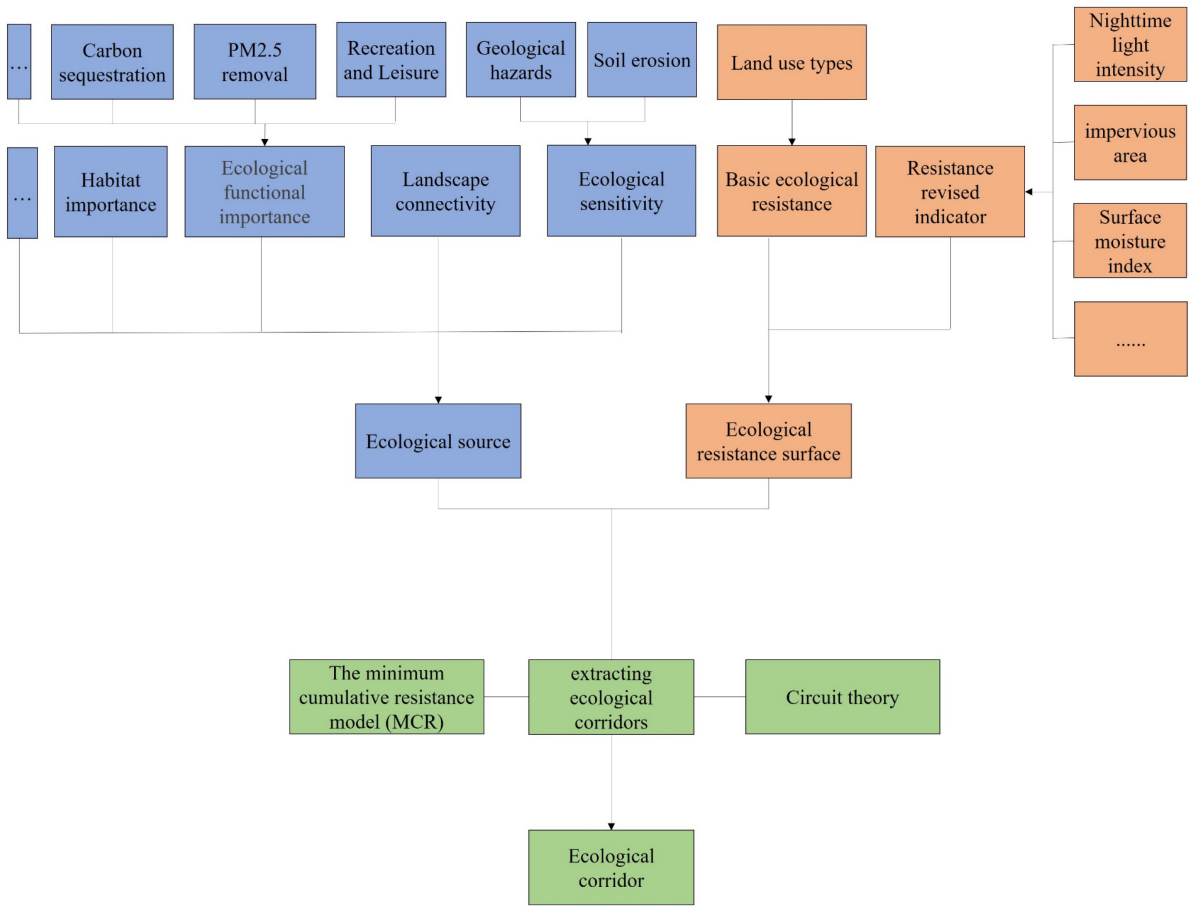

FIGURE 1 | The basic research paradigm of ecological network construction (blue boxes, identifying ecological sources; orange boxes, constructing ecological resistance surfaces; green boxes, extracting ecological corridors).

identifying the spatial range of ENs is still in the initial stage, and further improvements are still needed in the theoretical basis, identification methods and validity tests. This study proposed an approach to determine the width of ecological corridors based on the effective cumulative current values of ecological corridor simulated by circuit theory, in an attempt to improve the objectivity and spatial precision in determining the width of ecological corridor. The purpose of this study is to identify the key areas within the ENs based on the improved identification method of ENs spatial range. Then, according to the nature of the key areas, priority areas for conservation and restoration in the ENs of large urban agglomeration were identified.

The Shandong Peninsula urban agglomeration, located in the eastern coastal region of China, is one of the fastest growing urban agglomerations in China (Peng et al., 2020). During the past decades of development, it has experienced a rapid urbanization process, and the structure and function of the regional ecosystem have suffered a violent impact. This is also a common problem faced by other rapidly developing urban agglomeration. Taking the Shandong Peninsula urban agglomeration as an example, this study is based on a new approach to determine the ENs spatial range of the urban agglomeration, and to identify priority areas for conservation and restoration in the ENs. Specifically, this study has three research objectives: (1) to integrate MSPA and circuit theory to identify the spatial range and key areas of ENs in large urban agglomeration areas; (2) to identify priority conservation and restoration areas in ENs based on the nature of key areas; (3) to integrate important areas of ecosystem functions and key areas of ENs into ecological conservation and restoration implementation plans for large urban agglomeration. By focusing on priority areas, to develop implementation planning to promote the implementation efficiency of restoration and conservation measures in large urban agglomeration.

STUDY AREA AND DATA SOURCE

Study Area

The Shandong Peninsula urban agglomeration is one of the important urban agglomeration in northern China, located on the eastern coast of China and the southern flank of the Bohai Sea Rim. The specific scope of the Shandong Peninsula urban agglomeration varies depending on the claims made by the

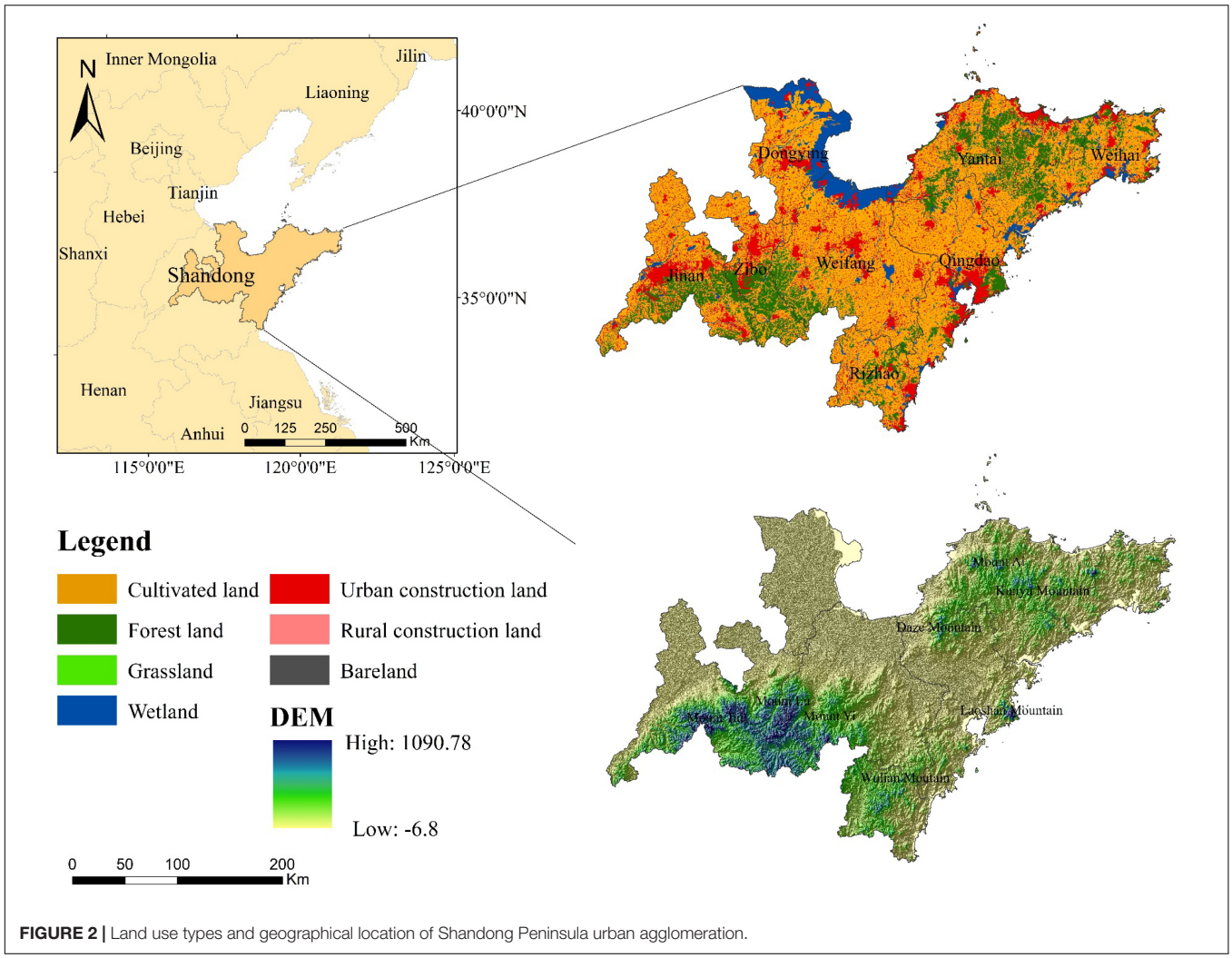

FIGURE 2 | Land use types and geographical location of Shandong Peninsula urban agglomeration.

government and scholars at different times. In this study, we adopt the widely accepted 8-city scenario proposed by Prof. Zhou Yixing in "Study on the Development Strategy of Shandong Peninsula Urban Agglomeration," including the coastal cities of Yantai, Weihai, Qingdao, Rizhao, Weifang, Dongying and the two non-coastal cities of Zibo and Jinan (**Figure 2**). The total land area of Shandong Peninsula urban agglomeration is about 73,000 km^2, accounting for 46.5% of the Shangdong province. By the end of 2018, the resident population of Shandong Peninsula urban agglomeration was 45,984,200, accounting for 45.77% of Shangdong province; the regional GDP was 4,891,191 billion yuan, accounting for 63.96% of Shandong province, and the per capita GDP was 106,400 yuan, 1.39 times of the province's average. Since 2,000, with the accelerated urbanization process, the ecological space within the urban agglomeration has been squeezed and degraded, and the biodiversity has been drastically reduced. Strict ecological protection and restoration measures must be taken to improve the ecological situation, maintain the ecological security of urban agglomerations and achieve sustainable regional development.

Data Source

Land use data, nighttime light index, normalized difference vegetation index (NDVI), leaf-area index (LAI), raster of averaged PM2.5 Concentrations, meteorological data (precipitation, temperature, wind speed), and road traffic data were applied to the study, and general information on each data is shown in **Table 1**. Among them, NDVI was obtained from the MOD13Q1 dataset based on the data time series from January to December 2018 to calculate the monthly average value of raster data that is produced every 16 days. LAI was obtained from the MOD15A2H dataset based on the data time series from January to March and September to December 2018 (i.e., in winter half-year) to calculate the average value of raster data that is produced every 8 days. The rest of the data were obtained by clipping from the downloaded raw data. Specifically, land use data were used for the calculation of habitat quality, habitat risk and MSPA; nighttime light index was used for constructing ecological resistance surfaces; NDVI and meteorological data were used for the calculation of the net primary productivity of vegetation; LAI and raster of averaged PM2.5 Concentrations were used

TABLE 1 | General status of data for study.

Name of data	Processing methods	Formats	Temporal reference	Data sources
Land use data	Clip	30 m*30 m raster	2018	http://www.resdc.cn/
Nighttime light index	Clip	1 km*1 km raster	2018	https://www.ngdc.noaa.gov/
NDVI	Clip	250 m*250 m raster	monthly average value in 2018	https://lpdaac.usgs.gov/
LAI	Clip	500 m*500 m raster	monthly average value in 2018	https://lpdaac.usgs.gov/
$PM_{2.5}$ concentrations	Clip	1 km*1 km raster	2018	http://fizz.phys.dal.ca/
Precipitation	Clip	1 km*1 km raster	2018	http://www.geodata.cn/
Temperature	Clip	1 km*1 km raster	2018	http://www.geodata.cn/
Wind speed	Clip	100 m*100 m raster	2018	https://globalsolaratlas.info/
Solar radiation	Clip	100 m*100 m raster	2018	https://globalsolaratlas.info/
Traffic data	Clip	vector	2018	https://lbs.amap.com/

for the calculation of PM2.5 removal function (according to the statistics, most of the PM2.5 occurs in the winter half year, so this study calculated the ability of vegetation to remove PM2.5 in the winter half year); road traffic data were used for the calculation of habitat quality, habitat risk. All data were converted into a consistent resolution (100 m * 100 m).

RESEARCH METHODOLOGY

Identifying Ecological Sources Based on Morphological Spatial Pattern Analysis and Habitat Quality

MSPA is an image processing method based on mathematical morphological principles such as erosion, expansion, open operation and closed operation to measure, identify and segment the spatial pattern of raster images (Soille and Vogt, 2009; Xiao et al., 2020; Huang X. et al., 2021). It can distinguish the type and structure of landscape more precisely. Combining with the current situation of landscape types in Shandong Peninsula urban agglomeration, natural landscapes with high ecosystem service value and less human interference, such as forest, grassland, water and wetland, were used as the foreground data for MSPA analysis. Cultivated land, construction land and bare land were used as the background data due to the lack of living environment for species to feed. According to the parameter settings of MSPA, the 30 × 30 m land use type raster map of Shandong Peninsula urban agglomeration was firstly converted into binary images of foreground and background, and then processed into seven types of landscape elements by Guidos Toolbox software to obtain core, islet, perforation, edge, bridge, loop, and branch.

Since MSPA only reflects the morphological and structural importance of landscape patches in the regional landscape pattern, it cannot evaluate the habitat suitability within the landscape patches. Therefore, based on the MSPA analysis, this study introduced the habitat quality model to further assess the habitat suitability of the core area, and identified the high habitat quality patches in the core area as ecological sources. The habitat quality module of the InVEST model (Sharp et al., 2016) was used to assess the habitat quality of the core area. It assesses the distribution and degradation of habitats in different landscapes based on the habitat quality calculated from the distance, intensity and response of different habitats to threat sources, and can reflect the state of biodiversity within a landscape patch and its potential level to provide survival conditions for species (Li et al., 2018; Sun et al., 2019). In this study, habitat quality was measured by the habitat quality module in InVEST3.1.2 model. The main parameters were set with reference to the example data of InVEST model, previous studies (Sharp et al., 2016; Li et al., 2018; Sun et al., 2019; Xu et al., 2019; Zhai et al., 2020) and actual situation within the study area, as shown in **Tables 2**, **3**.

TABLE 2 | Parameter settings for threat sources.

Threat	Maximum distance	Weight	Decay
Paddy field	6	0.5	Linear
Dryland	6	0.7	Linear
City	9	1	Exponential
Rural settlement	5	0.6	Exponential
Other construction land	4	0.6	Exponential
Road	4	0.5	Exponential
Bare land	4	0.3	Exponential

Constructing Ecological Resistance Surfaces Based on Habitat Risk

The scientific construction of ecological resistance surface is important for the accuracy of ENs identification. Past studies usually determined different ecological resistance values based on different land use types (Peng et al., 2018a,b; Huang et al., 2019). However, within urban agglomeration, landscape characteristics such as the degree of economic development and intensity of human activities vary greatly from region to region, leading to great landscape variability of the same land use type in different regions. Setting resistance values based only on land use types cannot objectively and accurately reflect the degree of landscape disturbance to biological flows. Therefore, this study introduced the habitat risk model to construct ecological resistance surface. The Habitat Risk Assessment (HRA) model is commonly used to evaluate the impact of human activities on ecosystem health, and can reflect the degree of human activities' disturbance to ecosystems. This fits perfectly with the connotation of ecological resistance surfaces. HRA is based on ecological risk theory and spatial overlay analysis, which combines the frequency and

TABLE 3 | Sensitivity coefficient of habitats to threat sources.

Land-use type	Habitat suitability score	Sensitivity to threats					
		Paddy field	Dryland	UC	RC	Road	Bare land
Paddy field	0.6	0	0.3	0.5	0.4	0.3	0.1
Dryland	0.4	0.3	0	0.5	0.4	0.3	0.1
Forest	1	0.8	0.5	1	0.9	0.7	0.3
Grassland	0.8	0.4	0.4	0.6	0.5	0.5	0.3
Wetland	0.9	0.7	0.7	0.9	0.8	0.5	0.3
UC	0	0	0	0	0	0	0
RC	0	0	0	0	0	0	0
Bare land	0	0	0	0	0	0	0

degree of threat of habitat threat factors, the degree of impact on habitat factors and self-restoration ability to simulate and assess the degree of disturbance to ecological land (Arkema et al., 2014; Duggan et al., 2015; Wyatt et al., 2017). In this study, the habitat risk was calculated by the habitat risk module in InVEST3.1.2 (Sharp et al., 2016). And the selection of habitat factors and threat sources were kept consistent with the habitat quality module, and the base parameters were set according to the HRA model guidelines, and the exposure, impact and risk were calculated as follows:

$$E = \frac{\sum_{i=1}^{N} \frac{e_i}{d_i * w_i}}{\sum_{i=1}^{N} \frac{1}{d_i * w_i}} \quad (1)$$

$$C = \frac{\sum_{i=1}^{N} \frac{c_i}{d_i * w_i}}{\sum_{i=1}^{N} \frac{1}{d_i * w_i}} \quad (2)$$

$$R_{ij} = \sqrt{(E-1)^2 + (C-1)^2} \quad (3)$$

$$R_i = \sum_{j=1}^{J} R_{ij} \quad (4)$$

In the formula, E denotes exposure, C denotes influence, Rij denotes the risk of habitat i caused by ecological threat factor j, Ri is the habitat risk value of habitat I, ei is the average ecological threat impact score of all patches of the threatened species, ci is the score of all plaques affected by the habitat factor, wi is the threat score for each grid, di is the data quality score, and N is the number of each habitat evaluation criterion.

However, it is clear from the calculation process of habitat risk that habitat risk can only reflect the ecological resistance value of ecological land. For non-habitats, this study introduced the strength of nighttime light index to reflect the spatial extent and activity intensity of human activities on biological flow. Nighttime light index effectively reflects the spatial extent and activity intensity of human activities in urban area (Yang et al., 2020), and wildlife would avoid areas usually with higher light intensity during their activities to avoid human threats (Gaston et al., 2013).

Identifying the Spatial Range of Ecological Corridors and Their Key Areas Based on Circuit Theory

Identifying the Spatial Range of Ecological Corridors

Circuit theory combines circuits in physics with ecology through random walk theory (McRae and Beier, 2007; McRae et al., 2008). In the process of species migration or dispersal, the landscape is considered as a conductive surface with low resistance in high permeability landscapes and high resistance in low permeability landscapes. The circuit theory model assumes that species migration or dispersal through different resistance values produces differential current densities by connecting source patches and creating cumulative current values as a depletion path (Peng et al., 2018a; Huang L. et al., 2021). Higher cumulative current values indicate better connectivity between the two ecological sources in the area, with more species or more frequent passage of a species through the area, i.e., more frequent use of the ecological corridor. Therefore, this method cannot only simulate the migration routes of organisms between ecological sources by current direction, but also determine the spatial range of ecological corridors by extracting the effective value of cumulative current values (current value > 0). In this study, the Linkage Mapper module (Version 2.0.0) in Circuitscape (McRae and Beier, 2007; McRae et al., 2008)[1] was used to identify the direction of ecological corridors, and corridor ranges were determined using the cumulative current value.

Identifying the Key Areas in Ecological Corridors

In circuit theory, the cumulative current value reflects the net migration of random wanderers. The higher the cumulative current value of a grid, the more important the grid is to the landscape. The areas of the corridor with the highest cumulative current density are called pinch points (McRae et al., 2008; Xiao et al., 2020; Yu et al., 2021), which indicate that species are more likely to pass through the area between habitats or that there are no other available pathways. If pinch points are removed or altered, this will have a very significant impact

[1] http://www.circuitscape.org/

on regional landscape connectivity. Therefore, pinch points are critical areas on ecological corridors and are priority areas for ecological conservation.

The area of the corridor with the highest cumulative current recovery value is called the barrier (Peng et al., 2018a). The ecological corridor at the barrier is actually in a fractured state, and the connectivity between ecological sources must be enhanced by ecological restoration measures. Therefore, barriers are fractured areas in ENs and are priority areas for ecological restoration. The pinchpoint mapper and barrier mapper modules in Circuitscape see text footnote 1were used to identify pinchpoint and barrier.

RESEARCH RESULTS

Spatial Distribution Characteristics of Ecological Sources in Shandong Peninsula Urban Agglomeration

Figure 3 shows the results of MSPA analysis. After spatial statistics, it can be found that the core areas account for about 11.04% of the total area of the study area and about 45.96% of the natural ecological space. They were distributed in clusters within the study area. The areas of high habitat quality in the study area (**Figure 4**) were more consistent with the core areas in terms of spatial distribution. And the ecological sources of the Shandong Peninsula urban agglomeration were obtained by extracting the habitat quality high value areas in the core areas. The ecological sources mainly consisted of forests and wetlands, with a total of 146 locations and a total area of 6,263.73 km^2, accounting for about 8.35% of the study area. In terms of spatial distribution (**Figure 5**), the ecological sources were concentrated in the hilly mountainous and coastal areas of the study area, and were distributed in five groups. The first is the Jinan-Zibo group, including the northern part of Mount Tai, Mount Lu and Mount Yi; the second is the Dongying-Weifang group, including the coastal wetlands of the two regions; the third is the Rizhao group, mainly the Wulian Mountain in Rizhao; the fourth is the Yantai-Weihai group, including the continuous hills of Kunyu Mountain, Mount Ai; The fifth group is the Yantai-Qingdao group, which includes Daji Mountain, Daze Mountain and Mount Cha in the border area between Yantai and Qingdao. In addition to the five groups, a few isolated patches such as Laoshan Mountain were also included. In general, ecological sources were scarce in the central part of the urban agglomeration, resulting in the fragmentation of ecological sources in the Shandong Peninsula urban agglomeration and long distances between source groups.

Spatial Differences in Ecological Resistance Surfaces in the Shandong Peninsula Urban Agglomeration

As shown in **Figure 6**, the spatial heterogeneity of ecological resistance surfaces in the Shandong Peninsula urban agglomeration integrating habitat risk and nighttime light index was significant, which fully reflected the scope and intensity of human activities within the urban agglomeration. Coastal cities such as Yantai, Weihai and Qingdao formed a continuous space of high resistance values along the coastline. Inland cities such as Jinan, Zibo and Weifang formed large-scale contiguous areas of high resistance value near their central urban areas. Small and medium-sized towns between major cities formed areas with the next highest resistance values. In addition, the transportation networks connecting cities and towns also

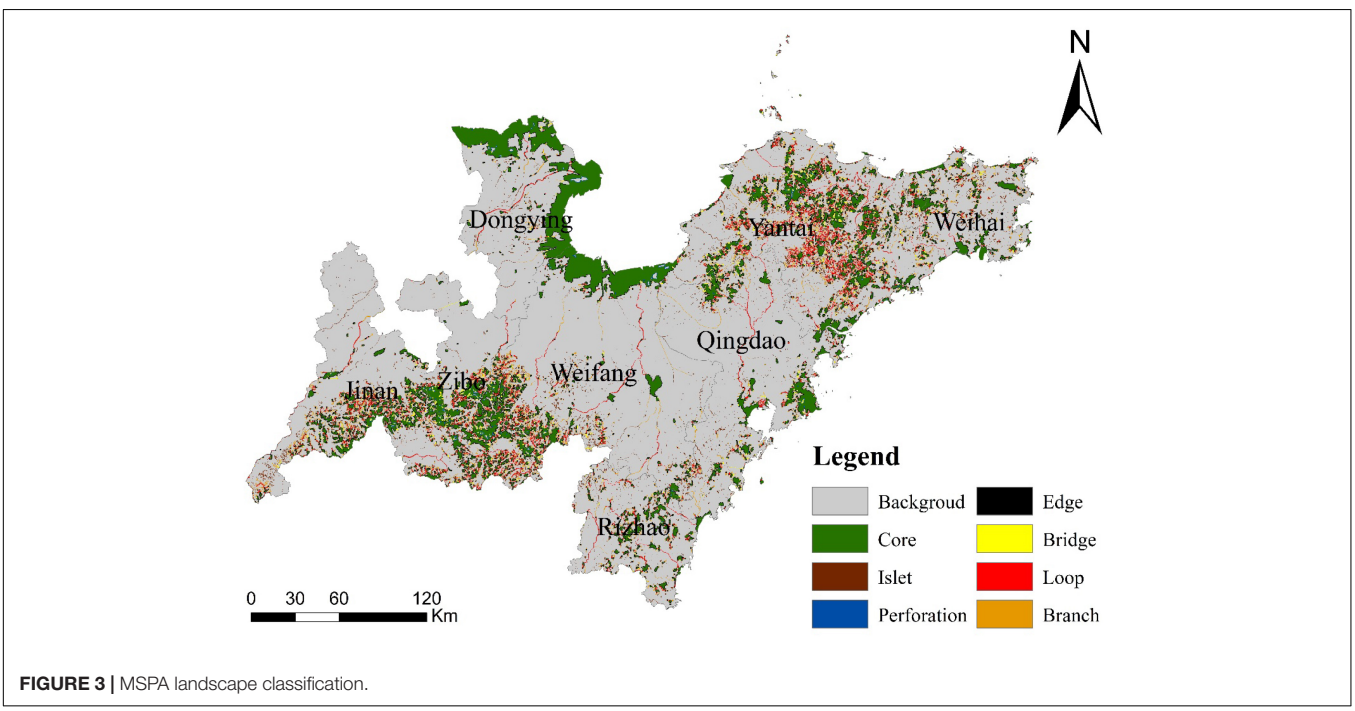

FIGURE 3 | MSPA landscape classification.

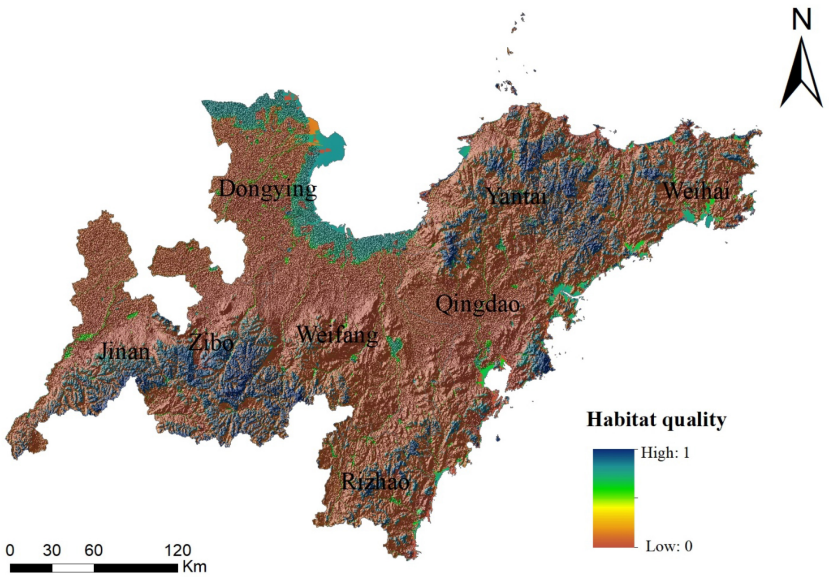

FIGURE 4 | Spatial differentiation of habitat quality in Shandong Peninsula urban agglomeration.

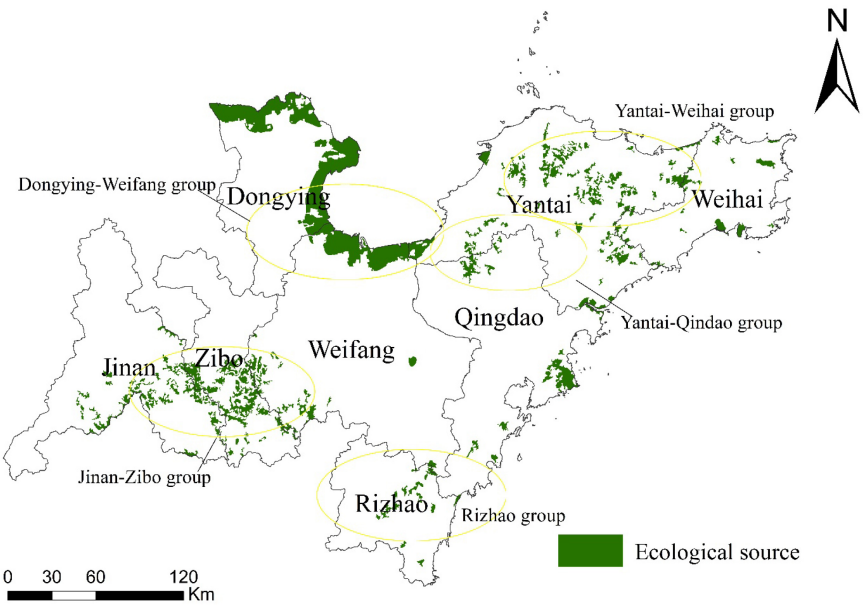

FIGURE 5 | Spatial distribution of ecological sources in Shandong Peninsula urban agglomeration.

have relatively high resistance values. The average resistance value within the urban agglomeration was 21.61. Among them, Qingdao had the highest average resistance value of 25.044, while Zibo, Jinan and Weihai had higher average resistance values than the regional average of 23.79/23.38/22.12. Yantai and Rizhao had the lowest average resistance values of 19.28 and 17.96, respectively. In general, the natural ecological space in the Shandong Peninsula urban agglomeration was squeezed into relatively closed ecological clusters by the contiguous urban space and the dense road traffic network. The inter-group connections were cut and hindered, resulting in a serious impact on the integrity and connectivity of the ecosystem within the urban agglomeration.

Spatial Distribution of Ecological Networks in Shandong Peninsula Urban Agglomeration

Based on the identification and calculation results of ecological sources and ecological resistance surfaces, combined with

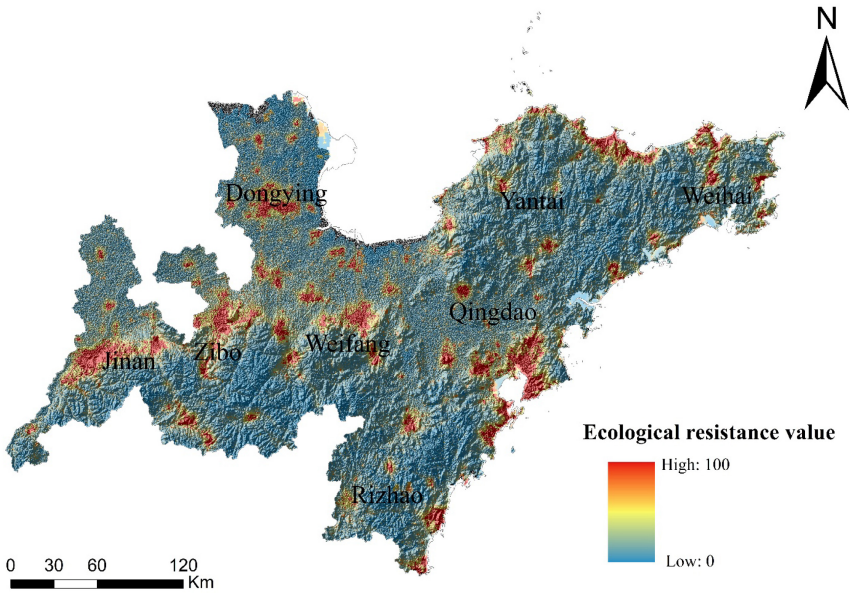

FIGURE 6 | Spatial differentiation of ecological resistance surface in Shandong Peninsula urban agglomeration.

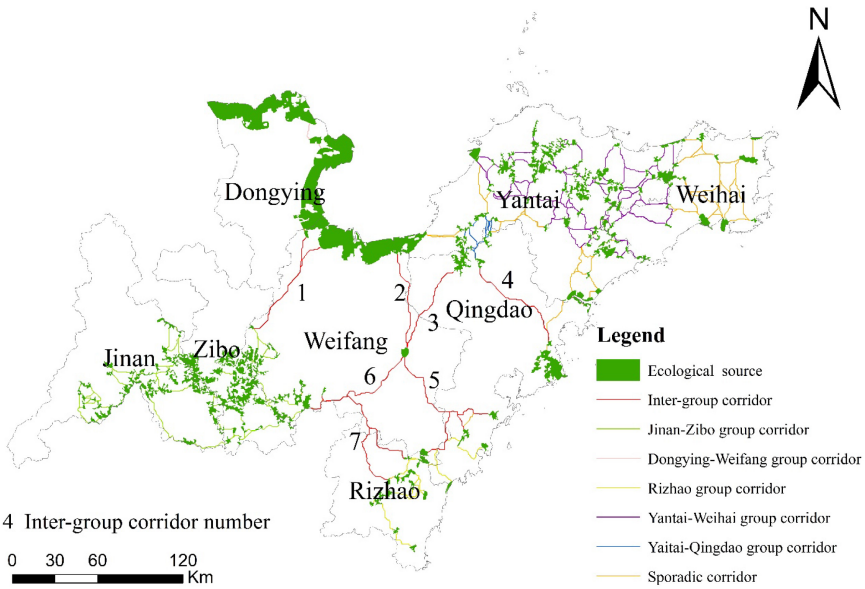

FIGURE 7 | Spatial orientation of ecological corridors in Shandong Peninsula urban agglomeration.

circuit theory calculations, the ecological corridors of Shandong Peninsula urban agglomeration were identified. As shown in **Figure 7**, the total length of ecological corridors in the Shandong Peninsula urban agglomeration was 2994.74 km, and the average length of ecological corridors in each ecological source group was 9.14 km, of which the average distance of ecological corridors in the Jinan-Zibo group was 7.22 km and the average distance in the Rizhao group was 18.27 km. The average length of the inter-group corridors was 76.86 km, among which the No. 1 inter-group corridor and No. 6 inter-group corridor were more than 80 km apart, indicating that the connection between the ecological source groups was weak, and the risk of disturbance and breakage was relatively high.

On the basis of the calculated ecological corridor orientation, the spatial range of the ecological corridor was obtained by calculating the cumulative current values between the sources and extracting the effective current values. As shown in **Figure 8**, the average value of cumulative current value of ecological corridors in urban agglomeration was 0.049, the highest value was 1, and the lowest value tends to be 0. The total area of ecological

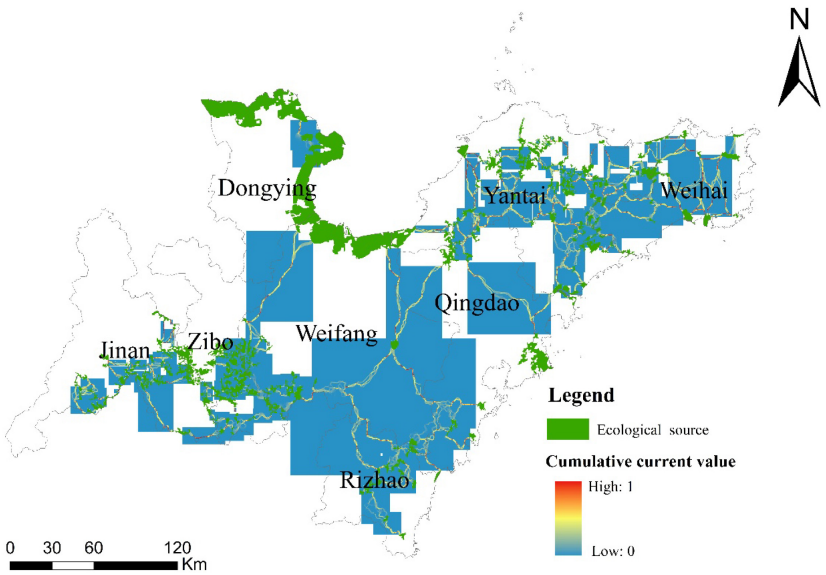

FIGURE 8 | Cumulative current value of ecological corridors in Shandong Peninsula urban agglomeration.

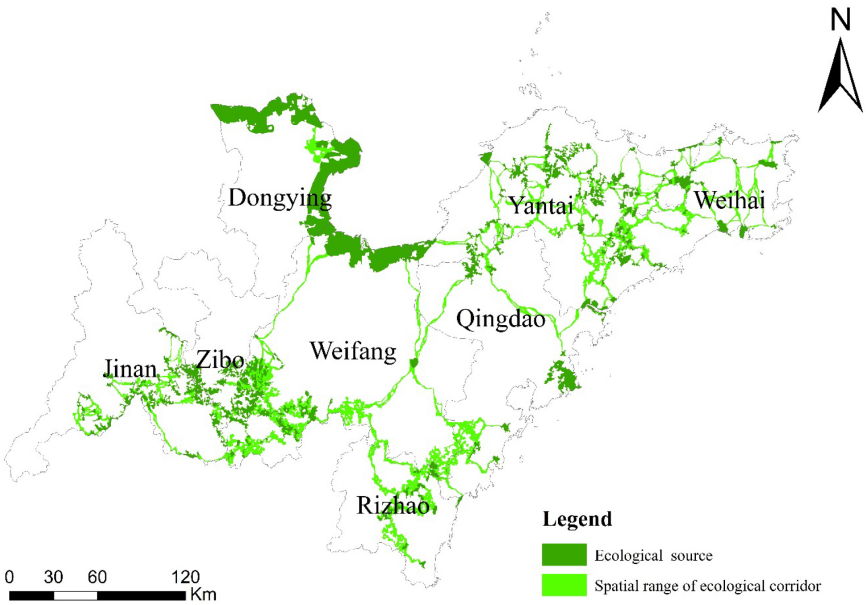

FIGURE 9 | Spatial distribution of ecological networks (ENs) in Shandong Peninsula urban agglomeration.

corridors was 5872.86 km^2. In general, the average width of ecological corridors within urban agglomeration was 1.96 km. However, the width of ecological corridors in different regions varies greatly. The average width of the inter-group corridors was 1.45 km, and the average width of the No. 1 inter-group corridor was the narrowest at 1.12 km, while the average width of the corridors in the Jinan-Zibo eco-source cluster was 3.18 km. This was mainly due to the fact that the inter-group corridors have to traverse human settlements with strong landscape heterogeneity, and the corridor space was severely squeezed, so they were mostly in a narrow linear configuration. On the other hand, most of the ecological corridors in the ecological source groups were natural ecological spaces, and the corridors were less disturbed and squeezed, so they were mostly faceted. This also indicates that biological activities in this area were unrestricted or little restricted, and can flow almost freely.

Integrating ecological sources and ecological corridors, the spatial range of the ENs of the Shandong Peninsula urban agglomeration was identified (**Figure 9**). The total area of the ENs was 12136.61 km^2, accounting for 16.18% of the

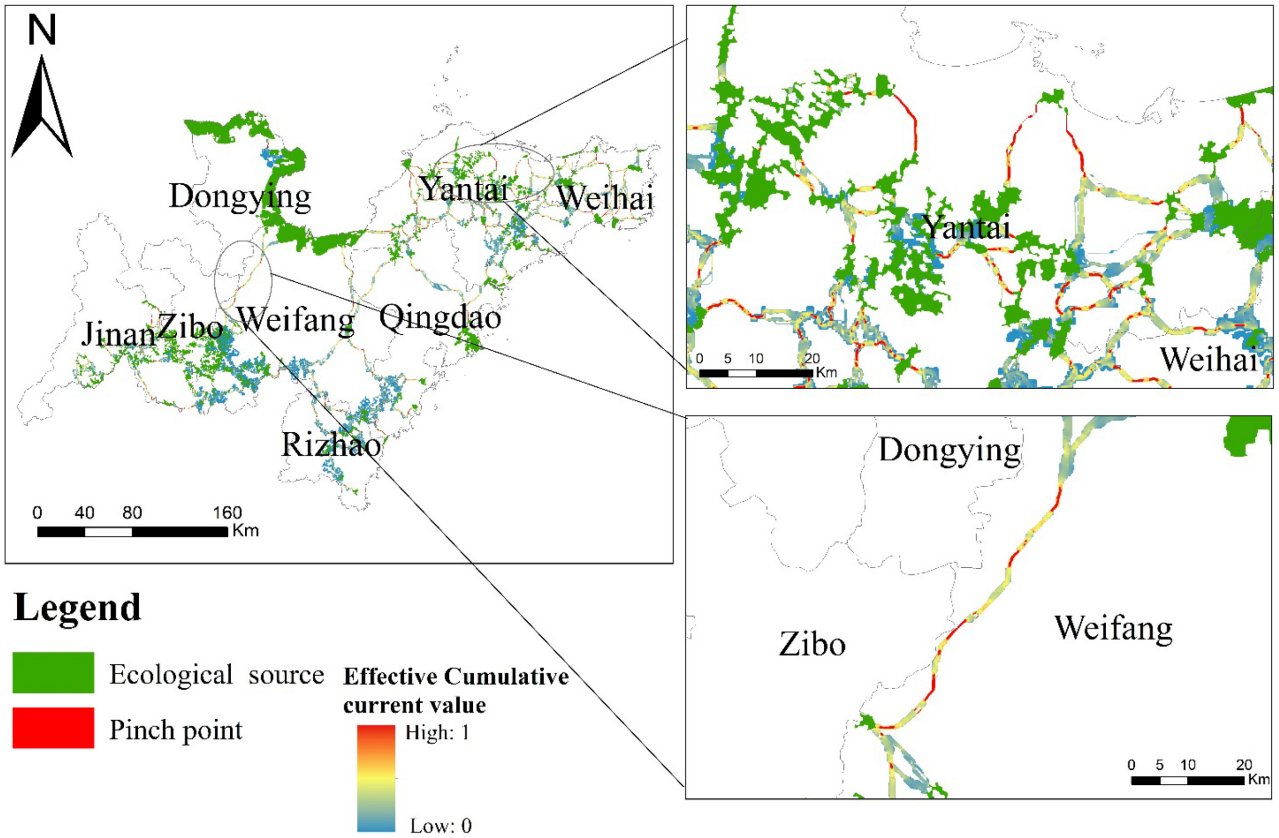

FIGURE 10 | Spatial distribution of conservation priority areas in the ENs of Shandong Peninsula urban agglomeration.

total area of the study area. Among them, they were mainly distributed in Dongying, Zibo and Yantai, accounting for 25.26/19.91/18.27%, respectively; Weihai, Rizhao and Weifang each accounted for about 15%; Jinan and Qingdao accounted for the lowest percentage, about 10% each. The overall ENs also shown the spatial characteristics that dense surrounding and scarcity in the middle, influenced by the concentrated distribution of ecological sources in the periphery of the urban agglomeration.

Priority Conservation and Restoration Areas in the Ecological Networks of Shandong Peninsula Urban Agglomeration

The priority conservation areas are the pinch points on the ecological corridor. As shown in **Figure 10**, the total area of the high value of cumulative current intensity (pinch points) was about 283.61 km^2, accounting for 2.33% of the total area of the ENs. The pinch points were concentrated on the inter-group corridors and the corridors within the Yantai-Weihai group. Most of these corridors passed through dense urban areas and were poorly replaceable; once the function of the pinch point was degraded or lost, it will affect the connection of the whole ENs. Therefore, including the pinch point areas into the priority conservation areas of the ENs and ensuring the smooth flow of ecological corridors in the pinch point areas was the key to ensure that the ecological corridors effectively perform their ecological functions.

The priority restoration area is the barrier on the ecological corridor. As shown in **Figure 11**, the high value areas of cumulative current recovery value (barriers) were mainly distributed in the eastern part of the central urban area of Jinan, the eastern part of the central urban area of Zibo, the eastern part of Qingdao, the southern part of the central urban area of Yantai and the southern part of the southwestern part of the central urban area of Weihai, with a total of 266 locations and a total area of 347.51 km^2, accounting for 2.86% of the total area of the ENs. Among them, there were 61 obstacle points with an area of more than 1 km^2, mainly distributed in the No. 1 inter-group corridor, No. 6 inter-group corridor and within the Yantai-Weihai ecological source group. These areas were densely populated with towns, concentrated contiguous construction land, intensive human activities, fragmented ecological land, narrow ecological corridors, and actual in a fractured state. Among them, the most urgent need for restoration measures was the area where pinch points and barriers overlap, with an area of 88.37 km^2. These areas were the only corridors for biological flow between sources, with no alternative paths, but at the same time were in a broken state, indicating that there

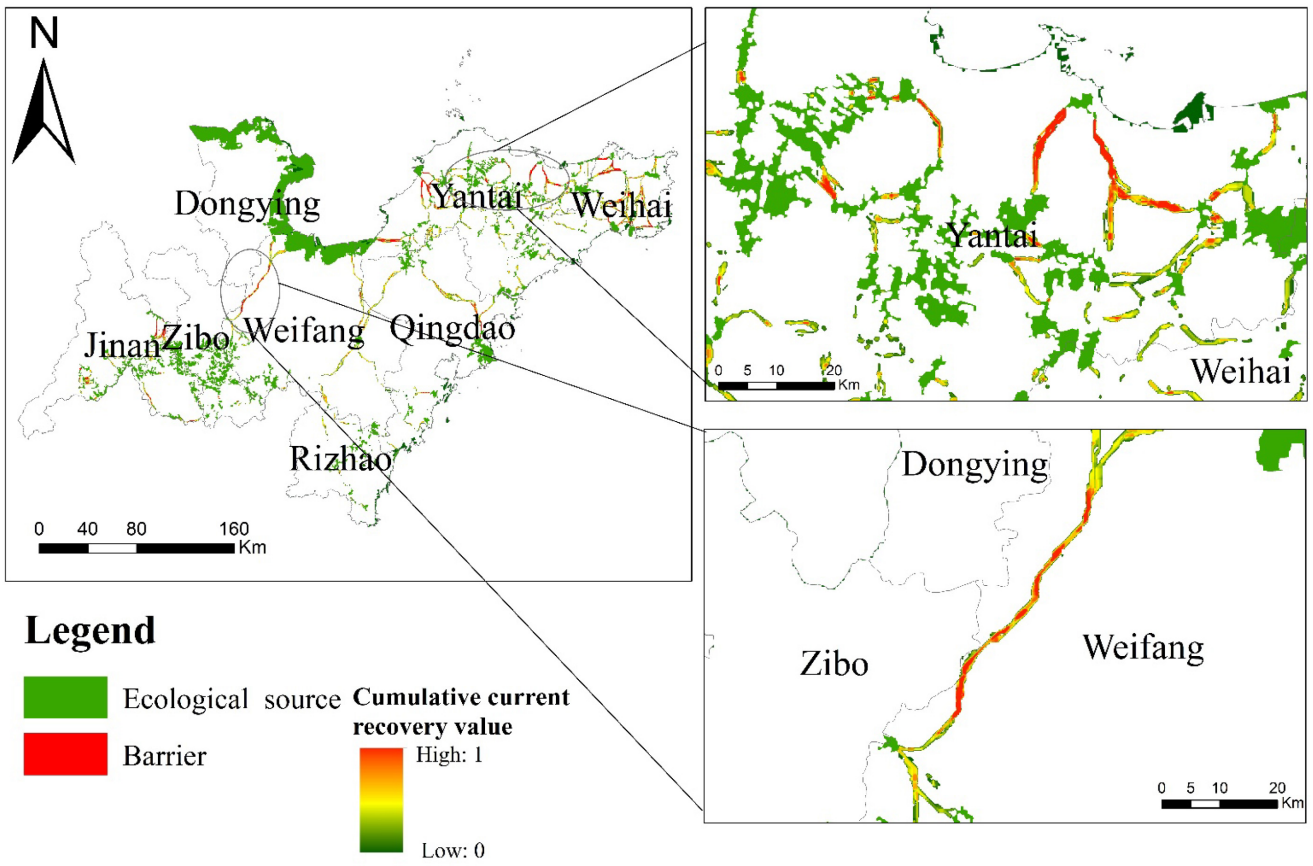

FIGURE 11 | Spatial distribution of restoration priority areas in the ENs of Shandong Peninsula urban agglomeration.

were no available paths between the ecological sources connected by this corridor. Therefore, if restoration measures were not taken in time, the connectivity of the urban agglomeration ecosystem and the effectiveness of ecological functions will be seriously affected.

In general, although the ENs in the Shandong Peninsula urban agglomeration consisted of large ecological sources and large-scale ecological corridors, the construction of ENs needs to focus on only a small part of the study area while maintaining the status quo. Most ecological corridors were in a reliable state, and the area that was in a broken state and must be restored does not exceed 350 km^2. Although it is difficult to maintain the status quo, which is needed to control the rate, scale and direction of urban expansion. However, by focusing on priority areas for restoration and conservation, it provides a viable option for ENs construction.

DISCUSSION AND CONCLUSION

The Role of Ecosystem Functionally Important Areas in Ecological Networks

In this study, we identified ecological sources based on MSPA analysis and habitat quality assessment, constructed ecological resistance surfaces based on habitat risk and nighttime light data, and identified ecological corridors based on circuit theory. In general, we constructed an ENs for the Shandong Peninsula urban agglomeration from the perspective of maintaining ecosystem connectivity. However, the ENs should promote nature conservation on the one hand, and take into account the human demand for ecological products on the other hand, especially in large urban agglomeration. Therefore, ENs should not only maintain the integrity and connectivity of ecosystems, but also maintain and promote the effective performance of ecosystem functions and the effective supply of ecosystem services. Ecosystem functions include four aspects such as production function, regulation function, habitat maintenance function and information function (O'Farrell and Anderson, 2010). Ecosystem functionally important areas are key areas within an ecosystem that can effectively perform ecosystem functions. In the past studies, ecosystem functionally important areas were often directly considered as ecological sources (Weber et al., 2006; Peng et al., 2018b). However, connecting ecosystem functionally important areas (e.g., water connotation areas and recreational recreation areas) using ecological corridors does not seem to promote ecosystem function per se. Considering the natural ecological conditions and ecological needs of the study

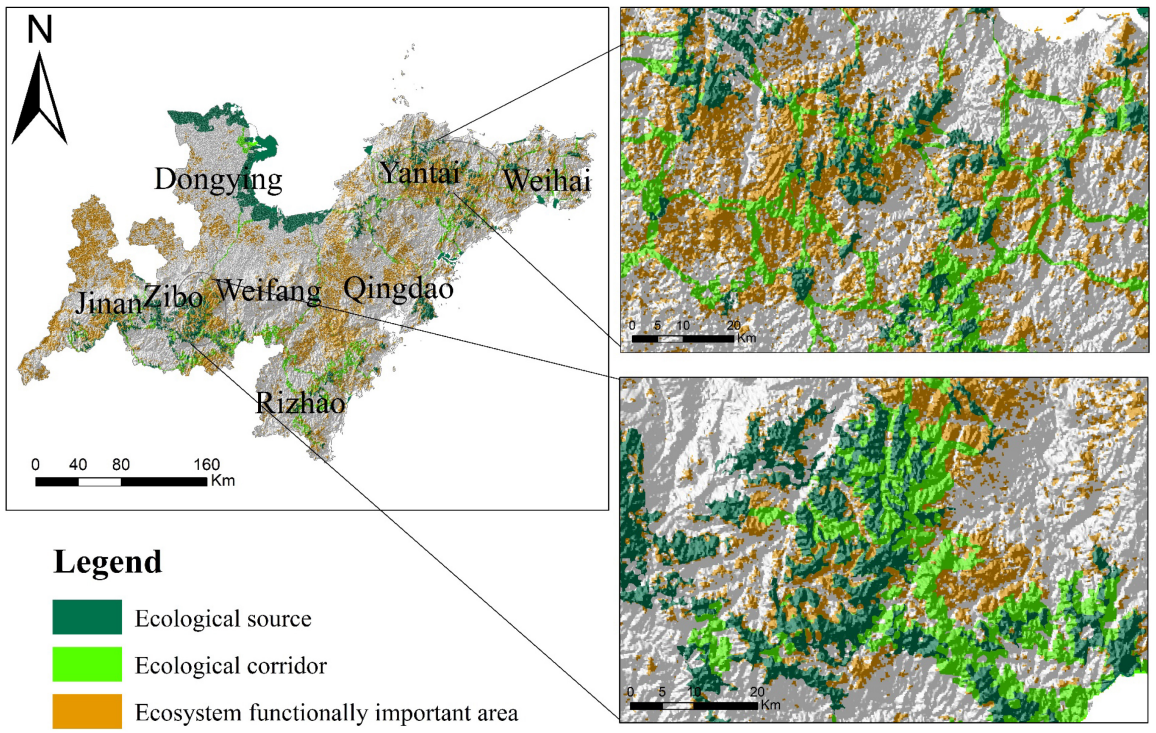

FIGURE 12 | Spatial overlap of ENs and ecosystem functionally important areas.

area, this study discusses the role of ecosystem functionally important area in the ENs by identifying important area of carbon sequestration function and PM2.5 removal function in the regulating function (the detailed calculation process in **Supplementary Material**).

In terms of spatial distribution (**Figure 12**), the scope and area of the ecosystem functionally important areas are much larger than the ecological sources. If the ecosystem functionally important areas are included in the ecological sources, it is likely to identify ineffective ecological corridors, increase the scale and protection cost of the ENs, and reduce the nature conservation value and efficiency. Looking at the spatial overlay of ecological networks and ecosystem functionally important areas, a clear spatial hierarchy can be found. The ecological sources are the core, the ecological corridors are the channels that disperse around the ecological sources, and the ecosystem functionally important areas surround them. Therefore, we consider the ecosystem functionally important areas as a low-intensity land use buffer around the ecological network, which protects the ENs from the high-intensity disturbances associated with urban development and is an important part of the ENs. It can also be considered as a transition area between the natural ecosystem represented by the ENs and the socio-economic system, which provides both a buffer zone for the protection of the ENs and an effective ecosystem service for human society.

Achieving nature conservation and maintaining ecosystem functions are two aspects of ENs, which should not be confused with each other but not completely separated. We believe that on the basis of constructing ENs that maintains regional biodiversity and regional ecosystem connectivity, integrating ecosystem functionally important areas into the ENs and acting as buffer zones for the core elements of the ENs can realize the integration of the structure and function of the ENs.

Implications for the Implementation Plan of Ecological Conservation and Restoration in Shandong Peninsula Urban Agglomeration

For different spatial elements in the ENs, according to the ecological characteristics of various spatial elements and their sensitivity to human activities, the implementation plan for ecological conservation and restoration of large urban agglomeration should develop different conservation and restoration measures. First, the ecological source areas that need strict conservation. For core habitats such as Mount Lu, Mount Yi and Kunyu mountain, ecological conservation measures must be strictly implemented to enhance the conservation and maintenance of habitat systems on the premise of ecological conservation; the intensity of human activities must be reduced as much as possible, and all large-scale production and construction activities are prohibited. Second, ecological corridors that need to be maintained and constructed. For the priority conservation areas on ecological corridors, land use type conversion should be strictly restricted to avoid the loss of ecological functions and affect the efficiency and stability of ENs connectivity. For the

priority restoration areas on ecological corridors, engineering measures such as returning farmland to forest and grass, ecological re-greening, and building wildlife corridors should be taken to restore corridor functions and improve the connectivity of ENs. Third, ecosystem functionally important areas that need to be maintained and protected. Destructive and high-intensity urban development should be avoided in these areas, and agricultural development, tourism development and other development and utilization activities should be carried out without destroying the corresponding ecological functions.

Limitations and Directions for Future Work

In China, ecosystem conservation and restoration has been elevated to a national strategy in response to the enormous threats to the country's natural ecosystem caused by rapid urban expansion over the past decades. Especially in large urban agglomeration, there is an urgent need to identify key ecological spaces and prioritize conservation and restoration. Based on the integration of MSPA and circuit theory, this study develops an integrated approach to identify the spatial range and key areas of ENs and integrate ecosystem functionally important areas into them to form a spatial scheme of ENs that both achieve nature conservation and maintain ecosystem functions. In the ENs identification, we improved the method of setting ecological resistance surface. Unlike most past studies that assigned ecological resistance values based on land use types, we constructed ecological resistance surfaces based on habitat risk and nighttime lighting data. This method takes into account the landscape variability of the same land type in different areas, which makes the setting of resistance values more objective. Based on the effective current intensity and cumulative recovery current values of the ecological corridor calculated by circuit theory, this study identified the width and key areas of the ecological corridor. Compared with most past studies that could only identify the direction of ecological corridors, this made the ENs no longer an abstract network of points and lines, but a spatially presentable landscape entity. And it allows ENs planning and ecological protection and restoration measures for large urban agglomeration to be implemented to specific patches. By focusing on priority conservation and restoration areas in ENs, the effectiveness and connectivity of ENs can be ensured as much as possible by concentrating ecological investments in a few priority areas with limited investments. In addition, we have explored the integration of ecologically important areas into ENs, rather than simply including ecologically important areas into ecological sources, to avoid the creation of ineffective corridors.

However, combined with the existing studies, we believe that there are still some shortcomings in this study that need to be further explored. The determination of the width of ecological corridors is still a difficult problem in ENs research (Weber et al., 2006; Wang et al., 2019; Huang L. et al., 2021). Research on ecological corridor width determination is not mature. This study took the effective current value of the ecological corridor calculated by the model as the spatial range of the ecological corridor. Although it avoids the subjectivity of indicator selection and spatial gradient setting in existing methods and improves the spatial precision of corridor identification, it does not take into account the landscape characteristics, spatial heterogeneity and functional effectiveness inside and outside the corridor. These are the key indicators that may affect the corridor width. Therefore, the accuracy and validity of ecological corridor width still need to be further tested and studied. The design of ecological corridors strictly depends on the spatial scale (Fichera et al., 2015; Liang et al., 2018), so what is the appropriate width of ecological corridors under different geographic environments and spatial scales? Further research should be conducted from different perspective and corridor ecological effect measurement. In addition, in-depth research is needed on the coupling and coordination of nature conservation and ecosystem functions in ENs. In addition to the simple inclusion of ecosystem functionally important areas into ecological networks, the coupling and coordination relationship between biodiversity conservation and multiple ecosystem functions, and the difference in sensitivity of different ecosystem functions to human activities should be explored.

CONCLUSION

Most previous studies on ENs can only determine the orientation of ecological corridors, and were not mature enough in determining their spatial range. In this study, an integrated approach based on MSPA analysis and circuit theory was developed for determining the spatial range of ENs of the Shandong Peninsula urban agglomeration and the priority areas for restoration and protection. The results shown that the ENs of the Shandong Peninsula urban agglomeration consists of 6,263.73 km^2 of ecological sources and 12136.61 km^2 of ecological corridors, accounting for about 16.18% of the total area of the study area. Ecological sources were distributed in groups, and ecological corridors were distributed in a network within each source group and in a narrow line between source groups. The priority conservation areas and priority restoration areas in the ENs were pinch points and barriers on the ecological corridors, respectively, with a total area of 542.75 km^2. Planners and the government should focus implementation planning on priority areas through effective restoration and protection measures, such as eco-redlining policies, eco-agriculture, and reforestation. This method can provide spatial guidance for the implementation of ENs and urban planning for the Shandong Peninsula urban agglomeration. This approach prioritizes ENs in a simple but effective way, which may help planners and the

government to implement ecological protection and restoration projects, and more funds and resources should be allocated to priority areas.

DATA AVAILABILITY STATEMENT

The raw data supporting the conclusions of this article will be made available by the authors, without undue reservation.

AUTHOR CONTRIBUTIONS

TZ and LH: conceptualization, methodology, software, writing—original draft preparation, formal analysis, and visualization. TZ: investigation, resources, data curation, writing—review and editing, supervision, project administration, and funding acquisition. Both authors have read and agreed to the published version of the manuscript.

FUNDING

This research was funded by the National Natural Science Foundation of China (grant no. 42101298).

SUPPLEMENTARY MATERIAL

The Supplementary Material for this article can be found online at: https://www.frontiersin.org/articles/10.3389/fevo.2022.828979/full#supplementary-material

REFERENCES

Afionis, S., Mkwambisi, D. D., and Dallimer, M. (2020). Lack of cross-sector and cross-level policy coherence and consistency limits urban green infrastructure implementation in Malawi. *Front. Environ. Sci.* 8:558619. doi: 10.3389/fenvs.2020.558619

Arkema, K. K., Verutes, G., Bernhardt, J. R., Clarke, C., Rosado, S., Canto, M., et al. (2014). Assessing habitat risk from human activities to inform coastal and marine spatial planning: a demonstration in Belize. *Environ. Res. Lett.* 9:114016. doi: 10.1088/1748-9326/9/11/114016

Coppola, E., Rouphael, Y., Pascale, S. D., Moccia, F. D., and Cirillo, C. (2019). Ameliorating a complex urban ecosystem through instrumental use of softscape buffers: proposal for a green infrastructure network in the metropolitan area of Naples. *Front. Plant Sci.* 10:410. doi: 10.3389/fpls.2019.00410

Cunha, N. S., and Magalhães, M. R. (2019). Methodology for mapping the national ecological network to mainland Portugal: a planning tool towards a green infrastructure. *Ecol. Indic.* 104, 802–818. doi: 10.1016/j.ecolind.2019.04.050

Dai, L., Liu, Y., and Luo, X. (2021). Integrating the MCR and DOI models to construct an ecological security network for the urban agglomeration around Poyang Lake, China. *Sci. Total Environ.* 754:141868. doi: 10.1016/j.scitotenv.2020.141868

D'Aloia, C. C., Naujokaitis-Lewis, I., Blackford, C., Chu, C., Curtis, J. M. R., Darling, E., et al. (2019). Coupled networks of permanent protected areas and dynamic conservation areas for biodiversity conservation under climate change. *Front. Ecol. Evol.* 7:27. doi: 10.3389/fevo.2019.00027

De Montis, A., Ganciu, A., Cabras, M., Bardi, A., Peddio, V., Caschili, S., et al. (2019). Resilient ecological networks: a comparative approach. *Land Use Policy* 89, 104207. doi: 10.1016/j.landusepol.2019.104207

Deng, J. S., Wang, K., Hong, Y., and Qi, J. G. (2009). Spatio-temporal dynamics and evolution of land use change and landscape pattern in response to rapid urbanization. *Landsc. Urban Plann.* 92, 187–198. doi: 10.1016/j.landurbplan.2009.05.001

Dong, J., Peng, J., Liu, Y., Qiu, S., and Han, Y. (2020). Integrating spatial continuous wavelet transform and kernel density estimation to identify ecological corridors in megacities. *Landsc. Urban Plann.* 199:103815. doi: 10.1016/j.landurbplan.2020.103815

Duggan, J. M., Eichelberger, B. A., Ma, S., Lawler, J. J., and Ziv, G. (2015). Informing management of rare species with an approach combining scenario modeling and spatially explicit risk assessment. *Ecosyst. Health Sustain.* 1, 1–18. doi: 10.1890/EHS14-0009.1

Elansky, N. F., Ponomarev, N. A., and Verevkin, Y. M. (2018). Air quality and pollutant emissions in the moscow megacity in 2005–2014. *Atmos. Environ.* 175, 54–64. doi: 10.1016/j.atmosenv.2017.11.057

Fichera, C. R., Laudari, L., and Modica, G. (2015). Application, validation and comparison in different geographical contexts of an integrated model for the design of ecological networks. *J. Agric. Eng.* 46, 52–61. doi: 10.4081/jae.2015.459

Gaston, K. J., Bennie, J., and Davies, T. W. (2013). The ecological impacts of nighttime light pollution: a mechanistic appraisal. *Biol. Rev.* 88, 912–927. doi: 10.1111/brv.12036

Hammad, A. A., and Tumeizi, A. (2012). Land degradation: socioeconomic and environmental causes and consequences in the eastern mediterranean. *Land Degrad. Dev.* 23, 216–226. doi: 10.1002/ldr.1069

Huang, L., Wang, J., Fang, Y., Zhai, T., and Cheng, H. (2021). An integrated approach towards spatial identification of restored and conserved priority areas of ecological network for implementation planning in metropolitan region. *Sustain. Cities Soc.* 69:102865. doi: 10.1016/j.scs.2021.102865

Huang, L. Y., Liu, S. H., Fang, Y., and Zou, L. (2019). Construction of Wuhan's ecological security pattern under the" quality-risk-requirement" framework. *J. Appl. Ecol.* 30, 615–626. doi: 10.13287/j.1001-9332.201902.014

Huang, X., Wang, H., Shan, L., and Xiao, F. (2021). Constructing and optimizing urban ecological network in the context of rapid urbanization for improving landscape connectivity. *Ecol. Indic.* 132:108319. doi: 10.1016/j.ecolind.2021.108319

Isaac, N. J., Brotherton, P. N., Bullock, J. M., Gregory, R. D., Boehning-Gaese, K., Connor, B., et al. (2018). Defining and delivering resilient ecological networks: nature conservation in England. *J. Appl. Ecol.* 55, 2537–2543. doi: 10.1111/1365-2664.13196

Jin, G., Chen, K., Liao, T., Zhang, L., and Najmuddin, O. (2020). Measuring ecosystem services based on government intentions for future land use in Hubei Province: implications for sustainable landscape management. *Landsc. Ecol.* 36, 2025–2042. doi: 10.1007/s10980-020-01116-3

Kong, F., Ban, Y., Yin, H., James, P., and Dronova, I. (2017). Modeling stormwater management at the city district level in response to changes in land use and low impact development. *Environ. Modell. Softw.* 95, 132–142. doi: 10.1016/j.envsoft.2017.06.021

Li, F., Wang, L., Chen, Z., Clarke, K. C., Li, M., and Jiang, P. (2018). Extending the SLEUTH model to integrate habitat quality into urban growth simulation. *J. Environ. Manag.* 217, 486–498. doi: 10.1016/j.jenvman.2018.03.109

Li, S., Wu, X., Zhao, Y., and Lv, X. (2020). Incorporating ecological risk index in the multi-process mcre model to optimize the ecological security pattern in a semi-arid area with intensive coal mining: a case study in northern china - sciencedirect. *J. Clean. Prod.* 247:119143. doi: 10.1016/j.jclepro.2019.119143

Liang, J., He, X., Zeng, G., Zhong, M., Gao, X., Li, X., et al. (2018). Integrating priority areas and ecological corridors into national network for conservation planning in China. *Sci. Total Environ.* 626, 22–29. doi: 10.1016/j.scitotenv.2018.01.086

Liquete, C., Kleeschulte, S., Dige, G., Maes, J., Grizzetti, B., Olah, B., et al. (2015). Mapping green infrastructure based on ecosystem services and ecological networks: a Pan-European case study. *Environ. Sci. Policy* 54, 268–280. doi: 10.1016/j.envsci.2015.07.009

Marchant, S. C. (2014). *Investing in Ecological Infrastructure: A Framework for Sustainable Development*. Brisbane, QLD: The University of Queensland, doi: 10.14264/UQL.2014.425

Masum, K. M., Mansor, A., Sah, S. A. M., and Lim, H. S. (2017). Effect of differential forest management on land-use change (luc) in a tropical hill forest of malaysia. *J. Environ. Manag.* 200, 468–474. doi: 10.1016/j.jenvman.2017.06.009

Mcdonald, R. I., Güneralp, B., Chun-Wei, H., Seto, K. C., and Mingde, Y. (2018). Conservation priorities to protect vertebrate endemics from global urban expansion. *Biol. Conserv.* 224, 290–299. doi: 10.1016/j.biocon.2018.06.010

McRae, B. H., and Beier, P. (2007). Circuit theory predicts gene flow in plant and animal populations. *Proc. Natl. Acad. Sci. U.S.A.* 104, 19885–19890. doi: 10.1073/pnas.0706568104

McRae, B. H., Dickson, B. G., Keitt, T. H., and Shah, V. B. (2008). Using circuit theory to model connectivity in ecology, evolution, and conservation. *Ecology* 89, 2712–2724. doi: 10.1890/07-1861.1

O'Farrell, P. J., and Anderson, P. M. (2010). Sustainable multifunctional landscapes: a review to implementation. *Curr. Opin. Environ. Sustain.* 2, 59–65. doi: 10.1016/j.cosust.2010.02.005

Pei, F., Li, X., Liu, X., Lao, C., and Xia, G. (2015). Exploring the response of net primary productivity variations to urban expansion and climate change: a scenario analysis for guangdong province in china. *J. Environ. Manag.* 150, 92–102. doi: 10.1016/j.jenvman.2014.11.002

Peng, J., Lin, H., Chen, Y., Blaschke, T., Luo, L., Xu, Z., et al. (2020). Spatiotemporal evolution of urban agglomerations in China during 2000–2012: a nighttime light approach. *Landsc. Ecol.* 35, 421–434. doi: 10.1007/s10980-019-00956-y

Peng, J., Pan, Y., and Liu, Y. (2018a). Linking ecological degradation risk to identify ecological security patterns in a rapidly urbanizing landscape. *Habitat Int.* 71, 110–124. doi: 10.1016/j.habitatint.2017.11.010

Peng, J., Tian, L., Liu, Y., Zhao, M., Hu, Y., and Wu, J. (2017). Ecosystem services response to urbanization in metropolitan areas: thresholds identification. *Sci. Total Environ.* 60, 706–714. doi: 10.1016/j.scitotenv.2017.06.218

Peng, J., Yang, Y., Liu, Y., Du, Y., Meersmans, J., and Qiu, S. (2018b). Linking ecosystem services and circuit theory to identify ecological security patterns. *Sci. Total Environ.* 644, 781–790. doi: 10.1016/j.scitotenv.2018.06.292

Peng, J., Zhao, S., Dong, J., Liu, Y., Meersmans, J., Li, H., et al. (2019). Applying ant colony algorithm to identify ecological security patterns in megacities. *Environ. Modell. Softw.* 117, 214–222. doi: 10.1016/j.envsoft.2019.03.017

Pierik, M. E., Dell'Acqua, M., Confalonieri, R., Bocchi, S., and Gomarasca, S. (2016). Designing ecological corridors in a fragmented landscape: a fuzzy approach to circuit connectivity analysis. *Ecol. Indic.* 67, 807–820. doi: 10.1016/j.ecolind.2016.03.032

Rebelo, A. G., Holmes, P. M., Dorse, C., and Wood, J. (2011). Impacts of urbanization in a biodiversity hotspot: conservation challenges in metropolitan cape town. *South Afr. J. Bot.* 77, 20–35. doi: 10.1016/j.sajb.2010.04.006

Salvati, L., Zambon, I., Chelli, F. M., and Serra, P. (2018). Do spatial patterns of urbanization and land consumption reflect different socioeconomic contexts in europe? *Sci. Total Environ.* 625, 722–730. doi: 10.1016/j.scitotenv.2017.12.341

Sharp, R., Tallis, H. T., Ricketts, T., Guerry, A. D., Wood, S. A., Chaplin-Kramer, R., et al. (2016). *InVEST+ VERSION+ User's Guide. The Natural Capital Project*.

Sigwela, A., Elbakidze, M., Powell, M., and Angelstam, P. (2017). Defining core areas of ecological infrastructure to secure rural livelihoods in South Africa. *Ecosyst. Serv.* 27, 272–280. doi: 10.1016/j.ecoser.2017.07.010

Soille, P., and Vogt, P. (2009). Morphological segmentation of binary patterns. *Pattern Recogn. Lett.* 30, 456–459. doi: 10.1016/j.patrec.2008.10.015

Su, Y., Chen, X., Liao, J., Zhang, H., Wang, C., Ye, Y., et al. (2016). Modeling the optimal ecological security pattern for guiding the urban constructed land expansions. *Urban For. Urban Green.* 19, 35–46. doi: 10.1016/j.ufug.2016.06.013

Sun, X., Jiang, Z., Liu, F., and Zhang, D. (2019). Monitoring spatio-temporal dynamics of habitat quality in Nansihu Lake basin, eastern China, from 1980 to 2015. *Ecol. Indic.* 102, 716–723. doi: 10.1016/j.ecolind.2019.03.041

Tang, F., Zhou, X., Wang, L., Zhang, Y., Fu, M., and Zhang, P. (2021). Linking ecosystem service and MSPA to construct landscape ecological network of the huaiyang section of the grand canal. *Land* 10:919. doi: 10.3390/land10090919

Wang, S., Liu, X., Wu, P., Feng, K., and Sun, L. (2019). Impacts of urban expansion on terrestrial carbon storage in china. *Environ. Sci. Technol.* 53, 6834–6844. doi: 10.1021/acs.est.9b00103

Wang, Y., and Pan, J. (2019). Building ecological security patterns based on ecosystem services value reconstruction in an arid inland basin: a case study in Ganzhou District, NW China. *J. Clean. Prod.* 241:118337. doi: 10.1016/j.jclepro.2019.118337

Weber, T., Sloan, A., and Wolf, J. (2006). Maryland's green infrastructure assessment: development of a comprehensive approach to land conservation. *Landsc. Urban Plann.* 77, 94–110. doi: 10.1016/j.landurbplan.2005.02.002

Wyatt, K. H., Griffin, R., Guerry, A. D., Ruckelshaus, M., Fogarty, M., and Arkema, K. K. (2017). Habitat risk assessment for regional ocean planning in the U.S. Northeast and Mid-Atlantic. *PLoS One* 12:e0188776. doi: 10.1371/journal.pone.0188776

Xiao, L., Cui, L., Jiang, Q., Wang, M., Xu, L., and Yan, H. (2020). Spatial structure of a potential ecological network in Nanping, China, based on ecosystem service functions. *Land* 9:376. doi: 10.3390/land9100376

Xu, Q., Zheng, X., and Zheng, M. (2019). Do urban planning policies meet sustainable urbanization goals? A scenario-based study in Beijing, China. *Sci. Total Environ.* 670, 498–507. doi: 10.1016/j.scitotenv.2019.03.128

Yang, J., Wang, Y., Xiu, C., Xiao, X., Xia, J., and Jin, C. (2020). Optimizing local climate zones to mitigate urban heat island effect in human settlements. *J. Clean. Prod.* 275:123767. doi: 10.1016/j.jclepro.2020.123767

Yang, R., Bai, Z., and Shi, Z. (2021). Linking morphological spatial pattern analysis and circuit theory to identify ecological security pattern in the loess plateau: taking Shuozhou City as an example. *Land* 10:907. doi: 10.3390/land10090907

Yu, H., Huang, J., Ji, C., and Li, Z. (2021). Construction of a landscape ecological network for a large-scale energy and chemical industrial base: a case study of Ningdong, China. *Land* 10:344. doi: 10.3390/land10040344

Zhai, T., Wang, J., Fang, Y., Qin, Y., Huang, L., and Chen, Y. (2020). Assessing ecological risks caused by human activities in rapid urbanization coastal areas: towards an integrated approach to determining key areas of terrestrial-oceanic ecosystems preservation and restoration. *Sci. Total Environ.* 708:135153. doi: 10.1016/j.scitotenv.2019.135153

Zhang, R., Pu, L., Li, J., Zhang, J., and Xu, Y. (2016). Landscape ecological security response to land use change in the tidal flat reclamation zone, China. *Environ. Monit. Assess.* 188, 1–10. doi: 10.1007/s10661-015-4999-z

Conflict of Interest: The authors declare that the research was conducted in the absence of any commercial or financial relationships that could be construed as a potential conflict of interest.

Publisher's Note: All claims expressed in this article are solely those of the authors and do not necessarily represent those of their affiliated organizations, or those of the publisher, the editors and the reviewers. Any product that may be evaluated in this article, or claim that may be made by its manufacturer, is not guaranteed or endorsed by the publisher.

frontiers in Environmental Science

ORIGINAL RESEARCH
published: 08 February 2022
doi: 10.3389/fenvs.2022.824254

Spatiotemporal Differentiation of Land Ecological Security and Its Influencing Factors: A Case Study in Jinan, Shandong Province, China

Jinhua Liu[1†], *Xiangyang Cao*[2†], *Lesong Zhao*[3], *Guanglong Dong*[1] *and Kun Jia*[1*]

[1]School of Management Engineering, Shandong Jianzhu University, Jinan, China, [2]School of Civil Engineering, Shandong Jiaotong University, Jinan, China, [3]School of Public Administration, South China Agricultural University, Guangzhou, China

Land ecological security plays an important role in the sustainable land resources utilization and social economic development. In this study, the Pressure-State-Response (PSR) model was constructed to measure the land ecological security pattern based on grids scale of Jinan from 2006 to 2016. Then, Moran's index was used to explore the spatial autocorrelation of the land ecological security score. Finally, the driving factors of land ecological security pattern differentiation in Jinan were revealed by using geographical detector method. The results showed that the level of land ecological security in Jinan, generally, decreased at the beginning and then gradually increased during the research periods. More specifically, land ecological security was represented as a downward trend in the central region and an upward trend in the southern mountainous area. The apparent regional heterogeneity of land ecological security level in Jinan showed the overall distribution pattern "low in the middle and high around" and the direction of urban expansion consistent with the low-level land ecological security. Land ecological security presented a significant spatial autocorrelation. The differentiation of land ecological security pattern was mainly driven by social and economic development factors, among which urban expansion was most important, so urban development should try to avoid occupying those areas with high level of land ecological security. From the study, the valuable information could be provided in the improvement of land ecosystem environment and in the facilitation of sustainable development.

Keywords: land ecological security, spatiotemporal differentiation, influencing factors, PSR model, geographical detector, Jinan

OPEN ACCESS

Edited by:
Fan Zhang,
Institute of Geographic Sciences and Natural Resources Research (CAS), China

Reviewed by:
Shanzhong Qi,
Shandong Normal University, China
Wei Liu,
Shandong Normal University, China

****Correspondence:***
Kun Jia
jiakun20@sdjzu.edu.cn

[†]These authors have contributed equally to this work

Specialty section:
This article was submitted to Conservation and Restoration Ecology, a section of the journal Frontiers in Environmental Science

Received: *29 November 2021*
Accepted: *04 January 2022*
Published: *08 February 2022*

Citation:
Liu J, Cao X, Zhao L, Dong G and Jia K (2022) Spatiotemporal Differentiation of Land Ecological Security and Its Influencing Factors: A Case Study in Jinan, Shandong Province, China. Front. Environ. Sci. 10:824254. doi: 10.3389/fenvs.2022.824254

1 INTRODUCTION

Land is the material basis for the survival and development of human society and the basic premise for the healthy development of an ecosystem (Zhang et al., 2007; Wu et al., 2019a; Liu et al., 2020). With the acceleration of industrialization and urbanization, human demand for land is increasing (Chen, 2007; Long et al., 2012; Wu and Zhang, 2012). Unreasonable land use not only makes more apparent the contradiction between increasing population and land use, but it also causes a series of ecological problems (Kim et al., 2009; Nunes et al., 2011). With the ecological problems attracting broad attention by the government, ecological security has gradually become a hot topic in the international ecological environment research field and a new theme of the sustainable development

of the human economy and society (Steffen et al., 2015). Numerous studies have been carried out worldwide and a series of significant developments have been achieved (Yang et al., 2018).

The concept of land ecological security originates from ecological security, representing the health of environment and sustainability of land resources and ecosystems, which can provide steady ecological services and meet ecological needs for future generations (Wen et al., 2021). Studies have shown that land use can greatly influence the regional environment and ecosystem services, and land ecological security is important to the ecosystem (Liu et al., 2019b; Wu et al., 2019b). Especially with the rapid increase of population, the excessive pursuit of economic benefits of land use has destroyed the land ecology to a certain extent. Conversely, land ecological destruction has increasingly restricted human social and economic activities, and reduced land sustainability. At present, many regions are in a critical period of ecological environment quality transformation (Cohen, 2006). As the capital of Shandong, Jinan is in the stage of rapid urbanization and is faced with considerable discussion on land use and ecological environmental protection (Qi et al., 2020; Liu et al., 2021a). The systematic evaluation and analysis of land ecological security and its influencing factors have important significance for ecological civilization construction and high-quality social economic development in Jinan.

In recent years, land ecological security has attracted much attention (Yan et al., 2015; Feng et al., 2018; Guo et al., 2021). From the research content, scholars mainly carry out land ecological security evaluation from different research scales, indexes, and methods (Li et al., 2014; Li et al., 2019a; Liu et al., 2019a; Yang and Cai, 2020). Research scales are generally divided into time scale and space scale. The time scale includes static and dynamic. The spatial scale is mainly concentrated on provinces, cities, counties, a few important economic zones, and watersheds. The evaluation indexes of land ecological security are mainly constructed by Pressure-State-Response (PSR), Economy-Environment-Society, and Driving Force-Pressure-State-Impact-Response (DPSIR) (Wolfslehner and Vacik, 2008; Sekovski et al., 2012; Geissdoerfer et al., 2017). The evaluation methods mainly include the comprehensive index method, matter element model, gray correlation method, ecological footprint method, TOPSIS method, etc. (Behzadian et al., 2012; Gong et al., 2012; Li et al., 2019b; Ma et al., 2019; Seyedmohammadi et al., 2019). The existing research has enriched the research content of land ecological security and promoted the process of ecological civilization construction. However, the current research mainly focuses on large-scale regions (city and country), and it is difficult to accurately express the evaluation results. It is imperative to analyze the land ecological security based on a spatial scale of grids. Besides, the difficulty of existing evaluation index in adapting to the regional characteristics of the study area will cause poor management of specific land. In addition, the core of land ecological security lies in effective identification of key influencing factors which include such factors as social-economic development and human activities that tend to be ignored in previous studies, and thus should be given a comprehensive consideration.

From what has been discussed above, this study analyzed the spatiotemporal differentiation of land ecological security and its influencing factors based on multi-source data in Jinan from 2006 to 2016. The evaluation index system was established at the beginning by the use of the PSR model reflecting the interaction mechanisms between the natural and the social ecosystem. Then, land ecological security was evaluated based on 1 km*1 km grids determining the index weights by the entropy weight and analytic hierarchy process (AHP) method, and the spatiotemporal pattern was analyzed thoroughly. Finally, the geographical detector method was employed to identify the dominant factors influencing the spatial differentiation of land ecological security from four aspects. The results can provide meaningful insights for sustainable land use and sustainable urban development, and facilitate decision-makers to formulate refined optimization countermeasures. The objectives of this study were (1) to evaluate the land ecological security and analyze the spatiotemporal pattern in Jinan; and (2) to investigate the influencing factors driving the spatial differentiation of land ecological security.

2 MATERIALS AND METHODS

2.1 Study Area

Jinan, located in the middle of the Shandong province in China, stands at the edge of a foothill and an alluvial plain with high topography in the south and low topography in the north (**Figure 1**). Its location close to the mountain Tai in the south and the Yellow River in the north makes the city vital to ecological environmental protection. Because of the "72 famous springs," it also has the reputation as a "Spring City." Meanwhile, it is one of the central cities in the south of Bohai Rim and the middle and lower reaches of the Yellow River.

2.2 Data Source

The data is divided into land spatial statistics and socio-economic statistics. The land spatial statistics obtained from the Jinan Land Resources Department and other relevant departments, include current land utilization statistics, land use annual alteration investigation statistics, investigation achievement of cultivated land backup resources, capital farmland delimitation, ecological function delimitation, biodiversity conservation, and ecological conservation district data. The socio-economic data was collected from Jinan Statistical Yearbook (for 2007, 2012, and 2017), the environmental collection bulletin, and the 13th Five-Year-Plan forestation development strategy. Through recalculation, the data is recalculated into 8460 grids (1 km*1 km).

2.3 Methodology

2.3.1 Establishment of PSR Model Index System

The study, based on the PSR model, selected 24 indicators to construct the land ecological security evaluation index system in Jinan (**Table 1**). Among the system, the direct influences on the land ecological security exerted by different utilization patterns

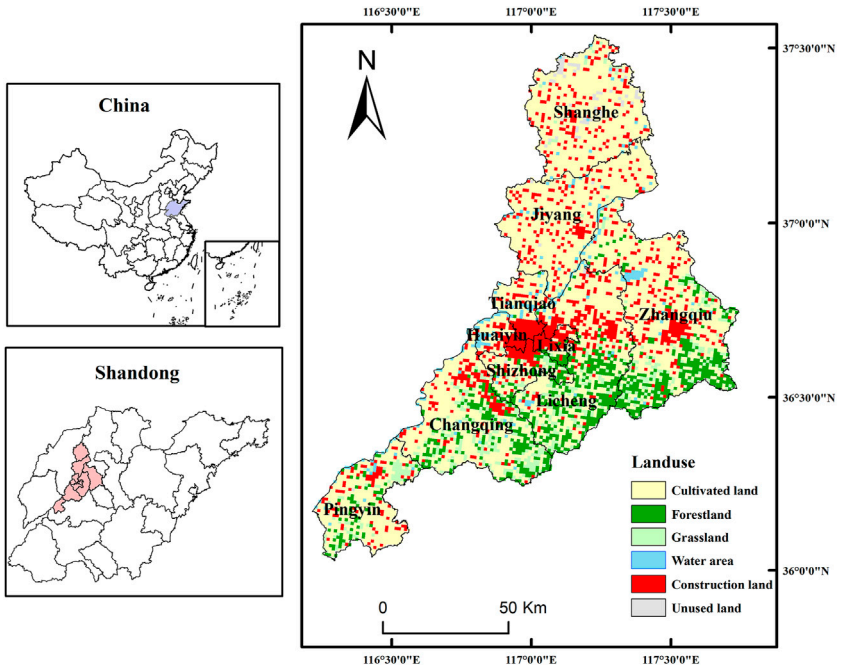

FIGURE 1 | Study area.

TABLE 1 | Land ecological security assessment indexes in Jinan.

Target	Project	Factor	Index	Scale	Attribute	Reference
Land ecological security	Pressure	Population	Population density	County/District	Negative	Ma et al. (2019)
			Population growth rate	County/District	Negative	Gao et al. (2018)
		Land	Per cultivated land chemical fertilizer	County/District	Negative	Ma et al. (2019)
			Per cultivated land pesticide	County/District	Negative	Li et al. (2019a)
			Proportion of aline-alkali soil	Grid	Negative	Chen et al. (2019)
		City	Urbanization rate	County/District	Negative	Liu et al. (2019a)
			Proportion of construction land	Grid	Negative	Wen et al. (2021)
	State	Resource	Per capita cultivated land	Grid	Positive	Ma et al. (2019)
			Per capita land resource backup	Grid	Positive	Li et al. (2019a)
			Proportion of transportation land	Grid	Negative	Liu et al. (2019a)
		Ecology	The forest coverage rate	Grid	Positive	Li et al. (2020)
			Proportion of water area	Grid	Positive	Wu et al. (2019a)
			Proportion of grassland	Grid	Positive	Feng et al. (2017)
			Spring group distribution	Grid	Positive	Yang et al. (2021)
		Economy	Yield per area under crops	County/District	Positive	Ma et al. (2019)
			Per capita GDP	County/District	Negative	Feng et al. (2017)
			Economic density	County/District	Negative	Ma et al. (2019)
	Response	Environment	Proportion of environment protection investment in GDP	County/District	Positive	Li et al. (2019a)
			Carbon emission per billion yuan in GDP	County/District	Negative	Feng et al. (2018)
		Policy	Proportion of forestation	Grid	Positive	Chen et al. (2019)
			Effective irrigation area	County/District	Positive	Gong et al. (2012)
			Natural reserve	Grid	Positive	Liu et al. (2019a)
		Industry	Proportion of primary industry in GDP	County/District	Positive	Su et al., 2011
			Proportion of tertiary industry in GDP	County/District	Positive	Wen et al. (2021)

can be reflected by the project "Pressure," from which the indexes were constructed from seven indicators: population density, population growth rate, per cultivated land chemical fertilizer, per cultivated land pesticide, proportion of aline-alkali soil, urbanization rate, and proportion of construction land. The project "State" indicated the current situation or future tendency of the target, containing ten indicators for the construction of the indexes: per capita cultivated land, per capita land resource backup, proportion of transportation land, forest coverage rate, proportion of water area, proportion

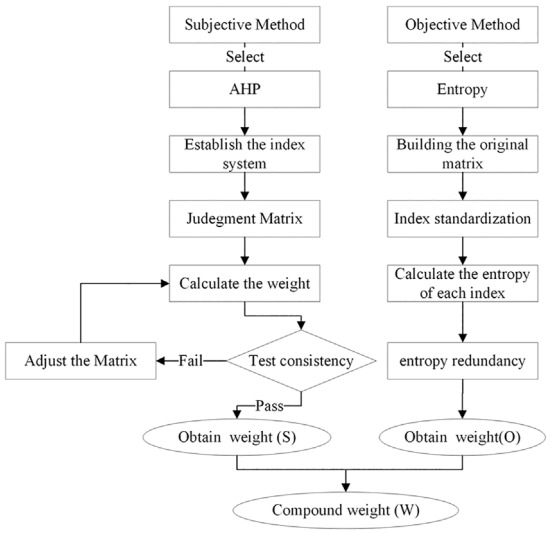

FIGURE 2 | Flow chart of weight determination.

of grassland, spring group distribution, yield per area under crops, per capita GDP, and economic density. "Response," another project in the system, representing the efforts made in environmental rehabilitation and adjustments, included seven more indicators to construct the indexes: proportion of environmental protection investment in GDP, carbon emission per billion yuan in GDP, proportion of forestation, effective irrigation area, natural reserve, proportion of primary industry in GDP, and proportion of tertiary industry in GDP. On the whole, the PSR model reflects the integration of nature, society, and human beings.

2.3.2 Standardization of the Index

Given the great dimensional variations between different indicators, we performed logarithmic transformation and standardized all evaluation indicators within each grid cell. In total, 13 positive indicators and 11 negative indicators were established considering the impact of each indicator on land ecological security. The formulas for standardization were indicated below (Zhang et al., 2017).

$$\text{Positive index}: X_{ij} = \frac{x_{ij} - min(x_{ij})}{max(x_{ij}) - min(x_{ij})} + 1 \quad (1)$$

$$\text{Negative index}: X_{ij} = \frac{max(x_{ij}) - x_{ij}}{max(x_{ij}) - min(x_{ij})} + 1 \quad (2)$$

where X_{ij} represents the realistic value of the jth indicator in the ith grid cell; X_{ij} represents the standardized value of X_{ij}; $min(x_{ij})$ and $min(x_{ij})$ represent the minimum and maximum value of X_{ij}.

2.3.3 Determination of Weights

The determination of weight plays a very important role in multi-index comprehensive evaluation. The methods of weight determination can be divided into subjective and objective. The main methods of subjective evaluation include Delphi, cycle score, AHP, and empirical estimation (Okoli and Pawlowski, 2004; Geist, 2010). The main methods of objective evaluation include factor analysis, cluster analysis, principal component analysis, and entropy weight method (Blashfield and Aldenderfer, 1978; Lansangan and Barrios, 2009; Li et al., 2010; Liu et al., 2021b). Subjective methods are easily limited and influenced by the judge's own conditions while objective methods cannot flexibly add the experience of experts. Therefore, this study usesd entropy weight method and AHP to determine the index weight so as to establish a scientific and reasonable index weight system (**Figure 2**). The formula of compound weight is shown in **formula 3**. The calculation results of compound weight were as follows (**Table 2**).

$$W_i = \alpha * S_i + (1 - \alpha) * O_i \quad (3)$$

where S_i represents the subjective weight of the ith indicator; O_i represents the objective weight of the ith indicator; W_i represents the compound weight of the ith indicator; and α is the balance coefficient of the two methods.

The result was based on the principle that the single score of each grid cell was calculated by multiplying the standardized data with the corresponding weight. Then, we added up all the scores of each indicator so as to get the results of land ecological security. The equation for this formulation was indicated below.

$$LES = \sum_{i=1}^{n} S_i * W_i \quad (4)$$

where LES represents the final result of land ecological security in each grid cell; S_i represents the security index of the ith indicator; and W_i represents the weight of the corresponding indicator. Higher LES values indicated better land ecological secure conditions in the area.

2.3.4 Classification of Land Ecological Security

In order to make the overall characteristics of land ecological security more prominent, the Jenks Natural Breaks method was used to classify the regional types (Feng et al., 2017; Liu et al., 2019a). The result further showed that the land ecological security of Jinan was divided into five levels: Secure (I), Sub-secure (II), Moderate (III), Sensitive (IV), and Severe (V) (**Table 3**).

2.3.5 Spatial Autocorrelation Analysis

Exploratory spatial data analysis was performed to quantify spatial heterogeneity, detect spatial autocorrelation patterns, and identify clusters of similar incidence and outliers (Oom and Pereira, 2013). Spatial autocorrelation analysis consists of global and local spatial autocorrelation. Global spatial autocorrelation can be observed by the global Moran's I statistic. However, the global statistic gives a measure of overall clustering but it is still under investigation as well in the location of clusters or outliers or the type of spatial correlation that may exist in the data. Therefore, a detailed characterization of the clustering characteristics of the land ecological security was conducted by local indicators of spatial

TABLE 2 | Land ecological security assessment weights in Jinan.

Index	Entropy	AHP	Compound
Population density	0.0085	0.0138	0.0125
Population growth rate	0.0652	0.0035	0.0210
Per cultivated land chemical fertilizer	0.0364	0.0171	0.0104
Per cultivated land pesticide	0.0222	0.0065	0.0182
Proportion of aline-alkali soil	0.0010	0.2906	0.0258
Urbanization rate	0.0262	0.0218	0.0077
Proportion of construction land	0.0239	0.0449	0.0616
Per capita cultivated land	0.0455	0.1061	0.0495
Per capita land resource backup	0.0793	0.0446	0.0307
Proportion of transportation land	0.0005	0.0971	0.0212
The forest coverage rate	0.0341	0.0499	0.1418
Proportion of water area	0.0131	0.0871	0.1001
Proportion of grassland	0.0007	0.0140	0.1201
Spring group distribution	0.1494	0.0274	0.1301
Yield per area under crops	0.0399	0.0609	0.0141
Per capita GDP	0.0363	0.0200	0.0119
Economic density	0.0071	0.0066	0.0064
Proportion of environment protection investment in GDP	0.0559	0.0162	0.0197
Carbon emission per billion yuan in GDP	0.0860	0.0040	0.0187
Proportion of forestation	0.0571	0.0410	0.0127
Effective irrigation area	0.0708	0.0050	0.0116
Natural reserve	0.0074	0.0111	0.1125
Proportion of primary industry in GDP	0.0645	0.0072	0.0196
Proportion of tertiary industry in GDP	0.0689	0.0036	0.0220

TABLE 3 | Land ecological security classification.

Level	Value	Characteristics of the ecosystem
Secure (I)	1.42–2	The land ecosystem service function is perfect and the structure is complete; the ecological environment is very good, and there are basically no ecological problems
Sub-secure (II)	1.34–1.42	The function of the ecosystem is well-protected; could rehabilitate itself naturally if damaged; no distinct ecological problems
Moderate (III)	1.27–1.34	The function of land ecosystem starts degenerating; its structure changed slightly but still can maintain its fundamental function; easy to deteriorate but still easy to restore
Sensitive (IV)	1.22–1.27	Half of the service function land ecosystem has been invalidated; the environment and structure of the ecosystem are seriously damaged; hard to be rehabilitated and restored
Severe (V)	1–1.22	The service function of land ecosystem is basically lost; ecological environment is severely deteriorating; the structure of the ecosystem has been substantially damaged; very difficult to be rehabilitated and restored

autocorrelation (LISA) and Moran scatterplots. The formulas were indicated below.

$$\text{Moran's I} = \frac{\sum_{i=1}^{n}\sum_{j=1}^{n} w_{ij}\,(x_i - u)\left(x_j - u\right)}{\sum_{i=1}^{n}\sum_{j=1}^{n} w_{ij} \times \frac{1}{n}\sum_{i=1}^{n}(x_i - u)} \tag{5}$$

$$\text{Local Moran's I} = \frac{(x_i - u)}{S^2}\sum_{j=1}^{n} w_{ij}\left(x_j - u\right) \tag{6}$$

$$S^2 = \frac{1}{n}\sum_{i}^{n}(\mathrm{x}_i - u)^2 \tag{7}$$

$$u = \frac{1}{n}\sum_{i=1}^{n} x_i \tag{8}$$

where n represents the number of all grid cells; Xi and Xj represents the observation of location i and j, respectively; Wij represents the element of the spatial weights matrix w corresponding to the observation pair (i,j), and represents the component that incorporates "space." The scores of both indexes range from −1 to 1, but Moran's I demonstrate that the positive mean grid cells with similar values cluster together, as well as the negative means grid cells with dissimilar values. The nature of spatial association can be categorized into four types: "High-High" (I, first quadrant) and "Low-Low" (III, third quadrant) with spatial cluster of similar grid cells; "Low-High" (II, second quadrant) and "High-Low" (IV, fourth quadrant) with spatial cluster of dissimilar grid cells.

2.3.6 Geographical Detector Analysis

Geographical detector is a statistical method to detect spatial differentiation and reveal the driving factors behind it (Yang et al., 2019; Zhu et al., 2020). There are spatial differences in land ecological security which is affected by many factors. For an illustrative purpose, this study quantitatively explored the dominant factors driving the spatial differentiation of land

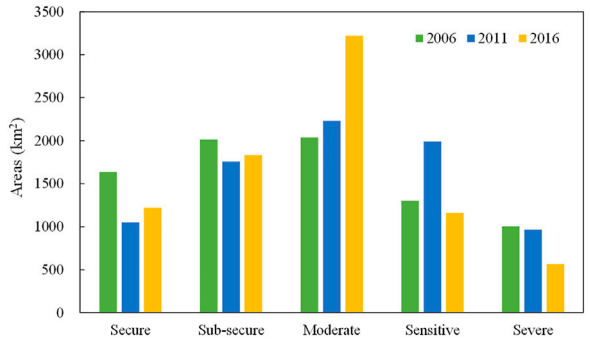

FIGURE 3 | Areas of land ecological security levels in Jinan from 2006 to 2016.

ecological security level by using the geographical detector in different periods. In this method, the larger the q-statistic, the stronger the explanatory power of the factor. The q-statistic ranges from 0 to 1. The calculation formula was as follows:

$$q = 1 - \frac{1}{N\sigma^2}\sum_{h=1}^{L} N_h \sigma_h^2 \tag{9}$$

where h represents the classes of variables; N and N_h represent the number of grid cells within the entire region and subregion h, respectively; σ^2 and σ_h^2 represent the variances of the entire region and subregion h, respectively.

3 RESULTS

3.1 Variation of Land Ecological Security Structure

In 2006, moderate and sub-secure regions covered an area of 4,054.39 km^2, accounting for over half of the study area (**Figure 3**). Specifically, moderate security areas added up to 2,039.35 km^2 taking the largest proportion of the entire city (i.e., 25.5%); what's more, sub-secure areas added up to 2,015.04 km^2 accounting for 25.19%. In 2011, the area of moderate security area reached 2231.19 km^2, accounting for 27.89% of the total area and followed by sensitive area, accounting for 24.90%. Both of the two areas respectively increased by 9.41 and 52.78% compared to 2006. However, secure areas covered an area of 1,050.79 km^2, decreasing by 35.79% from 2006. Sub-secure and severe areas covered about 1,758.75 and 966.31 km^2 respectively, accounting for 21.99 and 12.08% of the total area, decreasing by 12.72 and 3.77%, respectively. On the whole view, the land ecological security of Jinan decreased from 2006 to 2011. Specifically, levels of secure and sub-secure areas were converted into moderate and sensitive areas while some scattered instances of severe areas were converted to sensitive.

In 2016, secure areas added up to 1,219.03 km^2, increasing by 16.01% from 2011. Sub-secure areas covered about 1,832.13 km^2 accounting for 22.91% of the total area, and increasing by 4.17% from 2011. Moderate areas added up to 3,220.01 km^2 and accounted for 40.26% of the total area, increasing by 44.32% from 2011. Sensitive and severe areas covered 1,159.82 and 567.76 km^2 accounting for 14.50 and 7.10%, decreasing by 41.77 and 41.24% respectively compared to 2011. The results show that the overall condition of land ecological security has improved from 2011. All these changes are benefited from Jinan's great emphasis on environmental protection. The awareness of environmental protection has been widely publicized among the people and heavily polluted industries have been forced to move outside of the middle region of Jinan. Furthermore, since the establishment of 12th Five-Year Plan of China, the local government worked hard in upgrading the tertiary industry as the predominant so as to improve the land ecological security.

3.2 Analysis of Spatiotemporal Pattern

The land ecological security of Jinan has continuously changed with the development and construction of the city. The land ecological security of Jinan was characteristically low in the middle, but relatively high in the surrounding areas. The ecological security in the middle region was overwhelmingly negative categorized at the severe level. In contrast, the east, west, south, and north regions were categorized in a positive ecological condition. This was because most construction had been concentrated in the middle region, which is the political, economic, and cultural center of Jinan.

In 2006, the situation of land ecological security was better in Jinan, and the main types were moderate and sub-secure (**Figure 4A**). The levels of land ecological security varied from different regions. More specifically, land ecological security in the central regions (Lixia, Shizhong, Huaiyin, Tianqiao, and the north of Licheng) was represented as severe and sensitive, influenced by the high population density, high urbanization rate, and almost full load of land carrying capacity. Land ecological security was represented as secure and sub-secure in the southern regions (the south of Licheng, Zhangqiu, and Changqing) due to the regions' status as the ecological conservation area where the forests and water area were widely distributed and human activities were very little. In the middle and north of Jiyang and Zhangqiu, land ecological was mainly represented as moderate and sensitive, which could be because the development of secondary and tertiary industries led to many human activities in the region, seriously interfering with the ecological environment. The land ecological security was represented as sensitive in the middle and west of Changqing and the middle and north of Pingyin. In a word, the rapid development in the region may cause a negative ecological security situation.

In 2011, the overall land ecological security of Jinan worsened (**Figures 4B**). The ecological security of the north exhibited a mostly moderate pattern. In particular, the general ecological security of Shanghe decreased. In contrast, the land ecological security of Jiyang improved with fewer areas categorized as sensitive or severe. Decision-makers in the Jiyang strengthened controls on environmental governance, increased the environmental protection investment, shut down heavily polluting industries, and reduced carbon emission gradually to improve the ecological condition. The land ecological security of

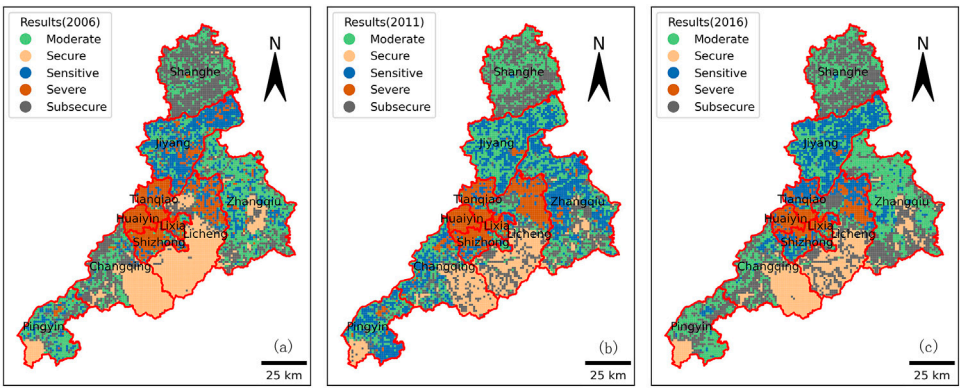

FIGURE 4 | Land ecological security of Jinan from 2006 to 2016. **(A–C)** represent the results in 2006, 2011 and 2016.

the south also deteriorated. Specifically, the ecological effect in the fringe of the area weakened with fewer areas classified as secure and moderate. The land ecological security of the east also deteriorated, with a wide occurrence of sensitive areas. The ecological condition of the middle of Zhangqiu worsened because of the rapid development of the secondary industries, in conjunction with little environmental investment. Conversely, the south of Zhangqiu was in a better ecological condition, possessing more water area and woodlands. Furthermore, the ecological condition of the west seriously declined due to the rapid development of secondary and tertiary industries resulting in a decrease of per capita cultivated land and increase of transportation land.

In 2016, areas classified as Severe dropped in the middle region of Jinan and were converted to Sensitive, especially in the north of the Licheng (**Figure 4C**). This trend was also observed in the Tianqiao and Shizhong. The overall ecological condition improved as demonstrated by Shanghe. The area with land ecological security represented as moderate in the middle region changed distinctly and then converted into a considerable proportion of sub-secure areas, which was due to a rapid increase in environmental protection investment, predominant development of the tertiary industry, and allocating more resources for afforestation to improve ecological security. The improvement of land ecological security in the east of Jinan City was attributed to the implementation of Zhangqiu's policy of not sacrificing nature reserves and reducing carbon emission. At the same time, the strict management measures also improved land ecological security in the south of Jinan. The areas characterized as sensitive decreased by 87.78% and the areas characterized as moderate increased in the west of Jinan.

Generally speaking, the spatial difference of land ecological security in Jinan was obvious. The level of ecological security in the central built-up area was low. In recent years, the areas with land ecological security represented as severe continues to increase, and the scope of increase is basically consistent with the direction of urban expansion. Due to the underdevelopment of the area, the southern ecological conservation area was of great significance to maintain the ecological balance. As it is difficult to recover from the damage, the area was a key area for strengthening control. The situation of land ecological security in Jiyang, northern Zhangqiu, and western Changqing was poor, while it in the south of Shanghe and Pingyin was good. Urbanization not only improved people's living standards but also caused the incomplete structure and irreversible function of regional land ecosystem. Coordinating the relationship between economic development and ecological protection, strengthening the supervision of key ecological protection areas will significantly improve the level of land ecological security in Jinan.

3.3 Exploration of Spatial Agglomeration Characteristics

The weight matrix based on a spatial distance relationship was established by employing the data from the evaluation results of land ecological security in 2006, 2011, and 2016. Applying the Global Moran's index method, the Moran's I index of the comprehensive value of land ecological security of Jinan was computed, after which the values were visualized in scatter plots. In said plots, the X-axis represents the observational value (i.e., standardization), and the Y-axis represents the weighted mean of the values surrounding the observational value (**Figure 5**).

The Moran's I values of land ecological security were 0.879, 0.847, and 0.886 in 2006, 2011, and 2016, respectively, and its statistical significance was tested via the Monte Carlo simulation method. The result indicated a significant spatial autocorrelation ($p < 0.01$), confirming a distinct global positive spatial correlation within the land ecological security of Jinan, illustrating continuity and dependency between the 1 km × 1 km grid cells. Regions with similar land ecological security conditions tended to cluster together. Moran's I decreased from 2006 to 2011, indicating a weakening correlation between the level of land ecological security and spatial distribution, thus resulting in polarization and stronger local autocorrelation. However, Moran's I increased from 2011 to 2016, and correlations strengthened once again.

Taken together, the spatial association was classified as "High-High" (H-H) and "Low-Low" (L-L) for clusters of similar grid cells, while "Low-High" (L-H) and "High-Low"

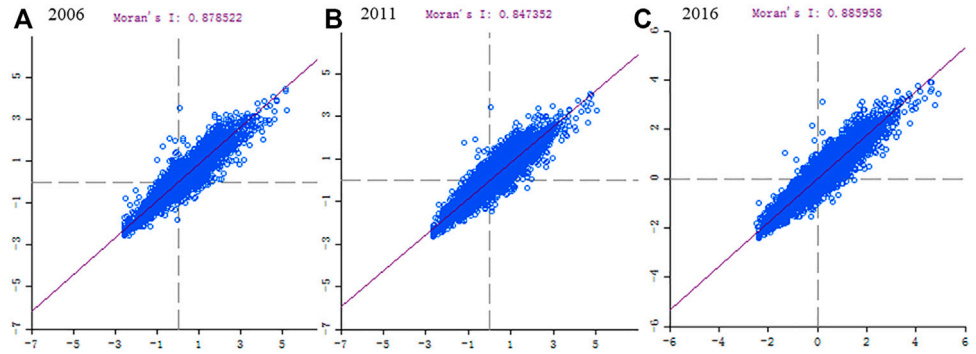

FIGURE 5 | Scatter plot of Global Moran's index derived from Jinan's land ecological security in different years. **(A–C)** represent the results in 2006, 2011 and 2016.

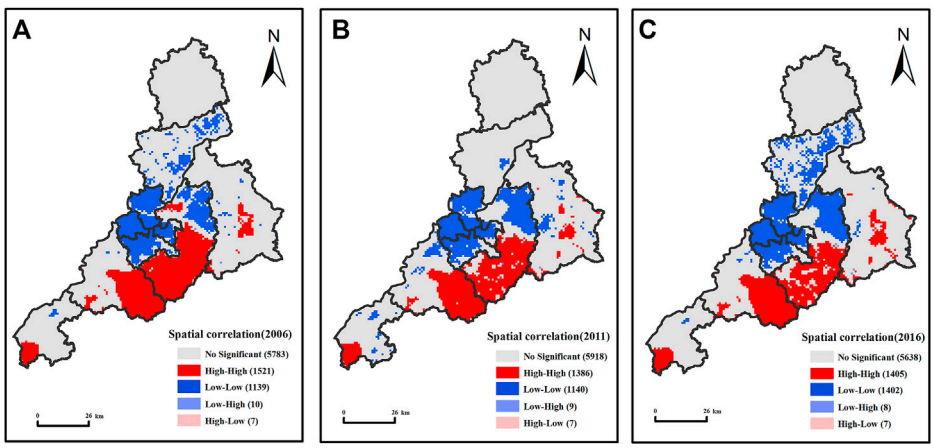

FIGURE 6 | Spatial correlation of land ecological security condition in different years. **(A–C)** represent the results in 2006, 2011 and 2016.

(H-L) for clusters of dissimilar grid cells. The H-H classification represents grid cells with values as high as the surrounding cells. This type of grid cells was mainly observed in the southeast of the Changqing district, the south of Licheng district, the middle of Zhangqiu district, as well as the southwest of Pinyin county (**Figure 6**). These observations corresponded with the land ecological security conditions discussed above, indicating that areas of high ecological security conditions were often classified as H-H. From 2006 to 2016, the number of H-H areas in the south Licheng district decreased consistently, and so did the number of secure-level areas. It is mainly because of the fast development of tourism, more and more human activities increased the incidence of natural hazards, thus resulting in a more vulnerable ecosystem. In contrast, the number of H-H type areas increased in the Zhangqiu district since 2011, which was consistent with improvements in Zhangqiu district's ecological condition. This was attributed to the intervention of decisions makers, leading to more resource allocation and attention to environmental protection and sustainable economic development.

L-L type areas represent regions where the values were as low as the surrounding ones. This type of grid cells was mainly observed in Shizhong, Lixia, Huaiyin, Tianqiao, and the east of the Licheng district. L-L type areas often corresponded with areas of severe land ecological security condition. Changes could be observed from 2006 to 2016. For instance, there was an inversion in the number of L-L type areas from 2006 to 2011, after which a large proportion of L-L type areas reemerged from 2011 to 2016. Both trends were observed within the Jiyang district. H-L type and L-H type areas represented a very small proportion of the study area, mostly interspersed in the periphery of H-H type and L-L type areas. Also, a large proportion of non-significant areas was observed mostly in the Shanghe and Pinyin counties, and most of the Zhangqiu district.

3.4 Identification of Influencing Factors

The spatial differentiation of land ecological security is affected by many factors. For that reason, it is of great significance to identify the main driving factors for the formulation of regional refine control measures. The results were shown in **Table 4**. At the significance level of 1%, the factor with q-statistic greater than 0.25 was selected as the

TABLE 4 | Geographical detector factors of land ecological security in Jinan from 2006 to 2016.

Factor category	Impact factors	q (2006)	q (2011)	q (2016)
Stress level of resources and environment	Population density	0.232	0.248	0.286
	Natural population growth rate	0.230	0.200	0.171
	Application amount of chemical fertilizer per unit land	0.076	0.258	0.084
	Application amount of pesticide per unit land	0.127	0.117	0.255
Ecological governance efforts	Proportion of environmental protection investment in GDP	0.100	0.171	0.221
	Carbon emissions per billion yuan of GDP	0.165	0.249	0.330
	Ecological protection area	0.127	0.098	0.104
	Proportion of ecological afforestation area	0.222	0.168	0.173
	Effective irrigation area	0.207	0.217	0.185
Resource endowment	Forest coverage	0.439	0.231	0.288
	Proportion of grassland area	0.001	0.100	0.157
	Distribution of spring group	0.049	0.006	0.013
	Specific gravity of saline alkali land	0.001	0.018	0.002
	Proportion of water area	0.042	0.039	0.025
	Grain yield per unit area	0.063	0.112	0.147
	Per capita cultivated land area	0.213	0.246	0.290
	Per capita land reserve resources	0.187	0.143	0.322
Social and economic development level	Agricultural economic added value	0.224	0.287	0.321
	Proportion of tertiary industry	0.191	0.260	0.180
	Economic density	0.213	0.289	0.174
	Proportion of construction land	0.560	0.606	0.614
	Urbanization rate	0.213	0.251	0.294
	Per capita GDP	0.168	0.229	0.125

dominant factor. The main driving factors corresponding to different time points are also changing. The main influencing factors in 2006 were the proportion of construction land and forest coverage. The main factors in 2011 were the proportion of construction land, economic density, agricultural economic added value, proportion of tertiary industry, fertilizer application per unit of cultivated land, and urbanization rate. The main factors in 2016 were the proportion of construction land, carbon emissions per billion yuan of GDP, per capita land reserve resources, agricultural economic value added, urbanization rate, per capita cultivated land area, forest coverage, population density, and pesticide application per unit of cultivated land.

There is a great correlation between resource and environment stress level and land ecological security. The increasing q value of population density indicated that the influence of population on the differentiation of land ecological security was increasing. In contrast, the q value of natural population growth rate was decreasing, which indicated that its influence was gradually weakening. Compared with 2006, the q value of chemical fertilizer and pesticide application per unit cultivated land increased in 2016. Cultivated land played an increasingly important role in maintaining the structure and function balance of the ecosystem. The change of population development level also had a great impact on land ecological status. Especially in recent years, the consumption of resources has been increasing for the rapid increase of population in the central area of Jinan.

Ecological governance is of great significance to alleviate the pressure of land ecological security and maintain the state of ecological security. In the study periods, the q values of the proportion of environmental protection investment in GDP were 0.100, 0.171, and 0.221, respectively. The q values of carbon emissions per billion yuan GDP were 0.165, 0.249, and 0.330, respectively. Their continuous growth indicated that the impact of economic and industrial structure transformation on land ecological security differentiation was increasing. Take Shanghe as an example; its proportion of environmental protection investment in GDP increased, and the level of land ecological security in the region improved significantly. Compared with 2006, the q values of ecological protection area, proportion of ecological afforestation area, and effective irrigation area decreased in 2016, which indicated that their impact on the spatial differentiation of land ecological security was weakened.

The influence degree of resource endowment factors on the spatial differentiation of land ecological security is different. The strongest explanatory factor was forest coverage. The q values were 0.439, 0.231, and 0.288, respectively, which indicated that the impact of this factor on land ecological security was weakened. The ecological status of areas with high forest coverage, such as the south of Licheng and the southeast of Changqing, was better.

The level of social and economic development has the strongest explanation for the spatial differentiation of land ecological security. During the study periods, the proportion of construction land had the greatest impact on land ecological security and its q values were 0.560, 0.606, and 0.614, respectively. The expansion of construction land has changed the structure of land cover and land ecosystem. The q values of agricultural economic added value and urbanization rate increased continuously, which showed that the explanatory power was increasing. The q values of per capita GDP were 0.168, 0.229, and 0.125, respectively. The q values of the proportion of the tertiary industry were 0.191, 0.260, and 0.180, respectively. The q values of economic density were 0.213, 0.289, and 0.174, respectively. The explanation degree of these three factors to spatial heterogeneity showed the characteristics of first increasing and then decreasing.

4 DISCUSSION

Land ecological security plays an important role in regional socio-economic development and ecological environment protection. The land ecological security level was evaluated and the spatiotemporal differentiation was analyzed in Jinan from 2006 to 2016. Results showed that the land ecological security decreased first and then increased, and the level was improved in 2016 compared with those in previous years. This finding was consistent with many studies which the land ecological security was also presented as an upward trend in general (Hu et al., 2019; Yang et al., 2021). This is closely related to China's recent emphasis on ecological and environmental protection. Meanwhile, obvious spatial differentiation of land ecological security within Jinan was found in our study. In fact, land ecological security has also been reported to show regional characteristics (Wen et al., 2021). Taking Jinan as an example, to study its land ecological security is not only conducive to the proposal of land optimization countermeasures but also conducive to alleviate the land contradiction in Jinan and improve the path of urban sustainable development. At the same time, it also provides a practical reference for the research of other cities.

The relationship between land ecological security and influencing factors is very complicated (Feng et al., 2018). In our study, the social and economic development, especially the construction land proportion, was found to have more explanatory power on land ecological security differentiation than other factors. Related studies also indicated that human activities have significant impact on regional land ecological security over natural factors (Yang et al., 2020; Wen et al., 2021). In addition, the results of this study also showed that the main driving factors were different at different time points. In 2006, resource endowment and socio-economic development level had the greatest impact on land ecological security differentiation. In 2011, the level of social and economic development restricted the improvement of land ecological security. In 2016, the spatial differentiation of land ecological security was largely explained by the intensity of ecological governance, the level of population development and the level of social and economic development. Therefore, only by formulating corresponding land ecological security optimization schemes at different times can we better serve urban sustainable development. Only by paying attention to the image of human activities on land ecological security can we realize the win-win situation of regional ecological protection and economic and social development.

Based on the grid scale, the spatial and temporal distribution pattern and driving factors of land ecological security in Jinan were analyzed, which further detailed the characteristics of regional land ecological security structure. However, due to the influence of data acquisition, the index system constructed failed to consider the regional ecological protection policy, public ecological cognition level, and other factors. Meanwhile, it is necessary to continually explore how to better realize the fusion of data at different scales, especially the rasterization of social-economic data to improve the research accuracy. In addition, although this study explored the driving factors of urban land ecological security, it failed to consider the interaction among the factors. These problems will be the important direction of future research, and multi-methods could be combined to better reveal the interactions between land ecological security and influencing factors.

5 CONCLUSION

Taking the grid as the evaluation unit, this study analyzed the spatiotemporal evolution characteristics and spatial differentiation law of land ecological security of Jinan in different years. The main conclusions are as follows:

(1) The level of land ecological security decreased first and then gradually increased from 2006 to 2016 in Jinan. Among them, the security level in the central region showed a downward trend, and gradually improved in the southern mountainous area.
(2) There was obvious heterogeneity of land ecological security level in Jinan. The overall distribution pattern was "low in the middle and high around." The direction of urban expansion was consistent with the low-level land ecological security.
(3) There was a distinct global spatial positive correlation within the land ecological security. Roughly 15% of the surface of Jinan had low-value agglomeration, whereas roughly 17% exhibited high-value agglomeration. In addition, distribution patterns matched spatial agglomeration characteristics.
(4) There were differences in the driving factors of spatial differentiation of land ecological security in Jinan. Generally, the explanatory power of the level of social and economic development on the spatial differentiation of land ecological security was higher than other factors. Among them, the construction land proportion had the strongest explanatory power. Urban development should try to avoid occupying areas with high level of land ecological security.

DATA AVAILABILITY STATEMENT

The original contributions presented in the study are included in the article/Supplementary Material, further inquiries can be directed to the corresponding author.

AUTHOR CONTRIBUTIONS

JL and KJ designed the study, LZ was responsible for data collection and processing, XC and GD completed the analysis of the results and the writing of the manuscript, XC and KJ are responsible for the revision of the manuscript.

FUNDING

This research was funded by the National Natural Science Foundation of China (No. 41801173), the Science and Technology Project of the Housing and Rural Development Department in Shandong Province (No. 2019-R4-1), and the Doctoral Fund of Shandong Jianzhu University (No. X21011Z).

REFERENCES

Behzadian, M., Khanmohammadi Otaghsara, S., Yazdani, M., and Ignatius, J. (2012). A State-Of The-Art Survey of TOPSIS Applications. *Expert Syst. Appl.* 39, 13051–13069. doi:10.1016/j.eswa.2012.05.056

Blashfield, R. K., and Aldenderfer, M. S. (1978). The Literature on Cluster Analysis. *Multivariate Behav. Res.* 13, 271–295. doi:10.1207/s15327906mbr1303_2

Chen, W., Chi, G., and Li, J. (20192019). The Spatial Association of Ecosystem Services with Land Use and Land Cover Change at the County Level in China, 1995-2015. *Sci. Total Environ.* 669, 459–470. doi:10.1016/j.scitotenv.2019.03.139

Chen, J. (2007). Rapid Urbanization in China: A Real challenge to Soil protection and Food Security. *Catena* 69, 1–15. doi:10.1016/j.catena.2006.04.019

Cohen, B. (2006). Urbanization in Developing Countries: Current Trends, Future Projections, and Key Challenges for Sustainability. *Technol. Soc.* 28, 63–80. doi:10.1016/j.techsoc.2005.10.005

Feng, Y., Liu, Y., and Liu, Y. (2017). Spatially Explicit Assessment of Land Ecological Security with Spatial Variables and Logistic Regression Modeling in Shanghai, China. *Stoch. Environ. Res. Risk Assess.* 31, 2235–2249. doi:10.1007/s00477-016-1330-7

Feng, Y., Yang, Q., Tong, X., and Chen, L. (2018). Evaluating Land Ecological Security and Examining its Relationships with Driving Factors Using GIS and Generalized Additive Model. *Sci. Total Environ.* 633, 1469–1479. doi:10.1016/j.scitotenv.2018.03.272

Gao, P. P., Li, Y. P., Sun, J., and Li, H. W. (2018). Coupling Fuzzy Multiple Attribute Decision-Making with Analytic Hierarchy Process to Evaluate Urban Ecological Security: A Case Study of Guangzhou, China. *Ecol. Complexity* 34, 23–34. doi:10.1016/j.ecocom.2018.03.001

Geissdoerfer, M., Savaget, P., Bocken, N. M. P., and Hultink, E. J. (2017). The Circular Economy - A New Sustainability Paradigm? *J. Clean. Prod.* 143, 757–768. doi:10.1016/j.jclepro.2016.12.048

Geist, M. R. (2010). Using the Delphi Method to Engage Stakeholders: A Comparison of Two Studies. *Eval. Program Plann.* 33, 147–154. doi:10.1016/j.evalprogplan.2009.06.006

Gong, J., Liu, Y., and Chen, W. (2012). Land Suitability Evaluation for Development Using a Matter-Element Model: A Case Study in Zengcheng, Guangzhou, China. *Land Use Policy* 29, 464–472. doi:10.1016/j.landusepol.2011.09.005

Guo, D., Wang, D., Zhong, X., Yang, Y., and Jiang, L. (2021). Spatiotemporal Changes of Land Ecological Security and its Obstacle Indicators Diagnosis in the Beijing-Tianjin-Hebei Region. *Land* 10, 706. doi:10.3390/land10070706

Hu, M., Li, Z., Yuan, M., Fan, C., and Xia, B. (2019). Spatial Differentiation of Ecological Security and Differentiated Management of Ecological Conservation in the Pearl River Delta, China. *Ecol. Indicators* 104, 439–448. doi:10.1016/j.ecolind.2019.04.081

Kim, H., Kim, S., and Dale, B. E. (2009). Biofuels, Land Use Change, and Greenhouse Gas Emissions: Some Unexplored Variables. *Environ. Sci. Technol.* 43, 961–967. doi:10.1021/es802681k

Lansangan, J. R. G., and Barrios, E. B. (2009). Principal Components Analysis of Nonstationary Time Series Data. *Stat. Comput.* 19, 173–187. doi:10.1007/s11222-008-9082-y

Li, M., Sun, H., Singh, V., Zhou, Y., and Ma, M. (2010). Agricultural Water Resources Management Using Maximum Entropy and Entropy-Weight-Based TOPSIS Methods. *Entropy* 21, 364–1228. doi:10.3390/e21040364

Li, X., Tian, M., Wang, H., Wang, H., and Yu, J. (2014). Development of an Ecological Security Evaluation Method Based on the Ecological Footprint and Application to a Typical Steppe Region in China. *Ecol. Indicators* 39, 153–159. doi:10.1016/j.ecolind.2013.12.014

Li, H., Zhao, Y., and Zheng, F. (2020). The Framework of an Agricultural Land-Use Decision Support System Based on Ecological Environmental Constraints. *Sci. Total Environ.* 717, 137149. doi:10.1016/j.scitotenv.2020.137149

Li, J. X., Chen, Y.-N., Xu, C.-C., and Li, Z. (2019a). Evaluation and Analysis of Ecological Security in Arid Areas of Central Asia Based on the Emergy Ecological Footprint (EEF) Model. *J. Clean. Prod.* 235, 664–677. doi:10.1016/j.jclepro.2019.07.005

Li, Z. T., Yuan, M.-J., Hu, M.-M., Wang, Y.-F., and Xia, B.-C. (2019b). Evaluation of Ecological Security and Influencing Factors Analysis Based on Robustness Analysis and the BP-DEMALTE Model: A Case Study of the Pearl River Delta Urban Agglomeration. *Ecol. Indicators* 101, 595–602. doi:10.1016/j.ecolind.2019.01.067

Liu, C., Wu, X., and Wang, L. (2019a). Analysis on Land Ecological Security Change and Affect Factors Using RS and GWR in the Danjiangkou Reservoir Area, China. *Appl. Geogr.* 105, 1–14. doi:10.1016/j.apgeog.2019.02.009

Liu, W., Zhan, J., Zhao, F., Yan, H., Zhang, F., and Wei, X. (2019b). Impacts of Urbanization-Induced Land-Use Changes on Ecosystem Services: A Case Study of the Pearl River Delta Metropolitan Region, China. *Ecol. Indicators* 98, 228–238. doi:10.1016/j.ecolind.2018.10.054

Liu, R., Dong, X., Zhang, P., Zhang, Y., Wang, X., and Gao, Y. (2020). Study on the Sustainable Development of an Arid Basin Based on the Coupling Process of Ecosystem Health and Human Wellbeing under Land Use Change-A Case Study in the Manas River Basin, Xinjiang, China. *Sustainability* 12, 1201. doi:10.3390/su12031201

Liu, P., Hu, Y., and Jia, W. (2021a). Land Use Optimization Research Based on FLUS Model and Ecosystem Services-Setting Jinan City as an Example. *Urban Clim.* 40, 100984. doi:10.1016/j.uclim.2021.100984

Liu, W., Zhan, J., Zhao, F., Wei, X., and Zhang, F. (2021b). Exploring the Coupling Relationship between Urbanization and Energy Eco-Efficiency: A Case Study of 281 Prefecture-Level Cities in China. *Sustain. Cities Soc.* 64, 102563. doi:10.1016/j.scs.2020.102563

Long, H., Li, Y., Liu, Y., Woods, M., and Zou, J. (2012). Accelerated Restructuring in Rural China Fueled by 'Increasing vs. Decreasing Balance' Land-Use Policy for Dealing with Hollowed Villages. *Land Use Policy* 29, 11–22. doi:10.1016/j.landusepol.2011.04.003

Ma, L., Bo, J., Li, X., Fang, F., and Cheng, W. (2019). Identifying Key Landscape Pattern Indices Influencing the Ecological Security of Inland River Basin: The Middle and Lower Reaches of Shule River Basin as an Example. *Sci. Total Environ.* 674, 424–438. doi:10.1016/j.scitotenv.2019.04.107

Nunes, A. N., De Almeida, A. C., and Coelho, C. O. A. (2011). Impacts of Land Use and Cover Type on Runoff and Soil Erosion in a Marginal Area of Portugal. *Appl. Geogr.* 31, 687–699. doi:10.1016/j.apgeog.2010.12.006

Okoli, C., and Pawlowski, S. D. (2004). The Delphi Method as a Research Tool: An Example, Design Considerations and Applications. *Inf. Manage.* 42, 15–29. doi:10.1016/j.im.2003.11.002

Oom, D., and Pereira, J. M. C. (2013). Exploratory Spatial Data Analysis of Global MODIS Active Fire Data. *Int. J. Appl. Earth Observation Geoinformation* 21, 326–340. doi:10.1016/j.jag.2012.07.018

Qi, S., Guo, J., Jia, R., and Sheng, W. (2020). Land Use Change Induced Ecological Risk in the Urbanized Karst Region of North China: A Case Study of Jinan City. *Environ. Earth Sci.* 79, 280. doi:10.1007/s12665-020-09036-w

Sekovski, I., Newton, A., and Dennison, W. C. (2012). Megacities in the Coastal Zone: Using a Driver-Pressure-State-Impact-Response Framework to Address Complex Environmental Problems. *Estuarine, Coastal Shelf Sci.* 96, 48–59. doi:10.1016/j.ecss.2011.07.011

Seyedmohammadi, J., Sarmadian, F., Jafarzadeh, A. A., and McDowell, R. W. (2019). Development of a Model Using Matter Element, AHP and GIS Techniques to Assess the Suitability of Land for Agriculture. *Geoderma* 352, 80–95. doi:10.1016/j.geoderma.2019.05.046

Steffen, W., Richardson, K., Rockström, J., Cornell, S. E., Fetzer, I., Bennett, E. M., et al. (2015). Planetary Boundaries: Guiding Human Development on a Changing Planet. *Science* 347, 1259855. doi:10.1126/science.1259855

Su, S., Li, D., Yu, X., Zhang, Q., Xiao, R., Zhi, J., et al. (2011). Assessing Land Ecological Security in Shanghai (China) Based on Catastrophe Theory. *Stoch. Environ. Res. Risk Assess.* 25, 737746. doi:10.1007/s00477-011-0457-9

Wen, M., Zhang, T., Li, L., Chen, L., Hu, S., Wang, J., et al. (2021). Assessment of Land Ecological Security and Analysis of Influencing Factors in Chaohu Lake Basin, China from 1998-2018. *Sustainability* 13, 358. doi:10.3390/su13010358

Wolfslehner, B., and Vacik, H. (2008). Evaluating Sustainable forest Management Strategies with the Analytic Network Process in a Pressure-State-Response Framework. *J. Environ. Manage.* 88, 1–10. doi:10.1016/j.jenvman.2007.01.027

Wu, K.-y., and Zhang, H. (2012). Land Use Dynamics, Built-Up Land Expansion Patterns, and Driving Forces Analysis of the Fast-Growing Hangzhou Metropolitan Area, Eastern China (1978-2008). *Appl. Geogr.* 34, 137–145. doi:10.1016/j.apgeog.2011.11.006

Wu, Y., Tao, Y., Yang, G., Ou, W., Pueppke, S., Sun, X., et al. (2019a). Impact of Land Use Change on Multiple Ecosystem Services in the Rapidly Urbanizing Kunshan City of China: Past Trajectories and Future Projections. *Land Use Policy* 85, 419–427. doi:10.1016/j.landusepol.2019.04.022

Wu, Z., Lei, S., He, B.-J., Bian, Z., Wang, Y., Lu, Q., et al. (2019b). Assessment of Landscape Ecological Health: A Case Study of a Mining City in a Semi-arid Steppe. *Int. J. Environ. Res. Public Health* 16, 752. doi:10.3390/ijerph16050752

Yan, J., Xia, F., and Bao, H. X. H. (2015). Strategic Planning Framework for Land Consolidation in China: A Top-Level Design Based on SWOT Analysis. *Habitat Int.* 48, 46–54. doi:10.1016/j.habitatint.2015.03.001

Yang, Y., and Cai, Z. (2020). Ecological Security Assessment of the Guanzhong Plain Urban Agglomeration Based on an Adapted Ecological Footprint Model. *J. Clean. Prod.* 260, 120973. doi:10.1016/j.jclepro.2020.120973

Yang, Q., Liu, G., Hao, Y., Coscieme, L., Zhang, J., Jiang, N., et al. (2018). Quantitative Analysis of the Dynamic Changes of Ecological Security in the Provinces of China through Emergy-Ecological Footprint Hybrid Indicators. *J. Clean. Prod.* 184, 678–695. doi:10.1016/j.jclepro.2018.02.271

Yang, J., Song, C., Yang, Y., Xu, C., Guo, F., and Xie, L. (2019). New Method for Landslide Susceptibility Mapping Supported by Spatial Logistic Regression and GeoDetector: A Case Study of Duwen Highway Basin, Sichuan Province, China. *Geomorphology* 324, 62–71. doi:10.1016/j.geomorph.2018.09.019

Yang, Y., Song, G., and Lu, S. (2020). Assessment of Land Ecosystem Health with Monte Carlo Simulation: A Case Study in Qiqihaer, China. *J. Clean. Prod.* 250, 119522. doi:10.1016/j.jclepro.2019.119522

Yang, R., Du, W., and Yang, Z. (2021). Spatiotemporal Evolution and Influencing Factors of Urban Land Ecological Security in Yunnan Province. *Sustainability* 13, 2936. doi:10.3390/su13052936

Zhang, M. A., Borjigin, E., and Zhang, H. (2007). Mongolian Nomadic Culture and Ecological Culture: On the Ecological Reconstruction in the Agro-Pastoral Mosaic Zone in Northern China. *Ecol. Econ.* 62, 19–26. doi:10.1016/j.ecolecon.2006.11.005

Zhang, F., Liu, X., Zhang, J., Wu, R., Ma, Q., and Chen, Y. (2017). Ecological Vulnerability Assessment Based on Multi-Sources Data and SD Model in Yinma River Basin, China. *Ecol. Model.* 349, 41–50. doi:10.1016/j.ecolmodel.2017.01.016

Zhu, L., Meng, J., and Zhu, L. (2020). Applying Geodetector to Disentangle the Contributions of Natural and Anthropogenic Factors to NDVI Variations in the Middle Reaches of the Heihe River Basin. *Ecol. Indicators* 117, 106545. doi:10.1016/j.ecolind.2020.106545

Conflict of Interest: The authors declare that the research was conducted in the absence of any commercial or financial relationships that could be construed as a potential conflict of interest.

Publisher's Note: All claims expressed in this article are solely those of the authors and do not necessarily represent those of their affiliated organizations, or those of the publisher, the editors, and the reviewers. Any product that may be evaluated in this article, or claim that may be made by its manufacturer, is not guaranteed or endorsed by the publisher.

frontiers in Ecology and Evolution

ORIGINAL RESEARCH
published: 11 February 2022
doi: 10.3389/fevo.2022.841943

Assessment of Grassland Ecosystem Services and Analysis on Its Driving Factors: A Case Study in Hulunbuir Grassland

*Minhuan Li[1], Xiaoyu Wang[2,3] and Jiancheng Chen[1]**

[1] School of Economics and Management, Beijing Forestry University, Beijing, China, [2] College of Resource Environment and Tourism, Capital Normal University, Beijing, China, [3] Key Laboratory of 3D Information Acquisition and Application of Ministry, Capital Normal University, Beijing, China

OPEN ACCESS

Edited by:
Fan Zhang, Institute of Geographic Sciences and Natural Resources Research, Chinese Academy of Sciences (CAS), China

Reviewed by:
Yanmin Teng, Dongguan University of Technology, China
Zhe Zhao, Liaoning University, China
Yi Xie, Museum of Beijing Forestry University, China

***Correspondence:**
Jiancheng Chen
chenjc_bjfu@126.com

Specialty section:
This article was submitted to Conservation and Restoration Ecology, a section of the journal Frontiers in Ecology and Evolution

Received: *23 December 2021*
Accepted: *07 January 2022*
Published: *11 February 2022*

Citation:
Li M, Wang X and Chen J (2022) Assessment of Grassland Ecosystem Services and Analysis on Its Driving Factors: A Case Study in Hulunbuir Grassland. Front. Ecol. Evol. 10:841943. doi: 10.3389/fevo.2022.841943

Grassland is the largest terrestrial ecosystem in China, and its ecological environment is currently facing several challenges. The service assessment of scientific and effective grassland ecosystem and in-depth analysis of its change mechanism is of great significance to clarify its protection demand and spatial optimization layout. This study used a set of quantitative surrogate biophysical indicators to evaluate the capability of grassland ecosystem services (i.e., carbon fixation, soil protection, water purification and provision, and biodiversity conservation) in the Hulunbuir grassland from 2000 to 2015 and use econometric models to explore their dynamic change mechanism. The results showed that from 2009 to 2012, the grassland ecosystem service value significantly declined, and from 2013 to 2015, its value significantly improved, but the overall level was still lower than that of 2000. The factor that has the highest degree of impact on grassland ecosystem services is the soil potassium content, and there is a significant positive correlation. This is mainly due to the important role of potassium in the photosynthesis of grassland plants; the least influential factors are social economic factors such as population and gross domestic product (GDP). It shows that the sparsely populated grassland ecosystem is not sensitive to these factors. In addition, climate, topography, and grassland management policies all have a significant impact on grassland ecosystem services. Against the backdrop of intensified pressure on ecological grassland protection and surging market demand for livestock products based on grassland resource input, the sustainable development of grassland areas needs to improve the supply capacity of grassland while ensuring its ecological security, so as to realize a win-win situation for its ecological and production functions.

Keywords: ecosystem services, spatial distribution, driving mechanism, Hulunbuir, grassland

INTRODUCTION

With population growth and economic and social development, the human use and transformation of Earth surface ecosystems have reached unprecedented levels, with net primary productivity taking up more than 20% of the net primary productivity of the global ecosystem; however, this expression is highly heterogeneous, with some areas reaching even more than 60%

(Zhang et al., 2017). Human interference and utilization have exerted profound impacts on the natural ecosystem, leading to ecological environment degradation, which is mainly manifested in, for example, reductions in biodiversity and productivity, desertification, soil and nutrient loss, and water pollution (Liebig et al., 2010; Castellani et al., 2017; Wang et al., 2019; Zhao et al., 2019). Continuous ecosystem supply is an important guarantee for the sustainable development of human society, mainly in the form of ecosystem services (ESs). Ecosystems and ESs, in the process of material and energy flow forming and maintaining human survival in the ecosystem, depending on the natural environment and utility for input to the social economic system through useful material and energy (e.g., products) and as a necessary environment for human survival conditions (e.g., improving the environment and water and biodiversity conservation) (Daily, 1997; Reid et al., 2005; Zagonari, 2016). The quantitative assessment of ESs is not only an important basis for supporting decisions for the rational utilization of regional resources, ecological protection, and sustainable social and economic development but also an important index for investigating the supply capacity of ecosystems and identifying the *status quo* of their ecological functions and production functions (Burkhard et al., 2013; Woodruff and Bendor, 2016). As the largest terrestrial ecosystem in China, grassland accounts for over 40% of the total land area species, which is an important part of the national green ecological barrier and ecological security. An ecological function is always the first function of grassland; the protection of the ecological grassland security is also a key task of the implementation of the 18th National Congress of the Communist Party of China to vigorously promote the construction of ecological civilization, and as an important part of the life community of "mountains, rivers, forests, fields, lakes, and grasses"; the grassland ecosystem plays an increasingly important role in maintaining the national ecological security. For example, in terms of water conservation, grassland occupies nearly 40% of water conservation function areas in China (Wang et al., 2017). The water conservation capacity of grassland is 40–100 times that of cultivated land and 0.5–3 times that of forest land. The water conservation capacity of grassland is 58.5% higher than that of forest land for runoff retention and 88.5% higher than that of forest land for sediment reduction. In terms of carbon fixation, grassland, as an important carbon-storing terrestrial vegetation ecosystem, is a huge carbon reservoir in China. Most of the carbon storage of grassland ecology is concentrated in the underground roots and soil of the grassland, and the carbon storage of grassland accounts for 17% of the national land carbon storage (Fang et al., 2010; Deng et al., 2017). Giving full play to the carbon storage function of grassland is of great significance for China's independent emission-reduction program and maintaining the carbon balance of the natural system. In addition, grassland plays an important role in windbreak and sand fixation, soil and water conservation, biodiversity, and carbon fixation. In this context, the scientific and effective assessment of ES was carried out for the grassland ecosystem, and its change mechanism was analyzed in depth. It is of great significance to clarify the needs of grassland protection, optimize the spatial layout, and realize the harmonious development between humans and nature.

Currently, the ES assessment mainly comprises three types of methods, namely, the benefit transfer, model, and quantitative index methods. Among these, the benefit transfer method was derived from Costanza et al. (1997), and it is mainly based on research of various types of land area and per unit area ES values or the product of the physical-quality parameters of the various types of ESs (Plummer, 2009). Benefit transfer, although less demanding in terms of data amounts and simpler, has higher corresponding uncertainty results and a lack of a solid scientific foundation and was thus put into question (Eigenbrod et al., 2010; Koschke et al., 2012). The model method is based on ESs provided by the ecological and social economic foundation of the development of the comprehensive evaluation method; among them, the InVEST and ARIES models are the most widely used (Daily et al., 2009). Although the model method to evaluate ESs value is, in theory, the most complete, data demand is higher, and it is often difficult for it to fully obtain the desired results in practice. The quantitative index is based on laws of the ecology principle for different ESs, and the corresponding algorithm is briefly formulated to define its value. This method focuses on the space unit and the practicability and accuracy of ESs. In practice, both the feasibility and accuracy of the operation results are high, this method thus having more extensive applications (Carreño et al., 2012). On this basis, this study used a set of quantitative surrogate biophysical indicators to evaluate the capability of grassland ESs in the Hulunbuir grassland in 2001–2015, considering that the grassland ecosystem has more natural attributes, and the framework of the grassland ecological service established in this study mainly includes carbon fixation, soil protection, water purification and provision, and biodiversity conservation. This method takes into account the operability and accuracy of the evaluation of ESs, and at the same time, combines the econometric model to explore its change mechanism and provides decision support for the management of the ecological environment of the grassland area.

The rest of this article is organized as follows: First, the research area is introduced in section "Study Area." Then, in section "Data and Methodology," we focused on the methodology and data sources. In section "Results," we further reported and analyzed the estimated results and the factors affecting ESs. Finally, in section "Conclusion and Discussion," we provided the discussion and conclusions of this article.

STUDY AREA

The Hulunbuir grassland is located northwest of Hulunbuir, Inner Mongolia Autonomous Region, and it is one of the four major grasslands of the world. It has a coverage of 100,000 km^2 and is mainly divided into six types, namely, mountain meadow, mountain meadow grassland, hill meadow grassland, plain hill arid grassland, sandy vegetation grassland, and lowland meadow grassland. There are over 3,000 rivers, over 500 lakes, over 1,600 plant species, over 500 animal species, over 30 million mu of arable land, and over 18 million livestock (e.g., horse

and pieces). However, in recent years, 66% of all pastures have degraded, which were manifested as three lows and one imbalance (i.e., low productivity, low coverage, low proportion of high-quality forage, and ecological and production dysfunction); industrial development is in urgent need for transformation and upgrading. Research on the grassland is correspondingly typical and representative. Therefore, based on assessing the grassland ES function and exploring its change mechanism, the Hulunbuir grassland was chosen as the study area in this study, which mainly includes five counties of Hulunbuir, namely, Xin Barag Right, Xin Barag Left, Prairie Chenbarhu, Hailar, and Ewenki Autonomous; the research in this region provide decision support for eco-environmental management in grassland regions (**Figure 1**).

DATA AND METHODOLOGY

Data

The data used in this research mainly come from the Resource Environment and Science Data Center[1]. In this study, we selected MOD17A2 data from MODIS product data, which have provided 1 km spatial resolution around the global land surface since 2000 and can be downloaded for free from http://www.ntsg.umt.edu/. MOD17A2 data are based on the net primary production (NPP) estimation model built by means of the Biome Biochemical Model (BIOME-BGC) model and a light-utilization model (Zhao and Running, 2010). According to research needs, this study extracted the data of MOD17A2 products of two tiles (i.e., h25v05 and h26v05) from 2000 to 2015 covering the Hulunbuir grassland with a spatial resolution of 1 km. On the basis of the MODIS Reprojection Tool (MRT) and the Cygwin platform, MODIS data were extracted and assembled. NPP source data in the Hierarchical Data Format (HDF) were converted into the GeoTIFF format, and the final image based on Python was converted and cropped. In addition, the data of the land-use raster component come from the Chinese Academy of Sciences (2000, 2005, 2010, 2015). Taking into account the time availability of parameter data in the evaluation of influencing factors in this study, the time range of this study is set to 2000–2015.

Methodology

Assessment of Grassland Ecosystem Services

In this study, grassland ES capacity was investigated, and its change mechanism is deeply explored mainly on the basis of the quantitative index method (**Figure 2**), based on the ecological principles and laws of different ESs, a quantitative index system is established, and economic analysis methods of multiple regression models are introduced to determine the important factors that affect ESs. These studies are based on the assumption that the capacity of an ES is directly related to the amount of biology covering Earth. The NPP of the grassland was taken as the index of the amount of biology and production, and the evaluation system of ESs was constructed. Through the measuring method, NPP was transformed into the equivalent of the ESs on a raster scale of 1 km × 1 km and was spatialized by using ArcGIS software. The selection of the index refers to previous studies (Barral and Oscar, 2012; Carreño et al., 2012; Zhang et al., 2017).

Furthermore, the process of variable determination is shown as follows:

(1) Net primary production (NPP).

Net primary production refers to the total amount of organic matter accumulated by photosynthesis per unit area per unit time in green plants after deducting autotrophic respiration. It can represent well the capacity of grassland biomass and original production, and the production and accumulation process within the ecosystem can also influence the formation and balance of ESs. In existing research, NPP estimation methods mainly include site-based actual observation, traditional climate statistical models, remote-sensing-based eco-physiological process models, and light-utilization models. As remote-sensing and geographic information systems are constantly being developed and applied, the NPP estimation model based on remote-sensing information is important to study the NPP.

(2) NPP coefficient of variation (VC_{NPP}).

VC_{NPP} represents the annual variation of NPP, which can be calculated by using the ENVI5.0 software.

(3) Soil erodibility factor (K).

K is the soil erosion factor that can be calculated through the model of the erosion-productivity impact calculator (EPIC) from the study by Vadas et al. (2006):

$$K = \left\{0.2 + 0.3e\left[-0.0256Sa\left(1\frac{Si}{100}\right)\right]\right\}\left(\frac{Si}{C+Si}\right)^{0.3}\left\{1.0 - \frac{0.25C}{C+e^{(3.72+2,95c)}}\right\}$$

$$\left\{1.0 - \frac{0.7(1-\frac{Sa}{100})}{(1-\frac{Sa}{100}) + e^{(-5.51+22.91-\frac{Sa}{100})}}\right\}$$

where S_a, S_i, S_l, and c represent the percentages of sand, clay, silt, and organic matter in the soil.

(4) Slope (F_{slo}).

This is specifically located in the spatial analysis module of the ArcGIS 10.2 software by means of 1:250,000 digital elevation model (DEM) image data provided by the Chinese Academy of Sciences (grid size was 1 km × 1 km, the numbers of rows and columns of each image were 1,201 × 1,801, and all maps were rectangles with the same size). Slope data could be obtained by merging the grids, transforming the projections, and dividing the watershed boundaries for DEM maps.

(5) Coefficient of soil permeability (F_{sic}).

F_{sic} is the coefficient of soil permeability, and 13 species of soil series were divided by the United States Department of Agriculture based on the soil texture. According to the subsequence of soil particle classification [in ascending sequence: clay (heavy), silty clay, clay, silty clay loam, clay loam, silt, silty loam, sandy clay, loam, sandy clay, sandy loam, loam sand, and sand], F_{sic} was assigned to 1/13, 2/13, 3/13, . . ., 1.

(6) Precipitation (F_{pre}) and air temperature (F_{tem}).

F_{pre} and F_{tem} represent the precipitation and air temperature, respectively. Specifically, in the geostatistical analysis module using the ArcGIS 10.2 software, the grid dataset of precipitation

[1]https://www.resdc.cn/

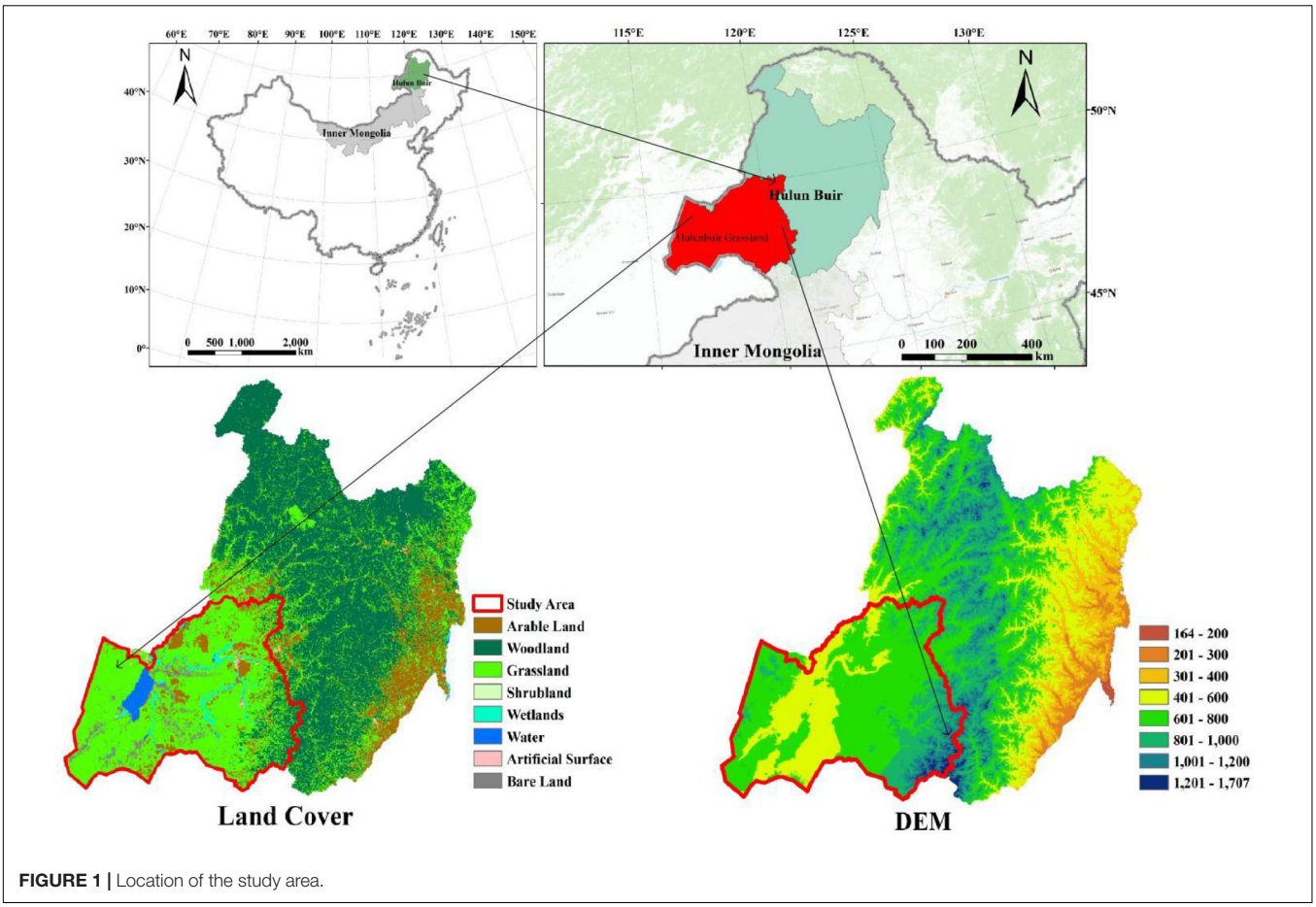

FIGURE 1 | Location of the study area.

and temperature can be obtained by spatial interpolation on the basis of daily observational data from the China Meteorological Data Network. The spatial resolution was 1 km.

(7) Surface roughness (D).

D is surface roughness, which can be calculated by $D = 1/\cos(\theta)$, in which θ is the slope of the radian. Both D and θ could be calculated in the spatial analysis module using the ArcGIS 10.2 software on the basis of DEM data.

Since all variables were normalized to the difference between the maximal and minimal values between 2000 and 2015, they all changed ranging from 0 to 1. Total ESs are the sum of all ESs, and results are dimensionless data.

Analysis of the Driving Mechanism

To deeply explore the change mechanism of grassland ESs, we introduced a multiple regression model used in the economic analysis, and the key indicators were determined on the basis of relevant research, which is shown as:

$$ESit = \beta 0 + \beta 1 slopeit + \beta 2 temit + \beta 3 preit + \beta 4 sunit$$
$$+\beta 5 d2waterit + \beta 6 d2highwit + \beta 7 soil\_nit + \beta 8 soil\_pit$$
$$+\beta 9 soil\_kit + \beta 10 unitpopit + \beta 11 unitgdpit + \beta 12 gfgit + \varepsilon it$$

where E_{Sit} represents the total amount of grassland ESs on grid units in each period; *slope* represents the slope; *tem* represents the annual average temperature; *pre* represents the annual precipitation; *sun* represents the sunshine time; *d2water* means the distance from a water source; *d2highw* is the distance from an expressway; *soil_n* represents the amount of nitrogen (N) in soil; *soil_p* represents the amount of phosphorus (P) in soil; *soil_k* represents the amount of the potassium (K) in soil; $unit_{pop}$ represents the population density; $unit_{gdp}$ represents the gross domestic product (GDP) density; *rfg* represents the policy of decaying farmland to grassland; *i* represents the basic analysis unit; and *t* represents the year.

RESULTS

Net Primary Production Changes

According to data of the Hulunbuir grassland NPP from 2000 to 2015, extracted on the basis of the MOD17A2 product, the major years are shown in **Figure 3**. NPP saw a trend of partial improvement and overall deterioration after 2000. The decline in NPP was mainly concentrated in the areas bordering East and West Piedmont and the plain of Greater Khingan, which showed degradation from forest steppes to meadow grassland and desert grassland; the ecological restoration level of the western border with Mongolia is weak, and the value of NPP is generally below 200. NPP in 2015 was also lower than that in 2000, but still better

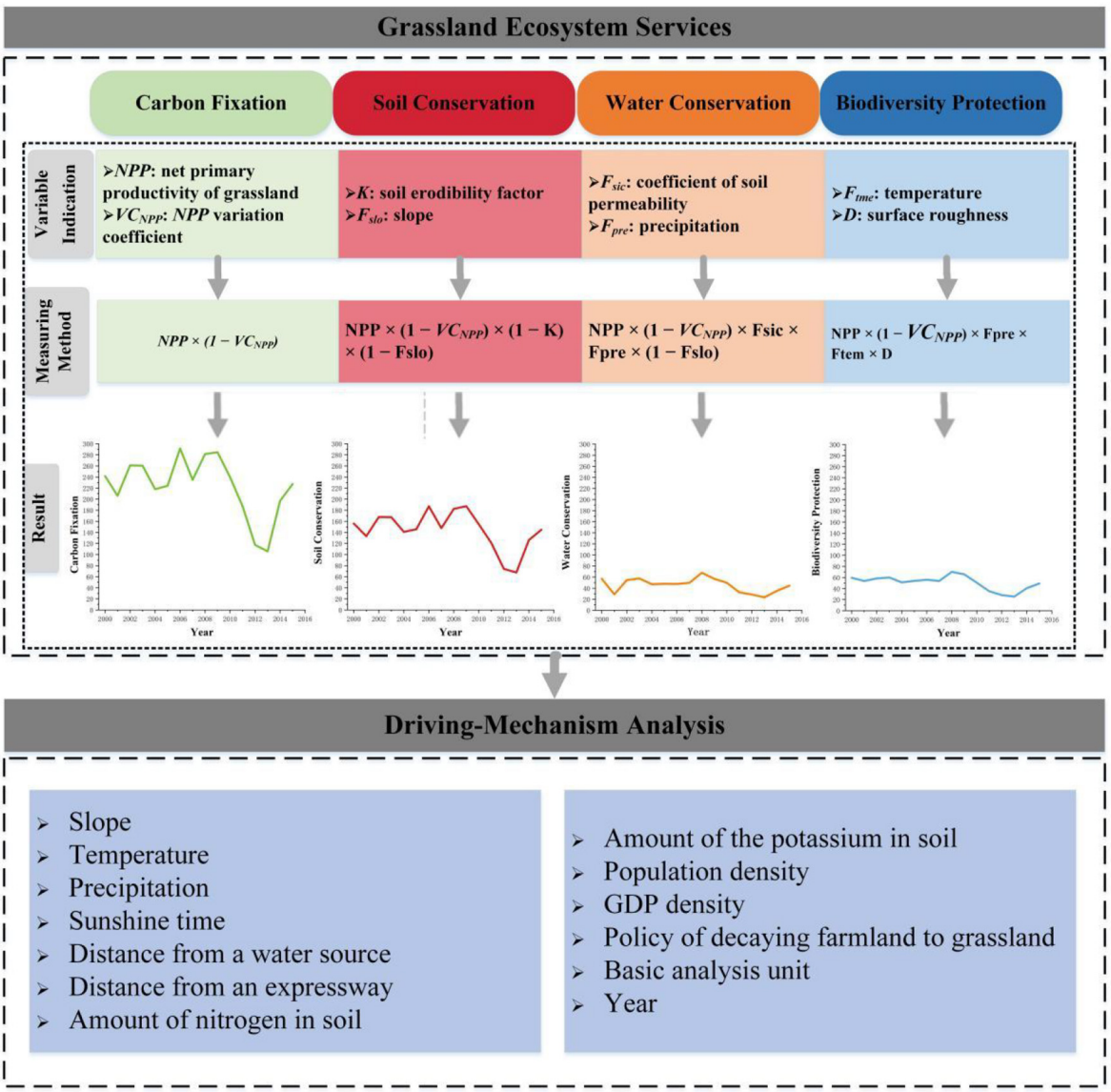

FIGURE 2 | The changing mechanism of grassland ecosystem services.

than in 2005 and 2010. Overall, the ecological security of the Hulunbuir grassland is still greatly threatened.

Changes in Grassland Ecosystem Services

From NPP data from 2000 to 2015, dynamic changes in grassland ESs in Hulunbuir from 2000 to 2015 were obtained by combining the evaluation index and calculation method in **Figure 2**. By calculating the average value and sum of the four ES types of carbon fixation, namely, carbon fixation, soil protection, water purification and provision, and biodiversity conservation in Hulunbuir from 2000 to 2015 (dimensionless data), it is found that the carbon fixation ability of the study area is relatively outstanding, accounting for about half of the overall ESs. Correspondingly, the two ESs of water conservation and biodiversity protection are relatively weak; from the perspective of time evolution, the ES level of Hulunbuir grassland has shown a clear downward trend, and related ecological improvement work urgently needs to be strengthened (**Figure 4**).

The various ESs are displayed in a more detailed and intuitive view of the time trend change graph. The grassland ES indicators generally show a slow undulating upward trend from 2000 to 2009 and show a rapid decline in 2010–2015 and a trend of later recovery. The changing trend of the overall ESs of each index is basically the same; especially, from 2009 to 2013, the downward trend is more obvious. During this period, the

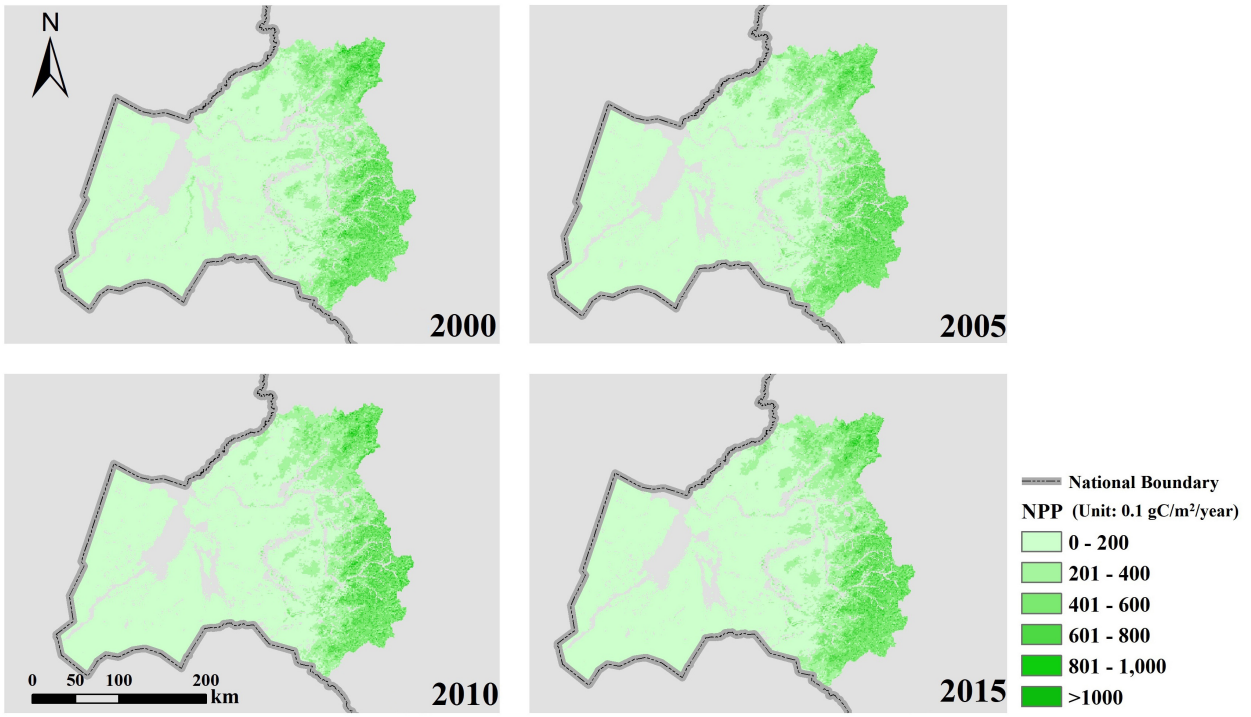

FIGURE 3 | NPP changes in 2000–2015.

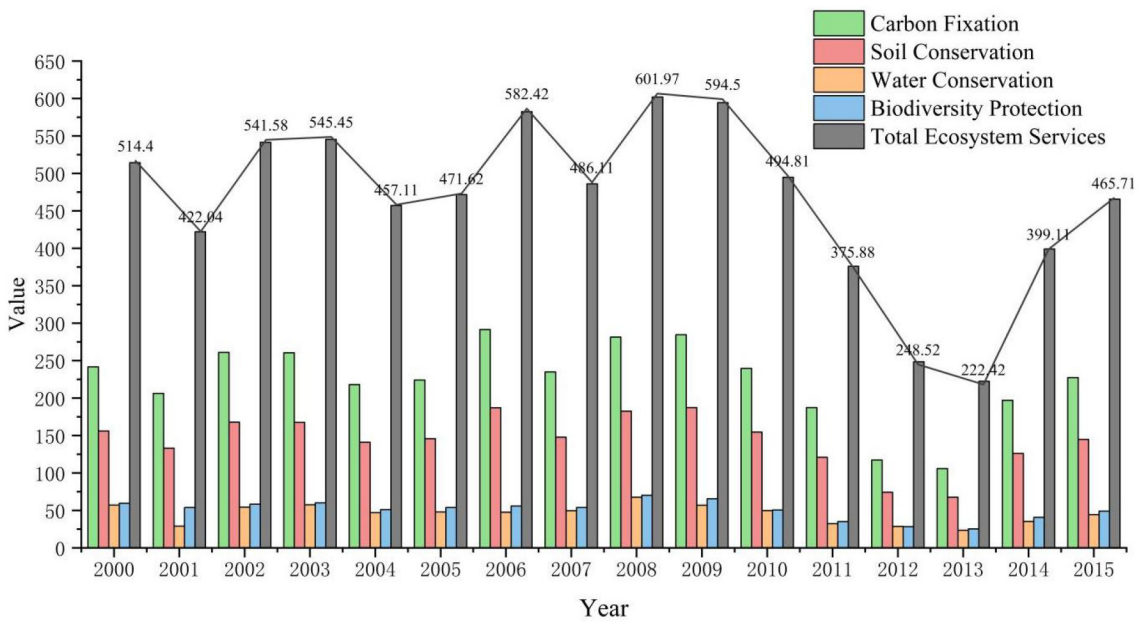

FIGURE 4 | The changing trend of Hulunbuir ecosystem service from 2000 to 2015.

grassland ecological environment deteriorated, and the grassland ecological supply capacity was significantly weakened; in 2008, the level of Hulunbuir ES reached the highest value of 601.97, and it fell to the lowest value of 222.42 in 2013. The main reason behind this was the natural and extensive management of grassland resources during 2010–2013, which caused serious degradation of pastures.

To visualize the ESs of the main years in the time series, refer to **Figure 5**. We could find that the spatial distribution of each ES type is similar, but the spatial distribution of different

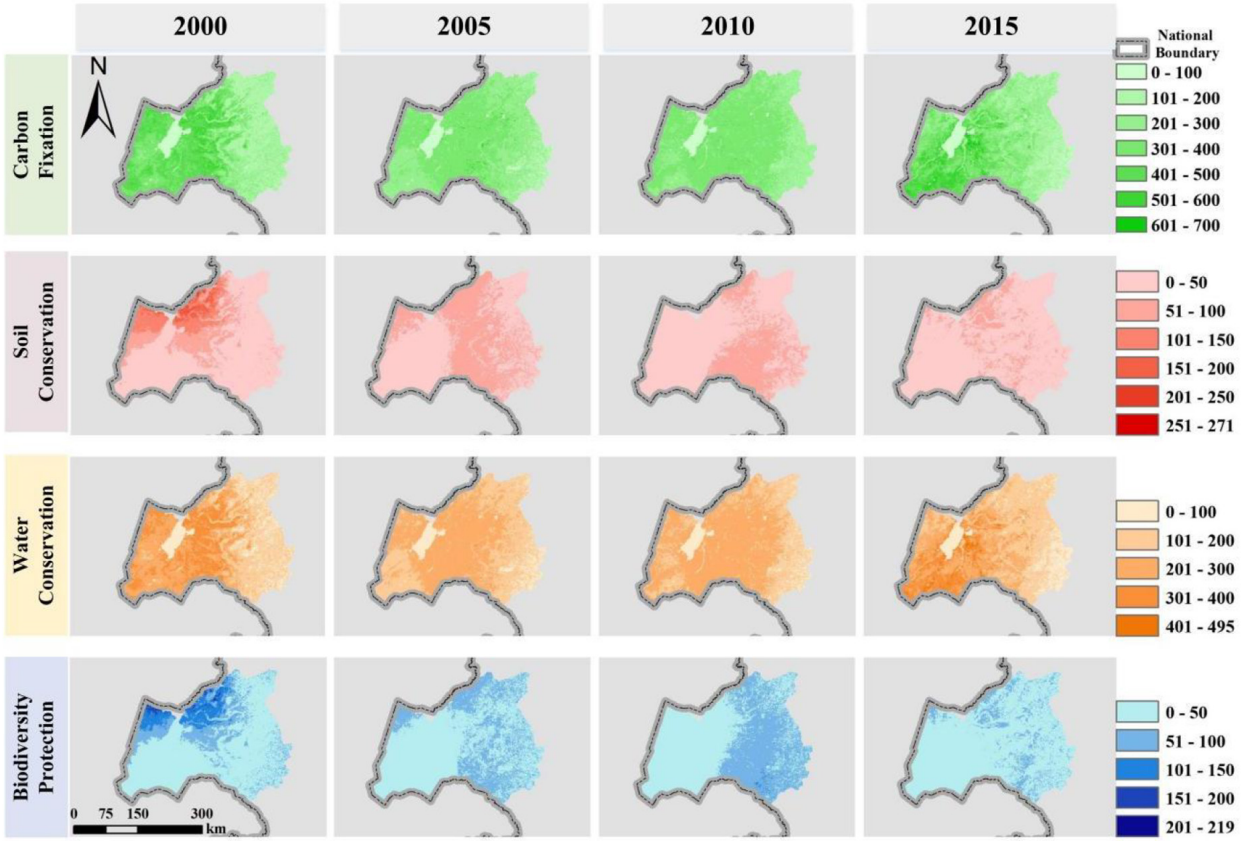

FIGURE 5 | Spatial distributions of ecosystem services in 2000–2015.

ESs has some differences. From the perspective of the time change, the value of ESs in each time period is in a state of concentrated distribution of early extreme values and an even distribution in the later period. The value of carbon fixation is generally higher in the west than in the east, and as time evolves, the distribution of values is more even; while the value of soil conservation is generally higher in the east than in the west, the spatial distribution of water conservation values is more even, but the western value is relatively high; biodiversity protection from the concentrated distribution of the extreme value of ESs in the northern region in 2000 to a low value in 2015 showed a difference between east and west.

In general, the spatial and temporal changes in the Hulunbuir grassland area have experienced the concentrated distribution of higher ESs in the northwestern region and gradually eased the uniform distribution changes in the eastern region. This is mainly due to the ecological restoration work in recent years.

Analysis of the Driving Mechanism

Analysis results of the driving mechanisms on changes in grassland ESs in Hulunbuir are shown in **Table 1**. The results showed that the model passed the 1% significance test, which indicated that the overall fitting is better. Among natural environmental factors, slope, temperature, annual precipitation, and lighting time all passed the 1% significance test, which showed that the above variables could affect changes in grassland ESs. The coefficient of variables shows that temperature variables have a smaller influence on grassland ESs mainly because the temperature is a stable and less dynamic factor and does not greatly change within a short amount of time. The coefficient of the precipitation variable was significantly positive, which indicated that precipitation has a significant positive effect on the growth of grassland vegetation and the increase in grassland ESs. The coefficient of the slope variable was negative, which shows that the higher the slope is, the worse the growth of grassland vegetation is; the smoother the slope is, the better the growth of grassland vegetation is. The coefficient of the sunshine time variable was also negative, indicating that, when sunshine time exceeds a certain limit, the heat flux of the soil, transformed by the absorbing solar shortwave radiation, accelerates the evaporation of soil moisture, which is unfavorable to the growth of grassland vegetation. The research by Hu et al. (2019) obtained a similar conclusion.

Among topographical factors, the distance from a water source was significantly positive, indicating that it is an important factor in explaining grassland ESs. Water sources are an important factor for grassland growth. As the distance to a water source increases, the more fragile the grassland

TABLE 1 | Results of panel model regression.

Driving factor	Coefficient	Standard error	*t* Value	*P* > | t|	95%
slope	0.118***	0.001	−96.79	0.000	[–0.121, –0.116]
tem	0.007***	0.000	17.52	0.000	[0.006, 0.007]
pre	0.132***	0.003	43.05	0.000	[0.126, 0.138]
sun	0.354***	0.007	−51.42	0.000	[–0.368, –0.341]
d2 water	0.729***	0.004	176.96	0.000	[0.720, 0.737]
d2 highw	0.068***	0.002	−34.02	0.000	[–0.072, –0.064]
soil_n	1.632***	0.004	−373.22	0.000	[–1.640, –1.624]
soil_p	0.470***	0.005	−104.65	0.000	[–0.480, –0.461]
soil_k	2.749***	0.009	319.03	0.000	[2.733, 2.767]
unitpop	0.002***	0.000	−37.90	0.000	[–0.002, -0.003]
unitgdp	0.001	0.000	1.17	0.242	[0.000, 0.001]
rfg	0.369***	0.001	−274.21	0.000	[–0.371, –0.366]
Constant	0.213***	0.001	53.42	0.000	[0.204, 0.220]
Prob > Fstatistic	0.000				

**** indicate the significance test of 10, 5, and 1%, respectively.*

ecosystem becomes, and the worse the grassland growth is. The distance from expressways and grass area per unit area is negatively affected, and this variable represents the degree to which grassland is disturbed by human activities. The nearer an expressway is, the more disturbed the grassland is by human activities, the worse the environment of grassland vegetation growth is, and the smaller the unit area of grassland is.

Among soil attribute factors, N, P, and K variables all passed the 1% significance test, in which the K variable had a significant positive effect on the growth of grassland ESs, while the N variable and P variable have an obvious negative influence. Related studies also showed that K is involved in the activation of over 60 enzyme systems, photosynthesis, the transportation of assimilation products, carbohydrate metabolism, and protein synthesis in the process of plant growth and development. Therefore, lodging, drought, and disease resistance can be improved, especially since the effect of the K fertilizer on the growth of leguminous forage is obvious (Read and Pratt, 2012).

Among social economic factors, the variable of GDP density could not explain the changes in grassland ES well. Although the variable of population density passed the significance test, the coefficient showed that it has a slightly negative effect on grassland ESs. As the population grows, urbanization deepens, rural populations shift to the cities, and the expansion of urban areas inevitably attacks the grassland ecosystem.

Among policy factors, analysis results showed that the policy of returning farmland to grassland has a negative effect on grassland ESs, which indicated that policy implementation has not played an expected role in the improving of the grassland ecological environment. Although we only took the policy of returning grazing to grassland as representative in this study, this variable passed a significant test, indicating that there is a strong correlation between the grassland ecological protection policy and the grassland ecological environment. Relevant studies also showed that the implementation of policies such as "grazing ban and conservation for purpose" and "returning grazing to grassland" has played a role in alleviating ecological pressure on natural grassland. However, the economic functions of the grassland system are neglected, which constrained the development of animal husbandry and the improvement of living standards of people to a certain extent. Illegal grazing is still prohibited, overgrazing is not fundamentally contained, and the resettlement program of ecological migration is not yet perfected, inflicting more poverty on people of herds. After the country has implemented ecological compensation, the current herdsmen who mainly rely on animal husbandry production, only rely on compensation to broaden their employment channels, and it will take a longer time to achieve the purpose of changing their lifestyles. However, relevant national policies are of great significance for enhancing the vitality of the regional economy and mobilizing the enthusiasm of farmers and herdsmen for production. In the process of implementing the policy, there have been some problems, such as quadratic disequilibrium in the process of policy resource distribution, a lack of effective supervision of the compensation fund, and the contradiction between ecological and economic benefits and between ecological welfare and benefits. Although the essence of implementing a grass-livestock balance policy is to ease the contradiction between ecological and productive functions, there are problems with implementing ecological protection and construction projects that make it difficult to form specific and feasible effective programs. Partial problems exist: there is no organic integration with innovations in the development model of grassland in pastoral areas, and there is a lack of balance between ecological and economic functions; clarifying and solving these problems is the next main task.

CONCLUSION AND DISCUSSION

This study used a set of quantitative surrogate biophysical indicators to evaluate the capability of grassland ESs (i.e., carbon fixation, soil protection, water purification and provision, and biodiversity conservation) in the Hulunbuir grassland in

2000–2015. This was connected with the econometric model, location, and land use from the natural environment, terrain, soil properties, and policy aspects of in-depth analysis on its change mechanism, basically leading to the following conclusion: grassland ES assessment results showed that, in 2009–2012, each downward trend of the ES index was more obvious; in 2013 and 2015, indicators K improved but were still below the 2000 level overall. The K content of the soil is an important factor affecting ESs and needs to be focused on in future grassland conservation. Social and economic factors such as population and GDP have a relatively small impact on grassland ecosystems with natural attributes, but the intensity of grassland grazing also needs to be considered to prevent the degradation of grassland ecosystem functions caused by overgrazing. In addition, climatic, topographic, soil, socioeconomic, and grassland-management policies all have a significant impact on grassland ESs. Among them, factors such as increased precipitation, distance from water sources, and potash use all play a positive role in improving grassland ESs. In recent years, in the view of the prairie regions of worsening of the ecological environment, the continuous reduction in grassland area, and grassland quality problems such as decreasing area, the state has carried out many ecological protection and construction projects for the implementation of a series of policies for the protection of grassland ecology. However, the grassland area is shrinking, and the grassland ecological deterioration trend is not fundamentally curbed, and the ecological protection policy did not achieve the desired effect and partly inhibits the growth of the regional economy, so it is difficult to improve the people's living standards with the contradiction between the ecological protection and economic growth.

Since 2003, China's grain output has been on the rise and increased for the 12th year in 2015, which is of great positive significance to ensuring Chinese self-sufficiency in grain rations and maintaining food security (Wang et al., 2018). For nearly 10 years, China has imported beef and mutton, liquid milk, and milk powder almost every year; its self-sufficiency grain rate dropping is a serious threat to national food security (Huang et al., 2017). On the other hand, due to domestic food not matching actual market demand, it is much less popular than imported food. Due to the grain-production inventory overload, autumn grain purchases at the end of 2015, China's three major staple food stocks were recorded high; in the agricultural-product market, excessive food products exist between the supply of and higher demand for animal food products. Meanwhile, China imported more than 100 million tons of grain in 2015. Under the impact of the high national grain-production inventory and the continuous increase in imported grain, the purchase price of grain in China has dropped to different degrees, and the income of growing grain has decreased. In addition, due to the backward agricultural production mode in China, an increase in the grain yield can only rely on the extensive resource input, including the massive consumption of water resources, and the extensive use of fertilizers and pesticides, which have caused a series of environmental problems and made it difficult to achieve sustainable development.

The main reason for problems of agricultural structures in China, such as the structures of grain production and consumption not matching, extensive resources, the unreasonable layout of agricultural production, and agricultural industry proportion coordination, is that agricultural production equal to "production" has yet to change its traditional thinking, backward agricultural production mode, and has not been paying enough attention to grassland productivity. In grassland areas, the contradiction between ecology and production function produces the contradiction of supply and demand on the market, so it is required to adjust agricultural structures and modes of production while protecting grassland ecological security to achieve the optimal allocation of grassland resources, reasonably and fully utilizing the grass production function, and improving the supply of high-quality animal products on the market. All these in order to meet the growing demand of people for a better life, speed up the development of the grass industry and improve the level of pastoral life and the vitality of the regional economic development, so as to realize the sustainable development of grassland areas. In 2015, Central File No. 1, for the first time, put forward speeding up the development of grass-based livestock husbandry in combination with support grass planting, and feeding is combined with planting and raising modes to promote the combination of grain, cash crops, the coordinated development of grass ternary planting structures, and the protection of grassland to realize a win-win of ecological and economic benefits.

DATA AVAILABILITY STATEMENT

The raw data supporting the conclusions of this article will be made available by the authors, without undue reservation.

AUTHOR CONTRIBUTIONS

ML wrote the article and did the laboratory analysis. XW contributed to the field analysis, while the latter also conceptualized the research. ML, XW, and JC provided conceptual and editorial inputs on the manuscript and discussed field methodology. All authors contributed to the article and approved the submitted version.

FUNDING

This study was supported by the Strategic Priority Research Program of the Chinese Academy of Sciences (XDA23070402).

ACKNOWLEDGMENTS

We are also grateful to reviewers for their helpful comments on the manuscript.

REFERENCES

Barral, M. P., and Oscar, M. N. (2012). Land-use planning based on ecosystem service assessment: A case study in the Southeast Pampas of Argentina. *Agric. Ecosyst. Environ.* 154, 34–43. doi: 10.1016/j.agee.2011.07.010

Burkhard, B., Crossman, N., Nedkov, S., Petz, K., and Alkemade, R. (2013). Mapping and modelling ecosystem services for science, policy and practice. *Ecosyst. Serv.* 4, 1–3. doi: 10.1016/j.ecoser.2013.04.005

Carreño, L., Frank, F., and Viglizzo, E. (2012). Tradeoffs between economic and ecosystem services in Argentina during 50 years of land-use change. *Agric. Ecosyst. Environ.* 154, 68–77. doi: 10.1016/j.agee.2011.05.019

Castellani, V., Sala, S., and Benini, L. (2017). Hotspots analysis and critical interpretation of food life cycle assessment studies for selecting eco-innovation options and for policy support. *J. Clean. Prod.* 140, 556–568. doi: 10.1016/j.jclepro.2016.05.078

Costanza, R., d'Arge, R., de Groot, R., Farber, S., Grasso, M., Hannon, B., et al. (1997). The value of the world's ecosystem services and natural capital. *Nature.* 387, 253–260. doi: 10.1038/387253a0

Daily, C. C. (1997). *Nature's Service: Societal Dependence on Natural Ecosystems.* Washington, DC, USA: Island Press.

Daily, G. C., Polasky, S., and Goldstein, J. (2009). Ecosystem services in decision making: time to deliver. *Front. Ecol. Environ.* 7:21–28. doi: 10.1890/080025

Deng, X., Gibson, J., and Wang, P. (2017). Quantitative measurements of the interaction between net primary productivity and livestock production in Qinghai Province based on data fusion technique. *J. Clean. Prod.* 142, 758–766. doi: 10.1016/j.jclepro.2016.05.057

Eigenbrod, F., Armsworth, P. R., Anderson, B. J., Heinemeyer, A., Gillings, S., Roy, D. B., et al. (2010). Error propa-gation associated with benefits transfer-based mapping of ecosystem services. *Biol. Conserv.* 143, 2487–2493. doi: 10.1016/j.biocon.2010.06.015

Fang, J., Yang, Y., Ma, W., Mohammat, A., and Shen, H. (2010). Ecosystem carbon stocks and their changes in China's grasslands. *Sci. China Life Sci.* 53, 757–765. doi: 10.1007/s11427-010-4029-x

Hu, Z., Zhao, Z., Zhang, Y., Jing, H., Gao, S., and Fang, J. (2019). Does 'Forage–Livestock Balance' policy impact ecological efficiency of grasslands in China? *J. Clean. Prod.* 207, 343–349. doi: 10.1016/j.jclepro.2018.09.158

Huang, J., Wei, W., Cui, Q., and Xie, W. (2017). The prospects for china's food security and imports: will china starve the world via imports? *J. Integr. Agric.* 16, 2933–2944. doi: 10.1016/S2095-3119(17)61756-8

Koschke, L., Fürst, C., Frank, S., and Makeschin, F. (2012). A multi-criteria approach for an integrated land-cover-based assessment of ecosystem services provision to support landscape planning. *Ecol. Indic.* 21, 54–66. doi: 10.1016/j.ecolind.2011.12.010

Liebig, M. A., Gross, J. R., Kronberg, S. L., and Phillips, R. L. (2010). Grazing management contributions to net global warming potential: A long-term evaluation in the Northern Great Plains. *J. Environ. Qual.* 39, 799–809. doi: 10.2134/jeq2009.0272

Plummer, M. L. (2009). Assessing benefit transfer for the valuation of ecosystem services. *Front. Ecol. Environ.* 7:38–45. doi: 10.1890/080091

Read, J. J., and Pratt, R. G. (2012). Potassium influences forage bermudagrass yield and fungal leaf disease severity in Mississippi. Online. *Forage Grazinglands* 10, *. doi: 10.1094/FG-2012-0725-01-RS

Reid, W. V., Watson, R. T., Rosswall, T., Steiner, A., Mooney, H. A., Arico, S., et al. (2005). *Millennium Ecosystem Assessment: Ecosystems and Human Well Being - Synthesis Report*. Washington DC: Island Press.

Vadas, P. A., Krogstad, T., and Sharpley, A. N. (2006). Modeling phosphorus transfer between labile and nonlabile soil pools. *Soil Sci. Soc. Am. J.* 70:736. doi: 10.2136/sssaj2005.0067

Wang, J., Zhang, Z., and Liu, Y. (2018). Spatial shifts in grain production increases in china and implications for food security. *Land Use Policy* 74, 204–213. doi: 10.1016/j.landusepol.2017.11.037

Wang, P., Deng, X., and Jiang, S. (2019). Global warming, grain production and its efficiency: Case study of major grain production region. *Ecol. Indic.* 105, 563–570. doi: 10.1016/j.ecolind.2018.05.022

Wang, Z., Deng, X., Song, W., Li, Z., and Chen, J. (2017). What is the main cause of grassland degradation? A case study of grassland ecosystem service in the middle-south Inner Mongolia. *Catena.* 150, 100–107. doi: 10.1016/j.catena.2016.11.014

Woodruff, S. C., and Bendor, T. K. (2016). Ecosystem services in urban planning: Comparative paradigms and guidelines for high quality plans. *Landsc. Urban Plan.* 152, 90–100. doi: 10.1016/j.landurbplan.2016.04.003

Zagonari, F. (2016). Using ecosystem services in decision-making to support sustainable development: Critiques, model development, a case study, and perspectives. *Sci. Total Environ.* 54, 25–32. doi: 10.1016/j.scitotenv.2016.01.021

Zhang, L., Lü, Y., Fu, B., Dong, Z., Zeng, Y., and Wu, B. (2017). Mapping ecosystem services for China's ecoregions with a biophysical surrogate approach. *Landsc. Urban Plan.* 161, 22–31. doi: 10.1016/j.landurbplan.2016.12.015

Zhao, M., and Running, S. W. (2010). Drought-Induced Reduction in Global Terrestrial Net Primary Production from 2000 through 2009. *Science.* 329, 940–943. doi: 10.1126/science.1192666

Zhao, Z., Wang, G., Chen, J., Wang, J., and Zhang, Y. (2019). Assessment of climate change adaptation measures on the income of herders in a pastoral region. *J. Clean. Prod.* 208, 728–735. doi: 10.1016/j.jclepro.2018.10.088

Conflict of Interest: The authors declare that the research was conducted in the absence of any commercial or financial relationships that could be construed as a potential conflict of interest.

The reviewer YX declared a shared affiliation, with no collaboration, with several of the authors JC and ML to the handling editor at the time of the review.

frontiers in Environmental Science

ORIGINAL RESEARCH
published: 11 March 2022
doi: 10.3389/fenvs.2022.847719

Spatial Analysis of Agricultural Eco-Efficiency and High-Quality Development in China

Guofeng Wang, Lingchen Mi, Jinmiao Hu and Ziyu Qian*

Faculty of International Trade, Shanxi University of Finance and Economics, Taiyuan, China

High-quality development has become a new requirement for China's social and economic development. As an important industry related to the national economy and people's livelihood, achieving high-quality development in agriculture has become the most urgent task currently facing agriculture. This study focuses on agricultural eco-efficiency to indicate spatial distribution of high-quality development based on agricultural input–output data from 2001 to 2019 and the SBM-Undesired model; this study focuses on Agricultural Eco-efficiency, a key indicator related to the high-quality development of agriculture, to measure the temporal and spatial evolution of Agricultural Eco-efficiency. The results show that the Agricultural Eco-efficiency has increased from 0.363 in 2001 to 0.818 in 2019, with a growth rate of 125.34%, and the provinces with higher agricultural eco-efficiency are mainly located in the eastern regions. In addition, there is a U-shaped change trend between Agricultural Eco-efficiency and the total output value of agriculture, forestry, animal husbandry, and fishery. In other words, the provinces with the total output value of agriculture, forestry, animal husbandry, and fishery in the low range and high range enjoy higher Agricultural Eco-efficiency. Compared with the eastern region, the middle reaches of Yellow River and middle reaches of Yangtze River have great potential to reduce carbon emissions. In order to achieve high-quality agricultural development, it is necessary to pay attention to key indicators for improving Agricultural Eco-efficiency, and the technology development of the central and western regions will be very useful to decrease the gap.

Keywords: agricultural eco-efficiency, high-quality development, spatial analysis, carbon emission, carbon neutrality

OPEN ACCESS

Edited by:
Fan Zhang,
Institute of Geographic Sciences and Natural Resources Research (CAS), China

Reviewed by:
Ehsan Elahi,
Shandong University of Technology, China
Tianhe Sun,
Hebei University of Economics and Business, China
Qing Zhou,
Huazhong Agricultural University, China

****Correspondence:***
Guofeng Wang
wanggf@sxufe.edu.cn

Specialty section:
This article was submitted to Land Use Dynamics, a section of the journal Frontiers in Environmental Science

Received: *03 January 2022*
Accepted: *16 February 2022*
Published: *11 March 2022*

Citation:
Wang G, Mi L, Hu J and Qian Z (2022) Spatial Analysis of Agricultural Eco-Efficiency and High-Quality Development in China. Front. Environ. Sci. 10:847719. doi: 10.3389/fenvs.2022.847719

INTRODUCTION

In 2021, the COP 26 UN Climate Change Conference in Glasgow highlighted a crucial time mode for mankind's positive actions and explained that the next 10 years will be a crucial last window. If we do not take positive actions in time, humans and the Earth will face unimaginable natural disasters, such as sea level rise and biological extinction. Global warming of 2°C will have a wide-ranging and serious impact on humans and nature (Liu, 2019). One-third of the world's population will be regularly exposed to severe high temperatures, thus causing health problems and increasing death rates related to high temperatures. In addition, almost all warm water coral reefs will be destroyed, and Arctic sea ice will completely melt at least one summer every 10 years, generating devastating effects on the wildlife and communities they support. The latest "Emissions Gap Report" released by the United Nations Environment Program (UNEP) shows that despite the global climate ambitions and "net

zero" commitments, the total amount of fossil fuels that countries plan to produce in 2030 is still more than double the amount of fossil fuels that are required to achieve the 1.5°C temperature control target of the Paris Agreement. The fossil fuels that governments around the world plan to produce in 2030 are about 110% higher than the production level required to achieve the global 1.5°C temperature control target and 45% higher than the production level required to achieve the 2°C temperature control target. Compared with the previous assessment, this production gap remains basically unchanged (Ji and Hoti, 2021).

Agriculture is one of the most sensitive fields affected by climate change (Elahi et al., 2021a), and climate change may cause China's agriculture to be more vulnerable. In addition to carbon dioxide, agricultural production also causes a large amount of methane and nitrous oxide emissions (Chen et al., 2020). In comparison with carbon dioxide, the two greenhouse gases methane and nitrous oxide are 20 and 310 times more capable of causing global warming than carbon dioxide, respectively. Agriculture is facing pressures and major challenges to alleviate and adapt to climate change and feed the huge population around the globe (Zhao et al., 2017; Abid et al., 2019; Van et al., 2019). The promotion of sustainable agriculture is an important means to adapt to climate change, reduce greenhouse gas emissions in agriculture, and alleviate the problem of deforestation caused by food demand (Han et al., 2018).

The ecological development of the agricultural industry is an important feature of achieving green and sustainable development of agriculture. The ecologicalization of the agricultural industry requires integrating the development of primary, secondary, and tertiary industries of agriculture, making full use of resources, and coordinating the relationship between economy, society, and ecology (Chen et al., 2021). Among them, the realization of ecological development of the agricultural primary industry is the key to achievement of ecological development of the entire agricultural industry. Agricultural eco-efficiency is not only the core indicator of green development of agriculture but also one of the important measures to fulfill agricultural modernization (Pang et al., 2016; Elahi et al., 2019a; Elahi et al., 2020). Sustainable Development Goals (SDGs) consider no poverty, zero hunger, and good health and wellbeing as the first three goals for achieving sustainable development, which shows the significance of realizing the three goals for human development; the sustainable development of agriculture is the key to achieve the three goals (Balezentis et al., 2016). From the perspective of global agricultural development, all countries have entered into comprehensive agricultural modernization with mechanization, improved varieties, chemistry, electrification, and informationization as the main content. Circular agriculture and low-carbon agriculture have become crucial methods to achieve sustainable agricultural development (Czyzewski et al., 2021). On the one hand, various countries have developed a variety of circular agriculture models, including material reuse models, resource reduction models, and waste utilization models (Elahi et al., 2019b). On the other hand, low-carbon agriculture mainly achieves low-carbon development goals through rational use of chemical fertilizers, water-saving irrigation, and energy-saving farming (Ke et al., 2012). With the tightening of resource environment constraints, agriculture in various countries around the world is moving toward green transformation, and China is no exception. In 2015, China formulated the "Zero Growth Action Plan of Chemical Fertilizer and Pesticide by 2020," implementing the policy of "one control, two reduction" on chemical fertilizer use (Qu et al., 2021). According to the data from the Ministry of Agriculture and Rural Affairs of People's Republic of China, the action of zero increase in the use of chemical fertilizers and pesticides since 2015 has achieved initial results. By the end of 2020, the reduction and efficiency enhancement of chemical fertilizers and pesticides have successfully helped achieve the expected goals. The chemical fertilizer utilization rate of the three staple crops of rice, wheat, and corn was 40.1%, which increased by 5 percentage points from 2015 (Bai and Tao, 2017). However, the further realization of green development is a challenge facing China's agriculture (Deng and Gibson, 2019).

Through analyzing the relationship between agricultural eco-efficiency and industrial green development, this study will propose a spatial heterogenous scheme of agricultural industrial green development.

This study is organized as follows: *Literature Review* consists of the literature review, *Methodology and Data* consists of methodology and data, *Results and Discussion* explains the results and discussion, and the final *Policy Implications* explains the policy implication.

Literature Review

The efficiency theory focuses on analyzing the conflict between the effectiveness of resources and infinity of human desires. "Pareto efficiency" is the earliest and widely recognized theory of resource utilization efficiency in economics (Charnes et al., 1978) "The New Palgrave Dictionary of Economics" states that the efficiency refers to the efficiency of resource utilization; subsequently, Samuelson and Nordhaus pointed out that efficiency means that there is no waste. When there is a state in which society has to increase the output of a certain product at the cost of damaging or reducing the output of another product, then such production is effective, and the indicated efficiency is the "optimal" state of the described resource usage. However, with the development of economic research theory and development practice, the concept of "efficiency" has not been an exactly unified definition. Although "Pareto efficiency" can show the possibility boundary of realizing effective allocation of resources, it cannot identify different distributions between actual and effective allocation of resources and cannot provide a feasible expansion path. Therefore, most scholars use the concept of reflecting resource utilization and allocation to study efficiency when using the concept of efficiency, and this connotation has gradually been recognized (Coelli and Rao, 2012). At this time, efficiency research not only reflects the actual use and allocation of resources but also maps the "optimal" state of resource

utilization. Based on the different emphasis of investigating resource utilization, efficiency is divided into two parts: utilization efficiency and production efficiency (Zeng et al., 2020). Therefore, the general meaning of efficiency refers to the ratio of the relationship between limited production resources and what can be provided for human consumption under certain production conditions and technical levels (Zhong et al., 2020).

The concept of eco-efficiency originated from abroad and was first proposed by German scholars, and it integrates the concept of economic and ecological two-way efficiency (Baum and Bienkowski, 2020). It is used to measure the relationship between economic value change and environmental impact caused by a certain change. With the deepening of research in China and abroad, the concept of ecological efficiency is getting perfect. The concept recognized by academics is that based on necessary materials and products and services that could improve the quality of life, human beings achieve the goal of coordinated coupling between the environment and economy. Agricultural eco-efficiency is the specific application of eco-efficiency in the agricultural field. Taking the sustainable use of agricultural resources as the core and considering the realization of resource conservation and pollutant emission reduction as the goal, it is an indicator that evaluates the comprehensive performance of agricultural production and economy on the basis of meeting human needs for agricultural products (Magarey et al., 2019). The goal of Agricultural Eco-efficiency is to realize the efficient utilization of resources in the process of agricultural production, focusing on measuring the relationship between resources in the natural ecology and agricultural economic production. In other words, it refers to the simultaneous realization of multiple goals of high efficiency of agricultural production, reduction of resource input, and decrease of waste loss in the process of agricultural production (Reith and Guidry, 2003). Its main features contain the following five aspects: to achieve efficient use of resources and maximize the use of renewable resources, to avoid environmental losses caused by the production process to the local and surrounding environment, to produce expected agricultural products, to maintain biodiversity, and to make rapid adjustments to social, economic, and environmental impacts. (Golas et al., 2020). Based on the abovementioned research interpretation, the connotation of Agricultural Eco-efficiency can be summarized into three levels. The first level is that Agricultural Eco-efficiency demonstrates a research method for the regulation and control of the entire production process of agriculture. To increase the overall output level of agriculture, we must find ways to improve the utilization efficiency of various input elements in the agricultural system. Therefore, in this state, it not only reduces the use of chemical fertilizers and pesticides and other productive materials in the agricultural production process but also relies more on technologies (mixed planting, crop rotation, and the complementarity of agriculture and animal husbandry, etc.) to effectively increase the level of agricultural output (Todorovic et al., 2018). The second level is that Agricultural Eco-efficiency should be a key goal pursued by agricultural production. The level of Agricultural Eco-efficiency means the level of utilization efficiency of agricultural resources, and the improvement of utilization efficiency characterizes the reduction of pollutants discharged into the environment. The improvement of ecological efficiency is based on reducing the adverse effects in the system as a "reward". Its improvement can effectively reduce the input of fossil fuels, chemical fertilizers, and other agricultural materials in the agricultural production process, decrease the entire agricultural production cost, and indirectly increase the agricultural income (Czyzewski et al., 2021). Therefore, the level of Agricultural Eco-efficiency is not only consistent with the entire ideological connotation and extension of sustainable agricultural development but also an indispensable development goal for the ecologicalization of the agricultural industry. At the third level, Agricultural Eco-efficiency is a vital means of assessing the sustainable development capability in the process of agricultural production (Gava et al., 2020). It can effectively evaluate ecological and economic performance, thus providing an important method for evaluation.

Agricultural Eco-efficiency is an important measurement indicator for sustainable agricultural development. It focuses on the coupling of the ecological and economic objectives in the agricultural production process, and based on the maximization of expected output and the minimization of undesired output, the increase in output and reduction of pollutants are realized. Existing studies have discussed the connotation of Agricultural Eco-efficiency, which will provide an important basis for this research. However, the adoption of any technology is dependent on the sociopsychological behavior of people (Elahi et al., 2021b).

There are certain differences in the measurement methods of Agricultural Eco-efficiency due to different disciplines. In terms of methods, they mainly include ratio method, life cycle assessment (Soteriades et al., 2016), ecological footprint analysis (Wackernagel and Galli, 2007), energy analysis (Wang and Zhao, 2021), data envelopment analysis (Tone and Tsutsui, 2009), and stochastic frontier analysis (Guo et al., 2020), etc.

The ratio method is the earliest measurement method, which has gradually faded out of the field of vision of scholars. Early methods of eco-efficiency evaluation mainly used the ratio of economic value of products to the environmental impact of products (Ke et al., 2012), and the more common calculation formula was proposed by the World Business Council for Sustainable Development (WBCSD).

$$\text{Eco} - \text{efficiency} = \frac{\text{Economic Value of Products}}{\text{Environmental Impact of Products}} \quad (1)$$

The particularity of using the ratio method to calculate Agricultural Eco-efficiency is mainly manifested in the fact that in the entire agricultural production process, not only will the use of chemical fertilizers and pesticides cause negative effects, such as pesticide residues and soil compaction, but also due to the carbon sequestration effect of the crop itself; the absorption of toxic gases will generate a positive effect (Lwin et al., 2017). Therefore, in the calculation process, the formula is deformed as follows:

$$\text{Agricultural Eco} - \text{efficiency} = \frac{\text{Economic Value of Agricultural Products}}{\begin{array}{l}\text{Negative Evironmental Effects}\\ -\text{ Positive Evironmental Effects}\end{array}} \quad (2)$$

The ratio method characterizes the possible negative impacts of economic development on the environment to a certain extent. However, the defect of this indicator is that it only considers the impacts on the output side and completely ignores the description of the input side, but for agriculture, the resource and environmental impacts are generated precisely on the input side. Therefore, this method has gradually faded out of scholars' research horizons.

Life cycle assessment is a method that originated in the 1960s. Due to resource consumption and oil crisis, it has had serious impacts on social and economic development. However, Chinese and foreign academic research evaluation methods were limited to a few concentrated environmental load methods (Soteriades, A.D. et al., 2016). In the 1990s, with the gradual deepening of sustainable development research, the method of life cycle assessment appeared. The detailed definition is given by the International Society for Environmental Toxicology and Chemistry and the International Organization for Standardization (Fridrihsone et al., 2020). Specifically, it refers to evaluating the potential impacts of energy and resource consumption and waste pollutants generated during the entire production process (from raw material extraction, material preparation, to the product becoming waste) of products (Holka, 2020). The quantification of life cycle assessment appeared in 1990. It is an ecological scarcity method developed by Swiss researchers. Its calculation formula is as follows:

$$\frac{\text{Ecopoints}}{kg} = \frac{Emissions_A}{Emissions_T} \times \frac{1}{Emissions_T}. \quad (3)$$

Among them, the subscript A represents the actual environmental load, and the subscript T represents the environmental load in an ideal state.

In the process of calculation based on the life cycle assessment, the whole process needs to be measured, especially in the calculation of Agricultural Eco-efficiency as it is difficult to define the boundary, and the data of the whole analysis process are more complicated. At the same time, the comparative analysis mechanism between regions needs to be further deepened.

Ecological footprint analysis was first proposed by Rees, a Canadian ecologist, in the early 1990s and then developed and improved by Wackernagel. It mainly compares the overall loss caused by human production activities to nature and converts it into the corresponding land area through the conversion coefficient. Moreover, this value is compared with the overall amount of supply that nature can provide to human beings, and it is determined whether the regional economic development is within the carrying range of the ecosystem (Costa et al., 2018) based on the comparison result. If the area of productivity required by human activities is greater than the amount that nature can provide for humans, at this time, it is in a situation of over-utilization of ecological resources. The use of ecological footprint analysis is simple and globally comparable. However, this method has some shortcomings, which are manifested in the lack of data on the actual consumption of products of various biological resources in the calculation. Therefore, it is easy to cause errors when using different product usage data for substitution (Wackernagel and Galli, 2007). In addition, there is lack of groundwater resource measurement in the account coverage, and no attention is paid to the quality of the land in the production process.

Energy analysis was put forward by Odum, a famous American ecologist, in the 1980s, focusing on the quantitative evaluation of the "nature–economy–society" complex system. This method mainly takes energy as the core of the research, uses the energy conversion rate to convert the different types and the same types of energy in the ecosystem into the same standard solar energy value to evaluate the energy value of various energies within the system (Wang and Zhao, 2021), comprehensively analyzes the energy value (material flow, currency flow, information flow, etc.), and assesses the structure, benefit, and function of the ecosystem. Based on energy analysis, the changes in the natural environment and carrying capacity over a period of time (Llinas et al., 2021), sustainable development capabilities, and energy usage could be evaluated.

The energy analysis takes into consideration the value of economy, resources, and the environment as a whole and makes up for the difficulties of traditional economics in resource pricing and measurement. However, the energy analysis also has the problems such that the energy conversion rate will change greatly with the change of regions, and the evaluation indexes are relatively single.

Stochastic frontier analysis is a type of parametric analysis. It has been widely used to measure the efficiency in different research topics. This method was proposed by Farrell in 1957, and by 1977, Aigner, Meeusen, and Van DenBroeck conducted independent research on this method (Li et al., 2021). In the process of measuring Agricultural Eco-efficiency, the first step is to determine the form of the production function. Then, the difference value between the actual production output level and the maximum expected output level is calculated based on the specific form of the production function. Finally, the inefficiency term and the random error term are separated. This method is considered to be a commonly used evaluation method of Agricultural Eco-efficiency.

Data envelopment analysis is currently the most widely used method for evaluating Agricultural Eco-efficiency. This method was proposed by Charnes, Cooper, and Rhodes in 1978 and can evaluate the effectiveness of decision-making units (Liu et al., 2020) with multiple inputs and multiple outputs. This method does not need to emphasize the specific form of the model, is more convenient to use, and does not require dimensional processing of the data.

Owing to the difference in various disciplines, there are certain differences in the measurement methods of Agricultural Eco-efficiency. However, every calculation method has its own pros and cons. Therefore, it is necessary to conduct an in-depth

analysis of the measurement framework system of Agricultural Eco-efficiency and seek a measurement method that is more suitable for resource-environmental constraints.

METHODOLOGY AND DATA

SBM Model With Undesired Output

The DEA–Slack-Based Model (DEA-SBM) can break the shortcomings of input–output angle selection and radial improvement of traditional BCC and CCR models so that the efficiency values can be better measured based on non-angular, non-radial, and actual slack variables to the target. The specific model is as follows:

$$min_{\lambda,s^-,s^+}\rho = \frac{1-\frac{1}{m}\sum_{i=1}^{m}\frac{s_i^-}{x_{i0}}}{1+\frac{1}{s}\sum_{r=1}^{s}\frac{s_r^+}{y_{r0}}}. \tag{4}$$

$$\text{s.t. } x_0 = X\lambda + s^- \tag{5}$$

$$y_0 = Y\lambda - s^+ \tag{6}$$

$$\lambda \geq 0, s^- \geq 0, s^+ \geq 0 \tag{7}$$

Among them, λ represents the weight vector; s^- s^+ represents excess input and insufficient output, respectively; x_0 y_0 represents the input and output of each decision-making unit, respectively; and X, Y is the input and output matrix, respectively; $X = [x_1, ..., x_n] \in R^{m\times n}$, $Y = [y_1, ..., y_n] \in R^{s\times n}$. It is assumed that X > 0, Y > 0 and ρ is the efficiency value that needs to be calculated.

It is assumed that there are n production decision making units (DMUs) in the agricultural evaluation system, and each DMU comprises the following three sets of vectors: input vector $x \in R^m$, expected output vector $y^e \in R^a$, and undesired output vector $y^n \in R^b$ Among them, m, a, b represents the types of input–output elements. The matrices $X = [x_1, \cdots, x_n]\epsilon R^{m\times n}$, $Y^e = [Y_1^e, \cdots, Y_n^e]\epsilon R^{a\times n}$, $Y^n = [Y_1^n, \cdots, Y_n^n]\epsilon R^{b\times n}$, and $X > 0, Y^e > 0, Y^n > 0$are defined, and the possible set of system production based on constant returns to scale (CRS) is defined as follows:

$$\begin{cases} \rho^* = min\dfrac{1-\dfrac{1}{m}\sum_{i=J}^{m}\dfrac{d_i^-}{x_{i0}}}{1+\dfrac{1}{a+b}\left(\sum_{r=1}^{a}\dfrac{d_r^e}{y_{r0}^e}+\sum_{h=1}^{b}\dfrac{d_h^n}{y_{h_0}^n}\right)} \\ s.t.\ x_0 = X\lambda + D^-,\ y_0^e = Y^e\lambda - D^e,\ y_0^n = Y^n\lambda + D^n \\ D^- \geq 0, D^e \geq 0, D^n \geq 0, \lambda \geq 0 \end{cases} . \tag{8}$$

In **Eq. 8**, D^-, D^e, D^n represents the slack variable of the input, expected output, and undesired output, respectively. ρ^* indicates the target value of the Agricultural Eco-efficiency of the production decision-making units, $\rho^*\epsilon$ (0,1).

Data

The research object of this study focuses on the agricultural planting industry in a narrow sense. In order to measure the Agricultural Eco-efficiency, land, labor, machinery, irrigation water, pesticide, chemical fertilizer, agricultural film, and agricultural diesel are selected as input elements. In addition, agriculture itself has the value of ecosystem services so that agricultural carbon emissions and agricultural non-point sources are selected as undesired outputs. The specific indicator system is shown in **Table 1**.

This study conducted research on 31 provinces, municipalities, and autonomous regions in China (excluding Hong Kong, Macao, and Taiwan). The data of indicators are obtained from "China Rural Statistical Yearbook," "China Statistical Yearbook," and China's social and economic big data research platform.

RESULTS AND DISCUSSION

Overall Trends in Agricultural Eco-Efficiency

The growth trend of Agricultural Eco-efficiency is obvious; the provincial Agricultural Eco-efficiency in 2001 and 2012 is shown in **Figure 1**. From 2001 to 2019, the Agricultural Eco-efficiency showed an increased trend. The average value of Agricultural Eco-efficiency increased from 0.363 to 0.818, with a growth of 125.34%. All 31 provinces in the mainland are classified into three groups, namely, the eastern, central, and western. Overall, the provinces with higher Agricultural Eco-efficiency are mainly located in the eastern region, such as Zhejiang, Shanghai, Shandong, and Jiangsu. In 2019, the provinces mentioned above all equaled to 1. These provinces feature small agricultural output or a well-developing economy. For example, Zhejiang and Shanghai are two typical provinces with small agricultural output, and the gross domestic product (GDP) ranks at the upper level in China. In contrast, most provinces in the western region feature with low Agricultural Eco-efficiency, and these regions are characterized by a relatively high agricultural output and less developed economics. For instance, in 2001, Qinghai, Shanxi, Ningxia, and Gansu were the four provinces with lowest Agricultural Eco-efficiency. Nevertheless, the growth rate of Agricultural Eco-efficiency in the western region is faster than that in the eastern region, and there are significant differences in Agricultural Eco-efficiency among different provinces. For instance, as a typical representative of the western region, the Agricultural Eco-efficiency of Qinghai was 0.081 in 2001, while it increased to 1 in 2019.

However, it is interesting that although most regions in the western provinces had relatively low Agricultural Eco-efficiency, they were very likely to enjoy higher growth rates. Such rapid growth can be attributed to technology increase and urbanization. Due to rapid technology increase, the increase of Agricultural Eco-efficiency was generally faster than that of other regions. For example, the Agricultural Eco-efficiency of Shaanxi increased from 0.196 to 1, with an average growth rate of 21.59%. In addition, with the increased pace of urbanization, a large number of people tend to live in cities, and more machinery and equipment are put into production, which effectively improves the Agricultural Eco-efficiency.

TABLE 1 | Agricultural Eco-efficiency indicator system.

Indicator type	Indicator name	Indicator description	Unit
Input	Land input	Total sown crop area	Thousand hectares
	Machinery input	Total agricultural machinery power	10 thousand kilowatts
	Labor input	Primary industry practitioners *(total agricultural output value/total agriculture, forestry, animal husbandry, and fishery output value)	10 thousand people
	Chemical fertilizer input	Chemical fertilizer consumption	10 thousand tons
	Agricultural water input	Irrigation water consumption	Ton
	Pesticide input	Pesticide consumption	10 thousand tons
	Agricultural film input	Agricultural film consumption	10 thousand tons
Expected output	Total agricultural output value	Total agricultural output value	100 million yuan
	Ecosystem services	Ecosystem service value	10 thousand yuan
Undesired output	Agricultural carbon emissions	Total carbon emissions of chemical fertilizers, pesticides, agricultural films, agricultural diesel oil, agricultural irrigation, and agricultural sowing	The following carbon emission sources and their emission coefficients are selected: chemical fertilizer 0.8956 (kg/kg), pesticide 4.9341 (kg/kg), agricultural films 5.18 (kg/kg), diesel oil 0.5927 (kg/kg), agricultural sowing 312.6 (kg/km2), and agricultural irrigation 20.476 (kg/hm2)
	Comprehensive index of agricultural non-point source pollution	Calculated by the entropy method	—

There is a U-shaped change trend between the Agricultural Eco-efficiency and the total output value of agriculture, forestry, animal husbandry, and fishery. In other words, the provinces with the total output value of agriculture, forestry, animal husbandry, and fishery in the low range and high range enjoy higher Agricultural Eco-efficiency. For example, the total output value of agriculture, forestry, animal husbandry, and fishery in Zhejiang, Xinjiang, and Tibet is in the low range, and their Agricultural Eco-efficiency values in 2019 were all 1. Similarly, Shandong, Jiangsu, and other provinces are the regions with a high range of the total output value of agriculture, forestry, animal husbandry, and fishery, and their Agricultural Eco-efficiency all equaled to 1.

Provincial Agricultural Eco-efficiency Inequality

We also measure the provincial Agricultural Eco-efficiency inequality in **Figure 2**, and it can be found that Agricultural Eco-efficiency inequality declines with the growth of economics in China. At the provincial level, Agricultural Eco-efficiency inequality could be divided into three tiers. The first tier is the provinces with the Agricultural Eco-efficiency of 1, including Beijing, Shanghai, Hainan, and Tibet; these provinces featured with low agricultural output or high gross domestic production from 2001–2019, and the Agricultural Eco-efficiency of these four provinces was equal to 1. The second tier is the regions that did

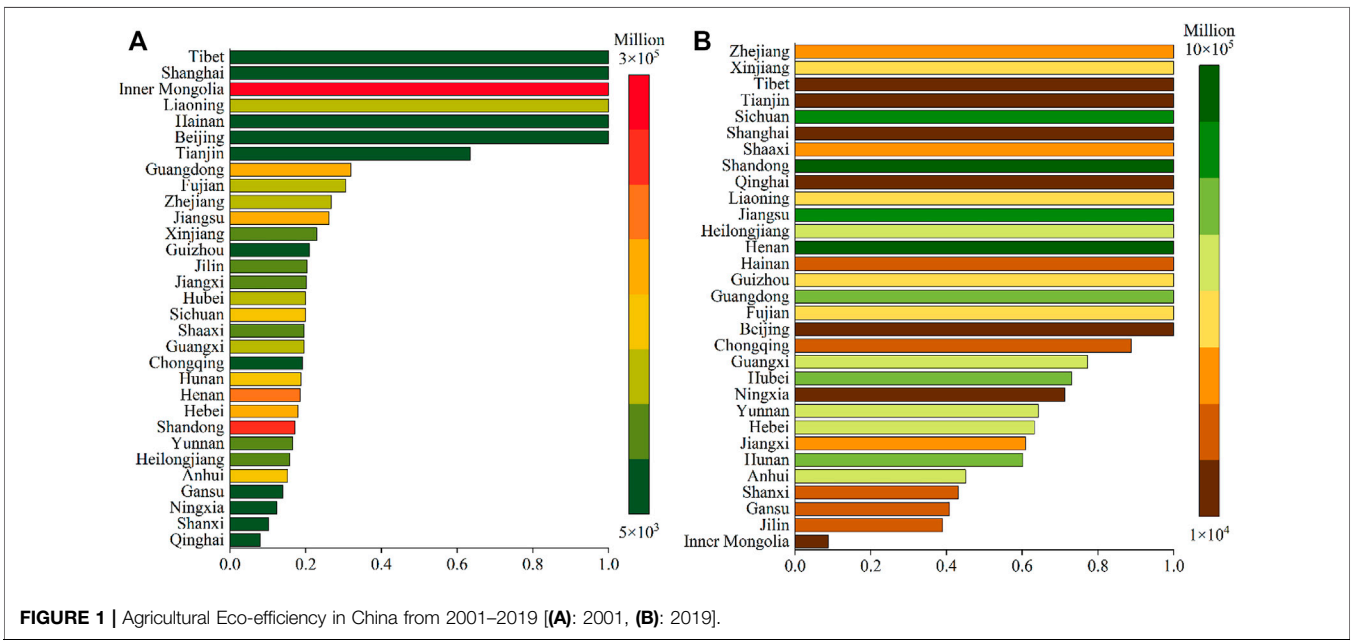

FIGURE 1 | Agricultural Eco-efficiency in China from 2001–2019 [**(A)**: 2001, **(B)**: 2019].

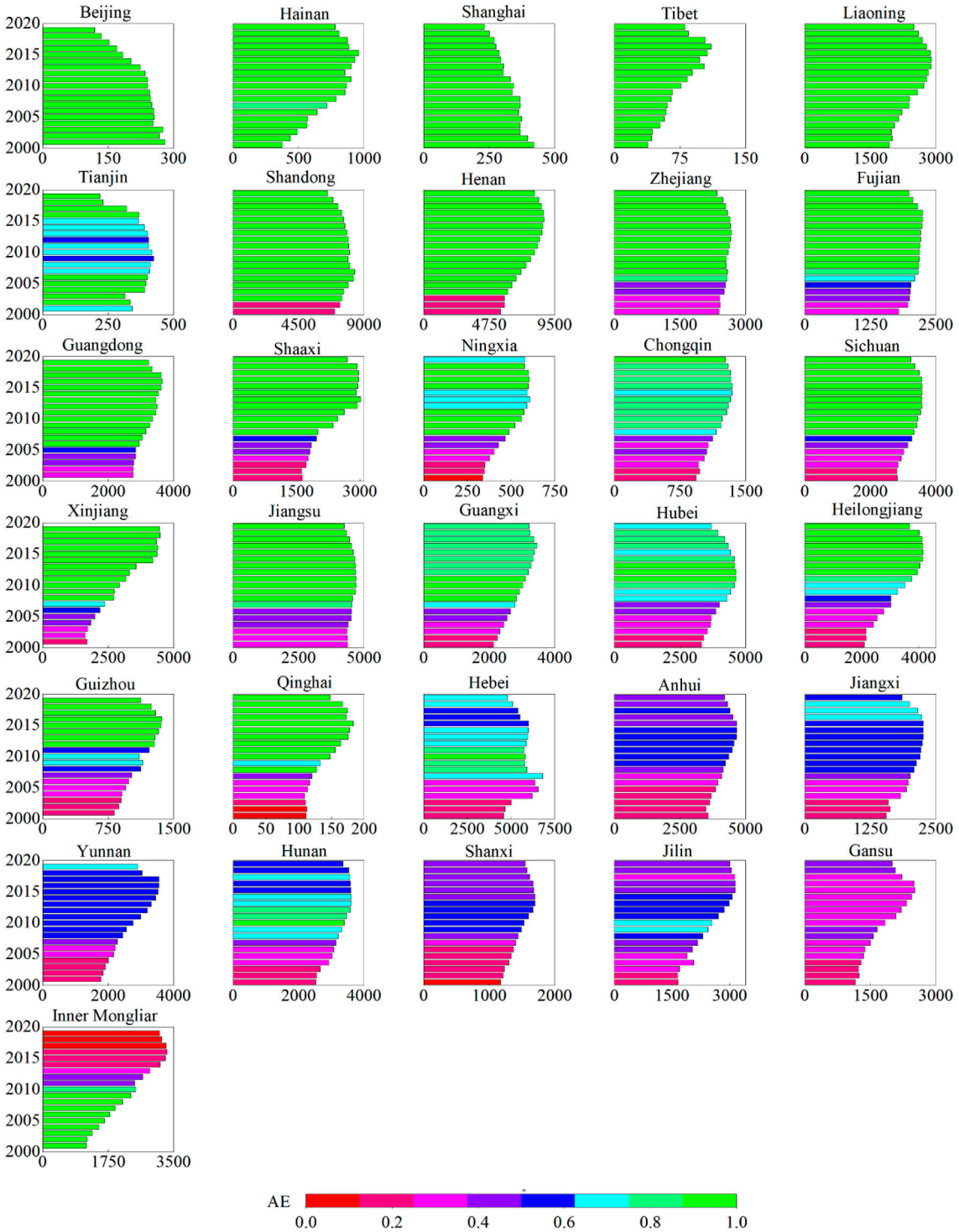

FIGURE 2 | Agricultural Eco-efficiency in different provinces from 2001–2019.

not start with an Agricultural Eco-efficiency of 1, but reached 1 in 2019, including 14 provinces. Many of these provinces are China's main grain producing areas, such as Shandong and Henan. This shows that with the implementation of China's ecological civilization construction, agricultural green development has become the mainstream of development, and Agricultural Eco-efficiency inequality between provinces is gradually decreasing. The third tier is provinces that have consistently failed to achieve an Agricultural Eco-efficiency of 1, such as Shanxi, Jilin, Gansu, and Inner Mongolia. These

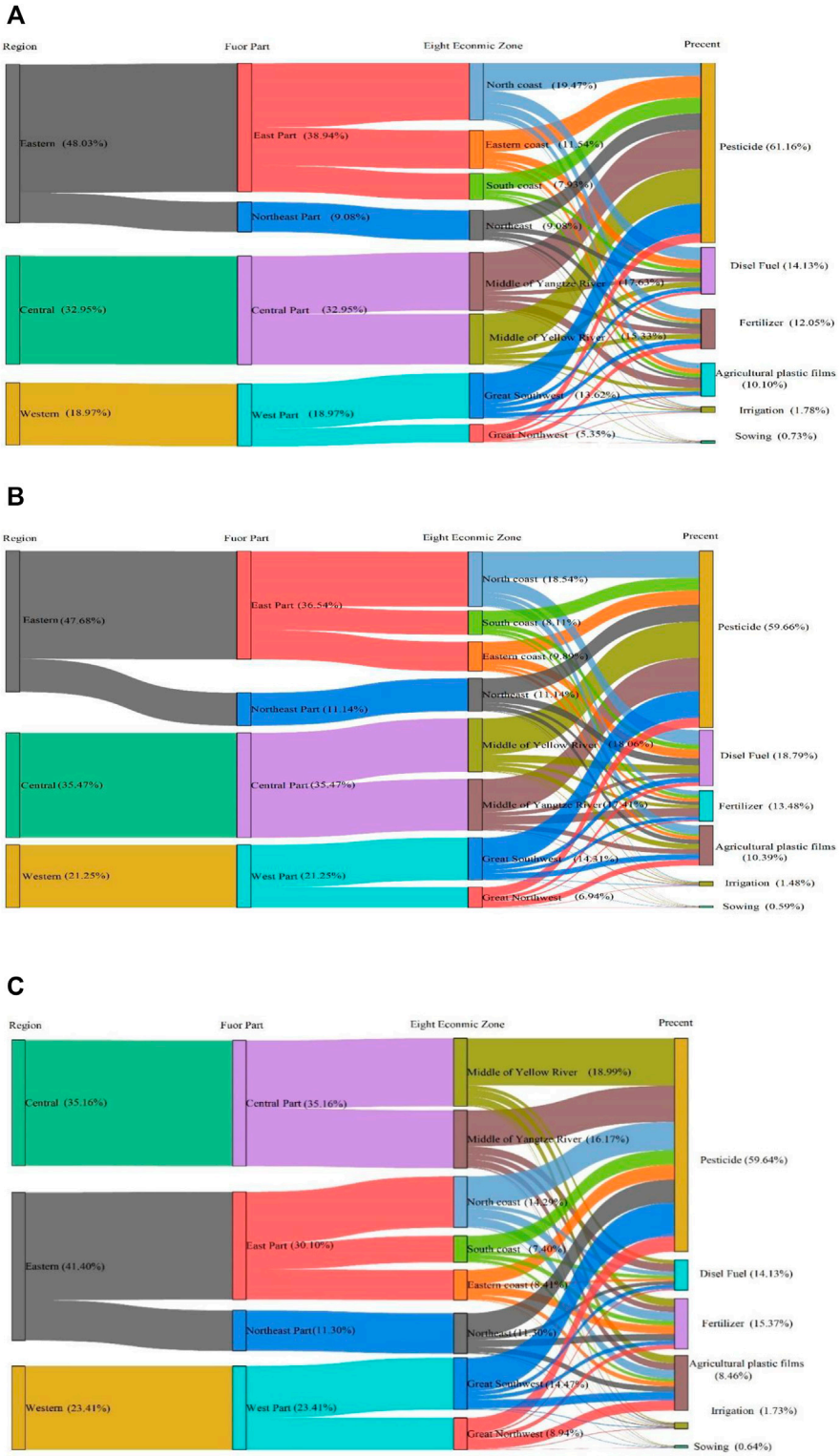

FIGURE 3 | Agricultural Carbon Emission Flow from 2001–2019 [**(A)**: 2001, **(B)**: 2010, **(C)**: 2019].

provinces are characterized with less developed economics. From 2001–2019, Agricultural Eco-efficiency inequality declined; to increase Agricultural Eco-efficiency, appropriate reduction measures should be taken by encouraging low-carbon and low–non-point source pollution production style. For instance, reduced fertilizer and pesticide use could influence Agricultural eco-efficiency inequality.

Drivers of Agricultural Eco-efficiency Inequality

The influencing factors of Agricultural Eco-efficiency inequality could date back to the source of undesired outputs. In **Figure 3**, pesticide, diesel fuel, fertilizer, agricultural plastic films, irrigation, and sowing are the main undesired output sources. The main source of carbon dioxide emitted during agricultural production was pesticides. In 2019, carbon dioxide from the pesticides accounted for 59.64% of total emissions, followed by fertilizer (15.37%), diesel fuel (14.13%), agricultural plastic films (8.46%), irrigation (1.73%), and sowing (0.64%). From the perspective of major carbon dioxide emission regions, provinces in the eastern region emitted the highest level of carbon dioxide, accounting for 41.40% in 2019, followed by the central (35.16%) and the western (23.41%) regions. In view of the distribution of the four major parts and the eight major economic zones, the eastern is divided into the east part and northeast part. The east part accounted for 30.10% of carbon dioxide emissions and the northeast part occupied 11.30%. Among the eight major economic zones, the middle reaches of Yellow River took up the highest carbon dioxide emissions, reaching 18.99%. This is closely linked to the important agricultural production bases in this economic zone such as Henan, Shandong, and other provinces. The economic zone that ranked second in terms of emissions was the middle reaches of Yangtze River (16.17%), which fully confirms that the Yellow River Basin and the Yangtze River Basin are the main agricultural planting areas in China. Such performance of agricultural carbon emission was primarily due to increase of planting area. With the implementation of the green development strategy, the agricultural carbon emissions are expected to decrease.

In terms of time and space, the proportion of carbon dioxide emitted by agricultural production has decreased in the eastern region and the share in the Central and Western regions has increased. From the perspective of spatial change, from 2001 to 2019, carbon emissions in the eastern region showed a downward trend, from 48.03% in 2001 to 47.68% in 2010 and 41.4% in 2019, with a decrease of 6.63%. Specifically, the main reason for the change was the decline in the east part, especially due to the rapid urbanization of the eastern provinces, such as Beijing and Shanghai, which has caused part of the agricultural land to be replaced by urban land. What is more special is that the percentage of carbon emissions in the northeast part has shown an increasing trend, increasing by 2.22% from 2001 to 2019, mainly caused by the use of pesticides and machinery in northeast China. In addition, the shares of agricultural carbon emissions in the central and west part have shown an increasing trend, with 32.95%–35.16% in the central and 18.97%–23.41% in the western region.

To achieve carbon neutrality, the Chinese government should pay more attention to agriculture, especially for Agricultural Eco-efficiency. National Agricultural Eco-efficiency increased by 125.34% from 2001 to 2019, and all provinces experienced rapid growth. Due to the implementation of green development policy and urbanization, Agricultural Eco-efficiency inequality is expected to decrease in China, and great efforts should be paid to deal with this problem in the future.

Our results highlight the influencing factors affecting Agricultural Eco-efficiency. The eastern region always enjoys high Agricultural Eco-efficiency; in 2001, Agricultural Eco-efficiency in Shanghai was 12.35 times higher than that of Qinghai, also characterized with low agricultural output. The Agricultural Eco-efficiency will exist for a very long time in China, the green development strategy will give an opportunity for sustainable agricultural development, and the technology development of the central and western regions will be very useful to bridge the gap. Furthermore, compared with the eastern region, the middle reaches of Yellow River and middle reaches of Yangtze River have great potential in reducing carbon emissions. The output of grain and meat in the Yellow River Basin accounts for one-third of the country's output, and the Yangtze River Basin is a land of fish and rice in China. The grain produced in the Yellow River Basin and the Yangtze River Basin accounts for more than 60% of the country's production. Therefore, taking these two regions as key emission reduction regions will be significant to agricultural eco-efficiency improvement.

POLICY IMPLICATIONS

Given the outputs of agriculture, the government should focus on guiding the planting type. The changing planting type should join the government and farmer together. For the government, a more greener planting guide should be given. A model of agricultural development in harmony with nature, such as combining planting and raising, intensive farming, and using land for cultivation, should be formed. Focusing on the adaptation of the development of the planting and breeding industry to the carrying capacity of the resources and environment, efforts should be taken to solve the outstanding problems of the dirty, chaotic, and poor rural environment, such as reducing livestock manure, crop stalks, and other planting and breeding wastes. According to the cyclical development concept of "planting industry drives breeding industry; breeding industry promotes planting industry," taking local consumption, energy recycling, and comprehensive utilization as the main line and considering equal emphasis on economic, ecological, and social benefits as the guide, the operation mode of government support, enterprise operation, social participation, and promotion of the whole county should be adopted to build a coordinated development model of planting and breeding that combines intensive, standardization, organization, and socialization. In addition, it is necessary to explore comprehensive and overall solutions for waste recycling of the planting and breeding industry in typical counties, and form a long-term mechanism of county-rural enterprise linkage and construction management operation, so as to effectively prevent

and control agricultural non-point source pollution, improve the efficiency of agricultural resource utilization, promote the transformation of agricultural development mode, and boost sustainable agricultural development.

It is necessary to continue to reduce the use of chemical fertilizers and pesticides and increase their efficiency. On the one hand, the government should further promote the development of soil testing, formula fertilization, unified control of crop diseases and insect pests, and whole-process green prevention and control and improve farmers' awareness and skills of scientific fertilization and pesticide use, thus reducing the use of fertilizers and pesticides. On the other hand, it is also important to integrate and promote green and efficient technologies, such as deep application of chemical fertilizers by machinery, simultaneous sowing of fertilizer and integration of water and fertilizer, and applying green prevention and control technologies such as ecological regulation, biological control, and physical and chemical control. In addition, quality standards for agricultural inputs, such as chemical fertilizers and pesticides, should be revised and strictly implemented so as to strictly control the use of high-toxicity and high-risk pesticides and develop and promote new products and advanced fertilization and application machinery, such as high-efficiency and slow-controlled release fertilizers; high-efficiency, low-toxicity, and low-residue pesticides; and biological fertilizers and pesticides.

CONCLUDING REMARKS

Carbon neutrality is not a constraint on economic growth but an important source of China's total factor productivity growth. It will promote rapid changes in China's economic growth momentum and growth model in the new development stage. These carbon node industries include both production-oriented industries and consumer-oriented industries, which are not completely overlapped with traditional high-energy consuming industries. The core of agricultural emission peaking and carbon neutrality is to promote the transformation of the agricultural development mode to a comprehensive green and low-carbon mode. The results show that the provinces in the central and western region had a low value of Agricultural Eco-efficiency in China, and the middle reaches of Yellow River is the key zone of carbon emissions and non-point source pollution control, so it is necessary to effectively improve agriculture based on the improvement of Agricultural Eco-efficiency. Agriculture, as a basic industry, plays an important role in the whole socioeconomic development. In the process of supporting agricultural development, agriculture will produce "desirable" products, such as grain, fruit, and other products, and "undesirable" outputs, such as greenhouse gases, such as carbon dioxide, methane, and nitrogen dioxide. Taking these undesired factors into account in agricultural production is of great significance to accurately quantify agricultural inputs and outputs and provide important parameters for the next step of promoting greener Chinese agriculture.

Although our study produced some informative findings, there still exist some limitations of this study. This study focuses on agricultural planting, innovatively taking agricultural ecosystem services as expected outputs, and considering carbon emissions and non-point source pollution as undesired outputs. However, agriculture will also produce undesired outputs, such as methane and nitrous oxide, which will be introduced into our research as new variables in the future.

DATA AVAILABILITY STATEMENT

The raw data supporting the conclusion of this article will be made available by the authors, without undue reservation.

AUTHOR CONTRIBUTIONS

LM and JH conceived the study and wrote the manuscript. GW and ZQ analyzed data for figures and table. All authors contributed to manuscript development and edited the final version.

FUNDING

This study was supported by funding from the National Science Foundation of China (72003111) and the Strategic Priority Research Program of Chinese Academy of Sciences, (Grant No. XDA23070400).

REFERENCES

Abid, M., Scheffran, J., Schneider, U. A., and Elahi, E. (2019). Farmer Perceptions of Climate Change, Observed Trends and Adaptation of Agriculture in Pakistan. *Environ. Manage.* 63, 110–123. doi:10.1007/s00267-018-1113-7

Bai, H., and Tao, F. (2017). Sustainable Intensification Options to Improve Yield Potential and Eco-Efficiency for rice-wheat Rotation System in China. *Field Crops Res.* 211, 89–105. doi:10.1016/j.fcr.2017.06.010

Baležentis, T., Li, T., Streimikiene, D., and Baležentis, A. (2016). Is the Lithuanian Economy Approaching the Goals of Sustainable Energy and Climate Change Mitigation? Evidence from DEA-Based Environmental Performance Index. *J. Clean. Prod.* 116, 23–31. doi:10.1016/j.jclepro.2015.12.088

Baum, R., and Bieńkowski, J. (2020). Eco-Efficiency in Measuring the Sustainable Production of Agricultural Crops. *Sustainability* 12, 1418. doi:10.3390/su12041418

Charnes, A., Cooper, W. W., and Rhodes, E. (1978). Measuring the Efficiency of Decision Making Units. *Eur. J. Oper. Res.* 2, 429–444. doi:10.1016/0377-2217(78)90138-8

Chen, R., Zhang, R., Han, H., and Jiang, Z. (2020). Is Farmers' Agricultural Production a Carbon Sink or Source? - Variable System Boundary and Household Survey Data. *J. Clean. Prod.* 266, 122108. doi:10.1016/j.jclepro.2020.122108

Chen, X., Liu, X., Gong, Z., and Xie, J. (2021). Three-stage Super-efficiency DEA Models Based on the Cooperative Game and its Application on the R&D green Innovation of the Chinese High-Tech Industry. *Comput. Ind. Eng.* 156, 107234. doi:10.1016/j.cie.2021.107234

Coelli, T., and Rao, P. (2012). Assessing the Welfare Effects of Microfinance in Vietnam: Empirical Results from a Quasi-Experimental Survey. *J. Dev. Stud.* 48, 619–632. doi:10.1080/00220388.2011.638051

Costa, M. P., Schoeneboom, J. C., Oliveira, S. A., Viñas, R. S., and de Medeiros, G. A. (2018). A Socio-Eco-Efficiency Analysis of Integrated and Non-integrated Crop-Livestock-Forestry Systems in the Brazilian Cerrado Based on LCA. *J. Clean. Prod.* 171, 1460–1471. doi:10.1016/j.jclepro.2017.10.063

Czyżewski, B., Matuszczak, A., Grzelak, A., Guth, M., and Majchrzak, A. (2021). Environmental Sustainable Value in Agriculture Revisited: How Does Common Agricultural Policy Contribute to Eco-Efficiency? *Sustain. Sci.* 16, 137–152. doi:10.1007/s11625-020-00834-6

Deng, X., and Gibson, J. (2019). Improving Eco-Efficiency for the Sustainable Agricultural Production: A Case Study in Shandong, China. *Technol. Forecast. Soc. Change* 144, 394–400. doi:10.1016/j.techfore.2018.01.027

Elahi, E., Khalid, Z., and Weijun, C. (2020). The Public Policy of Agricultural Land Allotment to Agrarians and its Impact on Crop Productivity in Punjab Province of Pakistan. *Land Use Pol.* 90, 104324. doi:10.1016/j.landusepol.2019.104324

Elahi, E., Khalid, Z., Tauni, M. Z., Zhang, H., and Lirong, X. (2021a). Extreme Weather Events Risk to Crop-Production and the Adaptation of Innovative Management Strategies to Mitigate the Risk: A Retrospective Survey of Rural Punjab, Pakistan. *Technovation* 4, 102255. doi:10.1016/j.technovation.2021.102255

Elahi, E., Weijun, C., Jha, S. K., and Zhang, H. (2019b2019b). Estimation of Realistic Renewable and Non-renewable Energy Use Targets for Livestock Production Systems Utilising an Artificial Neural Network Method: A Step towards Livestock Sustainability. *Energy* 183 (Sep.15), 191–204. doi:10.1016/j.energy.2019.06.084

Elahi, E., Weijun, C., Zhang, H., and Abid, M. (2019a2019a). Use of Artificial Neural Networks to rescue Agrochemical-Based Health Hazards: A Resource Optimisation Method for Cleaner Crop Production. *J. Clean. Prod.* 238, 117900. doi:10.1016/j.jclepro.2019.117900

Elahi, E., Zhang, H., Lirong, X., Khalid, Z., and Xu, H. (2021b). Understanding Cognitive and Socio-Psychological Factors Determining Farmers' Intentions to Use Improved Grassland: Implications of Land Use Policy for Sustainable Pasture Production. *Land Use Policy* 102, 105250. doi:10.1016/j.landusepol.2020.105250

Fridrihsone, A., Romagnoli, F., and Cabulis, U. (2020). Environmental Life Cycle Assessment of Rapeseed and Rapeseed Oil Produced in Northern Europe: A Latvian Case Study. *Sustainability* 12, 5699. doi:10.3390/su12145699

Gołaś, M., Sulewski, P., Wąs, A., Kłoczko-Gajewska, A., and Pogodzińska, K. (2020). On the Way to Sustainable Agriculture-Eco-Efficiency of Polish Commercial Farms. *Agriculture* 10, 438. doi:10.3390/agriculture10100438

Guo, B., He, D., Zhao, X., Zhang, Z., and Dong, Y. (2020). Analysis on the Spatiotemporal Patterns and Driving Mechanisms of China's Agricultural Production Efficiency from 2000 to 2015. *Phys. Chem. Earth, Parts A/B/C* 120, 102909. doi:10.1016/j.pce.2020.102909

Han, H., Zhong, Z., Wen, C., and Sun, H. (2018). Agricultural Environmental Total Factor Productivity in China under Technological Heterogeneity: Characteristics and Determinants. *Environ. Sci. Pollut. Res.* 25, 32096–32111. doi:10.1007/s11356-018-3142-4

Holka, M. (2020). Assessment of Carbon Footprint and Life Cycle Costs of Winter Wheat (Triticum Aestivum L.) Production in Different Soil Tillage Systems. *Appl. Ecol. Env. Res.* 18, 5841–5855. doi:10.15666/aeer/1804_58415855

Ji, H., and Hoti, A. (2021). Green Economy Based Perspective of Low-Carbon Agriculture Growth for Total Factor Energy Efficiency Improvement. *Int. J. Syst. Assur. Eng. Manag.* doi:10.1007/s13198-021-01421-3

Ke, Y., Rusong, W., Chuanbin, Z., and Jing, L. (2012). Review of Eco-Efficiency Accounting Method and its Applications. *Acta Eco Sin* 32, 3595–3605. doi:10.5846/stxb201104280564

Li, Z., Sarwar, S., and Jin, T. (2021). Spatiotemporal Evolution and Improvement Potential of Agricultural Eco-Efficiency in Jiangsu Province. *Front. Energ. Res.* 9, 2021040431. doi:10.3389/fenrg.2021.746405

Liu, J., Jin, X., Xu, W., Gu, Z., Yang, X., Ren, J., et al. (2020). A New Framework of Land Use Efficiency for the Coordination Among Food, Economy and Ecology in Regional Development. *Sci. Total Environ.* 710, 135670. doi:10.1016/j.scitotenv.2019.135670

Liu, W. (2019). The Data Source of This Study Is Web of Science Core Collection? Not Enough. *Scientometrics* 121, 1815–1824. doi:10.1007/s11192-019-03238-1

Llinàs, F. O., Tello Aragay, E., Murray Mas, I., Jover-Avellà, G., and Marull López, J. (2021). Socio-Ecological Transition in a Mediterranean Agroecosystem: What Energy Flows Tell Us about Agricultural Landscapes Ruled by Landlords, Peasants and Tourism (Mallorca, 1860-1956-2012). *Ecol. Econ.* 190, 107206. doi:10.1016/j.ecolecon.2021.107206

Lwin, C. M., Nogi, A., and Hashimoto, S. (2017). Eco-Efficiency Assessment of Material Use: The Case of Phosphorus Fertilizer Usage in Japan's Rice Sector. *Sustainability* 9, 1562. doi:10.3390/su9091562

Magarey, R. D., Klammer, S. S., Chappell, T. M., Trexler, C. M., Pallipparambil, G. R., and Hain, E. F. (2019). Eco-efficiency as a Strategy for Optimizing the Sustainability of Pest Management. *Pest Manag. Sci.* 75, 3129–3134. doi:10.1002/ps.5560

Gava, O., Bartolini, F., Venturi, F., Brunori, G., and Pardossi, A. (2020). Improving Policy Evidence Base for Agricultural Sustainability and Food Security: A Content Analysis of Life Cycle Assessment Research. *Sustainability* 12 (3), 1033. doi:10.3390/su12031033

Pang, J., Chen, X., Zhang, Z., and Li, H. (2016). Measuring Eco-Efficiency of Agriculture in China. *Sustainability* 8, 398. doi:10.3390/su8040398

Qu, Y., Lyu, X., Peng, W., and Xin, Z. (2021). How to Evaluate the Green Utilization Efficiency of Cultivated Land in a Farming Household? A Case Study of Shandong Province, China. *Land* 10, 789. doi:10.3390/land10080789

Reith, C. C., and Guidry, M. J. (2003). Eco-Efficiency Analysis of an Agricultural Research Complex. *J. Environ. Manage.* 68, 219–229. doi:10.1016/S0301-4797(02)00161-5

Soteriades, A. D., Stott, A. W., Moreau, S., Charroin, T., Blanchard, M., Liu, J., et al. (2016). The Relationship of Dairy Farm Eco-Efficiency with Intensification and Self-Sufficiency. Evidence from the French Dairy Sector Using Life Cycle Analysis, Data Envelopment Analysis and Partial Least Squares Structural Equation Modelling. *Plos One* 11, e0166445. doi:10.1371/journal.pone.0166445

Todorović, M., Mehmeti, A., and Cantore, V. (2018). Impact of Different Water and Nitrogen Inputs on the Eco-Efficiency of Durum Wheat Cultivation in Mediterranean Environments. *J. Clean. Prod.* 183, 1276–1288. doi:10.1016/j.jclepro.2018.02.200

Tone, K., and Tsutsui, M. (2009). Network DEA: A Slacks-Based Measure Approach. *Eur. J. Oper. Res.* 197, 243–252. doi:10.1016/j.ejor.2008.05.027

Van, T., Elahi, E., and Zhang, L. (2019). Historical Perspective of Climate Change in Sustainable Livelihoods of Coastal Areas of the Red River Delta, Nam Dinh, Vietnam. *Int. J. Clim. Chang Str* 11 (5), 687–695. doi:10.1108/IJCCSM-02-2018-0016

Wackernagel, M., and Galli, A. (2007). An Overview on Ecological Footprint and Sustainable Development: A Chat with Mathis Wackernagel. *Int. J. Eco* 2, 1–9. doi:10.2495/ECO-V2-N1-1-9

Wang, Y., and Zhao, G. (2021). A Joint Use of Life Cycle Assessment and Emergy Analysis for Sustainability Evaluation of an Intensive Agro-System in China. *Environ. Dev. Sustain.* 17 (12), 2822–2835. doi:10.1007/s10668-021-01929-5

Zeng, L., Li, X., and Ruiz-Menjivar, J. (2020). The Effect of Crop Diversity on Agricultural Eco-Efficiency in China: A Blessing or a Curse? *J. Clean. Prod.* 276, 124243. doi:10.1016/j.jclepro.2020.124243

Zhao, X., Zhang, X., Li, N., Shao, S., and Geng, Y. (2017). Decoupling Economic Growth from Carbon Dioxide Emissions in China: A Sectoral Factor Decomposition Analysis. *J. Clean. Prod.* 142, 3500–3516. doi:10.1016/j.jclepro.2016.10.117

Zhong, Z., Peng, B., Xu, L., Andrews, A., and Elahi, E. (2020). Analysis of Regional Energy Economic Efficiency and its Influencing Factors: A Case Study of Yangtze River Urban Agglomeration. *Sustainable Energ. Tech. Assessments* 41 (7–9), 100784. doi:10.1016/j.seta.2020.100784

Conflict of Interest: The authors declare that the research was conducted in the absence of any commercial or financial relationships that could be construed as a potential conflict of interest.

Publisher's Note: All claims expressed in this article are solely those of the authors and do not necessarily represent those of their affiliated organizations, or those of the publisher, the editors, and the reviewers. Any product that may be evaluated in this article, or claim that may be made by its manufacturer, is not guaranteed or endorsed by the publisher.

frontiers in Ecology and Evolution

ORIGINAL RESEARCH
published: 11 March 2022
doi: 10.3389/fevo.2022.844437

Integrating Landscape Connectivity and Natural-Anthropogenic Interaction to Understand Karst Vegetation Restoration: A Case Study of Guizhou Province, China

Kexin Huang[1,2], Li Peng[1,2], Xiaohui Wang[1,2] and Tiantian Chen[3]*

[1] College of Geography and Resources, Sichuan Normal University, Chengdu, China, [2] Key Laboratory of Land Resources Evaluation and Monitoring in Southwest, Ministry of Education, Sichuan Normal University, Chengdu, China, [3] College of Geography and Tourism, Chongqing Normal University, Chongqing, China

OPEN ACCESS

Edited by:
Jinyan Zhan,
Beijing Normal University, China

Reviewed by:
Qiuwen Zhou,
Guizhou Normal University, China
Miaomiao Xie,
China University of Geosciences, China

***Correspondence:**
Li Peng
pengli@imde.ac.cn

Specialty section:
This article was submitted to Conservation and Restoration Ecology, a section of the journal Frontiers in Ecology and Evolution

Received: *28 December 2021*
Accepted: *31 January 2022*
Published: *11 March 2022*

Citation:
Huang K, Peng L, Wang X and Chen T (2022) Integrating Landscape Connectivity and Natural-Anthropogenic Interaction to Understand Karst Vegetation Restoration: A Case Study of Guizhou Province, China. Front. Ecol. Evol. 10:844437. doi: 10.3389/fevo.2022.844437

Because of implementation of ecological projects, the restoration of vegetation not only changes the typological composition and spatial structure of the landscape, but also improves the regional ecosystem function. The present study considered the effects of natural-anthropogenic factors and landscape connectivity on vegetation restoration. It also explored the impact and underlying mechanisms by which structural changes in landscape connectivity affect vegetation coverage in the karst region of Guizhou Province and provided a novel perspective for the maintenance of regional ecological security. We used morphological spatial pattern analysis (MSPA) and integrated valuation of ecosystem services and tradeoffs (InVEST) and circuit theory to identify ecological networks and explore the changes in landscape structure. We performed a Theil-Sen Median trend analysis and a Mann-Kendall (MK) trend test to determine spatiotemporal variations in vegetation coverage. We conducted a coupling analysis to discover correlations between the average cumulative current density (CCD) and the normalized difference vegetation index (NDVI) in various karst landform counties. We also implemented a geographical detector to detect the factors affecting the NDVI trend and disclose interactions among factors. The results showed that (1) Though the total area of forests and core areas was reduced, the ecological networks and landscape connectivity steadily improved. (2) Areas with improved vegetation coverage accounted for 77.77% of the total. By contrast, the degraded areas covered 14.28% while the remaining 7.95% was stable. (3) The relationships between the average CCD and the NDVI were inconsistent among various geomorphological counties. The counties with the highest proportions of karst landforms presented with negative correlations between the average CCD and the NDVI in 2005 and positive correlations between these parameters in 2018. (4) The NDVI trend was influenced by several factors. Of these, anthropogenic activity played a dominant role. Nevertheless, changes in landscape connectivity was also implicated. Attention should be paid to the impact of landscape connectivity on ecological restoration. The foregoing results indicated that the

rocky desertification projects effectively improved landscape connectivity and vegetation coverage and provided a reference for developing policies establishing and maintaining ecological security of the karst ecosystem and coordinating sustainable development in this region.

Keywords: circuit theory, ecological network, geographical detector, Guizhou Province, landscape connectivity, karst vegetation restoration

INTRODUCTION

Vegetation comprises the hub of material circulation and energy exchange in ecosystems and prevents ecological degradation. Elucidating the spatiotemporal patterns in vegetation cover and the impact of climate change and human activity on it helps clarify the effects of ecosystem restoration and facilitates the sustainable development of terrestrial ecosystems (Peng et al., 2021). The normalized difference vegetation index (NDVI) is commonly used in remote sensing estimation of vegetation coverage (Lagomasino et al., 2015). It comprehensively reflects vegetation type (Zhang et al., 2013), growth status, and coverage density in an observation area. Thus, it is widely used in the dynamic monitoring of vegetation coverage (Zhu et al., 2019). The NDVI time series data are used to study variations in vegetation and their response to external disturbances, which is of great value in identifying the ecological benefits of the ecosystem and is very important in global change research.

Patch corridor matrix model can be used to describe landscape structure heterogeneity and reflect the landscape pattern (Forman and Wilson, 1995), which helps clarify landscape structure, function, and dynamic change (Feyissa and Gebremariam, 2018). Landscape connectivity describes the connections among landscape elements within a spatial pattern or ecological process (Uroy et al., 2019), and this connection may be species or gene flow between biological communities or the exchange of materials and energy between landscape elements (Forman and Godron, 1986; Taylor et al., 1993). It also lays theoretical and empirical foundations for elucidating the relationships among spatial patterns and for ecological network planning (An et al., 2021). It usually comprises both structural and functional connectivity (Tischendorf and Fahrig, 2000). Structural connectivity measures the structural characteristics of the landscape such as its size, shape, and habitat patch locations. It reflects the spatial pattern of the physical connections among landscape patches, but does not consider ecological processes (Carlier and Moran, 2019). Functional connectivity is based on the biological and ecological processes among patches determined by observation, experimentation, and model predictions (Salgueiro et al., 2021). The regional landscape structure may be reconstructed by restoring existing (Williams and Baker, 2012) or introducing new landscape elements (Haider et al., 2016), adjusting their spatial configuration, and enhancing landscape connectivity (Dondina et al., 2018). In this manner, the security of the regional landscape pattern is established and maintained. Several tools are available to depict landscape connectivity. Carlier and Moran (2019) used morphological spatial pattern analysis (MSPA) for the comprehensive description of the structural connectivity among linear and spatial habitats. Dai et al. (2021) combined Minimum Cumulative Resistance (MCR) and Duranton and Overman Index (DOI) models to identify ecological networks and maintain landscape connectivity. Circuit theory identifies ecological networks by assigning different degrees of significance to various physical variables. It integrates the strengths of the random walking and graph theories (McRae, 2006). Gao J. et al. (2021) integrated ecosystem services and the circuit theory to portray landscape connectivity and identify karst ecological networks. An et al. (2021) took both structural connectivity and functional connectivity into consideration, using the integrative method of MSPA and circuit theory to construct and optimize the ecological networks, which has greater ecological significance.

LeGrand (1973) first paid attention to the ecological problems in karst regions. Guizhou Province is typical and representative of the karst area in Southwestern China (Tian et al., 2017). Karstification and high intensity development and construction make the phenomenon of landscape isolation in karst region increasingly serious (Peng et al., 2018). Rocky desertification impoverishes ecosystems, destroys natural habitats, and impedes regional sustainable development (Huang et al., 2010). With the decrease of the connectivity of multiple landscape patches, the free migration of species and the normal ecological circulation process of landscape were hindered. Since the onset of the 21st century, several large-scale ecological protection and construction projects have been initiated in China and have achieved positive results. In Guizhou Province, the long-term rocky desertification project has involved extensive tree planting and afforestation and has significantly increased forest and grass coverage (Liao et al., 2018). Nevertheless, it is also necessary to determine the changes in landscape structure caused by these projects and assess the impact that these modifications have on ecosystem function. Prior studies on karst regions mainly evaluated the impact of vegetation restoration from the perspective of climate change and human activity and confirmed that anthropogenic factors play major roles (Cai et al., 2014; Peng et al., 2021). However, the landscape pattern strongly influences landscape function and ecological processes (Pausas, 2003). Hence, it is necessary to consider its impact on variations in vegetation from the perspective of landscape connectivity.

The ecological restoration project has been implemented in Guizhou Province since approximately 2,000. However, vegetation may have to pass through several succession stages until its ecological function is optimized. For this reason, the present study was initiated in 2005. The ecological networks were mapped according to the patch corridor matrix model using MSPA and the integrated valuation of ecosystem services

and tradeoffs (InVEST) and circuit theory models. Based on MODIS NDVI data, the spatiotemporal pattern of vegetation coverage and the stability of ecosystem functions was analyzed by Theil-Sen trend analysis and the Mann-Kendall (MK) trend test. Correlations between the average cumulative current density (CCD) and the normalized difference vegetation index (NDVI) in various karst counties were evaluated. The factors and their interactions influencing the NDVI trends were revealed with geographical detectors. This study aims to clarify the mechanisms by which the karst areas in Guizhou Province respond to changes in landscape connectivity. Additionally, it will present evidence of the efficacy of the ecological restoration projects in these regions.

MATERIALS AND METHODS

Study Area

Guizhou Province is in the eastern part of the Yunnan-Kweichow Plateau in the karst region of Southwestern China (24°37′–29°13′N, 103°36′–109°35′E) (**Figure 1**). Its total area is 17.62×10^4 km^2 of which ∼70% is karst. The regional climate is subtropical humid monsoon. The average annual temperature is 10–18°C and the annual precipitation is 1,000–1,500 mm. Carbonate rocks are widely distributed in Guizhou Province. The ecosystem structure is complex, the spatial heterogeneity and ecological sensitivity are high, the environmental capacity is low, and the habitat is fragile. Guizhou is the only province in China lacking plains. Its average elevation is ∼1,100 m. Plateaus and mountains account for ∼87% of the total area. Long-term human activity has intensified rocky desertification there. Guizhou Province has been the focus of national rocky desertification and ecological restoration projects since 2000.

Data Source

The datasets used in this study included land use data for 2005 and 2018, a digital elevation model (DEM), and ground meteorological data derived from the Resources and Environmental Science and Data Center of the Chinese Academy of Sciences.[1] The annual mean precipitation and temperature data were obtained from the China Surface Climatic Data Daily Dataset (v. 3.0) of the National Meteorological Science Data Center[2] and were calculated by inverse distance weighting (IDW) interpolation. The NDVI data were obtained using the MOD13Q1 product of the Land Processes Distributed Active Archive Center of NASA.[3] The MODIS reprojection tool (MRT[4]) was used to extract the NDVI data and convert them to a raster file. ArcGIS 10.4 software was used to obtain the largest NDVI per pixel per year and the NDVI of each county-level administrative region. County-level afforestation data were acquired from the China Forestry and Grassland Statistical Yearbook.[5] Socioeconomic data were procured from the Guizhou Statistical Yearbook.[6] The research framework is shown in **Figure 2**.

Identification of Core Area Patches by the Morphological Spatial Pattern Analysis Method

Morphological spatial pattern analysis is a classification processing method based on mathematical morphology. It analyzes the topological relationship of an image at the pixel level. MSPA divides the pixels of a binary image into seven mutually exclusive landscape elements (Soille and Vogt, 2009). Using the MSPA method to extract ecological patches requires no indicator selection or complex data processing.

Forestland coverage accounts for ∼53% of the total area in Guizhou Province. Areas with relatively less human disturbance are primarily mosaic communities dominated by forests. The ecological function of forestland is greater than that of other vegetation communities and thus partially determines the state of the entire ecosystem. For the restoration and reconstruction of karst regions, although other biological and engineering measures also play a certain role in ecological regulation, it is difficult to overcome the main contradiction that leads to the degradation of karst ecosystems, that is, the problem of water conservation. Forestland has a richer hierarchical structure than other vegetation, and its water conservation function is much higher than that of other vegetation. Therefore, forestlands were selected as foreground elements while other land use types were used as background elements. A binary image was generated and GuidosToolbox software[7] was used to identify the seven MSPA-based landscape elements, namely, core, bridge, edge, branch, loop, islet, and perforation. The core is the source of various ecological processes. Bridges are linear elements connecting various core area patches representing landscape connectivity. Edges are transition zones between the external perimeters of the core area and the non-forest landscape area. Branches are narrow regions connected to the core areas. Loops are the internal access points of material and energy exchange within a single core area. Islets are isolated small patches with low landscape connectivity. Perforations are the interior perimeters of a core area patch. Here, we used GuidosToolbox to assess forestland connectivity, adopted an eight-connectivity analysis, and set the edge width to three (Gao J. et al., 2021).

Ecological Resistance Surface Identification

The resistance surface is the basis of ecological network identification and represents the resistance that various animal species must overcome when they move in space. Here, habitat quality was calculated with the habitat quality module in the InVEST model. The resistance surface was the reciprocal of the habitat quality as the latter indicates high biodiversity and low species resistance. The resistance surface extracted by this method was relatively more ecologically significant

[1] http://www.resdc.cn/

[2] http://data.cma.cn/

[3] https://www.usgs.gov/

[4] https://modis-land.gsfc.nasa.gov/tools.html

[5] https://navi.cnki.net/knavi/yearbooks/YGFDS/detail?uniplatform=NZKPT

[6] https://navi.cnki.net/knavi/yearbooks/YGUIZ/detail

[7] https://forest.jrc.ec.europa.eu/en/activities/lpa/gtb/

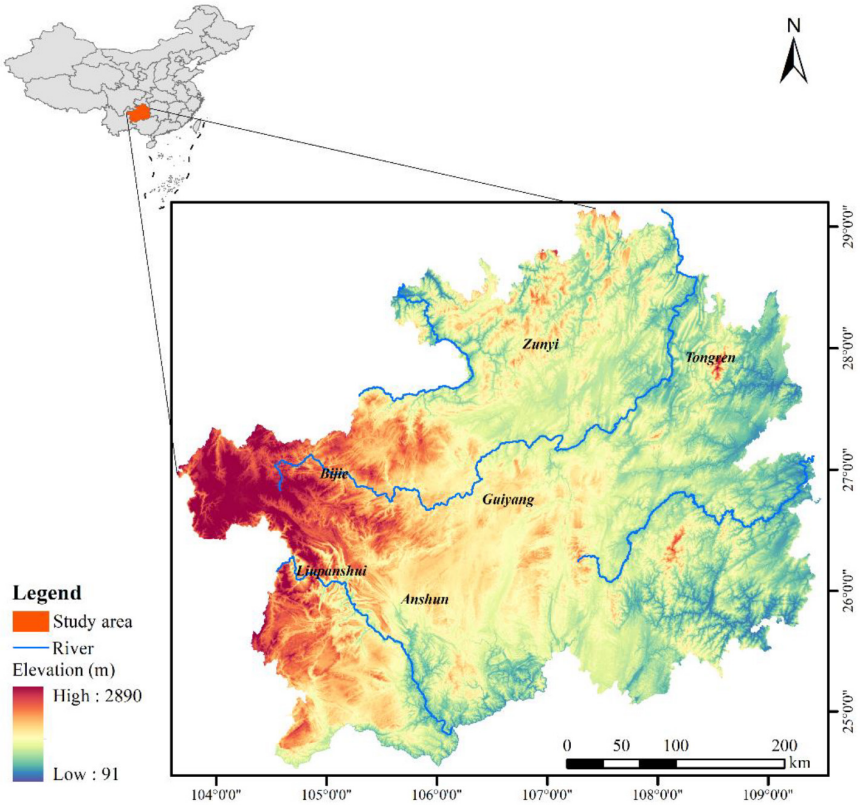

FIGURE 1 | Study site in Guizhou Province.

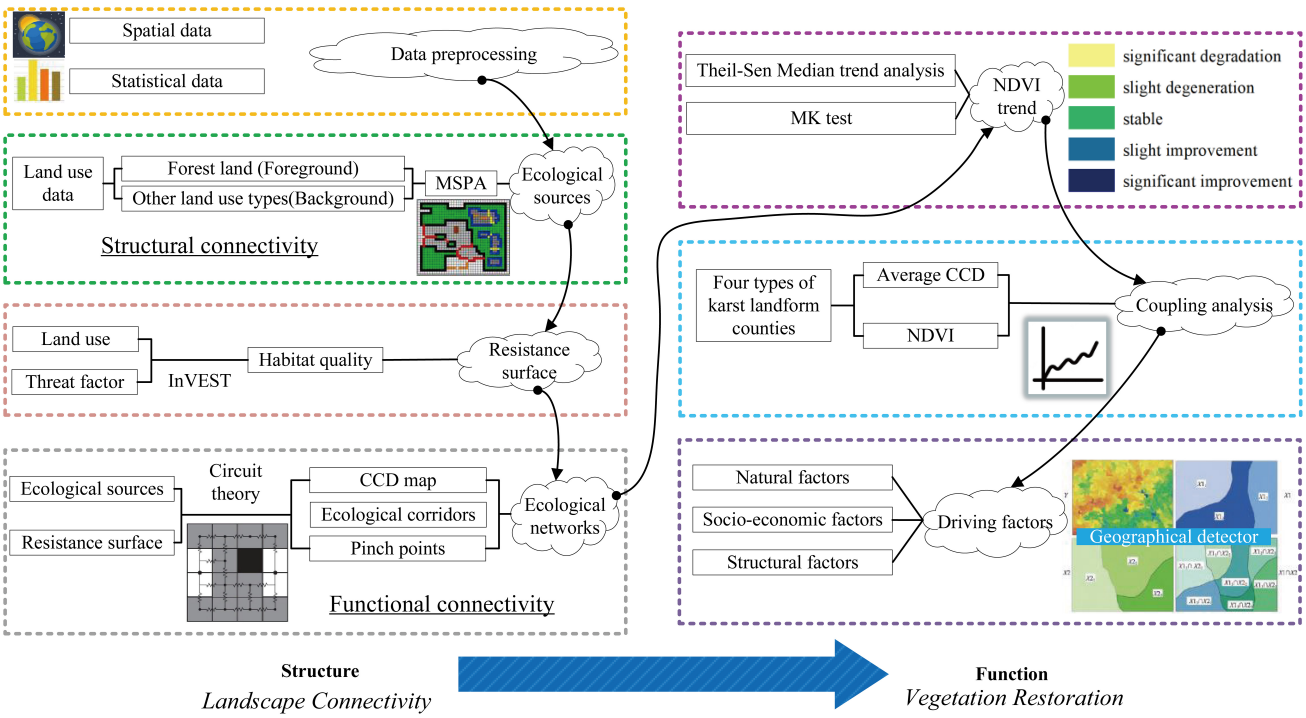

FIGURE 2 | Study methodology.

(Peng et al., 2018). Space limitations prohibit description of the calculation processes here.

Ecological Networks Identification

Circuit theory treats landscape as an electrical circuit. Heterogeneous landscapes may be viewed as circuits containing a series of nodes and resistors. Ecological corridors link ecological sources and usually consist of belt-like areas with specific widths. In the raster data, the CCD is defined as the amount of current flowing through a single pixel, and it can reflect the probability that a wanderer will move along a certain node or path. With the increase of the circuit path number, the effective resistance of the parallel circuit decreases and the corresponding current increases. That is to say, when resistance to the movement of species in the landscape decreases, CCD will increase, meaning that functional connectivity will also improve. Prior studies regarded ecological corridors as optimal paths for species migration (Beaujean et al., 2021; Fan et al., 2021). However, not all species may accurately identify the optimal path they must follow to reach their habitat destinations. Therefore, certain suboptimal paths are potential ecological flow corridors. Based on random walk characteristics of species in landscape, circuit theory can provide multiple potential corridors. This is better aligned with the behavioral characteristics of species (Ciudad et al., 2021). Besides, circuit theory model also can be used to identify "pinch points" corresponding to areas with high CCD in the voltage diagrams. Pinch point is the area with good connectivity between source areas, which is very important to maintain the connection of the whole ecological networks. Animal species either prefer to move through them or do so because there are no alternate paths. If a pinch point is removed or changed, it may significantly affect landscape connectivity (McRae et al., 2008; Cushman et al., 2013). Besides, circuit theory can provide a basis for improving the quality of existing corridors and patches and identifying key conservation and restoration areas, thereby helping to control and improve biological and abiotic flows and improve the efficiency of other important ecological processes and services (Taylor et al., 2006). In this study, Circuitscape 4.0 software[8] and Linkage Mapper[9] were applied to calculate the CCD and create voltage diagrams across the landscape based on available node and resistance surface data.

Theil-Sen Median Trend Analysis and Mann-Kendall Trend Test

A combination of Theil-Sen Median trend analysis and the MK trend test analyzes patterns of variation in vegetation over extended time series (Fensholt and Proud, 2012; Fensholt et al., 2012; Jiang et al., 2015). Theil-Sen Median trend analysis is a non-parametric statistical method used to calculate trends in variation (Healy et al., 1983). Its slope was used here to evaluate improvement and degradation in the vegetation of Guizhou Province between 2005 and 2018. The formula is as follows:

$$S_{NDVI} = median\left(\frac{NDVI_a - NDVI_b}{a-b}\right), 2005 \le b < a \le 2018 \quad (1)$$

where S_{NDVI} is the slope of the Theil-Sen median and $NDVI_b$ and $NDVI_a$ are the NDVI for years b and a. $S_{NDVI} > 0$ indicates a rising trend while $S_{NDVI} \le 0$ indicates a falling trend.

The MK trend test is also a non-parametric statistic measuring the significance of S_{NDVI}. Its input samples need not conform to certain distributions and it is not susceptible to the interference of outliers. The MK trend test has also been proposed to study patterns of variation in vegetation over extended time series (Jiang et al., 2015). The significance level $|Z| > u_{1-\alpha/2}$ indicates that the time series significantly varies at the α level. Here, the significance of the S_{NDVI} from 2005 to 2018 was measured at the 0.05 confidence level.

Division of Karst Landform Counties

As there are extensive karst landforms in Guizhou Province, lithology strongly affects the heterogeneity of landscape structure and function. The 88 counties of Guizhou Province were divided into four categories according to their proportions of carbonate rocks. Lin (2001) divided the counties of Guizhou Province into four classes based on their proportions of karst area. The county categories were: (a) higher proportion of karst landforms; (b) lower proportion of karst landforms; (c) interlaced karst and non-karst landforms; and (d) non-karst landforms. According to this classification system, the 88 counties in Guizhou Province were reclassified by lithology data and changes in administrative division. Sixty-two counties had >60% karst area, seven had karst area in the range of 50–60%, another seven had interlaced karst and non-karst landforms in an area ratio of 25–50%, and the remaining 12 were non-karst counties.

Geographical Detector Model

The geographical detector is a spatial statistic model proposed by Wang et al. (2010). It has been used to quantify the influences of potential driving factors on geographical phenomena based on spatial variance analysis (Wang et al., 2016, 2017; Gao F. et al., 2021). Our aim was to investigate the effects of structural changes in regional landscape connectivity on key ecological processes and ecosystem functions. To this end, we selected three dynamic indicators representing changes in spatial structure, namely, the rates of change in the core, bridge, and average CCD. However, the NDVI was also related to climatic, surface, and human activity factors. Therefore, we added the following control variables: annual average and temperature, urbanization growth rate, land surface relief, percentage of carbonate rocks, areas of artificial afforestation and closing hillsides to facilitate afforestation, and rates of change in GDP per capita and population density. The pixel-level NVDI slope was calculated for Guizhou Province and the average slope of each county unit was calculated as the dependent variable by using the zonal statistics method in ArcGIS. Factor and interaction detectors were used and they indicated which factors had the most significant impact on the slope of NDVI. They also disclosed the interactive effects among various pairs of factors.

Factor Detector

The factor detector calculates the *q*-value which quantifies the impact of potential driving factors on the spatiotemporal trend in

[8]https://circuitscape.org/downloads/

[9]https://linkagemapper.org

NDVI variation. The influence of q on the spatiotemporal trend in NDVI variation increases with its value:

$$q = 1 - \frac{\sum_{h=1}^{L} N_h \sigma_h^2}{N\sigma^2} = 1 - \frac{SSW}{SST} \quad (2)$$

$$SSW = \sum_{h=1}^{L} N_h \sigma_h^2 \quad (3)$$

$$SST = N_{\sigma^2} \quad (4)$$

where N is study area comprising N units layered into h = 1, 2, 3, …L strata. Stratum h comprises N_h units. σ^2 and $\sigma_h{}^2$ are the global variance of the dependent variable of the study area and the variances of the dependent variables in the sub-areas, respectively. SSW and SST are the "within sum of squares" and "total sum of squares," respectively. The q-value is in the range of 0–1.

Interaction Detector

The interaction detector indicates whether two factors strengthen or weaken each other. It compares their combined and separate contributions (Wang et al., 2010). The model categorized five interactive effects (**Table 1**).

RESULTS

Identification of Ecological Sources and Resistance Surface

In 2005 and 2018, the Guizhou Province forestland occupied 94,781.33 and 93,082.51 km^2, respectively. The changes in morphological spatial pattern were most evident in Central and Western Guizhou Province. By contrast, the other regions remained relatively stable. The proportions of various landscape elements in the foreground area were also stable. The proportion of perforation decreased by 0.48%. The core area was 57,806.25 and 56,870.55 km^2 in 2005 and 2018, respectively, and occupied mainly the northeastern and southeastern parts of the study area. However, there were also small dispersive core areas and the landscape was fragmented (**Figure 3**). Cores with areas >10 km^2 (based on MSPA) were defined as ecological sources. They were entered into the circuit theory model for landscape connectivity analysis (Gao J. et al., 2021). There were 453 and 507 core patches extracted as ecological sources in 2005 and 2018, respectively. Overall, the ecological sources were large but fragmented. This finding was consistent with the distribution characteristics of typical karst landform vegetation.

Connectivity of the landscape ecological flow must overcome resistance contributed by various influencing factors in the space. As is shown in **Figure 4**, the average ecological resistance values in Guizhou were 1.2039 and 1.2074 in 2005 and 2018, respectively. Thus, ecological resistance rose slightly but nonetheless remained low. The areas with strong resistance were located mainly in the urban areas of Guiyang, Zunyi, Kaili, and Liupanshui City and their environs. The habitat quality of these areas was zero. Hence, they showed infinite resistance.

TABLE 1 | Interactions between covariate pairs.

Description	Interaction
$q(A\cap B) < \text{Min}(q(A), q(B))$	Weakened and non-linear
$\text{Min}(q(A), q(B)) < q(A\cap B) < \text{Max}(q(A), q(B))$	Weakened and univariate
$q(A\cap B) > \text{Max}(q(A), q(B))$	Strengthened and bivariate
$q(A\cap B) = q(A) + q(B)$	Independent
$q(A\cap B) > q(A) + q(B)$	Strengthened and non-linear

Identification of Ecological Networks and Their Variations

The ecological networks (**Figures 5A,B**) showed that the numbers of ecological sources and corridors in Guizhou Province increased overall and the potential corridors were extended. In Guiyang City, the ecological sources and corridors became scattered and their numbers decreased. Hence, urbanization markedly contributed to the change in vegetation cover in Guizhou Province. However, this degradation was ecologically compensated in remote areas. In 2018, small forest patches appeared in the southwest and they improved the landscape connectivity of the surrounding area. **Figures 5C,D** show the CCD values for 2005 and 2018. The maximum and average CCD were 1,681.94 and 58.49, respectively, in 2005 and 1,896.97 and 81.74, respectively, in 2018. Though the total forestland area and the core area decreased, there was overall improvement in forest landscape connectivity in Guizhou Province. **Figure 5D** shows that the positions of most pinch points in Western Guizhou remained unchanged. However, their ranges narrowed. Thus, resistance around the pinch points decreased and landscape connectivity improved in Western Guizhou. New pinch points appeared in Northeastern Guizhou. Therefore, the ecological resistance around them increased and the landscape connectivity deteriorated.

The Variation in Trends of Vegetation Coverage

Integration of the Theil-Sen Median trend analysis and the MK trend test reflects variations in the vegetation trends of Guizhou Province. Regions with $S_{NDVI} = 0$ do not exist. Therefore, we created the categories according to real S_{NDVI} conditions. Areas with S_{NDVI} in the range of -0.0005 to 0.0005 were rated as stable. Areas with $S_{NDVI} \geq 0.0005$ were rated as improved. Areas with $S_{NDVI} < 0.0005$ were rated as degraded. The results of the MK trend test were classified as significant ($Z > 1.96$ or $Z < -1.96$) or insignificant ($-1.96 \leq Z \leq 1.96$) variations and categorized into five grades (**Table 2**).

Overall, the NDVI improved; however, greening and degradation may have occurred in different areas. Regions with improved vegetation far exceeded degraded ones in Guizhou Province between 2005 and 2018 (**Figure 6**). Regions with significantly improved vegetation coverage were located primarily in Northwestern and Southwestern Guizhou Province.

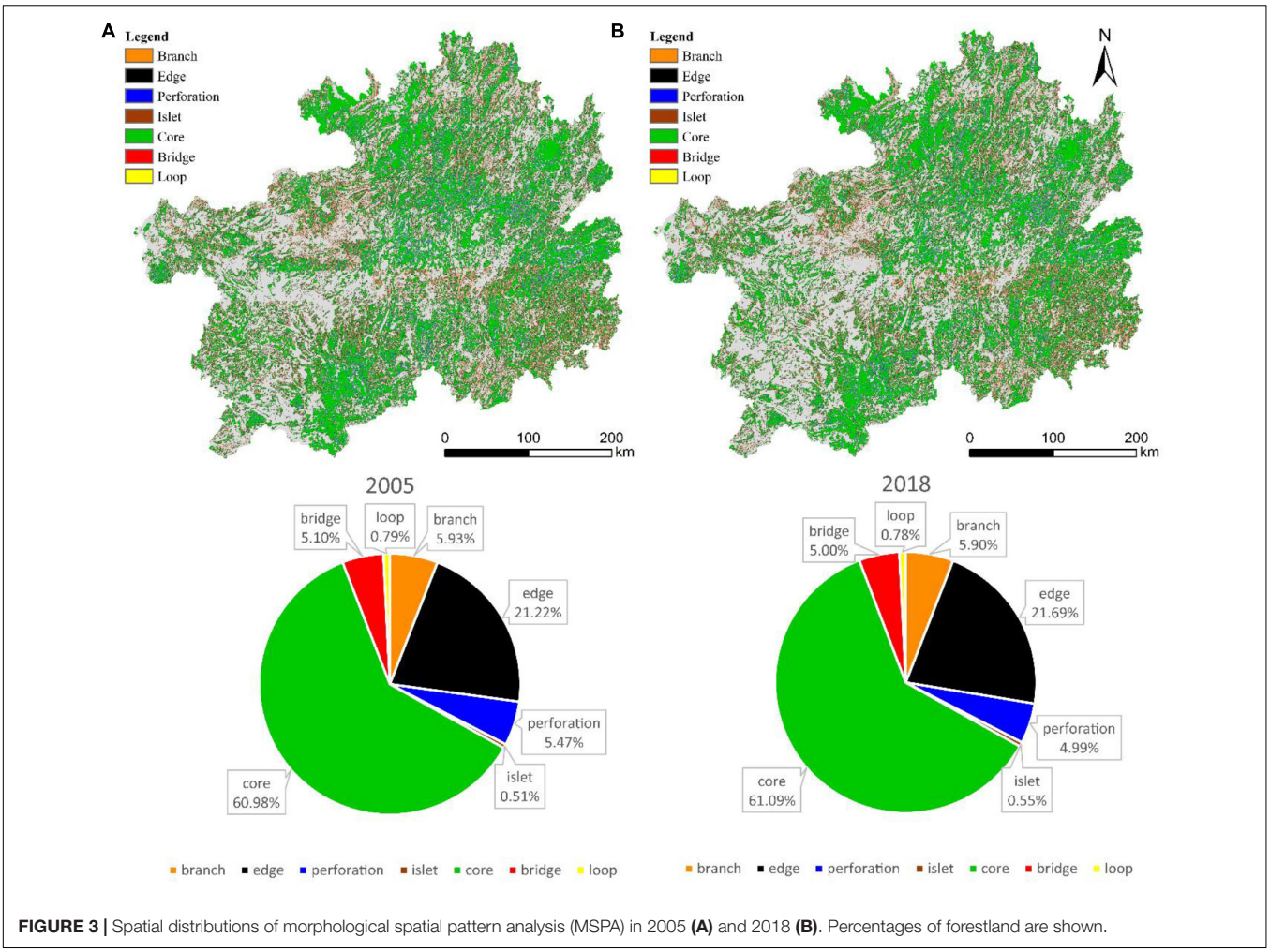

FIGURE 3 | Spatial distributions of morphological spatial pattern analysis (MSPA) in 2005 **(A)** and 2018 **(B)**. Percentages of forestland are shown.

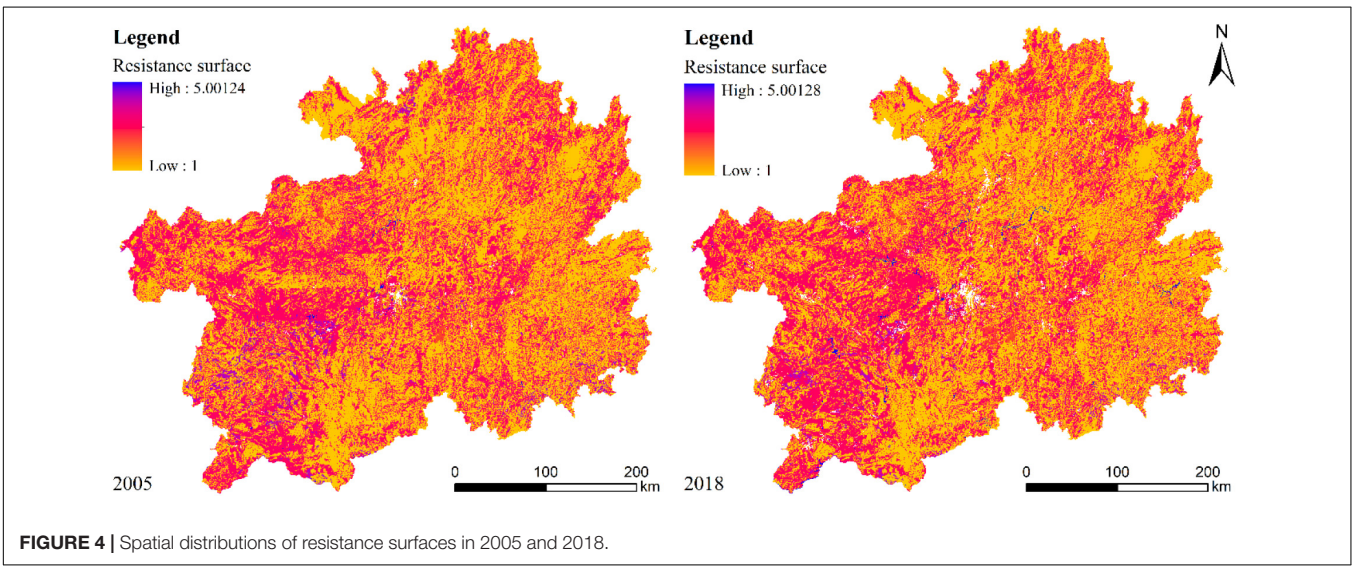

FIGURE 4 | Spatial distributions of resistance surfaces in 2005 and 2018.

Regions with slightly improved vegetation coverage showed a dispersive distribution. Regions with stable or slightly degraded vegetation coverage were distributed mostly in Central and Eastern Guizhou Province. Regions with severe degradation were distributed mainly in Guiyang City, Xingyi City, Zunyi City, and Kaili City.

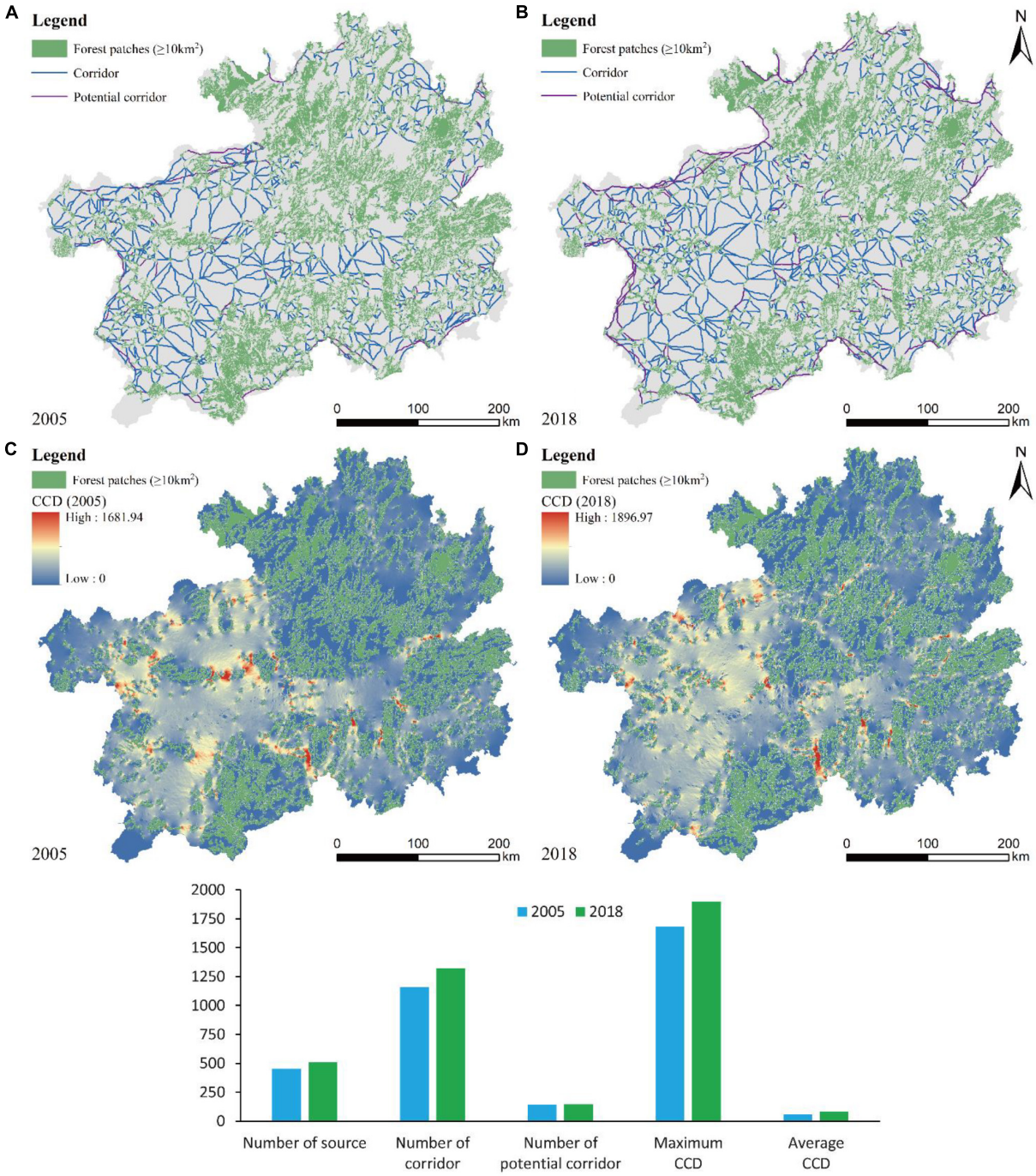

FIGURE 5 | (A,B) Spatial distributions of ecological sources and corridors in 2005 and 2018. **(C,D)** Cumulative current density (CCD) maps for 2005 and 2018.

TABLE 2 | Normalized difference vegetation index (NDVI) trend variations in Guizhou Province.

S_{NDVI}	Z	Trend variation	Area percentage (%)
≥0.0005	≥1.96	Significant improvement	28.81%
≥0.0005	−1.96 to 1.96	Slight improvement	48.96%
−0.0005 to 0.0005	−1.96 to 1.96	Stable or no significant variation in vegetation	7.95%
<0.0005	−1.96 to 1.96	Slight degradation	12.43%
<0.0005	<−1.96	Significant degradation	1.85%

Coupling Analysis of Landscape Connectivity and Normalized Difference Vegetation Index

Landscape structure influences the representation of landscape function. Coupling analysis identifies the relationship between landscape connectivity and NDVI at the statistical level and reflects regional ecological security. According to the result of the division of karst landform counties, we then explored the correlations between the average CCD values and the NDVI in the various karst counties in 2005 and 2018. **Figure 7** shows that in general, the average CCD values increased especially for counties with higher proportions of karst areas. Their average CCD were relatively low in 2005 and had significantly increased by 2018. In 2018, the NDVI for most counties had gradually improved relative to those of 2005. Hence, the ecological environment was sustainably developed. Certain counties with higher proportions of karst landforms were not conducive to the growth or restoration of vegetation because of high levels of urbanization or high proportions of carbonate rocks. Hence, their average CCD and NDVI had declined over time.

The trend of the eight fitting lines for 2005 and 2018 demonstrated inconsistent correlations between the average CCD and the NDVI of the counties with different geomorphologies. The average CCD and the NDVI were positively correlated for the counties with non-karst landforms and those with interlaced karst and non-karst landforms. For the counties with lower proportions of karst landforms, the average CCD was negatively correlated with the NDVI in 2005 and 2018, but negative correlation alleviated in 2018. For the counties with higher proportions of karst landforms, the average CCD and the NDVI were negatively correlated in 2005 but positively correlated in 2018. The rocky desertification projects improved the landscape connectivity and positively changed the NDVI in areas with widespread karst landforms.

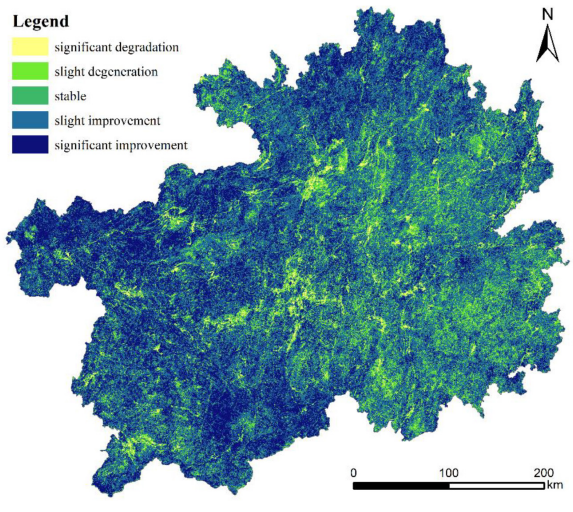

FIGURE 6 | Spatial S_{NDVI} distribution in Guizhou Province between 2005 and 2018.

Effects of Influencing Factors on Trends in Normalized Difference Vegetation Index Change

We described the statistical correlation between landscape connectivity and the NDVI. We also used metrology and a regression model to quantify the impact of this association. We selected the corresponding control variables, used S_{NDVI} as the dependent variable, and applied the factor detector to calculate the q-value for each factor on S_{NDVI} between 2005 and 2018. Seventy-five percent of the q-values were statistically significant at the 1% level (**Table 3**). The order of the q-values corresponding to each factor was: $X_5 > X_3 > X_6 > X_4 > X_1 > X_2 > X_7 > X_8 > X_{12} > X_{11} > X_{10} > X_9$. Non-climatic factors are the main reasons for the observed general improvements in the vegetation of Guizhou Province. Urbanization growth rate, rate of change in GDP per capita, and population density all affect vegetation change in Guizhou Province to varying degrees. Urbanization promotes the adjustment of rural industrial structure, and a huge number of rural labor forces choose to work in non-agricultural industries, which increases per capita income and land utility intensive level. According to the 2019 Statistical Yearbook, the population in rural areas of Guizhou province decreased by 30.74% from 2005 to 2018, indicating the phenomenon of population outflow and significant reduction of human disturbance on rural land, which is beneficial to vegetation restoration. The reconstruction, restoration and protection of vegetation not only change the composition of landscape types, but also strongly affect the landscape structure. Closing hillsides to facilitate afforestation reduces anthropogenic disturbance of vegetation, and artificial afforestation also accelerates forest growth. The ecological benefits brought by ecological restoration projects are being reflected. Moreover, the relief degree of land surface and the proportion of carbonate rocks also influence variations in vegetation. Thus, ecological construction must be conducted based on local conditions to restore vegetation. The rates of change in average CCD and bridge also affected the change in the NDVI, which proved that the improvement of landscape connectivity also had a certain effect on vegetation change. The improvement of the connectivity of the landscape pattern is conducive to the improvement of the ecological function of the vegetation and the promotion of the ecological process.

Twelve factors and 33 of their interactions were evaluated using the interaction detector. **Table 4** shows that each factor had a different interactive effect. All interactions contributed bivariate or non-linear enhancement. Therefore, S_{NDVI} was the product of synergy among multiple factors. The interactions adding the highest q-values to S_{NDVI} were [urbanization growth rate ∩ annual average temperature] (q = 0.7477) and [urbanization growth rate ∩ annual average precipitation] (q = 0.7176). It indicates that the influence of temperature and precipitation on vegetation change will be enhanced in areas with high urbanization growth rate. Urbanization migrated the population to cities and towns and significantly altered vegetation which, in turn, reduced human activity, mitigated forest damage, and increased land abandonment in rural areas. Moreover, we found

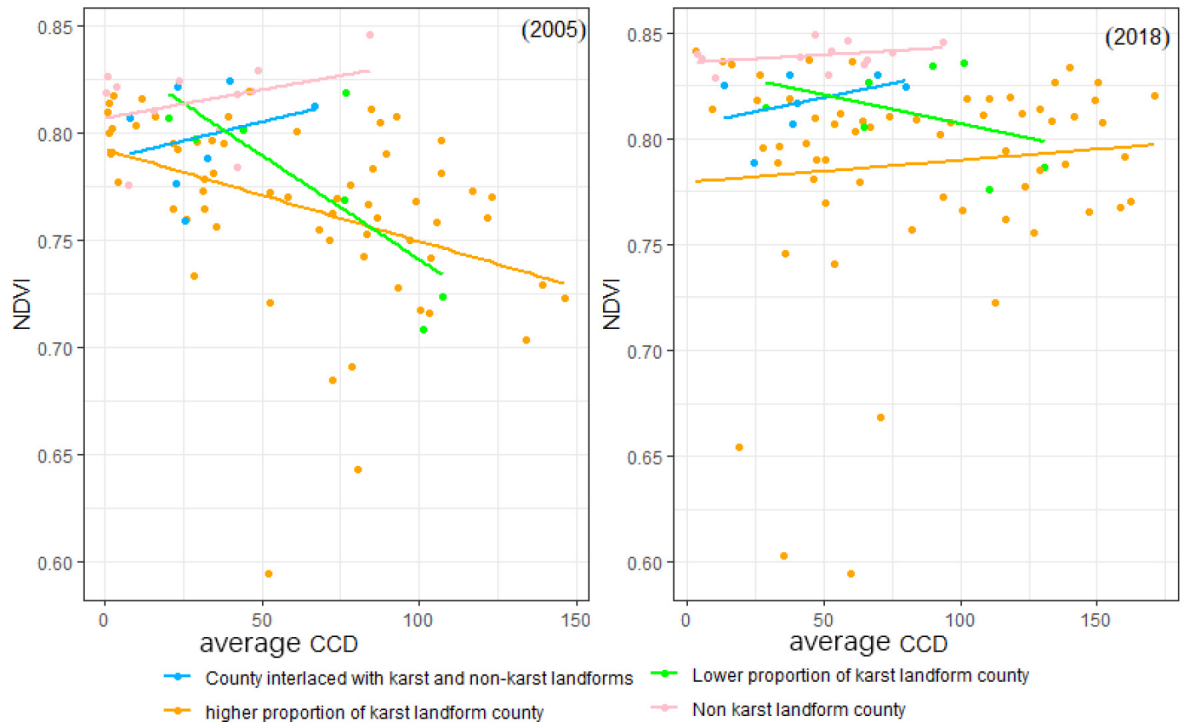

FIGURE 7 | Correlation analysis of average cumulative current density (CCD) and normalized difference vegetation index (NDVI) in counties with different geomorphic forms.

TABLE 3 | Factors influencing the *q*-value for the normalized difference vegetation index (NDVI) trend in Guizhou, 2005–2018.

Variable	*q*	Variable	*q*
X_1 = Rate of change in GDP per capita	0.2783***	X_7 = Annual average precipitation	0.2319***
X_2 = Rate of change in population density	0.2725***	X_8 = Annual average temperature	0.1936**
X_3 = Area of artificial afforestation	0.4023***	X_9 = Rate of change in core	0.1930
X_4 = Area of closing hillsides to facilitate afforestation	0.2963***	X_{10} = Rate of change in bridge	0.1427***
X_5 = Urbanization growth rate	0.5002***	X_{11} = Proportion of carbonate rocks	0.1911***
X_6 = Relief degree of land surface	0.3365***	X_{12} = Rate of change in average CCD	0.1914***

*** and **** indicate significance at the 5 and 1% levels, respectively.*

TABLE 4 | Effects of interactions among influencing factors on S_{NDVI} in Guizhou Province, 2005–2018.

Factor	X1	X2	X3	X4	X5	X6	X7	X8	X9	X10	X11	X12
X1												
X2	0.5014											
X3	0.5831	0.6038										
X4	0.6067	0.6064	0.414									
X5	0.6673	0.6225	0.7126	0.6321								
X6	0.5054	0.4442	0.5702	0.5246	0.5611							
X7	0.6352	0.6059	0.5576	0.4877	0.7176	0.5353						
X8	0.6648	0.522	0.5062	0.5651	0.7477	0.5729	0.4947					
X9	0.6312	0.5954	0.4965	0.4757	0.672	0.4697	0.5377	0.4836				
X10	0.5816	0.5113	0.5464	0.5098	0.6903	0.4866	0.3946	0.4571	0.3819			
X11	0.4037	0.4813	0.4314	0.3395	0.6444	0.367	0.367	0.3799	0.4425	0.335		
X12	0.4718	0.4972	0.5494	0.4725	0.6148	0.4601	0.5535	0.4651	0.4724	0.4921	0.371	

that the interactions between landscape connectivity (X_{10} and X_{12}) and other factors enhanced the variation in vegetation.

DISCUSSION

The core and forestland areas of Guizhou Province have decreased in response to natural factors and human activity. Moreover, landscape connectivity and the trends of vegetation coverage have also been markedly altered in Guizhou Province. Significant ecological sources and corridors have increased and overall landscape connectivity has improved. The area of vegetation significantly improved was much larger than that of vegetation degradation. Current studies have analyzed regional changes in vegetation by regarding natural and human factors. Nevertheless, they did not consider the impact of changes in landscape structure on ecological function and process. In this paper, rate of change in bridge representing structural connectivity and rate of change in average CCD representing functional connectivity are introduced into vegetation change analysis. According to the result of factor detector, although these two factors are not the dominant factors affecting vegetation change, their impact on landscape change is still significant. Circuit theory models simulate migration and diffusion in the biological flow within ecosystems, which use the random walking characteristic of electrons in a circuit. Species diffusion and migration may be predicted based on the current strength between source areas. Landscape elements and pinch points that strongly influence landscape connectivity may be effectively identified. MSPA and circuit theory model need only small amount of data required for calculation and the simple process, and integrate structural connectivity and functional connectivity between ecological source areas. This paper meets the needs of multi-species migration and is more consistent with the real situation of species movement. It provides a new method for quantitative identification of key areas in ecological networks and can provide scientific basis for ecological protection planning in karst area. However, landscape connectivity strongly depends on the scale characteristics of the research object. The ecological process and function of landscape spatial structure characteristics at different scales are different, and landscape connectivity varies greatly. Therefore, multi-scale studies on landscape connectivity need to be further explored, and more attention should be paid to the effect of landscape pattern on vegetation change.

In this study, we considered the positive impact of human activity and improvements in landscape connectivity on changes in vegetation. However, we ignored the significant degradation of the vegetation in certain areas. The impact of ecological engineering implementation on landscape connectivity and ecosystem processes and functions is complex. Large-scale afforestation may increase vegetation transpiration, consume more water, and reduce vegetation coverage in the afforestation area. Most artificially planted species are not indigenous and grow rapidly. Hence, they simplify the community structure, have a negative effect on biodiversity, and may interrupt or even reverse ecological succession. Afforestation reduces the incident light below the canopy, thereby attenuating photosynthesis in the understory plants. Changes in ecosystem types caused by urbanization, drought, and illegal logging and overgrazing may also lead to poor vegetation growth. At the same time, the National Forestry and Grassland Administration's Bulletin on the Status of Rocky Desertification in 2018 also indicated that local rocky desertification land is still expanding, causing vegetation degradation in some areas, and the prevention and control situation is grim. Environmental engineering must consider the original landscape structure and landscape connectivity improvement to produce beneficial ecological and economic results. As the karst ecological environment is fragile, forest, shrub, and grass collocation must be regarded as well. In the future research, we should evaluate the vegetation restoration situation in karst areas more comprehensively, and deeply explore the positive and negative effects of ecological restoration projects on regional vegetation changes.

A geographical detector accurately identifies the relationships and interactions among multiple factors and is widely used to analyze driving force mechanisms. We explored the changes in vegetation cover in response to the natural environment, human activity, and changes in landscape structure at the county scale. The change in vegetation cover was influenced mainly by anthropogenic factors. The urbanization growth rate strongly interacted with the annual mean precipitation and temperature. Urbanization has concentrated people in cities and towns. Reduced human activity in rural areas has decreased deforestation and/or increased land abandonment. Thus, an increase in urbanization can reinforce interactions among factors. Interactions among landscape connectivity and other factors also significantly increased the variation in vegetation. The geographical detector model is affected by a modifiable areal unit problem when it is used to analyze the factors influencing variation in vegetation including the scale and zoning effects. The number of layers also affects the results. Here, we selected several unsupervised classification discretization methods and quantities using the "optidisc" function in the GD package of R. We made comparisons to choose the optimal combinations of discretization methods to avoid the subjectivity of artificial classification. However, the influences of number and stratification method on the results remain to be established.

CONCLUSION

The MSPA indicated that the degree of fragmentation was still high for each element. However, the proportion of each element did not markedly change. Several cities with a high level of urbanization, their morphological spatial pattern changed significantly. By contrast, the other regions remained relatively stable. Ecological resistance was reduced in certain areas which led to improvements in the ecological resistance surface of biological migration, the path and quantity of ecological corridors, and landscape connectivity. The structure of the ecological networks steadily improved because the number of ecological sources and ecological corridors were both increased. Identification of the ecological networks enhanced

the function of the ecological barriers and provided guidance for future ecological protection and restoration programs in Guizhou Province.

The areas with improved vegetation coverage were substantially larger than the degraded areas in Guizhou Province in 2005–2018. The improved and degraded areas accounted for 77.77 and 14.28% of the total area, respectively. The remaining 7.95% was stable. We divided the 88 counties into four categories based on their karst landforms. Most of them were counties with higher proportions of karst landforms. A coupling analysis of the average CCD and the NDVI showed that they were generally higher in 2018 than 2005 for most counties. Nevertheless, the growing demands for economic development and the limitations of the karst environment lowered the average CCD and the NDVI for several counties with higher proportions of karst landforms. The average CCD and the NDVI were positively correlated for counties with non-karst and interlaced karst and non-karst landforms. In 2005, the average CCD and the NDVI were strongly negatively correlated for counties with lower proportions of karst landforms. By 2018, however, the average CCD and the NDVI were only weakly negatively correlated for these counties. For counties with higher proportions of karst landforms, the average CCD and the NDVI were negatively correlated in 2005 but positively correlated in 2018. It can be concluded that ecological restoration projects have a more obvious impact on counties with higher proportions of karst landforms. The rocky desertification problem and landscape connectivity have been improved.

Natural and socioeconomic factors as well as improvement in landscape connectivity significantly influenced the change in the NDVI. The interactive detector revealed that [urbanization growth rate ∩ annual average temperature] and [urbanization growth rate ∩ annual average precipitation] jointly drove the variation in vegetation in Guizhou Province. Therefore, the urbanized area is more likely to enhance the effects of temperature and precipitation than the rural area because the latter has a smaller population. In addition, interactions among landscape connectivity and other factors significantly enhance the spatial variations in vegetation. Thus, changes in landscape pattern play crucial roles in the restoration of vegetation in this region. Future research should investigate the coordinated development of urbanization and ecological restoration within the karst region.

DATA AVAILABILITY STATEMENT

The datasets presented in this study can be found in online repositories. The names of the repository/repositories and accession number(s) can be found in the article.

AUTHOR CONTRIBUTIONS

KH and LP performed the material preparation and data collection and analysis. KH wrote the first draft of the manuscript. All authors commented on previous versions of the manuscript, contributed to the study conception and design, read, and approved the final manuscript.

FUNDING

The research was supported by the National Natural Science Foundation of China (No. 42001090), the Guangxi Natural Science Foundation Program (No. 2020GXNSFDA238012), and the National Key Basic Research Program of China (973 Program) (No. 2015CB452706).

ACKNOWLEDGMENTS

We would like to thank Editage (www.editage.cn) for English language editing.

REFERENCES

An, Y., Liu, S., Sun, Y., Shi, F., and Beazley, R. (2021). Construction and optimization of an ecological network based on morphological spatial pattern analysis and circuit theory. *Landsc. Ecol.* 36, 2059–2076.

Beaujean, S., Nor, A. N. M., Brewer, T., Zamorano, J. G., Dumitriu, A. C., Harris, J., et al. (2021). A multistep approach to improving connectivity and co-use of spatial ecological networks in cities. *Landsc. Ecol.* 36, 2077–2093. doi: 10.1007/s10980-020-01159-6

Cai, H., Yang, X., Wang, K., and Xiao, L. (2014). Is forest restoration in the southwest China Karst promoted mainly by climate change or human-induced factors? *Remote Sen.* 6, 9895–9910. doi: 10.3390/rs6109895

Carlier, J., and Moran, J. (2019). Landscape typology and ecological connectivity assessment to inform Greenway design. *Sci. Total Environ.* 651, 3241–3252. doi: 10.1016/j.scitotenv.2018.10.077

Ciudad, C., Mateo-Sánchez, M. C., Gastón, A., Blazquez-Cabrera, S., and Saura, S. (2021). Landscape connectivity estimates are affected by spatial resolution, habitat seasonality and population trends. *Biodivers. Conserv.* 30, 1395–1413.

Cushman, S., Mcrae, B., Adriaensen, F., Beier, P., Shirley, M., and Zeller, K. (2013). *Key Topics in Conservation Biology 2*. Hoboken, NJ: Wiley-Blackwell.

Dai, L., Liu, Y., and Luo, X. (2021). Integrating the MCR and DOI models to construct an ecological security network for the urban agglomeration around Poyang Lake, China. *Sci. Total Environ.* 754:141868. doi: 10.1016/j.scitotenv.2020.141868

Dondina, O., Saura, S., Bani, L., and Mateo-Sánchez, M. C. (2018). Enhancing connectivity in agroecosystems: focus on the best existing corridors or on new pathways? *Landsc. Ecol.* 33, 1741–1756. doi: 10.1007/s10980-018-0698-9

Fan, F., Liu, Y., Chen, J., and Dong, J. (2021). Scenario-based ecological security patterns to indicate landscape sustainability: a case study on the Qinghai-Tibet Plateau. *Landsc. Ecol.* 36, 2175–2188. doi: 10.1007/s10980-020-01044-2

Fensholt, R., Langanke, T., Rasmussen, K., Reenberg, A., Prince, S. D., Tucker, C., et al. (2012). Greenness in semi-arid areas across the globe 1981–2007–an earth observing satellite based analysis of trends and drivers. *Remote Sens. Environ.* 121, 144–158.

Fensholt, R., and Proud, S. R. (2012). Evaluation of earth observation based global long term vegetation trends–comparing GIMMS and MODIS global NDVI time series. *Remote Sens. Environ.* 119, 131–147. doi: 10.1016/j.rse.2011.12.015

Feyissa, G., and Gebremariam, E. (2018). Mapping of landscape structure and forest cover change detection in the mountain chains around Addis Ababa:

the case of Wechecha Mountain, Ethiopia. *Remote Sens. Appl. Soc. Environ.* 11, 254–264. doi: 10.1016/j.rsase.2018.07.008

Forman, R., and Godron, M. (1986). *Landscape Ecology*. New York, NY: John Wiley and Sons Ltd.

Forman, R., and Wilson, E. (1995). *Land Mosaics: The Ecology of Landscapes and Regions*. Cambridge: Cambridge University Press.

Gao, F., Li, S., Tan, Z., Wu, Z., Zhang, X., Huang, G., et al. (2021). Understanding the modifiable areal unit problem in dockless bike sharing usage and exploring the interactive effects of built environment factors. *Int. J. Geogr. Inf. Sci.* 35, 1905–1925. doi: 10.1080/13658816.2020.1863410

Gao, J., Du, F., Zuo, L., and Jiang, Y. (2021). Integrating ecosystem services and rocky desertification into identification of karst ecological security pattern. *Landsc. Ecol.* 36, 2113–2133. doi: 10.1007/s10980-020-01100-x

Haider, J. A., Höbart, R., Kovacs, N., Milchram, M., Dullinger, S., Huber, W., et al. (2016). The role of habitat, landscape structure and residence time on plant species invasions in a neotropical landscape. *J. Trop. Ecol.* 32, 240–249. doi: 10.1017/s0266467416000158

Healy, M., Hoaglin, D., Mosteller, F., and Tukey, J. (1983). Understanding robust and exploratory data analysis. *Biometrics* 39:1126.

Huang, Q., Li, M., Chen, C., Mao, K., Chen, Z., Li, F., et al. (2010). "Assessment of land degradation in Guizhou Province, Southwest China using AVHRR/NDVI and MODIS/NDVI data," in *Proceedings of the 2010 18th International Conference on Geoinformatics* (Beijing: Peking University).

Jiang, W., Yuan, L., Wang, W., Cao, R., Zhang, Y., and Shen, W. (2015). Spatio-temporal analysis of vegetation variation in the Yellow River Basin. *Ecol. Indic.* 51, 117–126. doi: 10.1016/j.ecolind.2014.07.031

Lagomasino, D., Price, R. M., Whitman, D., Melesse, A., and Oberbauer, S. F. (2015). Spatial and temporal variability in spectral-based surface energy evapotranspiration measured from Landsat 5TM across two mangrove ecotones. *Agricult. For. Meteorol.* 213, 304–316. doi: 10.1016/j.agrformet.2014.11.017

LeGrand, H. E. (1973). Hydrological and ecological problems of Karst regions. *Science* 179, 859–864. doi: 10.1126/science.179.4076.859

Liao, C., Yue, Y., Wang, K., Fensholt, R., Tong, X., and Brandt, M. (2018). Ecological restoration enhances ecosystem health in the karst regions of southwest China. *Ecol. Indic.* 90, 416–425. doi: 10.1016/j.ecolind.2018.03.036

Lin, J. (2001). The distributed area and the features analysis of karst and non karst landscape in Guizhou. *J. Guizhou Educ. Coll.* 12, 43–46.

McRae, B. H. (2006). Isolation by resistance. *Evolution* 60, 1551–1561. doi: 10.1554/05-321.1

McRae, B. H., Dickson, B. G., Keitt, T. H., and Shah, V. B. (2008). Using circuit theory to model connectivity in ecology, evolution, and conservation. *Ecology* 89, 2712–2724. doi: 10.1890/07-1861.1

Pausas, J. G. (2003). The effect of landscape pattern on Mediterranean vegetation dynamics: a modelling approach using functional types. *J. Veget. Sci.* 14, 365–374. doi: 10.1111/j.1654-1103.2003.tb02162.x

Peng, J., Jiang, H., Liu, Q., Green, S. M., Quine, T. A., Liu, H., et al. (2021). Human activity vs. climate change: distinguishing dominant drivers on LAI dynamics in karst region of southwest China. *Sci. Total Environ.* 769:144297. doi: 10.1016/j.scitotenv.2020.144297

Peng, J., Yang, Y., Liu, Y., Hu, Y. N., Du, Y., Meersmans, J., et al. (2018). Linking ecosystem services and circuit theory to identify ecological security patterns. *Sci. Total Environ.* 644, 781–790. doi: 10.1016/j.scitotenv.2018.06.292

Salgueiro, P. A., Valerio, F., Silva, C., Mira, A., Rabaça, J. E., and Santos, S. M. (2021). Multispecies landscape functional connectivity enhances local bird species' diversity in a highly fragmented landscape. *J. Environ. Manag.* 284:112066. doi: 10.1016/j.jenvman.2021.112066

Soille, P., and Vogt, P. (2009). Morphological segmentation of binary patterns. *Pattern Recogn. Lett.* 30, 456–459.

Taylor, P., Fahrig, L., Henein, K., and Merriam, G. (1993). Connectivity is a vital element of landscape structure. *Oikos* 68:571. doi: 10.1093/database/bav010

Taylor, P., Fahrig, L., and With, K. (2006). *Landscape Connectivity: A Return to the Basics*. Cambridge: Cambridge University Press, 29–43.

Tian, Y., Bai, X., Wang, S., Qin, L., and Li, Y. (2017). Spatial-temporal changes of vegetation cover in Guizhou Province, Southern China. *Chin. Geogr. Sci.* 27, 25–38. doi: 10.1007/s11769-017-0844-3

Tischendorf, L., and Fahrig, L. (2000). On the usage and measurement of landscape connectivity. *Oikos* 90, 7–19. doi: 10.1034/j.1600-0706.2000.900102.x

Uroy, L., Ernoult, A., and Mony, C. (2019). Effect of landscape connectivity on plant communities: a review of response patterns. *Landsc. Ecol.* 34, 203–225. doi: 10.3390/ijerph16214241

Wang, J. F., Li, X. H., Christakos, G., Liao, Y. L., Zhang, T., Gu, X., et al. (2010). Geographical detectors-based health risk assessment and its application in the neural tube defects study of the Heshun region, China. *Int. J. Geogr. Inf. Sci.* 24, 107–127. doi: 10.1080/13658810802443457

Wang, J.-F., Zhang, T.-L., and Fu, B.-J. (2016). A measure of spatial stratified heterogeneity. *Ecol. Indic.* 67, 250–256. doi: 10.1016/j.ecolind.2016.02.052

Wang, Y., Wang, S., Li, G., Zhang, H., Jin, L., Su, Y., et al. (2017). Identifying the determinants of housing prices in China using spatial regression and the geographical detector technique. *Appl. Geogr.* 79, 26–36. doi: 10.1016/j.apgeog.2016.12.003

Williams, M. A., and Baker, W. L. (2012). Spatially extensive reconstructions show variable-severity fire and heterogeneous structure in historical western United States dry forests. *Glob. Ecol. Biogeogr.* 21, 1042–1052. doi: 10.1111/j.1466-8238.2011.00750.x

Zhang, X., Liao, C., Li, J., and Sun, Q. (2013). Fractional vegetation cover estimation in arid and semi-arid environments using HJ-1 satellite hyperspectral data. *Int. J. Appl. Earth Observ. Geoinform.* 21, 506–512.

Zhu, C., Peng, W., Zhang, L., Luo, Y., Dong, Y., and Wang, M. (2019). Study of temporal and spatial variation and driving force of fractional vegetation cover in upper reaches of Minjiang River from 2006 to 2016. *Acta Ecol. Sin.* 39, 1583–1594.

Conflict of Interest: The authors declare that the research was conducted in the absence of any commercial or financial relationships that could be construed as a potential conflict of interest.

Publisher's Note: All claims expressed in this article are solely those of the authors and do not necessarily represent those of their affiliated organizations, or those of the publisher, the editors and the reviewers. Any product that may be evaluated in this article, or claim that may be made by its manufacturer, is not guaranteed or endorsed by the publisher.

frontiers in Ecology and Evolution

ORIGINAL RESEARCH
published: 14 March 2022
doi: 10.3389/fevo.2022.854497

Impacts of Future Climate and Land Use/Cover Changes on Water-Related Ecosystem Services in Changbai Mountains, Northeast China

Hebin Wang[1,2], Wen J. Wang[1], Lei Wang[1], Shuang Ma[1,3], Zhihua Liu[4], Wenguang Zhang[1], Yuanchun Zou[1] and Ming Jiang[1]*

[1] Northeast Institute of Geography and Agroecology, Chinese Academy of Sciences, Changchun, China, [2] University of Chinese Academy of Sciences, Beijing, China, [3] Key Laboratory of Geographical Processes and Ecological Security in Changbai Mountains, Ministry of Education, School of Geographical Sciences, Northeast Normal University, Changchun, China, [4] CAS Key Laboratory of Forest Ecology and Management, Institute of Applied Ecology, Chinese Academy of Sciences, Shenyang, China

Sustaining ecosystem services in alpine regions is a pressing global challenge given future accelerating environmental changes. Understanding how future climate change and land use/cover change (LUCC) drive ecosystem service will be important in this challenge. However, few studies have considered the combined effects of future climate change and LUCC on ecosystem services. We assessed water yield and soil retention services and their drivers in the Changbai mountains region (CBMR) from the 2020 to 2050s using the Integrated Valuation of Ecosystem Services and Trade-offs (InVEST) model and factor control experiments. Water yield decreased by 2.80% and soil retention increased by 6.14% over the 30 years. Climate change decreased water yield and increased soil retention, while LUCC decreased both water yield and soil retention. The interactive effects between climate change and LUCC had relatively small inhibitory effects on water yield and large facilitation effects on soil retention. Changes in water yield were mainly attributed to climate change, while soil retention was largely influenced by interaction. Our study highlights the individual and interactive contributions of future climate change and land use to ecosystem service in the mountains region, which can provide important information for informed future land management and policy making for sustaining diverse ecosystem services.

Keywords: water yield, soil retention, future climate change, land use and land cover change, interactive effects, InVEST model, CLUE-S model

OPEN ACCESS

Edited by:
Fan Zhang,
Institute of Geographic Sciences and Natural Resources Research (CAS), China

Reviewed by:
Dragos George Zaharescu, Georgia Institute of Technology, United States
Fengping Li, Jilin University, China
Huakun Zhou, Key Laboratory of Restoration Ecology in Cold Regions, Northwest Institute of Plateau Biology (CAS), China

***Correspondence:**
Wen J. Wang
wangwenj@iga.ac.cn

Specialty section:
This article was submitted to Environmental Informatics and Remote Sensing, a section of the journal Frontiers in Ecology and Evolution

Received: *14 January 2022*
Accepted: *21 February 2022*
Published: *14 March 2022*

Citation:
Wang H, Wang WJ, Wang L, Ma S, Liu Z, Zhang W, Zou Y and Jiang M (2022) Impacts of Future Climate and Land Use/Cover Changes on Water-Related Ecosystem Services in Changbai Mountains, Northeast China. Front. Ecol. Evol. 10:854497. doi: 10.3389/fevo.2022.854497

INTRODUCTION

Ecosystem services are benefits that people derive from natural ecosystems, and they act as an important bridge between natural ecosystems and human well-being (Steffen et al., 2015; Gomes et al., 2021). Since the twentieth century, the warming climate has triggered extreme weather, and population expansion and food security have led to urban and cropland expansion. These changes

have seriously affected ecosystem sustainability, and further led to the degradation and loss of ecosystem services (Buitenwerf et al., 2018). Therefore, a greater understanding of future global change trajectories and their effects on ecosystem services provided an important basis for future ecosystem management and decision-making.

Climate change and land use are direct drivers of many ecosystem services and can affect ecosystem distribution and thus determine ecosystem services supply (Kuglerová et al., 2020). Climate change also increases the frequency and severity of extreme events, such as high-winds and extreme temperature fluctuations than can alter ecosystem biophysical processes, and therefore ecosystem services. These events are expected to become even more serious threat in the next decade (Fezzi et al., 2015; Daneshi et al., 2021). Land use/cover change (LUCC) by human-induced directly affects ecosystem composition and configuration and ultimately their ability to provide ecosystem services (Fu et al., 2017; Augustynczik and Yousefpour, 2021). For instance, in alpine regions LUCC significantly affects ecosystem services through changing carbon balance and water flow (Lawler et al., 2014). Spatial changes in land use also have a significant impact on the future provision and location of ecosystem services (Ricke et al., 2018). Many studies have used LUCC as a proxy or visual representation of ecosystem service change to convey potential future development and assess environmental change (Ladouceur et al., 2021; Zambon et al., 2021). Numerous modeling studies on changes in ecosystem services and their contributing factors have been conducted, but typically they have focused on the independent effects of climate change or LUCC. Few studies have considered the combined impacts of climate and land use change on ecosystem services under future climate change conditions (Runting et al., 2017; Guo et al., 2020).

Mountains cover 22% of the earth's surface, are home to 915 million people, and provide a range of important ecosystem services, such as timber, water supply, and wildlife habitat (Romeo et al., 2015). Mountains experience higher rates of temperature rise than lowlands, therefore they are more sensitive to the effects of climate change, and they are also very susceptible to land use changes impacts due to their high elevation and slope, which in turn affect ecosystem function and services (Kim et al., 2017). Thus, more assessment and monitoring of ecosystem services in mountain areas are needed to maintain ecosystem health under increasing environmental change (Egan and Price, 2017; Bai et al., 2019). The Changbai mountains region (CBMR) is a dormant active volcano and provides a variety of ecological services to the region, such as water provision, habitat, tourism, and carbon sink. It is also the source of the Songhua River, the largest river in Northeast, and precipitation runoff from the mountains also provides important recharge for other local rivers (e.g., Yalu River and Heilongjiang River) (Song et al., 2020). However, the CBMR environment has experienced unprecedented climate change (warming and drying) and human disturbances (e.g., urbanization, reclamation, deforestation), which have profoundly altered ecosystem structure and function. Historical climate data and projections indicate that warming and drying of the CBMR region will become more pronounced in the future and will be accompanied by more frequent extreme weather events (Zhang et al., 2021). Additionally, tourism development and food security-induced urban expansion have changed the natural trajectory of the LUCC, creating a series of land and environmental problems such as land degradation and water pollution (Wang et al., 2021).

To achieve a balance between regional development and environmental protection in the CBMR, the Chinese government implemented a series of measures to improve the fragmented ecological environment [e.g., establishment of a National Nature Reserve in (1986) (Guo et al., 2014)], and then enacted several ecological restoration projects [e.g., Grain for Green Project in (1999) (Cao et al., 2009) and Natural Forest Protection Project in (2000) (Wei et al., 2014)]. Recent studies have shown that these land use decisions significantly enhanced the CBMR carbon sink, and reduced wind-sand erosion (Mao et al., 2019). Some studies also found increased woodlands cover reduced surface runoff, which in turn affected downstream water use patterns (Feng et al., 2022). However, these studies generally focused on past-to-present changes in ecosystem services, or the effects of ecological projects on a particular ecosystem service, and do not provide a comprehensive assessment on the combined impacts of climate change and land use decisions on ecosystem services under an uncertain future. Thus, a deeper understanding of how climate change and policy-driven LUCC affect ecosystem services and quantifying these drivers can inform future land use decisions and natural resource management.

We focus on two types ecosystem services in CBMR: water yield and soil retention services, the quality of them is an important criterion for assessing the ecological health of alpine regions. CBMR has high vegetation cover, requires considerable water for growth, and is highly susceptible to soil erosion from abundant summer precipitation and steep slope. To better understanding the combine effects of future climate change and LUCC on ecosystem services. We first simulated climate change and LUCC for CBMR in 2050, and then used the InVEST model to assess water yield and soil retention under future climate and land use scenarios. We address the following questions in the CBMR: (1) how do climate and land use change under high emission scenarios *SSP 8.5* and environmental protection policies, (2) how do ecosystem services change spatially and temporally, and (3) what are the individual and interactive effects of future climate and land use changes on water yield and soil retention?

MATERIALS AND METHODS

Study Area

Changbai mountain region (CBMR) is located in Northeast China (126.49°E to 129.64°E, 41.18°N to 43.70°N). It includes Helong, Linjiang, Fusong, Antu, and Changbai Counties and is dominated by alpine terrain, with the highest peak in Northeast China, Baiyun Peak (2, 666 m above sea level). The CBMR land area is approximately 2.42×10^4 km^2, accounting for 13% of Jilin Province, China (**Figure 1**). CBMR is characterized by a typical temperate continental monsoonal climate with hot and rainy

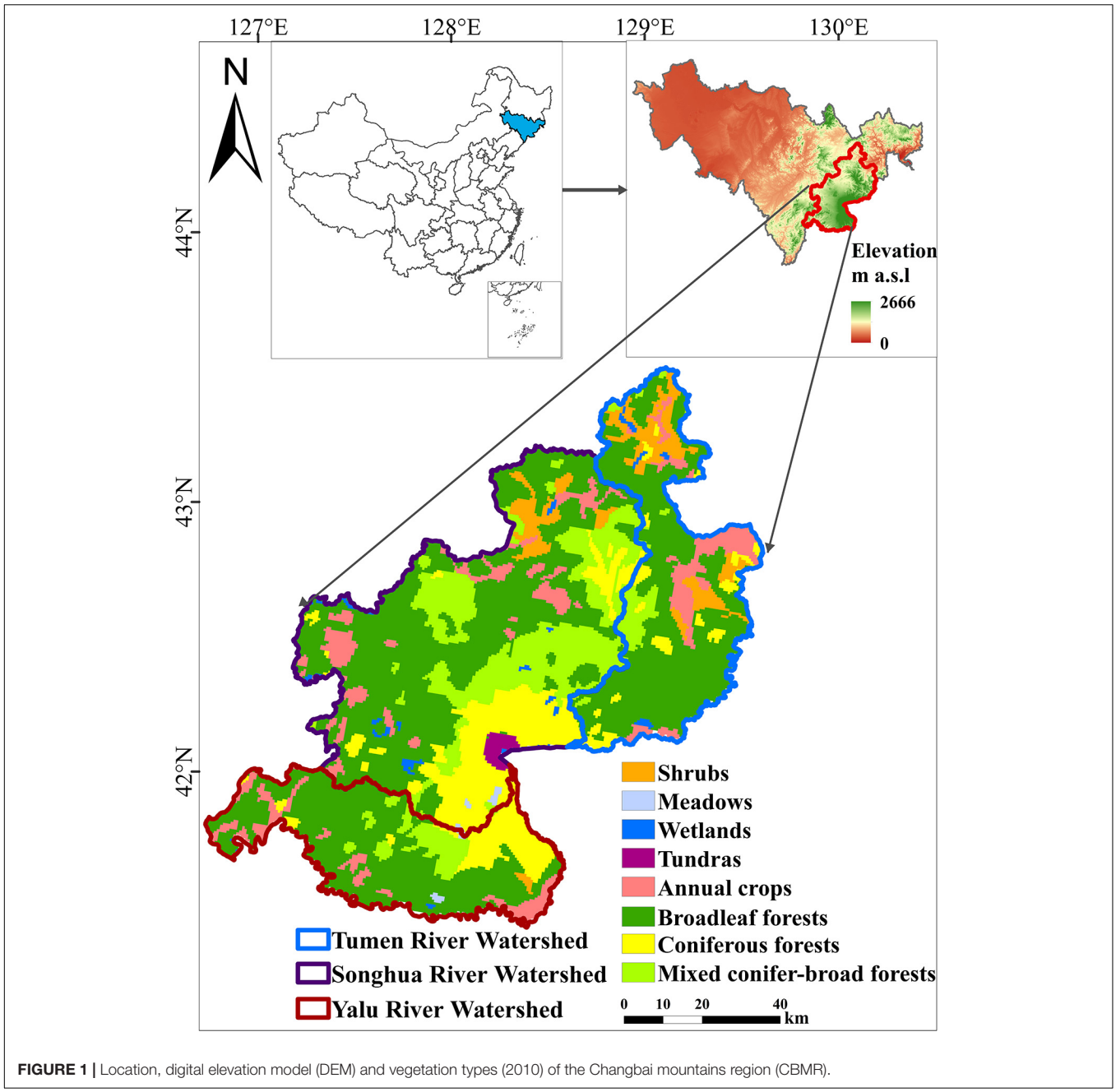

FIGURE 1 | Location, digital elevation model (DEM) and vegetation types (2010) of the Changbai mountains region (CBMR).

summers, and cold and dry winters. Over the past 30 years, the average annual temperature was 4.38°C, and the average annual precipitation was 742 mm (Wang et al., 2020).

Changbai mountain region can be divided into three watersheds based on terrain and catchment area (**Figure 1**). The Songhua River Watershed (SRW) is the largest (about 53.52%), and its main vegetation types are broadleaf, mixed conifer-broadleaf, and coniferous forests. The Yalu River Watershed (YRW) is the smallest (about 24.54%), and its main vegetation types are broadleaf and coniferous forests. The main vegetation types in the Tumen River basin (TRW) are broadleaf forests and annual cropland (**Figure 1**).

Current Climate and Land Use Data

The meteorological data were obtained from the China Meteorological Data Sharing Service,[1] and included daily temperature, precipitation, and solar radiation for 2016–2020 at 1 km resolution. Land use data at 30 m resolution for 2020 was obtained from the National Earth System Science Data Center.[2] Digital elevation model (DEM) data were obtained from the U.S. Geological Survey[3] at 90 m resolution.

[1]http://data.cma.cn/
[2]http://www.geodata.cn/
[3]http://www.usgs.gov/

Future Climate and Land Use Change Scenarios

We simulated future climate and land use scenarios for the 2050s (2045–2050). Since the high emission scenario (SSP 8.5) assumes a business-as-usual-high-end emissions scenario by the end of the century (Jacob et al., 2014), we used it to assess future climate change effects. The CLUE-S model was used to determine future land use based on historical trends, in which ecological protection policy was the main driving factor.

Future Climate Data

Future climates for the period 2045–2050 were obtained from the Coupled Model Intercomparison Project (Phase 6).[4] We assembled daily precipitation, minimum/maximum temperature, and radiation data according to predictions of the CESM1-BGC, CCSM4, CNRM-CM5, FGOALS-g2, MIROC5, and MRI-CGCM3 global models under the *SSP 8.5* scenario, and chosen these six models because they have been validated to have good applicability in the Changbai Mountains (Wang et al., 2019). Then, we regionalized it to 1 km resolution for CBMR using the WFR-ARW regional dynamical model.

Land Use/Cover Change Projections

The CLUE-S (The Conversion of Land Use and its Effects at Small Region Extent) model was used to simulate land use/cover in 2050. CLUE-S is a spatially explicit land use model that simulates dynamic competition between different land use types. It is based on high-resolution (usually better than 1 km) spatial image data and is suitable for simulating land use change at small and medium spatial scales. The model includes spatial and non-spatial modules. The non-spatial module calculates land use demand based on the analysis of natural, social and economic factors. The spatial module uses a raster system to translate these demands into land use changes based on probabilities and rules for different land use types (Verburg et al., 2002).

The model requires three main types of input data: location suitability, spatial policies and restrictions, and conversion settings. First, location suitability was determined by quantifying the relationship between land use/cover patterns and constraints (Land Management Policies) through logistic regression (Verburg et al., 2002). Secondly, spatial constraints were used to limit land use/cover variables by setting woodlands and wetlands as environmental constraints. Finally, conversion settings were determined by a land use conversion matrix of past time series. A detailed description of CLUE-S can be found in Verburg and Overmars (2009).

We validated model accuracy by comparing simulation results for 2000, 2010, and 2020 with satellite remote sensing data. The Kappa index was used to assess the consistency between the simulation results and remote sensing data (Vliet et al., 2011). The Kappa index was 0.8554, 0.8827, and 0.8814 in 2000, 2010, and 2020, respectively, which demonstrated that the CLUE-S simulation results were reliable, selected indexes and parameters conformed to requirements, and future simulation results were in accordance with development trends and had practical significance.

[4]https://esgf-node.llnl.gov/projects/cmip6/

Integrated Valuation of Ecosystem Services and Trade-Offs Model Parameterization

We used the Water Yield module and the Sediment Delivery Ratio module of the InVEST model to estimate ecosystem services under current and future scenarios. The Water Yield module is based on the Budyko curve and the Sediment Delivery Ratio module is based on the Revised Universal Soil Loss Equation (RUSLE), which are described in Appendix 1 (**Supplementary Material**). The InVEST model is mainly based on spatial data (land use data and climate data) and assesses the value of ecosystem services through empirical models. Due to its ease of accessibility and rich functionality, the model has been widely used in ecological and hydrological studies (Luetzenburg et al., 2020; Morán-Ordóez et al., 2021). All models were parameterized and tested at the CBMR (Xiao et al., 2002; Yu et al., 2018; Li et al., 2019). **Table 1** briefly describes the data sets used to assess the two ecosystem services. Details of the model parameterization can be found in Appendix 2 (**Supplementary Material**). The precipitation, temperature, and reference evapotranspiration datasets were spatially interpolated for all sites using the ArcGIS 10.3 platform with a spatial resolution of 1,000 m. A detailed description of the InVEST model can be found in Sharp et al. (2018).

Experimental Design

We designed a factor control analysis through controlling two influential factors of climate and land use to assess climate change, LUCC and their interactive effects on ecosystem services. We generated four simulation scenarios by integrating climate and land use scenarios at 2020s (2016–2020) and 2050s (2045–2050) (**Table 2**). Then we used the InVEST model to assess water yield and soil retention under the four simulated scenarios.

We determined the magnitude of effects of climate change and land use by the difference between the baseline scenario (Scenario 1) and the climate change only (Scenario 3) or LUCC only (Scenario 2) scenarios. We determine the combined climate and land use effects by the difference between the 2050s simulation scenario (Scenario 4) and the baseline scenario (Scenario 1), and then determined the interactive effects by subtracting the individual effects of climate change and LUCC from the combined effects.

RESULTS

Future Climate and Land Use Change

The CBMR climate became warmer and drier from the 2020 to 2050s, with 92% of the area warming, and about 56% showing a drying trend. Under the high emissions scenario, annual mean temperature increased from 5.25°C in the 2020s to 5.57°C in the 2050s, an increase of 6.10%, with the most pronounced

TABLE 1 | Data requirement for the integrated valuation of ecosystem services and trade-offs (InVEST) model (WY, Water Yield module; SDR, Sediment Delivery Ratio module).

Date	Type	Resolution	Data sources	Related module
Land use images	Raster	30 m	National Earth System Science Data Center (see text footnote 2)	WY, SDR
Vegetation images	Raster	30 m	National Earth System Science Data Center (see text footnote 2)	WY, SDR
Precipitation	Raster	1 km	National Meteorological Information Center (http://data.cma.cn/user/toLogin.html)	WY
Reference evapotranspiration	Raster	1 km	$ET_0 = 0.0013 \times 0.408 \times RA \times (T_{average} + 17) \times (T_{differences} - 0.0123P)^{0.76}$	WY
Soil depth	Raster	1 km	Harmonized World Soil Database (http://westdc.westgis.ac.cn/data)	WY
Plant available water content	Raster	30 m	PAWC = 0.301 × clay% + 0.369 × silt% + 0.045 × organic%	WY
DEM	Raster	90 m	U.S. Geological Survey (see text footnote 3)	SDR
Rainfall erosivity index	Raster	1 km	$R = 0.067P_d^{1.627}$	SDR
Soil erodibility	Raster	30 m	$K = \{0.2 + 0.3\exp[-0.25\text{sand}\,(1 - silt/100)]\}\left(\frac{silt}{clay+silt}\right)^{0.3}\left(1 - \frac{0.25 \times \text{organic}}{\text{organic}+\exp(3.72-0.95 \times \text{organic})}\right)\left(1 - \frac{0.7 \times sand}{sand+\exp(-5.51+22.9 \times sand)}\right)$	SDR

TABLE 2 | Land use and climate scenario settings.

	Land use 2020s	Land use 2050s
Climate 2020s	Scenario 1	Scenario 2
Climate 2050s	Scenario 3	Scenario 4

warming in the SRW. A decreasing annual precipitation trend was significant, lowering from 773 mm in the 2020s to 691 mm in the 2050s, a decrease of 10.65%. The decrease occurred mainly in TRW and SRW (**Figures 2A,B**).

Although the limits of environmental protection constraints such as the Natural Forest Protection Project in (2000) (Wei et al., 2014) and the Grain for Green Project in (1999) (Cao et al., 2009) were considered in the future land use simulation, significant changes occurred in the CBMR due to human disturbances. Woodlands, the dominant land cover type would decrease by 7.79% (1.87×10^3 km^2) and be converted mainly to cropland and grassland, with a significant decrease in SRW. Croplands, converted from woodland and barren land, would increase the most at 4.10% (0.98×10^3 km^2), mainly in SRW and YRW. Grasslands, built-lands and wetlands (natural and artificial) experienced varying degrees of increase, with 2.64% (0.64×10^3 km^2), 0.69% (0.16×10^3 km^2) and 0.63% (0.15×10^3 km^2), respectively (**Figures 2C,D**).

Ecosystem Service Changes

The CBMR showed a slight decreasing trend in water yield, from 617 mm/km^2 in the 2020s to 600 mm/km^2 in the 2050s, a decrease of 2.80%. The most pronounced decrease was in the eastern mountains, while the southern mountains showed a slight increase (**Figures 3**, **4**). Sub-regionally, TRW and SRW showed decreases in water yield (due to decreased precipitation), of 29 mm/km^2 (5.50%) and 37 mm/km^2 (5.91%) respectively, while YRW showed an increase, of 38 mm/km^2 (5.53%) (**Figures 3**, **4**).

Soil retention in the CBMR significantly increased (due to the decreased precipitation and interactive effects), from 390 t/km^2 in the 2020s to 414 t/km^2 in the 2050s, an increase of 6.14%. The increases were mainly in the eastern mountains, while decreases occurred in the northern hills (**Figures 3**, **4**). The largest increase occurred in the YRW, of 42.98 t/km^2 (7.66%), followed by SRW, of 26.08 t/km^2 (8.66%). In the TRW there was a significant decrease, of 8.23 t/km^2 (1.85%) (**Figures 3**, **4**).

Effects of Climate and Land Use

Climate change was the dominant factor affecting water yield changes in the CBMR, followed by interactive effects and LUCC. Interactive effects were the most significant driving factor for soil retention changes, followed by climate change and LUCC.

Individual Effects of Climate and Land Use

Climate change decreased water yield by 9.60 mm/km^2 for the whole region (1.55%) from the 2020s to 2050s, with most pronounced effects in the southern mountainous area (**Figures 5A**, **6**). Climate change decreased water yield by 3.50 and 3.63% in the TRW and the SRW, respectively, and increased water yield by 4.10% in the YRW. Climate change increased soil retention in the CBMR by 11.17 t/km^2 (2.86%) from the 2020 to 2050s, mainly in the northern hills (**Figures 5B**, **6**). Climate change increased soil retention in TRW and SRW by 1.85 and 6.71%, respectively, while in the YRW decreased by 1.08%.

Land use decreased water yield in the CBMR by 2.90 mm/km^2 (0.50%) from the 2020 to 2050s, mainly in the northern hills (**Figures 5A**, **6**). Land use had negative effects on water yield for all three watersheds, decreasing by 1.16, 1.60, and 0.63% in the TRW, SRW, and YRW, respectively. Land use also decreased soil retention in the CBMR by 8.14 t/km^2 (2.08%), mainly in the southern mountainous region (**Figures 5B**, **6**). Land use effects decreased soil retention by 2.35 and 6.18% in the TRW and SRW, respectively, while increasing it by 3.36% in the YRW.

Interactive Effects

Interactive effects between climate change and LUCC had significant impacts on CBMR future ecosystem services, with inhibitory effects on water yield and facilitation effects on soil retention. Interactive effects decreased water yield by 4.36 mm/km^2 (0.71%) from the 2020 to 2050s in the CBMR, with the most pronounced inhibitory effects occurring in the southern and eastern mountainous region (**Figures 5C**, **6**). Interactive effects increased soil retention by 20.22 t/km^2 (5.17%) from the 2020 to 2050s in the CBMR, mainly in the eastern and southern mountainous areas (**Figures 5D**, **6**).

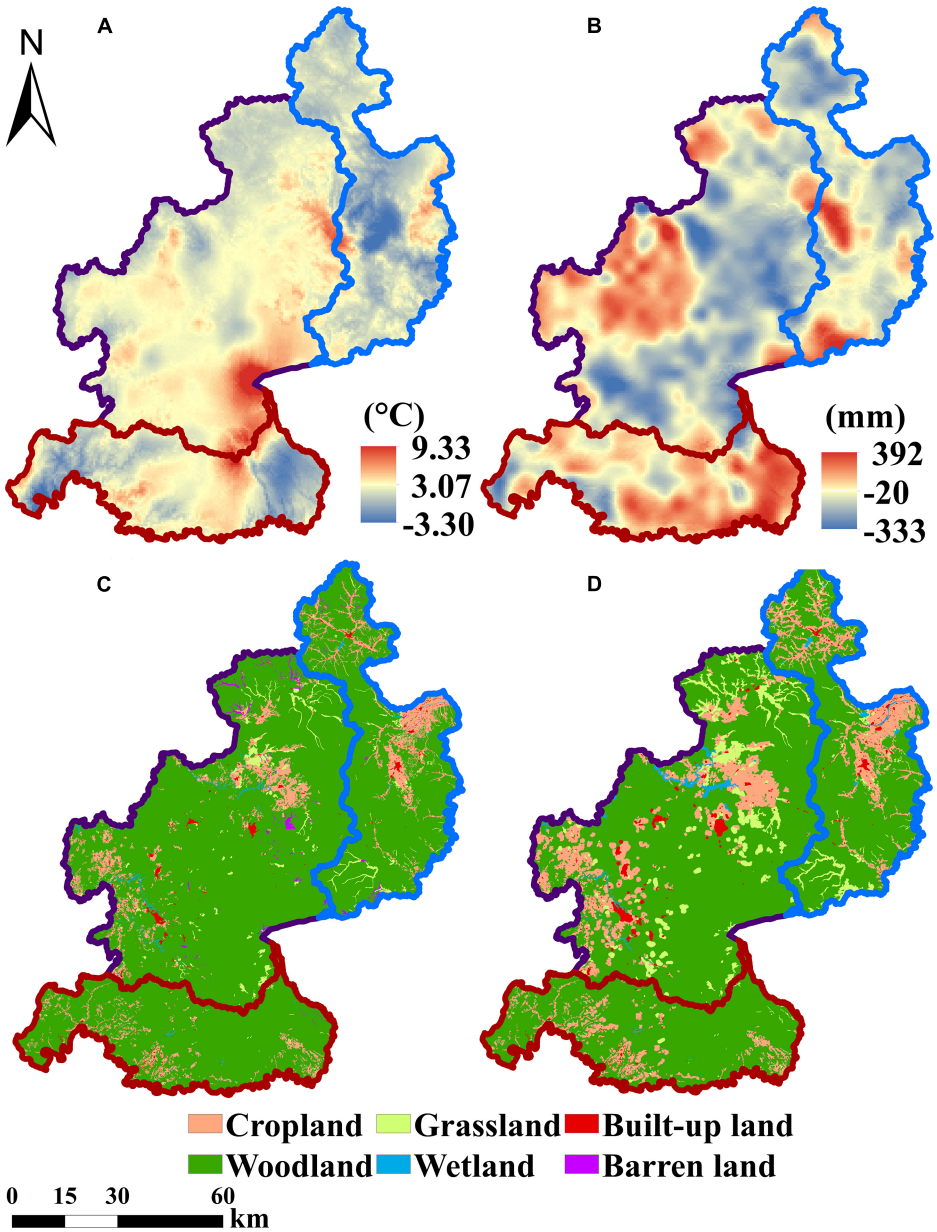

FIGURE 2 | Spatial changes in annual average temperature **(A)** and annual precipitation **(B)** and during 2020–2050s, spatial distributions of land use for year 2020 **(C)** and year 2050 **(D)**.

DISCUSSION

Water yield changes were mainly attributed to climate change, while soil retention was largely influenced by interactions. Recent studies noted that precipitation patterns directly determine water yield, especially in mountainous areas, where precipitation is the main recharge (Braun et al., 2019). For example, Yin et al. (2022) found that water yield changes in North China were more sensitive to precipitation than temperature, and the changes demonstrated a trend consistent with the precipitation change from 1995 to 2015. Tirupathi and Shashidhar (2020) found that a 9.5% precipitation increase led to a doubling in water yield during 2010–2040 under the Representative Concentration Pathways scenario 8.5 in the Krishna River basin of India. Meanwhile, increasing temperature can also alter evapotranspiration to exacerbate decreasing water yield (Bai et al., 2020). However, soil retention in mountainous areas was more susceptible to precipitation intensity due to the high altitude and slope effects (Soto et al., 2021). Decreased precipitation can diminish slope erosion and reduce soil scouring by affecting runoff (Qiu and Turner, 2013; O'Connor et al., 2019). Although the CBMR has a temperate

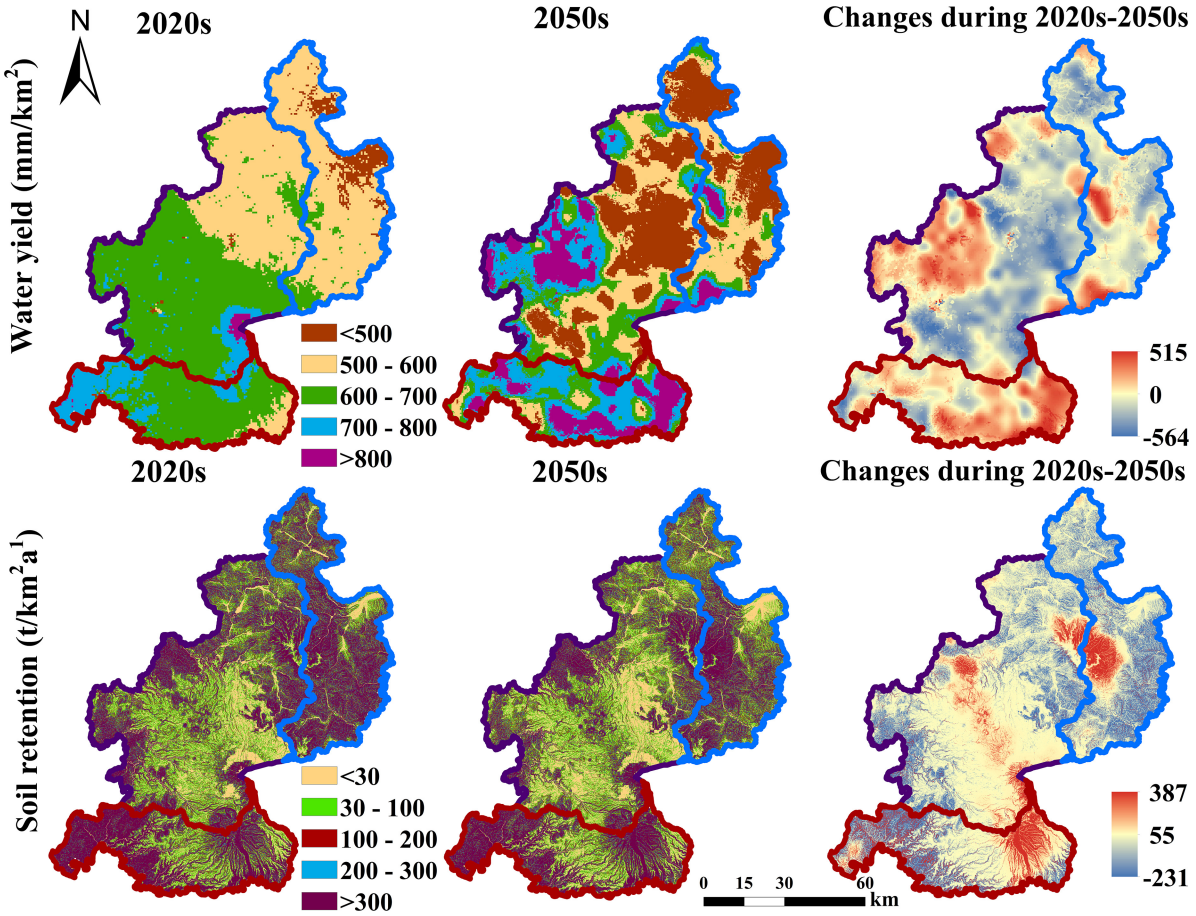

FIGURE 3 | Spatial distributions of water yield and soil retention in 2020 and 2050s and changes during 2020–2050s.

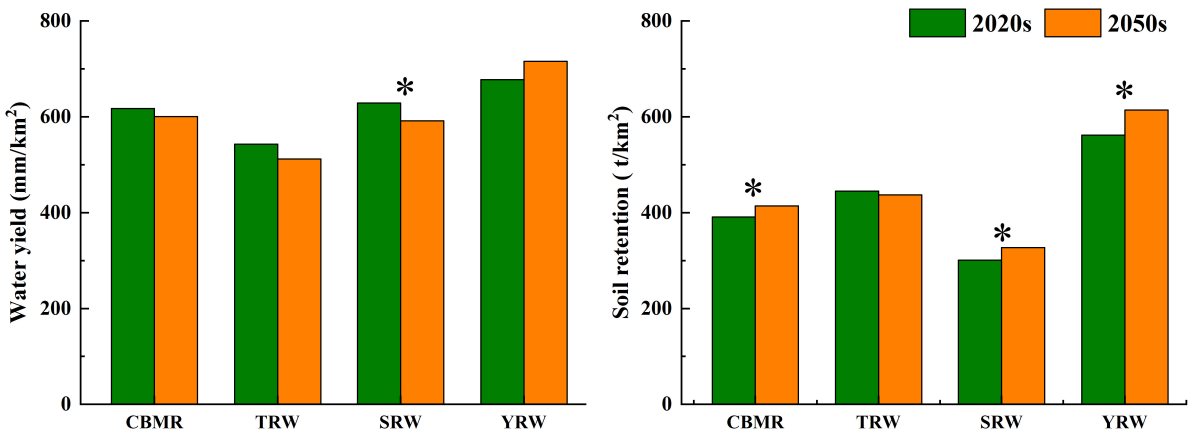

FIGURE 4 | Water yield and soil retention in 2020 and 2050s for the Changbai mountains region (CBMR) and three watersheds (the sign "*" indicated significant differences at the 0.05 level).

monsoonal continental climate, it is significantly influenced by topography and humid oceanic air flow. Precipitation is abundant throughout the year, especially from July to September (Li et al., 2019). Therefore, future warming and drying climates will continue to lead to increased soil retention in the CBMR. This is consistent with southern Europe, where Mediterranean (Ebro), Alpine (Adige), and continental (Sava) basins are expected to experience a 20%

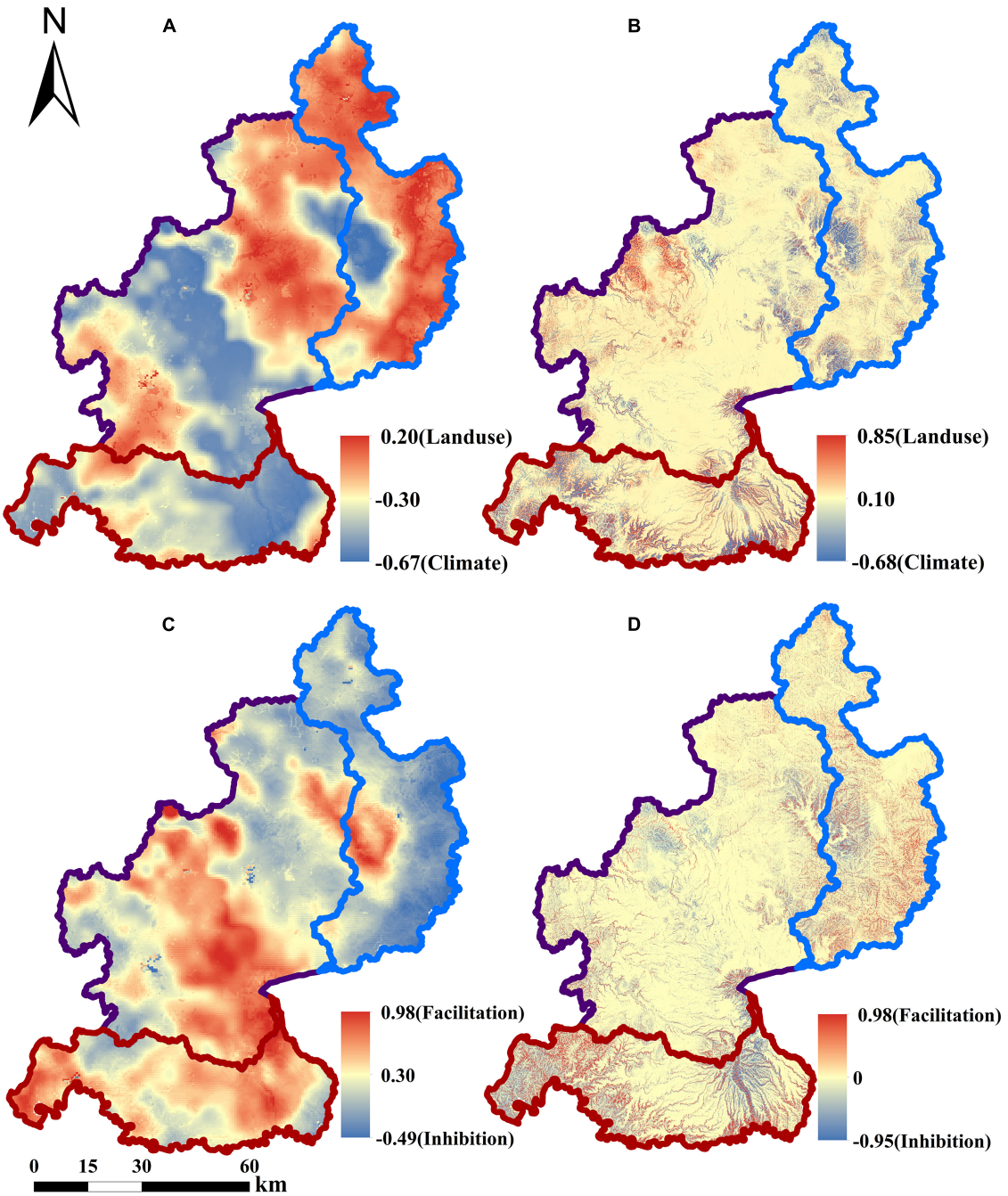

FIGURE 5 | Spatial distributions of the individual effects (**A**: Water yield; **B**: Soil retention) and interactive effects (**C**: Water yield; **D**: Soil retention) of LUCC and climate change.

increase in soil retention by 2050 due to a 40% decrease in water availability caused by climate change and irrigation (Jorda-Capdevila et al., 2019).

In our future land use simulation (2020–2050s), CBMR land use conversion area reached 18.20% despite the implementation of ecological restoration projects. Some studies have found that land use directly determined vegetation type, which further influenced surface runoff and evapotranspiration (Khorchania et al., 2020). The greatest land use changes predicted in our study were in the TRW and SRW, with a significant shift from woodlands to grasslands and croplands. These changes reduced watershed water yield because woodlands have a greater water storage capacity than other vegetation type (Grimm et al., 2013). Furthermore, some studies have found that the expanded croplands, especially an increase in paddy fields led a greater demand for irrigation, which would directly affect evaporation

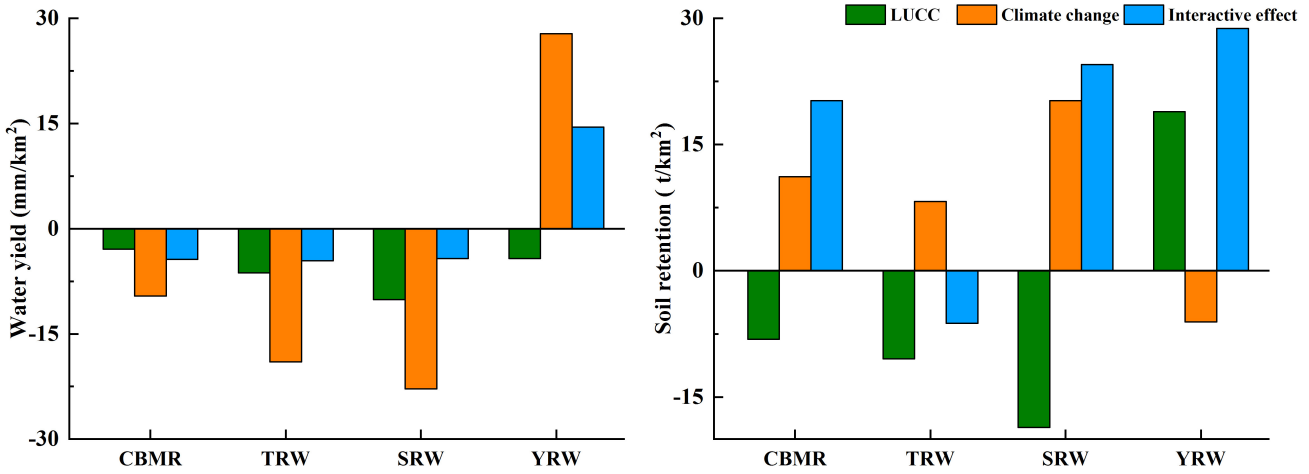

FIGURE 6 | The effect sizes of climate change, land use/cover change (LUCC) and their interaction on changes in water yield and soil retention during 2020–2050s for the Changbai mountains region (CBMR) and three watersheds.

and runoff, in turn decreasing water yield (Cord et al., 2017). In the TRW and SRW watersheds, future LUCC will similarly decrease soil retention. This is because in most regions, forest canopies have a stronger precipitation interception capacity than grasslands and annual crops, especially in mountainous areas, while the complex root system of woodlands also increases soil stability (Felipe-Lucia et al., 2020). For example, compared to our study, Xia et al. (2021) found that the GFGP project in the Liaohe River basin of China resulted in soil loss of 4.33×10^5–2.94×10^5 t/year from 2007 to 2015. In mountainous areas of Spain, the revegetation of Aragón between the mid-20th and early 21st centuries led to a significant increase in water supply (>1,000%) and soil retention (>400%) (Brunoa et al., 2021).

In the CBMR, climate change interacts with LUCC to significantly impact ecosystem services, especially soil retention on the landscape. Predicted future land use change-induced soil retention primarily occurred in the relatively low elevation of western and northern flanks, which were most vulnerable to climate change. Although woodland loss reduced soil retention, decreases in precipitation-based erodibility interact with the reduction of surface runoff to enhance soil retention (Morán-Ordóez et al., 2020). For water yield, future warmer and drier climates and decreased water holding capacity by ecosystems due to declining woodlands will exacerbate decreasing water yield (Krueger et al., 2019). For example, Clerici et al. (2019) used IPCC-LUCC scenarios to analyze the effects of LUCC and climate change on water provision and carbon storage in Colombian Andes from 2016 to 2046. The results showed that climate change scenarios had a greater impact on water availability than LUCC scenarios, and the interactive between climate change and LUCC significantly reduced the water provision.

It should be noted that there were several limitations in our study. First, our simulations of future climate did not consider the effects of mountain microclimates, which can increase climate uncertainty (Bagstad et al., 2013). Secondly, land use data resolution was 30 m, while the downloaded and simulated climate data was 1 km resolution, which may increase uncertainty of the simulation results (Zhang et al., 2019). However, our simulations predicted the climate and land use conditions in the CBMR over the next 30 years, and quantitatively assessed through factor control experiments the effects of climate and land use individually, interactively and in combination with ecosystem service changes. Our study can provide important information for government land use decisions and natural resource management in response to future environmental changes.

CONCLUSION

In the CBMR, we assessed water yield, soil retention and the factors controlling them from the 2020 to 2050s using the InVEST model and factor control analyses. Water yield decreased and soil retention increased significantly over the three decades. Climate change decreased water yield and increased soil retention, while LUCC decreased both water yield and soil retention. The interactive effects of climate change and LUCC had relatively small inhibitory effects on water yield and largely facilitated on soil retention. Changes in water yield were mainly attributed to climate change, while soil retention was largely influenced by interactions. Our results highlight the driver impacts of climate and land use on ecosystem services and provide important information for governments to develop land-use and ecological management policies to tackle future environmental changes.

DATA AVAILABILITY STATEMENT

The original contributions presented in the study are included in the article/**Supplementary Material**, further inquiries can be directed to the corresponding author.

AUTHOR CONTRIBUTIONS

HW and WW: conceptualization, writing, and editing. HW, WW, and ZL: methodology. HW, LW, SM, YZ, WZ, and MJ: data curation and analysis. All authors contributed to the article and approved the submitted version.

FUNDING

This study was jointly funded by the Development and Application of National Key Research and Development Plan (2019YFC0409102), the National Natural Science Foundation of China (U19A2023, 41871045, 41922006, and 41801081), the Chinese Academy of Sciences (Y7H7031001), the Natural Science Foundation of Jilin Province, China (20200201047JC), and the Key Laboratory of Geographical Processes and Ecological Security in Changbai Mountains, Ministry of Education.

SUPPLEMENTARY MATERIAL

The Supplementary Material for this article can be found online at: https://www.frontiersin.org/articles/10.3389/fevo.2022.854497/full#supplementary-material

REFERENCES

Augustynczik, A., and Yousefpour, R. (2021). Assessing the synergistic value of ecosystem services in European beech forests. *Ecosyst. Serv.* 49:101264. doi: 10.1016/j.ecoser.2021.101264

Bagstad, K. J., Semmens, D. J., Waage, S., and Winthrop, R. (2013). A comparative assessment of decision-support tools for ecosystem services quantification and valuation. *Ecosyst. Serv.* 5, 27–39. doi: 10.1016/j.ecoser.2013.07.004

Bai, P., Liu, X., Zhang, Y. Q., and Liu, C. M. (2020). Assessing the impacts of vegetation greenness change on evapotranspiration and water yield in China. *Water Resour. Res.* 56:e2019WR027019. doi: 10.1029/2019WR027019

Bai, Y., Ochuodho, T. O., and Yang, J. (2019). Impact of land use and climate change on water-related ecosystem services in Kentucky, USA. *Ecol. Indic.* 102, 51–64. doi: 10.1016/j.ecolind.2019.01.079

Braun, D., Jong, R., Schaepman, M. E., Furrer, R., Hein, L., Kienast, F., et al. (2019). Ecosystem service change caused by climatological and non-climatological drivers: a Swiss case study. *Ecol. Applic.* 29:e01901. doi: 10.1002/eap.1901

Brunoa, D., Sorandoab, R., Álvarez-Farizoa, B., Castellanoa, C., Céspedes, V., Gallardo, B., et al. (2021). Depopulation impacts on ecosystem services in Mediterranean rural areas. *Ecosyst. Serv.* 52:101369. doi: 10.1016/j.ecoser.2021.101369

Buitenwerf, R., Sandel, B., Normand, S., Mimet, A., and Svenning, J. C. (2018). Land surface greening suggests vigorous woody regrowth throughout European semi-natural vegetation. *Glob. Change Biol.* 24, 5789–5801. doi: 10.1111/gcb.14451

Cao, S. X., Chen, L., and Liu, Z. D. (2009). An investigation of Chinese attitudes toward the environment: case study using the Grain for Green Project. *Ambio* 38, 55–64. doi: 10.1579/0044-7447-38.1.55

Clerici, N., Cote-Navarro, F., Escobedo, F. J., Rubiano, K., and Villegas, J. C. (2019). Spatio-temporal and cumulative effects of land use-land cover and climate change on two ecosystem services in the Colombian Andes. *Sci. Total Environ.* 685, 1181–1192. doi: 10.1016/j.scitotenv.2019.06.275

Cord, A. F., Brauman, K. A., Chaplin-Kramer, R., Huth, A., Ziv, G., and Seppelt, R. (2017). Priorities to advance monitoring of ecosystem services using earth observation. *Trends Ecol. Evol.* 32, 416–428. doi: 10.1016/j.tree.2017.03.003

Daneshi, A., Brouwer, R., Najafinejad, A., Panahi, M., and Maghsood, F. F. (2021). Modelling the impacts of climate and land use change on water security in a semi-arid forested watershed using InVEST. *J. Hydrol.* 593:125621. doi: 10.1016/j.jhydrol.2020.125621

Egan, P., and Price, M. F. (2017). *Mountain Ecosystem Services and Climate Change*. Paris: The United Nations Educational, Scientific and Cultural Organization.

Felipe-Lucia, M. R., Soliveres, S., Penone, C., Fischer, M., Ammer, C., Boch, S., et al. (2020). Land-use intensity alters networks between biodiversity, ecosystem functions, and services. *Proc. Natl. Acad. Sci. U.S.A.* 117, 28140–28149. doi: 10.1073/pnas.2016210117

Feng, M. M., Zhang, W. G., Zhang, S. Q., Sun, Z. Y., Li, Y., Huang, Y. Q., et al. (2022). The role of snowmelt discharge to runoff of an alpine watershed: evidence from water stable isotopes. *J. Hydrol.* 604:127209. doi: 10.1016/j.jhydrol.2021.127209

Fezzi, C., Harwood, A. R., Lovett, A. A., and Bateman, I. J. (2015). Erratum: the environmental impact of climate change adaptation on land use and water quality. *Nat. Climate Change* 5, 255–260. doi: 10.1038/nclimate2585

Fu, Q., Li, B., Hou, Y., Bi, X., and Zhang, X. S. (2017). Effects of land use and climate change on ecosystem services in Central Asia's arid regions: a case study in Altay Prefecture, China. *Sci. Total Environ.* 607-608, 633–646. doi: 10.1016/j.scitotenv.2017.06.241

Gomes, E., Inácio, M., Bogdzevi, K., Kalinauskas, M., Karnauskaitė, D., and Pereira, P. (2021). Future land use changes and its impacts on terrestrial ecosystem services: a review. *Sci. Total Environ.* 781:147716. doi: 10.1016/j.scitotenv.2021.146716

Grimm, N. B., Chapin, F. S., Bierwagen, B., Gonzalez, P., Groffman, P. M., Luo, Y., et al. (2013). The impacts of climate change on ecosystem structure and function. *Front. Ecol. Environ.* 11:474–482. doi: 10.1890/120282

Guo, X. Y., Zhang, H. Y., Wang, Y. Q., and Clark, J. (2014). Mapping and assessing typhoon-induced forest disturbance in Changbai mountain national nature reserve using time series landsat imagery. *J. Mt. Sci.* 12, 404–406. doi: 10.1007/s11629-014-3206-y

Guo, Y. H., Fang, G. H., Xu, Y. P., Tian, X., and Xie, J. K. (2020). Identifying how future climate and land use/cover changes impact streamflow in Xinanjiang Basin, East China. *Sci. Total Environ.* 710:136275. doi: 10.1016/j.scitotenv.2019.136275

Jacob, D., Petersen, J., Eggert, B., Alias, A., Christensen, O. B., Bouwer, L. M., et al. (2014). EURO-CORDEX: new high-resolution climate change projections for European impact research. *Reg. Environ. Change* 14, 563–578. doi: 10.1007/s10113-013-0499-2

Jorda-Capdevila, D., Gampe, D., García, V. H., Ludwig, R., Sabater, S., Vergoñós, L., et al. (2019). Impact and mitigation of global change on freshwater-related ecosystem services in Southern Europe. *Sci. Total Environ.* 651, 895–908. doi: 10.1016/j.scitotenv.2018.09.228

Khorchania, M., Nadal-Romeroa, E., Tague, C., Lasantaa, T., Zabalzaa, J., Lana-Renaultc, N., et al. (2020). Effects of active and passive land use management after cropland abandonment on water and vegetation dynamics in the Central Spanish Pyrenees. *Sci. Total Environ.* 717:137160. doi: 10.1016/j.scitotenv.2020.137160

Kim, I., Arnhold, S., Ahn, S., Le, Q. B., Kim, S. J., Park, S. J., et al. (2017). Land use change and ecosystem services in mountainous watersheds: predicting the consequences of environmental policies with cellular automata and hydrological modeling. *Environ. Model. Softw.* 122:103982. doi: 10.1016/j.envsoft.2017.06.018

Krueger, E., Rao, P. S. C., and Borchardt, D. (2019). Quantifying urban water supply security under global change. *Glob. Environ. Change* 56, 66–74. doi: 10.1016/j.gloenvcha.2019.03.009

Kuglerová, L., Jyvsjrvi, J., Ruffing, C., Muotka, T., Jonsson, A., Andersson, A., et al. (2020). Cutting edge: a comparison of contemporary practices of riparian buffer retention around small streams in Canada, Finland, and Sweden. *Water Resour. Res.* 56:e2019WR026381. doi: 10.1029/2019WR026381

Ladouceur, E., Mcgowan, J., Huber, P., Possingham, H., Scridel, D., Klink, R. V., et al. (2021). An objective-based prioritization approach to support trophic

complexity through ecological restoration species mixes. *J. Appl. Ecol.* 59, 394–407. doi: 10.1111/1365-2664.13943

Lawler, J. J., Lewis, D. J., Nelson, E., Plantinga, A. J., Polasky, S., Withey, J. C., et al. (2014). Projected land-use change impacts on ecosystem services in the United States. *Proc. Natl. Acad. Sci. U.S.A.* 111, 7492–7497. doi: 10.1073/pnas.1405557111

Li, X. H., Farooqi, T. J. A., Jiang, C., Liu, S. R., and Sun, J. X. (2019). Spatiotemporal variations in productivity and water use efficiency across a temperate forest landscape of Northeast China. *Forest Ecosyst.* 6:22. doi: 10.1186/s40663-019-0179-x

Luetzenburg, G., Bittner, M. J., Calsamiglia, A., Renschler, C. S., Estrany, J., and Poeppl, R. (2020). Climate and land use change effects on soil erosion in two small agricultural catchment systems Fugnitz- Austria, CanRevull-Spain. *Sci. Total Environ.* 704:135389. doi: 10.1016/j.scitotenv.2019.135389

Mao, D. H., He, X. Y., Wang, Z. M., Tian, Y. L., Xiang, H. X., Yu, H., et al. (2019). Diverse policies leading to contrasting impacts on land cover and ecosystem services in Northeast China. *J. Clean. Prod.* 240:117961. doi: 10.1016/j.jclepro.2019.117961

Morán-Ordóez, A., Ameztegui, A., Cáceres, M. D., de-Miguelb, S., Lefèvref, F., Brotons, L., et al. (2020). Future trade-offs and synergies among ecosystem services in Mediterranean forests under global change scenarios. *Ecosyst. Serv.* 45:101174. doi: 10.1016/j.ecoser.2020.101174

Morán-Ordóez, A., Ramsauer, J., Coll, L., Brotons, L., and Ameztegui, A. (2021). Ecosystem services provision by Mediterranean forests will be compromised above 2°C warming. *Glob. Change Biol.* 27, 4210–4222. doi: 10.1111/gcb.15745

O'Connor, J., Santos, M. J., Rebel, K. T., and Dekker, S. C. (2019). The influence of water table depth on evapotranspiration in the Amazon arc of deforestation. *Hydrol. Earth Syst. Sci.* 23, 3917–3931. doi: 10.5194/hess-2019-47

Qiu, J. X., and Turner, M. G. (2013). Spatial interactions among ecosystem services in an urbanizing agricultural watershed. *Proc. Natl. Acad. Sci. U.S.A.* 110, 12149–12154. doi: 10.1073/pnas.1310539110

Ricke, K., Drouet, L., Caldeira, K., and Tavoni, M. (2018). Country-level social cost of carbon. *Nat. Climate Change* 8, 895–900. doi: 10.1038/s41558-018-0282-y

Romeo, R., Vita, A., Testolin, R., and Hofer, T. (2015). *Mapping the Vulnerability of Mountain Peoples to Food Insecurity*. Rome: FAO.

Runting, R. K., Bryan, B. A., Dee, L. E., Maseyk, F. J. F., Mandle, L., Hamel, P., et al. (2017). Incorporating climate change into ecosystem service assessments and decisions: a review. *Glob. Change Biol.* 23, 28–41. doi: 10.1111/gcb.13457

Sharp, R., Tallis, H. T., Ricketts, T., Guerry, A. D., Wood, S. A., Chaplin-Kramer, R., et al. (2018). *InVEST 3.5.0 User's Guide*. Arlington, VA: The Nature Conservancy.

Song, F., Su, F., Mi, C., and Sun, D. (2020). Analysis of driving forces on wetland ecosystem services value change: a case in Northeast China. *Sci. Total Environ.* 751:141778. doi: 10.1016/j.scitotenv.2020.141778

Soto, D. P., Donoso, P. J., Elgueta, C. Z., Ríos, A. I., and Promis, A. (2021). Precipitation declines influence the understory patterns in Nothofagus pumilio old-growth forests in northwestern Patagonia. *For. Ecol. Manag.* 491:119169. doi: 10.1016/j.foreco.2021.119169

Steffen, W., Richardson, K., Rockström, J., Cornel1, S. E., Fetzer, I., Bennett, E. M., et al. (2015). Planetary boundaries: guiding human development on a changing planet. *Science* 347:1259855. doi: 10.1126/science.1259855

Tirupathi, C., and Shashidhar, T. (2020). Investigating the impact of climate and land-use land cover changes on hydrological predictions over the Krishna river basin under present and future scenarios. *Sci. Total Environ.* 721:137736. doi: 10.1016/j.scitotenv.2020.137736

Verburg, P. H., and Overmars, K. P. (2009). Combining top-down and bottom-up dynamics in land use modeling: exploring the future of abandoned farmlands in Europe with the Dyna-CLUE model. *Landsc. Ecol.* 24, 1167–1181. doi: 10.1007/s10980-009-9355-7

Verburg, P. H., Veldkamp, W., and Limpiada, R. (2002). Modeling the spatial dynamics of regional land use: the CLUE-S model. *Environ. Manag.* 30, 391–405. doi: 10.1007/s00267-002-2630-x

Vliet, J. V., Bregt, A. K., and Hagen-Zanker, A. (2011). Revisiting kappa to account for change in the accuracy assessment of land-use change models. *Ecol. Model.* 222, 1367–1375. doi: 10.1016/j.ecolmodel.2011.01.017

Wang, L. J., Ma, S., Zhao, Y. G., and Zhang, J. C. (2021). Ecological restoration projects did not increase the value of all ecosystem services in Northeast China. *Forest Ecol. Manag.* 495:119340. doi: 10.1016/j.foreco.2021.119340

Wang, L., Wang, W. J., Du, H. B., Wu, Z. F., Shen, X. J., and Ma, S. (2020). Decreasing precipitation occurs in daily extreme precipitation intervals across China in observations and model simulations. *Climate Dyn.* 54, 2597–2612. doi: 10.1007/s00382-020-05120-w

Wang, L., Wang, W. J., Wu, Z. F., Du, H. B., Zong, S. W., and Ma, S. (2019). Potential distribution shifts of plant species under climate change in Changbai Mountains, China. *Forests* 10:498. doi: 10.3390/f10060498

Wei, Y. W., Yu, D. P., Lewis, B. J., Zhou, L., Zhou, W. M., Fang, X. M., et al. (2014). Forest carbon storage and tree carbon pool dynamics under natural forest protection program in northeastern China. *Chin. Geogr. Sci.* 24, 397–405. doi: 10.1007/s11769-014-0703-4

Xia, H. J., Kong, W. J., Zhou, G., and Sun, O. J. X. (2021). Impacts of landscape patterns on water-related ecosystem services under natural restoration in Liaohe River Reserve, China. *Sci. Total Environ.* 792:20. doi: 10.1016/j.scitotenv.2021.148290

Xiao, X., Boles, S., Liu, J., Zhuang, D., and Liu, M. (2002). Characterization of forest types in Northeastern China, using multi-temporal SPOT-4 VEGETATION sensor data. *Remote Sens. Environ.* 82, 335–348. doi: 10.1016/s0034-4257(02)00051-2

Yin, G. D., Wang, G. Q., Zhang, X., Wang, X., Hu, Q. H., Shrestha, S., et al. (2022). Multi-scale assessment of water security under climate change in North China in the past two decades. *Sci. Total Environ.* 805:150103. doi: 10.1016/j.scitotenv.2021.150103

Yu, X. F., Ding, S. S., Zou, Y. C., Xue, Z. S., and Lv, X. G. (2018). Review of rapid transformation of floodplain wetlands in Northeast China: roles of human development and global environmental change. *Chin. Geogr. Sci.* 28, 114–124.

Zambon, N., Johannsen, L. L., Strauss, P., Dostal, T., Zumr, D., Cochrane, T. A., et al. (2021). Splash erosion affected by initial soil moisture and surface conditions under simulated rainfall. *CATENA* 196:104827. doi: 10.1016/j.catena.2020.104827

Zhang, J. J., Gao, G. Y., Fu, B. J., and Gupta, H. V. (2019). Formulating an elasticity approach to quantify the effects of climate variability and ecological restoration on sediment discharge change in the Loess Plateau, China. *Water Resourc. Res.* 55, 9604–9622. doi: 10.1029/2019WR025840

Zhang, M. M., Bu, Z. J., Li, H. K., Liu, S. S., Chen, J., and Cui, Y. X. (2021). Hydrological variation recorded in a subalpine peatland of Northeast Asia since the little ice age and its possible driving mechanisms. *Sci. Total Environ.* 772:144923. doi: 10.1016/j.scitotenv.2020.144923

Conflict of Interest: The authors declare that the research was conducted in the absence of any commercial or financial relationships that could be construed as a potential conflict of interest.

frontiers in Ecology and Evolution

ORIGINAL RESEARCH
published: 23 March 2022
doi: 10.3389/fevo.2022.833389

Cooperation With Arbuscular Mycorrhizal Fungi Increases Plant Nutrient Uptake and Improves Defenses Against Insects

*Lu Yu[1], Wantong Zhang[1], Yiyi Geng[1], Kesi Liu[1] and Xinqing Shao[1,2]**

[1] College of Grassland Science and Technology, China Agricultural University, Beijing, China, [2] Qinghai Provincial Key Laboratory of Adaptive Management on Alpine Grassland, Xining, China

Plants have evolved various defense mechanisms to cope with biotic and abiotic stresses. Cooperation with microorganisms, especially arbuscular mycorrhizal fungi (AMF), strengthens the defense capabilities of host plants. To explore the effect of AMF on the growth of *Elymus* and the defenses against locust feeding, we designed a two-compartment device to connect or cut the mycelia and roots. We used this to investigate communication cues and pathways between donor and receiver plants. We found that AMF significantly increased the nitrogen content and decreased the carbon to nitrogen (C:N) ratio of donor plants and receiver plants and the carbon content of both. After the establishment of the common mycorrhizal network (CMN) with AMF between the two chambers, inoculations of donor plants challenged by locusts caused enhancement in four defense-related enzymes, namely, lipoxygenase, polyphenol oxidase, phenylalanine ammonia lyase, and β-1,3-glucanase, in the receiver plants. The main components of volatile organic compounds emitted by receiver plants were terpenoids. The findings indicated that AMF could not only improve plant growth but also activate the defense response of plants to insect feeding. Four defense enzymes, volatile organic compounds, and carbon and nitrogen content were involved in the defense response, and the mycelial network could act as a conduit to deliver communication signals.

Keywords: arbuscular mycorrhizal fungi, plant-insect-microbe interaction, plant evolution, volatile organic compounds, common mycelial network

OPEN ACCESS

Edited by:
Shiliang Liu,
Beijing Normal University, China

Reviewed by:
Xukun Su,
Research Center for Eco-Environmental Sciences (CAS), China
Shikui Dong,
Beijing Forestry University, China
Zhanhuan Shang,
Lanzhou University, China

****Correspondence:***
Xinqing Shao
shaoxinqing@163.com

Specialty section:
This article was submitted to Conservation and Restoration Ecology, a section of the journal Frontiers in Ecology and Evolution

Received: *11 December 2021*
Accepted: *08 February 2022*
Published: *23 March 2022*

Citation:
Yu L, Zhang W, Geng Y, Liu K and Shao X (2022) Cooperation With Arbuscular Mycorrhizal Fungi Increases Plant Nutrient Uptake and Improves Defenses Against Insects. Front. Ecol. Evol. 10:833389. doi: 10.3389/fevo.2022.833389

INTRODUCTION

Insects and terrestrial plants have cooperated for millions of years. Plants gain protection and pollination from insect species, and insects gain food from plants (Frew et al., 2017). However, herbivore feeding sometimes threatens the growth of plants and can lead to plant death (Kong et al., 2016); hence, plants have evolved mechanisms to sense herbivorous insects and their natural enemies and rapidly respond to attacks through signaling changes in morphology, physiology, and biochemistry. Challenged by herbivores, plants innovate evolutionarily with induced responses evolving into resistance (Karban, 2020). These relationships are regulated by soil microbes

(Wilkinson et al., 2019), and they affect the soil microbial communities in return (Rasmann et al., 2017; Tao et al., 2017; Garzo et al., 2020).

Arbuscular mycorrhizal fungi (AMF) from the phylum Glomeromycota establish symbiotic associations with 80% of terrestrial plants (Smith and Smith, 2011; Martin et al., 2017). This dates to 450 million years ago based on fossil and phylogenetic research (Smith and Read, 2010). AMF assist host plants to obtain more nutrients, such as phosphorus (P) and nitrogen (N), and plants provide carbohydrates to AMF in the form of sugar and lipids via exchange through arbuscules (Hodge and Storer, 2015; Hijikata et al., 2016; van der Heijden et al., 2016). Arbuscules are the primary sites for the exchange of nutrients between host plants and fungus (Caroline and Martin, 2013; Luginbuehl and Oldroyd, 2017). The benefits from AMF facilitate plant growth and strengthen plant resistance by influencing responses to abiotic stresses, such as drought, salinity, and extreme temperatures (Aliasgharzad et al., 2006; Mohamed et al., 2014; Delavaux et al., 2017), and biotic stresses, such as pathogens, herbivorous insects, and parasitic plants (Pineda et al., 2010; Cameron et al., 2013). Moreover, modifications of host plant phenotypes by AM fungi can impact insects affecting the plants (Meier and Hunter, 2018a; Garzo et al., 2020).

A key characteristic of AMF is the formation of common mycorrhizal networks (CMNs) by physically linking the individual roots of con- and heterospecific plants underground (Simard and Durall, 2004; Song et al., 2019). Symbionts of plants and mycorrhizae are capable of acquiring nutrients from other plants through CMNs (Giovannetti et al., 2001). The critical roles that mycorrhizas play in plant physiology, the production of primary or secondary metabolism and hormones, are necessary for individual growth and propagation (Smith and Read, 2010; Johnson and Gilbert, 2015). Research has demonstrated that CMNs deliver nutrients to accelerate the growth of adjacent plants (Smith and Read, 2010; Johnson and Gilbert, 2015), while also acting as a warning system of herbivore attacks and pathogens (Babikova et al., 2013; Song et al., 2019).

Volatile organic compounds (VOCs) as chemical signals are exuded by plants and released into the environment, affecting plant fitness and development indirectly (Unsicker et al., 2009; Bilas et al., 2021). Herbivore-induced VOCs emitted by attacked tissues are specific and stable signals that serve as warning signals to distant parts of the plant or its neighbors (Maffei, 2010; Tomczak et al., 2016; Hill et al., 2018; Meier and Hunter, 2018a,b; Velásquez et al., 2020). Plant defenselessness or resistance to mycorrhiza-induced pathogens and phytophagous insects has been reported (Gange et al., 2002; Barber, 2013; Bernaola et al., 2018). The positive (Pineda et al., 2010; Tomczak et al., 2016; Hill et al., 2018; Meier and Hunter, 2018a; Song et al., 2019) or negative (Vicari et al., 2002; Wang et al., 2015) effects that mycorrhiza induce have been documented. However, the ecological interactions that AMF have on aboveground plant–herbivore interactions in grassland ecosystems remain to be explored.

Locust outbreaks have occurred in many regions, lead to unpredictable agricultural outputs, and threaten human well-being (Cease et al., 2015; Zhang et al., 2019). The Tibetan Plateau, the highest area in the world, extending over 2.5 million km^2, has suffered severe locusts damage (Cao et al., 2004). *Elymus nutans* Griseb. is a perennial, dominant species in the Qinghai-Tibet Plateau, China (Chu et al., 2016). It plays an important role in animal husbandry and in the ecological balance of this region. Despite numerous pieces of evidence indicating AMF-induced resistance against herbivores (Hill et al., 2018; Frew et al., 2020; Garzo et al., 2020), the effects of AMF on triggering or evoking defense against locusts are unclear. The main aim was to investigate how the inoculation of *E. nutans* with *Funneliformis mosseae* affected the defense mechanisms of the plant against locusts. We hypothesized that (1) AMF would increase the concentrations of VOCs and defense enzymes, which enhance the host plant defense and induce reactions in neighboring plants, and (2) the CMNs act as the signal pathways.

MATERIALS AND METHODS

Study Organisms and Growth Conditions

Seeds of *E. nutans* and *Elymus sibiricus* Linn. were collected from the Tibetan Autonomous Prefecture of Haibei in Qinghai, China. It has a typical plateau continental climate and clay loam type soil. Precipitation is highest between June and September (Wei et al., 2021). The seeds were surface-sterilized with 10% H_2O_2 and rinsed three times before germination (Schweiger et al., 2014); then, they were sown and grown in a 3:2 mixture of clay and sand in a climate chamber (20°C, 12/12 h light/dark, 60–70% relative humidity). The soil was excavated (0–15 cm depth) in March 2020. After 2 weeks, 100 individuals (50 of *E. nutans* and 50 of *E. sibiricus*) were transferred into square plastic pots (30 cm length × 24 cm width × 12 cm depth) with a 2:1 mixture of soil and sand, and then autoclaved at 121°C for 2 h. They were stored in the dark at 4°C for 3 days and then transferred to a greenhouse (Tomczak et al., 2016). Each pot was watered with the same volume two times a week (1,800 ml/week/pot). The inoculum was mixed with the upper layer (3–4 cm) of the soil–sand mixture. Pots were randomly arranged in the greenhouse and replaced every 10 days during the growing period.

Funneliformis mosseae was purchased from the Beijing Academy of Agriculture and Forestry Sciences (No. BGCYN05), which were propagated with identified fungal spores and white clover (*Trifolium repens*) for 16 weeks in pots. The inoculant used in this experiment was a rhizosphere soil mixture of spores, extra-rhizome hyphae, and root segments of infected plants (containing 129 spores/g).

Locusts (*Locusta migratoria manilensis*) were collected from Yushu City, which is in the eastern part of Qinghai Province, China. The locusts were fed on wheat germ (∼16 g/day) and reared indoors at 28–30°C, 18/6 h (day/night), and 30–50% relative humidity (Veenstra et al., 2021). Fifth-instar locusts were used to attack grown plants (Wang et al., 2019).

Experimental Design

A rectangular pot (20 cm × 12 cm × 15 cm) was divided into two sections (I and II) using different nylon meshes to create a 2 cm air gap (**Figure 1**). Fifty seedlings of *E. nutans* as

donor plants and *E. sibiricus* as receiver plants were planted in sections I and II, respectively. Six treatments were implemented: (A) I and II separated by 35-μm nylon mesh to prevent plant roots from connecting but CMNs were allowed to pass through (35 μm + AMF); (B) I and II separated by 0.5-μm nylon mesh to prevent CMNs passing through (0.5 μm + AMF); (C) I and II blocked with 35-μm nylon mesh to prevent plant roots from connecting, while CMN could form connections with neighbors. Then, pots were immediately rotated to snap CMNs before insects attack (rotated 35 μm + AMF); (D) I and II with no mesh, allowing donor roots and CMNs to connect with receivers (0 μm + AMF); (E) I and II separated with 35-μm mesh to hinder donor and receiver roots interacting and without AMF inoculation (35 μm + AMF); (F) I and II with no barriers and AMF inoculation (0 μm + AMF). Treatments A, B, C, and D had 20 g *F. mosseae* added in section I, and E and F were inoculated with 20 g AMF that were autoclaved at 120°C for 2 h. All treatments had three replicates. Twelve weeks after AMF inoculation, the donor plants in section I were treated with fifth-instar locusts. To avoid donor airborne volatile signals communicating with receiver plants, we covered all receivers with polyethylene terephthalate (PET) bags before adult locusts were fed. Fifth-instar locusts were starved for 24 h before they were used in the experiment.

Collection of Plant Volatile Organic Compounds

Volatile organic compounds were collected from all receivers during the day (10:00–16:00) (Huang et al., 2020) using dynamic headspace for 24 h after locusts attacked donor plants. The air was filtered by activated carbon (produced by Beijing Chemical Reagent Company) and humidified with distilled water. A 50 mg sample of Porapak Q (80–100 mesh, Waters Corporation, Ireland) was filled into dried glass narrow tubes (0.5 cm in diameter and 8.0 cm in length), and both ends of the tubes were plugged with a clean glass fiber. The dried tower, PET bags, and Teflon tubes were placed in a constant temperature drying oven to remove odors. The receiver plants were put in PET bags (100 cm × 111 cm, which had low volatile emissions under high temperature and high-intensity light). After the air in the bag was drawn out by a pump, sampling collection started after 30 min, and extraction with a flow rate of 300 ml/min was conducted for 6 h for VOC collection. All treatments were repeated three times. The adsorbent was eluted with 4 ml n-hexane to a 2 ml sample bottle, and the samples were kept in a refrigerator at –20°C for later use (Fontana et al., 2009).

Analysis of Volatile Organic Compounds

Volatile organic compounds were identified with an Agilent 7890B Gas Chromatograph coupled with Agilent 7200 MSD spectrometer and a DB-5MS column (30 m × 0.25 mm × 0.25 μm film, J&W Scientific, Folsom, CA, United States); the carrier gas was helium at 1 ml/min, with splitless injection (injection temperature 220°C, injection volume 1 μl). The working conditions of gas chromatography (GC) were as follows. The carrier gas flow rate was 2.0 ml/min. A two-stage temperature increase method was adopted, with the initial temperature of 40°C for 1 min followed by a heating rate of 5°C/min to 180°C, then at 10°C/min to 270°C for 2 min. The working conditions of mass spectrometry (MS) were as follows: solvent delay 1 min; an electron impact ion source (EI source) was used; electron energy was 70 eV; interface temperature was 250°C; ion source temperature was 220°C; and scanning mass range was 40–600 m/z with the scanning time in 0.2 s (Fontana et al., 2009). Volatile compounds were initially identified by comparing mass spectra with real standards or data system libraries (NIST 08, National Institute of Standards and Technology, Gaithersburg, MD, United States, 2008).

Arbuscular Mycorrhizal Fungi Colonization and Leaf Nitrogen and Carbon Concentration

Plant Traits

Mycorrhizal Colonization Measurement

Mycorrhizal colonization was examined using the method of Phillips and Hayman (1970). We collected the random receiver plant roots from four treatments, washed them in distilled water to remove soil particles, cut them into 1 cm segments of ∼1 g, immersed them in 10% KOH, and heated them in water at 90°C for 60 min. The root segments were watered to eliminate the alkali, and the remaining alkali was neutralized in 2% hydrochloric acid. We added 0.05% trypan blue to stain the root segments, separated them from the acid solution by heating at 90°C for 30 min, and then immersed them in the mixture solution of glycerol/lactic/water acid (1:1:1) to destain for 24 h. The samples were observed under a regular optical microscope at 40× to examine mycorrhizal colonization (Song et al., 2019).

Mycorrhizal colonization (%) = Number of infected root bits/Total number of root bits observed × 100%

Leaf Carbon and Nitrogen Measurement

Leaf tissues were milled with a ball mill (Retsch MM400, Retsch, Haan, Germany); 0.15 g of the sieved plant sample was weighed, filled into a tin cup, and measured using an elemental analyzer (Vario MAX CNS, Elementar, Hanau, Germany).

Enzyme Assays

Polyphenol Oxidase Enzyme Extraction and Activity Assays

Leaf samples were collected after the insects were fed and were held at −20°C until enzyme extraction and activity assays. Fresh leaf tissue (0.1 g) was used for the next preparation step for the crude enzyme extraction. We added 1 ml of extract that was homogenized in an ice bath, it was centrifuged at 8,000 × *g* at 4°C for 10 min using a FastPrep Instrument high-speed benchtop homogenizer (MP Biomedicals, CA, United States), and we placed the supernatant on ice to determine its activity. Enzymatic activities were evaluated by a microplate reader (SpectraMax iD5, Molecular Devices, San Jose, CA, United States) at 410 nm.

Phenylalanine Ammonia Lyase Enzyme Extraction and Activity Assays

Fresh leaf tissue (0.1 g) was used for the next preparation step of the crude enzyme extraction. We added 1 ml of extract to

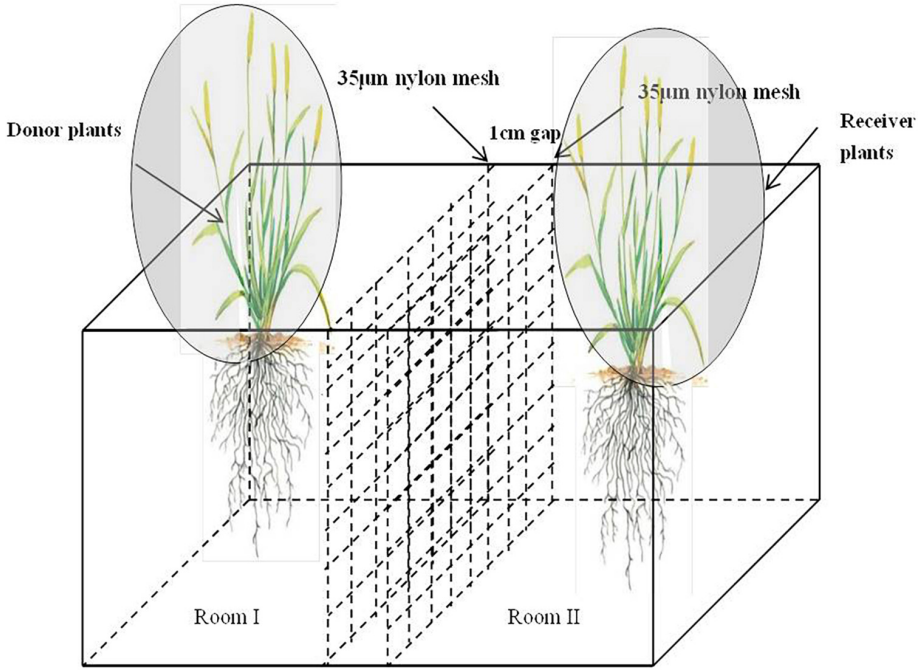

FIGURE 1 | Experimental setup.

homogenize it, centrifuged at 10,000 × *g* at 4°C for 10 min, placed the supernatant on ice to determine its activity, used a plant phenylalanine ammonia lyase (PAL) activity detection kit for activity determination (Solarbio Science and Technology Ltd., Beijing, China), and evaluated enzymatic activities using the microplate reader at 290 nm.

Lipoxygenase Enzyme Extraction and Activity Assays

Fresh leaf tissue (0.1 g) was used for the next preparation step of the crude enzyme extraction. We added 1 ml extraction solution for ice bath homogenization, centrifuged at 16,000 × *g* at 4°C for 20 min, and placed it on ice to test its activity. We used a plant lipoxygenase (LOX) activity detection kit for activity determination (Solarbio Science and Technology Ltd., Beijing, China) and evaluated enzymatic activities using the microplate reader at 234 nm.

β-1,3-Glucanase Enzyme Extraction and Activity Assays

Fresh leaf tissue (0.1 g) was used for the next preparation step of the crude enzyme extraction. According to the ratio of tissue quality and an extraction solution of 1:5 or 1:10, we weighed 0.1 g of leaf tissue, added 1 ml of extraction solution for ice bath homogenization, centrifuged at 16,000 × *g* at 4°C for 20 min, and placed the supernatant on ice. We used a plant β-1,3-glucanase activity detection kit (Solarbio Science and Technology Ltd., Beijing, China) and evaluated enzymatic activities with the microplate reader at 410 nm.

Statistical Analysis

Data (means ± SD, $n = 3$) were analyzed by Analysis of Variance (ANOVA) using R software version 4.1.0. Plant carbon and nitrogen content and enzyme activities were analyzed with a one-way ANOVA in the "agricolae" package of R. The VOC analysis was run using Microsoft Excel 2010, and the figures were produced with R and Origin 2018.

RESULTS

Inoculum Availability and Arbuscular Mycorrhizal Fungi Colonization

Arbuscular mycorrhizal fungi colonization was found in donor plants, with an average colonization rate of 13.34%. In treatment A, AMF colonization in the receiver plant was 5.98% (**Figures 2A,B**) which was significantly lower than the other three treatments. The mycelial hyphae freely passed through the 35-μm mesh, and the AMF colonization between the donor and the receiver plant was roughly the same in treatment B. With no mesh in treatment C, AMF also colonized in the receiver plants, and the colonization was significantly higher than that of the other three groups ($P < 0.05$). Treatment D was rotated before the insects were fed, so the donor and receiver plants were connected with the mycelial hyphae. The colonization rate of receiver plants was about 8.96%.

Plant Performance

The carbon content of donor plants inoculated with AMF significantly decreased (**Figures 3A,B**), while the nitrogen content increased ($P < 0.05$). Compared with the control (F), the carbon content in treatments A, B, C, and D decreased by 0.91, 0.47, 1.12, and 0.93%, respectively, while the nitrogen

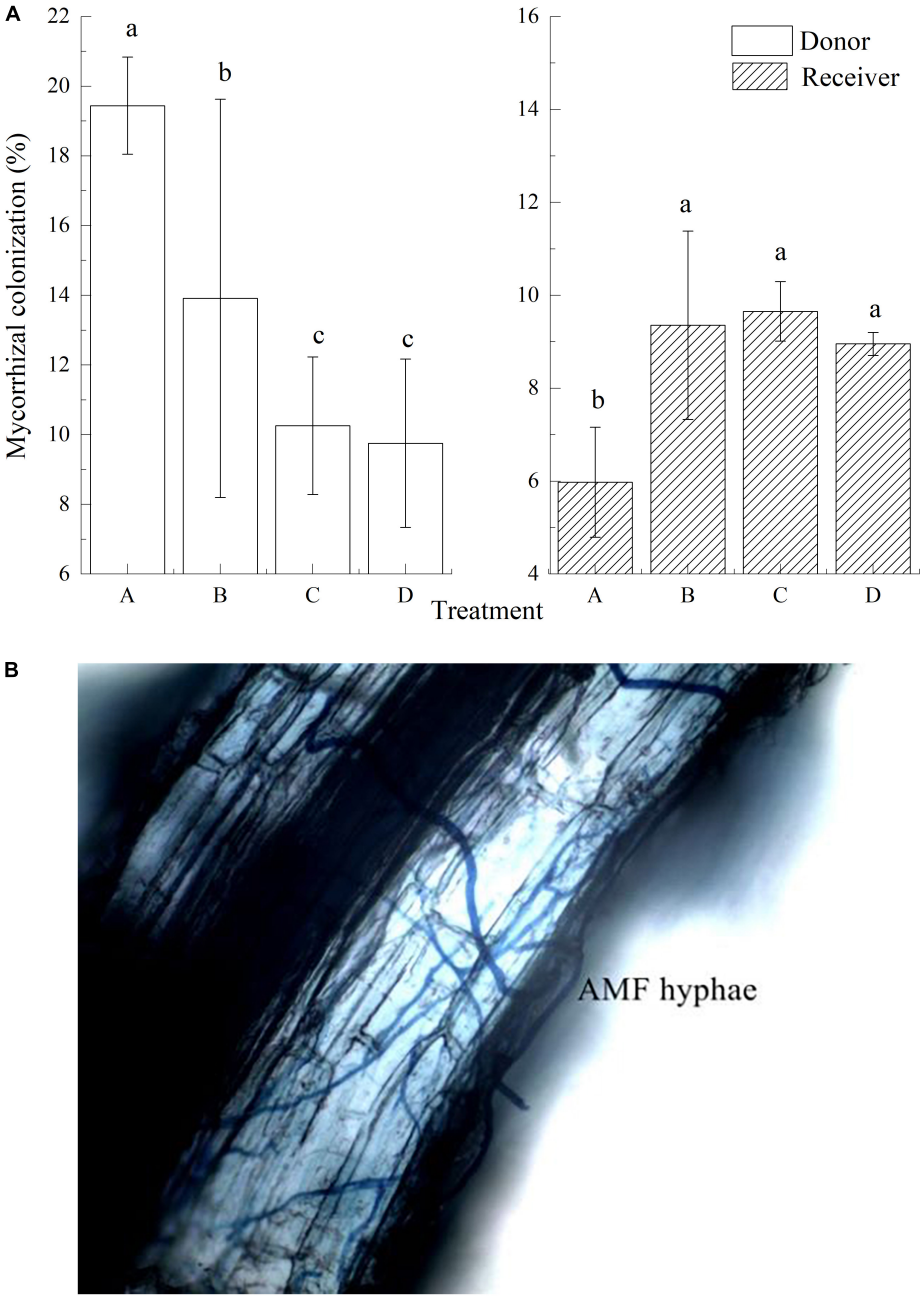

FIGURE 2 | Mycorrhizal colonization and AMF hyphae of donor and received plants in different treatments. Data are mean ± SD (n = 3); different letters indicate significant difference ($P < 0.05$).

content increased by 0.88, 1.64, 1.28, and 1.26%, respectively. With the presence of CMN, the carbon content of receiver plants in treatments B and C was significantly lower than that in treatment A, and the rank among them was A (39.30%) > C (38.90%) > B (38.54%). The nitrogen content in treatment B (1.37%) and treatment C (1.32%) was significantly higher than that in treatment A (0.99%). For non-mycorrhizal plants, the carbon and nitrogen content of receiver plants with roots (F) was higher than that of plants without roots ($P < 0.05$).

Compared with non-mycorrhizal donor plants, mycorrhizal plants showed a higher carbon to nitrogen (C:N) ratio ($P < 0.05$; **Figures 4A,B**), and the average C:N ratios in mycorrhizal plants and non-mycorrhizal plants were 40.11 and 42.57, respectively. The receiver plants showed the same result ($P < 0.05$). The C:N ratios in the receiver plants under treatments A and D were significantly higher than those under other treatments, and the maximum difference was 14.66%.

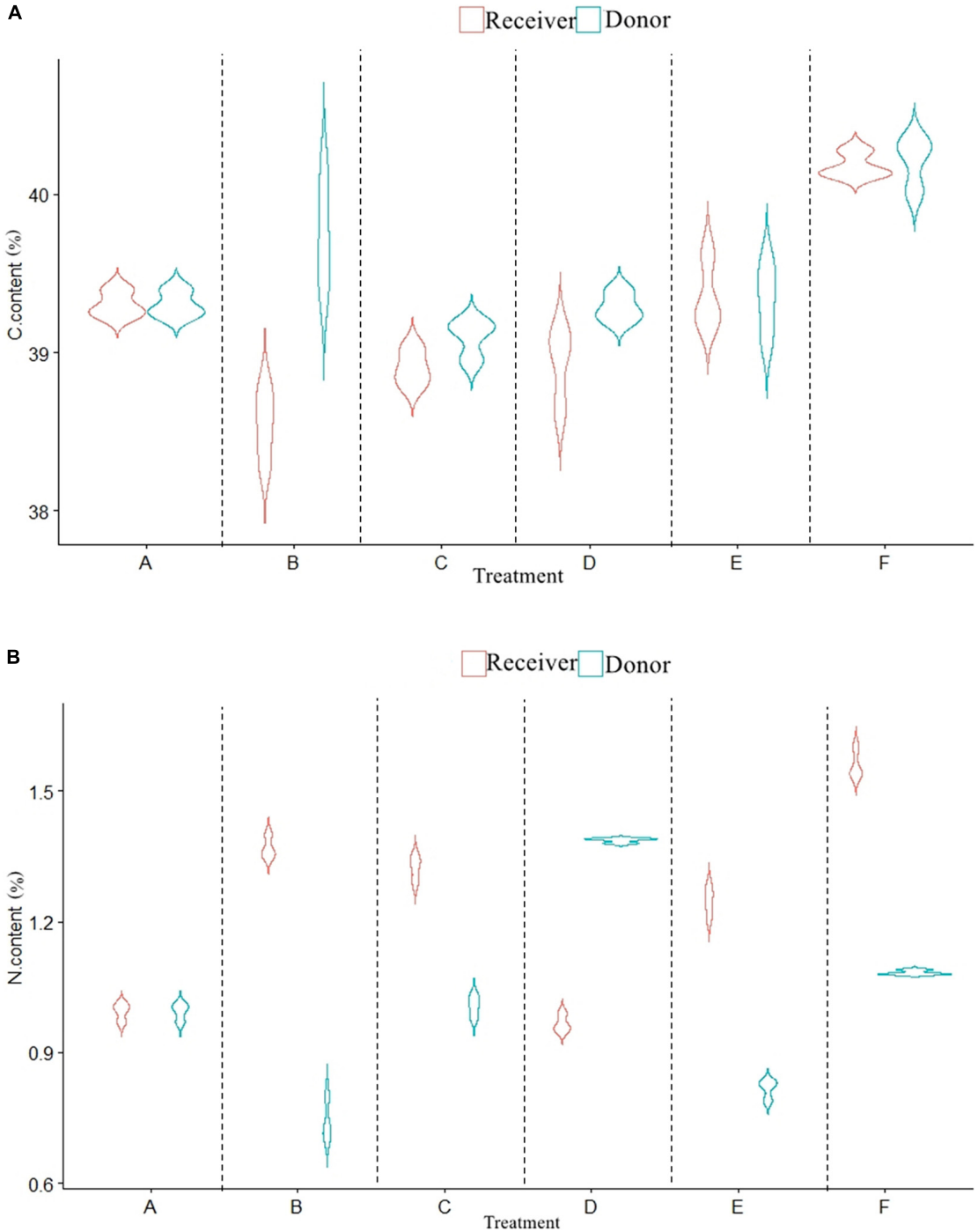

FIGURE 3 | Effects of AMF on C and N content of donor and receiver plants between different treatments. Data are mean ± SD (n = 3).

Defense Enzymes and Volatile Organic Compounds Affected by Arbuscular Mycorrhizal Fungi

In comparison with non-mycorrhiza (F), four leaf defense-related enzymes, namely, PAL, LOX, polyphenol oxidase (PPO), and β-1,3-glucanase, in the donor plants and receiver plants that were inoculated with AMF were all higher than those in non-mycorrhizal plants, and PPO of both had the most significant differences. Compared with treatments B and C, LOX and PPO in the receiver plants of treatment A (without AMF hyphae) were lower. Without root and hyphae connections in treatments D and E, the activities of the four enzymes in the donor and receiver plants were similar (**Figures 5A–D**).

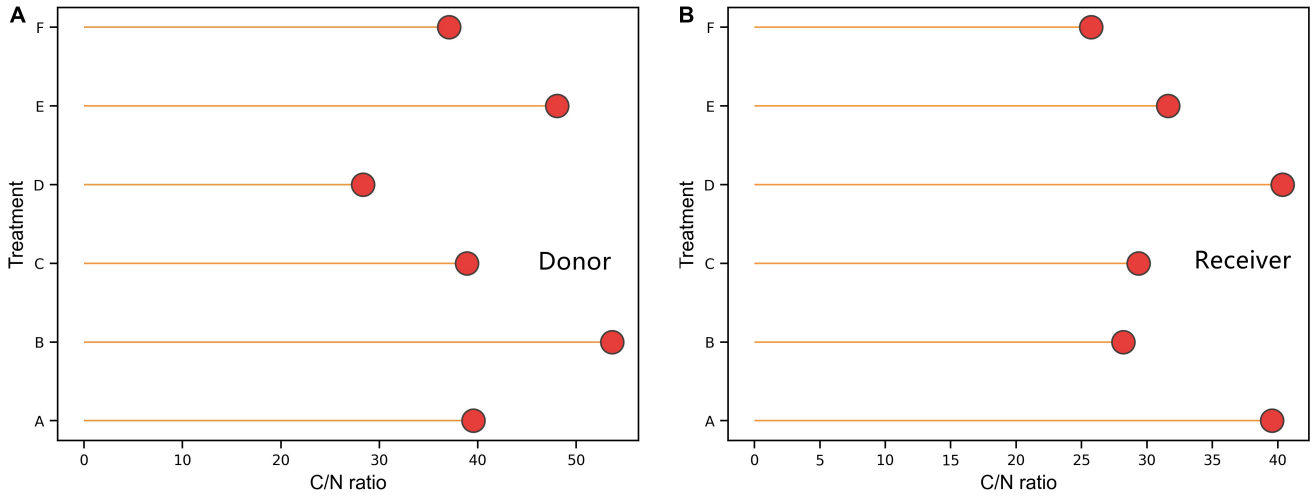

FIGURE 4 | Effects of AMF on the ratio of C and N content of donor and received plants. Data are mean ± SD (n = 3).

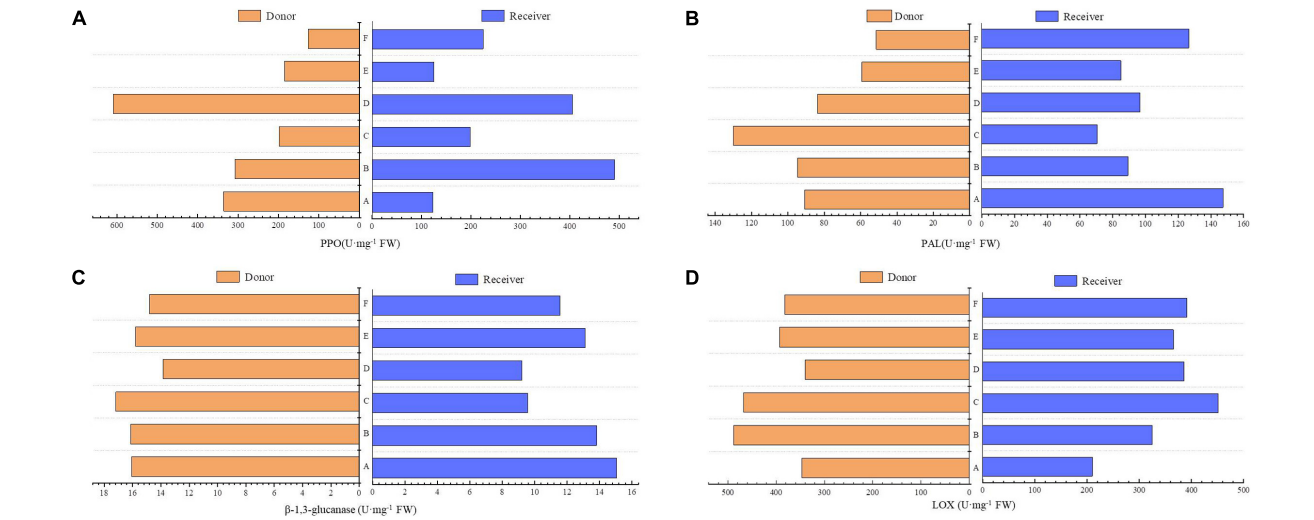

FIGURE 5 | Effects of AMF on enzymes of donor and receiver plants between different treatments. Data are mean ± SD (n = 3).

The main volatile compounds emitted by the receiver plants were terpenoids (**Table 1**). Treatment E emitted the most kinds of volatile compounds, 13 types, whereas Treatment F emitted the least, eight types. Except for treatment E, the relative content of acetophenone, 2′,4′- dimethyl-, from other treatments was the highest. Other treatments did not emit 1,4-diethylbenzene, *p*-xylene, and 2- ethyl-, but all had acetophenone, 2′,4′- dimethyl-, 4-ethylbenzaldehyde, β-cymene, and *p*-cymene. Compared with the non-inoculation treatment, AMF increased acetophenone, 2′,4′- dimethyl-, 4-ethylbenzaldehyde, cumene, phenethyl alcohol, β-cymene, *p*-cymene, and 2-phenyl-1-propanal. For AMF-mediated plants, treatment B and C connected by hyphae produced eight substances, which were acetophenone, 2′,4′- dimethyl-, 4-ethylbenzaldehyde, β-cymene, phenethyl alcohol, *p*-cymene, 4-ethyltoluene, and *p*-propyltoluene. Compared with treatment A, the relative content of 1-methyl-2-phenylcyclopropane, *p*-cymene, 2-phenyl-1-propanal, 4-ethyltoluene, and *p*-propyltoluene increased in the other three treatments.

Relationships Between Plant Defense Traits and Arbuscular Mycorrhizal Fungi Colonization

The linear regression showed that VOC blends and C:N ratio varied with AMF colonization (**Table 2**), but there were no significant interactions between them and AMF colonization. Defense enzymes also varied predictably with AMF colonization, while different from the positive relationships between the other three enzymes and AMF colonization, β-1,3-glucanase decreased with increasing AMF colonization ($P = 0.33$, $F = 1.01$), showing the opposite trend. Despite their effects were not very strong,

TABLE 1 | The concentration of plant volatile organic compounds in received plants.

NO.	Compounds	Chemical Abstracts Service (CAS)	Treatments					
			A	B	C	D	E	F
1	Acetophenone, 2′,4′-dimethyl-	89-74-7	34.76% ± 0.01	25.85% ± 0.08	33.28% ± 0.01	36.58% ± 0.02	18.09% ± 0.07	30.18% ± 0.05
2	2,5-Dimethylacetophenone	2142-73-6	18.67% ± 0.05			28.39% ± 0.01	20.76% ± 0.06	23.30% ± 0.04
3	4-Ethylbenzaldehyde.	4748-78-1	2.14% ± 0.00	1.55% ± 0.00	1.44% ± 0.00	0.62% ± 0.00	1.04% ± 0.00	
4	Cumene, p-ethyl-	4218-48-8	1.71% ± 0.00	0.66% ± 0.00	1.28% ± 0.00		0.41% ± 0.00	
5	1-Methyl-2-phenylcyclopropane	3145-76-4	0.92% ± 0.01		1.63% ± 0.00	1.02% ± 0.01		
6	β-Cymene	535-77-3	17.83% ± 0.00	5.77% ± 0.03	13.16% ± 0.03	16.69% ± 0.01	14.67% ± 0.02	12.44% ± 0.03
7	Phenethyl alcohol	60-12-8	2.27% ± 0.00	0.68% ± 0.00	4.04% ± 0.02		0.68% ± 0.00	
8	p-Cymenene	1195-32-0	3.67% ± 0.01	1.48% ± 0.01	5.06% ± 0.00	3.49% ± 0.01	3.36% ± 0.01	3.89% ± 0.01
9	2-Phenyl-1-propanal	93-53-8	0.85% ± 0.00	8.76% ± 0.04		0.83 ± 0.00	0.72% ± 0.00	
10	Cumene	98-82-8	3.20% ± 0.01	1.48% ± 0.01		0.96% ± 0.01		0.92% ± 0.00
11	Isobutenylbenzene	768-49-0	0.96% ± 0.01			1.04% ± 0.01		2.07% ± 0.00
13	4-Ethyltoluene	622-96-8	0.97% ± 0.01	2.03% ± 0.01	1.04% ± 0.01	0.71% ± 0.00	2.00% ± 0.01	
14	p-Propyltoluene	1074-55-1		0.82% ± 0.00	2.55% ± 0.00	0.84% ± 0.00	0.29% ± 0.00	
15	p-Cymene	99-87-6		6.46% ± 0.04				
17	Isopropyl palmitate	142-91-6				8.04% ± 0.05	5.59% ± 0.03	
18	Indane	496-11-7				0.79% ± 0.00		
19	Palmitoyl chloride	18919-94-3					0.55% ± 0.00	
20	2-Propenal	107-02-8					27.82% ± 0.08	
21	p-Xylene, 2-ethyl-	1758-88-9						1.12% ± 0.01
22	1,4-Diethylbenzene	105-05-5						26.07% ± 0.12

Values were mean ± SE (n = 3).

they also indicated that the increase in AMF colonization possibly influences plant defense.

DISCUSSION

Effects of Arbuscular Mycorrhizal Fungi on Plant Nutrition Uptake

Our findings showed that AMF inoculation significantly increased the total nitrogen content and decreased the total carbon in host plants. This can be explained by the fact that nearly 25% of the photosynthetic product of the host plant is supplied to the mycorrhiza (Hobbie, 2006; van der Heijden et al., 2006). Fungal hyphae can explore large volumes of soil, enter soil pores that are inaccessible to roots (Smith and Read, 1997), transfer nitrogen as arginine or urea from the soil to the roots of a host plant, and thereby enhance plant accumulation of nitrogen (Hodge et al., 2010; van der Heijden et al., 2015; Ingraffia et al., 2021). The C:N ratio in plants is an important indicator for studying insect resistance (Těšitel et al., 2021). Healthy and nutrient-rich plants are more resistant to the feeding of herbivores. By contrast, plants with weaker vitality and limited resources may be more vulnerable (Löser et al., 2021). Our findings indicate that the C:N ratios in those receiver plants with AMF were much higher than those plants with no inoculations. This is consistent with another study that showed mycorrhizal symbionts have negative effects on herbivores by changing the C:N ratio (Getman Pickering et al., 2021), as plants with higher C:N ratio may reduce their nutritional value and their attractiveness to herbivores (Bennett et al., 2016; Getman Pickering et al., 2021). The enhancement of defenses results from increased nutrient acquisition (Mhlongo et al., 2018) and changes in defensive trypsin inhibitors (Getman Pickering et al., 2021).

TABLE 2 | Results of linear model analyses of the effects of the availability of arbuscular mycorrhizal fungi (AMF) inoculum on volatile organic compounds (VOCs) blends, C:N ratio, and defense enzymes.

	AMF colonization			
	F	*P*	Slope	*y* Intercept
VOCs blends	0.21	0.66	0.06	6.72
C:N ratio	1.16	0.30	0.30	30.77
PPO	0.32	0.58	6.76	223.17
PAL	0.02	0.89	0.36	100.50
LOX	0.01	0.91	1.23	347.28
β-1,3-glucanase	1.01	0.33	-0.25	13.46

PPO, polyphenol oxidase; PAL, phenylalanine ammonia lyase; LOX, Lipoxygenase. The P-values indicate statistical significance (P < 0.05).

Effects of Arbuscular Mycorrhizal Fungi on Plant Defense to Insects

Mycorrhizae modify plant traits, including chemical resistance (Hartley and Gange, 2009). Two signal pathways mediated by jasmonic acid (JA) and salicylic acid (SA) respond to physical or biological damage (Zhao et al., 2009). Enzymes such as β-1,3-glucanase and PAL are key enzymes involved in the biosynthesis of the signal molecule of SA (Balog et al., 2017). As the final

enzymes of the main defense pathway, they directly participate in the synthesis of secondary metabolites related to plant defense and resistance (Selvaraj et al., 2020). Our results found that AMF led to an increase in the enzymatic activities of PPO, β-1,3-glucanase, PAL, and LOX, which has been shown in sweet pepper, tomato, and potato (Constabel and Barbehenn, 2008; Balog et al., 2017). Host plants show higher defenses, demonstrating that inoculation with AMF enhances the resistance of host plants to insects by improving enzymatic activities (Balog et al., 2017; Selvaraj et al., 2020). PPO and PAL increase to catalyze the production of poisonous quinone compounds via cross-linking proteins and carbohydrates, generating oxygen-free radicals (Bagy et al., 2019), and reducing the availability of protein (Selvaraj et al., 2020). The enhancement of melanin through PPOs can also increase the resistance of the cell wall to insects and pathogens (Zhao et al., 2009). LOX and PPO catalyze the initial reaction in the JA biosynthetic pathway, form hydroperoxides through catalytic reactions, and degrade hydroperoxides into reactive aldehydes and ketones through chemical reactions and enzymes (Bruinsma et al., 2009). An increase in PAL can promote the accumulation of phenolic substances and convert them into toxic compounds during oxidation (Bhonwong et al., 2009), and these phenolic substances are generally linked to plant resistances to insects (Frew et al., 2020).

Volatile organic compounds are important chemical signals for communication between phytophagous insects and their host plants (Liu and Brettell, 2019). In the arms race between plants and herbivores, any herbivore that can suppress plant-induced defense signals has increased fitness (Bruinsma et al., 2010; Zu et al., 2020). Plant–plant signals may have a fundamental impact on mycorrhizal plant–herbivore interactions at the community level and exert selective pressure on herbivore insects to evolve antagonistic mechanisms (Gilbert and Johnson, 2015). Plant compounds are complex mixtures of volatile gases that can directly repel herbivores and indirectly attract herbivore natural enemies (Huang et al., 2020). The amount and characteristics of the emitted plant VOCs vary from species to species (Zhao et al., 2009).

Various studies have revealed that AMF affect the interactions between plants and insects. Meier and Hunter (2019) reported that increasing cardenolides (a toxic substance) generated by milkweed inoculated with AMF decreased weights and growth rates of aphids. Velásquez et al. (2020) reported that an increase in (E)-2-hexenal, 3-hexenal, geraniol, benzaldehyde, and methyl salicylate associated with plant defenses has been shown in mycorrhizal plants linked to herbivore attacks. In *Plantago lanceolate* L., a large increase in volatile terpenoids mediated by AMF can assist in indirect defense against herbivore attacks (Fontana et al., 2009).

Our results showed that receiver plants that were linked to mycorrhizal donor plants released VOC emissions. Acetophenone, 2′,4′- dimethyl-, 4-ethylbenzaldehyde, cumene, phenethyl alcohol, β-cymene, *p*-cymene, and 2-phenyl-1-propanal were enhanced by AMF, indicating that AMF are capable of affecting the concentration and composition of plant secondary metabolites (Velásquez et al., 2020). As the most abundant and structurally diverse volatiles released by plants, terpenoids can drive interaction among insects, pathogens, and neighboring plants. Besides their role in direct and indirect defense, terpenoids affect defense-related signals released by the injured leaf to undamaged leaves through an internal system or to nearby plants through an external route (Sharma et al., 2017). In our study, mycorrhiza significantly improved and changed the relative content and composition of VOCs, such as cumene, phenethyl alcohol, 4-ethyltoluene, β-cymene, and 4-ethylbenzaldehyde. The majority of VOCs were terpenoids, which are combined with other compounds (green leaf volatiles, esters, aldehydes, and aromatic compounds) to enhance resistances (Kigathi et al., 2013; Kigathi et al., 2019). Among them, cumene affects the feeding of sucking herbivores (Gras et al., 2005) and primes defenses in *Brassica nigra* to white butterflies (Pashalidou et al., 2020). The specific effects of AMF on VOC emissions may be due to the differences in carbon allocation. Further, VOC emissions are mediated by interactions between plant hormones and secondary defense metabolites (Meier and Hunter, 2019).

The Signal Pathways of Defense Responses That Arbuscular Mycorrhizal Fungi Mediate

Root exudates and the fungal mycelia network mediate belowground plant communication (Guerrieri et al., 2002). Root exudates were excluded by a 2-cm gap in our devices, and our study showed that four defense-related enzymes and VOC emissions were higher in undamaged receiver plants, and the defensive substances induced by hyphal connections performed better compared with the control. This indicated that the defensive substances produced by the donor plants in different treatments were mainly transmitted through the mycelial network, demonstrating the importance of hyphae connection in the response of the receiver plants to the donor plants when harmed by insect pests (Barto et al., 2012). Studies have shown that the mycelial hyphae are a signal conduit (Babikova et al., 2013; Song et al., 2019). They transmit a series of signals and compounds between plants and trigger the response to organisms at various trophic levels (Babikova et al., 2013, 2014a; Alaux et al., 2020). Defense signals induced by herbivores can be transferred by a common mycelial network from injured plants to uninfected neighbors to enhance the resistance of injured individuals to herbivores and warn adjacent plants through CMN to prepare for future attacks without direct contact with herbivores. This early warning system may have a profound impact on trophic webs (Babikova et al., 2014b), especially plant–insect interactions (Barto et al., 2012).

Arbuscular mycorrhizal fungi induced host plant resistance to insects by facilitating the release of PPO, LOX, PAL, and β-1,3-glucanase and by mediating VOCs and C:N ratios. The common mycorrhizal network is an important pathway for transferring defense signals. Our findings showed that CMNs provide a potential approach for triggering defense responses in undamaged neighbors. Further studies are

warranted to validate the extent and nature of the defense responses to different herbivores.

DATA AVAILABILITY STATEMENT

The original contributions presented in the study are included in the article/**Supplementary Material**, further inquiries can be directed to the corresponding author.

AUTHOR CONTRIBUTIONS

XS and KL conceived the study, supervised the writing, and revised the manuscript. LY led the writing. WZ and YG contributed sections to the manuscript. All authors read and approved the final submission.

FUNDING

This study was supported by the National Natural Science Foundation of China (grant number 31971746), Major Science and Technology Projects in Qinghai Province (2018-NK-A2), and the Platform of Adaptive Management on Alpine Grassland-livestock System (2020-ZJ-T07).

SUPPLEMENTARY MATERIAL

The Supplementary Material for this article can be found online at: https://www.frontiersin.org/articles/10.3389/fevo.2022.833389/full#supplementary-material

Supplementary Figure S1 | The chromatograms of (1-Methylpropyl)benzene.

Supplementary Figure S2 | The chromatograms of 1-Methyl-2-phenylcyclopropane.

Supplementary Figure S3 | The chromatograms of 2,5-Dimethylacetophenone.

Supplementary Figure S4 | The chromatograms of 2,5-dimethylethylbenzene.

Supplementary Figure S5 | The chromatograms of 2-Phenyl-1-propanal.

Supplementary Figure S6 | The chromatograms of 2-Propenal.

Supplementary Figure S7 | The chromatograms of 4-Acetyl-m-xylene.

Supplementary Figure S8 | The chromatograms of 4-Ethyltoluene.

Supplementary Figure S9 | The chromatograms of Cumene, p-ethyl-.

Supplementary Figure S10 | The chromatograms of Cumene.

Supplementary Figure S11 | The chromatograms of Ethyl-benzaldehyde.

Supplementary Figure S12 | The chromatograms of Isobutenylbenzene.

Supplementary Figure S13 | The chromatograms of Isopropyl palmitate.

Supplementary Figure S14 | The chromatograms of p-Cymene.

Supplementary Figure S15 | The chromatograms of Phenethyl alcohol.

REFERENCES

Alaux, P., Naveau, F., Declerck, S., and Cranenbrouck, S. (2020). Common mycorrhizal network induced JA/ET genes expression in healthy potato plants connected to potato plants infected by phytophthora infestans. *Front. Plant Sci.* 11:602. doi: 10.3389/fpls.2020.00602

Aliasgharzad, N., Neyshabouri, M. R., and Salimi, G. (2006). Effects of arbuscular mycorrhizal fungi and *Bradyrhizobium japonicum* on drought stress of soybean. *Biologia* 6119, S324–S328. doi: 10.2478/s11756-006-0182-x

Babikova, Z., Gilbert, L., Bruce, T., Dewhirst, S. Y., Pickett, J. A., and Johnson, D. (2014a). Arbuscular mycorrhizal fungi and aphids interact by changing host plant quality and volatile emission. *Funct. Ecol.* 28, 375–385. doi: 10.1111/1365-2435.12181

Babikova, Z., Johnson, D., Bruce, T., Pickett, J., and Gilbert, L. (2014b). Underground allies: how and why do mycelial networks help plants defend themselves? *Bioessays* 36, 21–26. doi: 10.1002/bies.201300092

Babikova, Z., Gilbert, L., Bruce, T. J. A., Birkett, M., Caulfield, J. C., Woodcock, C. M., et al. (2013). Underground signals carried through common mycelial networks warn neighbouring plants of aphid attack. *Ecol. Lett.* 16, 835–843. doi: 10.1111/ele.12115

Bagy, H. M. M. K., Hassan, E. A., Nafady, N. A., and Dawood, M. F. A. (2019). Efficacy of arbuscular mycorrhizal fungi and endophytic strain *Epicoccum nigrum* ASU11 as biocontrol agents against blackleg disease of potato caused by bacterial strain *Pectobacterium carotovora* subsp. *Atrosepticum* PHY7. *Biol. Control* 134, 103–113. doi: 10.1016/j.biocontrol.2019.03.005

Balog, A., Loxdale, H. D., Bálint, J., Benedek, K., Szabó, K., Jánosi-Rancz, K. T., et al. (2017). The arbuscular mycorrhizal fungus *Rhizophagus* irregularis affects arthropod colonization on sweet pepper in both the field and greenhouse. *J. Pest Sci.* 90, 935–946. doi: 10.1007/s10340-017-0844-1

Barber, N. A. (2013). Arbuscular mycorrhizal fungi are necessary for the induced response to herbivores by *Cucumis sativus*. *J. Plant Ecol.* 6, 171–176. doi: 10.1093/jpe/rts026

Barto, E. K., Weidenhamer, J. D., Cipollini, D., and Rillig, M. C. (2012). Fungal superhighways: do common mycorrhizal networks enhance below ground communication? *Trends Plant Sci.* 17, 633–637. doi: 10.1016/j.tplants.2012.06.007

Bennett, A. E., Millar, N. S., Gedrovics, E., and Karley, A. J. (2016). Plant and insect microbial symbionts alter the outcome of plant–herbivore–parasitoid interactions: implications for invaded, agricultural and natural systems. *J. Ecol.* 104, 1734–1744. doi: 10.1111/1365-2745.12620

Bernaola, L., Cosme, M., Schneider, R. W., and Stout, M. (2018). Belowground inoculation with arbuscular mycorrhizal fungi increases local and systemic susceptibility of rice plants to different pest organisms. *Front. Plant Sci.* 9:747. doi: 10.3389/fpls.2018.00747

Bhonwong, A., Stout, M. J., Attajarusit, J., and Tantasawat, P. (2009). Defensive role of tomato polyphenol oxidases against cotton bollworm (*Helicoverpa armigera*) and beet armyworm (*Spodoptera exigua*). *J. Chem. Ecol.* 35, 28–38. doi: 10.1007/s10886-008-9571-7

Bilas, R. D., Bretman, A., and Bennett, T. (2021). Friends, neighbours and enemies: an overview of the communal and social biology of plants. *Plant Cell Environ.* 44, 997–1013. doi: 10.1111/pce.13965

Bruinsma, M., Posthumus, M. A., Mumm, R., Mueller, M. J., van Loon, J. J. A., and Dicke, M. (2009). Jasmonic acid-induced volatiles of *Brassica oleracea* attract parasitoids: effects of time and dose, and comparison with induction by herbivores. *J. Exp. Bot.* 60, 2575–2587. doi: 10.1093/jxb/erp101

Bruinsma, M., van Broekhoven, S., Poelman, E. H., Posthumus, M. A., Müller, M. J., van Loon, J. J., et al. (2010). Inhibition of lipoxygenase affects induction of both direct and indirect plant defences against herbivorous insects. *Oecologia* 162, 393–404. doi: 10.1007/s00442-009-1459-x

Cameron, D. D., Neal, A. L., van Wees, S. C. M., and Ton, J. (2013). Mycorrhiza-induced resistance: more than the sum of its parts? *Trends Plant Sci.* 18, 539–545. doi: 10.1016/j.tplants.2013.06.004

Cao, G., Tang, Y., Mo, W., Wang, Y., Li, Y., and Zhao, X. (2004). Grazing intensity alters soil respiration in an alpine meadow on the Tibetan plateau. *Soil Biol. Biochem.* 36, 237–243. doi: 10.1016/j.soilbio.2003.09.010

Caroline, G., and Martin, P. (2013). Cell and developmental biology of the arbuscular mycorrhiza symbiosis. *Annu. Rev. Cell Dev. Biol.* 29, 593–617.

Cease, A. J., Elser, J. J., Fenichel, E. P., Hadrich, J. C., Harrison, J. F., and Robinson, B. E. (2015). Living with locusts: connecting soil nitrogen, locust outbreaks, livelihoods, and livestock markets. *BioScience* 65, 551–558. doi: 10.1093/biosci/biv048

Chu, X. T., Fu, J. J., Sun, Y. F., Xu, Y. M., Miao, Y. J., Xu, Y. F., et al. (2016). Effect of arbuscular mycorrhizal fungi inoculation on cold stress-induced oxidative damage in leaves of *Elymus nutans* Griseb. *S. Afr. J. Bot.* 104, 21–29.

Constabel, C. P., and Barbehenn, R. (2008). "Defensive roles of polyphenol oxidase in plants," in *Induced Plant Resistance to Herbivory*, ed. A. Schaller (Dordrecht: Springer Netherlands), 253–270.

Delavaux, C. S., Smith Ramesh, L. M., and Kuebbing, S. E. (2017). Beyond nutrients: a meta-analysis of the diverse effects of arbuscular mycorrhizal fungi on plants and soils. *Ecology* 98, 2111–2119. doi: 10.1002/ecy.1892

Fontana, A., Reichelt, M., Hempel, S., Gershenzon, J., and Unsicker, S. B. (2009). The effects of arbuscular mycorrhizal fungi on direct and indirect defense metabolites of *Plantago lanceolata* L. *J. Chem. Ecol.* 35, 833–843. doi: 10.1007/s10886-009-9654-0

Frew, A., Powell, J. R., Hiltpold, I., Allsopp, P. G., Sallam, N., and Johnson, S. N. (2017). Host plant colonisation by arbuscular mycorrhizal fungi stimulates immune function whereas high root silicon concentrations diminish growth in a soil-dwelling herbivore. *Soil Biol. Biochem.* 112, 117–126. doi: 10.1016/j.soilbio.2017.05.008

Frew, A., Powell, J. R., and Johnson, S. N. (2020). Aboveground resource allocation in response to root herbivory as affected by the arbuscular mycorrhizal symbiosis. *Plant Soil* 447, 463–473. doi: 10.1007/s11104-019-04399-x

Gange, A. C., Stagg, P. G., and Ward, L. K. (2002). Arbuscular mycorrhizal fungi affect phytophagous insect specialism. *Ecol. Lett.* 5, 11–15. doi: 10.1046/j.1461-0248.2002.00299.x

Garzo, E., Rizzo, E., Fereres, A., and Gomez, S. K. (2020). High levels of arbuscular mycorrhizal fungus colonization on *Medicago truncatula* reduces plant suitability as a host for pea aphids (*Acyrthosiphon pisum*). *Insect Sci.* 27, 99–112. doi: 10.1111/1744-7917.12631

Getman Pickering, Z. L., Stack, G. M., and Thaler, J. S. (2021). Fertilizer quantity and type alter mycorrhizae-conferred growth and resistance to herbivores. *J. Appl. Ecol.* 58, 931–940. doi: 10.1111/1365-2664.13833

Gilbert, L., and Johnson, D. (2015). Plant-mediated 'apparent effects' between mycorrhiza and insect herbivores. *Curr. Opin. Plant Biol.* 26, 100–105. doi: 10.1016/j.pbi.2015.06.008

Giovannetti, M., Fortuna, P., Citernesi, A. S., Morini, S., and Nuti, M. P. (2001). The occurrence of anastomosis formation and nuclear exchange in intact arbuscular mycorrhizal networks. *New Phytol.* 151, 717–724. doi: 10.1046/j.0028-646x.2001.00216.x

Gras, E. K., Read, J., Mach, C. T., Sanson, G. D., and Clissold, F. J. (2005). Herbivore damage, resource richness and putative defences in juvenile versus adult *Eucalyptus* leaves. *Austral. J. Bot.* 53:33. doi: 10.1071/BT04049

Guerrieri, E., Poppy, G. M., Powell, W., Rao, R., and Pennacchio, F. (2002). Plant-to-plant communication mediating in-flight orientation of *Aphidius ervi*. *J. Chem. Ecol.* 28, 1703–1715.

Hartley, S. E., and Gange, A. C. (2009). Impacts of plant symbiotic fungi on insect herbivores: mutualism in a multitrophic context. *Annu. Rev. Entomol.* 54, 323–342.

Hijikata, N., Murase, M., Tani, C., Ohtomo, R., Osaki, M., and Ezawa, T. (2016). Polyphosphate has a central role in the rapid and massive accumulation of phosphorus in extraradical mycelium of an arbuscular mycorrhizal fungus. *New Phytol.* 2, 285–289.

Hill, E. M., Robinson, L. A., Abdul-Sada, A., Vanbergen, A. J., Hodge, A., and Hartley, S. E. (2018). Arbuscular mycorrhizal fungi and plant chemical defence: effects of colonisation on aboveground and belowground metabolomes. *J. Chem. Ecol.* 44, 198–208. doi: 10.1007/s10886-017-0921-1

Hobbie, E. A. (2006). Carbon allocation to ectomycorrhizal fungi correlates with belowground allocation in culture studies. *Ecology* 87, 563–569. doi: 10.1890/05-0755

Hodge, A., Helgason, T., and Fitter, A. H. (2010). Nutritional ecology of arbuscular mycorrhizal fungi. *Fungal Ecol.* 3, 267–273. doi: 10.1016/j.funeco.2010.02.002

Hodge, A., and Storer, K. (2015). Arbuscular mycorrhiza and nitrogen: implications for individual plants through to ecosystems. *Plant Soil* 386, 1–19. doi: 10.1007/s11104-014-2162-1

Huang, D., Sun, M., Han, M., Zhang, Z., Miao, Y., Zhang, J., et al. (2020). Volatile organic compounds (VOCs) regulate the spatial distribution of Lepidoptera insects in an orchard ecosystem. *Biol. Control* 149:104311. doi: 10.1016/j.biocontrol.2020.104311

Ingraffia, R., Saia, S., Giovino, A., Amato, G., Badagliacca, G., Giambalvo, D., et al. (2021). Addition of high C:N crop residues to a P-limited substrate constrains the benefits of arbuscular mycorrhizal symbiosis for wheat P and N nutrition. *Mycorrhiza* 31, 441–454. doi: 10.1007/s00572-021-01031-8

Johnson, D., and Gilbert, L. (2015). Interplant signalling through hyphal networks. *New Phytol.* 205, 1448–1453. doi: 10.1111/nph.13115

Karban, R. (2020). The ecology and evolution of induced responses to herbivory and how plants perceive risk. *Ecol. Entomol.* 45, 1–9. doi: 10.1111/een.12771

Kigathi, R. N., Weisser, W. W., Reichelt, M., Gershenzon, J., and Unsicker, S. B. (2019). Plant volatile emission depends on the species composition of the neighboring plant community. *BMC Plant Biol.* 19:58. doi: 10.1186/s12870-018-1541-9

Kigathi, R. N., Weisser, W. W., Veit, D., Gershenzon, J., and Unsicker, S. B. (2013). Plants suppress their emission of volatiles when growing with conspecifics. *J. Chem. Ecol.* 39, 537–545. doi: 10.1007/s10886-013-0275-2

Kong, H. G., Kim, B. K., Song, G. C., Lee, S., and Ryu, C. (2016). Aboveground whitefly infestation-mediated reshaping of the root microbiota. *Front. Microbiol.* 7:1314. doi: 10.3389/fmicb.2016.01314

Liu, H., and Brettell, L. E. (2019). Plant defense by VOC-induced microbial priming. *Trends Plant Sci.* 24, 187–189. doi: 10.1016/j.tplants.2019.01.008

Löser, T. B., Mescher, M. C., De Moraes, C. M., Maurhofer, M., and Rudi, K. (2021). Effects of root-colonizing fluorescent *Pseudomonas* strains on arabidopsis resistance to a pathogen and an herbivore. *Appl. Environ. Microbiol.* 87:e283120. doi: 10.1128/AEM.02831-20

Luginbuehl, L. H., and Oldroyd, G. E. D. (2017). Understanding the arbuscule at the heart of endomycorrhizal symbioses in plants. *Curr. Biol.* 17, 952–963.

Maffei, M. E. (2010). Sites of synthesis, biochemistry and functional role of plant volatiles. *S. Afr. J. Bot.* 76, 612–631. doi: 10.1016/j.sajb.2010.03.003

Martin, F. M., Uroz, S., and Barker, D. G. (2017). Ancestral alliances: plant mutualistic symbioses with fungi and bacteria. *Science* 6340:d4501.

Meier, A. R., and Hunter, M. D. (2018a). Mycorrhizae alter toxin sequestration and performance of two specialist herbivores. *Front. Ecol. Evol.* 6:33. doi: 10.3389/fevo.2018.00033

Meier, A. R., and Hunter, M. D. (2018b). Arbuscular mycorrhizal fungi mediate herbivore-induction of plant defenses differently above and belowground. *Oikos* 127, 1759–1775. doi: 10.1111/oik.05402

Meier, A. R., and Hunter, M. D. (2019). Mycorrhizae alter constitutive and herbivore-induced volatile emissions by milkweeds. *J. Chem. Ecol.* 45, 610–625. doi: 10.1007/s10886-019-01080-6

Mhlongo, M. I., Piater, L. A., Madala, N. E., Labuschagne, N., and Dubery, I. A. (2018). The chemistry of plant–microbe interactions in the rhizosphere and the potential for metabolomics to reveal signaling related to defense priming and induced systemic resistance. *Front. Plant Sci.* 9:112. doi: 10.3389/fpls.2018.00112

Mohamed, A. A., Eweda, W. E. E., Heggo, A. M., and Hassan, E. A. (2014). Effect of dual inoculation with arbuscular mycorrhizal fungi and sulphur-oxidising bacteria on onion (*Allium cepa* L.) and maize (*Zea mays* L.) grown in sandy soil under greenhouse conditions. *Ann. Agric. Sci.* 59, 109–118. doi: 10.1016/j.aoas.2014.06.015

Pashalidou, F. G., Eyman, L., Sims, J., Buckley, J., Fatouros, N. E., De Moraes, C. M., et al. (2020). Plant volatiles induced by herbivore eggs prime defences and mediate shifts in the reproductive strategy of receiving plants. *Ecol. Lett.* 7, 1097–1106.

Phillips, J. M., and Hayman, D. S. (1970). Improved procedures for clearing roots and staining parasitic and vesicular-arbuscular mycorrhizal fungi for rapid assessment of infection. *Trans. Br. Mycol. Soc.* 55:158. doi: 10.1016/S0007-1536(70)80110-3

Pineda, A., Zheng, S., van Loon, J. J. A., Pieterse, C. M. J., and Dicke, M. (2010). Helping plants to deal with insects: the role of beneficial soil-borne microbes. *Trends Plant Sci.* 15, 507–514. doi: 10.1016/j.tplants.2010.05.007

Rasmann, S., Bennett, A., Biere, A., Karley, A., and Guerrieri, E. (2017). Root symbionts: powerful drivers of plant above- and belowground indirect defenses. *Insect Sci.* 24, 947–960. doi: 10.1111/1744-7917.12464

Schweiger, R., Baier, M. C., and Mueller, C. (2014). Arbuscular Mycorrhiza-Induced shifts in foliar metabolism and photosynthesis mirror the developmental stage of the symbiosis and are only partly driven by improved phosphate uptake. *Mol. Plant Microbe Interact.* 27, 1403–1412. doi: 10.1094/MPMI-05-14-0126-R

Selvaraj, A., Thangavel, K., and Uthandi, S. (2020). Arbuscular mycorrhizal fungi (*Glomus intraradices*) and diazotrophic bacterium (Rhizobium BMBS) primed defense in blackgram against herbivorous insect (*Spodoptera litura*) infestation. *Microbiol. Res.* 231:126355. doi: 10.1016/j.micres.2019.126355

Sharma, E., Anand, G., and Kapoor, R. (2017). Terpenoids in plant and arbuscular mycorrhiza-reinforced defence against herbivorous insects. *Ann. Bot.* 119:w263. doi: 10.1093/aob/mcw263

Simard, S. W., and Durall, D. M. (2004). Mycorrhizal networks: a review of their extent, function, and importance. *Can. J. Bot.* 82, 1140–1165. doi: 10.1139/B04-116

Smith, F. A., and Smith, S. E. (2011). What is the significance of the arbuscular mycorrhizal colonisation of many economically important crop plants. *Plant Soil* 348, 63–79.

Smith, S. E. and Read, D. J. (1997) *Mycorrhizal symbiosis*. 2nd Edition, San Diego: Academic Press.

Smith, S. E., and Read, D. J. (2010). *Mycorrhizal Symbiosis*. London: Academic Press.

Song, Y., Wang, M., Zeng, R., Groten, K., and Baldwin, I. T. (2019). Priming and filtering of antiherbivore defences among *Nicotiana attenuata* plants connected by mycorrhizal networks. *Plant Cell Environ.* 42, 2945–2961. doi: 10.1111/pce.13626

Tao, L., Hunter, M. D., and de Roode, J. C. (2017). Microbial root mutualists affect the predators and pathogens of herbivores above ground: mechanisms, magnitudes, and missing links. *Front. Ecol. Evol.* 5:160. doi: 10.3389/fevo.2017.00160

Těšitel, J., Tahadlová, M., Lepš, J., and Hölzel, N. (2021). Linking insect herbivory with plant traits: phylogenetically structured trait syndromes matter. *J. Veg. Sci.* 32:e13061. doi: 10.1111/jvs.13061

Tomczak, V. V., Schweiger, R., and Müller, C. (2016). Effects of arbuscular mycorrhiza on plant chemistry and the development and behavior of a generalist herbivore. *J. Chem. Ecol.* 42, 1247–1258. doi: 10.1007/s10886-016-0785-9

Unsicker, S. B., Kunert, G., and Gershenzon, J. (2009). Protective perfumes: the role of vegetative volatiles in plant defense against herbivores. *Curr. Opin. Plant Biol.* 12, 479–485.

van der Heijden, M. G., de Bruin, S., Luckerhoff, L., van Logtestijn, R. S., and Schlaeppi, K. (2016). A widespread plant-fungal-bacterial symbiosis promotes plant biodiversity, plant nutrition and seedling recruitment. *ISME J.* 10, 389–399. doi: 10.1038/ismej.2015.120

van der Heijden, M. G. A., Martin, F. M., Selosse, M., and Sanders, I. R. (2015). Mycorrhizal ecology and evolution: the past, the present, and the future. *New Phytol.* 205, 1406–1423. doi: 10.1111/nph.13288

van der Heijden, M. G. A., Streitwolf-Engel, R., Riedl, R., Siegrist, S., Neudecker, A., Ineichen, K., et al. (2006). The mycorrhizal contribution to plant productivity, plant nutrition and soil structure in experimental grassland. *New Phytol.* 172, 739–752. doi: 10.1111/j.1469-8137.2006.01862.x

Veenstra, J. A., Leyria, J., Orchard, I., and Lange, A. B. (2021). Identification of gonadulin and insulin-like growth factor from migratory locusts and their importance in reproduction in *Locusta migratoria*. *Front. Endocrinol.* 12: 693068. doi: 10.3389/fendo.2021.693068

Velásquez, A., Vega-Celedón, P., Fiaschi, G., Agnolucci, M., Avio, L., Giovannetti, M., et al. (2020). Responses of *Vitis vinifera* cv. Cabernet Sauvignon roots to the arbuscular mycorrhizal fungus *Funneliformis mosseae* and the plant growth-promoting rhizobacterium *Ensifer meliloti* include changes in volatile organic compounds. *Mycorrhiza* 30, 161–170. doi: 10.1007/s00572-020-00933-3

Vicari, M., Hatcher, P. E., and Ayres, P. G. (2002). Combined effect of foliar and mycorrhizal endophytes on an insect herbivore. *Ecology*. 83, 2452–2464. doi: 10.2307/3071806

Wang, M. G., Bezemer, T. M., van der Putten. Wim. H., Biere, Arjen. (2015). Effects of the Timing of Herbivory on Plant Defense Induction and Insect Performance in Ribwort Plantain (*Plantago lanceolata L.*) Depend on Plant Mycorrhizal Status. *J. Chem. Ecol.*, 41, 1006–17. doi: 10.1007/s10886-015-0644-0

Wang, P., Yin, X., and Zhang, L. (2019). Plant Approach-Avoidance response in locusts driven by plant volatile sensing at different ranges. *J. Chem. Ecol.* 45, 410–419. doi: 10.1007/s10886-019-01053-9

Wei, X. T., Shi, Y. N., Qin, F. W., Zhou, H. K., and Shao, X. Q. (2021). Effects of experimental warming, precipitation increase and their interaction on AM fungal community in an alpine grassland of the Qinghai-Tibetan Plateau. *Eur. J. Soil Biol.* 102:103272.

Wilkinson, T. D. J., Miranda, J., Ferrari, J., Hartley, S. E., and Hodge, A. (2019). Aphids influence soil fungal communities in conventional agricultural systems. *Front. Plant Sci.* 10:895. doi: 10.3389/fpls.2019.00895

Zhang, L., Lecoq, M., Latchininsky, A., and Hunter, D. (2019). Locust and grasshopper management. *Annu. Rev. Entomol.* 64, 15–34. doi: 10.1146/annurev-ento-011118-112500

Zhao, L. Y., Chen, J. L., Cheng, D. F., Sun, J. R., Liu, Y., Tian, Z., et al. (2009). Biochemical and molecular characterizations of *Sitobion avenae*-induced wheat defense responses. *Crop Protect.* 28, 435–442. doi: 10.1016/j.cropro.2009.01.005

Zu, P., Boege, K., Del-Val, E., Schuman, M. C., Stevenson, P. C., Zaldivar-Riverón, A., et al. (2020). Information arms race explains plant-herbivore chemical communication in ecological communities. *Science* 368, 1377–1381. doi: 10.1126/science.aba296

Conflict of Interest: The authors declare that the research was conducted in the absence of any commercial or financial relationships that could be construed as a potential conflict of interest.

Publisher's Note: All claims expressed in this article are solely those of the authors and do not necessarily represent those of their affiliated organizations, or those of the publisher, the editors and the reviewers. Any product that may be evaluated in this article, or claim that may be made by its manufacturer, is not guaranteed or endorsed by the publisher.

frontiers | Frontiers in Environmental Science

ORIGINAL RESEARCH
published: 08 April 2022
doi: 10.3389/fenvs.2022.865883

An Analytical Framework on Utilizing Natural Resources and Promoting Urban–Rural Development for Increasing Farmers' Income Through Industrial Development in Rural China

Xiangzheng Deng[1], Guofeng Wang[2], Wei Song[1], Mingxin Chen[1], Yujie Liu[1], Zhigang Sun[1], Jinwei Dong[1], Tianxiang Yue[1] and Wenjiao Shi[1]*

[1]Institute of Geographic Science and Natural Resources Research, CAS, Beijing, China, [2]Shanxi University of Finance and Economics, Taiyuan, China

Lucid waters and lush mountains are invaluable assets. The countryside is an important carrier of these assets, and rural revitalization is a national strategy to meet the needs of the people. This study constructs the framework system for improving the efficiency of resource utilization, refining the effect of urban–rural integration, and optimizing the efficiency of industrial development for increasing farmers' income. The challenges facing rural revitalization are clarified, especially including limited space for the growth of cultivated land quantity and significant challenges for quality improvement, insufficient effective supply of labor resources, uneven spatial distribution of water resources, low utilization efficiency of agricultural water resources, and so on. Finally, it puts forward the possible direction of future policies for rural revitalization, which is mainly reflected in the transformation of resource utilization efficiency improvement from single element to multi-element, the development of an urban–rural integration effect from extensive to lean, and the optimization of the industrial enrichment efficiency from management to comprehensive service. The analytical framework of resource utilization, urban–rural integration development, and industrial enrichment will provide regulatory policies and theoretical support for the flow of urban–rural factors.

Keywords: rural revitalization, resource guarantee, integrated urban–rural development, prosperous industrial development, people enrichment, framework

OPEN ACCESS

Edited by:
Shiliang Liu,
Beijing Normal University, China

Reviewed by:
Wei Liu,
Shandong Normal University, China
Jialin Li,
Ningbo University, China
Zhe Zhao,
Liaoning University, China

****Correspondence:***
Xiangzheng Deng
dengxz@igsnrr.ac.cn

Specialty section:
This article was submitted to Land Use Dynamics, a section of the journal Frontiers in Environmental Science

Received: *30 January 2022*
Accepted: *09 March 2022*
Published: *08 April 2022*

Citation:
Deng X, Wang G, Song W, Chen M, Liu Y, Sun Z, Dong J, Yue T and Shi W (2022) An Analytical Framework on Utilizing Natural Resources and Promoting Urban–Rural Development for Increasing Farmers' Income Through Industrial Development in Rural China. Front. Environ. Sci. 10:865883. doi: 10.3389/fenvs.2022.865883

INTRODUCTION

Lucid waters and lush mountains are invaluable assets, and rural revitalization is an important concept for the development of China's ecological civilization put forward by Chinese communists after a century of development practice. It is a vivid expression of the dialectical and unified relationship between economic development and ecological protection and is a Chinese solution for the sustainable development of the world (Liu et al., 2020). As one of the most important carriers of lucid waters and lush mountains, the countryside is the distribution center of these resources, and the rural revitalization strategy must practice the concept of these resources being invaluable assets (Yuan et al., 2018). China's socialist construction has entered the second centenary goal. Xi Jinping, the general secretary of the Communist Party of China (CPC) Central Committee, pointed out that

"the key to moderate prosperity is fellow-villagers," the foundation of the construction of a moderately prosperous society and a modern country is in agriculture, the difficulties are in the countryside, and the key is in the peasants. To this end, under the strategic framework of rural revitalization, it is important to clarify the framework, challenges, and policy directions for resource utilization, urban–rural integration development, and industrial enrichment (Liu et al., 2020). From the perspective of the actual development situation, clarifying the framework of resource utilization, urban–rural integration development, and industrial enrichment can fundamentally solve the "three rural" problems to achieve the "three lives" coordination of production, life, and ecology and promote agriculture, the processing industry, and modern service industry. In 2021, the total output value of agriculture, forestry, animal husbandry, and fishery reached 9,286.34 billion yuan. Among them, the total output value of agriculture was 4,667.11 billion yuan, of forestry was 384.13 billion yuan, of animal husbandry was 2,832.90 billion yuan, and of fishery was 912.96 billion yuan. The total national grain output reached 1,365.7 billion jin—an increase of 26.7 billion jin over the previous year, an increase of 2% year-on-year, and remained at 1.3 for seven consecutive years. The national grain sowing area was 1.764 billion mu, an increase of 12.95 million mu over the previous year, an increase of 0.7% year-on-year, and maintained a growth trend for two consecutive years. The 14th Five-Year Plan period is an important stage for China to base itself on a new stage of development, implement the new development concept, build a new development pattern, promote high-quality development, and promote common prosperity. From the perspective of research needs, to accelerate the realization of rural revitalization, (Elahi et al., 2021) it is necessary to optimize the layout of resource utilization, clarify the integration path of the primary, secondary, and tertiary industries in rural areas, and identify the industrial system schemes for enriching the people.

LITERATURE REVIEW

The concept of resources arises from the development of the discipline of economics (Wackernagel and Galli, 2007). A resource is the general term for the creation of all human wealth. At the same time, since human beings create many resources, they are the products of the combination of nature, human beings, and culture (science and technology). Resources are a dynamic historical category. With the deepening of the human cognition and utilization level, the evolution of resources gradually shows the characteristics from natural resources to physical resources, from living resources to means of production, and from physical resources to non-physical resources (Rahim et al., 2014). For a long time, a variety of cognitions have been formed around natural resources and their classification. *The Great British Encyclopedia* states that human beings can use natural products, and the environmental elements that produce these components are collectively referred to as resources. UNESCO proposes that natural resources are obtained from the natural environment and used by human beings. The United Nations Environment Programme (UNEP) notes that natural resources are substances that, at a certain time, place, and technical level, can generate economic value and provide natural factors and conditions for the present and future welfare of human beings (Zhong et al., 2020). Natural resources are available to human beings and are the material basis for human survival and development. Natural resources include land, water, minerals, biology, climate, and oceans (Elahi et al., 2021). Resource-related research has received widespread attention in political, economic, social, cultural, and other fields, and targeted research has gradually developed into theories of resource allocation and dependence (Todorovic et al., 2018). The specific theoretical debate on the use of resources revolved around efficiency and fairness, condensing the theory of efficiency priority, fairness priority, and efficiency and fairness (Satterthwaite et al., 2010; Fridrihsone et al., 2020). Marx pointed out in *Das Kapital* that the increase in the productivity of labor was achieved by shortening the socially necessary labor time for the production of a certain product. From this idea, efficiency was the process of creating more resource values with shorter social labor time (Hassan et al., 2019). Arthur believed that efficiency characterized the maximum output from a given input, and the efficiency of resource utilization needed to focus more on effective allocation (Jedwab et al., 2017). Fairness involves a broader concept, encompassing both intragenerational equity and intergenerational equity. Intragenerational fairness is the equality of resource utilization rights and opportunities, and intergenerational fairness is the equality of resource utilization opportunities in the present and future generations. According to the different standards of identification efficiency, the Pareto optimality, impossibility theorem, Pigou theory, Kaldor–Hicks theory, and Samuelson test have appeared in academic debates (Ke et al., 2012).

Globally, the transformation of urban–rural relations is a real challenge that all developing countries need to face, and China is no exception (MacLean and Gudelj, 2006). Since the founding of New China, urban–rural relations have gradually changed along with the development of the socialist cause, and the urban–rural relations at different stages have promoted the modernization of the country. The urban–rural relations are entering the stage of "urban–rural integration" after experiencing the development stages of "supporting the city with the countryside" and "leading the countryside by the city." Marx and Engels applied the methodology of historical materialism to reveal the historical trend of separation, opposition, and integration of urban–rural relations. The increasing separation of urban and rural areas results from the role of productive forces and production relations (Costa et al., 2018). Along with the improvement of productive forces, the relationship between urban and rural areas will gradually move from separation and opposition to integration, and only by realizing the integration of urban and rural areas can we promote the all-round development of the people. Urban–rural integration is the only way to solve the main contradiction based on socialist characteristics. In its development process, it combines historical trends, value orientations, and ultimate goals. At present, there are fewer domestic and foreign resources and environmental

management frameworks (Wang and Zhao, 2021), and the existing resources are only a single resource, such as water resources. With the expansion of research elements, the framework of the collaborative management of resources has also been extended, such as the water–food–energy management framework (Han et al., 2018), the water–food–ecological association, and the earth boundary concept framework. However, the theoretical system of resources and environmental policies and management that integrates resource utilization, urban–rural integration development, and industrial enrichment needs to be studied.

ANALYTICAL FRAMEWORK

Industrial enrichment is inseparable from the development of rural industries, which is the foundation to achieve the strategic goals and tasks of rural revitalization and agricultural and rural modernization in 2035. In 1990, Xi Jinping systematically expounded the "large agriculture concept" in *Out of a Road to Develop Large Agriculture*, pointing out that large agriculture is a three-dimensional agricultural development toward multi-functional, open, and comprehensive development. The top-level goals of resource utilization, urban–rural integration development, and the industrial enrichment framework are efficiency improvement (Zeng et al., 2020), effect improvement, and efficiency optimization (Bai and Tao, 2017). Its development involves multi-scale model simulation, multi-element mechanism analysis, multi-process role inversion, and multi-dimensional path exploration.

Guaranteed Resource and Its Utilization Efficiency

The guaranteed resource is a fundamental support for urban–rural integration and industrial enrichment. In *Agriculture and Industrialization*, it is pointed out that the grain is the main factor in determining the location of industry, commerce, and other economic activities. With the change of technology and economic conditions, other resources have partially replaced the positioning of food in terms of resources, but before or after the Industrial Revolution, food resources still play a pivotal role. As a key area of grain production, the primary resource guarantee function of the countryside is the supply guarantee function of agricultural products (Deng and Gibson, 2019). Since the founding of the People's Republic of China, China's food guarantee capacity has been steadily improved due to the state's supportive policies for food production. With the improvement of living standards, people need higher quality agricultural products for a better life, which also puts forward a new proposition for rural resource protection, not only to ensure quantity but also to ensure quality, and to produce products that meet the needs of the people (Qu et al., 2021). For the rural revitalization strategy, the resource items involved in resource guarantee are diverse—including core elements such as labor, capital, water, and soil and more important resources such as the technology, virtual water, virtual soil, and hidden carbon—which are all indispensable in the process of realizing rural revitalization. Efficiency improvement is the core essence of resource guarantee, and clarifying the different resource guarantee roads for rural revitalization is the primary goal of the framework. "Efficiency" is a complex, dynamic concept; its management perspective is the ratio relationship between various input resources and outputs at a specific time, and it is inversely proportional to inputs and proportional to outputs (Guo et al., 2020). The improvement of supply-side efficiency is moving toward high-quality agricultural products, effectively promoting the transformation of the agricultural industry, and embarking on a standardized, large-scale, and green path (Li et al., 2021). In the transformation process, the improvement of the resource utilization efficiency is the primary goal (Gołaś et al., 2020). The improvement of demand-side efficiency is moving toward the integration of primary, secondary, and tertiary industries, promoting the optimal allocation of production factors among industries, regions, and agricultural entities, improving rural resource guarantee capabilities (Ji and Hoti, 2021), and proposing a Chinese system and plan under the multiple goals of food security, nutritional security, and resource and environmental constraints.

Integrated Development of Urban and Rural Areas and Its Effect Improvement

The integration of urban and rural areas is the path of resource guarantee and industrial enrichment. The *Opinions of the CPC Central Committee and the State Council on Establishing and Improving the System and Policy System for the Integration of Urban and Rural Development* points out that the integrated development of urban and rural areas is the only way for rural revitalization and agricultural and rural modernization. Rural revitalization is inseparable from various resources and elements. Urban–rural integration is characterized by the free flow of urban and rural elements, equal exchange, and rational allocation of public resources. The relationship between urban and rural areas is reconstructed through integration. The integrated development of urban and rural areas is the main driving force for breaking the contradiction between urban and rural areas, and it is also an important symbol of agricultural modernization. Effect improvement is an important issue of urban–rural integration; urban–rural integration has no template, especially in provinces with large differences in natural endowments and uneven development. Therefore, it is necessary to clarify the shortcomings of urban–rural integration and break the unequal barrier between resources and factors for regional development characteristics. Effect improvement aims to restrict the integration of urban and rural primary, secondary, and tertiary industries, focusing on changing

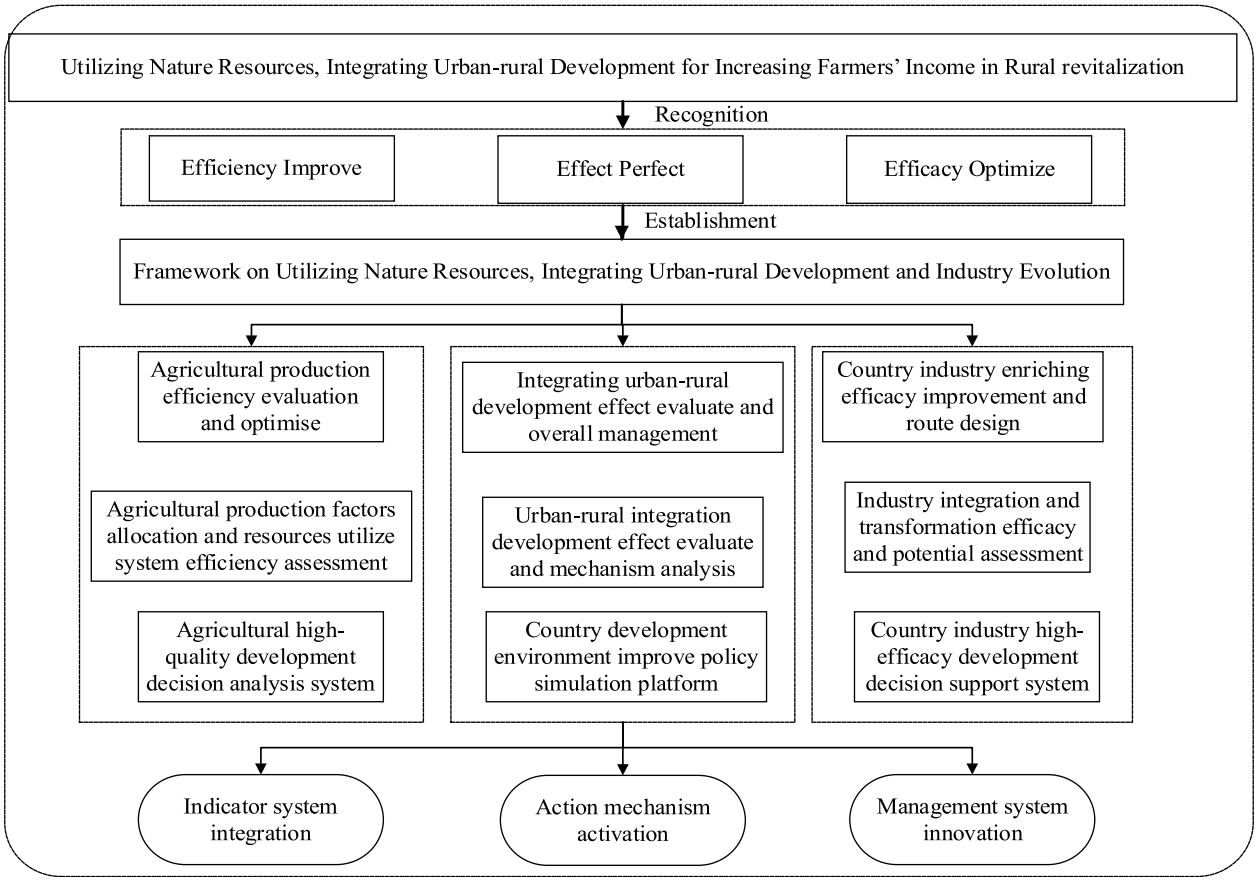

FIGURE 1 | Framework on Utilizing Nature Resources, Integrating Urban-rural Development for Increasing Farmers' Income in Rural revitalization.

the long-term unbalanced resource allocation mode, carrying out integration effect evaluation, exploring the overall management of resources, and revitalizing resources.

Strategy of Industrial Enrichment and Its Optimization Management

Industrial enrichment is the purpose of resource utilization and urban–rural integration, and these, in turn, are ultimately for the realization of industrial enrichment. The purpose of industrial prosperity is also to achieve industrial enrichment; whether it is the integrated development of the primary, secondary, and tertiary industries in rural areas or the realization of the development path of industrial ecology and ecological industrialization, it is constantly exploring the road to enrich the people in rural industries and achieving high-quality development by adjusting the industrial structure. The optimization management of industrial enrichment contains the concepts of space and time, and the realization of industrial enrichment is a systematic project. From the perspective of development geography, industrial enrichment is a function tending to the convergence of enriching the people, including the reform of the land property rights system, the increase of farmers' income and welfare, and the innovation of the agricultural industry. The optimization of industrial enrichment management needs to activate the main motivation, and there are many influencing factors for the promotion and adoption of the people enrichment industry, among which the cognition and perception of the farmer's main body have the greatest impact, especially the farmer's preference for industrial risk as the adopter. Under the influence of characteristics such as the education level and family structure, the subject decides on whether to adopt the people enrichment industry. Therefore, it is necessary to intervene in their cognition and perception. The optimization management of industrial enrichment needs to stimulate the main motivation. Optimizing management is the optimization of rural production, living, and ecological space, which involves industrial production and reproduction and requires the willpower of rural subjects to take action.

Analytical Framework for Resource Utilization, Urban–Rural Integrated Development, and Industrial Enrichment

Figure 1 is in view of the key and difficult issues of the "Agriculture, rural areas and farmers" problem and rural

revitalization, with the focus on the improvement of the resource utilization efficiency and the optimal management of agricultural production in rural revitalization, the integration of urban and rural development, and the improvement of the rural environment, the integration of rural industries and their transformation and development, etc. Through the analysis of the causal chain and efficiency transmission mechanism of "lucid waters and lush mountains are invaluable assets," we observed improving quality and efficiency, policies to enrich the people, environmental elements, industrial layout, and farmers' income increase and realizing the leap from empirical and theoretical combination, from case analysis to method summary, and from model simulation to policy simulation, including the original breakthrough of indicators, methods, and system tools. Specifically, in the efficiency evaluation of the agricultural production system, the core connotation of the improvement of the efficiency of the resource utilization system under the background of rural revitalization is clarified, the evaluation framework is established, the indicators, methods, models, and technical systems of the optimal management of resource utilization are innovated, and the modernization level of the agricultural production system and the management system is improved so as to promote the high-quality and high-efficiency development of agriculture. In terms of the evaluation of the effect of urban–rural integration development, the effect evaluation, mechanism analysis, and simulation platform of urban–rural integration development are integrated, the two-way flow and optimal allocation of capital and resource elements in the integration of urban and rural development are explored, the development of county urbanization, the smooth circulation of the urban and rural economy, the functional control of urban and rural land use, and the improvement of the rural environment are explored. In terms of the optimization and improvement of the efficiency of industrial integration and development, combining the background of national carbon neutrality goals (Van et al., 2019), carbon emission reduction, and climate change response based on the requirements of industrial ecology and ecological industrialization, the strategies for the prosperity of rural revitalization industries and farmers' income increases are explored, such as farmland transformation, land productivity improvement (Zhao et al., 2017), agricultural landscape diversity conservation, and biomass energy development so as to provide decision-making support for solving the "Agriculture, rural areas and farmers" problems and practicing the rural revitalization strategy.

SITUATIONS AND SOLUTIONS

There are still challenges in China's resource utilization system and urban–rural integration system to serve the industrial enrichment system. From the founding of the People's Republic of China in 1949 to the reform and opening up in 1978 and then to the establishment of a moderately prosperous society in 2020, New China has solved the food security problem of 1.4 billion people, and China's resource guarantee capacity has made great progress. At the 2020 Central Rural Economic Work Conference, Xi Jinping clearly emphasized that "it is necessary to firmly grasp the initiative in food security, and grain production should be grasped every year". Whether it is the "seventeen consecutive abundances" of grain supply or the substantial improvement of the efficiency of production factors and the level of technical efficiency, resources always play an important supporting role in ensuring the production capacity, and resource utilization, urban–rural integration development, and the industrial enrichment system are moving toward agricultural modernization. The "14th Five-Year Plan for National Economic and Social Development of the People's Republic of China and the Outline of Long-term Goals for 2035" clearly defines the binding indicators for the comprehensive production capacity of grains, and the grain production capacity should be ensured to be more than 1.3 trillion kilograms, which reflects the improvement of the comprehensive security capacity. At the same time, with the limited growth space of arable land resources, the insufficient effective supply of labor, and the tightening of constraints such as water resources, China is also facing many challenges in resource utilization and urban–rural integration development to achieve an industrial enrichment system.

Limited Increase Room of Cultivated Land and the Great Challenge of Quality Improvement

China's crop planting areas show a trend of increasing initially and then decreasing, and the growth space of the cultivated land quantity is limited. The results of relevant studies show that in order to ensure the balance between supply and demand of agricultural products, the planting area of crops needs 3.5 billion mu, but the area of crops available for actual use in China is only 2.5 billion mu; thus, the arable land gap is still 1 billion mu. From 2010 to 2015, the sown area increased from 158.579 million hectares to 166.829 million hectares, and from 2015 to 2019, the sown area showed a downward trend, with an "inverted U-shaped" growth. In 2019, the amount of agricultural land in Inner Mongolia and Tibet remained at a high level, and the number of cultivated lands accounted for 11.19 and 5.1% (**Figure 2A**). It is difficult to increase production by the traditional way to increase the land area, and the land resources that can be developed into arable land resources are extremely limited.

The challenge of improving the quality of a cultivated land is enormous. Under the dual circulation pattern, especially under the impact of the COVID-19 outbreak and the intensification of international political risks, the uncertainty of the supply of foreign grain resources of "two resources and two markets" has intensified. In addition, the demand for arable land resources to increase production capacity and improve the quality of cultivated land is critical. However, the contradiction of more people and less land in China leads to the long-term adoption of high input and overload operation of agriculture. From the

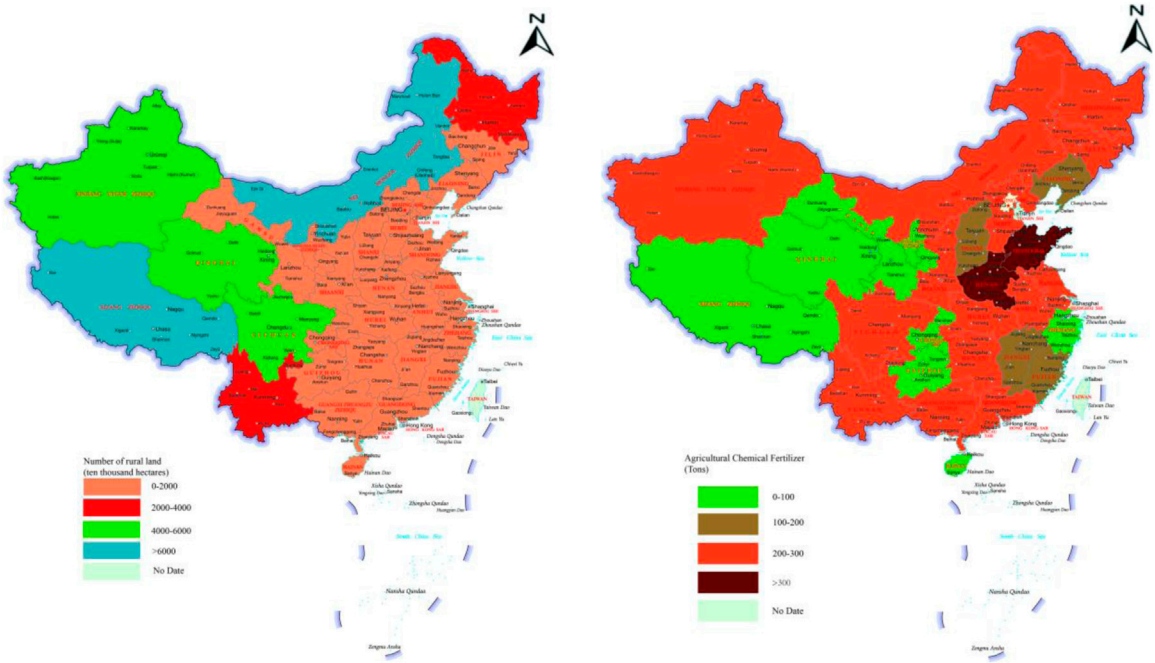

FIGURE 2 | The area of agricultural land and the pure volume of agricultural chemical fertilizers in 2019. [**(A)** Agricultural land area; **(B)** Agricultural chemical fertilizer].

perspective of the pure amount of agricultural chemical fertilizers in various provinces, municipalities, and autonomous regions, the amount of chemical fertilizer application in the main grain-producing areas is still maintained at a high level, of which the pure amount of agricultural fertilizers in Henan, Shandong, and other large agricultural provinces is more than 3 million tons (**Figure 2B**) so that the soil fertility degradation is serious, the organic matter content is low, and the solution of problems such as relatively poor soil strength requires a long period of time, and the quality improvement challenge is significant.

Insufficient Effective Supply of Labor Resources

The imbalance between urban and rural development has exacerbated the flow of labor to cities and towns; thus, the supply of rural labor is insufficient. With the rapid progress of urbanization construction in China, resources continue to accumulate, and migrant workers have become an important way for farmers to increase their income. The young and middle-aged rural labor force is accelerating to flow into cities with more favorable conditions. The problems of "aging" and "hollowing out" in rural areas have intensified, and "who will cultivate the land" has become a hot topic in the work of agriculture, rural areas, and farmers. In 2019, the rural population of China was 551.62 million, and provinces with a rural population of more than 30 million were clustered in Yunnan, Guangxi, Hunan, Wuhan, Hubei, and Jiangsu (**Figure 3A**). After the 1970s, it was the main force of rural land cultivation, the shortage of labor supply led to the serious problem of arable land famine.

The quality of rural labor supply is low, and it is difficult for farmers to master science and technology and agricultural machinery to meet the needs of modern agriculture. Farmers are important promoters of agricultural modernization, and new professional farmers can actively adapt to the needs of agricultural production and industrial development, but from the actual situation of development, the stock and flow of new professional farmers are insufficient. In addition, there are great differences in the development of total mechanical power in different provinces. In 2019, the total national power of agricultural machinery was 102,758.3 kWh. In major agricultural provinces of production, such as Shandong and Henan, the total power level of agricultural machinery was much higher than that of Ningxia, Qinghai, and other provinces (**Figure 3B**). Coupled with the ability and speed of rural labor, to master the new mechanization is relatively low, it is difficult to meet the needs of agricultural modernization.

Uneven Spatial Distribution of Water Resources and Inefficient Utilization of Multiple Agricultural Resources

China has a vast territory, diverse climate types, and spatial heterogeneity in resource distribution. In 2020, the national total amount of water resources was 3,160.52 billion cubic meters, ranking at the forefront of the world, but the per capita water resources were far from reaching the world average. Agriculture, as a "big household" in China's water

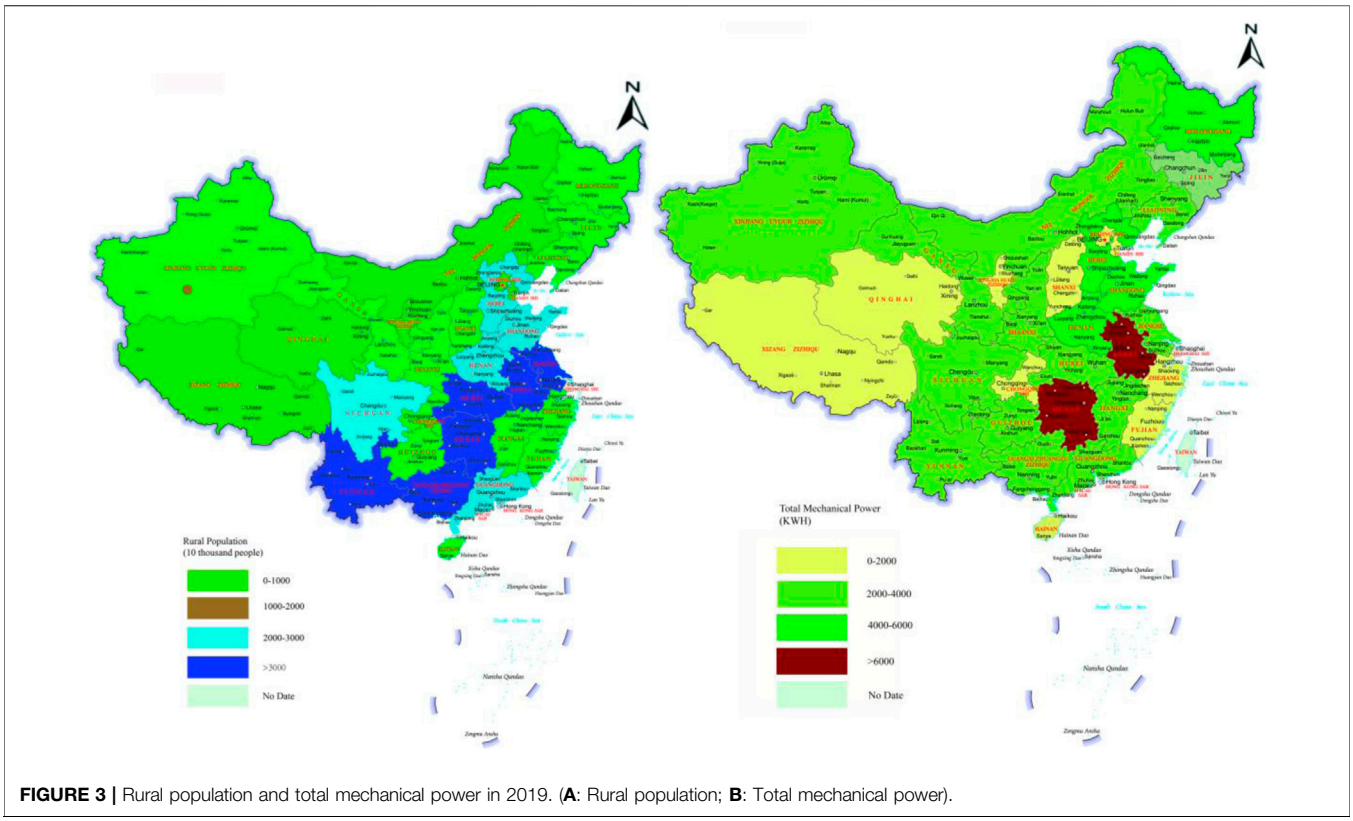

FIGURE 3 | Rural population and total mechanical power in 2019. (**A**: Rural population; **B**: Total mechanical power).

TABLE 1 | Agricultural water consumption and the effective utilization coefficient of farmland irrigation water in 2020.

Province	Total water use (m^3)	Agricultural water use (m^3)	Effective utilization coefficient of farmland irrigation water	Province	Total water use (m^3)	Agricultural water use (m^3)	Effective utilization coefficient of farmland irrigation water
Entire country	5812.9	3612.4	0.565	Henan	237.1	123.5	0.617
Beijing	40.6	3.2	0.75	Hubei	278.9	139.1	0.528
Tianjin	27.8	10.3	0.72	Hunan	305.1	195.8	0.541
Hebei	182.8	107.7	0.675	Guangdong	405.1	210.9	0.514
Shanxi	72.8	41	0.551	Guangxi	261.1	186.9	0.509
Inner Mongolia	194.4	140	0.564	Hainan	44	33.4	0.572
Liaoning	129.3	79.6	0.592	Chongqing	70.1	29	0.504
Jilin	117.7	83	0.602	Sichuan	236.9	153.9	0.484
Heilongjiang	314.1	278.4	0.613	Guizhou	90.1	51.8	0.486
Shanghai	97.5	15.2	0.738	Yunnan	156	110	0.492
Jiangsu	572	266.6	0.616	Tibet	32.2	27.4	0.451
Zhejiang	163.9	73.9	0.602	Shaanxi	90.6	55.6	0.579
Anhui	268.3	144.5	0.551	Gansu	109.9	83.7	0.57
Fujian	183	99.7	0.557	Qinghai	234.3	17.7	0.501
Jiangxi	244.1	161.9	0.515	Ningxia	70.2	58.6	0.551
Shandong	222.5	134	0.646	Xinjiang	570.4	46.2	0.57

resource utilization, occupies 62.1% of the total water consumption. The spatial mismatch between water resources and land resources is severe, which poses challenges to resource utilization, urban–rural integration development, and industrial enrichment. In 2019, the utilization efficiency of farmland irrigation water resources in China was 0.559. Although the water resource utilization efficiency of Beijing (0.75), Tianjin (0.72), Shanghai (0.738), and other provinces exceeded 0.7, the national overall agricultural water resource utilization efficiency was low, and there is a large room for

improvement compared with the level of 0.7 to 0.8 in developed countries (**Table 1**).

POLICY IMPLICATIONS

Resource utilization, urban–rural integration development, and industrial enrichment are organic combinations, and the three are mutually supportive and premised. Resource utilization is the foundation and starting point of urban–rural integration and industrial enrichment, and industrial enrichment is the purpose of resource utilization and urban–rural integration.

The Improvement of Resource Utilization Efficiency Has Been Transitioned From Single Element to Multi-Element

Resource guarantee is the security involving the whole chain of rural revitalization, and resource guarantee involves a variety of resource items, including core elements such as labor, capital, water, and land. It also includes technology, virtual water, virtual soil, and hidden carbon resources. The improvement of the resource utilization efficiency needs to leap from single element to multi-element, promoted by zones (industrial zone and ecological zone), by classification (characteristic type and promotion type), and by points (concentrated breakthrough point and delayed promotion point), and strive to improve the utilization efficiency of all elements of landscapes, forests, fields, lakes, and grasses. In the process of rural revitalization, it is necessary to optimize rural production, living and ecological space, accurately identify rural resource backgrounds, focus on rural development of the present situation and function orientation, emphasize foresight, rationality, and overall planning, reasonably delimit the efficiency of transition track, identify changes of the inflection point, give full play to the leading of national spatial planning development, and adjust measures to local conditions to explore the resource use efficiency promotion mode and path. In addition, it is supposed to strengthen the exploration of the potential of rural resources, promote the intensive use of land resources, revitalize idle rural land, optimize urban and rural land resources, increase efforts to transform hollow villages, and carry out land resource integration and improvement. It should also focus on soil improvement, soil fertility cultivation, water and fertilizer conservation, pollution control, and restoration to break the time and space constraints on water resources, improve the production and security capacity of cultivated land, strengthen land circulation to realize the "removal of cages for birds" of rural land resources, and revitalize idle houses and lands in rural areas. In this way, the construction of "small county and big city" will be rapidly promoted, population agglomeration will be promoted, the efficient use of natural resources will be promoted with a systematic concept, and the potential of land, water, forest, and other element resources will be further released.

The Integrated Development of Urban and Rural Areas Has Changed From Extensive to Lean Improvement

To promote the integration of urban and rural industries, it is supposed to further realize industrial prosperity and accelerate the development of primary, secondary, and tertiary industries. In terms of the product layer, the agricultural industry chain should be lengthening vertically, and a one-stop industrial chain of agricultural production, processing, and derivative manufacturing should be created to enhance the added value of agriculture. In terms of the industry layer, on the one hand, the agricultural production structure should be adjusted to produce more high-quality agricultural products that meet the people's needs for a better life. On the other hand, it is necessary to promote agricultural technological innovation, increase the guidance for agricultural technological innovation, pay attention to the incentives for agricultural machinery innovation, according to local conditions, and use new information technology to continuously improve the modern agricultural system. In terms of the guarantee layer, it needs to promote the equalization of urban and rural infrastructure, realize the common prosperity of urban and rural areas, improve the rural garbage disposal system, accelerate the construction of the rural infrastructure, improve the garbage disposal system, and promote the concept of green life and production. In terms of the culture layer, it is supposed to integrate rural cultural advantages, promote cultural integration between urban and rural areas, protect and inherit excellent rural culture, build cultural exchange platforms between urban and rural areas, and strengthen life and cultural exchanges between urban and rural areas to better promote the effect of urban and rural integration from extensive to lean. In terms of the factor layer, the circulation channels of urban and rural factors should be unblocked so that more high-quality products from the countryside can flow to the cities, and more capital from the cities can be injected into the countryside to complement each other's advantages.

Industrial Enrichment Has Marched From Routine Management to Comprehensive Services

In the process of industrial enrichment, attention should be paid to play the leading role of the agricultural industry. In accordance with the principle of "suitable farming, suitable animal husbandry, and suitable travel," the development concept of large-scale agriculture should be set up, the demonstration and driving effect of enriching the people by the industry should be paid attention, the restricting factors of the development path of enriching the people should be identified, the demonstration project/demonstration site construction scheme of enriching the people should be put forward, and the unique optimization road of enriching the people by the industry should be explored. From management to service, it is the change of the management strategy and the speculation on

who to serve and what kind of service to provide. High-quality industrial enrichment service is to provide farmers with selective services. Their needs may be very different for different farmers. Therefore, it is necessary to understand the missing items on the road of industrial enrichment, provide good "technological packages," sort out and actively participate in the transformation of new industries, carefully design effective services, drive the endogenous desire for self-development, carry out performance evaluation, diagnose the shortcomings, vulnerability, and resilience in the development process of "industrial enrichment," identify elasticity, thresholds, and inflection points, so as to provide scientific criteria for path identification and evaluation, and formulate a blueprint for industrial enrichment.

DATA AVAILABILITY STATEMENT

The datasets presented in this article are not readily available because the authors do not have permission to share data. Requests to access the datasets should be directed to GW, wanggf@sxufe.edu.cn.

AUTHOR CONTRIBUTIONS

All authors listed have made a substantial, direct, and intellectual contribution to the work and approved it for publication. XD: Conceptualization, and manuscript; GW and WS: Manuscript editing and manuscript review; MC, YL, and ZS: Manuscript review; JD, TY, and WS: Methodology and manuscript editing.

FUNDING

This research was supported by the Strategic Priority Research Program of the Chinese Academy of Sciences (Grant No. XDA23070400).

REFERENCES

Bai, H., and Tao, F. (2017). Sustainable Intensification Options to Improve Yield Potential and Eco-Efficiency for rice-wheat Rotation System in China. *Field Crops Res.* 211, 89–105. doi:10.1016/j.fcr.2017.06.010

Costa, M. P., Schoeneboom, J. C., Oliveira, S. A., Viñas, R. S., and de Medeiros, G. A. (2018). A Socio-Eco-Efficiency Analysis of Integrated and Non-integrated Crop-Livestock-Forestry Systems in the Brazilian Cerrado Based on LCA. *J. Clean. Prod.* 171, 1460–1471. doi:10.1016/j.jclepro.2017.10.063

Deng, X., and Gibson, J. (2019). Improving Eco-Efficiency for the Sustainable Agricultural Production: A Case Study in Shandong, China. *Technol. Forecast. Soc. Change* 144, 394–400. doi:10.1016/j.techfore.2018.01.027

Elahi, E., Khalid, Z., Tauni, M. Z., Zhang, H., and Lirong, X. (2021). Extreme Weather Events Risk to Crop-Production and the Adaptation of Innovative Management Strategies to Mitigate the Risk: A Retrospective Survey of Rural Punjab, Pakistan. *Technovation* (4), 102255. doi:10.1016/j.technovation.2021.102255

Elahi, E., Zhang, H., Lirong, X., Khalid, Z., and Xu, H. (2021). Understanding Cognitive and Socio-Psychological Factors Determining Farmers' Intentions to Use Improved Grassland: Implications of Land Use Policy for Sustainable Pasture Production. *Land Use Policy* 102, 105250. doi:10.1016/j.landusepol.2020.105250

Fridrihsone, A., Romagnoli, F., and Cabulis, U. (2020). Environmental Life Cycle Assessment of Rapeseed and Rapeseed Oil Produced in Northern Europe: A Latvian Case Study. *Sustainability* 12, 5699. doi:10.3390/su12145699

Gołaś, M., Sulewski, P., Wąs, A., Kłoczko-Gajewska, A., and Pogodzińska, K. (2020). On the Way to Sustainable Agriculture-Eco-Efficiency of Polish Commercial Farms. *Agriculture* 10, 438. doi:10.3390/agriculture10100438

Guo, B., He, D., Zhao, X., Zhang, Z., and Dong, Y. (2020). Analysis on the Spatiotemporal Patterns and Driving Mechanisms of China's Agricultural Production Efficiency from 2000 to 2015. *Phys. Chem. Earth, Parts A/B/C* 120, 102909. doi:10.1016/j.pce.2020.102909

Han, H., Zhong, Z., Wen, C., and Sun, H. (2018). Agricultural Environmental Total Factor Productivity in China under Technological Heterogeneity: Characteristics and Determinants. *Environ. Sci. Pollut. Res.* 25, 32096–32111. doi:10.1007/s11356-018-3142-4

Hassan, S. T., Xia, E., Khan, N. H., and Shah, S. M. A. (2019). Economic Growth, Natural Resources, and Ecological Footprints: Evidence from Pakistan. *Environ. Sci. Pollut. Res.* 26, 2929–2938. doi:10.1007/s11356-018-3803-3

Jedwab, R., Christiaensen, L., and Gindelsky, M. (2017). Demography, Urbanization and Development: Rural Push, Urban Pull and Urban Push? *J. Urban Econ.*

Ji, H., and Hoti, A. (2021). Green Economy Based Perspective of Low-Carbon Agriculture Growth for Total Factor Energy Efficiency Improvement. *Int. J. Syst. Assur. Eng. Manag.* doi:10.1007/s13198-021-01421

Li, Z., Sarwar, S., and Jin, T. (2021). Spatiotemporal Evolution and Improvement Potential of Agricultural Eco-Efficiency in Jiangsu Province. *Front. Energ. Res.* 9. doi:10.3389/fenrg.2021.746405

Liu, J., Jin, X., Xu, W., Gu, Z., Yang, X., Ren, J., et al. (2020). A New Framework of Land Use Efficiency for the Coordination Among Food, Economy and Ecology in Regional Development. *Sci. Total Environ.* 710, 135670. doi:10.1016/j.scitotenv.2019.135670

Liu, Y., Zang, Y., and Yang, Y. (2020). China's Rural Revitalization and Development: Theory, Technology and Management. *J. Geogr. Sci.* 30, 1923–1942. doi:10.1007/s11442-020-1819-3

Lwin, C. M., Nogi, A., and Hashimoto, S. (2017). Eco-Efficiency Assessment of Material Use: The Case of Phosphorus Fertilizer Usage in Japan's Rice Sector. *Sustainability* 9, 1562. doi:10.3390/su9091562

MacLean, R. C., and Gudelj, I. (2006). Resource Competition and Social Conflict in Experimental Populations of Yeast. *Nature* 441, 498–501. doi:10.1038/nature04624

Qu, Y., Lyu, X., Peng, W., and Xin, Z. (2021). How to Evaluate the Green Utilization Efficiency of Cultivated Land in a Farming Household? A Case Study of Shandong Province, China. *Land* 10, 789. doi:10.3390/land10080789

Rahim, H. L., Abidin, Z. Z., Ping, S. D. S., Alias, M. K., and Muhamad, A. I. (2014). Globalization and its effect on world poverty and inequality. *GJMBR* 1 (2), 9–13.

Satterthwaite, D., McGranahan, G., and Tacoli, C. (2010). Urbanization and its Implications for Food and Farming. *Phil. Trans. R. Soc. B* 365, 2809–2820. doi:10.1098/rstb.2010.0136

Todorović, M., Mehmeti, A., and Cantore, V. (2018). Impact of Different Water and Nitrogen Inputs on the Eco-Efficiency of Durum Wheat Cultivation in Mediterranean Environments. *J. Clean. Prod.* 183, 1276–1288. doi:10.1016/j.jclepro.2018.02.200

Van, T., Elahi, E., Zhang, L., Magsi, H., Trung, Q., Hoang, T. M., et al. (2019). Historical Perspective of Climate Change in Sustainable Livelihoods of Coastal Areas of the Red River Delta, Nam Dinh, Vietnam. *INT. J. CLIM. CHANG STR* 11 (5), 687–695.

Wackernagel, M., and Galli, A. (2007). An Overview on Ecological Footprint and Sustainable Development: A Chat with Mathis Wackernagel. *Int. J. Eco* 2, 1–9. doi:10.2495/ECO-V2-N1-1-9

Wang, Y., and Zhao, G. (2021). A Joint Use of Life Cycle Assessment and Emergy Analysis for Sustainability Evaluation of an Intensive Agro-System in China. *Environ. Dev. Sustain.* doi:10.1007/s10668-021-01929-5

Yuan, J., Lu, Y., Ferrier, R. C., Liu, Z., Su, H., Meng, J., et al. (2018). Urbanization, Rural Development and Environmental Health in China. *Environ. Develop.* 28, 101–110. doi:10.1016/j.envdev.2018.10.002

Zeng, L., Li, X., and Ruiz-Menjivar, J. (2020). The Effect of Crop Diversity on Agricultural Eco-Efficiency in China: A Blessing or a Curse? *J. Clean. Prod.* 276, 124243. doi:10.1016/j.jclepro.2020.124243

Zhao, X., Zhang, X., Li, N., Shao, S., and Geng, Y. (2017). Decoupling Economic Growth from Carbon Dioxide Emissions in China: A Sectoral Factor Decomposition Analysis. *J. Clean. Prod.* 142, 3500–3516. doi:10.1016/j.jclepro.2016.10.117

Zhong, Z., Peng, B., Xu, L., Andrews, A., and Elahi, E. (2020). Analysis of Regional Energy Economic Efficiency and its Influencing Factors: A Case Study of Yangtze River Urban Agglomeration. *Sustainable Energ. Tech. Assessments* 41 (7–9), 100784. doi:10.1016/j.seta.2020.100784

Conflict of Interest: The authors declare that the research was conducted in the absence of any commercial or financial relationships that could be construed as a potential conflict of interest.

Publisher's Note: All claims expressed in this article are solely those of the authors and do not necessarily represent those of their affiliated organizations, or those of the publisher, the editors, and the reviewers. Any product that may be evaluated in this article, or claim that may be made by its manufacturer, is not guaranteed or endorsed by the publisher.

frontiers | Frontiers in Environmental Science

ORIGINAL RESEARCH
published: 08 April 2022
doi: 10.3389/fenvs.2022.848134

Ecological Efficiency of Grass-Based Livestock Husbandry Under the Background of Rural Revitalization: An Empirical Study of Agro-Pastoral Ecotone

Dawei He[1], Xiangzheng Deng[2,3], Gui Jin[4], Xinsheng Wang[1], Yali Zhang[2], Zhigang Sun[2], Wenjiao Shi[2] and Zhe Zhao[5]*

[1]Hubei Engineering Research Center for Remote Sensing Technology in Agriculture, Hubei University, Wuhan, China, [2]Institute of Geographic Sciences and Natural Resources Research, Chinese Academy of Sciences, Beijing, China, [3]University of Chinese Academy of Sciences, Beijing, China, [4]School of Economics and Management, China University of Geosciences, Wuhan, China, [5]School of Economics, Liaoning University, Shenyang, China

OPEN ACCESS

Edited by:
Fan Zhang,
Institute of Geographic Sciences and Natural Resources Research (CAS), China

Reviewed by:
Wei Liu,
Shandong Normal University, China
Jialin Li,
Ningbo University, China

***Correspondence:**
Xiangzheng Deng
dengxz@igsnrr.ac.cn

Specialty section:
This article was submitted to Land Use Dynamics, a section of the journal Frontiers in Environmental Science

Received: *04 January 2022*
Accepted: *28 January 2022*
Published: *08 April 2022*

Citation:
He D, Deng X, Jin G, Wang X, Zhang Y, Sun Z, Shi W and Zhao Z (2022) Ecological Efficiency of Grass-Based Livestock Husbandry Under the Background of Rural Revitalization: An Empirical Study of Agro-Pastoral Ecotone. Front. Environ. Sci. 10:848134. doi: 10.3389/fenvs.2022.848134

As the starting point of addressing the issue of "agriculture, rural areas, and farmers" for a new era, a rural revitalization strategy is necessary and suits the realistic demand for high-quality development. At present, agro-pastoral ecotone in China is facing a series of ecological degradation and environmental pollution problems. The measurement and analysis of ecological efficiency play an important role in promoting the sustainable development of the agro-pastoral ecotone. Based on the theoretical discussion and empirical calculation, this study took Tongliao as a case area to explore the ecological efficiency issue. Firstly, the ecological efficiency of grass-based livestock husbandry in Tongliao from 2000 to 2019 was calculated by the DEA method, then the dynamic change of efficiency was dissected by the Malmquist index, and finally, multiple factors affecting the ecological efficiency of grass-based livestock husbandry were evaluated by Tobit model. The results showed that the ecological efficiency of grass-based livestock husbandry in the counties of Tongliao showed a growing trend from 2000 to 2019, and the average ecological efficiency increased from 0.88 to 1.17. The total factor ecological efficiency of the counties in Tongliao had increased year by year from 2000 to 2019, and it mainly depended on technological progress. The implementation of the national ecological protection policy and the increase of the output value and number of persons employed in grass-based livestock husbandry has significantly improved the ecological efficiency. However, the increase in the number of livestock, especially in the case of exceeding the carrying capacity of the grassland, was not conducive to the protection of grassland ecology. The key to realizing the revitalization of grass-based livestock husbandry in the future is to promote the coordinated development of economy and ecology through the improvement of management level and large-scale and standardized livestock breeding.

Keywords: rural revitalization, ecological efficiency, grass-based livestock husbandry, DEA method, agro-pastoral ecotone

1 INTRODUCTION

The 19th National Congress of the Communist Party of China put forward the general requirements for a rural revitalization strategy: "thriving businesses, pleasant living environments, social etiquette and civility, effective governance, and prosperity". The Outline of the 14th Five-Year Plan (2021–2025) for National Economic and Social Development and Vision 2035 of the People's Republic of China further proposed to prioritize the development of agriculture and rural areas and promote all-round rural revitalization. In the new period of promoting the effective connection between poverty alleviation and rural revitalization, rural industry and ecology are the basis of achieving this goal. As a modern industry under the coordination of industrial ecology and ecological industrialization, grass-based livestock husbandry is an important link to realize rural revitalization and the ecological construction of civilization. In the process of traditional agricultural production, economic benefits have always been placed first (Deng and Gibson, 2018; Lv et al., 2021). However, with the increasing demand for food in China, excessive development and utilization of land resources directly lead to a series of ecological problems, such as soil erosion, land degradation, water pollution, and so forth (Tian et al., 2021). In the northern agro-pastoral ecotone with frequent drought, poverty agglomeration, and fragile ecology, the change of the rural human-land relationship is very demanding (Shi et al., 2018). The agro-pastoral ecotone has an important strategic position in China's territorial space, and it should focus on coordinating multiple objectives such as society, environment, and ecology, (Zhang et al., 2020). Under tight pressure on resources and the environment, choosing a sustainable mode of rural industrial development to meet hundreds of millions of farmers' yearnings for a better life is an important goal of the efforts concerning "agriculture, rural areas, and farmers" and rural revitalization strategy (Sun et al., 2015).

Thriving businesses is the primary goal and focus of implementing a rural revitalization strategy, but in the process of rural industrial development, the connotation analysis and evaluation criteria of "thriving businesses" is missing. Under the guidance of high-quality development of agriculture and rural areas, this study brought "ecological efficiency" into the evaluation criteria of "thriving businesses" as a specific starting point to realize rural revitalization at the industrial level (Yin et al., 2014). This means realizing the sustainable development of rural areas in the unity of economic benefits and environmental benefits and providing inexhaustible power for rural revitalization. Ecological efficiency was first defined as obtaining the maximum economic value with minimized resource input and environmental cost (Schaltegger and Sturm, 1990). Domestic scholars have carried out various research to define the connotation of ecological efficiency from the aspects of social economy, resource utilization, energy consumption, product price, and so on (Yin et al., 2014; Liu et al., 2020; Tan and Lin, 2020). Existing research on ecological efficiency in China and abroad mainly includes two aspects: the calculation of and the application of ecological efficiency. The calculation methods of ecological efficiency mainly include the ratio method, index system method, and mathematical model method. The ratio method is considered to be the most basic method for measuring ecological efficiency (Zhou et al., 2018). However, the single ratio method assumes that the optimal solution has been considered, cannot distinguish the effects of different environments, and cannot provide a set of optimal solutions for decision-makers. It is only applicable to the analysis of mutually independent objects (Zhao et al., 2017). The index system method is the main method used to evaluate ecological efficiency, but there are some problems such as incomplete index and subjectivity, which can be made up for by calculating ecological efficiency by the mathematical model (Deng and Gibson 2019; Guo et al., 2020). Data Envelopment Analysis (DEA) evaluates the relative effectiveness of the same type of decision-making units based on multi-index input and multi-index output. Through automatic weighting to reduce the subjectivity of environmental index weighting, the combination of multi-input and multi-output can be explained clearly, therefore it is widely used in the calculation of ecological efficiency (Rebolledo-Leiva et al., 2019). In the application of ecological efficiency, the existing research can be summarized to micro-level, mesoscale level, and macro-level, which focuses on enterprises, industries, and regions, respectively, (Arabi et al., 2014; Koskela et al., 2015; Bonfiglio et al., 2017; Jin et al., 2018; Xing et al., 2018). The research at the macro level includes the differences and causes of ecological efficiency in different regions, the analysis of the competitive advantage of regional long-term development, and the temporal and spatial changes of inter-regional ecological efficiency (Yue et al., 2017; Yang and Yang, 2019).

Most research on ecological efficiency focuses on the planting industry, with little research on grass-based livestock husbandry, especially in the agro-pastoral ecotone. In the adjustment of the planting structure of "grain, industrial, and forage crops", the development of grass-based livestock husbandry in the northern agro-pastoral ecotone is of great significance to improve the efficiency of resource utilization and agricultural production. Accurate and objective ecological efficiency assessment can reflect the main problems in the development of grass-based livestock husbandry, coordinate agricultural development and ecological environment protection, and promote regional sustainable development and rural revitalization. This study took Tongliao, which is located in the northeast section of the northern agro-pastoral ecotone, as a case area to evaluate the change of ecological efficiency of grass-based livestock husbandry and identify the key influencing factors. At the same time, this study analyzed the actual level of thriving businesses under the rural revitalization strategy and discusses the coordinated development path of resource conservation and sound ecosystem, which aimed to provide decision support for rural industrial development.

2 THEORETICAL FRAMEWORK AND METHODS

2.1 Development of Grass-Based Livestock Husbandry Under the Goal of Thriving Businesses

"Thriving businesses" is a development goal based on the production function of rural areas. It strives to promote the integrated development of rural primary, secondary, and tertiary industries based on advantageous industries according to local conditions and aims to enhance farmers' income and enhance the international competitiveness of agriculture at the same time. "Thriving businesses" has become an essential prerequisite for the realization of agricultural and rural modernization. The northern agro-pastoral ecotone is an important production space for the coordination of the agro-grassland system and cropland system. With further adjustment of the proportion of planting area of "grain, industrial, and forage crops", the quality and efficiency of the foraging industry are gradually improved, and the growing grass-based livestock husbandry has become an important support for the industrial revitalization of the agro-pastoral ecotone. However, due to the expansion of the scope of human activities, there are a series of problems in the agro-pastoral ecotone, such as land degradation, water pollution, ecological disruption, and so on, which leads to a fragile ecological environment and increasingly prominent conflict between humans and the land. The development of grass-based livestock husbandry is highly dependent on the ecological environment. In the tradeoff between production function and ecological function of grassland, only the high-quality development mode of "ecological priority" can realize the sustainable development of grass-based livestock husbandry and provide a solid guarantee for the rural revitalization in the agro-pastoral ecotone.

2.2 Interpretation of Ecological Efficiency of Grass-Based Livestock Husbandry

"Economic efficiency" is an important standard to measure the limited social resources to meet people's practical needs from the perspective of income and cost, and it has gradually become the focus of social development. However, with social and economic development, human beings have a higher level of demand for livelihood. Under the constraints of resources and environmental carrying capacity, we begin to pay attention to improving production efficiency and at the same time reducing the impact on the environment. The "ecological efficiency" of coordinating economic and environmental benefits has gradually become the focus of efficiency research. In 1990, ecological efficiency was clearly defined for the first time as "people achieve the goal of maximizing economic value on the premise of minimizing resource input and environmental costs on the basis of the added value and environmental impact of economic activities" (Schaltegger and Synnestvedt, 2002). Subsequently, government departments and academia carried out a series of studies and discussions on the concept and connotation of ecological efficiency. The World Business Council for Sustainable Development (WBCSD) defined ecological efficiency as "On the basis of ensuring the quality and needs of human life, provide products or services with competitive prices by controlling the environmental impact and resource consumption in the life cycle within the carrying capacity of the Earth". This definition has been widely accepted and promoted by the Organization for Economic Co-operation and Development (OECD). In this definition, ecological efficiency is regarded as the ratio of input to output, which means that the output (the value of services and products) must be maximized in the production process while the consumption of resources and the impact on the environment must be minimized.

Domestic scholars extended the connotation of ecological efficiency from various perspectives, including social economy, resource utilization, energy consumption, product price, and so on (Ma et al., 2018; Liu et al., 2020; Dong et al., 2020). It is generally believed that ecological efficiency is an important index to characterize the construction level of ecological civilization and the ability of sustainable development (Hu et al., 2019). The essence of ecological efficiency is to minimize the negative impact on resources and the environment in the process of pursuing economic benefits, that is, to exchange the minimum resource input for the maximum economic output. It is emphasized in the National Agricultural Sustainable Development Plan (2015–2030) that the sustainable development of agriculture is the fundamental guarantee and priority area of China's sustainable development. The ecological efficiency of grass-based livestock husbandry is the embodiment of ecological efficiency in the field of agriculture, and the improvement of ecological efficiency has become an important way to promote the sustainable development of grass-based livestock husbandry (Yin et al., 2014; Liu et al., 2018). The key to achieving the sustainable development of grass-based livestock husbandry is to reduce the consumption of resources and the negative impact on the ecosystem by production activities, and finally achieve a win-win situation of both economic and ecological benefits. The agro-pastoral ecotone still faces the arduous tasks of resource-saving and environmental protection, grass-based livestock husbandry with high ecological efficiency takes into account both ecological and economic benefits, which is the inevitable way to realize the revitalization of rural industry.

2.3 Evaluation Methods of Ecological Efficiency

2.3.1 Ecological Efficiency

Data Envelopment Analysis (DEA), proposed by Charnes, Cooper, and Rhodes, is a production analysis method to measure technical efficiency through linear programming (Charnes et al., 1978). The DEA model adopts the concept of mathematical programming to determine whether the multi-input and multi-output decision-making unit (DMU) is located on the "production Frontier" of the production

possibility set and then identify the relative effectiveness of the decision-making unit.

Suppose there are n ($n = 1, 2, 3, \ldots, N$) decision-making units of grass-based livestock husbandry production, and the output of j ($j = 1, 2, 3, \ldots, J$) factors is obtained by using the input of i ($i = 1, 2, 3, \ldots, I$) factors in every period of t ($t = 1, 2, \ldots, T$). In the input-output index system, it is expressed by x and y, respectively, then the input-output index of n grass-based livestock husbandry production decision-making units in t period can be expressed as $x_{n,j}^{\ i}$, $y_{n,j}^{\ i}$. Without considering the change of time dimension, the input-output data of decision-making unit i can usually be recorded as $x_i = (x_{1n}, x_{2n}, x_{3n}\ldots, x_{mn})$, $y_i = (y_{1n}, y_{2n}, y_{3n}\ldots, y_{sn})$, $n = 1, 2, \ldots, N$. The model under this data recording mode can be expressed as follows:

Based on the CCR model, the non-Archimedean infinitesimal ε, relaxation variable S_j^- and residual variable S_j^+ are introduced, and the efficiency linear programming model of DMU_0 is expressed as follows:

$$\min \theta^{CCR} - \varepsilon\left(\sum_{i=1}^{m} s_i^- + \sum_{i=1}^{m} s^+\right)$$

$$s.t.\begin{cases} \sum_{j=1}^{n} \lambda_j X_{ij} + s_i^- = \theta^{CCR} X_0 \\ \sum_{j=1}^{n} \lambda_j Y_{ij} - s_i^+ = Y_0 \\ \lambda_j \geqq 0,\ j = 1, 2, \ldots, n \\ s^- \geqq 0, s^+ \geqq 0 \end{cases}$$

Where, λ_j is the weight variable, and the DMU_0 optimal solution is θ^*、λ^*、S^{*+}、S^*. If it satisfies $\theta^* = 1$ and $S^{*+} = S^{*-} = 0$, then $DMU0$ is DEA efficient, indicating that both scale and technology are effective; If $S^{*+} \neq 0$ or $S^{*-} \neq 0$, then DMU_0 is weakly DEA efficient, indicating that scale and technology are not efficient at the same time; if $\theta^* < 1$, DMU_0 is non-DEA efficient, neither scale efficient nor technical efficient, and the closer the efficiency value is to 1, the higher the relative efficiency of DEA.

The super-efficiency DEA model is the ranking and analysis of the points on the Frontier (technical efficient units) based on the traditional DEA model. The realization path is that when some points are in the efficiency Frontier, it is necessary to exclude this point when evaluating the efficiency of one point (such as point A), and several other points on the Frontier reconstitute a new efficiency Frontier curve, in which case the efficiency value of the point is greater than 1. By analogy, the efficiency values of all the sets of points on the production frontiers can be obtained, respectively. The formula is as follows:

$$\begin{cases} \min\left[\theta^{SUP} - \varepsilon\left(\sum_{i=1}^{m} s_i^- + \sum_{i=1}^{s} s_r^+\right)\right] \\ \sum_{j=1, j\neq k}^{n} \lambda_j X_{ij} + s_i^- \leq \theta^{SUP} X_0 \\ \sum_{j=1, j\neq k}^{n} \lambda_j Y_{ij} - s^+ \leq Y_0 \\ \lambda_j \geqq 0,\ j = 1, 2, \ldots, n, s^- \geqq 0, s^+ \geqq 0 \end{cases}$$

Where, θ is super-efficiency, $s^-(s^- \geq 0)$ is the relaxation variable, $s^+(s^+ \geq 0)$ is the residual variable, and ε is the non-Archimedean infinitesimal. Based on the DEA model under the premise of constant return to scale (CRS) described in the above formula, $\theta = 1$ indicates that the ecological efficiency of the decision-making unit is on the "production Frontier" of the production possible set, that is, the technology of the decision-making unit is effective. On this basis, by introducing the constraint $\sum_{j=1}^{k} \lambda_j = 1$, it can be transformed into a more realistic DEA model of variable return to scale (VRS).

2.3.2 Total Factor Ecological Efficiency

Malmquist productivity was originally proposed by the Swedish economist Sten Malmquist (1953), through the concept of scaling factor to construct the consumption quantity index, and then applied by Caves et al. (1982) to the production analysis of constructing the productivity index through the ratio of the distance function. However, due to the lack of a method to measure the distance index at the initial stage, the Malmquist index exists only in the form of theory, and then Färe and Grosskopf (1992) applied the theoretical index of Malmquist productivity to practical calculation through the DEA method. The Malmquist productivity index is defined based on the benchmark technology. The Malmquist productivity indices of t and $t+1$ with reference to technology are:

$$M_t\left(x^t, y^t, x^{t+1}, y^{t+1}\right) = \frac{D_C^t\left(x^{t+1}, y^{t+1}\right)}{D_C^t\left(x^t, y^t\right)}$$

$$M_{t+1}\left(x^t, y^t, x^{t+1}, y^{t+1}\right) = \frac{D_C^{t+1}\left(x^{t+1}, y^{t+1}\right)}{D_C^{t+1}\left(x^t, y^t\right)}$$

Since periods t and $t+1$ are symmetrical in economic meaning, the Malmquist productivity index is defined as the geometric average of the two periods of total factor productivity according to the ideal index idea:

$$M\left(x^t, y^t, x^{t+1}, y^{t+1}\right) = \left(M_t \cdot M_{t+1}\right)^{1/2} = \left[\frac{D_C^t\left(x^{t+1}, y^{t+1}\right)}{D_C^t\left(x^t, y^t\right)} \frac{D_C^{t+1}\left(x^{t+1}, y^{t+1}\right)}{D_C^{t+1}\left(x^t, y^t\right)}\right]^{1/2}$$

Using the method proposed by Ray and Desli (1997), it can be further decomposed into changes in technical efficiency, technological progress, and scale efficiency. The decomposition process is as follows:

$$M_t\left(x^t, y^t, x^{t+1}, y^{t+1}\right) = \frac{D_V^{t+1}\left(x^{t+1}, y^{t+1}\right)}{D_V^t\left(x^t, y^t\right)} \times \left[\frac{D_V^t\left(x^t, y^t\right)}{D_V^{t+1}\left(x^t, y^t\right)} \frac{D_V^t\left(x^{t+1}, y^{t+1}\right)}{D_V^{t+1}\left(x^{t+1}, y^{t+1}\right)}\right]^{1/2} \times \left[\frac{D_C^t\left(x^{t+1}, y^{t+1}\right)/D_V^t\left(x^{t+1}, y^{t+1}\right)}{D_C^t\left(x^t, y^t\right)/D_V^t\left(x^t, y^t\right)} \frac{D_C^{t+1}\left(x^{t+1}, y^{t+1}\right)/D_V^{t+1}\left(x^{t+1}, y^{t+1}\right)}{D_C^{t+1}\left(x^t, y^t\right)/D_V^{t+1}\left(x^t, y^t\right)}\right]^{1/2} = TE\Delta_{RD} \times TP\Delta_{RD} \times SE\Delta_{RD}$$

Where, $D^t\left(x_t, y_t\right)$ is the distance between the actual output and the production Frontier in t period, TE represents pure technical efficiency, TP represents technological progress, and SE represents scale efficiency.

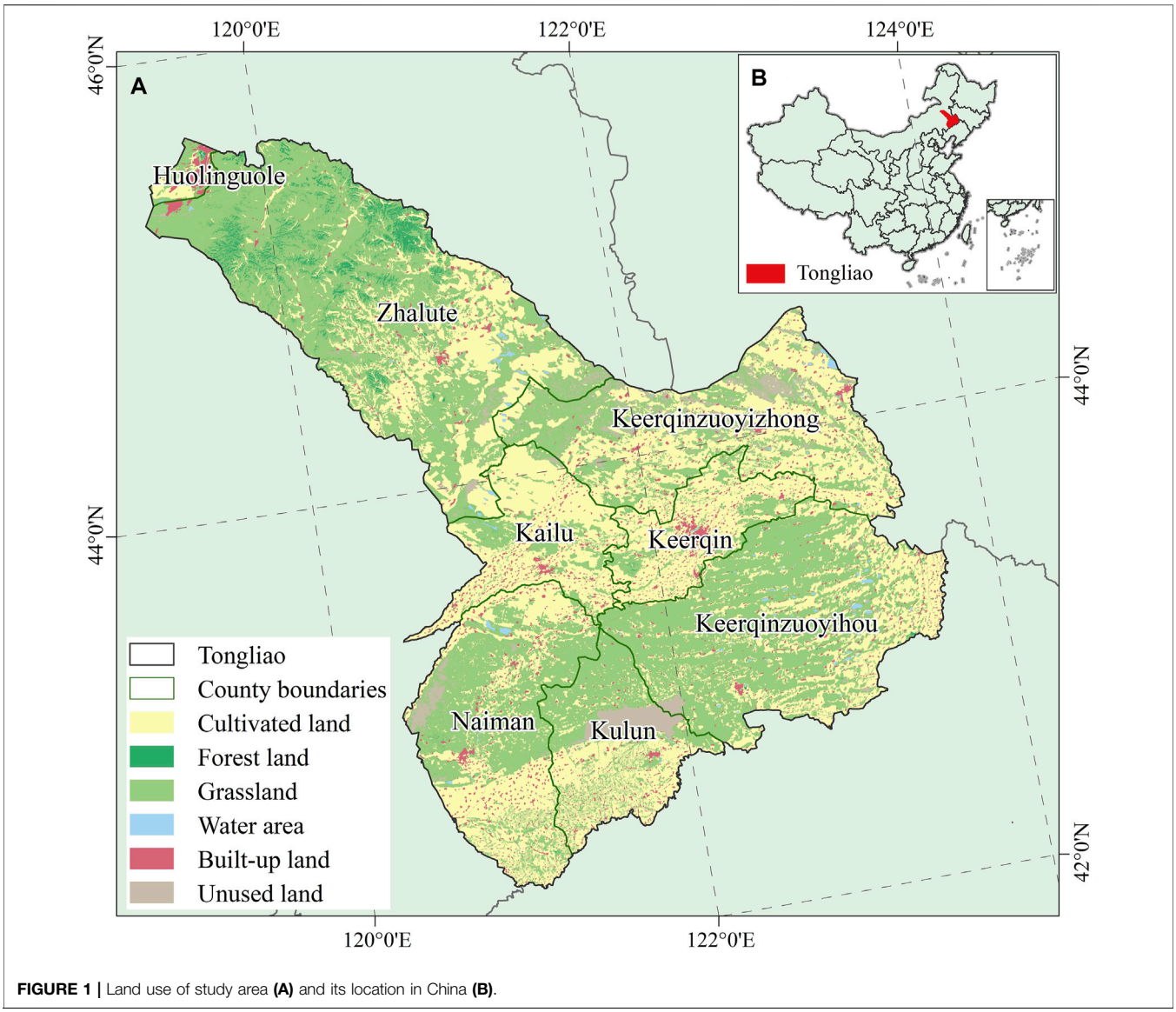

FIGURE 1 | Land use of study area **(A)** and its location in China **(B)**.

The decomposition method comprehensively analyzes the temporal and spatial changes of the total factor ecological efficiency of grass-based livestock husbandry production DMU from three dimensions: the distance from the production Frontier, the movement characteristics of the production Frontier in different periods, and the time variation characteristics of returns to scale. The super-efficiency DEA model can reflect the relative efficiency of each DMU at a certain time but cannot reflect the change of ecological efficiency over time. On the other hand, the Malmquist index reveals the changing trend over time through the change of ecological efficiency relative to the previous time point, but it is unable to compare the difference of ecological efficiency of each DMU.

2.3.3 Influencing Factors of Ecological Efficiency

The analysis of the influencing mechanism of the leading factors on the ecological efficiency of grass-based livestock husbandry in the agro-pastoral ecotone is a supplement to the calculation of ecological efficiency, the characterization of spatio-temporal pattern, and the correlation simulation of regional units. As a variable with boundaries, the ecological efficiency of grass-based livestock husbandry is difficult estimate without bias by traditional analysis methods such as OLS, so it is necessary to use the Tobit regression model to estimate it. The Tobit model uses a piecewise function to accurately estimate the restricted dependent variables of truncation or censorship to avoid the potential risk of biased and inconsistent estimation. The formula is as follows:

$$Y_i = \begin{cases} a_0 + \sum_k a_k X_{ki} + \varepsilon_i, Y_i > 0 \\ 0, Y_i > 0 \end{cases}$$

Where, Y_i represents the ecological efficiency of grass-based livestock husbandry in different periods in area i, X_{ki} represents the variable of influencing factors, α_0 is the constant term, α_k is the regression coefficient of influencing factors, and ε_i is the error term that obeys normal distribution. When $Y_i>0$, the actual observed value is taken; when $Y_{it}\leq 0$, the observed value is truncated to 0.

3 EMPIRICAL ANALYSIS

3.1 Study Area

The agro-pastoral ecotone in northern China ranges from Hulun Buir at the western foot of the Daxing'an Mountains to the southwest to the Ordos and northern Shaanxi, and is in the transitional zone between semi-arid and semi-humid areas. The agro-pastoral ecotone is an important ecological security barrier in China, and the main types of land use are grassland, cultivated land, forest, and desert. Tongliao is in the eastern part of Inner Mongolia Autonomous Region and the hinterland of Horqin grassland, with desert, grassland, wetland, and sparse forest (**Figure 1**). With the richest biodiversity in the sparse forest and grassland of Horqin, Tongliao is an important commodity grain base and animal husbandry production base in China because of its rich resources and good natural conditions. However, the continuous expansion of human activities has increased the burden on the local environment, and ecological problems such as lake shrinkage and grassland degradation have emerged. In the implementation of the rural revitalization strategy, the development of grass-based livestock husbandry is facing severe challenges, and there is an urgent need to balance the conflict between human beings and the environment. In recent years, the implementation of major ecological projects such as "returning grazing to grassland" and "banning grazing and rearing" shows that China attaches great importance to sustainable development. However, in order to achieve the goal of "thriving businesses," the development of grass-based livestock husbandry in Tongliao still needs to improve ecological efficiency. On the premise of minimizing the environmental impact, Tongliao should enhance the added value of grass-based livestock husbandry and promote the revitalization of grass-based livestock husbandry to lay a solid foundation for realizing rural revitalization.

3.2 Data Sources

In the evaluation of ecological efficiency, the economic acquisition in the ecosystem is usually taken as the output index and the resource consumption as the input index. In addition, the consumption of grassland resources is the main impact on the environment in the process of grass-based livestock husbandry development. Therefore, the fixed asset investment of grass-based livestock husbandry, employed population, and grassland net primary productivity (NPP) of each county were taken as the input index, and the added value of grass-based livestock husbandry was taken as the output index. The index system for evaluating the ecological efficiency of grass-based livestock husbandry in Tongliao is shown in **Table 1**.

Plants absorb and release carbon through photosynthesis and respiration, and the difference of carbon formed is the organic matter accumulated by plants. NPP in **Table 1** is the total amount of organic matter accumulated per unit area of grassland per unit time, reflecting the coverage of grassland in this area. The data were obtained from the Resource and Environmental Science data Center of the Chinese Academy of Sciences, which was used to reflect the ecological status of grassland and the development conditions of grass-based livestock husbandry in each county. In the process of grass-based livestock husbandry development, the input is mainly to provide forage for livestock, and the output is to obtain the added value through the operation of grass-based livestock husbandry. Therefore, combined with the current research results, the following factors affecting the ecological efficiency of grass-based livestock husbandry were selected: proportion of output value of grass-based livestock husbandry, the proportion of employed persons in grass-based livestock husbandry, national policy (returning grazing to grassland, grass-livestock balance) and the number of livestock in stock. The relevant data were obtained from *Inner Mongolia Statistical Yearbook* (2001–2020) and *Tongliao Statistical Yearbook* (2001–2020).

3.3 Ecological Efficiency of Grass-Based Livestock Husbandry

3.3.1 Spatio-Temporal Change of Ecological Efficiency

The results showed that there are significant spatial differences in the ecological efficiency of grass-based livestock husbandry in Tongliao (**Table 2**). In 2000, the overall level of ecological efficiency was low, among which Keerqin had the highest ecological efficiency (1.18) and Huolinguole had the lowest ecological efficiency (0.45). This indicated that the development of grass-based livestock husbandry in Keerqin coordinated ecological and economic benefits better than other counties, but the ecological efficiency of grass-based livestock husbandry in each county still needs to be improved. By 2019, the ecological efficiency of all counties increased greatly, the average ecological efficiency increased from 0.88 to 1.17, and the ecological efficiency of Huolinguole increased the most, which indicated that the ecological efficiency of grass-based livestock husbandry in the agro-pastoral ecotone of northern China showed a dynamic growing trend. According to the average ecological efficiency of each region in the five periods from 2000 to 2019, Tongliao can be divided into three grades: the highest level includes Keerqin District, Keerqinzuoyihou Banner, Kailu County, and Keerqinzuoyizhong Banner with ecological efficiency greater than 1. The lowest level included Huolinguole City whose ecological efficiency was less than 0.8. The middle level included Kulun Banner, Naiman Banner, and Zhalute Banner. The ecological efficiency of grass-based livestock husbandry in Kulun and Huolinguole is significantly lower than that in other

TABLE 1 | Evaluation index of ecological efficiency of grass-based livestock husbandry in each county of Tongliao.

Category	Constitute	Index	Maximum value	Minimum value	Average value	Standard deviation
Output	Output value	Output value of grass-based livestock husbandry	60.01	0.56	22.05	16.63
Input	Capital	Total power of agricultural machinery	139.8	1.55	61.15	44.76
	Labor	Number of employed persons	26.94	0.25	11.65	6.74
	Land	NPP	442.71	45.89	186.21	94.35
	Public infrastructure	Number of senior high schools	58	5	23.72	13.13
		Number of persons engaged in health care institutions	8,364	314	1,521.41	1755.21
Influencing factor	Structural variable	Proportion of output value of grass-based livestock husbandry	0.75	0.01	0.30	0.18
		Proportion of employed persons in grass-based livestock husbandry	0.78	0.11	0.59	0.19
	Policy variable	Policy of returning grazing to grassland	0 (before 2003), 1 (after 2003)			
		Policy of grass-livestock balance	0 (before 2005), 1 (after 2005)			
	Other	Number of livestock in stock	247.53	9.56	112.51	64.11

TABLE 2 | Ecological efficiency of grass-based livestock husbandry in counties of Tongliao.

Year	Keerqin District	Huolinguole city	Kailu county	Kulun banner	Naiman banner	Zhalute banner	Keerqin-zuoyizhong banner	Keerqin-zuoyihou Banner
2000	1.18	0.45	1.03	0.64	0.83	0.95	0.89	1.05
2005	1.43	0.37	1.24	0.77	0.81	0.81	0.98	1.09
2010	1.61	0.77	1.33	0.75	0.78	0.87	1.01	1.11
2015	1.78	0.81	1.52	0.87	0.97	1.03	1.07	1.25
2019	1.83	0.79	1.47	0.93	1.02	0.99	1.13	1.21

TABLE 3 | Malmquist index and its decomposition of counties in Tongliao from 2000 to 2019.

County	Comprehensive technical efficiency	Technological progress	Pure technical efficiency	Scale efficiency	Total factor ecological efficiency
Keerqin District	0.91	1.24	0.91	1.00	1.14
Keerqinzuoyizhong Banner	1.14	1.31	1.08	1.05	1.50
Keerqinzuoyihou Banner	1.00	1.42	1.00	1.00	1.42
Kailu County	1.00	1.60	1.00	1.00	1.60
Kulun Banner	1.11	1.09	0.98	1.14	1.21
Naiman Banner	0.99	1.07	0.92	1.07	1.06
Zhalute Banner	1.05	1.17	1.01	1.04	1.23
Huolinguole city	1.00	1.29	1.00	1.00	1.29
Average	1.02	1.26	0.99	1.04	1.29

counties, which indicated that the production level of grass-based livestock husbandry was at a low level. However, from 2000 to 2019, the ecological efficiency increased by 45.31 and 75.55%, respectively, second only to Keerqin District, and there was still room for further improvement in the ecological efficiency of grass-based livestock husbandry.

3.3.2 Decomposition and Change of Total Factor Ecological Efficiency

The average annual Malmquist index and its decomposition of counties in Tongliao from 2000 to 2019 are shown in **Table 3**. The growth rate of total factor ecological efficiency of all counties in the table was more than 1, and the overall ecological efficiency showed an upward trend. This reflected the development of grass-based livestock husbandry has gradually changed from factor-driven to innovation-driven, and the development of grass-based livestock husbandry in the agro-pastoral ecotone has increasingly coincided with the ecological environment. The comprehensive technical efficiency of Keerqin District and Naiman Banner is less than 1, indicating that the comprehensive technical efficiency shows a downward trend from 2000 to 2019. The value of Keerqinzuoyihou Banner, Huolinguole City, and Kailu County is 1, which indicated that its comprehensive technical efficiency was relatively stable, while the comprehensive technical efficiency of other counties showed an increasing trend. The change of comprehensive technical efficiency was mainly caused by pure technical efficiency and scale efficiency, and the changing trend of scale efficiency was roughly the same as that of comprehensive

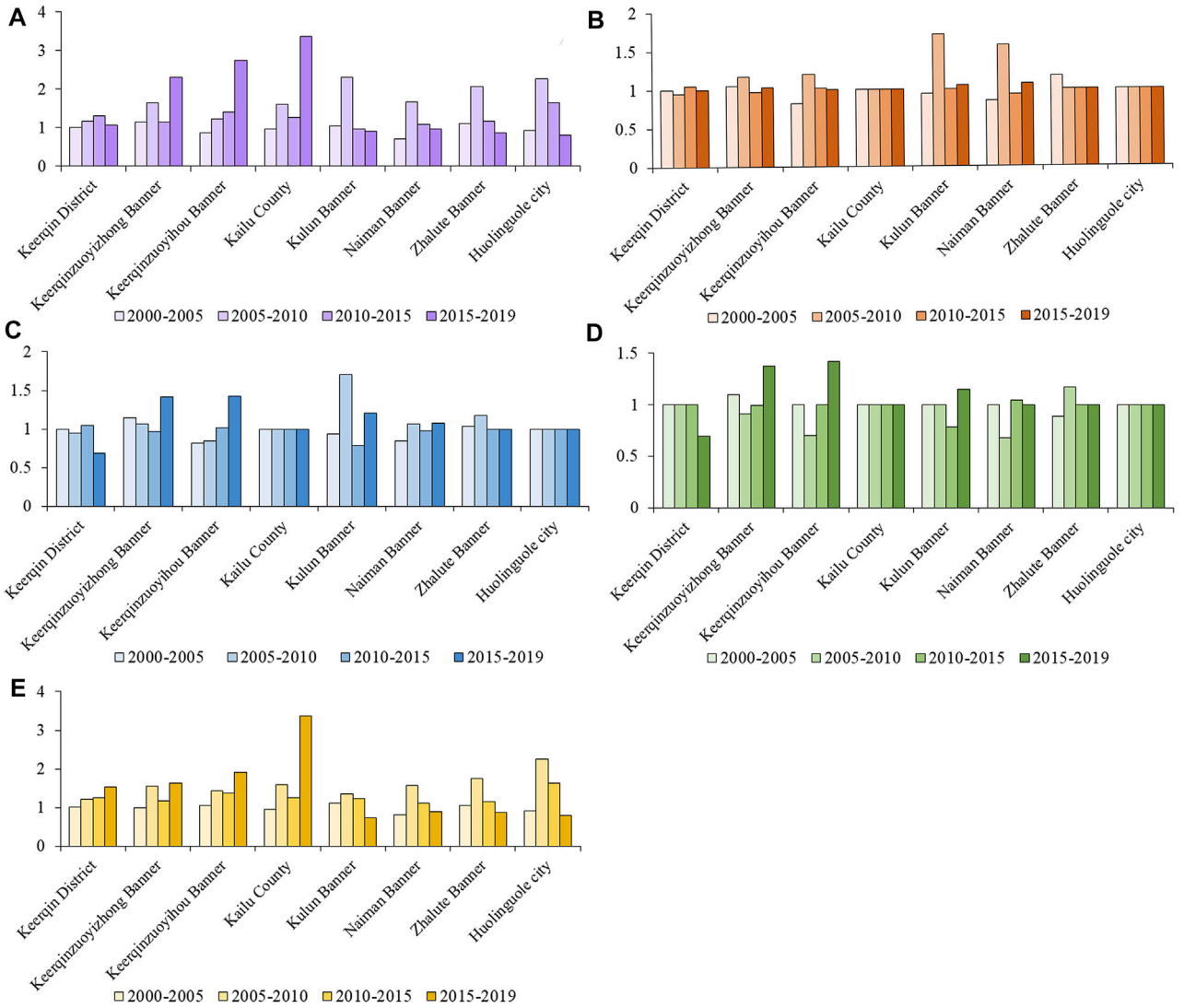

FIGURE 2 | Annual Malmquist index and its decomposition of counties in Tongliao. **(A–E)** showed the changes of total factor ecological efficiency, scale efficiency, comprehensive technical efficiency, pure technical efficiency, and technological progress, respectively.

technical efficiency. The change of pure technical efficiency showed that only Keerqinzuoyizhong Banner and Zhalute Banner show an increasing trend, which demonstrated that the production management of grass-based livestock husbandry in Tongliao from 2000 to 2019 was relatively insufficient and the input of production factors was not reasonable. The growth rate of technological progress in each county was more than 1, which implied that the growth of TFP in Tongliao mainly depended on the improvement of technological progress, and further showed that the key to promoting sustainable development of regional grass-based livestock husbandry lay in the research and development of advanced technology of grass-based livestock husbandry and the popularization of high-quality germplasm resources.

Overall, the efficiency fluctuation of each county reflected the uneven regional development of total factor ecological efficiency in the agro-pastoral ecotone. From 2000 to 2019, the efficiency of Keerqin District, Zhalute Banner, and Huolinguole City increased at first and then decreased. It was speculated that the main reason was the adjustment of economic structure with 2012 as the turning point. The growth rate of the added value of grass-based livestock husbandry slowed down, and the number of employed persons of grass-based livestock husbandry began to decline. Keerqinzuoyizhong Banner, Keerqinzuoyihou Banner, Kailu County, Kulun Banner, and Naiman Banner showed large fluctuations (increased-decreased-increased), and their fluctuations were closely related to the changes of NPP (**Figure 2**). The fastest change of total factor ecological efficiency was Keerqinzuoyihou Banner with an increasing growth rate, and the smallest fluctuations were Keerqin District and Kulun Banner, as shown in **Figure 2A**. Keerqin District, Keerqinzuoyihou Banner, and Kailu County are

TABLE 4 | Average Malmquist index and its decomposition in Tongliao.

Year	Comprehensive technical efficiency	Technological progress	Pure technical efficiency	Scale efficiency	Total factor ecological efficiency
2000–2005	0.97	0.99	1.00	0.97	0.96
2005–2010	1.08	1.57	0.92	1.17	1.70
2010–2015	0.97	1.27	0.98	1.00	1.24
2015–2019	1.08	1.29	1.06	1.02	1.39
Average	1.02	1.26	0.99	1.04	1.29

TABLE 5 | Regression results of Tobit model.

Factors	Coefficient	Standard error	T Value	95% confidence interval
Number of senior high schools	0.063	0.070	0.91	[–0.074,0.200]
Number of persons engaged in health care institutions	0.223***	0.062	3.59	[0.100,0.347]
Proportion of output value of grass-based livestock husbandry	0.001	0.013	0.01	[–0.026,0.026]
Proportion of employed persons in grass-based livestock husbandry	0.329**	0.120	2.73	[0.090,0.567]
Policy of returning grazing to grassland	–0.093***	0.027	–3.40	[–0.147,0.039]
Policy of grass-livestock balance	0.146**	0.058	2.53	[0.032,0.260]
Number of livestock in stock	0.255***	0.063	4.05	[0.130,0.379]
Constant term	0.592***	0.153	3.87	[0.289,0.896]
Significance Prob>chi2	0.000			

*Note: *, **, ***indicate significance at the level of 10, 5, and 1% confidence levels, respectively.*

important agricultural and livestock product bases and commodity grain bases in the country, and their grass-based livestock husbandry development is relatively stable. In the future, we need to focus on promoting new technologies, new varieties, and new models, form new growth points and promote the modernization and high-quality development of grass-based livestock husbandry.

The annual average Malmquist index and its decomposition of each county in Tongliao are shown in **Table 4**. The efficiency of all kinds in 2019 was higher than that in 2000, and the increase of efficiency in 2015–2010 was obviously higher than that in the other stages. The average annual growth rate of total factor ecological efficiency was 29.3%, the interannual fluctuation of the growth rate was large, but it showed an upward trend. Technological progress from 2005 to 2019 was the main reason for the improvement of total factor ecological efficiency, therefore future grass-based livestock husbandry production in Tongliao should further promote the mechanization level and technical level of grass-based livestock husbandry. The average annual growth rate of comprehensive technical efficiency was 2.3%, which indicated that there was still a lack of effective coordination mechanism in the development of grass-based livestock husbandry, so it was difficult to improve the ecological efficiency of the region. From the perspective of pure technical efficiency, it showed an increasing trend only in the period from 2015 to 2019, indicating that the production management of grass-based livestock husbandry in Tongliao made little contribution to the improvement of total factor ecological efficiency before 2015, which was also the main problem in the development of grass-based livestock husbandry in the agro-pastoral ecotone. The scale efficiency showed an alternating trend of decrease and increase, which meant that the production scale of grass-based livestock husbandry in Tongliao has not yet reached the optimal level, and the input structure of industrial factors did not match the production scale.

3.3.3 Analysis on Influencing Factors of Ecological Efficiency

In this study, the Tobit model was used to analyze the impact of various factors on ecological efficiency (**Table 5**). The model passed the significance test with a confidence level of 99%, indicating a good degree of fit. Among the variables of public infrastructure, the number of senior high schools and the number of persons engaged in health care institutions did not pass the significance test, which revealed that the level of social health care and education had no significant impact on the ecological efficiency of grass-based livestock husbandry in each county of Tongliao. Among the structural variables, the proportion of output value of grass-based livestock and the proportion of employed persons in grass-based livestock husbandry passed the significance test with a confidence level of 99 and 95%, respectively, and the coefficient was positive. It showed that the increase of the proportion of output value and employed persons could significantly improve the ecological efficiency of grass and animal husbandry in this area. The number of livestock in stock has passed the significance test with a confidence level of 99%, and the coefficient was negative, which demonstrated the increase in the number of livestock (especially beyond the ecological carrying capacity of grassland) was not conducive to the protection of grassland ecological environment.

Among the policy variables, both "returning grazing to grassland" and "grass-livestock balance" have passed the significance test with a confidence level of 99%, indicating that the national policy had a significant positive impact on ecological protection and sustainable development of the

northern agro-pastoral ecotone. At present, there are a series of ecological problems in the agro-pastoral ecotone in China, such as grassland degradation, soil desertification, and so on. In order to ensure the ecological security of grassland and enhance the effectiveness of resource utilization, the central government has invested a large amount of money and implemented several major construction projects for ecological protection. In recent years, the Inner Mongolia Autonomous Region has issued a series of reform measures to strengthen the protection of grassland ecology in response to the policy call of the CPC Central Committee to protect grassland and restore the ecology. Among them, the policy of "returning grazing to grassland" and "grass-livestock balance" is the most representative. The results showed that compared with the "grass-livestock balance," "returning grazing to grassland" had a more positive impact on ecological efficiency (Hu et al., 2019; Liu et al., 2020). This was mainly due to the differences in the core ideas and practical operation of the two policies: "returning grazing to grassland" to keep the ecosystem in an ideal state without human intervention and to realize the natural restoration of grassland ecology by banning grazing and resting grazing; "grass-livestock balance" aimed to realize the dynamic balance between forage supply and livestock demand within a certain range of time and space, and to reduce the burden of grassland by "determining livestock-carrying capacity according to grass production". To realize the sustainable development of agro-pastoral ecotone, it is necessary to construct the coordinated development system of grassland ecology and production function and reduce the negative impact of ecological engineering construction. At the same time, we should pay more attention to innovating the development model of grass-based livestock husbandry, and improving the production level of local grass-based livestock husbandry under the premise of ensuring ecological security, so as to realize the sustainable development of the agro-pastoral ecotone.

4 CONCLUSIONS AND DISCUSSION

4.1 Conclusions

In the new era, agricultural space is the core component of territorial space, agricultural production is the focus of rural revitalization, and the improvement of agricultural production efficiency is an important way to improve agricultural quality and efficiency. Based on the requirements for agricultural green development in the context of rural revitalization, this study was guided by the goal of the revitalization of grass-based livestock husbandry, taking Tongliao as a study area, carried out the analysis on spatiotemporal patterns and influencing factors of the ecological efficiency of grass-based livestock husbandry.

The results showed that: 1) from 2000 to 2019, the overall production efficiency of grass-based livestock husbandry in Tongliao showed an increasing trend, with the average efficiency increasing from 0.88 to 1.17. Among them, the ecological efficiency of Keerqin District, Keerqinzuoyihou Banner, Kailu County, and Keerqinzuoyizhong Banner has been higher than that of other counties for a long time. 2) According to the Malmquist index and its decomposition, the total factor ecological efficiency, comprehensive technical efficiency, and scale efficiency in 2019 have been generally improved compared with 2000, and the average annual growth rate of the total factor ecological efficiency of grass-based livestock husbandry was 29.3%. Moreover, the improvement of the total factor ecological efficiency of Tongliao mainly depended on technological progress, and the growth of efficiency from 2005 to 2010 was significantly higher than that of other stages. 3) The output of grass-based livestock husbandry, the number of livestock in stock, and the grass-livestock balance were the main factors that determine the improvement of the ecological efficiency of grass-based livestock husbandry. The influence of public infrastructure variables, structural variables, and policy variables on the ecological efficiency of grass-based livestock husbandry showed significant differences. However, after combining various influencing factors, it was found that ecological protection and sustainable development of the environment still had a significant positive impact on the development of grass-based livestock husbandry.

4.2 Discussion

Through the analysis of the development level of grass-based livestock husbandry in Tongliao, there are still two problems in the development of grass-based livestock husbandry in the agro-pastoral ecotone. The first is that the ecological efficiency of grass-based livestock husbandry is uneven. The resource advantage in the agro-pastoral ecotone has not yet been transformed into an economic advantage. There are obvious spatial differences in the development endowment and ecological protection measures of grass-based livestock husbandry (Zhou et al., 2019), which makes the ecological efficiency of grass-based livestock husbandry has great regional differences. The second is that the ecological efficiency of grass-based livestock husbandry has been low for a long time. The continuous excessive input of energy, water, and pasture resources has achieved rapid growth in forage and livestock production, but also led to the deterioration of the ecological environment, which is not conducive to the improvement of the ecological efficiency of grass-based livestock husbandry (Shi et al., 2018).

Agro-pastoral ecotone is an ecologically sensitive and fragile area, the rapid population growth and intense human activity bring food pressure and ecological degradation and form a situation of forced transformation in the construction and development of ecological husbandry (Li et al., 2021). Based on the main conclusions of this research, the following policy implications are proposed to promote the revitalization of the grass-based livestock husbandry in the agro-pastoral ecotone: Firstly, the development mode of agro-pastoral ecotone should be changed, to prioritize ecological and green development, improve the ecological efficiency of grass-based livestock husbandry, and support high-quality development of agriculture. Specifically, extensive production and management models should be transformed, and the relationship between economic development, resource conservation, and environmental protection of the grass-based livestock husbandry should be properly handled. Secondly, regional decision-makers should pay more attention to spatial differentiation and promote the

coordinated improvement of the ecological efficiency of grass-based livestock husbandry in the ecotone between agriculture and animal husbandry. Specifically, decision-makers should combine regional resource endowments and economic development levels to formulate differentiated agricultural development strategies. At the same time, it is necessary to maintain coordination and interaction between regions, learn from the advanced experience of grass and animal husbandry production in other regions, and ensure the coordinated improvement of ecological efficiency of grass-based livestock husbandry in different counties. Finally, government departments should support the ecologically inefficient areas of grass-based livestock husbandry, to "prescribe the right medicine for a symptom". For areas with low land-use efficiency, local government should promote the transformation of pastures in breeding areas, strengthen the development and utilization of local superior and characteristic varieties, promote advanced and applicable breeding techniques, and build a batch of standardized, modern, and large-scale breeding farms. For areas with fragile ecology and high pressure on resources and environment, local government should change the way of using grassland, implement modest scale breeding models such as "summer and autumn grazing, winter and spring house feeding", and thoroughly implement the grassland ecological protection subsidy and reward policy.

DATA AVAILABILITY STATEMENT

The datasets presented in this article are not readily available because the authors do not have permission to share data. Requests to access the datasets should be directed to DH, hedw09@163.com.

AUTHOR CONTRIBUTIONS

All authors listed have made a substantial, direct, and intellectual contribution to the work and approved it for publication. DH: Data Analysis and Manuscript. XD and GJ: Manuscript Editing and Manuscript Review. XW, YZ, and ZS: Manuscript Review. WS and ZZ: Methodology and Manuscript Editing.

FUNDING

This research was supported by the Strategic Priority Research Program of the Chinese Academy of Sciences (Grant No. XDA23070400).

REFERENCES

Arabi, B., Munisamy, S., Emrouznejad, A., and Shadman, F. (2014). Power Industry Restructuring and Eco-Efficiency Changes: A New Slacks-Based Model in Malmquist-Luenberger Index Measurement. *Energy Policy* 68, 132–145. doi:10.1016/j.enpol.2014.01.016

Bonfiglio, A., Arzeni, A., and Bodini, A. (2017). Assessing Eco-Efficiency of Arable Farms in Rural Areas. *Agric. Syst.* 151, 114–125. doi:10.1016/j.agsy.2016.11.008

Caves, D. W., Christensen, L. R., and Diewert, W. E. (1982). The Economic Theory of Index Numbers and the Measurement of Input, Output, and Productivity. *Econometrica* 50, 1393–1414. doi:10.2307/1913388

Charnes, A., Cooper, W. W., and Rhodes, E. (1978). Measuring the Efficiency of Decision Making Units. *Eur. J. Oper. Res.* 2 (6), 429–444. doi:10.1016/0377-2217(78)90138-8

Deng, X., and Gibson, J. (2019). Improving Eco-Efficiency for the Sustainable Agricultural Production: a Case Study in Shandong, China. *Technol. Forecast. Soc. Change* 144, 394–400. doi:10.1016/j.techfore.2018.01.027

Deng, X., and Gibson, J. (2018). Sustainable Land Use Management for Improving Land Eco-Efficiency: a Case Study of Hebei, China. *Ann. Oper. Res.* 290, 265–277. doi:10.1007/s10479-018-2874-3

Dong, Y., Jin, G., and Deng, X. (2020). Dynamic Interactive Effects of Urban Land-Use Efficiency, Industrial Transformation, and Carbon Emissions. *J. Clean. Prod.* 270, 122547. doi:10.1016/j.jclepro.2020.122547

Färe, R., and Grosskopf, S. (1992). Malmquist Productivity Indexes and fisher Ideal Indexes. *Econ. J.* 102, 158–160. doi:10.2307/2234861

Guo, B., He, D., Zhao, X., Zhang, Z., and Dong, Y. (2020). Analysis on the Spatiotemporal Patterns and Driving Mechanisms of China's Agricultural Production Efficiency from 2000 to 2015. *Phys. Chem. Earth, Parts A/B/C* 120 (1), 102909. doi:10.1016/j.pce.2020.102909

Hu, Z., Zhao, Z., Zhang, Y., Jing, H., Gao, S., and Fang, J. (2019). Does 'Forage-Livestock Balance' Policy Impact Ecological Efficiency of Grasslands in China? *J. Clean. Prod.* 207, 343–349. doi:10.1016/j.jclepro.2018.09.158

Jin, G., Deng, X., Zhao, X., Guo, B., and Yang, J. (2018). Spatiotemporal Patterns in Urbanization Efficiency within the Yangtze River Economic Belt between 2005 and 2014. *J. Geogr. Sci.* 28 (8), 1113–1126. doi:10.1007/s11442-018-1545-2

Koskela, M. (2015). Measuring Eco-Efficiency in the Finnish forest Industry Using Public Data. *J. Clean. Prod.* 98, 316–327. doi:10.1016/j.jclepro.2014.04.042

Li, S., Zhu, C., Lin, Y., Dong, B., Chen, B., Si, B., et al. (2021). Conflicts between Agricultural and Ecological Functions and Their Driving Mechanisms in Agroforestry Ecotone Areas from the Perspective of Land Use Functions. *J. Clean. Prod.* 317 (3), 128453. doi:10.1016/j.jclepro.2021.128453

Liu, W., Zhan, J., Li, Z., Jia, S., Zhang, F., and Li, Y. (2018). Eco-efficiency Evaluation of Regional Circular Economy: A Case Study in Zengcheng, Guangzhou. *Sustainability* 10 (2), 453. doi:10.3390/su10020453

Liu, Y., Zou, L., and Wang, Y. (2020). Spatial-temporal Characteristics and Influencing Factors of Agricultural Eco-Efficiency in China in Recent 40 Years. *Land Use Policy* 97 (5), 104794. doi:10.1016/j.landusepol.2020.104794

Lv, F., Deng, L., Zhang, Z., Wang, Z., Wu, Q., and Qiao, J. (2021). Multiscale Analysis of Factors Affecting Food Security in China, 1980-2017. *Environ. Sci. Pollut. Res.* 29, 6511–6525. doi:10.1007/s11356-021-16125-1

Ma, X., Wang, C., Yu, Y., Li, Y., Dong, B., Zhang, X., et al. (2018). Ecological Efficiency in China and its Influencing Factors-A Super-efficient SBM Metafrontier-Malmquist-Tobit Model Study. *Environ. Sci. Pollut. Res.* 25, 20880–20898. doi:10.1007/s11356-018-1949-7

Malmquist, S. (1953). Index Numbers and Indifference Surfaces. *Trabajos De Estadistica* 4 (2), 209–242. doi:10.1007/BF03006863

Ray, S., and Desli, E. (1997). Productivity Growth, Technical Progress, and Efficiency Change in Industrialized Countries: Comment. *Am. Econ. Rev.* 87 (5), 1033–1039.

Rebolledo-Leiva, R., Angulo-Meza, L., Iriarte, A., González-Araya, M. C., and Vásquez-Ibarra, L. (2019). Comparing Two CF+DEA Methods for Assessing Eco-Efficiency from Theoretical and Practical Points of View. *Sci. Total Environ.* 659, 1266–1282. doi:10.1016/j.scitotenv.2018.12.296

Schaltegger, S., and Sturm, A. (1990). Ökologische rationalität: ansatzpunkte zur ausgestaltung von ökologieorientierten managementinstrumenten. *Die Unternehmung* 44 (4), 273–290.

Schaltegger, S., and Synnestvedt, T. (2002). The Link between 'green' and Economic success: Environmental Management as the Crucial Trigger between Environmental and Economic Performance. *J. Environ. Manage.* 65 (4), 339–346. doi:10.1006/jema.2002.0555

Shi, W., Liu, Y., and Shi, X. (2018). Contributions of Climate Change to the Boundary Shifts in the Farming-Pastoral Ecotone in Northern China since 1970. *Agric. Syst.* 161 (3), 16–27. doi:10.1016/j.agsy.2017.12.002

Sun, Z., Wang, Q., Xiao, Q., Batkhishig, O., and Watanabe, M. (2015). Diverse Responses of Remotely Sensed Grassland Phenology to Interannual Climate Variability over Frozen Ground Regions in Mongolia. *Remote Sensing* 7 (1), 360–377. doi:10.3390/rs70100360

Tan, R., and Lin, B. (2020). The Influence of Carbon Tax on the Ecological Efficiency of China's Energy Intensive Industries-A Inter-fuel and Inter-factor Substitution Perspective. *J. Environ. Manage.* 261 (1), 110252. doi:10.1016/j.jenvman.2020.110252

Tian, P., Li, J., Cao, L., Pu, R., Wang, Z., Zhang, H., et al. (2021). Assessing Spatiotemporal Characteristics of Urban Heat Islands from the Perspective of an Urban Expansion and green Infrastructure. *Sust. Cities Soc.* 74 (13), 103208. doi:10.1016/j.scs.2021.103208

Xing, Z., Wang, J., and Zhang, J. (2018). Expansion of Environmental Impact Assessment for Eco-Efficiency Evaluation of China's Economic Sectors: An Economic Input-Output Based Frontier Approach. *Sci. Total Environ.* 635, 284–293. doi:10.1016/j.scitotenv.2018.04.076

Yang, L., and Yang, Y. (2019). Evaluation of Eco-Efficiency in China from 1978 to 2016: Based on a Modified Ecological Footprint Model. *Sci. Total Environ*. 662, 581–590. doi:10.1016/j.scitotenv.2019.01.225

Yin, K., Wang, R., An, Q., Yao, L., and Liang, J. (2014). Using Eco-Efficiency as an Indicator for Sustainable Urban Development: A Case Study of Chinese Provincial Capital Cities. *Ecol. Indicators* 36 (1), 665–671. doi:10.1016/j.ecolind.2013.09.003

Yue, S., Yang, Y., and Pu, Z. (2017). Total-factor Ecology Efficiency of Regions in China. *Ecol. Indicators* 73, 284–292. doi:10.1016/j.ecolind.2016.09.047

Zhang, Y., LuZhou, Y. Q., Zhou, Q., and Wu, F. (2020). Optimal Water Allocation Scheme Based on Trade-Offs between Economic and Ecological Water Demands in the Heihe River Basin of Northwest China. *Sci. Total Environ.* 703, 134958. doi:10.1016/j.scitotenv.2019.134958

Zhao, Y., Wang, S., Ge, Y., Liu, Q., and Liu, X. (2017). The Spatial Differentiation of the Coupling Relationship between Urbanization and the Eco-Environment in Countries Globally: A Comprehensive Assessment. *Ecol. Model.* 360, 313–327. doi:10.1016/j.ecolmodel.2017.07.009

Zhou, C., Shi, C., Wang, S., and Zhang, G. (2018). Estimation of Eco-Efficiency and its Influencing Factors in Guangdong Province Based on Super-SBM and Panel Regression Models. *Ecol. Indicators* 86, 67–80. doi:10.1016/j.ecolind.2017.12.011

Zhou, J., Xu, Y., Gao, Y., and Xie, Z. (2019). Land Use Model Research in Agro-Pastoral Ecotone in Northern China: A Case Study of Horqin Left Back Banner. *J. Environ. Manage.* 237 (4), 139–146. doi:10.1016/j.jenvman.2019.02.046

Conflict of Interest: The authors declare that the research was conducted in the absence of any commercial or financial relationships that could be construed as a potential conflict of interest.

Publisher's Note: All claims expressed in this article are solely those of the authors and do not necessarily represent those of their affiliated organizations, or those of the publisher, the editors and the reviewers. Any product that may be evaluated in this article, or claim that may be made by its manufacturer, is not guaranteed or endorsed by the publisher.

frontiers | Frontiers in Environmental Science

ORIGINAL RESEARCH
published: 14 April 2022
doi: 10.3389/fenvs.2022.843920

Estimation and Influencing Factor Analysis of Carbon Emissions From the Entire Production Cycle for Household consumption: Evidence From the Urban Communities in Beijing, China

Jiabin Wang[1], *Wenjie Hui*[1], *Lian Liu*[1], *Yuping Bai*[1,2]*, *Yudong Du*[1] *and Jiajin Li*[1]

[1]School of Land Science and Technology, China University of Geosciences, Beijing, China, [2]Institute of Geographic Sciences and Natural Resources Research, Chinese Academy of Sciences (CAS), Beijing, China

OPEN ACCESS

Edited by:
Jinyan Zhan,
Beijing Normal University, China

Reviewed by:
Guofeng Wang,
Shanxi University of Finance and Economics, China
Zhongxiao Sun,
China Agricultural University, China

***Correspondence:**
Yuping Bai
baiyp@cugb.edu.cn

Specialty section:
This article was submitted to Conservation and Restoration Ecology, a section of the journal Frontiers in Environmental Science

Received: *27 December 2021*
Accepted: *22 February 2022*
Published: *14 April 2022*

Citation:
Wang J, Hui W, Liu L, Bai Y, Du Y and Li J (2022) Estimation and Influencing Factor Analysis of Carbon Emissions From the Entire Production Cycle for Household consumption: Evidence From the Urban Communities in Beijing, China. Front. Environ. Sci. 10:843920. doi: 10.3389/fenvs.2022.843920

Household carbon emissions (HCEs) in urban communities are significant sources of China's total carbon emissions and contribute to global warming and climate change dramatically. This study aims to estimate the HCEs and investigate their influential factors based on a total of 185 household survey data collected from three typical types of urban communities in Beijing: traditional communities, unit communities, and commercial housing communities with the application of the consumer lifestyle approach analysis and econometrics model. The results show that unit communities contribute to the highest direct carbon emissions and the commercial housing communities produce the most indirect carbon emissions, with the traditional communities emitting the lowest carbon emissions both directly and indirectly. The highest direct carbon emissions of households are found in unit communities at 723.79 $kgCO_2$ per month, followed by commercial communities at 580.01 $kgCO_2$, and finally the traditional communities with 526.44 $kgCO_2$ direct carbon emissions monthly. And the highest monthly indirect carbon emissions of households are found in commercial communities at 707.70 $kgCO_2$, followed by unit communities at 669.38 $kgCO_2$, and finally with 554.85 $kgCO_2$ indirect carbon emissions monthly in traditional communities. It concludes that the community type affects HCE characteristics and their driving factors significantly. Household income, household population, and the ownership of cars increase HCE in more than one type of community. Scientific research work-related population, community environment satisfaction, housing area have positive effects, while community convenience has negative impacts on HCEs in one certain type of community. Policy implications tailored to general and specific community types are proposed as the guidance of carbon reduction and community transformation finally. This study contributes to the understanding of the impact of community attributes on HCEs and proposes some methods for microregional carbon emission reduction and the ecological transformation of urban communities.

Keywords: household carbon emissions, survey, consumer lifestyle approach, community type, influencing factors, Beijing

INTRODUCTION

Over the years, the emission of greenhouse gases (GHGs) especially CO_2 is confirmed as the primary reason for global warming (Eckstein et al., 2017). With the climate change caused by global warming, natural disasters and extreme weather are more likely to appear in those years (Calleja-Agius et al., 2021; Marlon et al., 2021). In 2020, China accounts for 27.2% of global energy consumption and 31.8% of global carbon emissions (BP 2021). Besides large amounts of industrial energy consumption, the daily life of communities has become a significant producer of greenhouse gases (Anderson et al., 2016; Lin et al., 2013; Yang and Chen, 2011; Yang, S. et al., 2018). The household carbon emissions (HCEs) accounted for 30–40% of China's national total emission between 2000 and 2010 (Li et al., 2019). And the proportion shows a trend of growth (Wang and Yang, 2014). To protect the environment and to explore the path of community ecological construction and transformation development, CO_2 emissions need to be controlled (Liu et al., 2021).

China emphasized the concept of carbon peak and carbon neutral recently and it is essential for environmental health. However, a broad and profound economic and social systemic change is needed to achieve it (Huo et al., 2021; Zhang and Hanaoka, 2021). Higher requirements have been given for the promotion of new-type ecological civilization construction and the realization of healthy and high-quality development (Bai et al., 2019; Deng, 2021; Lin and Zhu, 2021). As the capital of China, Beijing is in the process of transforming from a general city to an ecological city, and it is also faced with the challenges above, which will inevitably become obstacles to its development. Given its special urban nature and development orientation, it has a great demand for urban community transformation (Yang, Q. et al., 2018; Yang, S. et al., 2018). During its urbanization, the overexpansion of population, increasingly congested traffic, housing prices continuing to rise, resources and environmental carrying capacity are seriously insufficient (Wang et al., 2021), and much more carbon emission has been brought into Beijing with a high concentration of people and energy-consumed industries. The reduction of HCE will play a significant role in this section, and ecological communities will be the key to reduce regional carbon emissions. Recently, scholars start to set their sights on HCEs and discover methods to regulate carbon emission from a more micro perspective.

The results of studies on carbon emission carried out worldwide were impressive in the last 2 decades (Davis and Caldeira, 2010; Yang and Chen, 2011; Sun and Huang, 2020; Wang et al., 2021). Aside from the influence of carbon emission on global warming, there are some studies on the impact of carbon emission on public health and environmental protection (Yang, Q. et al., 2018; Yang, S. et al., 2018). In China, studies on carbon emission developed rapidly and HCE studies began after 2008 in different regions (Qin, 2009). Studies on HCE developed rapidly throughout these years, and huge progress was made (Ye et al., 2017; Zhang et al., 2021). In related studies, the growing household consumption level was confirmed as the main reason of the increase in emissions and waste (Wilson et al., 2013; Zhang et al., 2020). The community-level carbon emission research started at the same time as household level. At the same time, due to the large scale and variety of local communities, ecological community construction is expected to become a major way to break the bottleneck of its development, so it has a typical research significance. To reduce residents' carbon emissions and promote low-carbon community construction is to strengthen the construction of a low-carbon society, an important way to promote the development of low-carbon communities and an important measure to mitigate global warming.

Existing studies confirm that HCEs are divided into direct and indirect carbon emissions (Liu et al., 2011; Zhang et al., 2015). However, the academic circle has not formed a strict unified standard for the estimation boundary of household direct and indirect carbon emissions. In general, direct carbon emissions refer to those that are obtained from energy consumption, such as fossil fuels and electricity. Indirect carbon emissions refer to the carbon emission from consumer goods and services, including food, clothes, and furniture, caused by the energy consumption during industrial production (Bin and Dowlatabadi, 2005; Liu et al., 2011; Zhang et al., 2015; Chen et al., 2019). Another point of view is that HCEs can be divided into three tiers. Tier 1 is direct carbon emissions, including only fossil fuels that directly produce carbon emissions; Tier 2 and tier 3 are indirect carbon emissions; tier 2 is energy consumption that does not directly emit carbon emissions, such as electricity and heating. Tier 3 are emissions from products and services (Matthews et al., 2008; Kenny and Gray, 2009; Andrew and Cortese, 2011; Zhao, 2019).

As for the influential factors of HCEs, socioeconomic factors, household characteristics, and geographic factors are widely considered (Li et al., 2016; Yang et al., 2016; Zhang et al., 2015). On the basis of previous studies, Zhang et al. (2015) summarized that the household income, age, household size, education level, household location, gender, and rebound effects are major influencing factors of HCEs. However, fewer studies have taken community attributes into consideration. Gu et al. (2013) illustrated the disparity in transport energy consumption of different residential communities. In Yang et al. (2016)'s study, HCEs are relevantly inequal in different communities, and this is due to the different level of infrastructure construction and commuting distance. Rong et al. (2020) demonstrated the influence of the built environment on HCEs. More profound influential factors on community attributes are looking forward to being examined in the following HCE studies (Rong et al., 2020; Yang et al., 2016).

The consumer lifestyle approach (CLA) was first proposed by Bin and Dowlatabadi (2005) for exploring consumer-related energy consumption and carbon emission. In China, the term CLA was first carried out in the same year (Wei et al., 2007). In

previous studies, CLA was considered to be more efficient by combining the advantages of the input–output model and emission coefficient method (ECM), but it is complicated to apply (Zhang et al., 2015). CLA provides an integrated evaluation framework that is a clear understanding of the interaction factors affecting consumers, personal determinants, household characteristics, consumer choices, and consequences. Previous studies are more focused on the overall carbon emissions of communities (Adalilar et al., 2015; Rong et al., 2020), and CLA contributes to correlating carbon emissions with residents' lifestyles, revealing effective pathways for the government to formulate effective policies of energy conservation and emission reduction targeting urban communities.

In this paper, different structures of CO_2 emissions among three types of communities are estimated based on household survey questionnaires, and the influencing factors on the carbon emission of residents in different communities are identified. In our research, communities are classified differently and the factors involved, especially the factors of HCEs, are different from early studies. This paper contributes to the previous studies with the following perspectives: we explore new boundaries of HCE evaluation based on traditional studies with the selection of typical and distinctive communities. In addition, we focus more upon community residential services as well as attributes and their connections with HCEs, instead of simply explaining their structural features. Through our research, we hope to reveal the differences in HCE and their influential factors, respectively, between typical communities. Then, we can explore the eco-transformation solutions for the significant influential factors.

The remainder of this paper is organized as follows: in *Study Area*, the research area is introduced, in *Methodology and Data*, the relevant data are collected and analyzed, and the corresponding mathematical method is introduced. In *Results*, the results of HCE characteristics and driving factors in different communities are presented. The obtained results are discussed in *Discussions*; the policy implications obtained from this research are drawn in *Policy Implications*. *Conclusion* draws conclusions.

STUDY AREA

Beijing is the capital of China with the Global Positioning System (GPS) coordinates of 39°55′0.0048″N and 116°22′59.9916″E, which is located in the northern part of the North China Plain. Because of its dynamic economy, high-level urbanization construction, and strong innovation capability, Beijing has become an important engine for the economic development of north China. As the political, economic, and cultural center of China, Beijing has a large population of more than 20 million and a high GDP per capita, reaching up to 164,889 yuan in 2020 according to the National Bureau of Statistics (China Statistical Yearbook, 2021). Relying on a long history and a developed economy, Beijing has several different types of communities with distinctive characteristics: traditional communities, unit communities, and commercial housing communities. Due to the excellent protection of traditional buildings, a large number of houses and traditional communities built in the Ming and Qing dynasties have been preserved in Beijing. In addition, because of historical reasons, there are unit communities that are developed and uniformly allocated by the government and commercial communities, which are developed by commercial companies and allocated by the market. These three types of communities have obvious differences in lifestyles, consumption patterns, resource utilization styles, ecological adaptation, and public services. However, with the target of sustainable development, these three communities are facing the same challenge: ecological transformation. As widely recognized, the concept of the ecological community is committed to seeking harmony among people, society, and the environment (Dalton et al., 2007; Maliene et al., 2008; Roseland, 2012), and energy-saving and emission reduction in residential areas are thus one inevitable pathway for the ecological transformation of communities (Yang et al., 2016). For the reason that the study of community ecological transformation requires different types of research samples, Beijing has become a natural testing ground for studying the ecological transformation of communities in the process of ecological civilization construction and urban–rural integration development.

METHODOLOGY AND DATA

HCEs in communities can be divided into direct carbon emissions and indirect carbon emissions, of which the direct carbon emissions are building energy consumption system and transportation system emissions (Wei et al., 2007), as shown in **Figure 1**.

The estimation of direct carbon emissions was based on the ECM. Indirect carbon emissions are estimated by the conceptual model of consumers' lifestyle and input–output method after the carbon emission coefficients of eight types of household expenditures were determined, and the carbon emissions implied in the production of products and services obtained by households in the process of consumption were calculated.

Estimation of Household Direct CO_2 Emissions

Direct carbon emissions in this paper refer to those produced from the energy consumption process of cooking, heating, lighting, and transportation, which were calculated from 2 sources: building energy consumption system and transportation system.

Carbon Emissions From Building Energy Consumption System

According to the Intergovernmental Panel on Climate Change (IPCC) Guidelines for National Greenhouse Gas Inventories 2017 and "China Energy Statistical Yearbook", the energy consumed by communities in Beijing can be divided into three categories: residential electricity, gas, and heating. The accounting formula is (Fan et al., 2013; Liang et al., 2013; Chancel, 2014)

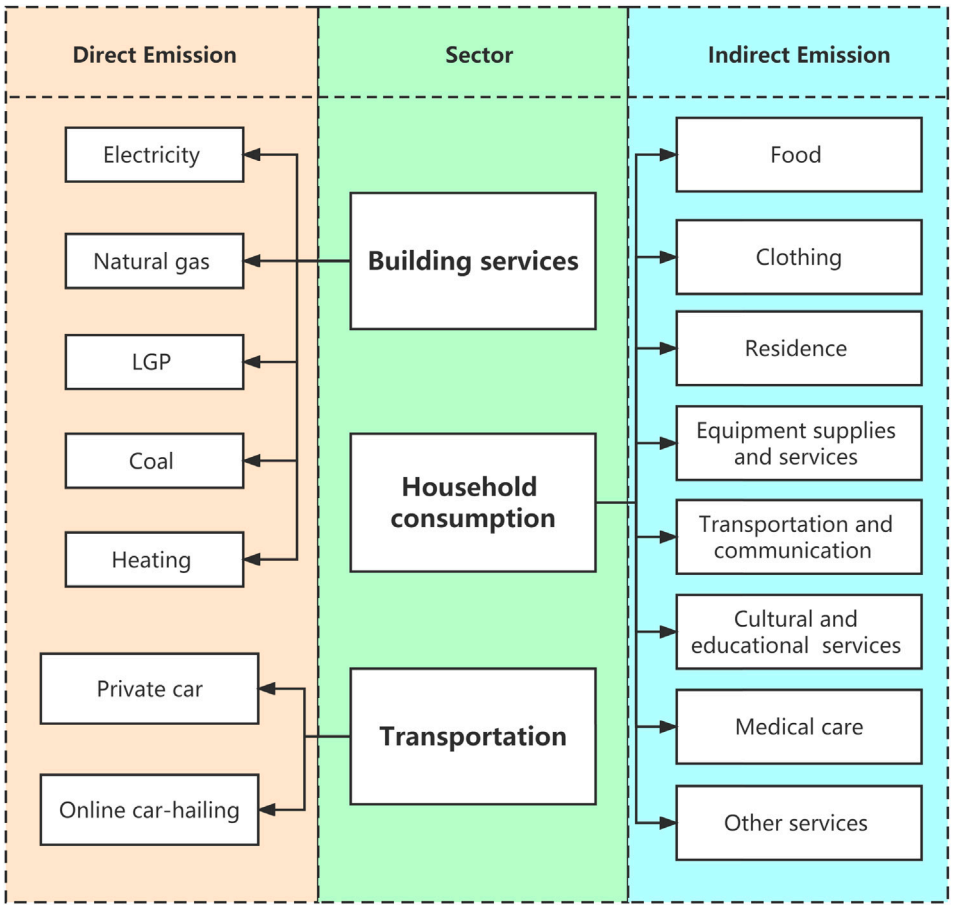

FIGURE 1 | Boundary of household carbon emissions' estimation system.

$$E_i = \sum_i^n F_i \times EF_i$$

where E_i is the carbon emissions generated by the monthly average i energy consumption of households; F_i is the monthly average energy consumption of i consumption; EF_i is the carbon emission factor of i energy consumption; and i is the energy type. The carbon emission factors are based on the method used by the IPCC (2006), and their main data and data sources are shown in the following **Table 1**:

Carbon Emissions From Transportation System

Private cars, online car-hailing, motorcycles, buses, planes, trains, bicycles, and electric cars are the significant means of transportation used by modern families. Carbon emission accounting in the category of community microresearch should have clear regional boundaries. Residents often travel beyond the community boundaries by long-distance vehicles such as planes and trains, so the carbon emissions generated are not included in this research, and these transportation modes are not considered. In recent years, Beijing has adopted a series of traffic management measures on motorcycles and implemented regulations banning motorcycles on many road sections from 2021, which has gradually reduced the number of families traveling by motorcycle. Shared bikes, private bikes, buses, and subways are commonly used, but their carbon emissions are low and data are not readily available. The carbon emissions of electric vehicles are accounted for in the building energy system in the form of household electricity consumption. To sum up, this paper only considers private cars and online car-hailing, which have high carbon emissions and are frequently used by residents for daily travel, and establishes a carbon emission model by referring to relevant literature (Yang et al., 2016) and the data required is declared in **Table 2**.

Carbon Emissions From Private Car

$$E_{pc} = \frac{Cost_{gas}}{Price_{gas}} \times EF_{gas}$$

where E_{pc} refers to the average monthly carbon emissions generated by driving a private car; $Cost_{gas}$ is family monthly gasoline expenditure per capita; $Price_{gas}$ is the price of gasoline; and EF_{gas} is the carbon emission factor of gasoline.

Carbon Emissions From Online Car-Hailing

$$E_{hailing} = D_{hailing} \times GC_{hailing} \times (1 - vacant) \times EF_{gas}$$

where $E_{hailing}$ is the carbon emission generated by a family getting a car-hailing service every month; $D_{hailing}$ is the distance in kilometers that a family travels by ride-hailing per week; $GC_{hailing}$ is the car-hailing gasoline consumption amount; *vacant* is the vacancy rate; and EF_{gas} is the carbon emission factor of fuel when hailing a car.

Estimation of Household Indirect CO_2 Emissions

Indirect carbon emission refers to the carbon emission indirectly generated by residents in the process of obtaining consumer goods and services to meet the needs of household food, clothing, housing, and transportation. The paper adopts the consumer lifestyle method (Feng et al., 2011; Wang and Yang, 2014; Chen et al., 2019) to determine the carbon emission coefficient of household consumption for accounting.

The common practice is based on the classification of the "China Energy Statistical Yearbook," dividing the household consumption expenditure for food, clothing, supplies and services, healthcare, transportation, communication, education, culture and entertainment, eight housing, and other goods and services with reference to Wei et al. (2007) and others, each corresponding to one or more of the production departments. In this paper, our divisions of household consumption departments are shown in **Table 3**. The ratio of production carbon emission to the output value of multiple industries is used to represent the carbon emission coefficient of each type of expenditure, and the indirect carbon emission generated by consumption expenditure is determined by combining consumption.

The input–output method is a frequently used optimization method in the application of CLA in China in recent years (Zhang et al., 2015). It is a common method to quantify and estimate carbon emissions (Wang et al., 2019). It was originally established by the American economist W. Leontief, and Bicknell et al. (1998) applied it and explained the principle reasonably. It determines the carbon emission coefficient by considering the correlation between industries, which can reflect the change of carbon emission caused by the change of one or more industries.

The formula is listed as follows:

$$C = FY = F'(I - A)^{-1}Y$$

where C is the carbon emission of household indirect energy consumption; F represents the implied carbon emission intensity of departments in the n × n input–output table; F′ represents the departments' direct carbon emission intensity; A is the direct consumption coefficient matrix of the n × n input–output table; I is the same order of the identity matrix as A; Y is the column vector, representing the expenditure of the family; $(I - A)^{-1}$ is the Leontief inverse matrix, which shows the impact on all other departments when there are technological changes in a sector of the national economy.

Data Sources

In order to simplify the calculation and consider the availability of data, this paper uses the carbon emission coefficient of standard coal to calculate the carbon emission of industry production (Tu and Liu, 2014). Since the input–output table is published every 5 years, the input–output table used in this paper comes from the relevant data of the 2017 Beijing Input–Output Table, and the energy consumption of various industries comes from the "2018 Beijing Statistical Yearbook." The household characteristics of Beijing residents, including basic household information, household energy consumption, the consumption of life services, community life satisfaction, and residents' decision-making behavior evaluation, were collected by a questionnaire survey.

The community type should have its representative characteristic and distinct characteristic. Based on community classification in the existing research results, this article first embarks from the community property, which could be divided into the traditional community, unit community, and commercial housing community, and selected the Beijing six rings of those three types of typical communities as the data sampling objects. The distribution of survey samples is shown in **Figure 2**. The survey covered six districts and 11 streets in Beijing, namely, the inner city (Dongcheng and Xicheng) and the inner-city suburbs (Chaoyang, Haidian, and Shijingshan). We adopted the method of random sampling, and distributed roughly the same number of questionnaires to each target community, which were scattered in space and did not overlap each other. Moreover, due to the randomness of questionnaire distribution, the interference of some subjective factors could be well avoided. Since the survey was conducted by a one-to-one interview, the authenticity and accuracy of data acquisition were also guaranteed. Thus, the differences of the community location, management mode, and residents' income class make the selection of the three communities believed to have the significance of horizontal comparative analysis.

Based on the existing research and experts' opinions, the questionnaire of our survey was divided into five modules: the basic information of individuals and families, information of household energy consumption, information of household life service consumption, community life satisfaction, and residents' decision-making behavior evaluation. The rationality and feasibility of the questionnaire were determined through a pre-survey through online channels, and the survey was officially started after several revisions. In the early stage of the survey, questionnaires were collected through field visits and one-to-one interviews. In the later stage, due to the impact of the COVID-19, questionnaires were collected through the Internet. Finally, we collected 185 valid household samples.

This paper defines influencing factors such as housing satisfaction and participation in energy conservation and environmental protection based on the existing data obtained from the questionnaire. From the family and community levels,

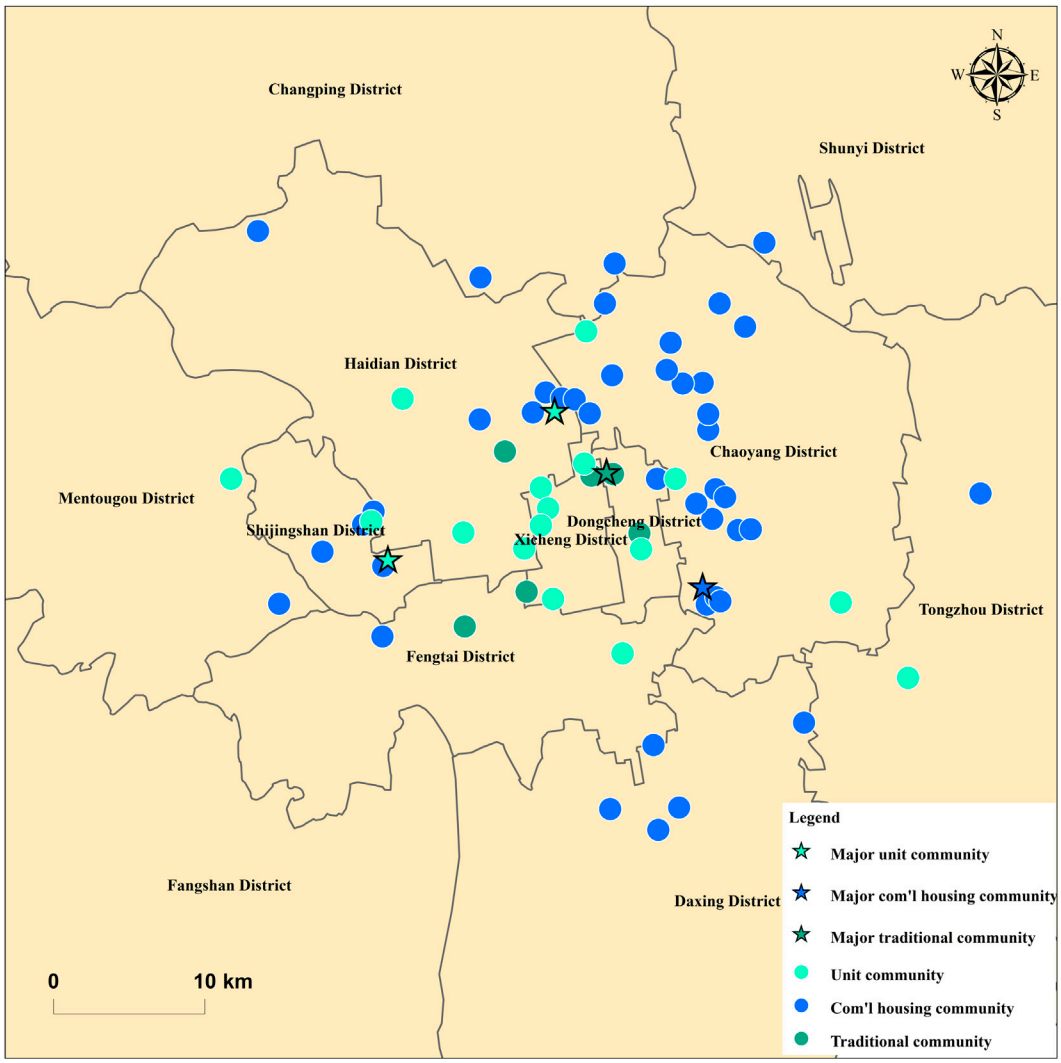

FIGURE 2 | Distribution of the 185 selected household samples.

TABLE 1 | Carbon emission factor of energy.

Energy type i	Carbon emission factor	Unit	Data sources
Electricity	1.00	$kgCO_2/kWh$	Carbon Emission Factors of the North Grid in 2016
Natural gas	2.09	$kgCO_2/m^3$	IPCC Guidelines for National Greenhouse Gas Inventories 2006
Liquefied petroleum gas (LPG)	43.21	$kgCO_2/can$	IPCC Guidelines for National Greenhouse Gas Inventories 2006
Coal	1.98	$kgCO_2/kg$	IPCC Guidelines for National Greenhouse Gas Inventories 2006
Heating	27.50	$kgCO_2/m^2$	Building Energy Research Center, Tsinghua University

we assumed that there are a total of 17 influence factors, including the family monthly income, family structure, engaged in scientific research work, age structure, level of education, floor, housing area, travel mode, air conditioning temperature settings, environment satisfaction, housing satisfaction, energy conservation, environmental protection, activity participation, degree of willingness to participate in community management, community facilities, and car ownership.

Empirical Models

Referring to the cross-sectional data model of the influencing factors of carbon emissions in existing studies, we took the total carbon emissions of traditional communities, unit communities, and commercial housing communities as dependent variables and studied the impact of the influencing factors on carbon emissions by applying econometrics analysis. The basic model is preliminarily set as

TABLE 2 | Data declaration of transportation carbon emissions estimation.

Data declaration	Sources
Household expenditure on gasoline of private car (month)	Micro survey data
Price of gasoline	National Development and Reform Commission
Carbon emission factor of gasoline	IPCC 2006
frequency on car-hailing services (week)	Micro survey data
Average distance of riding car-hailing services	Micro survey data
Gasoline consumption per km of hailing-car and its vacant rate	National average data

TABLE 3 | Related sectors of consumer expenditure.

Number	Consumer expenditure	Related sectors
1	Food	Processing of food from agricultural products, manufacture of foods, manufacture of wine, beverage and refined tea, manufacture of cigarettes and tobacco
2	Clothing	Manufacture of textile, manufacture of textile wearing apparel and ornament
3	Residence	Construction, manufacture of non-metallic mineral products, manufacture of fabricated metal products, renting and leasing activities and business services
4	Equipment supplies and services	Processing of timbers, manufacture of wood, bamboo, rattan, palm, and straw products, manufacture of furniture, manufacture of electrical machinery and equipment
5	Transportation and communication	Manufacture of computer, communication equipment and other electronic equipment, information transmission, software and information technology services, manufacture of motor vehicles, manufacture of railway locomotives, building of ships and boats, manufacture of air and spacecrafts and other transportation equipment
6	Cultural and educational goods and services	Manufacture of paper and paper products, printing, reproduction of recording media, manufacture of articles for culture, education, artwork, sport and entertainment activities, education, culture, sports, and entertainment
7	Medical care	Healthcare and social works
8	Other services	Wholesale and retail trade, accommodation and restaurants, resident services, repair, and other services

TABLE 4 | The definitions of variables in regression analysis.

Variable	Variable symbol	Definitions
Total carbon emissions	y_1	The sum of direct and indirect carbon emissions
Direct carbon emissions	y_2	Household carbon emissions caused from energy consumption
Indirect carbon emissions	y_3	Household carbon emissions caused from services consumption
Total monthly income	x_1	Monthly total income in a household (yuan)
Total household population	x_2	one member = 1, two members = 2, three members = 3, four members = 4, five or more than five members = 5
Engaged in scientific research related work	x_3	Engaged in scientific research = 1, otherwise = 0
Age structure	x_4	Proportion of the youth population to the total number of families aged 18–65
Education Level	x_5	Average education level, primary school and below = 0, junior high school = 1, senior high school or technical secondary school = 2, junior college = 3, bachelor's degree = 4, master's degree and above = 5
Floor	x_6	Floor of household
Housing area	x_7	Housing area for residential construction (m^2)
Trip mode	x_8	Car or online car-hailing = 0, otherwise = 1
The temperature setting of air conditioner	x_9	Air-conditional temperature set in summer <21°C = 1, 22–24°C = 2, 25–27°C = 4, 28°C and above = 5
Housing satisfaction	x_{10}	Average value of house type, area, and lighting satisfaction
Participation in energy conservation and environmental protection activities	x_{11}	Average value of trip mode, air conditioning temperature, environmental decoration, garbage sorting, and community management willingness
Ownership of cars	x_{12}	Household with car = 1, otherwise = 0
Permanent residents	x_{13}	Inhabitant in the community = 1, otherwise = 0
Job involvement	x_{14}	The percentage of adults in households who are working
Urban residents	x_{15}	Permanent urban residence certificate = 1, otherwise = 0
Lighting	x_{16}	To the south = 1, otherwise = 0
Community convenience satisfaction	x_{17}	Average value of the accessibility to supermarket, subway and employment place (accessible in 20 min by walking = 1, otherwise = 0)

TABLE 5 | Basic characteristics of three typical communities.

Community type	Sample size (person)	Average family size (*)	Average age structure (*)	Average level of education (*)	Average household income (yuan)	Satisfaction with community environment (*)	Satisfaction with supporting facilities (*)
Traditional community	54	3.33	0.72	1.92	13,280	3.37	3.15
Unit community	53	4.33	0.78	2.70	19,877	3.71	3.81
Commercial housing community	78	2.60	0.94	3.61	34,415	3.88	3.76

*Note: Satisfaction with community environment is calculated with the average level of the surrounding environment and environmental protection work in community; Satisfaction with supporting facilities is calculated with the average level of seven kinds of facilities needed for daily life in community. The definitions of other indicators with * are consistent with* ***Table 4****. Average family size, both satisfactions and average level of education are valued by the full mark of 5. Average age structure ranges from 0 to 1.*

$$y = \beta_0 + \beta_1 x_1 + \beta_2 x_2 + \ldots + \beta_{16} x_{16} + \varepsilon$$

where x_1, x_2,……, x_{16} is the independent variables as follows (**Table 4**) and y is the total residential carbon emission in the three types of communities. The definitions of variables are shown in the following **Table 4**.

It is assumed that the observed individuals of the cross-sectional data are independent and there is no autocorrelation. Therefore, the Variance Inflation Factor (VIF) test, Breusch-Pagan (BP) test, and White test are carried out on the explained variables, respectively, and some factors that have negative effects on the model are removed by stepwise regression. Taking the traditional community as an example, we first test the multicollinearity of independent variables. The correlation matrices of the independent variables and variance inflation factor in the multiple regression model both indicate that there is no multicollinearity in the independent variables. The p-value of the BP test is 0.000, indicating that the independent variable has heteroscedasticity, so the heteroscedasticity robust standard error is added for correction.

After the modification, the two-stage least square method (2SLS) command was applied to it, and it was found that the estimators of the two models had little difference, and there was no endogeneity problem. For further verification, environmental satisfaction was set to be an endogenous variable. According to the coefficient of the correlation matrix, it is found that the correlation between environmental satisfaction and infrastructure satisfaction of tool variables is 0.599, which is suitable to be a tool variable of environmental satisfaction. Assuming that all other variables are exogenous, the 2SLS was used for regression. The results of Anderson Canon. Corr. LM Statistic and Cragg–Donald Wald F Statistic show that the instrumental variables pass the over recognition and just recognition tests. Also, for the test, namely, the results of the Minimum Eigenvalue statistic, its value 32.2022 significantly rejected the null hypothesis of the existence of weak instrumental variables. We also carried out the Durbin Wu Hausman (DWH) test to test the endogeneity of explanatory variables because of heteroscedasticity, and all the results above proved that the original hypothesis is verified without an endogeneity problem and all variables are considered exogenous. A more robust model is selected under the condition that there is no significant difference in estimated values and no significant difference in parameters.

RESULTS

Basic Characteristics of the Three Typical Communities

From the data gathered in the survey, the basic characteristics of the three typical communities (traditional community, unit community, and commercial housing community) are portrayed in **Table 5**.

As shown, the community type affects its attributes significantly. The residents of traditional communities share the lowest income among the three types of communities. At the same time, this kind of community lacks labor-aged people more than the other two, with an average age structure of 0.72. The commercial housing community appears to have a much younger age structure of 0.94 and a higher level of education, at 3.61; thus, the respondents in this kind of community share the highest average income of 34,415. The family pattern of 2 or 3 members is common in commercial housing communities. The satisfaction with the community environment there is highest, while those with supporting facilities came in second place among three communities, respectively, at 3.88 and 3.76.

Characteristics of Carbon Emissions of Different Communities

Figure 3 illustrates the estimation of direct carbon emissions in three typical communities. The estimation of indirect carbon emissions of the three typical communities is exhibited in **Table 6** and **Figure 4**, and the structure of that is demonstrated in **Figure 5**.

Estimated direct carbon emissions are presented with the quantitative relation of unit community > commercial housing community > traditional community, while indirect carbon emissions are presented with the quantitative relation of commercial housing community > unit community > traditional community.

The average monthly direct carbon emissions of households in the unit community are the largest at 723.79 $kgCO_2$, followed by the commercial housing community at 580.01 $kgCO_2$ and traditional community at 526.44 $kgCO_2$. Between its two subsystems, the building energy consumption system accounts for the maximum proportion, which takes more than 70% of direct carbon emissions in all three communities. The

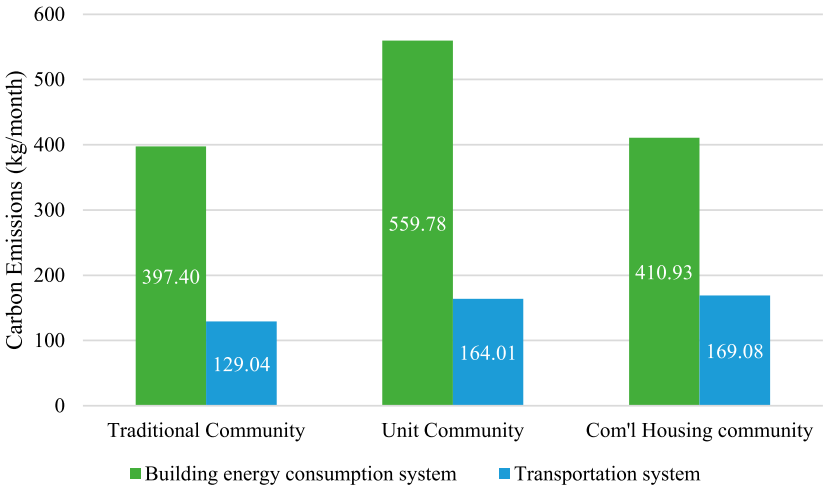

FIGURE 3 | Direct carbon emissions per month in three typical communities.

TABLE 6 | Estimation of indirect carbon emissions of three typical communities (kg/month).

Community type	Food	Clothing	Residence	Equipment supplies and services	Transportation and communication	Cultural and educational goods and services	Medical care	Other services	Total amount of indirect carbon emission
Traditional community	201.40	86.05	85.44	51.34	24.32	43.54	48.98	13.78	554.85
Unit community	187.70	123.32	84.96	53.15	51.52	114.89	33.05	20.80	669.38
Commercial housing community	187.30	126.96	155.33	67.51	41.34	58.79	33.23	37.25	707.70

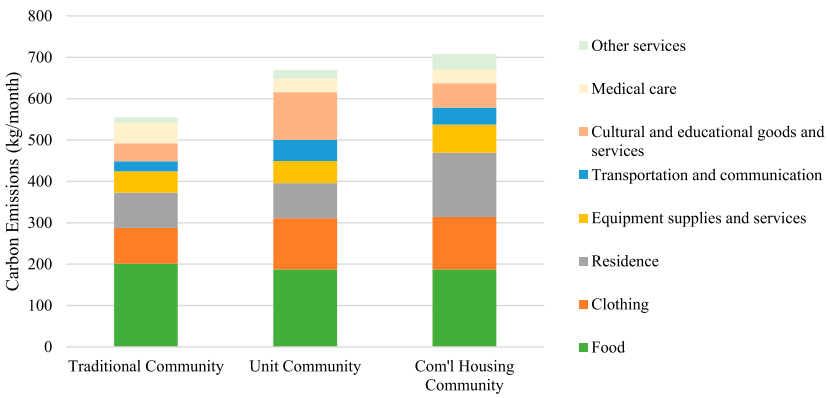

FIGURE 4 | Indirect carbon emissions per month in three typical communities.

transportation carbon emissions correspondingly take less than 30% of direct carbon emissions in all three communities. With the largest population scale, households in unit communities produce 559.78 $kgCO_2$ monthly from the building energy consumption system. On the contrary, households in traditional and commercial communities produce much lower carbon emissions from building energy consumption at 397.40 and 410.93 $kgCO_2$, respectively, mainly because of their smaller family size. The transportation carbon emissions in the traditional community are the lowest with 129.04 $kgCO_2$ per

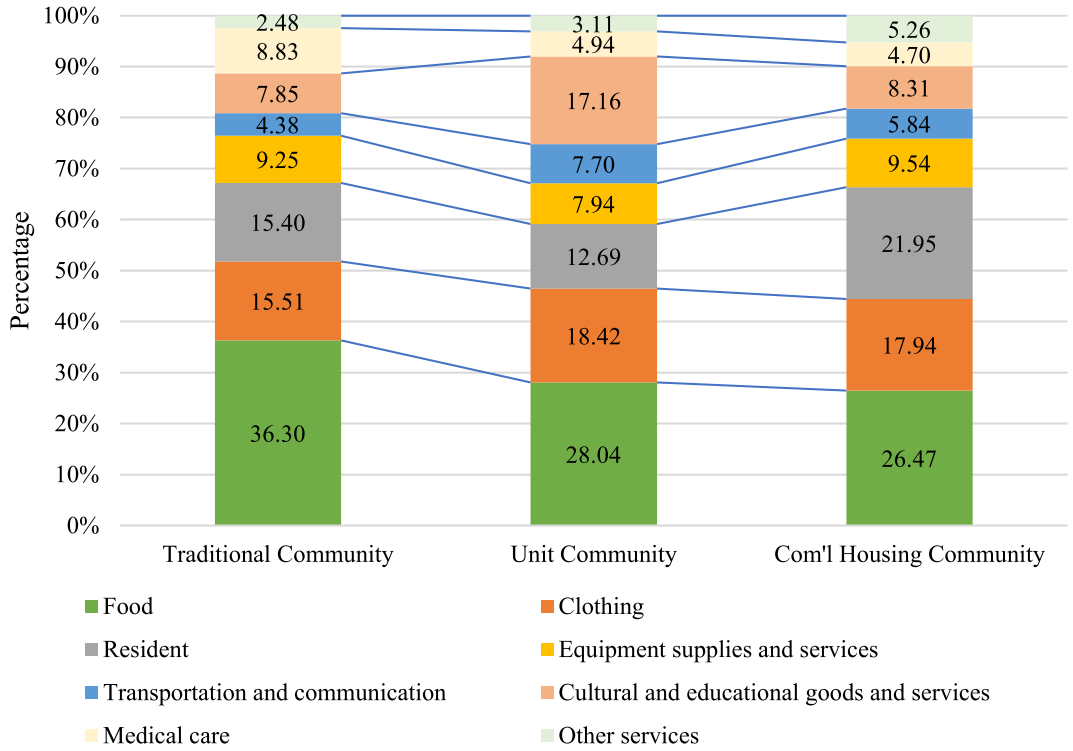

FIGURE 5 | Composition of indirect carbon emissions in three typical communities.

month, and that is mainly because the residents there are older and mostly retired without work-related mobility and the level of transportation carbon emissions in unit communities and commercial housing communities is flat, both estimated slightly more than 160 $kgCO_2$ per month.

The average monthly indirect carbon emissions of households in the commercial housing community are largest at 707.70 $kgCO_2$, followed by the unit community at 669.38 $kgCO_2$, and traditional community at 554.85 $kgCO_2$. Food consumption occupies more than 20% share of indirect carbon emissions in all three communities, numerically at 201.40, 187.70, and 187.30 $kgCO_2$, respectively, per month. Food, clothing, and residents are the three major sectors of indirect carbon emissions, occupying more than 10% separately, and altogether near 60% of indirect carbon emissions in all three communities. The indirect carbon emissions of the other 5 household consumption sectors are found much lower on the whole. Different communities witness a significant disparity in their indirect carbon emission structure. Residents in traditional communities produce much fewer carbon emissions from clothing consumption, with only 86.05 $kgCO_2$ per month, while those in the other two communities are both more than 120 $kgCO_2$ monthly. That is mainly because more aged citizens live in traditional communities and they often spent their expenses sparingly and lack the passion for purchasing new clothes. As illustrated in the analysis of direct carbon emissions, traditional community residents also produce the lowest amount of carbon emissions in transportation and communication sectors, numerically about half of the other two's levels. Traditional communities are more likely spatial aggregations in separation from the consumerism of modern society; residents there prefer a traditional and frugal living style, and thus, they choose to consume more on necessary daily needs and spend less on other sectors. Reasonably, expenses on medical care in traditional communities account for its largest constitution of the indirect carbon emission structure among three types of communities. Overall, the indirect carbon emission structures of unit communities and commercial communities are similar. No significant differences can be found in carbon emissions from food, clothing, and medical care consumption of these two kinds of communities. However, residents in commercial housing communities hold the highest income; therefore, the total indirect carbon emissions of consumption there is correspondingly the largest. Residents there tend to expend more on the fixture and repairing, which is included in residence consumption compared to others. The carbon emissions produced by expenditure on cultural and educational goods and services is highest in unit communities, more than ones from resident consumption there, which is probably because residents there are most likely former high-qualified staff of state-owned enterprises

TABLE 7 | Regression analysis results of HCEs in three typical communities.

	Total HCEs	Coef.	St.Err.	*p*-value	Sig
Traditional Community	Population	0.139	0.083	0.102	
	Salary	2.659	0.455	0	***
	car_own	0.117	0.047	0.017	**
	Area	0.201	0.519	0.7	
	sci_research	0.249	0.088	0.007	***
	Convenient	0.17	0.136	0.217	
	EnvironSat	0.217	0.093	0.024	**
	Working	−0.005	0.106	0.961	
	Constant	−0.165	0.133	0.219	
	N	54			
	R-squared	0.645			
	F	37.687			
Unit Community	Population	0.261	0.001	0.001	***
	Salary	1.611	0	0	***
	car_own	0.139	0.005	0.005	***
	Area	0.563	0	0	***
	sci_research	0.016	0.75	0.75	
	Convenient	−0.324	0.003	0.003	***
	EnvironSat	−0.124	0.331	0.331	
	Working	−0.04	0.688	0.688	
	Constant	0.385	0.003	0.003	***
	N	53			
	R-squared	0.649			
	F	28.557			
Commercial Housing Community	Population	0.22	331.174	0.028	**
	Salary	0.463	300.483	0	***
	car_own	0.076	167.396	0.15	
	Area	0.563	1667.189	0.24	
	sci_research	0.041	125.545	0.336	
	Convenient	0.072	245.645	0.401	
	EnvironSat	0.099	292.165	0.335	
	Working	0.234	519.253	0.154	
	Constant	−0.131	544.574	0.479	
	N	78			
	R-squared	0.304			
	F	8.739			

*Note: ***p < 0.01, **p < 0.05, *p < 0.1. Population represents total household population, salary represents total monthly income, car_own represents ownership of cars, area represents housing area, sci_research represents engaged in scientific research related work, convenient represents community convenience satisfaction, environSat represents housing satisfaction.*

or colleges in China and perform cultural consumption more frequently.

Combining and comparing the direct and indirect carbon emissions, it can be found that the unit community owns the highest total carbon emissions among three types of communities, which is 1393.17 $kgCO_2$, followed by commercial housing community with 1287.71 $kgCO_2$, and the lowest in traditional community, which is 1081.29 $kgCO_2$. Among them, the average indirect carbon emissions of the three types of communities exceeded direct carbon emissions, indicating that indirect carbon emissions accounted for a greater proportion of HCEs in the general community. However, according to the above calculation results, the indirect carbon emission of traditional community is 28.41 kg higher than direct carbon emission, while the indirect carbon emission of unit community is 54.41 kg lower than direct carbon emission. The indirect carbon emission of commercial housing communities is much higher than direct carbon emission, reaching 127.69 kg.

Analysis of Household Carbon Emission Influential Factors

We further conducted the econometric regression model to examine the influential factors of total carbon emissions in three different types of communities. The results showed that the monthly income in households has shown a significant positive correlation with total carbon emissions in three communities, which means that the household income increases total carbon emissions (**Table 7**). Results also indicated that income is one of the most important factors influencing HCEs. In three types of communities, one enhanced standard unit of income increases 2.659, 1.611, and 0.463 of total HCEs, respectively. Household population plays a vital role in HCEs in unit communities and commercial housing communities. Compared to income, this variable increases HCEs both directly and indirectly. When the household population in unit communities and commercial housing communities increased by one unit, more 0.261 and 0.22 HCEs will be

emitted. However, our research shows that its impact on HCEs in traditional communities is much weaker than the other two and is not strong enough to be significant. The obtained also depicts that car ownership is positively correlated with HCEs in both traditional communities and unit communities, at the level of 5% and 1%, respectively. It was also reported that the households with cars in these two communities produce more 0.117 and 0.139 of HCEs than those without cars monthly. However, car ownership is not in a statistically significant positive correlation with HCEs in commercial housing communities.

In addition to universal influential factors in more than one type of community, each community owns some unique driving factors of HCEs there, which reflects their varied attributes and other characteristics. In traditional communities, there existed significant positive correlations between engaged in scientific research-related work and environmental satisfaction and HCEs. In unit communities, the housing area is positively correlated with carbon emissions while community convenience is negatively correlated with HCEs. Besides income and household population, no other unique significant correlations can be found between HCEs and other variables; the personnel involved in scientific research have a significant impact at the 1% level, and each additional unit of personnel involved in scientific research in the family will increase HCEs in traditional communities by 0.249. Carbon emissions are positively correlated with environmental satisfaction at the level of 0.05, and every unit increases in environmental satisfaction will increase carbon emissions by 0.217. In unit communities, there existed a positive correlation between the housing area and HCEs, and this impact is significant under the 1% level, and every 1 standard unit increase in the housing area increases carbon emissions by 0.563. The degree of convenience is proven to decrease carbon emissions significantly in unit communities. Each added degree of community convenience can reduce 0.324 of HCEs here.

During the process of the linear regression model, there are some other influential factors of HCEs that can be enlightening to us, although they were not statistically significant enough in each kind of community. The results suggest a positive correlation between the household population on the average level of education and carbon emissions in the commercial housing communities, but in the unit communities and traditional communities, this correlation turns out to be negative.

DISCUSSIONS

From our HCE estimation model, we draw the conclusion that both direct and indirect carbon emissions in three communities are distinctive, and those differences are detailed and showed the unique features of typical sort of communities clearly. In comparison, existing studies concentrate more on exploring the changes of HCEs cross-time and the inequality between urban and rural areas (Donglan et al., 2010; Feng et al., 2011; Wang and Yang, 2014; Chen et al., 2019). Our study design is based on a new vision concerning the inequality of HCEs in communities, and what we obtained declares that the phenomenon of unbalanced HCEs can occur in more microspatial units than urban and rural, or developed and developing, places. As for the quantitative relationship of two carbon sources, it is widely accepted that indirect carbon emissions account for most or the majority of HCEs (Zhang et al., 2015; Yin et al., 2020), but this study found that although the average amount of indirect carbon emissions in three communities is more than direct carbon emissions, the households in unit communities produce more direct carbon emissions than indirect ones while the remaining two types of community indirect carbon emissions are more than direct carbon emissions. A possible explanation is that with the application of clean production and energy-saving technologies (Khan et al., 2019), the embedded carbon intensities in industrial production are much lower in Beijing recently, and the defined calculating boundary of carbon emissions in different studies plays a role in the disparity of their findings. Our results provide insights for revealing the different quantitative relations of direct and indirect HCEs in different kinds of communities, which can be heuristic in future studies. More than one kind of community presents a positive correlation between car ownership and HCEs.

In terms of influencing factors, existing studies suggested that household expenditure or income is one of the most important driving factors of carbon emissions (Pachauri, 2004; Weber and Matthews, 2008; Xu et al., 2015; Li et al., 2016) which was consistent with our results. It is believed that income affects the purchasing power of households, differing their lifestyles and characteristics of consumption structure to shape their carbon emissions indirectly. Higher incomes are closely associated with high-quality life, as well as higher daily expenditure.

The household population is also recognized to have a significant positive correlation with HCEs in many papers (Qu et al., 2013; Xue, 2020; Yang and Liu, 2017). It is reasonable that the more members in a household, the more HCEs foreseeable to emit because people are the dual subjects of both basic energy and living services or goods consumption. However, from what we attained in this study, because it was lacking young family members, the carbon emissions in traditional community households are not significantly correlated with the household population. A possible explanation is that young family members seldom settle in traditional communities for long with their parents, leaving fewer energy needs in households there. Since that, it presents that the permanent population in households is a better choice for future studies. On the whole, the HCE drivers suiting all kinds of communities in this paper are the household income and household permanent population to a certain extent. Similar to Lyons et al. (2012), we find that the household income is a more significant driving force of HCEs in households than the household population.

The impact of car ownership on HCEs shows a significant positive effect in both traditional communities and unit communities. The daily use of vehicles increases HCEs from transportation (Wang and Liu, 2015; Xu et al., 2015), but it is worth mentioning that car ownership shapes lifestyle and personal decisions dramatically in modern society, from which more carbon emissions can be produced. In commercial housing communities, the impact of car ownership on HCEs is also

positive but not statistically significant enough. Only 20.5% of residents choose car driving or car-hailing as their major travel decisions, while the percentage of private car owners here is 65.3%, which verifies that cars are not frequently used here for daily transportations. Besides, the large composition of consumption-induced indirect HCEs in carbon emissions structures there inhibits the positive effect of transportation carbon emissions in some means.

The other significant influential factors of HCEs obtained from our study are the scientific research work-related population, community environment satisfaction, housing area, and community convenience, which belongs to one certain kind of communities.

In traditional communities, scientific research work-related population and community environmental satisfaction are proven to increase HCEs here. The personnel involved in scientific research participate in more cultural and educational services and spend more in this field. At the same time, the carbon emission intensity of cultural and educational activities has also been confirmed to have a significant improvement in recent years. Additionally, the personnel involved in scientific research are generally highly educated, which may have more requirements for the quality of life and more frequent traffic activities (Büchs and Schnepf, 2013; Han et al., 2015) and such people may have a more luxurious lifestyle. These characteristics of people in those occupations are contrary to the overall structure of the main residents in the traditional communities, who are older and prefer a simple life and single carbon energy consumption concentrated in the basic daily consumption activities, making this factor significantly stimulate the carbon emissions of traditional communities to rise. This also suggests that households living in environmentally sound communities could have higher incomes and are able to pursue a better quality of life, but that higher environmental satisfaction in such communities may not be proportional to higher energy conservation awareness.

In unit communities, housing areas increase but the community convenience reduces HCEs significantly. This is mainly because the larger the residential area, the more the fixed devices, and the more energy needed (Li et al., 2019). When heating equipment is used, more energy is needed to achieve the same effect, so carbon emissions will consequently increase. Due to the frequent short-haul transmission between households and workplaces in this certain type of communities, the improvement of community convenience can reduce a lot of transportation carbon emissions there (Yang et al., 2016). This sheds a light on the importance of urban convenience in the means of carbon reduction (Rong et al., 2018).

Our study portrays the distinction between these three typical communities in Beijing *via* a new perspective: carbon emissions and their driving factors. From the aspect of carbon emissions, traditional communities emit the lowest total carbon emissions among the three types of communities, which is caused by the low mobility of its residents and their limited life quality demands. The commercial housing community takes the highest part of indirect carbon emission in the three kinds of communities, which suggests that the residents there are more likely wealthy and expect high life quality during daily living. The unit communities should be ones with both the largest household scale and total carbon emissions. As for the carbon emissions' influential factors, they indicate that traditional communities and unit communities are a characteristic with most significant drivers and can be regulated with carbon restriction targets through multiple pathways. However, each of these two types of communities is very distinctive; carbon emissions in traditional communities are concentrated on community environment and human-related factors, like community environment satisfaction and scientific research work-related population,. while those in unit communities are more tightly related with community functions, such as convenience and housing area. Commercial housing communities are correspondingly the most complex or unknown type of community among these three types of communities with less obvious drivers. The following studies need to concentrate on these kinds of communities more from multi-angles to dig the mechanism behind their complexity.

Considered as important emitters of carbon emissions, households gain the great attention of scholars in recent years. In recent studies, the necessary data are mostly gathered from the microsurvey and their quality and quantity are highly connected with the credibility of study results (Zhang et al., 2015). To study HCEs more accurately and profoundly, more available related data should be provided with open access. Due to the limited resources, our research needs more effective samples to revise itself as with many survey studies. The following studies should enlarge the scale of the samples and re-examine the conclusions, and more classification of households should be taken into consideration in the future. Further studies exploring the interrelation between HCEs and community attributes can concentrate more on the concept of eco-community, establishing widely applicable models of community carbon emissions and estimating their eco-efficiency. Furthermore, we can evaluate the community management mode, and propose reasonable decision-making intention, treat the community as an independent unit to manage carbon emissions.

POLICY IMPLICATIONS

According to the results obtained in our study, concrete policies can be proposed to deal with carbon emissions in different communities specifically. Food consumption accounts for the largest share of indirect carbon emissions from eight types of consumption. Household food purchasing should be based on the principle of an appropriate amount; avoiding waste as much as possible, the consumption mode of unit community and commercial housing community is more diversified, and the quality requirements of daily life, clothing, and daily necessities are higher. It should mainly guide the rational consumption of these two types of community residents, thrift, and form a correct consumption concept. Residents in traditional communities are generally older and have simple lifestyles, which prefer needy daily consumption. We should add health equipment and provide exercise places, which can reduce medical consumption-induced HCEs to some extent. The commercial housing community and unit community residents' lifestyles are relatively complex and diverse; guiding their green

consumption to alleviate carbon emissions is more important. In particular, it is necessary to strengthen the investment in infrastructure in the unit communities. In the unit communities, improving the convenience of the community will greatly reduce the utilization rate of transportation tools or the frequency of the use of private cars. Under the condition of improving the same convenience, the unit community can achieve a better emission reduction effect than the other two communities.

On the whole, the following policy implications based on universal influential factors in three types of the community also need wide attention. With the steady growth of per capita disposable income, the level of indirect carbon emissions will remain high. Relevant policies should be promoted to improve the consumption structure of residents, encourage and guide green consumption, and reduce the proportion of consumption of goods with high carbon emissions. In our research, it is found that the residents' living habits are one of the important factors affecting community carbon emissions. The government needs to strengthen the publicity of environmental protection and improve the residents' living habits. At the same time, the residents' consumption behavior can also be restrained by controlling energy prices within a reasonable range. In addition, promoting the development and utilization of renewable energy promotes the technology research and development and achieves the transformation of solar energy, tidal energy, and wind energy as well and realizes the technological breakthrough and practical application as soon as possible. More investment, development, and utilization of low-energy-consumption equipment. At the same time, the government will improve the coverage and utilization rate of low-carbon equipment through subsidies or tax exemption for low-carbon equipment in order to phase out traditional household equipment with low energy efficiency and high energy consumption. Manufacturers should be encouraged to continuously develop and launch household equipment with higher energy efficiency and lower energy consumption. Then, low-carbon transformation should be carried out at the community level to reduce carbon emissions without reducing the residents' living standards.

CONCLUSION

This paper mainly analyzed the different characteristics of HCEs in three kinds of typical communities in Beijing and driving factors behind them, aiming to assist the ecological transformation of urban communities. During our research, we tried to examine the interaction between community attributes and HCEs and provide implications for policymakers to congratulate carbon emissions specifically on microspatial units: communities. Based on a micro survey conducted with 185 samples, we utilized the ECM method and input–output revised CLA method to evaluate HCEs in the traditional, unit, and commercial housing communities from direct and indirect portions. Then, we applied the econometric regression model to explore the influential factors behind their disparity.

The results suggested that direct carbon emissions are actually with the quantitative relation of the unit community (723.79 $kgCO_2$) > commercial housing community (580.01 $kgCO_2$) > traditional community (526.44 $kgCO_2$), while indirect carbon emissions are with the quantitative relation of the commercial housing community (707.70 $kgCO_2$) > unit community (669.38 $kgCO_2$) > traditional community (554.85 $kgCO_2$). The structure of carbon emissions in three kinds of communities is distinctive dramatically, and diverse and reliable factors were found. It was proven that the household income is the universal driver that increases HCEs in all three types of communities. Household population affects carbon emissions positively in the unit communities and commercial housing communities. Car ownership increases HCEs in traditional communities and unit communities significantly. A set of demographic, economic, and community attribute factors is the unique driver of HCEs in one certain type of community. The scientific research work-related population and community environment satisfaction increase HCEs in traditional communities. Housing areas increase, but the community convenience reduces HCEs in unit communities effectively. There are also some non-significant factors that have mentionable impacts on HCEs, like the average education level of households.

DATA AVAILABILITY STATEMENT

The raw data supporting the conclusions of this article will be made available by the authors, without undue reservation.

AUTHOR CONTRIBUTIONS

JW conducted and performed research, collected the partial data and estimated the carbon emissions and wrote the main body of this paper; WH collected the partial data and wrote the abstract and introduction of this paper and went through some sectional works; LL collected the partial data and performed the analysis of the influential factors and wrote the part of data and methodology; YB contributed to revising and finalizing the paper; YD collected the partial data and contributed to write the study area of this paper; JL analyzed the influential factors and did partial graphic works.

FUNDING

This research was supported by National Natural Science Foundation of China (Grant No. 72004215) and National Natural Science Foundation of China (Grant No. 72104223).

REFERENCES

Adalilar, S. N., Alkibay, S., and Eser, Z. (2015). Ecovillages as a Destination and a Study of Consumer Approaches to Ecovillages. *Proced. Econ. Finance* 23, 539–546. doi:10.1016/s2212-5671(15)00561-4

Anderson, T. R., Hawkins, E., and Jones, P. D. (2016). CO2, the Greenhouse Effect and Global Warming: from the Pioneering Work of Arrhenius and Callendar to Today's Earth System Models. *Endeavour* 40 (3), 178–187. doi:10.1016/j.endeavour.2016.07.002

Andrew, J., and Cortese, C. (2011). Accounting for Climate Change and the Self-Regulation of Carbon Disclosures. *Account. Forum* 35, 130–138. Elsevier. doi:10.1016/j.accfor.2011.06.006

Bai, Y., Deng, X., Gibson, J., Zhao, Z., and Xu, H. (2019). How Does Urbanization Affect Residential CO2 Emissions? an Analysis on Urban Agglomerations of China. *J. Clean. Prod.* 209, 876–885. doi:10.1016/j.jclepro.2018.10.248

Bicknell, K. B., Ball, R. J., Cullen, R., and Bigsby, H. R. (1998). New Methodology for the Ecological Footprint with an Application to the New Zealand Economy. *Ecol. Econ.* 27 (2), 149–160. doi:10.1016/s0921-8009(97)00136-5

Bin, S., and Dowlatabadi, H. (2005). Consumer Lifestyle Approach to US Energy Use and the Related CO2 Emissions. *Energy policy* 33 (2), 197–208. doi:10.1016/s0301-4215(03)00210-6

BP (2021) The BP Statistical Review of World Energy. Available at: http://www.bp.com/statisticalreview (accessed 28 July 2021)

Büchs, M., and Schnepf, S. V. (2013). Who Emits Most? Associations between Socio-Economic Factors and UK Households' home Energy, Transport, Indirect and Total CO2 Emissions. *Ecol. Econ.* 90, 114–123.

Calleja-Agius, J., England, K., and Calleja, N. (2021). The Effect of Global Warming on Mortality. *Early Hum. Dev.* 155, 105222. doi:10.1016/j.earlhumdev.2020.105222

Chancel, L. (2014). Are Younger Generations Higher Carbon Emitters Than Their Elders? *Ecol. Econ.* 100, 195–207. doi:10.1016/j.ecolecon.2014.02.009

Chen, C., Liu, G., Meng, F., Hao, Y., Zhang, Y., and Casazza, M. (2019). Energy Consumption and Carbon Footprint Accounting of Urban and Rural Residents in Beijing through Consumer Lifestyle Approach. *Ecol. Indicators* 98, 575–586. doi:10.1016/j.ecolind.2018.11.049

Dalton, M., Jiang, L., Pachauri, S., and O'Neill, B. C. (2007). *Demographic Change and Future Carbon Emissions in China and India, Unpublished Update of the 16 March 2007 Draft Presented at the Annual Meeting of the Population*. New York, NY: Association of America, 29–31.

Davis, S. J., and Caldeira, K. (2010). Consumption-based Accounting of CO2 Emissions. *Proc. Natl. Acad. Sci.* 107 (12), 5687–5692. doi:10.1073/pnas.0906974107

Deng, S. (2021). Exploring the Relationship between New-type Urbanization and Sustainable Urban Land Use: Evidence from Prefecture-Level Cities in China. *Sustain. Comput. Inform. Syst.* 30, 100446. doi:10.1016/j.suscom.2020.100446

Donglan, Z., Dequn, Z., and Peng, Z. (2010). Driving Forces of Residential CO2 Emissions in Urban and Rural China: An index Decomposition Analysis. *Energy Policy* 38 (7), 3377–3383. doi:10.1016/j.enpol.2010.02.011

Eckstein, D., Künzel, V., and Schäfer, L. (2017). *Global Climate Risk Index 2018*. Bonn, Germany: Germanwatch.

Fan, J.-L., Liao, H., Liang, Q.-M., Tatano, H., Liu, C.-F., and Wei, Y.-M. (2013). Residential Carbon Emission Evolutions in Urban-Rural Divided China: An End-Use and Behavior Analysis. *Appl. Energ.* 101, 323–332. doi:10.1016/j.apenergy.2012.01.020

Feng, Z.-H., Zou, L.-L., and Wei, Y.-M. (2011). The Impact of Household Consumption on Energy Use and CO2 Emissions in China. *Energy* 36 (1), 656–670. doi:10.1016/j.energy.2010.09.049

Gu, Z. H., Sun, Q., and Wennersten, R. (2013). Impact of Urban Residences on Energy Consumption and Carbon Emissions: An Investigation in Nanjing, China. *Sustain. Cities Soc.* 7, 52–61. doi:10.1016/j.scs.2012.11.004

Han, L., Xu, X., and Han, L. (2015). Applying Quantile Regression and Shapley Decomposition to Analyzing the Determinants of Household Embedded Carbon Emissions: Evidence from Urban China. *J. Clean. Prod.* 103, 219–230. doi:10.1016/j.jclepro.2014.08.078

Huo, T., Ma, Y., Cai, W., Liu, B., and Mu, L. (2021). Will the Urbanization Process Influence the Peak of Carbon Emissions in the Building Sector? A Dynamic Scenario Simulation. *Energy and Buildings* 232, 110590. doi:10.1016/j.enbuild.2020.110590

Kenny, T., and Gray, N. F. (2009). Comparative Performance of Six Carbon Footprint Models for Use in Ireland. *Environ. impact Assess. Rev.* 29 (1), 1–6. doi:10.1016/j.eiar.2008.06.001

Khan, Z., Sisi, Z., and Siqun, Y. (2019). Environmental Regulations an Option: Asymmetry Effect of Environmental Regulations on Carbon Emissions Using Non-linear ARDL. *Energy Sourc. A: Recovery, Utilization, Environ. Effects* 41 (2), 137–155. doi:10.1080/15567036.2018.1504145

Li, J., Huang, X., Yang, H., Chuai, X., Li, Y., Qu, J., et al. (2016). Situation and Determinants of Household Carbon Emissions in Northwest China. *Habitat Int.* 51, 178–187. doi:10.1016/j.habitatint.2015.10.024

Li, J., Zhang, D., and Su, B. (2019). The Impact of Social Awareness and Lifestyles on Household Carbon Emissions in China. *Ecol. Econ.* 160, 145–155. doi:10.1016/j.ecolecon.2019.02.020

Liang, L., Wu, W., Lal, R., and Guo, Y. (2013). Structural Change and Carbon Emission of Rural Household Energy Consumption in Huantai, Northern China. *Renew. Sustain. Energ. Rev.* 28, 767–776. doi:10.1016/j.rser.2013.07.041

Lin, B., and Zhu, J. (2021). Impact of China's New-type Urbanization on Energy Intensity: A City-Level Analysis. *Energ. Econ.* 99, 105292. doi:10.1016/j.eneco.2021.105292

Lin, T., Yu, Y., Bai, X., Feng, L., and Wang, J. (2013). Greenhouse Gas Emissions Accounting of Urban Residential Consumption: a Household Survey Based Approach. *PloS one* 8 (2), e55642. doi:10.1371/journal.pone.0055642

Liu, L.-C., Wu, G., Wang, J.-N., and Wei, Y.-M. (2011). China's Carbon Emissions from Urban and Rural Households during 1992-2007. *J. Clean. Prod.* 19 (15), 1754–1762. doi:10.1016/j.jclepro.2011.06.011

Liu, X., Guo, P., Yue, X., Zhong, S., and Cao, X. (2021). Urban Transition in China: Examining the Coordination between Urbanization and the Eco-Environment Using a Multi-Model Evaluation Method. *Ecol. Indicators* 130, 108056. doi:10.1016/j.ecolind.2021.108056

Lyons, S., Pentecost, A., and Tol, R. S. J. (2012). Socioeconomic Distribution of Emissions and Resource Use in Ireland. *J. Environ. Manag.* 112, 186–198. doi:10.1016/j.jenvman.2012.07.019

Maliene, V., Howe, J., and Malys, N. (2008). Sustainable Communities: Affordable Housing and Socio-Economic Relations. *Local Economy* 23 (4), 267–276. doi:10.1080/02690940802407989

Marlon, J. R., Wang, X., Mildenberger, M., Bergquist, P., Swain, S., Hayhoe, K., et al. (2021). Hot Dry Days Increase Perceived Experience with Global Warming. *Glob. Environ. Change* 68, 102247. doi:10.1016/j.gloenvcha.2021.102247

Matthews, H. S., Hendrickson, C. T., and Weber, C. L. (2008). *The Importance of Carbon Footprint Estimation Boundaries*. ACS Publications.

Pachauri, S. (2004). An Analysis of Cross-Sectional Variations in Total Household Energy Requirements in India Using Micro Survey Data. *Energy policy* 32 (15), 1723–1735. doi:10.1016/s0301-4215(03)00162-9

Qin, C. J. P. X. Z. (2009). Impacts of Household Pattern on Carbon Emission [J]. *Chin. J. Popul. Sci.* 5.

Qu, J., Zeng, J., Li, Y., Wang, Q., Maraseni, T., Zhang, L., et al. (2013). Household Carbon Dioxide Emissions from Peasants and Herdsmen in Northwestern Arid-alpine Regions, China. *Energy Policy* 57, 133–140. doi:10.1016/j.enpol.2012.12.065

Rong, P., Zhang, L., Qin, Y., Xie, Z., and Li, Y. (2018). Spatial Differentiation of Daily Travel Carbon Emissions in Small- and Medium-Sized Cities: An Empirical Study in Kaifeng, China. *J. Clean. Prod.* 197, 1365–1373. doi:10.1016/j.jclepro.2018.06.205

Rong, P., Zhang, Y., Qin, Y., Liu, G., and Liu, R. (2020). Spatial Differentiation of Carbon Emissions from Residential Energy Consumption: A Case Study in Kaifeng, China. *J. Environ. Manage.* 271, 110895. doi:10.1016/j.jenvman.2020.110895

Roseland, M. (2012). *Toward Sustainable Communities: Solutions for Citizens and Their Governments*. New Society Publishers.

Sun, W., and Huang, C. (2020). How Does Urbanization Affect Carbon Emission Efficiency? Evidence from China. *J. Clean. Prod.* 272, 122828. doi:10.1016/j.jclepro.2020.122828

Tu, H., and Liu, C. (2014). *Calculation of CO2 Emission of Standard Coal*. Coal Qual. Technol. [Epub ahead of print].

Wang, C., Zhan, J., Li, Z., Zhang, F., and Zhang, Y. (2019). Structural Decomposition Analysis of Carbon Emissions from Residential Consumption in the Beijing-Tianjin-Hebei Region, China. *J. Clean. Prod.* 208, 1357–1364. doi:10.1016/j.jclepro.2018.09.257

Wang, C., Zhan, J., Zhang, F., Liu, W., and Twumasi-Ankrah, M. J. (2021). Analysis of Urban Carbon Balance Based on Land Use Dynamics in the Beijing-Tianjin-Hebei Region, China. *J. Clean. Prod.* 281, 125138. doi:10.1016/j.jclepro.2020.125138

Wang, Z., and Liu, W. (2015). Determinants of CO2 Emissions from Household Daily Travel in Beijing, China: Individual Travel Characteristic Perspectives. *Appl. Energ.* 158, 292–299. doi:10.1016/j.apenergy.2015.08.065

Wang, Z., and Yang, L. (2014). Indirect Carbon Emissions in Household Consumption: Evidence from the Urban and Rural Area in China. *J. Clean. Prod.* 78, 94–103. doi:10.1016/j.jclepro.2014.04.041

Weber, C. L., and Matthews, H. S. (2008). Quantifying the Global and Distributional Aspects of American Household Carbon Footprint. *Ecol. Econ.* 66 (2-3), 379–391. doi:10.1016/j.ecolecon.2007.09.021

Wei, Y.-M., Liu, L.-C., Fan, Y., and Wu, G. (2007). The Impact of Lifestyle on Energy Use and CO2 Emission: An Empirical Analysis of China's Residents. *Energy Policy* 35 (1), 247–257. doi:10.1016/j.enpol.2005.11.020

Wilson, J., Tyedmers, P., and Spinney, J. E. L. (2013). An Exploration of the Relationship between Socioeconomic and Well-Being Variables and Household Greenhouse Gas Emissions. *J. Ind. Ecol.* 17 (6), 880–891. doi:10.1111/jiec.12057

Xu, X., Tan, Y., Chen, S., Yang, G., and Su, W. (2015). Urban Household Carbon Emission and Contributing Factors in the Yangtze River Delta, China. *PLOS ONE* 10 (4), e0121604. doi:10.1371/journal.pone.0121604

Xue, Y. (2020). Empirical Research on Household Carbon Emissions Characteristics and Key Impact Factors in Mining Areas. *J. Clean. Prod.* 256, 120470. doi:10.1016/j.jclepro.2020.120470

Yang, J., and Chen, B. (2011). Using LMDI Method to Analyze the Change of Industrial CO2 Emission from Energy Use in Chongqing. *Front. Earth Sci.* 5 (1), 103–109. doi:10.1007/s11707-011-0172-3

Yang, Q., Liu, G., Hao, Y., Coscieme, L., Zhang, J., Jiang, N., et al. (2018). Quantitative Analysis of the Dynamic Changes of Ecological Security in the Provinces of China through Emergy-Ecological Footprint Hybrid Indicators. *J. Clean. Prod.* 184, 678–695. doi:10.1016/j.jclepro.2018.02.271

Yang, S., Wang, Y., Ao, W., Bai, Y., and Li, C. (2018). Prediction and Analysis of CO2 Emission in Chongqing for the protection of Environment and Public Health. *Ijerph* 15 (3), 530. doi:10.3390/ijerph15030530

Yang, T., and Liu, W. (2017). Inequality of Household Carbon Emissions and its Influencing Factors: Case Study of Urban China. *Habitat Int.* 70, 61–71. doi:10.1016/j.habitatint.2017.10.004

Yang, Z., Fan, Y., and Zheng, S. (2016). Determinants of Household Carbon Emissions: Pathway toward Eco-Community in Beijing. *Habitat Int.* 57, 175–186. doi:10.1016/j.habitatint.2016.07.010

Ye, H., Ren, Q., Hu, X., Lin, T., Xu, L., Li, X., et al. (2017). Low-carbon Behavior Approaches for Reducing Direct Carbon Emissions: Household Energy Use in a Coastal City. *J. Clean. Prod.* 141, 128–136. doi:10.1016/j.jclepro.2016.09.063

Yin, X., Hao, Y., Yang, Z., Zhang, L., Su, M., Cheng, Y., et al. (2020). Changing Carbon Footprint of Urban Household Consumption in Beijing: Insight from a Nested Input-Output Analysis. *J. Clean. Prod.* 258, 120698. doi:10.1016/j.jclepro.2020.120698

Zhang, H., Shi, X., Cheong, T. S., and Wang, K. (2020). Convergence of Carbon Emissions at the Household Level in China: a Distribution Dynamics Approach. *Energ. Econ.* 92, 104956. doi:10.1016/j.eneco.2020.104956

Zhang, J., Li, F., Sun, M., Sun, S., Wang, H., Zheng, P., et al. (2021). Household Consumption Characteristics and Energy-Related Carbon Emissions Estimation at the Community Scale: A Study of Zengcheng, China. *Clean. Responsible Consumption* 2, 100016. doi:10.1016/j.clrc.2021.100016

Zhang, R., and Hanaoka, T. (2021). Deployment of Electric Vehicles in China to Meet the Carbon Neutral Target by 2060: Provincial Disparities in Energy Systems, CO2 Emissions, and Cost Effectiveness. *Resour. Conservation Recycling* 170, 105622. doi:10.1016/j.resconrec.2021.105622

Zhang, X., Luo, L., and Skitmore, M. (2015). Household Carbon Emission Research: an Analytical Review of Measurement, Influencing Factors and Mitigation Prospects. *J. Clean. Prod.* 103, 873–883. doi:10.1016/j.jclepro.2015.04.024

Zhao, R. (2019). Carbon Emission Assessment of an Urban Community. *Appl. Ecol. Environ. Res.* 17 (6). doi:10.15666/aeer/1706_1367313684

Conflict of Interest: The authors declare that the research was conducted in the absence of any commercial or financial relationships that could be construed as a potential conflict of interest.

Publisher's Note: All claims expressed in this article are solely those of the authors and do not necessarily represent those of their affiliated organizations, or those of the publisher, the editors and the reviewers. Any product that may be evaluated in this article, or claim that may be made by its manufacturer, is not guaranteed or endorsed by the publisher.

frontiers | Frontiers in Environmental Science

ORIGINAL RESEARCH
published: 16 May 2022
doi: 10.3389/fenvs.2022.876414

How to Control Coastal Zone Through Spatial Planning? Taking the Construction of the Spatial Monitoring Index System of the Coastal Zone in China as an Example

Zelian Guo[1], Yecui Hu[1,2], Yuping Bai[1], Lei Yang[3] and Jieyong Wang[4]**

[1]School of Land Science and Technology, China University of Geosciences, Beijing, China, [2]Key Lab of Land Consolidation and Rehabilitation, Ministry of Natural Resources of the People's Republic of China, Beijing, China, [3]Land Consolidation and Rehabilitation Center, Ministry of Natural Resources of the People's Republic of China, Beijing, China, [4]Institute of Geographic Sciences and Natural Resources Research, Chinese Academy of Sciences, Beijing, China

OPEN ACCESS

Edited by:
Jinyan Zhan,
Beijing Normal University, China

Reviewed by:
Yanxu Liu,
Beijing Normal University, China
Guanghui Jiang,
Beijing Normal University, China
Chen Zeng,
Huazhong Agricultural University, China

***Correspondence:**
Yecui Hu
huyc@cugb.edu.cn
Jieyong Wang
wjy@igsnrr.ac.cn

Specialty section:
This article was submitted to Land Use Dynamics, a section of the journal Frontiers in Environmental Science

Received: *15 February 2022*
Accepted: *01 April 2022*
Published: *16 May 2022*

Citation:
Guo Z, Hu Y, Bai Y, Yang L and Wang J (2022) How to Control Coastal Zone Through Spatial Planning? Taking the Construction of the Spatial Monitoring Index System of the Coastal Zone in China as an Example. Front. Environ. Sci. 10:876414. doi: 10.3389/fenvs.2022.876414

Due to its fragile ecological environment and superior natural and location conditions, coastal areas are receiving extensive attention all over the world. Scientific space control is needed to ensure the harmonious development of the "human-land-ocean" system in this region. The monitoring index system is a crucial grasp of the national territory use control; it is also one of the main contents in the reform of China's planning system in the new era. Therefore, based on the strategic idea of land–sea overall management and the concept of "life community of human, mountains, rivers, forests, farmlands, lakes, grasslands, and ocean", this study puts forward three connotations of the index system of coastal spatial planning from the perspective of "function-structure-elements." Then, adopting the methods of "multiple planning integration" and expert consultation and using the research idea of "setting control objectives, contents, and indicators," an index system suitable for coastal space control is constructed. The results show that the index system puts forward 33 sub-indexes for coastal ecological space, living space, and production space and provides a basis for the high-quality development of coastal space through the restrictions and requirements on the total amount, bottom line, boundary, conversion, and quality of various spatial elements. This study can provide a basis for formulation, implementation, and later monitoring of coastal spatial planning and provide an index reference for the management of coastal areas in other countries in the world.

Keywords: coastal zone space use control, monitoring index system, land–sea overall management, multiple planning integration, China's coastal areas

INTRODUCTION

The coastal zone, located at the junction of land and sea ecosystems, is rich in natural resources. It has been the link of foreign exchange between countries for a long time because of its superior geographical location, which is of great strategic significance (Bax et al., 2021; Yan et al., 2021; Yu et al., 2021). In China, since the reform and opening up in 1978, coastal areas have attracted many people and capital, leading to rapid development of the region as China's valuable shoreline (Wang

et al., 2018). In 2018, coastal areas accounted for 12.93% of the national area, carrying 43.96% of the population and creating 53.47% of the GDP. However, like other countries around the world, there are a series of problems affecting sustainable development due to rapid urbanization and industrialization in this region (Alam et al., 2021; Smith et al., 2021). The problems of China's coastal zone are mainly reflected in the rough use of coastal zone production space resources and unreasonable industrial structure (Chen and Qian, 2020; Nie et al., 2021; Su and Liang, 2021), increased environmental pollution and impaired ecological functions in coastal zone eco-spaces (Lin and Yu, 2018; Zhao et al., 2021), and the lack of living space infrastructure in the coastal zone, leading to a poor level of living (Zhang et al., 2021).

The developed countries in the world have studied the coastal zone since the 1950s and made provisions on shoreline construction and coastal protection through coastal zone laws and regulations. In 1972, the United States promulgated the coastal zone management act, which was the world's first comprehensive coastal zone management regulation and marked the beginning of modern integrated coastal zone management (Humphrey et al., 2000). Since then, countries all over the world have carried out comprehensive management of coastal zones (Goodhead and Aygen, 2007; Batista et al., 2017; Yuan and Chang, 2021). The Netherlands attaches great importance to the functional connection of land and sea, so they implemented unified management of this area (Vanalphen, 1995). In 1998, South Korea formulated and implemented the National Coastal Management Plan, which covers the coastal waters and offshore land. Through the coastal zone survey conducted every 5 years, the problems realized in the implementation of the plan can be found in time (Lee, 1998). England introduced the East Inshore and Offshore Marine Plans in 2014, which proposes 11 goals and sets monitoring indicators for each goal. By calculating the completion rate of each index, the implementation effect of the plan is reviewed every 3 years (Guo, 2020). Japan divided the coastal zone into coastal preservation zone, general public coast, and other coastal zones and defined the management subject of each zone. Although many departments manage the coastal zone space, zoning can make the authority between departments and the spatial scope clear. It can be seen that the formulation and implementation of coastal zone spatial planning has become the focus of coastal zone management all over the world (Grafton et al., 2019). Reasonable land space use control of the coastal zone can promote the harmonious development of different functional spaces, which is an urgent problem to be solved in China at this stage.

Before 2018, the functions of China's coastal zone use control were administered by different departments, which issued multiple spatial control plans for different control objectives. These plans provide basic contents and valuable experience for the construction of coastal zone spatial planning. At the same time, they also had problems such as overlapping control contents and low management efficiency, which cannot control the coastal zone accurately. Although Guangdong, Shandong Province, and other regions have successively formulated coastal zone protection plans in recent years, relevant work was carried out before the establishment of the Ministry of Natural Resources. Therefore, in terms of specific management actions and decisions, they cannot play a supporting role in coastal zone spatial planning. In 2013, the concept of "life community of mountains, rivers, forests, farmlands, lakes, and grasslands" was put forward in China, which emphasizes the natural law within the life community and shows that all elements are generally connected and interact with each other. In this case, it is urgent for a department to be responsible for the control of all space uses within the territory and carry out unified protection and systematic management of mountains, rivers, forests, farmlands, lakes, and grasslands. In 2018, China established the Ministry of Natural Resources and the Department of Territorial Space Use Control. Later, the government issued a document entitled "several opinions on establishing a territory planning system and supervising its implementation." It is pointed out that in the future, China will implement territorial use control on all land space zoning and classify it based on territorial space planning. This study marks the full development of the construction of China's territory planning system and shows that the use control in the new era emphasizes the control of land and sea, all elements of natural resources, and all types of land use.

In the context of the reform of the space control system, an important task in coastal areas is to formulate coastal zone planning. As the only special plan involving the sea, this spatial planning needs to get rid of the ideal of land and sea respective control and promote the realization of land and sea overall planning. Therefore, we should not only consider the relationship between land and sea and combine it with land spatial planning but also meet the administrative requirements of the marine coastal zone so as to balance and integrate the information from multiple stakeholders of land and sea. Coastal zone planning involves different aspects of the "human-land-ocean" system, and the concept of "life community of mountains, rivers, forests, farmlands, lakes, and grasslands" has been most fully reflected in this region. The contents of control include coastline management and control and ecological restoration, fishery space supply and management, coastal zone industrial parks and marine economy, marine disaster prevention, special management and control of rivers entering the sea, improvement of coastal human settlements, etc. It has great strategic significance for coastal areas and national development.

Execution is the source of vitality of spatial planning. As an important basis for spatial planning management and implementation evaluation, the index system is the quantitative embodiment of the core ideas and key tasks of planning (Zhou et al., 2018; Gun et al., 2020) and is considered to be the transmission tool with the best execution effect (Li et al., 2019). If operational monitoring indicators cannot be found, the spatial planning of land and sea is bound to stay at the theoretical level. Therefore, under the background of compiling the special plan of the coastal zone area, it is urgent to build a set of scientific control index systems to provide supervision and guarantee for the implementation of control in this area.

Based on the elements of the life community contained in the coastal zone and from the perspective of system theory, this study

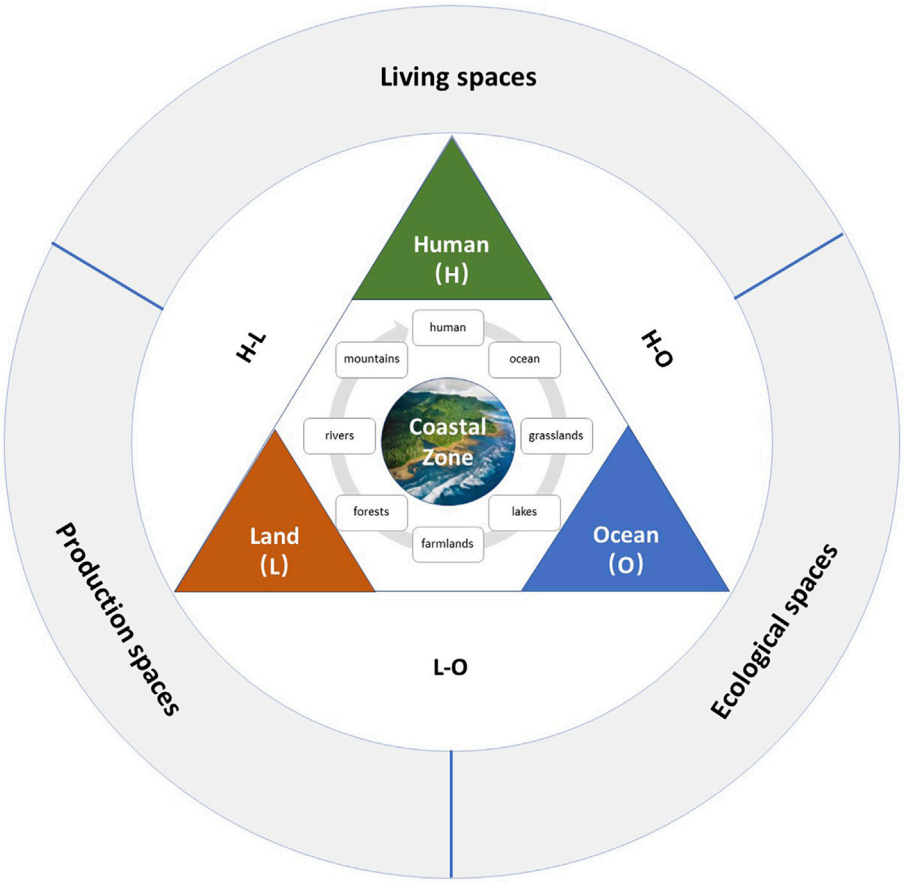

FIGURE 1 | Theoretical basis of the index system construction.

aims to design a set of index systems that can not only serve the reasonable protection and utilization of single elements but also reasonably control the structure and relationship between elements. The government can monitor the spatial utilization of the coastal zone effectively; understand the impact of land space utilization on the society, economy, and ecology of the region; and correct the unreasonable utilization direction timely, improving the implementation effect of coastal zone spatial planning. The research results can serve the use control of China's coastal zone; provide the basis for the formulation, implementation, and later monitoring of coastal zone land spatial planning; and provide index reference for the management of coastal zone areas in other countries in the world.

THEORETICAL FRAMEWORKS

Theoretical Basis

The coastal zone space is a huge and complex life system. The concept of "human-land-ocean" composite system and "life community of mountains, rivers, forests, farmlands, lakes, and grasslands" are fully reflected in this area. 1) In 2003, "land–ocean interactions in the coastal zone" (LOICZ) were listed as the core program of the International Geosphere Biosphere Program (IGBP) and the national human dimension of global environmental change (IHDP) (LOICZ working document, 2003). Studies have shown that the impact of human activities on the global environment is more intense than natural changes (Linton and Warner, 2003; Bullimore, 2014). Therefore, the second stage of LOICZ takes human activities and their impact on land–sea interaction as a new central theme. In densely populated coastal areas, the classical L–O interaction framework is replaced by the L–O–H interaction framework (**Figure 1**) to reflect the great impact of human activities on land and sea systems. Among them, the L–O–H interaction includes the H–L interaction reflecting the relationship between man and earth, H–O interaction reflecting the relationship between man and sea, and L–O interaction reflecting the relationship between land and sea (Xu et al., 2016). These three relationships converge in coastal areas to build a complex system. 2) Similarly, China has also proposed the concept of "life community of mountains, rivers, forests, farmlands, lakes, and grasslands" in 2013. This concept fully absorbs the ideas of sustainable development theory and ecosystem management theory, discusses the natural law in the community of life, provides an important theoretical basis

for the overall cognition of nature and the treatment of the relationship between man and ecological environment, and has become an important methodology for promoting the construction of ecological civilization in China at present and in the future. Combined with the characteristics of coastal areas, this study extends the concept to "human, mountains, rivers, forests, farmlands, lakes, grasslands, and ocean life community" and uses this idea to guide the construction process of the index system.

Based on the aforementioned ideas, the coastal zone space is a huge and complex life system, so it conforms to the theoretical logic of "function-structure-element". Among them, elements such as human, sea, and land (including mountains, rivers, forests, farmlands, lakes, and grasslands) are not only the basic constituent unit of the system but also the basis and carrier of the system. There are certain connections between the elements. The interrelated elements form the system according to a certain structure. The change of elements and structure will cause the change of system function, indicating that both elements and structure serve functional purpose. Conversely, at the beginning of the formation of the structure, it is necessary to clarify the functional objectives of the system so as to adopt the corresponding structure and control the elements. Therefore, based on these ideas, this study starts to construct the index system.

Connotation of the Index System

To build the index system, we first need to clarify the object of coastal zone use control, that is, the territorial space of the coastal zone so that the index system can be clearly implemented. A territorial space is a cross complex integrating entity space, function space, and management space (Yue and Wang, 2019). According to the theoretical viewpoint of "function-structure-element" in system theory, it can be seen that function space is the fundamental object of territorial space use control, and the structure comprising system elements is the basis of system function realization.

From the perspective of function, space utilization can be divided into three categories: production space, living space, and ecological space. Among them, production space is an area that provides industrial products, agricultural products, and service products, which pursues intensive land use and efficient output. Living space is an area that provides human living, consumption, leisure, and entertainment and pursues the convenience of service and livability. Ecological space is an area that provides ecological products and services. It plays an important role in regulating, maintaining, and ensuring regional ecological security and pursues the good development of ecological environment. The policy points out that by 2035, China should "basically form a space pattern with intensive and efficient production space, livable and appropriate living space, and beautiful ecological space", which is the strategic goal of the Chinese government in the territorial space use control at the present stage and also the ultimate goal of the index system of this study. The policy objectives determine the key direction of the monitoring system. Therefore, this study divides the index system into three subsystems: ecological space, living space, and production space, also known as "ecological–production–living space" (Cui et al., 2018).

From the perspective of elements, territory use is reflected in more specific land/sea use types that constitute the ecological–production–living space, that is, the space utilization types of mountains, rivers, forests, farmlands, lakes, grasslands, seas, and cities in the concept of life community. Separately, the ecological space comprises forest land, grassland, wetland, and other ecological elements; production space consists of various spatial elements used in agriculture, fishery, industry, service industry, and other industries; living space comprises spatial elements closely related to human life. These specific land/sea use categories occupy a certain area in space and are staggered, showing a specific spatial structure, and there will be conversion among the elements. Generally, the ecological element types are often occupied by the element types of the other two spaces because the benefits cannot be directly expressed. Cultivated land in the production space is also an element type that is easy to be occupied. These phenomena will lead to the transformation of the internal structure of ecological–production–living space and affect the harmony of its functions, so the specific spatial elements that are in a weak position are often strictly protected. Therefore, this study infers from the theory of "element structure function", and it holds that in order to achieve the functional goal of "production, ecology, and living space", we need to refine from two major elements: element and structure.

MATERIALS AND METHODS

Research Area

The coastal zone is a strip area with a certain width extending from the coastline to both sides of the land and sea, and the scope of it has not been uniformly defined so far. The Millennium Ecosystem Assessment Project points out that the coastal zone is "the interface between the ocean and the land, extends to the middle of the continental shelf, and includes all areas affected by marine factors in the continental direction (Millennium Ecosystem Assessment, 2005). LOICZ defines the coastal zone as extending from 200 m land elevation to 200 m isobath (LOICZ working document, 2003). Alves et al. (2013) hold the view that the coastal zone takes the high tide line as the center, extends 2 km to the land area, and then extends to the sea area to the territorial sea boundary (the territorial sea baseline extends 12 nautical miles to the sea). However, Awosika and Marone (2000) and Glavovic et al. (2015) considered that the extension of the coastal zone to the sea side should reach the boundary line of the exclusive economic zone (the baseline of the territorial sea extends 200 nautical miles to the sea). At present, the view from the Environmental Council of the Organization for International Economic Cooperation and Development (OECD) is widely accepted internationally. It proposes that the definition and scope of the coastal zone need to be changed according to the problems dealt with and the objectives of management. In China, the national conditions with prominent contradiction between human and territorial

Name of spatial planning	Planning positioning	Control objectives	Index system
Major Function Oriented Zoning planning	Strategic, basic and restrictive planning of China's national land space development	• Clear development pattern • Optimize spatial structure • Improve space efficiency • Promoting regional coordination • Enhance sustainable development capacity	(1) development intensity; (2) the amount of national arable land reserved; (3) urban space area; (4) rural residential area; (5) forest land tenure; (6) forest coverage
Marine Major Function Oriented Zoning planning	Basic and restrictive planning of marine space development	• Optimizing the pattern of Marine Spatial Development • Improve the efficiency of marine space utilization • Strengthen the construction of marine ecological civilization	(1) marine development intensity; (2) retention rate of continental natural coastline; (3) proportion of prohibited development areas in the area of sea areas under management; (4) proportion of excellent water quality (class I & II) in coastal water; (5) proportion of marine protected areas in the managed sea area
Territorial planning	It is a strategic, comprehensive and basic plan to make overall arrangements for the development, protection and renovation of land space	• Optimize development pattern • Promoting regional coordination • Safeguard Homeland Security • Building a maritime power • Enhancing sustainable development capacity	(1) the amount of national arable land reserved; (2) total water consumption; (3) national Land development intensity; (4) proportion of excellent water quality in seven major river basins in China; (5) water quality compliance rate of key rivers and lakes water functional areas; (6) forest coverage; (7) grassland comprehensive vegetation coverage; (8) wetland area; (9) urban space area; (10) the density of highway and railway network; (11) newly increased water and soil loss control area
land use master planning	A programmatic document for the implementation of the strictest land management system	• Strictly protect cultivated land • Economical and intensive land use	(1) the amount of national arable land reserved; (2) protected area of basic farmland; (3) the scale of urban and rural construction land; (4) the scale of arable land occupied by new construction; (5) per capita area of urban industrial and mining land; (6) the scale of supplement arable land through consolidation, reclamation and development; (7) the total scale of construction land; (8) the scale of urban industrial and mining land; (9) the scale of new construction land; (10) the scale of agricultural land occupied by new construction
The urban planning (Shanghai)	Basis for urban construction and management	• people oriented • Optimize layout • Ecological Civilization • Cultural inheritance • Classification guidance	(1) the total scale of construction land; (2) the amount of national arable land reserved; (3) the area of permanent basic farmland protection; (4) the area of construction land used of per unit of GDP; (5) community public service facilities can reach the coverage rate within 15 minutes' walk; (6) more than 400 square meters of green space, square and other public development space can reach the coverage rate within 5 minutes' walk; (7) the area of historical and cultural area; (8) the density of road network; (9) water surface ratio of rivers and lakes; (10) per capita park green space area; (11) forest coverage; (12) compliance rate of water functional area; (13) per capita refuge area of emergency shelter
marine functional zoning	Integrated, basic and binding documents for China's marine space development, control and comprehensive management	• Protection of the marine environment • Maintain fishery sea • Controlling marine development	(1) proportion of marine protected areas; (2) proportion of offshore marine protected areas; (3) the area of sea functional area for mariculture; (4) reclamation scale for construction; (5) proportion of reserves in coastal waters; (6) retention rate of continental natural coastline; (7) length of coastline to be renovated
marine ecological environment protection planning	Guiding planning of the marine sector	• Protect and improve the quality of ecological environment	(1) the proportion of rivers entering the sea eliminate inferior class V water bodies; (2) length of coastal zone remediation; (3) coastal wetland restoration area; (4) the proportion of marine protected areas in the area under jurisdiction; (5) area proportion of marine ecological red line area; (6) artificial ecosystem of rare and endangered species; (7) natural shoreline retention rate; (8) wetland area
ecological environment protection planning	Guide strategic arrangements in the field of ecological and environmental protection	• Protect and improve the quality of ecological environment	(1) Proportion of excellent water quality (class I & II) in coastal waters; (2) forest coverage; (3) forest volume; (4) wetland area; (5) grassland comprehensive vegetation coverage; (6) protection rate of key wildlife species; (7) natural shoreline retention rate; (8) newly increased desertification land control area; (9) newly increased water and soil loss control area
grassland protection, construction and utilization planning	Overall planning to guide the protection and construction of grassland in China	• Developing grassland industry • Protecting grassland ecology	(1) accumulated grassland fence area; (2) improved grassland area; (3) artificial grass planting area; (4) area of newly built Grassland Nature Reserve; (5) accumulative control of the "three modernizations" grassland area; (6) rate of grazing prohibition, rest grazing and rotational grazing on available grassland
fishery planning	Guiding documents for fishery development	• Developing fishery economy • Guarantee product supply • Maintain resource security	(1) fishery output value; (2) added value of fishery; (3) proportion of output value of fishery secondary and tertiary industries; (4) domestic marine fishing output; (5) mariculture area; (6) national aquatic germplasm resources protection zone; (7) number of aquatic biological nature reserves above the provincial level
forest land protection and utilization plan	Guiding document for national forest land protection and utilization	• Comprehensive protection of forest land • Rational utilization of forest land	(1) forest tenure; (2) quota of forest land requisition and occupation; (3) forest land tenure; (4) forest productivity; (5) proportion of key public welfare forest land; (6) key commodity forest land ratio
wetland protection plan	Guiding documents for wetland protection	• Expand wetland area • Enhance wetland function • Protect wetland ecology	(1) wetland area; (2) natural wetland retention rate; (3) number of new wetland nature reserves; (4) wetland protection rate; (5) protection rate of key wildlife species; (6) restoration of various degraded wetland areas
port planning	An important basis for guiding port construction management and effective utilization of port resources	• Enhance industrial functions • Improve port layout	(1) port throughput; (2) length of port shoreline; (3) length of wharf and port industrial shoreline; (4) length of deep water shoreline

FIGURE 2 | China's existing spatial planning index system.

space determine that the scope of coastal zone use control cannot be too broad but needs fine management. Considering China's administrative system and population density, it is practical to take the township scale as the basic unit for the control of the coastal zone. Townships are widely distributed in the coastal zone, which is not only conducive to scientific research of the researchers but also convenient for managers to make overall arrangements and take action (Wen and Liu, 2019). For example, the Regulations on the Administration of Coastal Zone Protection and Utilization implemented in 2018 in Fujian Province states that the coastal zone refers to the intersection zone between the sea and the land, including the coastal land extending to the areas within the administrative divisions of the township and the nearshore sea extending to the baseline of the territorial sea. For the convenience of management, the coastal zone in this study also follows this scope.

Research Data

In the process of territorial space use control in China, many departments have issued spatial plans for different control objectives. These plans are important means of national space governance and space policy tools for effectively regulating social, economic, and environmental factors. At present, China's spatial planning system is a complex "planning matrix" comprising multi-type and multilevel spatial planning, mainly including major function-oriented zoning planning (including ocean) issued by the Development and Reform Commission; territorial planning and land use master planning issued by the Ministry of Land and Resources; urban planning issued by the Ministry of Housing and Urban–Rural Department; marine functional zoning and marine ecological environment protection planning issued by State Oceanic Administration; ecological environment protection planning issued by the Ministry of Environmental Protection; grassland protection, construction, and utilization planning and fishery planning issued by the Ministry of Agriculture; forest land protection and utilization planning and wetland protection planning issued by the State Forestry Administration; and special plans such as port planning issued by the Ministry of Transport. On the basis of these plans, a network space planning system of "horizontal juxtaposition and vertical to the end" has been formed (Liu and Wang, 2016). These plans have played a vital role in each stage of national land use control in China, and their index system provides a reference for the construction of the coastal spatial planning index system. **Figure 2** shows the planning orientation, control objectives, and core indicators of China's spatial planning. These are also the realistic basis and data source for "multiple planning integration" to build the coastal zone spatial planning index system.

Due to the differences of regulation subjects, value orientation, and regulation objectives, there are two principal problems in China's existing spatial planning index system (**Figure 2**). First, there are overlapping control contents among different plans. For example, for the control of arable land, the indicator of "the Amount of Cultivated Land Reserved" is set in the major function-oriented zoning planning, territorial planning, land use master planning, and urban planning; for the control of forest land, the indicator of "forest coverage" is set in the major function-oriented zoning planning, territorial planning, and ecological environment protection planning; for grassland control, territorial planning and ecological environment protection planning have set the indicator of "grassland comprehensive vegetation coverage" and so on. Second, there are different values of the same index. For example, for the index of "the amount of national arable land reserved", the land use master plan (2006–2020) stipulates that it will reach 120.33 million hectares by 2020, while the national land planning outline (2016–2030) requires this value to be 124.33 million hectares. This situation can not only show the importance of the index, but it also leads to management contradictions and reduces control efficiency. Meanwhile, there are control gaps in these planning index systems. For example, these spatial planning index systems rarely involve controlling coastal living space and tourism land. For the spatial control gap, we should deeply understand its control connotation and determine the corresponding control indicators.

Research Methods

Based on the theoretical basis and connotation of coastal zone territorial spatial control, this study constructs the coastal zone spatial planning index system according to the path of "setting control objectives, setting control contents, and then setting control indicators" (**Figure 3**).

First, this study needs to determine the goal of the coastal zone monitoring index system, that is, to serve the high-quality development of the coastal zone. Second, starting from the territorial space function undertaken by ecological–production–living space, this study explores the classification system and its elements of ecological–production–living spaces in the coastal zone, and it constitutes the control content of the index system together with the structure of ecological–production–living spaces.

Among them, in order to realize the function of ecological-production-living spaces, the main control of elements is their total amount, bottom line, and quality; for the structure, it is to control the boundaries of different elements and the conversion between them. 1) Boundary is the spatial relationship between territorial space elements. It is divided according to different purposes to ensure that development, utilization, and protection activities can only be carried out in a specific space. 2) Conversion represents the dynamic conversion process between different territorial space types. Abandoning the previous concept of focusing only on the conversion of agricultural land use, we need to pay attention to the mutual conversion within the "mountains, rivers, forests, farmlands, lakes, grasslands, and sea" life community at this stage. 3) The total quantity is the control of the quantity state of specific elements and the expected target value. 4) The bottom line is the minimum standard and minimum defense line that must be maintained for land types with an important protection value. Breaking this standard will affect the country's food security or ecological security and cause irreparable losses. 5) Quality is a kind of index that reflects the environmental quality, the quality of people's life, and socioeconomics in the coastal space. The purpose is to evaluate the impact caused by the implementation of the index.

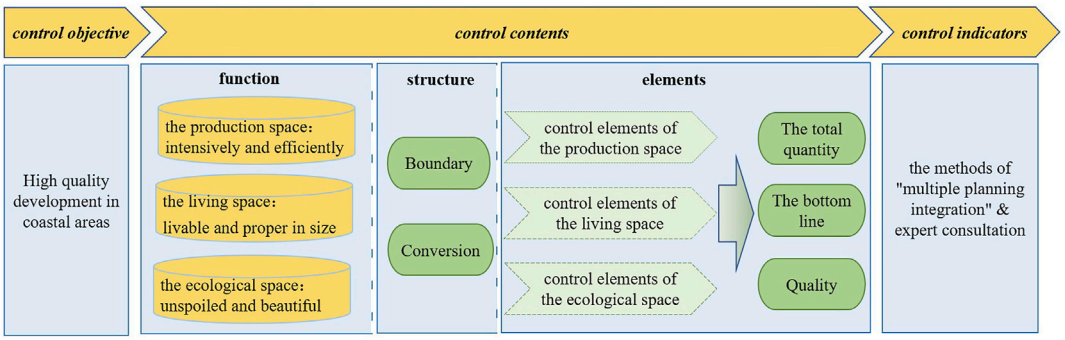

FIGURE 3 | Construction idea of the coastal zone spatial control index system.

Finally, combined with the existing "multiplanning" index system in China, this study supplements the content of the control gap, determines the core indicators applicable to ecological–production–living spaces, and then constructs the coastal zone spatial control index system to serve the high-quality development of the coastal zone space.

Multiple Planning Integration

Due to the overlapping and other contradictions in the index system of multiple departments, the National Development and Reform Commission, the Ministry of Land and Resources, the Ministry of Environmental Protection, and the Ministry of Housing and Urban–Rural Development of China jointly proposed to carry out the pilot work of "multiregulation integration" throughout the country in 2014. Since then, under the leadership of the government, all sectors of society have begun to explore "multi-compliance and integration", with the purpose of absorbing the core points of various plans, coordinating the conflicts between plans, and building a unified land and space planning to allocate space resources more effectively.

As the coastal zone involves land–sea space, the life community of "landscape, forest, field, lake, grass, and sea" is fully reflected here. Generally, this area is regarded as the "main battlefield" to realize the land–sea overall management and "multiregulation integration". At present, Chinese scholars have practiced the construction of a terrestrial multi-compliance index system (Bai and Tian, 2016; Wu et al., 2018); some scholars also explore the integration of marine spatial planning into a land-based multiplanning system (An et al., 2019; Yue et al., 2019), and they also developed and constructed the overall framework of comprehensive coastal zone planning (Jiang et al., 2018). However, the research on monitoring indicators of coastal space use control is still blank. Therefore, based on the existing spatial planning index system, this study constructs the spatial monitoring index system of land and sea overall management (**Figure 4**).

Expert Consultation

After analyzing the "multiple planning" index system, this study first screened the key indexes according to the index selection principle and obtained the preliminary scheme of the "multiple planning" index database, including 55 basic indexes. In order to further screen the key indicators that play a practical role in coastal zone space control, this study further carries out expert consultation. In total, 12 experts from institutions of universities, local natural resource departments, enterprises in coastal areas, and other units were invited to determine the priority of monitoring indicators by understanding the stakeholders' cognition of coastal zone use control, and it supplements the key contents in urgent need of supervision in the actual development of coastal zone areas through consultation.

RESEARCH RESULTS

Classification of "Production–Living–Ecological Spaces" in the Coastal Zone

Considering the overall structure and constituent elements of production–living–ecological spaces, the control content can cover all elements of the coastal zone. Chinese scholars have made many useful explorations on the classification of it (Huang et al., 2017; Liu et al., 2017; Cui et al., 2018; Huang et al., 2020). Referring to the research of Hu et al. (2020) and Zou et al. (2018), this study comprehensively classifies production–living–ecological spaces in the coastal zone involving 16 key-controlled land types (**Table 1**).

Among them, the coastal production space is related to the industrial structure. It is an area with the leading function of providing industrial products, agricultural products, and service products, mainly including agricultural land, land for forestry, land for animal husbandry, sea for fishery production, industrial and mining land, and land for transportation. The coastal living space is related to carrying and ensuring human settlement. It is an area with the leading function of providing human residence, consumption, leisure, and entertainment, and it mainly includes land for urban construction, land for tourism and entertainment, and land for special purpose. The coastal ecological space is an area providing ecological products and ecological services, mainly including ecological land of prohibited construction, ecological

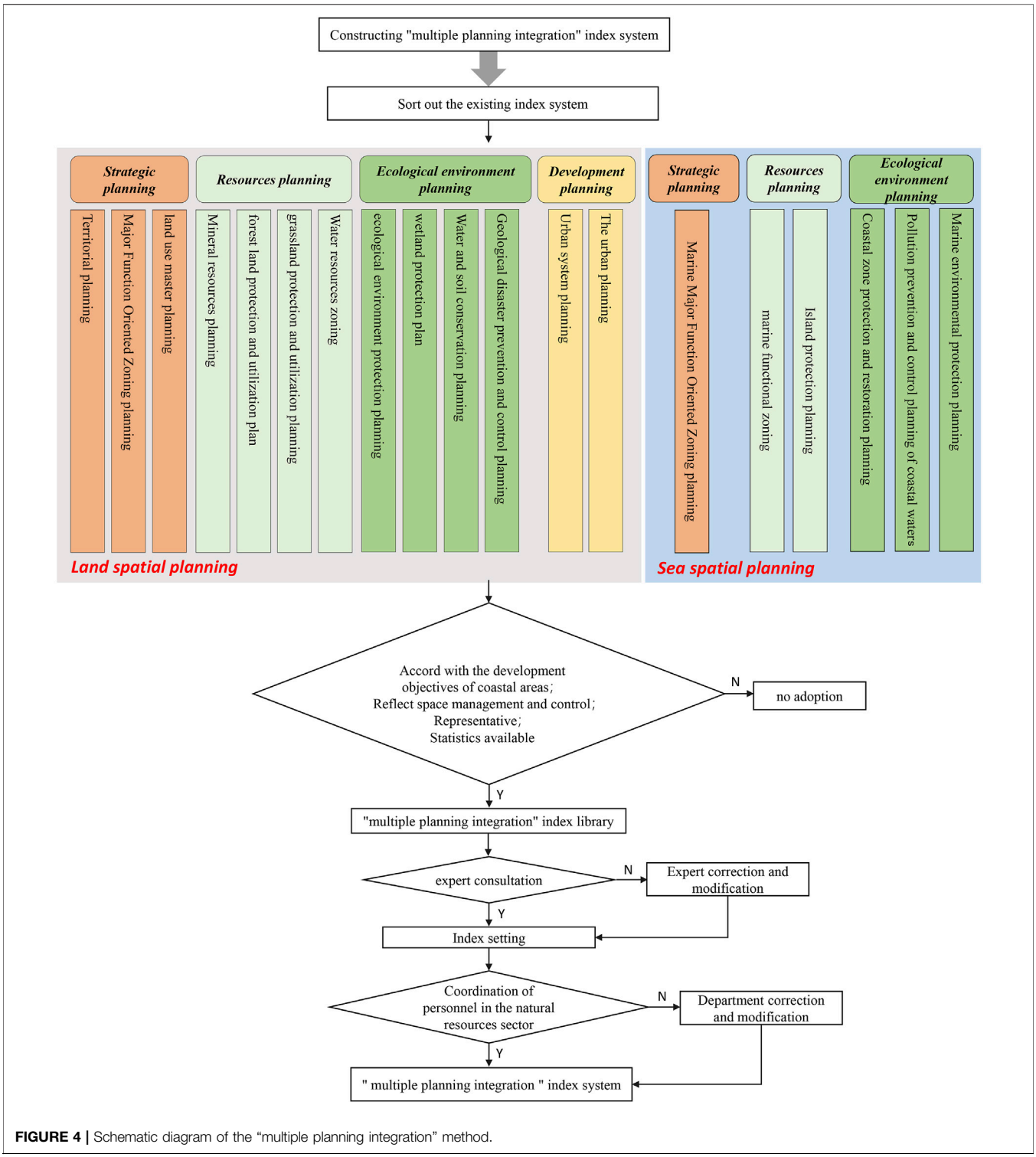

FIGURE 4 | Schematic diagram of the "multiple planning integration" method.

land allowed for moderate construction, and ecological land of nurturing protective.

Establishment of the Index Database

The indicators of the existing spatial planning are connected with the core management land-sea types of production-living-ecological spaces, and a coastal zone control index database is built, as shown in **Figure 5**.

It can be found that the control content of the existing spatial planning index system can cover all land–sea types of national land space. The index system of the Development and Reform Commission, the Ministry of Land and Resources, the Ministry of

TABLE 1 | Classification of "production-living-ecological spaces" in the coastal zone and its controlled land types.

Space types		Spatial classification and interpretation	Land-sea use type
Coastal production space	Agricultural land	It refers to the land used for the cultivation of agricultural products such as grain, fruit, tea, and rubber and its supporting or ancillary land	Arable land
	Land for forestry	It refers to timber forest, economic forest, bamboo forest land, slash land, and nursery that can be used for wood forest supply	Forest land
	Land for animal husbandry	It refers to the land used for livestock, animal husbandry, and other breeding	Grassland
	Sea for fishery production	It refers to the water area used for fishery production or service fishery production	Sea for fishery
	Industrial and mining land	It refers to the land for the supply of industrial products and commercial services and the production land for mining, quarrying, sand quarries, salt fields, brick kilns, and tailing stacking outside cities and towns	Industrial and mining land
	Land for transportation	It refers to the land used for transportation lines and stations outside towns and villages	Traffic land
Coastal living space	Land for urban construction	It refers to urban land, rural residential areas, commercial service construction, and other land	Urban and rural construction land
	Land for urban construction		
	Land for tourism and entertainment	It refers to the land used to meet the daily leisure and entertainment needs of residents	Tourism land
	Land for special-purpose	It refers to the land outside cities and towns for military facilities, infrastructure, waste disposal space, etc.	Land for infrastructure
Coastal ecological space	Ecological land of prohibited construction	It refers to the land that is indispensable for maintaining ecological security and prohibits any commercial development activities	Ecological land for water and soil resources protection
			Ecological land for species diversity protection
	Ecological land allowed for moderate construction	It refers to the land that mainly plays ecological functions and allows human beings to make appropriate or conditional use of it	Controlled land of coastal wetland
			Controlled land of natural shoreline
			Controlled land of sand source
			Controlled land of estuarine
	Ecological land of nurturing protective	It not only refers to the land with degraded ecological function but plays an important role in maintaining regional ecological balance	Land of ecological restoration

Housing and Urban-Rural Department, and the State Oceanic Administration can fully cover production–living–ecological spaces which are the four main departments of national land spatial use control in China's coastal zone.

Results of the Coastal Zone Monitoring Index System

The indexes with high frequency and key control effects in the index library were preliminarily screened and then 20 key spatial types of indexes were determined through expert consultation. In addition, 13 key indicators are supplemented according to expert opinions. The coastal zone monitoring index system includes 33 monitoring indicators, as shown in **Table 2**.

1) Index system of production space in the coastal zone: ensures the total quantity of resources and the efficiency of production land.

In order to maintain China's food security and ensure a controllable scale and quality of cultivated land, "the amount of arable land reserved" and "protected area of basic farmland" are proposed. In order to ensure the sustainable development of forestry, animal husbandry, fishery, and mining, indicators such as "forest coverage," "forest productivity," "grassland comprehensive vegetation coverage," "area of sea functional area for mariculture," and "per capita area of urban industrial and mining land" are set respectively. For the traffic land, two indicators of "the density of highway and railway network" and "the length of port shoreline" are set to ensure the regional traffic convenience of the coastal zone and promote the development of the industrial economy.

2) Index system of living space in the coastal zone: ensuring human security and people's happiness.

For land for urban construction, the area and structure of urban and village space should be reasonably arranged, and the occupation of cultivated land and ecological land by new construction should be strictly limited; we set the indicators of "scale of urban and rural construction land," "scale of arable land occupied by new construction," and "scale of reclamation for construction land." Tourism and entertainment space focuses on enhancing tourist experience and maintaining the scenic spot environment. This study combines scholars' research on tourism (Liang and Ding, 2002; Zhang and Tan, 2002; Papageorgiou, 2016; Yang et al., 2021), constructed "length of hydrophilic shoreline," and "construction rate of tourism service facilities" to improve the convenience and quality of coastal tourism activities. Special living land mainly refers to the control of infrastructure land (including waste disposal and another related land). Its control connotation is to ensure residential safety and environmental friendliness of the coastal zone. This study inherits the index of "per capita refuge area of emergency shelter" and supplements the three indexes of "construction level of flood discharge and drainage

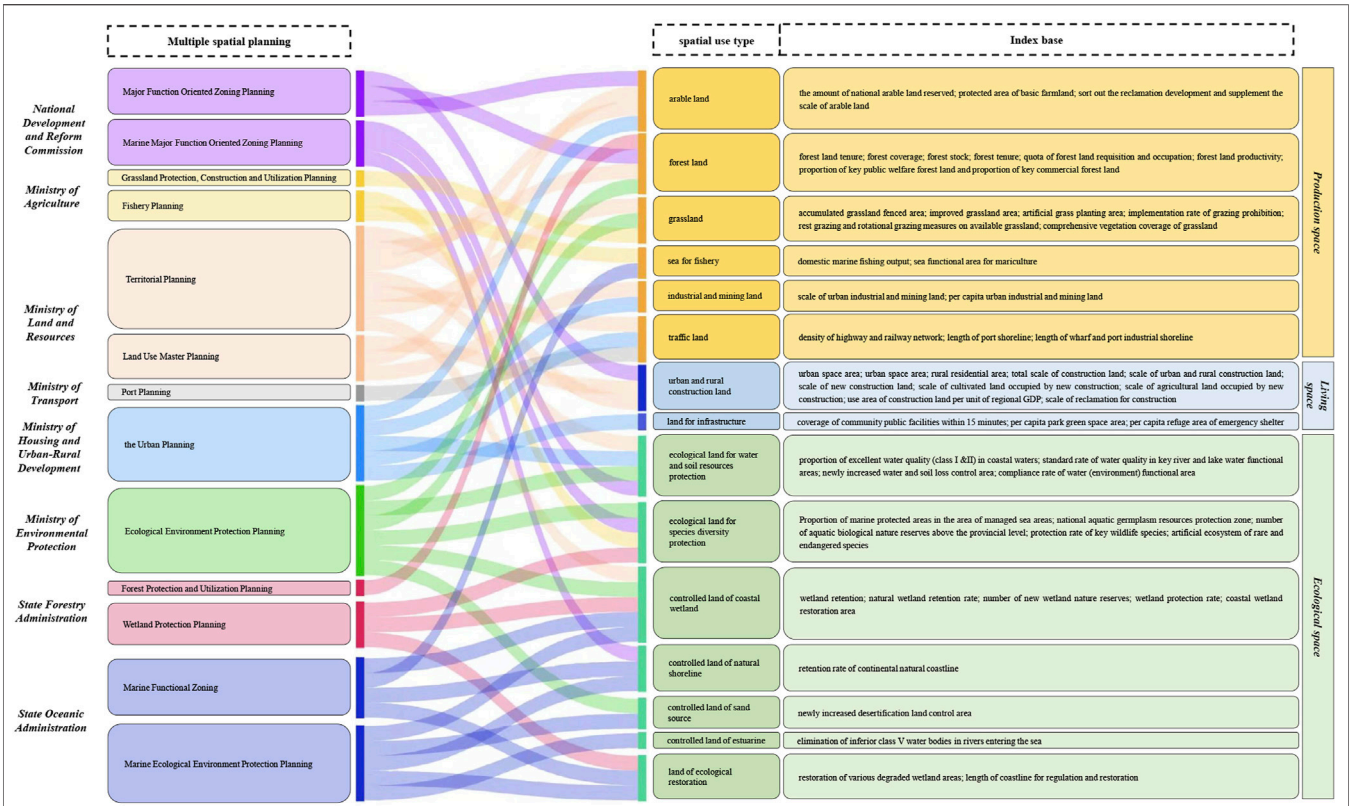

FIGURE 5 | The index system of spatial planning is connected with production-living-ecological spaces. Notes for **Figure 5**: (1) we use different colors to represent the government departments of spatial planning in the column of "multiple spatial planning"; (2) three colors are used to distinguish the "production, ecology, and living space" and its elements on the right side; (3) the lines indicates the flow direction of the existing spatial planning index system.

facilities," "treatment rate of domestic sewage," and "armless treatment rate of domestic waste," in order to maintain the residential safety of the coastal zone and strictly control the treatment of urban waste.

3) Index system of ecological spatial in the coastal zone: maintaining coastal zone ecological security.

Prohibited ecological land refers to the land that is indispensable to maintaining ecological security and prohibited from any commercial development activities. This study inherits the indicators of "newly increased water and soil loss control area," "proportion of excellent water quality (class I and II) in coastal waters," and "protection rate of key wildlife species" in the index database, focusing on the strict protection of species resources in water and soil ecologically fragile areas and coastal zones. Controlled ecological land refers to the land that mainly plays ecological functions and allows humans to make appropriate or conditional use. This study inherits the index of "wetland retention area" in the index library. At the same time, due to the importance of mangroves for maintaining the coastal wetland ecosystem, the index of "mangrove area" is supplemented. In addition, this study adopts three indexes in the index library, such as "natural shoreline retention rate," "newly increased desertification land control area," and "elimination of inferior class V water bodies in rivers entering the sea," in order to control the spatial types of natural shoreline, sand source, and estuary. Ecological conservation land refers to the land with degraded natural ecological functions but plays a key role in maintaining regional ecological balance. For the ecological restoration of the coastal zone, the existing spatial planning often uses the index of "length of remediation and restoration of the coastal zone". Since the coastal zone area involves a range of space from the coastline to the sea and land, this index is adjusted to "remediation of the coastal zone area" to monitor the ecological restoration of land. By improving the stability and resilience of ecological patches, the purpose of unspoiled and beautiful in ecological space can be achieved.

The report's "several opinions on establishing and supervising the implementation of the national land spatial planning system" clearly points out that it is necessary to "scientifically and orderly coordinate the layout of ecological, agricultural, urban, and other functional spaces; delimit the spatial control boundaries such as ecological protection red line, permanent basic farmland, and urban development boundary; and various sea area protection lines, in order to strengthen the bottom-line constraints". Therefore, based on the index base with factor control as the core, this study supplements the indicators related to the regional control boundary of production–living–ecological spaces, and the

TABLE 2 | Construction results of the coastal zone spatial planning monitoring index system.

Control objectives	Control elements	Order number	Monitoring indicators	Indicator attribute	Indicator source
The production space: intensively and efficiently	—	1	Development intensity of production space (%)	Total quantity	Add
		2	Area of permanent basic farmland boundary (km^2)	Boundary	Add
	Arable land	3	The amount of arable land reserved (million ha)	Bottom line	Index database
		4	Protected area of basic farmland (million ha)	Bottom line	Index database
	Forest land	5	Forest coverage (%)	Bottom line	Index database
		6	Forest productivity (m^3/ha)	Total quantity	Index database
	Grassland	7	Grassland comprehensive vegetation coverage (%)	Total quantity	Index database
	Sea for fishery	8	Area of sea functional area for mariculture (million ha)	Bottom line	Index database
	Industrial and mining land	9	Per capita area of urban industrial and mining land (million ha)	Quality	Index database
	Traffic land	10	The density of highway and railway network (%)	Quality	Index database
		11	The length of port shoreline (km)	Total quantity	Index database
The living space: livable and proper in size	—	12	Development intensity of living space (%)	Quality	Add
		13	Area of urban development boundary (km^2)	Boundary	Add
	Urban and rural construction land	14	Scale of urban and rural construction land (million ha)	Total quantity	Index database
		15	The scale of arable land occupied by new construction (million ha)	Conversion	Index database
		16	Scale of reclamation for construction land (million ha)	Conversion	Index database
	Tourism land	17	Length of hydrophilic shoreline (km)	Quality	Add
		18	Construction rate of tourism service facilities (%)	Quality	Add
	Land for infrastructure	19	Treatment rate of domestic sewage (%)	Quality	Add
		20	Harmless treatment rate of domestic waste (%)	Quality	Add
		21	Construction level of flood discharge and drainage facilities	Quality	Add
		22	Per capita refuge area of emergency shelter (km^2)	Quality	Index database
The ecological space: unspoiled and beautiful	—	23	Development intensity of ecological space (%)	Bottom line	Add
		24	Ecological protection red line area (km^2)	Boundary	Add
	Ecological land for water and soil resource protection	25	Newly increased water and soil loss control area (km^2)	Quality	Index database
		26	Proportion of excellent water quality (class I and II) in coastal waters (%)	Quality	Index database
	Ecological land for species diversity protection	27	Protection rate of key wildlife species (%)	Quality	Index database
	Controlled land of coastal wetland	28	Wetland retention area (million ha)	Bottom line	Index database
		29	Mangrove area (million ha)	Bottom line	Add
	Controlled land of natural shoreline	30	Natural shoreline retention rate (%)	Bottom line	Index database
	Controlled land of sand source	31	Newly increased desertification land control area (million ha)	Quality	Index database
	Controlled land of estuarine	32	Elimination of inferior class V water bodies in rivers entering the sea (accomplished)	Quality	Index database
	Land of ecological restoration	33	Remediation of coastal zone area (million ha)	Quality	Add

intensity of land–sea development and implements the land space use control transmission mechanism of " zoning + index". Finally, we suggest that the management department controls the coastal territorial space according to the attribute of indicators. That is, government departments should strictly restrict the indicators of bottom line, boundary, and conversion and further improve the indicators of total amount and quality on the basis of reaching the expected objectives so as to make the control of the indicators more efficient and achieve the goal of high-quality development of coastal territorial space.

DISCUSSION AND CONCLUSION

At present, Chinese governments are actively promoting the preparation and implementation of national land spatial planning. It is a major deployment made by the Chinese central government to establish a land spatial planning system and supervise its implementation, integrate spatial planning such as main functional area planning, land use planning, and urban and rural planning into a unified land spatial planning, and realize "multi-compliance and integration". It is a major deployment made by the Chinese central government to achieve "multi-regulation integration" and establish a national land spatial planning system and supervise its implementation.

From the perspective of systems theory, this study puts forward an idea of constructing the monitoring index system of coastal use control. By connecting with the research hotspot of "production–living–ecological spaces," the index system can be implemented. Specifically, taking the monitoring index system of coastal zone spatial planning as the research object, this study explores the new requirements for territorial spatial planning from the perspective of land–sea planning. From the perspectives of "zoning + indicators," using the method of "multi-regulation integration," this study puts forward the overall construction idea of controlling" objectives-contents-monitoring indicators," constructs a systematic and hierarchical coastal zone spatial planning index system, which can make intensive and efficient production space, livable living space, and beautiful ecological space in coastal areas. First, it divides the production-living-ecological spaces in the coastal zone and determines the key spatial type of control, that is, the main contents of the control. By sorting out the existing spatial planning index system, the key controlled land types correspond to the existing index basis one by one, the duplicate indexes are deleted, and the blank indexes are supplemented to construct the coastal zone spatial planning index system. This study finds that some spatial elements play a prominent role in China's territory use control, such as arable land, forest land, urban construction land, ecological land, and marine aquaculture functional area. This situation shows that under the previous separation of land and sea, the focus of China's coastal zone space control is to protect inland food production land and ecological land. Moreover, due to the different natural nature of land and sea, the control of land area is more refined, and the control of sea area and living space quality is relatively lacking. At present, the main contradiction in the Chinese society has become the contradiction between the people's growing need for a better life and unbalanced and insufficient development. Therefore, on the premise of paying attention to food security and ecological security in coastal areas, the construction of living land for people's high-quality needs to be enhanced in the future. This study can provide theoretical reference for the coastal zone spatial planning and enrich the coastal zone use control system. In the future management process, policy executors should manage coastal zone areas according to local conditions and add characteristic indicators or delete invalid indicators for specific areas, which will have a better effect.

This study only provides an idea of constructing the index system. However, the classification of production–living–ecological spaces is still in the exploratory stage at present, which means that the relationship between "function" and "element" is still unclear in the construction idea of the index system. In reality, a spatial use element may correspond to more than one function. For example, cultivated land mainly not only plays the function of food production, but it also plays ecological function. In the future, the classification and index determination of ecological–production–living spaces still need to be further explored in order to enhance the practicability of the research. In addition, the indicators applicable to territorial space under different scales are different. In the future, the indicator system of different administrative levels should be determined from the coastal zone of national, provincial, city, county, and township. The construction of an index system is a complex systematic project. It is necessary to clarify the responsibilities and positioning in land and space planning as soon as possible, jointly promote the research on land and space planning indicators in coastal zone, provide strong support for land and space monitoring and early warning mechanism in coastal zone, and comprehensively build a safe, efficient, harmonious, competitive, and sustainable coastal zone space.

DATA AVAILABILITY STATEMENT

The original contributions presented in the study are included in the article/Supplementary Material, further inquiries can be directed to the corresponding authors.

AUTHOR CONTRIBUTIONS

ZG, JW, and YH: conceptualization, methodology, writing—original draft preparation, formal analysis, and visualization. ZG, LY, and YB: investigation, resources, and data curation. JW and YH: writing—review and editing, supervision, project administration, and funding acquisition. All authors have read and agreed to the published version of the manuscript.

FUNDING

This work was supported by the National Natural Science Foundation of China (grant number 41877034), the Fundamental Research Funds for the Central Universities (grant number 2652018036), and a projected entitled "Construction of Monitoring Indicators for Space Use Control in Coastal Zone" funded by the National Marine Data and Information Service, Ministry of Natural Resources of People's Republic of China.

REFERENCES

Alam, M. W., Xiangmin, X., Ahamed, R., Mozumder, M. M. H., and Schneider, P. (2021). Ocean Governance in Bangladesh: Necessities to Implement Structure, Policy Guidelines, and Actions for Ocean and Coastal Management. *Reg. Stud. Mar. Sci.* 45, 101822. doi:10.1016/j.rsma.2021.101822

Alves, F. L., Sousa, L. P., Almodovar, M., and Phillips, M. R. (2013). Integrated Coastal Zone Management (ICZM): a Review of Progress in Portuguese Implementation. *Reg. Environ. Change* 13 (5), 1031–1042. doi:10.1007/s10113-012-0398-y

An, T. T., Zhu, Q. L., Yue, Q., and Liu, N. N. (2019). Exploring the Questions and Approaches about Multiple Spatial Planning's Integration on marine Spatial Planning in China. *Trans. Oceanology Limnology* 3, 28–35. (in Chinese). doi:10.13984/j.cnki.cn37-1141.2019.03.004

Awosika, L., and Marone, E. (2000). Scientific Needs to Assess the Health of the Oceans in Coastal Areas: a Perspective of Developing Countries. *Ocean Coastal Manage.* 43 (8-9), 781–791. doi:10.1016/S0964-5691(00)00062-4

Bai, W., and Tian, Z. Q. (2016). Establishment of the Indicator System for Yulin Land Space Planning. *J. Land Resour. Inf.* 3, 41–45. (in Chinese).

Bax, N., Novaglio, C., Maxwell, K. H., Meyers, K., McCann, J., Jennings, S., et al. (2021). Ocean Resource Use: Building the Coastal Blue Economy. *Rev. Fish. Biol. Fish.* 32, 189–207. doi:10.1007/s11160-021-09636-0

Bullimore, B. (2014). Problems and Pressures, Management and Measures in a Site of marine Conservation Importance: Carmarthen Bay and Estuaries. *Estuarine, Coastal Shelf Sci.* 150, 288–298. doi:10.1016/j.ecss.2014.05.005

Chen, X., and Qian, W. (2020). Effect of marine Environmental Regulation on the Industrial Structure Adjustment of Manufacturing Industry: An Empirical Analysis of China's Eleven Coastal Provinces. *Mar. Pol.* 113, 103797. doi:10.1016/j.marpol.2019.103797

Cui, J. X., Gu, J., Sun, J. W., and L, J. (2018). The Spatial Pattern and Evolution Characteristics of the Production, Living and Ecological Space in Hubei Provence. *China Land Sci.* 32 (08), 67–73. (in Chinese). doi:10.11994/zgtdkx.20180723.121720

Glavovic, B., Limburg, K., Liu, K.-K., Emeis, K.-C., Thomas, H., Kremer, H., et al. (2015). Living on the Margin in the Anthropocene: Engagement Arenas for Sustainability Research and Action at the Ocean-Land Interface. *Curr. Opin. Environ. Sustainability* 14, 232–238. doi:10.1016/j.cosust.2015.06.003

Goodhead, T., and Aygen, Z. (2007). Heritage Management Plans and Integrated Coastal Management. *Mar. Pol.* 31 (5), 607–610. doi:10.1016/j.marpol.2007.03.005

Grafton, R. Q., Doyen, L., Béné, C., Borgomeo, E., Brooks, K., Chu, L., et al. (2019). Realizing Resilience for Decision-Making. *Nat. Sustain.* 2 (10), 907–913. doi:10.1038/s41893-019-0376-1

Guo, Y. C. (2020). Experience Learned from English East Inshore and Offshore Marine Plans. *Ocean Develop. Manage.* 37 (02), 19–25. (in Chinese).

Guo, Z., Hu, Y., and Zheng, X. (2020). Evaluating the Effectiveness of Land Use Master Plans in Built-Up Land Management: A Case Study of the Jinan Municipality, Eastern China. *Land Use Policy* 91, 104369. doi:10.1016/j.landusepol.2019.104369

Hu, H., Huang, P. Y., and Zhang, M. M. (2020). Classification System of Ecological-Living-Industrial Spaces in Coastal Zone Based on the Coordinated Land-Sea Development. *Ocean Develop. Manage.* 37 (05), 14–18. (in Chinese).

Huang, A., Xu, Y., Lu, L., Liu, C., Zhang, Y., Hao, J., et al. (2020). Research Progress of the Identification and Optimization of Production-Living-Ecological Spaces. *Prog. Geogr.* 39 (03), 503–518. (in Chinese). doi:10.18306/dlkxjz.2020.03.014

Huang, J. C., Lin, H. X., and Qi, X. X. (2017). A Literature Review on Optimization of Spatial Development Pattern Based on Ecological-Production-Living Space. *Prog. Geogr.* 36 (03), 378–391. (in Chinese). doi:10.18306/dlkxjz.2017.03.014

Humphrey, S., Burbridge, P., and Blatch, C. (2000). US Lessons for Coastal Management in the European Union. *Mar. Pol.* 24 (4), 275–286. doi:10.1016/S0308-597x(00)00003-8

Jiang, Y. M., Li, J. L., Ma, R. F., Wu, D. D., Wang, T. F., and Ye, M. Y. (2018). Integrated Control of Coastal Zone Based on the Multiple Planning Integration. *China Land Sci.* 32 (02), 34–39. (in Chinese). doi:10.11994/zgtdkx.20180224.145740

Lee, J. (1998). Policy Issues and Management Framework of Chinhae Bay, Republic of Korea. *Ocean Coastal Manage.* 38 (2), 161–178. doi:10.1016/S0964-5691(97)00071-9

Li, B., Wang, Z., Chai, J., and Zhang, D. (2019). Index System to Assess Implementation of Strategic Land Use Plans in China. *Land Use Policy* 88, 104148. doi:10.1016/j.landusepol.2019.104148

Liang, X. C., and Ding, D. S. (2002). Trends of Overseas Studies of Ocean and Coastal Tourism. *J. Nat. Resour.* 06, 783–791. (in Chinese).

Lin, Q., and Yu, S. (2018). Losses of Natural Coastal Wetlands by Land Conversion and Ecological Degradation in the Urbanizing Chinese Coast. *Sci. Rep.* 8, 15046. doi:10.1038/s41598-018-33406-x

Linton, D. M., and Warner, G. F. (2003). Biological Indicators in the Caribbean Coastal Zone and Their Role in Integrated Coastal Management. *Ocean Coastal Manage.* 46 (3-4), 261–276. doi:10.1016/S0964-5691(03)00007-3

Liu, J. L., Liu, Y. S., and Li, Y. R. (2017). Classification Evaluation and Spatial-Temporal Analysis of "Production-Living-Ecological" Spaces in China. *Acta Geographica Sinica* 72 (07), 1290–1304. (in Chinese). doi:10.11821/dlxb201707013

Liu, Y. S., and Wang, J. Y. (2016). Theoretical Analysis and Technical Methods of "multiple Planning Integration" in the Rural to Urban Transition Period in China. *Prog. Geogr.* 35 (5), 529–536. (in Chinese). doi:10.18306/dlkxjz.2016.05.001

LOICZ working document (2003). *Version II: LOICZ Future-Beyond 2002.04*. Den Burg, Netherlands: LOICZ.

Milanés Batista, C., Suárez, A., and Botero Saltarén, C. M. (2017). Novel Method to Delimitate and Demarcate Coastal Zone Boundaries. *Ocean Coastal Manage.* 144, 105–119. doi:10.1016/j.ocecoaman.2017.04.021

Millennium Ecosystem Assessment (2005). *Ecosystems and Human Well-Being: Wetlands and Water Synthesis*. Washington, DC: World Resource Institute. Available at: http://www.millenniumassessment.org/en/index.html.

Nie, X., Wu, J., Zhang, W., Zhang, J., Wang, W., Wang, Y., et al. (2021). Can Environmental Regulation Promote Urban Innovation in the Underdeveloped Coastal Regions of Western China? *Mar. Pol.* 133, 104709. doi:10.1016/j.marpol.2021.104709

Papageorgiou, M. (2016). Coastal and marine Tourism: A Challenging Factor in Marine Spatial Planning. *Ocean Coastal Manage.* 129, 44–48. doi:10.1016/j.ocecoaman.2016.05.006

Smith, A. J., Barber, J., Davis, S., Jones, C., Kotra, K. K., Losada, S., et al. (2021). Aquatic Contaminants in Solomon Islands and Vanuatu: Evidence from Passive Samplers and Microtox Toxicity Assessment. *Mar. Pollut. Bull.* 165, 112118. doi:10.1016/j.marpolbul.2021.112118

Su, H., and Liang, B. (2021). The Impact of Regional Market Integration and Economic Opening up on Environmental Total Factor Energy Productivity in Chinese Provinces. *Energy Policy* 148, 111943. doi:10.1016/j.enpol.2020.111943

van Alphen, J. (1995). The Voordelta Integrated Policy Plan: Administrative Aspects of Coastal Zone Management in the Netherlands. *Ocean Coastal Manage.* 26 (2), 133–150. doi:10.1016/0964-5691(95)00018-W

Wang, B., Xin, M., Wei, Q., and Xie, L. (2018). A Historical Overview of Coastal Eutrophication in the China Seas. *Mar. Pollut. Bull.* 136, 394–400. doi:10.1016/j.marpolbul.2018.09.044

Wen, C. X., and Liu, J. X. (2019). Review and Prospect of Coastal Zone Planning Based on Land and Sea Integration. *Planners* 7, 5–11. (in Chinese).

Wu, J., Song, Y., Lin, J., and He, Q. (2018). Tackling the Uncertainty of Spatial Regulations in China: An Institutional Analysis of the "Multi-Plan Combination". *Habitat Int.* 78, 1–12. doi:10.1016/j.habitatint.2018.07.002

Xu, X., Li, X., Chen, M., Li, X., Duan, X., Zhu, G., et al. (2016). Land-ocean-human Interactions in Intensively Developing Coastal Zone: Demonstration of Case Studies. *Ocean Coastal Manage.* 133, 28–36. doi:10.1016/j.ocecoaman.2016.09.006

Yan, D., Yao, X., Li, J., Qi, L., and Luan, Z. (2021). Shoreline Change Detection and Forecast along the Yancheng Coast Using a Digital Shoreline Analysis System. *Wetlands* 41 (4), 47. doi:10.1007/s13157-021-01444-3

Yang, W., Cai, F., Liu, J., Zhu, J., Qi, H., and Liu, Z. (2021). Beach Economy of a Coastal Tourist City in China: A Case Study of Xiamen. *Ocean Coastal Manage.* 211, 105798. doi:10.1016/j.ocecoaman.2021.105798

Yu, G., Liao, Y., Liao, Y., Zhao, W., Chen, Q., Kou, J., et al. (2021). Research on Integrated Coastal Zone Management Based on Remote Sensing: A Case Study of Guangxi Beibu Gulf. *Reg. Stud. Mar. Sci.* 44, 101710. doi:10.1016/j.rsma.2021.101710

Yuan, W., and Chang, Y.-C. (2021). Land and Sea Coordination: Revisiting Integrated Coastal Management in the Context of Community Interests. *Sustainability* 13 (15), 8183. doi:10.3390/su13158183

Yue, Q., Xu, W., Li, Y. N., Teng, X., Dong, Y. E., and Hu, H. (2019). Integrating marine Functional Zoning into 'Multiple-Plan Integration' from the Perspective of Territorial Space. *J. Mar. Dev. Manag.* 36 (06), 3–6. (in Chinese).

Yue, W. Z., and Wang, T. Y. (2019). Rethinking on the Basic Issues of Territorial and Spatial Use Control in China. *China Land Sci.* 33 (08), 8–15. (in Chinese). doi:10.11994/zgtdkx.20190722.151305

Zhang, M., Chen, Y., Hu, W., Deng, N., and He, W. (2021). Exploring the Impact of Temperature Change on Residential Electricity Consumption in China: The 'crowding-Out' Effect of Income Growth. *Energy and Buildings* 245, 111040. doi:10.1016/j.enbuild.2021.111040

Zhang, R. Q., and Tan, Y. Y. (2002). Study on Development and protection of Coastal Tourism. *Coastal Eng.* 04, 60–65. (in Chinese).

Zhao, X., Zhang, Q., He, G., Zhang, L., and Lu, Y. (2021). Delineating Pollution Threat Intensity from Onshore Industries to Coastal Wetlands in the Bohai Rim, the Yangtze River Delta, and the Pearl River Delta, China. *J. Clean. Prod.* 320, 128880. doi:10.1016/j.jclepro.2021.128880

Zhou, S. T., Zhai, G. F., and Shi, Y. J. (2018). Indicator-based Monitoring Framework of Spatial Planning in England and its Inspirations. *Int. Urban Plann.* 33 (05), 126–131. (in Chinese). doi:10.22217/upi.2017.245

Zou, L. L., Wang, J. Y., and Hu, X. D. (2018). An Classification Systems of Production-Living-Ecological Land on the County Level: Theory Building and Empirical Research. *China Land Sci.* 32 (04), 59–66. (in Chinese). doi:10.11994/zgtdkx.20180410.150611

Conflict of Interest: The authors declare that the research was conducted in the absence of any commercial or financial relationships that could be construed as a potential conflict of interest.

frontiers | Frontiers in Ecology and Evolution

ORIGINAL RESEARCH
published: 18 May 2022
doi: 10.3389/fevo.2022.901873

Assessment of Sectoral Virtual Water Flows and Future Water Requirement in Agriculture Under SSP-RCP Scenarios: Reflections for Water Resources Management in Zhangye City

Yifei Wang[1,2,3], *Haowei Wu*[4] *and Zhihui Li*[1,2,3]*

[1] Institute of Geographic Sciences and Natural Resources Research, Chinese Academy of Sciences, Beijing, China, [2] Key Laboratory of Land Surface Pattern and Simulation, Chinese Academy of Sciences, Beijing, China, [3] University of Chinese Academy of Sciences, Beijing, China, [4] School of Soil and Water Conservation, Beijing Forestry University, Beijing, China

OPEN ACCESS

Edited by:
Jinyan Zhan,
Beijing Normal University, China

Reviewed by:
Qing Zhou,
Huazhong Agricultural University, China
Gui Jin,
China University of Geosciences Wuhan, China

***Correspondence:**
Zhihui Li
lizhihui@igsnrr.ac.cn

Specialty section:
This article was submitted to Environmental Informatics and Remote Sensing, a section of the journal Frontiers in Ecology and Evolution

Received: *22 March 2022*
Accepted: *11 April 2022*
Published: *18 May 2022*

Citation:
Wang Y, Wu H and Li Z (2022) Assessment of Sectoral Virtual Water Flows and Future Water Requirement in Agriculture Under SSP-RCP Scenarios: Reflections for Water Resources Management in Zhangye City. Front. Ecol. Evol. 10:901873. doi: 10.3389/fevo.2022.901873

Water scarcity is a core issue that constraints the high-quality development of arid areas in northwestern China. Zhangye is an oasis city located in the Heihe River Basin in northwestern China. It is populated with an agriculture-dominated economy and faces more and more serious water crises. Virtual water is an indicator that can measure the embodied water in the traded products, which has been widely applied for making rational policies for water resources management. In addition, clarifying water requirements in agricultural sectors under future climate change scenarios is essential to develop more appropriate adaptation strategies. From this perspective, this study aims to evaluate and compare virtual water flows among various sectors in Zhangye for the years 2012 and 2017 with a single regional input-output model and to further clarify the future water requirement tendency in agriculture during 2020–2050 under different shared socioeconomic pathways and representative concentration pathways (SSP-RCP) scenarios. The results showed that the planting sector directly contributed most of the total water consumption with the highest direct coefficient of 3307.5 m^3/yuan in 2012, whereas the manufacture of food products and tobacco processing sector had the largest proportion of indirect water consumption (99%) mainly from intermediate inputs of agricultural products. Water consumption intensity of all sectors on average decreased by 22% during 2012–2017, indicating an increasing water utilization efficiency in economic industries. Household consumption also can improve water utilization efficiency as the major pathway for final consumption (86.4% in 2017). Water scarcity in Zhangye was becoming increasingly prominent since virtual water net exports were higher than local consumption, especially in the agriculture, manufacturing, and energy supply industries. Moreover, under climate change scenarios, we found the highest level of water requirement per unit area occurred in 2000, but it still had an incremental potential by 2050, especially in SSP585. The high requirement intensity and

large-scale maize planting caused a rising tendency of total crop water requirement with an annual increasing rate of 8.4% from 1980 to 2050. This makes it possible to adapt to climate change through scientific management measures and technical means. We further made policy implications for adaptive management of water resources in Zhangye.

Keywords: virtual water, input-output analysis, crop water requirement, CMIP6, scenario analysis, Zhangye

INTRODUCTION

Water scarcity is a severe challenge to sustainable development worldwide. Water supply is becoming increasingly limited, especially in developing countries, due to the uncertainty of global climate change, the continuous rise in population and food demand, and a shift in consumption patterns toward more water-intensive products (Qasemipour and Abbasi, 2019; Arunrat et al., 2022). In northwestern China, which is mostly dominated by arid areas, water scarcity has been seriously exacerbated by the imbalance of water availability and water demand during rapid industrialization and urbanization (Zhang and Anadon, 2014; Zheng et al., 2020). High-quality development in arid areas largely depends on the water availability of inland rivers and effective management measures (Deng and Zhao, 2015; Jin et al., 2018; Wang and Wei, 2019; Wang H. et al., 2022). Arid areas are particularly sensitive to climate change, which causes ecological deterioration, frequent drought events, and water yield changes (Gain and Wada, 2014; Wu et al., 2017). Illustrating the dual impacts of climate change and socioeconomic development on water supply demand patterns is important for realizing adaptive management of water resources. Virtual water theory is widely applied in the research of water resources management by revealing the occupancy of production and domestic water in the socioeconomic system (Shi and Zhan, 2015; Zhang et al., 2019). However, characterizing the current water consumption and its future tendency under global climate change from the perspective of virtual water remains a major challenge. It plays a significant role in promoting sustainable water resources management and regional high-quality development.

The conception of virtual water was first proposed by Allan (1998), which refers to the amount of water resources during the production of products and services. Virtual water is different from physical water and exists "invisibly." In the early twentieth century, virtual water was applied to conduct a virtual water strategy in northwest arid areas of China. Water resources are the material basis for survival. Physical water is distributed unevenly and is difficult to transport. Therefore, transferring water resources within industrial sectors and trade among regions in the form of virtual water are the fundamental patterns of the water cycle in socioeconomic systems (Liu et al., 2020). Research applying virtual water theory has gradually extended from food circulation and food security strategy in international trade to sectoral connection and regional trade (Dong et al., 2014; Zhang et al., 2017; Zhang et al., 2019). Virtual water theory has provided a promising solution to alleviate the uneven distribution of water resources by sectoral transfer and regional trade of water resources.

Quantifying virtual water mainly includes two methods, namely, (1) classifying products and (2) then calculating the consumption of virtual water based on the production tree (Chapagain et al., 2006). As it is difficult to quantify water consumption of industrial products in a complex process and its intermediate consumption and final consumption cannot be distinguished (Zhang et al., 2019), this method is merely applied to virtual water measurement of primary agricultural products (such as crops and livestock) at the micro level. Another method is an input-output (IO) analysis. An IO table can describe both the input and output relationship of industrial sectors and the distribution of final products in detail. An IO table with water accounts embedded helps to clarify virtual water flows among various sectors, products, and services from the entire national economic system (Qasemipour et al., 2020; Xu and Li, 2020). For example, Zhao et al. (2010) analyzed the virtual water trade in Heihe River Basin (HRB) based on the IO analysis. Feng et al. (2014) specifically clarified the water footprint of major industries in the upper, middle, and lower reaches of the Yellow River Basin with a multiregional input-output model (MRIO). Du et al. (2021) combined the MRIO model and complex network theory to identify the structure of provincial virtual water trade. Generally, the IO analysis is applied to the research on industrial transformation and resources allocation at the macroeconomic level. However, it cannot describe production details due to data limits. Recently, an integrated method has been popularized by adding satellite accounts with detailed sectoral information to the IO model (Wu et al., 2017; Zhang et al., 2017), which is significant for improving the data availability and promoting research at a finer scale.

Previous studies have extended virtual water theory based on calculating virtual water and analyzing trade flows. Some studies focused on the evolution trends of water utilization and the patterns of regional virtual water trade (Dong et al., 2014; Zhang et al., 2016). Some studies also investigated driving factors of virtual water flows and their resource and environment effects, then analyzed tradeoffs of development in the socioeconomic system and environmental system by connecting with land use and carbon footprint (Zheng et al., 2019; Wang et al., 2021). Furthermore, sustainable management schemes of water resources were discussed in the field of water scarcity, utilization efficiency, and regional industrial advantages (Li et al., 2019; Wang and Wei, 2019; Islam et al., 2021). Previous studies have found that there is a significant correlation between virtual water trade and regional water scarcity. Virtual water flows increasingly from water-scarce developing regions to water-rich developed regions (Deng et al., 2021; Zhai et al., 2021). This phenomenon is

detrimental to the decoupling development of economic growth and resource utilization. Sandström et al. (2018) considered that reducing virtual water imports by replacing imported crops with local crop production contributes to balancing water resources in water-scarce countries and constructing global sustainable food systems. However, few studies have investigated water scarcity based on the comprehensive perspective of sectoral water allocation and virtual water trade to clarify management strategies of water-intensive industries in water-scarce regions.

In addition, clarifying how climate change will affect crop water requirements during agricultural production is important to help alleviate water scarcity. Crop water requirement was mostly analyzed and used for estimation of water footprint and virtual water content through the CROPWAT model (Deng et al., 2020; Qasemipour et al., 2020; Long et al., 2021). Nevertheless, with the continuous warming of the global climate, increasing variability in climatic factors, such as changes in temperature and precipitation, will significantly affect water consumption in the food production system and bring more challenges to water management (Bocchiola et al., 2013; Arunrat et al., 2020). Especially, understanding crop water requirement changes under future climate change at the local scale is essential to adaptive water management strategies in the region where agricultural production depends on both rainfall (green water) and irrigation water (blue water) (Rosenzweig et al., 2014; Arunrat et al., 2022). Currently, a number of studies have been conducted to analyze water footprints and virtual water content of crops under the combined shared socioeconomic pathways (SSPs) and representative concentration pathways (RCPs) scenarios (Wada and Bierkens, 2014; Arunrat et al., 2022; Li et al., 2022). However, regarding the variations in water requirement of crop production in climate change scenarios, the results differ or contradict each other (Zhuo et al., 2016). Therefore, evaluating crop water requirements under local climate change conditions is becoming necessary. Zhangye City in the HRB is a typical water-scarce region in northwestern China. Scholars have fully been discussing the supply and demand of water resources and their utilization strategies in the HRB (Wu et al., 2017; Zhang et al., 2017; Wang and Wei, 2019). However, it is still blank to identify water consumption and its response mechanism under the complex systematic changes caused by future climate. This is vitally beneficial for predicting future water utilization and flexibly adjusting management schemes of water resources.

Taking adaptive management of water resources to alleviate water supply demand pressure is essential in water-scarce regions. In this study, Zhangye City in the HRB was selected as a case area. The objectives were to analyze water consumption and virtual water flows among regional trade and sectoral transfer in Zhangye using an IO model and further specifically clarify crop water requirement in agricultural sectors using the CROPWAT model and its changing tendency in the future under the SSP-RCP scenarios. Finally, we proposed policy implications for adaptive management of water resources in Zhangye City from the perspectives of industrial transformation, efficiency improvement, and virtual water trade.

MATERIALS AND METHODS

Study Area

The HRB is the second largest inland river basin in China (**Figure 1A**). The water supply of the HRB mainly comes from atmospheric precipitation and meltwater in Qilian Mountain. Zhangye City is located in the northeast of Gansu Province. It is a typical large city located in the upper and middle reaches of the HRB (**Figure 1B**). It covers an area of 42,000 km^2, between latitude 37°28'N to 39°57'N and longitude 97°20'E to 102°12'E. Zhangye administratively covers Ganzhou, Linze, Minle, Shandan, Gaotai, and Su'nan counties (**Figure 1C**). The topography of Zhangye slopes from the northeast to the southwest, with the elevation ranging from 1,144 to 5,583 m (**Figure 1C**). Qilian Mountain stands along the northwest-southeast boundary of Zhangye with an average elevation of 3,200 m. In the middle reaches, Hexi Corridor plain is the biggest oasis in the HRB, covering 38% of the total area in Zhangye. Desert grassland and Gobi Desert cover the north of the city. Therefore, Zhangye has enjoyed the unique landform of deserts and oasis. It has an arid and semiarid climate. The high temperature and more than 80% of the precipitation are mainly concentrated from May to September. With the elevation decreasing, the annual average precipitation gradually decreases from 450 to 100 mm, whereas the annual average temperature increases from −16.3 to 8.9°C from southeast to northwest (**Figure 1B**). The plain in the middle usually has the highest temperature and the most abundant precipitation.

In the middle reaches, the vast Hexi Corridor plain is a major agricultural area in the HRB, benefiting from flat terrain, rich light and heat resources, and the large range of temperatures between day and night. Agricultural irrigation accounts for 88% of the total water consumption in Zhangye. Water scarcity is the key factor restricting agricultural production. However, unreasonable industrial structure and increasing domestic demand have further exacerbated the contradiction of water supply and demand, as well as a series of ecological and environmental problems such as desertification and salinization. Thus, alleviating the contradiction of water supply and demand in the view of virtual water under climate change can benefit regional high-quality development.

Data

Economic Data to Construct the Input-Output Table

The 2012 IO table of Zhangye was collected from the data prepared by Wu et al. (2017), based on which the 2017 IO table was further compiled through a non-survey approach. It consists of 39 sectors, including agriculture, mining, manufacturing, construction, and service industries, and their subordinate sectors. The classification of sectors depends on National Economical Industry Classification (GB/T 4754-2017) and data availability. There are two types of data required for implementing the IO model, including the economic production and consumption data and the water consumption statistics. Data on total output, added value, and final consumption at county-level sectors were collected and calculated from statistical

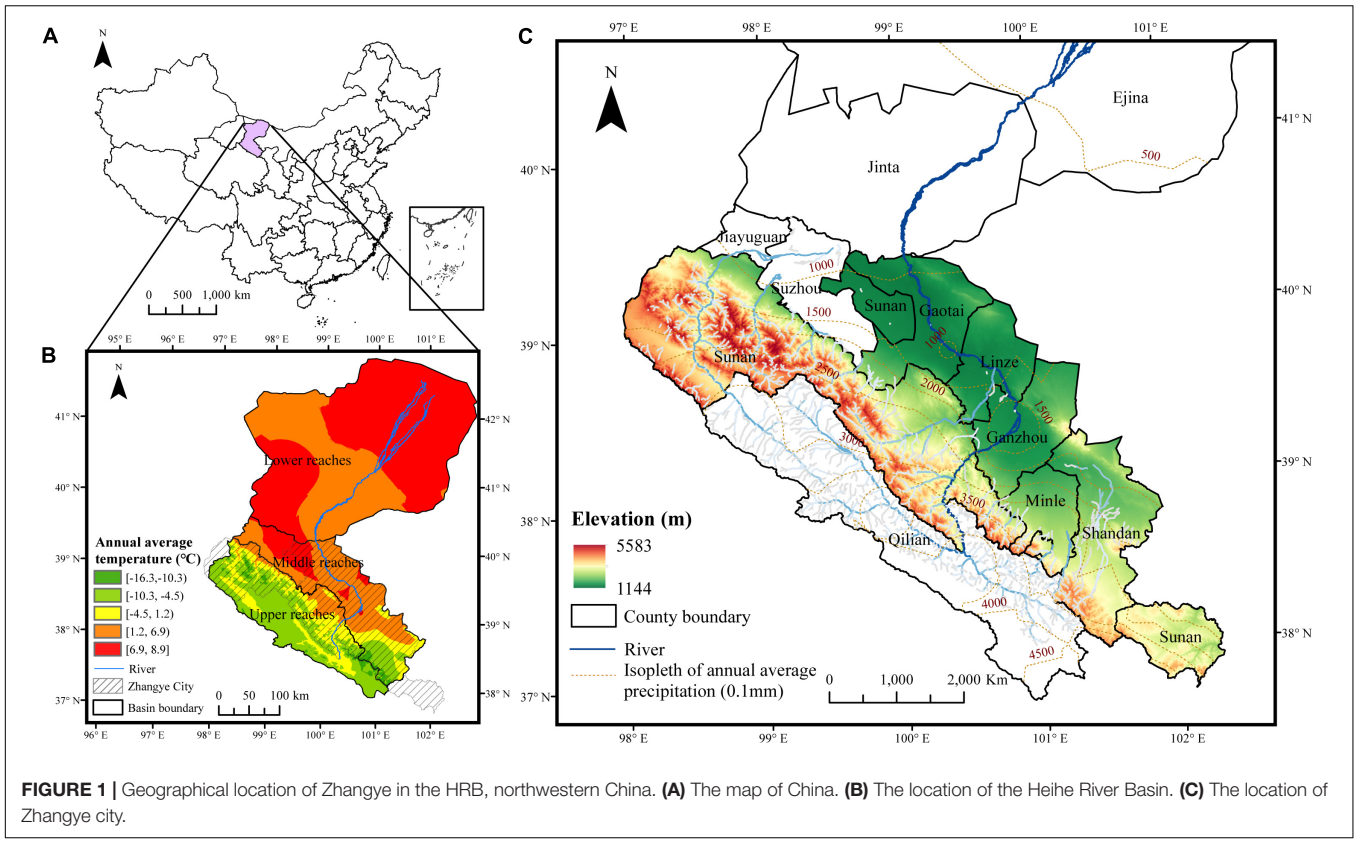

FIGURE 1 | Geographical location of Zhangye in the HRB, northwestern China. **(A)** The map of China. **(B)** The location of the Heihe River Basin. **(C)** The location of Zhangye city.

yearbooks. Water consumption data in Zhangye were derived from the water resources bulletin. Among each sector, data for the agriculture and construction industry were collected directly, whereas data for other industries were calculated based on water consumption per unit of GDP, industrial output value, and water consumption amounts at the national level and city level. Then, we corrected data through the total water consumption of industries and tested the data using sectoral water quota and product outputs in Zhangye. An intermediate input matrix was obtained using the RAS technique to adjust the bilateral proportion of intermediate inputs and intermediate outputs, as well as to calculate several iterations with the constraints of row and column sums. We finally obtained the IO tables with water accounts embedded in Zhangye in 2012 and 2017.

Climate Data

Historical climate data (1980–2020) were obtained from the National Meteorological Information Center.[1] It provides a daily dataset of surface climate data (V3.0), including maximum temperature, minimum temperature, average relative humidity, average wind speed, and sunshine hours. Future climate data were from the Coupled Model Intercomparison Project (CMIP6) multimode climate scenario data.[2] The Sixth Assessment Report of the Intergovernmental Panel on Climate Change has adopted a new set of emission scenarios developed using SSPs (Pedersen et al., 2021). SSPs include five scenarios (SSP1: sustainability; SSP2: middle of the road; SSP3: regional rivalry; SSP4: inequality; and SSP5: fossil fuel development), which represent different combinations of mitigation and adaptation challenges and a set of qualitative storylines and quantitative development indicators, including population, economy, education, city, and technology (O'Neill et al., 2017; Huang et al., 2019). The CMIP has conducted remarkable work in designing climate model standards and developing shared climate simulation data to support new scientific issues of climate change. The new phase CMIP6 proposed a new projection scenario, which combines different SSPs and RCPs, which makes future scenarios more reasonable (Eyring et al., 2016; Simpkins, 2017). Climate models are key tools to simulate climate change scenarios. The CMIP6 has provided various outputs of multi-series climate models, where ESM and Earth models have been confirmed to have significant improvement in simulation performance for extreme temperature and precipitation in arid and semiarid areas (Karim et al., 2020; Lim Kam Sian et al., 2021; Wang L. et al., 2022). In this study, we selected data for the period 2020–2050 from four core scenarios integrated by MPI-ESM1-2-HR and EC-Earth3-Veg models (SSP126: the green road with low radiation forcing; SSP245: the middle road with moderate radiation forcing; SSP370: the rocky road with moderate radiation forcing; and SSP585: the highway with high radiation forcing). By using climate output data from these scenarios to adjust the parameters of the Penman-Monteith combination equation, we predicted the trend of

[1]http://data.cma.cn/

[2]https://esgf-node.llnl.gov/projects/cmip6/

Output / Input		Intermediate consumption				Final consumption				Total output
		Sector 1	..	Sector n	**Total**	Household	Government	Capital	Net export	
Intermediate inputs	Sector 1									
	…									
	Sector n									
	Total									
Value added										
Total input										
Water consumption										

FIGURE 2 | An IO table with water accounts embedded.

agricultural crop water requirement in Zhangye under different scenarios in the future.

Methods

The Input-Output Model of Water Consumption

The IO model forms a matrix to describe the quantitative relationship of input and output in various economic sectors across time. Recently, the IO model with water accounts embedded (**Figure 2**) has been widely applied in research on water resources management because of its advantages in structured data and unique correlation analysis. Calculating the sectoral water consumption relies on several key coefficients. The direct water consumption coefficient represents the amount of physical water consumed by sectoral per unit output value during production. Apart from the direct water consumption, intermediate products and services provided by other sectors also consume water invisibly. It is regarded as indirect water and reflected by the indirect water consumption coefficient. The sum of the direct water consumption coefficient and indirect water consumption coefficient is equal to the total water input coefficient. It refers to the total amount of water consumption to provide a final product of sectoral per unit output value.

$$d_j = \frac{W_j}{X_j},\ j = 1, 2, ..., n \tag{1}$$

$$t = d + k \tag{2}$$

$$t = d(I - A)^{-1} \tag{3}$$

$$a_{ij} = \frac{x_{ij}}{X_j},\ i = 1, 2, , n,\ j = 1, 2, ..., n \tag{4}$$

$$W = d(I - A)^{-1}Y\ \ tY \tag{5}$$

$$VW = t * \hat{Y} \tag{6}$$

$$TVW = VW - VW^T \tag{7}$$

In Eq. 1, d_j is the direct water consumption coefficient of sector j, W_j is the direct water consumption of sector j, X_j is the total output value of sector j, and n represents the number of sectors. In Eq. 2, direct water consumption coefficients of all sectors constitute the row vector d, and t and k represent the row vectors of total water input coefficients and indirect water consumption coefficients, respectively. In Eqs 3 and 4, I is an identity matrix of order n. a_{ij} is the technical coefficient, referring to the product's value provided by sector i when producing per unit output value in sector j. x_{ij} is the product's value in sector j provided by sector i. Technical coefficients of all sectors constitute the direct IO coefficients matrix A. $(I - A)^{-1}$ is known as the Leontief inverse matrix. It links direct water consumption coefficients d and total water input coefficients t, reflecting the relationship between the direct and total input when considering the intermediate inputs from other sectors. In Eq. 5, the row vector t of total water input coefficients was multiplied by the column vector Y of final consumption in sectoral products. On the right side of Eq. 5, the total water consumption W in the macro national economic system includes water consumption from the household, government, capital, import, and export. In Eqs 6 and 7, we obtained the total water consumption matrix VW by multiplying the row vector t and the intermediate IO matrix $\hat{Y}$ among sectors. We further established the sectoral transfer matrix TVW of virtual water by subtracting matrix VW from its transpose matrix.

CROPWAT Model for Crop Water Requirement Calculation

CROPWAT model is an approach to calculate crop evapotranspiration using crop coefficients and meteorological and soil data to obtain crop water requirements. Agriculture is the largest sector of water consumption in Zhangye. Thus, we assumed non-agricultural sectors are not sensitive to climate change and only investigated the impact of climate change on the water consumption in agricultural sectors to simplify our calculation. As the water content of crops contains only 0.1–1% of evapotranspiration, the accumulative evapotranspiration during the growth period is approximately equal to the crop

water requirement. We used CROPWAT 8.0 developed by Joss Swennenhuis for the Water Resources Development and Management Service of FAO[3] to calculate the crop water requirement of two typical crops (wheat and maize) in Zhangye. The calculations were as follows:

$$ET_c = \sum_{d_{plant}}^{d_{harvest}} ET_{c,d} \quad (8)$$

$$ET_{c,d} = ET_{0,d} * K_c \quad (9)$$

$$ET_{0,d} = \frac{0.408\triangle (R_n - G) + \gamma \frac{900}{T+273} u_2 (e_s - e_a)}{\triangle + \gamma(1 + 0.34u_2)} \quad (10)$$

In Eq. 8, we defined the crop water requirement as ET_c. It is the accumulation of daily crop water requirements, namely, $ET_{c,d}$, during the entire growth period from the initial stage to the end of the late-season stage. In Eq. 9, $ET_{c,d}$ was calculated by the reference evapotranspiration $ET_{0,d}$ and the crop coefficient K_c. The reference evapotranspiration $ET_{0,d}$, also named the reference crop water requirement, was calculated by the Penman-Monteith combination method recommended by FAO. The equation of the Penman-Monteith combination is shown in Eq. 10, where R_n is the net radiation at the crop surface (MJ·m^{-2}·day^{-1}), G is the soil heat flux density (MJ·m^{-2}·day^{-1}), T is daily air temperature (°C), u_2 is the daily wind speed at 2 m height (m/s), e_s and e_a represent saturation vapor pressure and actual vapor pressure (kPa), respectively, $\triangle$ is the slope curve of vapor pressure (kPa/°C), and γ is the psychrometric constant (kPa/°C).

The crop coefficient K_c incorporates the effects of crop characteristics and soil evaporation to reflect the difference in crop water requirement influenced by crop types, planting areas, and soil and climate conditions. K_c coefficients differ in different growth stages, including the initial stage (K_{cini}), the mid-season stage (K_{cmid}), and the end of the late-season stage (K_{cend}). FAO has provided stages length of various planting periods and reference K_c coefficients of various crops globally under non-stressed, well-managed, and subhumid climates (RH_{min}45%, $u_2$2 m/s), as well as adjustment methods of crop coefficients in different growth stages.

$$K_{cmid} = K_{cmid(Tab)} [0.04 (u_2 - 2) - 0.0004 (RH_{min} - 45)] \left(\frac{h}{3}\right)^{0.3} \quad (11)$$

$$K_{cend} = K_{cend(Tab)} [0.04 (u_2 - 2) - 0.0004 (RH_{min} - 45)] \left(\frac{h}{3}\right)^{0.3} \quad (12)$$

$$RH_{min} = 100 \frac{e^0 (T_{\text{dew}})}{e^0 (T_{\max})} \quad (13)$$

In Eqs 11 and 12, K_{cmid}, K_{cend} were adjusted by reference coefficients $K_{cmid(Tab)}$, $K_{cend(Tab)}$. No adjustment was required when $K_{cend(Tab)}$ 0.45. K_{cini} was determined comprehensively by the magnitude and time interval of wetting events, soil texture, and reference evapotranspiration. RH_{min} is daily minimum relative humidity (%), u_2 is the daily wind speed at 2 m height (m/s), and h is plant height during the growth stage (m). In Eq. 13, e^0 (T_{dew}) and e^0 ($T_{\max}$) represent the saturation vapor pressure under mean dewpoint temperature and mean daily maximum air temperature, respectively. In arid and semiarid climates, T_{dew} can be replaced by subtracting 2°C from the average value of $T_{\min}$.

Based on this, we got K_c coefficients of wheat and maize in Zhangye in different growth stages. We showed growth stages length and K_c coefficients curves of wheat and maize in Zhangye (**Table 1** and **Figure 3**). We also obtained the accumulative crop water requirement per unit area during the entire growth period, ET_c(m^3/hm^2). In Eq. 14, we further calculated the total crop water requirement, namely, the virtual water content of the crop, VWC_c(m^3) by combining with yield per unit area Y_c and crop yield A_c.

$$VWC_c = \frac{ET_c}{Y_c} \times A_c \quad (14)$$

TABLE 1 | Growth stages length of wheat and maize in Zhangye (unit: days).

Growth stage	Initial stage	Rapid stage	Mid-season stage	End of the late season stage
Wheat	20	20	60	30
Maize	30	40	60	30

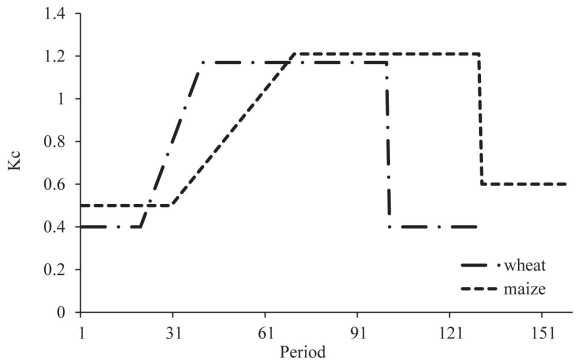

FIGURE 3 | Crop coefficients **K_c** curves of wheat and maize in Zhangye.

RESULTS

Water Consumption of Different Industrial Sectors

By analyzing the composition of water consumption coefficients of each industrial sector calculated by the IO model, we found the structure and intensity of water consumption when providing sectoral final products (**Table 2**). Planting was the largest water consumption sector, whose direct consumption accounted for the most. The direct water consumption coefficient (d) of the planting sector was 3,307.47 m^3/yuan in 2012 and 2,311.78 m^3/yuan in 2017, more than 100 times higher than

[3]https://www.fao.org/land-water/databases-and-software/cropwat/

TABLE 2 | Water consumption coefficients of Zhangye industrial sectors in 2012 and 2017 (unit: m^3/yuan).

Industrial sectors and codes		*d*		*k*		*t*	
		2012	2017	2012	2017	2012	2017
Planting (PA)		3307.5	2311.8	134.1	86.4	3441.6	2398.2
Non-planting agriculture (NPA)		253.1	246.0	193.3	139.3	446.4	385.3
Mining industry (B)	Coal mining and dressing.	6.2	2.3	23.5	26.7	29.6	29.0
	Metallic ore mining and dressing.	21.3	7.9	22.1	33.4	43.5	41.4
	Non-metallic minerals mining and dressing.	45.3	16.8	20.5	15.8	65.8	32.5
Manufacturing industry (C)	Manufacture of food products and tobacco processing.	6.9	2.6	527.3	472.3	534.2	474.8
	Sawmills and furniture.	3.1	1.2	89.6	97.7	92.7	98.9
	Pater and products, printing, and record medium reproduction.	37.3	13.8	50.8	43.6	88.1	57.4
	Petroleum processing, coking, and nuclear fuel processing.	22.5	0.0	0.1	0.0	22.6	0.0
	Chemical industry.	38.1	14.1	10.2	14.8	48.3	28.9
	Non-metallic mineral products.	7.3	2.7	15.4	15.8	22.7	18.5
	Metal smelting and pressing.	30.8	11.4	33.3	38.5	64.1	50.0
	Metal products.	2.7	1.0	47.9	35.7	50.6	36.7
	Equipment manufacturing.	1.5	0.6	34.7	29.6	36.2	30.2
Electricity, heat, gas, and water supply industry (D)	Electricity and heat production and supply.	68.4	25.3	6.9	5.6	75.2	30.9
	Gas production and supply.	0.0	31.3	0.0	0.0	0.0	31.3
	Water production and supply.	27.1	10.1	19.5	17.1	46.6	27.1
Construction industry (E)		5.1	0.6	42.8	26.6	47.9	27.2
Service industry (S)	Transport, storage, and post services	1.7	4.1	38.6	21.2	40.3	25.3
	Telecommunication, computer, and software services.	1.0	2.4	14.6	9.4	15.5	11.8
	Wholesale and retail trade services	2.8	7.0	8.8	6.7	11.7	13.7
	Accommodation and food serving.	10.1	25.1	50.9	51.3	61.0	76.4
	Finance.	0.9	2.1	15.7	12.1	16.6	14.3
	Real estate.	0.9	2.1	11.5	8.3	12.4	10.4
	Rental and business services.	4.2	10.3	15.9	10.4	20.0	20.8
	Scientific research and technology.	2.3	5.8	15.4	10.3	17.7	16.1
	Water, environment, and public facilities management.	4.2	10.5	63.7	41.8	68.0	52.3
	Residential and social services.	2.1	5.3	31.4	21.5	33.6	26.9
	Education. Health, social security, and welfare. Cultural, sporting, and recreational services.	0.9	2.3	15.9	9.5	16.8	11.9
	Public management and social organization.	4.2	10.5	16.5	11.3	20.7	21.8

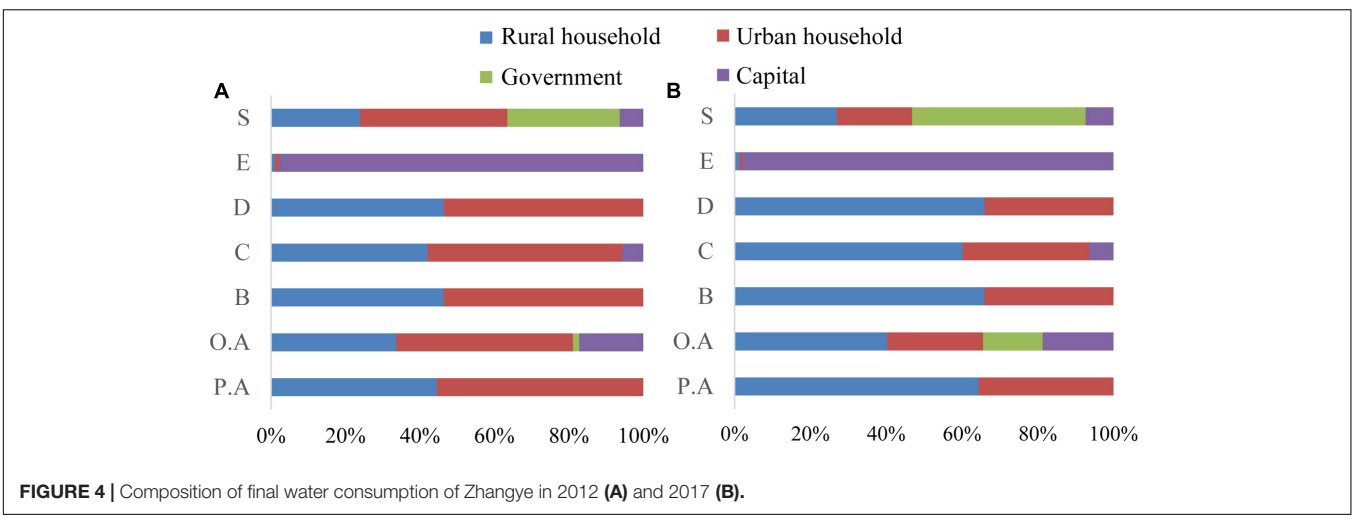

FIGURE 4 | Composition of final water consumption of Zhangye in 2012 **(A)** and 2017 **(B)**.

that of other sectors. Furthermore, the direct consumption coefficients (d) were relatively higher in sectors, including non-metallic minerals mining and dressing, chemical industry, and electricity and heat production and supply, which were regarded as direct water consumption sectors along with agriculture. In contrast, coal mining and dressing sector sectors in the manufacturing industry (other than the chemical industry and petroleum and coking processing sector), and all sectors in construction and service industries were all indirect water consumption-dominated sectors. Specifically, the service industry rarely consumed water directly. The direct consumption coefficients (d) were less than 1 m^3/yuan in 2012 in service sectors, including finance, real estate, telecommunication, computer and software services, and education, health, cultural, and sporting services. The manufacture of food products and tobacco processing sector was the second-largest water consumption sector after agriculture. It had the highest indirect water consumption coefficient (k) among all sectors with 527.31 m^3/yuan in 2012 and 472.25 m^3/yuan in 2017, accounting for approximately 99% of its total water input coefficient. Besides, the indirect consumption coefficients (k) were generally higher than the direct consumption coefficients (d) in the construction and service sectors, and coal mining and dressing sectors, accounting for 93.5, 80, and 86% of their total water input coefficients (t), respectively. These sectors consumed water mainly from intermediate inputs of products and services and were regarded as indirect water consumption sectors.

Water consumption intensity in all sectors averagely decreased by 22% in 2017 compared with 2012 (**Table 2**). Specifically, the total water input coefficient (t) of the electricity and heat production and supply sector decreased the most by 58.9%, followed by the non-metallic minerals mining and dressing sector by 50.5%. As the largest water consumption sector, the total water input coefficient (t) of planting decreased by 30.3%. Conversely, the direct consumption coefficients (d) of the service industry increased significantly by 1.5 times, and water consumption intensity in wholesale and retail trade services and accommodation and food-serving services increased by 17.6 and 25.2%, respectively. Although total water consumption intensity decreased, some indirect water consumption coefficients (k) still increased in sectors, including the chemical industry, coal mining and dressing, metallic ore mining and dressing, and metal smelting and pressing. These sectors alleviated their own water stress by increasing intermediate inputs from other sectors. Our results showed that water utilization efficiency in most of the sectors in Zhangye has increased. However, direct water consumption intensity in the service industry was increasing with its gradual increasing proportion in economic industries, which has restricted the water utilization efficiency in the service industry.

Analysis of water resources consumption from the viewpoint of the consumer side showed that household consumption was the major pathway for final consumption in Zhangye (**Figure 4**). Households accounted for 80.6 and 86.4% of total final consumption in 2012 and 2017, respectively, and consumed the total water from planting, mining, and electricity, heat, gas, and water supply industries. The proportion of urban and rural household consumption in final consumption changed from 5:3 in 2012 to 4:5 in 2017 with the rapid urbanization. Therefore, the structure of water consumption from households converted from rural dominant to urban dominant. Water consumption from the capital was dominant in the construction industry, accounting for 98% of sectoral output. Additionally, water consumption from the capital was also distributed in non-planting agriculture, manufacturing (such as general and special-purpose machinery), and service (such as telecommunication, computer, and software services) industries. The government consumed water (59%) mostly in the non-planting agricultural sector. It was also the major pathway for final consumption in public utility sectors, including public management and social organization, transport, storage and post services, and education, health, cultural, and sporting services. However, the proportion of water consumption by the government decreased from 5% in 2012 to 2% in 2017, which was occupied to the increasing household consumption.

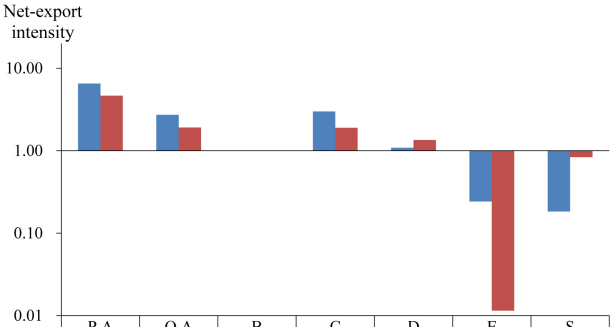

	P.A	O.A	B	C	D	E	S
2012	6.53	2.72	-2.82	3.00	1.08	0.24	0.18
2017	4.64	1.91	-16.75	1.90	1.34	0.01	0.84

FIGURE 5 | Net export intensity of virtual water of different sectors in Zhangye in 2012 and 2017. Positive value represents net exports, while negative value represents net imports.

Virtual Water Trade and Sectoral Transfer

Regional trade of virtual water in Zhangye was generally in the direction of net exports (**Figure 5**). We calculated the proportion of net flows to local water consumption to represent the intensity of the virtual water trade. Virtual water net-export sectors accounted for most of the economic industries of Zhangye. Specifically, the intensity of virtual water net exports was greater than 1 in agriculture, manufacturing, and electricity, heat, gas, and water supply industries. Virtual water net exports were higher than local consumption in these industries due to a large amount of water consumption and commodity exports, especially in the manufacture of food products and the tobacco processing sector. However, virtual water trade in coal mining and dressing, and most manufacturing sectors like non-metallic mineral products sector was in the direction of virtual water net imports with high external dependence on water utilization. From 2012 to 2017, the virtual water net import intensity in the mining industry (especially coal mining and dressing sector) has increased by 4.9 times with a higher external dependence. Moreover, the intensity of virtual water net exports in most sectors has declined

TABLE 3 | Sectoral transfer of virtual water of Zhangye in 2017.

Industry code	A	B	C	D	E	S	Net outputs
A	0.000	−0.002	5.003	−0.014	0.080	0.157	5.224
B	0.002	0.000	0.097	0.014	0.017	−0.002	0.128
C	−5.003	−0.097	0.000	−0.036	0.232	0.088	−4.815
D	0.014	−0.014	0.036	0.000	0.011	0.048	0.095
E	−0.080	−0.017	−0.232	−0.011	0.000	−0.029	−0.370
S	−0.157	0.002	−0.088	−0.048	0.029	0.000	−0.261
Net inputs	−5.224	−0.128	4.815	−0.095	0.370	0.261	0.000

except for service and electricity, heat, gas, and water supply industries. The direction of virtual water trade has even changed from net imports to net exports in service sectors, including finance, accommodation, and food-serving services, scientific research and technical services, and education, health, cultural, and sporting services. This indicates the increasing output value and export advantages in the service industry. Although the tendency of virtual water net exports in Zhangye has been alleviated over the past 5 years, it was still much higher than local consumption. Virtual water outflows hidden in products and services will continue to exacerbate water scarcity in Zhangye.

Some basic sectors have provided virtual water through intermediate inputs of products and services to support economic industries. We analyzed virtual water transfer among different industrial sectors in Zhangye based on the sectoral transfer matrix (**Table 3**). Virtual water net output sectors were commonly basic for social development, especially in agriculture, mining, and electricity, heat, gas, and water supply industries, whereas others were net input sectors. Virtual water transfer between agriculture and manufacturing industries was the largest (5×10^8 m^3) in 2017, which was 91.8% of the total net transfer due to plenty of intermediate inputs from agriculture to the manufacture of food products and the tobacco processing sector. Another major source of virtual water transfer was the electricity, heat, gas, and water supply industry, where 50.2% of water output was provided to the service industry in 2017. Additionally, the mining industry has exported virtual water to manufacturing and construction industries and received it from the service industry through infrastructure services and financing and technical support. However, since construction and service were indirect water consumption industries, they received virtual water from various sectors and depended on more intermediate products and services of manufacturing (62.9%) and agriculture (60.0%) industries, respectively.

The Trend of Crop Water Requirement Under SSP-RCP Scenarios

Crop water requirement per unit area (ET_c) of wheat and maize had an incremental potential under the foreseeable climate change scenarios (**Figure 6**). In the historical years, ET_{wheat} and ET_{maize} increased from 1980 to 2000, then decreased from 2000 to 2020. The peak of ET_{wheat} and ET_{maize} were 5.3 and 3.6% higher than that in 1980, respectively. ET_{maize} was approximately 1.5 times that of ET_{wheat} with a widening gap. In the following three decades, compared with the historical

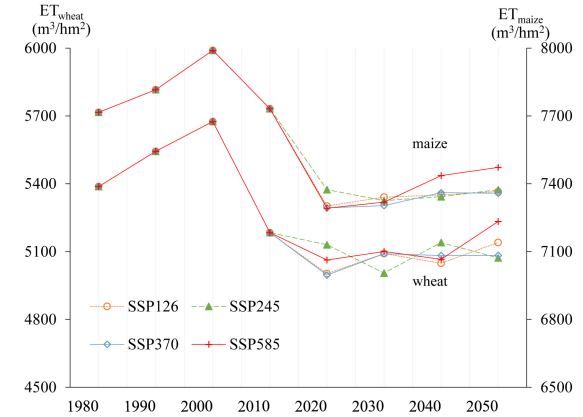

FIGURE 6 | Crop water requirement per unit area (ET_c) of wheat and maize in Zhangye under different SSP-RCP scenarios during 1980–2050.

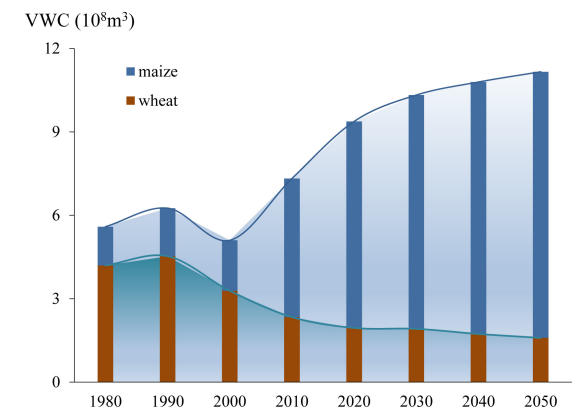

FIGURE 7 | Virtual water content of crops (VWC_c) in Zhangye during 1980–2050.

average level in recent 40 years, ET_{wheat} and ET_{maize} would decrease by nearly 5% with the impacts of climate change under SSP-RCP scenarios. However, ET_{wheat} and ET_{maize} would still show an increasing trend from 2020 to 2050. According to four SSP-RCP scenarios, crop water requirement per unit area varied from high to low and appeared in the scenarios of SSP585 > SSP245 > SSP126 > SSP370. This showed that crop water requirement per unit area would be higher under higher radiation forcing and rapid socioeconomic scenarios. Specifically, ET_{wheat} and ET_{maize} were expected to reach the highest and increase rapidly under the SSP585 scenario. The results indicated that the water requirement intensity of crops would increase after 2020 as the extreme climate events occurred frequently and temperature changed substantially under high fossil-fueled development and radiation forcing level.

The total crop water requirement or virtual water of crops (VWC_c) under the SSP-RCP scenarios was further calculated by time-series forecasted crop yields and water requirement per unit area. It showed that VWC_c was increasing with an annual rate of 8.4% from 1980 to 2050 dominated by maize water consumption

(**Figure 7**). The trend of virtual water content varied similarly under four scenarios. Taking SSP126 scenario as an example, though the crop water requirement per unit area was highest in 2000, the total virtual water content of maize and wheat was the lowest at the same time, then gradually increased since 2000. Specifically, VWC_{wheat} and VWC_{maize} in Zhangye increased by nearly 70% during 1980–2020. As the planting proportion of wheat and maize changed from 117:27 to 61:156 during the past four decades, VWC_{wheat} decreased while VWC_{maize} increased with the adjusted planting areas and yield changes. VWC_{maize} in 2020 had reached 4.3 times that in 1980. During 2020–2050, VWC_{wheat} would continue to decrease by 0.61%, whereas VWC_{wheat} would increase by 0.96% annually. Under predictable climate change in the future, total virtual water content of crops would constantly rise dominated by maize water consumption with an average annual rate of 6.3%, which varies slower than the historical period, but 99.7% higher than that in the year 1980.

Our results showed that crop water requirement in agricultural sectors represented by maize and wheat had been increasing over the past four decades because of cultivation structure adjustment and high intensity of water requirement of maize. According to Zhang et al. (2017), water consumption for maize and wheat planting sectors accounted for more than 60% of total agricultural water consumption of Zhangye in 2012. Therefore, the large-scale maize planting has caused large-scale irrigation water consumption. This kind of agricultural planting pattern with large water consumption made water scarcity of Zhangye increasingly prominent. Although crop water requirement per unit area was predicted lower than historical level, total virtual water content was higher, indicating that long-term climate change makes it possible to increase agricultural irrigation water consumption. If the current agricultural planting pattern with large water consumption continues for long, climate change and large-scale maize planting will exacerbate the risk of water utilization in the future.

CONCLUSION AND DISCUSSION

Global warming has exacerbated the uncertainty of frequent extreme climate events and seriously threatened sustainable water utilization. The irrational water utilization structure of the socioeconomic system in Zhangye made local water scarcity prominent. In this study, we applied the IO model to analyze water consumption and virtual water linkages among different economic sectors and used CROPWAT model to estimate future crop water requirement under different SSP-RCP scenarios for an agriculture-dominated region Zhangye. Based on the IO analysis, we found that planting sector was the largest water consumption sector dominated by direct consumption in all economic industries of Zhangye. Others consumed water mainly from intermediate products and services, especially in sectors including manufacture of food products and tobacco processing, coal mining and dressing, construction, and service. Water consumption intensity in most sectors decreased from 2012 to 2017 except service industry restricted by its higher direct water consumption. On the side of final consumption, changing household behavior of water consumption was essential to improve water utilization efficiency. Economic industries of Zhangye obviously relied on sectors with higher outputs of virtual water, including agriculture, mining, and electricity, heat, gas, and water supply. Nevertheless, the amount of virtual water net exports was much higher than that of local consumption. By using CROPWAT model combined with future climate data, we found that water requirement per unit area of maize and wheat reached the highest in 2000 and would increase after 2020, especially in SSP585 scenario. Under long-term climate change scenarios, the high intensity of water requirement and large-scale planting of maize would increase crop water requirement in agricultural sectors.

Our study extends the previous study that water intensity and final consumption are major factors of virtual water transfer in China (Wang et al., 2021). Specifically, the result of sectoral water consumption intensity decreasing during 2012–2017 indicates the increasing water utilization efficiency in economic industries. This was mainly driven by the effective water-saving measures in agriculture, electricity production and supply, and non-metallic minerals mining and dressing sector. Recently, it can be inferred that the total amount control of water resources and the constraints from industrial water quota of Zhangye have played an important role in improving sectoral water management. As for final consumption, household consumption is the major pathway for final consumption; thus, household behavior of saving water can effectively guide production and business activities. We also consider that both high intensity of virtual water net exports and the increasing tendency of agricultural water consumption will exacerbate water scarcity of Zhangye currently and even in the future, and are detrimental to tackle with climate risks. This finding is consistent with the existing view that water resources distribute unevenly with virtual water outflows more in water-scarce region (Deng et al., 2021; Zhai et al., 2021). Such water consumption structure is abnormal and needs to be improved through regional trade. Additionally, we calculated virtual water content of maize and wheat based on CROPWAT model, which was 32.5% lower than that of the total water consumption in maize and wheat planting sectors by using MRIO model (Zhang et al., 2017). This confirms that the result of virtual water content is reasonable to reflect water consumption of the two agricultural subsectors to a certain extent. Crop water requirement per unit area depends on regional climatic conditions and crop varieties; moreover, virtual water content of crops is also affected by agricultural material inputs, irrigation intensity, planting arrangement, and cropland management measures. Our analysis showed that under SSP-RCP scenarios crop water requirement per unit area would be lower than historical level, but virtual water content of crops would be higher. This indicates that scientific management measures and technical means are expected to reduce virtual water content effectively and benefit for climate change adaptation in agricultural sectors.

We further propose several implications for water resources adaptive management of Zhangye. Our findings revealed different characteristics of water consumption in various industries, which is helpful to make differentiated strategies for

industrial structure transformation. Zhangye is an agriculture-dominated city; thus, agriculture has great water-saving potential and should take more responsibility. This can reduce both the highest amount of direct water consumption in agriculture and indirect water consumption in manufacture of food products and tobacco processing sector. Specifically, the planting proportion of maize and other high-water-consumptive crops should be appropriately reduced through cultivation structure adjustment. Agricultural irrigation efficiency can be promoted by improving irrigation and water conservancy and applying water-saving technologies. In 2017, water-saving irrigation area of Zhangye was 1,873 km^2, reaching the highest level in Gansu Province. Micro-irrigation and low-pressure pipe irrigation have been used to increase water-saving irrigation area by 59.5%, but spray irrigation, drip irrigation, and canal anti-seepage have not been widely applied, which are expected to reduce per unit irrigation area by nearly 30% referring to the existing water-saving irrigation demonstration. Then, water resources saved in agriculture can be reasonably used in the secondary and tertiary industries through water rights trading. For example, saved water in agricultural irrigation can be replaced for industrial production. Additionally, an extended producer responsibility guides producers to select upstream raw materials with lower water consumption and environmental pollution as intermediate inputs. Then, excessive water consumption of intermediate products can be avoided that was provided by basic industries like agriculture, and electricity, heat, gas, and water supply. As for the development in mining and most manufacturing sectors, it will not exacerbate local water consumption directly due to their net import direction of virtual water trade. In spite of this, they should focus more on reducing water environment pollution and discharge during production activities. Construction and service industries have lower water consumption but smaller scale in economic industries of Zhangye. Our analysis showed an incremental developing tendency in service industry that was reflected by the rising intensity of water consumption and virtual water net exports. Service industry should further develop toward the structure of resource saving and technical innovation by improving production technology and management modes.

Zhangye has met unprecedented opportunities and developing moments from the belt and road to make better use of both domestic and international markets and resources. Our analysis of virtual water trade indicated that adopting virtual water strategy rationally is important to transform the unbalanced situation of increasing exports of virtual water flow and local water scarcity. Therefore, taking measures to build a sustainable virtual water trade pattern will help alleviate the contradiction of local water supply and demand. Specifically, in the economic industries of Zhangye, most sectors export more virtual water than they import, especially in agriculture, manufacturing, and electricity, heat, gas, and water supply industries. It is obvious that most of the products produced in these sectors are water intensive. In the view of regional trade, on the one hand, the pattern of virtual water trade can be adjusted by reducing exports and increasing imports of water-intensive products like crops, processed food, and energy supply. On the other hand, while optimizing industrial structure to develop the scale of secondary and tertiary industries, international market should also be broadened to expand the exported competitive advantage of service industry with high economic added value. Moreover, considering that most economic industries consumed water indirectly, the industrial demand for water-intensive products and services can be transferred outside the region by promoting imports of intermediate products and services, including crops and energy supply. As the first pilot of water-saving cities in China, Zhangye has conducted active exploration in water resources allocation, water rights trading, and water saving and intensive utilization. However, facing the increasingly local water scarcity and serious threat from climate change, adaptive water resources management is necessary to change the focus of water management from resources themselves to adaptability improvement of social and economic systems (Jin et al., 2020). Our implications are expected to promote optimal allocation of water resources and contribute to the high-quality development of the water-saving city Zhangye. Although our analysis improved the understanding of virtual water consumption and transfer among sectors and future crop water requirement changes in Zhangye, there are several limitations that require future research. One of the limitations in our study is that specific direction of virtual water trade in Zhangye has not been described due to the lack of universal methods and comprehensive data for MRIO tables at city level. Using gravity models combined with field survey data to reveal internal trade relationships of virtual water may help improve our research (Zheng et al., 2021). Another limitation is that for future virtual water estimation under different climate change scenarios we only consider the agricultural sectors. However, climate change is a complex system that affects more than just water utilization for agriculture. In spite of this, our findings of agricultural crop water requirement can nevertheless be extended to water consumption tendency in the socioeconomic system as agriculture is the largest water consumption sector. Consequently, our findings recommend that effective measures can help alleviate the increasing water scarcity and realize adaptive management of water resources in Zhangye. It further motivates research on response mechanism of water utilization and management to future climate change. Our research provides significant reference for sustainable utilization of water resources and high-quality development of Zhangye under the background of climate change mitigation and adaptation.

DATA AVAILABILITY STATEMENT

The raw data supporting the conclusions of this article will be made available by the authors, without undue reservation.

AUTHOR CONTRIBUTIONS

ZL and YW contributed to conception and design of the study. YW organized the database and wrote the first draft of the manuscript. ZL and HW performed the analysis and wrote sections of the manuscript. All authors contributed to manuscript revision, read, and approved the submitted version.

FUNDING

This research was financially supported by the Young Scientists Fund of the National Natural Science Foundation of China (Grant No. 71804175), the NSFC-Yunnan Joint Fund Key Support Project (Grant No. U2102208), and the Major Program of the National Natural Science Foundation of China (Grant No. 41890824).

REFERENCES

Allan, J. A. (1998). Virtual water: a strategic resource global solutions to regional deficits. *Groundwater* 36, 545–546. doi: 10.1111/j.1745-6584.1998.tb02825.x

Arunrat, N., Pumijumnong, N., Sereenonchai, S., Chareonwong, U., and Wang, C. (2020). Assessment of climate change impact on rice yield and water footprint of large-scale and individual farming in Thailand. *Sci. Total Environ.* 726:137864. doi: 10.1016/j.scitotenv.2020.137864

Arunrat, N., Sereenonchai, S., Chaowiwat, W., and Wang, C. (2022). Climate change impact on major crop yield and water footprint under CMIP6 climate projections in repeated drought and flood areas in Thailand. *Sci. Total Environ.* 807:150741. doi: 10.1016/j.scitotenv.2021.150741

Bocchiola, D., Nana, E., and Soncini, A. (2013). Impact of climate change scenarios on crop yield and water footprint of maize in the Po valley of Italy. *Agric. Water Manage.* 116, 50–61. doi: 10.1016/j.agwat.2012.10.009

Chapagain, A. K., Hoekstra, A. Y., and Savenije, H. H. (2006). Water saving through international trade of agricultural products. *Hydrol. Earth Syst. Sci.* 10, 455–468. doi: 10.5194/hess-10-455-2006

Deng, C., Zhang, G., Li, Z., and Li, K. (2020). Interprovincial food trade and water resources conservation in China. *Sci. Total Environ.* 737:139651. doi: 10.1016/j.scitotenv.2020.139651

Deng, J., Li, C., Wang, L., Yu, S., Zhang, X., and Wang, Z. (2021). The impact of water scarcity on Chinese inter-provincial virtual water trade. *Sustain. Prod. Consum.* 28, 1699–1707. doi: 10.1016/j.spc.2021.09.006

Deng, X., and Zhao, C. (2015). Identification of water scarcity and providing solutions for adapting to climate changes in the Heihe River Basin of China. *Adv. Meteorol.* 2015:279173. doi: 10.1155/2015/279173

Dong, H., Geng, Y., Fujita, T., Fujii, M., Hao, D., and Yu, X. (2014). Uncovering regional disparity of China's water footprint and inter-provincial virtual water flows. *Sci. Total Environ.* 500, 120–130. doi: 10.1016/j.scitotenv.2014.08.094

Du, R., Zheng, X., Tian, L., Liu, K., Qian, L., Wu, Q., et al. (2021). A study on drivers of water consumption in China from a complex network perspective. *Front. Phys.* 9:769420. doi: 10.3389/fphy.2021.769420

Eyring, V., Bony, S., Meehl, G. A., Senior, C. A., Stevens, B., Stouffer, R. J., et al. (2016). Overview of the Coupled Model Intercomparison Project Phase 6 (CMIP6) experimental design and organization. *Geosci. Model Dev.* 9, 1937–1958. doi: 10.5194/gmd-9-1937-2016

Feng, K., Hubacek, K., Pfister, S., Yu, Y., and Sun, L. (2014). Virtual scarce water in China. *Environ. Sci. Technol.* 48, 7704–7713. doi: 10.1021/es500502q

Gain, A. K., and Wada, Y. (2014). Assessment of future water scarcity at different spatial and temporal scales of the Brahmaputra River Basin. *Water Resour. Manage.* 28, 999–1012. doi: 10.1007/s11269-014-0530-5

Huang, J., Qin, D., Jiang, T., Wang, Y., Feng, Z., Zhai, J., et al. (2019). Effect of fertility policy changes on the population structure and economy of China: from the perspective of the shared socioeconomic pathways. *Earth Future* 7, 250–265. doi: 10.1029/2018EF000964

Islam, K. N., Kenway, S. J., Renouf, M. A., Wiedmann, T., and Lam, K. L. (2021). A multi-regional input-output analysis of direct and virtual urban water flows to reduce city water footprints in Australia. *Sust. Cities Soc.* 75:103236. doi: 10.1016/j.scs.2021.103236

Jin, G., Deng, X., Zhao, X., Guo, B., and Yang, J. (2018). Spatiotemporal patterns in urbanization efficiency within the Yangtze River Economic Belt between 2005 and 2014. *J. Geogr. Sci.* 28, 1113–1126. doi: 10.1007/s11442-018-1545-2

Jin, G., Shi, X., Zhang, L., and Hu, S. (2020). Measuring the SCCs of different Chinese regions under future scenarios. *Renew. Sustain. Energy Rev.* 130:109949. doi: 10.1016/j.rser.2020.109949

Karim, R., Tan, G., Ayugi, B., Babaousmail, H., and Liu, F. (2020). Evaluation of historical CMIP6 model simulations of seasonal mean temperature over Pakistan during 1970–2014. *Atmosphere* 11:1005. doi: 10.3390/atmos11091005

Li, M., Cao, X., Liu, D., Fu, Q., Li, T., and Shang, R. (2022). Sustainable management of agricultural water and land resources under changing climate and socio-economic conditions: a multi-dimensional optimization approach. *Agric. Water Manage.* 259:107235. doi: 10.1016/j.agwat.2021.107235

Li, Y., Zhang, Z., and Shi, M. (2019). What should be the future industrial structure of the Beijing-Tianjin-Hebei city region under water resource constraint? An inter-city input-output analysis. *J. Clean Prod.* 239:118117. doi: 10.1016/j.jclepro.2019.118117

Lim Kam Sian, K. T. C., Wang, J., Ayugi, B. O., Nooni, I. K., and Ongoma, V. (2021). Multi-decadal variability and future changes in precipitation over southern africa. *Atmosphere* 12:742. doi: 10.3390/atmos12060742

Liu, X., Shi, L., Engel, B. A., Sun, S., Zhao, X., Wu, P., et al. (2020). New challenges of food security in Northwest China: water footprint and virtual water perspective. *J. Clean Prod.* 245:118939. doi: 10.1016/j.jclepro.2019.118939

Long, A., Yu, J., He, X., Deng, X., Su, S., Zhang, J., et al. (2021). Linking local water consumption in inland arid regions with imported virtual water: approaches, application and actuators. *Adv. Water Resour.* 151:103906. doi: 10.1016/j.advwatres.2021.103906

O'Neill, B. C., Oppenheimer, M., Warren, R., Hallegatte, S., Kopp, R. E., Pörtner, H. O., et al. (2017). IPCC reasons for concern regarding climate change risks. *Nat. Clim. Change* 7, 28–37. doi: 10.1038/nclimate3179

Pedersen, J. S. T., Santos, F. D., van Vuuren, D., Gupta, J., Coelho, R. E., Aparício, B. A., et al. (2021). An assessment of the performance of scenarios against historical global emissions for IPCC reports. *Glob. Environ. Change* 66:102199. doi: 10.1016/j.gloenvcha.2020.102199

Qasemipour, E., Abbasi, A., and Tarahomi, F. (2020). Water-saving scenarios based on input–output analysis and virtual water concept: a case in Iran. *Sustainability* 12:818. doi: 10.3390/su12030818

Qasemipour, E., and Abbasi, A. (2019). Virtual water flow and water footprint assessment of an arid region: a case study of South Khorasan province. *Iran. Water* 11:1755. doi: 10.3390/w11091755

Rosenzweig, C., Elliott, J., Deryng, D., Ruane, A. C., Müller, C., Arneth, A., et al. (2014). Assessing agricultural risks of climate change in the 21st century in a global gridded crop model intercomparison. *Proc. Natl. Acad. Sci. U. S. A.* 111, 3268–3273. doi: 10.1073/pnas.1222463110

Sandström, V., Lehikoinen, E., and Peltonen-Sainio, P. (2018). Replacing imports of crop based commodities by domestic production in Finland: potential to reduce virtual water imports. *Front. Sustain. Food Syst.* 12:67. doi: 10.3389/fsufs.2018.00067

Shi, C., and Zhan, J. (2015). An input–output table based analysis on the virtual water by sectors with the five northwest provinces in China. *Phys. Chem. Earth. Parts A/B/C* 79, 47–53. doi: 10.1016/j.pce.2015.03.004

Simpkins, G. (2017). Progress in climate modelling. *Nat. Clim. Change* 7, 684–685. doi: 10.1038/nclimate3398

Wada, Y., and Bierkens, M. F. (2014). Sustainability of global water use: past reconstruction and future projections. *Environ. Res. Lett.* 9:104003. doi: 10.1088/1748-9326/9/10/104003

Wang, F., Cai, B., Hu, X., Liu, Y., and Zhang, W. (2021). Exploring solutions to alleviate the regional water stress from virtual water flows in China. *Sci. Total Environ.* 796:148971. doi: 10.1016/j.scitotenv.2021.148971

Wang, H., Wang, W. J., Wang, L., Ma, S., Liu, Z., Zhang, W., et al. (2022). Impacts of future climate and land use/cover changes on water-related ecosystem services in Changbai mountains, Northeast China. *Front. Ecol. Evol.* 10:854497. doi: 10.3389/fevo.2022.854497

Wang, L., Zhang, J., Shu, Z., Wang, Y., Bao, Z., Liu, C., et al. (2022). Evaluation of the ability of CMIP6 global climate models to simulate precipitation in the Yellow River Basin China. *Front. Earth Sci.* 9:751974. doi: 10.3389/feart.2021.751974

Wang, S., and Wei, Y. (2019). Water resource system risk and adaptive management of the Chinese Heihe River Basin in Asian arid areas. *Mitig. Adapt. Strateg. Glob Change* 24, 1271–1292. doi: 10.1007/s11027-019-9839-y

Wu, F., Bai, Y., Zhang, Y., and Li, Z. (2017). Balancing water demand for the Heihe River basin in Northwest China. *Phys. Chem. Earth. Parts A/B/C* 101, 178–184. doi: 10.1016/j.pce.2017.07.002

Xu, M., and Li, C. (2020). *Application of the Water Footprint: Water Stress Analysis and Allocation*. Singapore: Springer.

Zhai, Y., Bai, Y., Shen, X., Ji, C., Zhang, T., and Hong, J. (2021). Can grain virtual water flow reduce environmental impacts? Evidence from China. *J. Clean Prod.* 314:127970. doi: 10.1016/j.jclepro.2021.127970

Zhang, C., and Anadon, L. D. (2014). A multi-regional input–output analysis of domestic virtual water trade and provincial water footprint in China. *Ecol. Econ.* 100, 159–172. doi: 10.1016/j.ecolecon.2014.02.006

Zhang, X., Liu, J., Zhao, X., Yang, H., Deng, X., Jiang, X., et al. (2019). Linking physical water consumption with virtual water consumption: methodology, application and implications. *J. Clean Prod.* 228, 1206–1217. doi: 10.1016/j.jclepro.2019.04.297

Zhang, Y., Zhou, Q., and Wu, F. (2017). Virtual water flows at the county level in the Heihe River Basin. *China. Water* 9:687. doi: 10.3390/w9090687

Zhang, Z., Yang, H., and Shi, M. (2016). Spatial and sectoral characteristics of China's international and interregional virtual water flows–based on multi-regional input–output model. *Econ. Syst. Res.* 28, 362–382. doi: 10.1080/09535314.2016.1165651

Zhao, X., Yang, H., Yang, Z., Chen, B., and Qin, Y. (2010). Applying the input-output method to account for water footprint and virtual water trade in the Haihe River basin in China. *Environ. Sci. Technol.* 44, 9150–9156. doi: 10.1021/es100886r

Zheng, H., Többen, J., Dietzenbacher, E., Moran, D., Meng, J., Wang, D., et al. (2021). Entropy-based Chinese city-level MRIO table framework. *Econ. Syst. Res.* 1–26. doi: 10.1080/09535314.2021.1932764

Zheng, H., Zhang, Z., Zhang, Z., Li, X., Shan, Y., Song, M., et al. (2019). Mapping carbon and water networks in the north China urban agglomeration. *One Earth* 1, 126–137. doi: 10.1016/j.oneear.2019.08.015

Zheng, X., Huang, G., Liu, L., Zheng, B., and Zhang, X. (2020). A multi-source virtual water metabolism model for urban systems. *J. Clean Prod.* 275:124107. doi: 10.1016/j.jclepro.2020.124107

Zhuo, L., Mekonnen, M. M., and Hoekstra, A. Y. (2016). Consumptive water footprint and virtual water trade scenarios for China — With a focus on crop production, consumption and trade. *Environ. Int.* 94, 211–223. doi: 10.1016/j.envint.2016.05.019

Conflict of Interest: The authors declare that the research was conducted in the absence of any commercial or financial relationships that could be construed as a potential conflict of interest.

Publisher's Note: All claims expressed in this article are solely those of the authors and do not necessarily represent those of their affiliated organizations, or those of the publisher, the editors and the reviewers. Any product that may be evaluated in this article, or claim that may be made by its manufacturer, is not guaranteed or endorsed by the publisher.

frontiers | Frontiers in Environmental Science

ORIGINAL RESEARCH
published: 03 June 2022
doi: 10.3389/fenvs.2022.900908

Quantifying Carbon Sequestration Service Flow Associated with Human Activities Based on Network Model on the Qinghai-Tibetan Plateau

Qingbo Wang[1], Shiliang Liu[1], Fangfang Wang[1], Hua Liu[1], Yixuan Liu[1], Lu Yu[1], Jian Sun[2], Lam-Son Phan Tran[3] and Yuhong Dong[4]*

[1]State Key Laboratory of Water Environment Simulation, School of Environment, Beijing Normal University, Beijing, China, [2]Institute of Geographical Sciences and Natural Resources Research, Chinese Academy of Sciences, Beijing, China, [3]Institute of Genomics for Crop Abiotic Stress Tolerance, Department of Plant and Soil Science, Texas Tech University, Lubbock, TX, United States, [4]Research Institute of Forestry, Chinese Academy of Forestry, Key Laboratory of Tree Breeding and Cultivation of State Forestry Administration, Beijing, China

The flow of ecosystem services between regions as a result of the mismatch of supply and demand has increasingly become a new research focus. Clarifying the spatial regularity of ecosystem service flow is of great significance for realizing regional sustainable development and improving human well-being. This study applied a network model to map the interregional carbon flow based on the supply and demand of carbon sequestration service, and the driving effect of various driving factors was further analyzed. The results showed that the demand for carbon sequestration service on the Qinghai-Tibet Plateau increased steadily from 2000 to 2019, resulting in an increasingly significant difference between supply and demand with more than 20 million tons. In the carbon sequestration service flow network, the number of defined deficit nodes increased to 22 in 2010, but decreased to 21 in 2019. The interrupted edges continued to increase to 16, and the network density dropped to 0.022. The carbon sequestration service flow network on the northeastern parts of the Qinghai-Tibet Plateau was severely damaged. With the high-quality development of animal husbandry, the impact of grazing intensity on the difference between the supply and demand of carbon sequestration service has been weakened. When urbanization reached a certain level, the driving effects of urbanization and agricultural activities increased significantly. The study provided a reference for the use of network models to analyze ecosystem service flow, and provided a theoretical basis and data support for local ecological management decisions.

Keywords: Carbon Sequestration, Supply and demand, network model, Spatial flow, Geographical detector

OPEN ACCESS

Edited by:
Lei Deng,
Northwest A&F University, China

Reviewed by:
Jianjun Cao,
Northwest Normal University, China
Xinzhu Zheng,
China University of Petroleum, China

****Correspondence:***
Shiliang Liu
shiliangliu@bnu.edu.cn

Specialty section:
This article was submitted to Environmental Informatics and Remote Sensing, a section of the journal Frontiers in Environmental Science

Received: *21 March 2022*
Accepted: *17 May 2022*
Published: *03 June 2022*

Citation:
Wang Q, Liu S, Wang F, Liu H, Liu Y, Yu L, Sun J, Tran L-SP and Dong Y (2022) Quantifying Carbon Sequestration Service Flow Associated with Human Activities Based on Network Model on the Qinghai-Tibetan Plateau. Front. Environ. Sci. 10:900908. doi: 10.3389/fenvs.2022.900908

1 INTRODUCTION

Since the concept of 'ecosystem service' was put forward in the 1970s (Holdren and Ehrlich, 1974; Westman, 1977), it has been continuously developed through further study and evaluation by many scholars (Costanza et al., 1997; Daily, 1997). The widely accepted definition refers to the benefits that humans derive from ecosystems. These benefits are classified as the supply services that provide food, freshwater, production and living materials, cultural services that promote spiritual pleasure and

civilized development, support services, and regulation services that maintain the operation and development of the ecosystems (Millennium Ecosystem Assessment, 2005). Carbon sequestration service is an important regulation service that plays an important role in slowing down the rise of atmospheric CO_2 concentration, regulating global climate, and maintaining global carbon balance, which captures carbon in atmosphere through the carbon sequestration function of ecosystems and fixes the captured carbon to offset part of the CO_2 emitted by humans into the atmosphere (Yang et al., 2019; Zhai et al., 2021). However, as population growth and economic development have led to the increase in the demand for carbon resources (Adams et al., 2020), resource consumption and ecological damage have far exceeded the tolerance of the ecosystem, seriously affecting the sustainability of carbon resources (Abbasi et al., 2021). Ecosystem carbon sequestration service have become one of the most concerned focuses in the ecosystem service research.

As a hotspot and Frontier of ecological research, the study of ecosystem services has been continuously deepened in recent decades. The initial studies were conducted from the ecological perspective, focusing more on the structure, processes and functions of ecosystem (Kremen et al., 2007; Reiss et al., 2009). Some researchers conducted dynamic evaluation of ecosystem services through model simulation (Yapp et al., 2010; Robards et al., 2011), while others estimated the value of different types of ecosystem services in different regions from the perspective of ecological economics (Kontogianni et al., 2010; Zander and Straton, 2010). However, it was difficult to put forward scientific management policies only for ecosystem services supply without considering whether human's demand for ecosystem services has been met. Therefore, in recent years, more and more attention has been paid to the study of the supply and demand of ecosystem services and their balance. Kroll et al. (2012) quantified and mapped the supply and demand of three essential provisioning services, energy, food, and water, along the rural–urban gradient of the eastern German region by using land use, soil, climate, population, energy consumption and other data. Burkhard et al. (2012) constructed a matrix linking spatially explicit biophysical landscape units to ecosystem service supply and demand, and used remote sensing, land survey and socio-economic data to analyze the spatial pattern of ecosystem service supply and demand and their balance. Yang et al. (2012) analyzed the balance between the supply and demand of grain, oil and meat production services in the Yellow River Basin based on county-level statistical data, and visualized the spatial data. These studies demonstrated the spatial mismatch between the supply and demand of ecosystem services, which meant the ecosystem services provided by the region were not used to meet the needs of human society in the same region. In consequence, it is necessary to study the whole process of ecosystem services from generation to use, and clarify the flow process from supply to demand, so as to determine the impact on the human well-being.

Ecosystem service flow, defined as the movement of services from supply areas to benefit areas, can establish a spatio-temporal connection between the supply and demand of ecosystem services (Schirpke et al., 2019a). Therefore, clarifying the transmission path and flow of the ecosystem services is conducive to improving the accuracy of ecosystem service assessment. The formation of services flow mainly depends on the spatial heterogeneity of factors such as ecosystem structure, habitat condition, utilization degree, and the increasing demand of human beings at different levels is the fundamental driving force of ecosystem service flow (Azam and Mohsen, 2021). The direction and intensity of service flow reflect the regional differences in the level of social and economic development (Zank et al., 2016). At present, the research on ecosystem service flow mainly focused on the construction of the theoretical framework (Maass et al., 2005; Palomo et al., 2013), the analysis of service value (Turner et al., 2012; Wang et al., 2021), and spatial correlation analysis of supply and demand (Serna-Chavez et al., 2014). Although it was clear that the source and sink of ecosystem services need to go through a process of spatial flow, the existing studies have not accurately described the flow. Despite the difficulties, research needs to be continued. Only in this way can we accurately link the supply and demand of ecosystem services and provide a scientific basis for scientific and reasonable management policies.

Networks are composed of nodes that represent specific objects, and edges that represent relations between nodes, which can depict many systems that emphasize linkages between components and dynamics (Reza et al., 2021). To date, the network model has been widely used in the field of ecosystem service. For instance, Dee et al. (2017) proposed that using meta-networks to assess how drivers and management actions will impact ES directly and indirectly. Field and Parrott (2017) constructed a conceptual schematic of the multi-ES network to assess landscape connectivity and resilience. In addition, network model had great potential in ecosystem service flow research. Wang et al. (2020) demonstrated the effectiveness of the network model in mapping ESF by constructing a freshwater service flow network for the Yanhe watershed in China. Using networks to identify and regard the supply and demand of ecosystem services as the starting point and end point of the spatial flow can support connectivity assessment, determine the service flow transmission path and help identify spatial and temporal changes (Feurer et al., 2021). The ecosystem services network can assist in making ecological protection decisions by identifying where ecosystem services is most or least connected, and which nodes and edges are the most important.

The Qinghai-Tibetan Plateau has unique ecological significance not just for the natural ecosystems, but also for human society. As an important geographic and ecological unit, the changes in the ecosystems of the Qinghai-Tibet Plateau have a significant impact on the global environment. For the purposes of this study, we adapted the definition of ecosystem service flow from Bagstad et al. (2013) as the transmission of carbon from ecosystems to humans with a spatio-temporal connection between carbon supply and benefit areas. Therefore, the aims of this study were to: 1) quantify and map the spatio-temporal patterns on the supply and demand of carbon sequestration service from 2000 to 2019; 2) construct the carbon sequestration service flow network on the Qinghai-Tibet Plateau; 3) analyze the driving factors of difference between

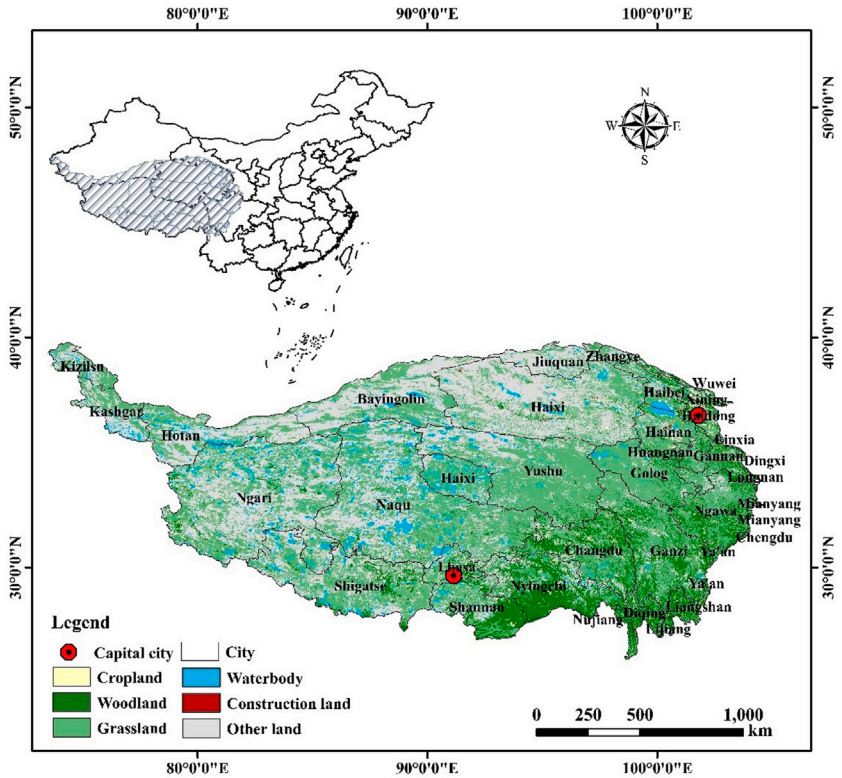

FIGURE 1 | Study area.

supply and demand of carbon sequestration service and discuss implications for resource management. The study contributed to a better understanding of the objective laws governing spatial flow of carbon sequestration service in regional ecosystems as well as providing theoretical basis and data support for regional carbon management, which was critical to the ecological management and sustainable development of the Qinghai-Tibet Plateau.

2 DATA SOURCES AND METHODS

2.1 Study Area

The Qinghai-Tibet Plateau (QTP) is located in the Southwest China (73°18′E~104°46′E, 26°00′N~39°46′N) (**Figure 1**) and is the world's largest and most unique geographical unit, accounting for about 26.8% of the land area in China. With an average altitude of more than 4000 m, it is known as the "third pole" of the Earth. The region belongs to a typical continental plateau climate area with low air temperature, strong solar radiation and distinct dry and rainy seasons. The mean annual precipitation ranges from 415 to 515 mm, and the mean annual temperature varies from -2.2 to 0°C. Precipitation and average annual temperature decline from the southeast to the northwest of the Plateau. As one of the most important agricultural and pastoral areas in China, the QTP is abundant in grassland resources, accounting for 50.43% of the country's total grassland area. The average annual carbon storage reaches 37.61 Pg C, accounting for 63.2% of the total grassland carbon storage in China, which is vital to maintain ecological security of China and the global carbon cycle (Li et al., 2019).

Administratively, the Qinghai-Tibetan Plateau covers six provinces including Xinjiang, Gansu, Qinghai, Tibet, Yunnan and Sichuan. Since 1949, the population has grown rapidly. By the end of 2019, the total population has reached 26.85 million. The expansion of agriculture and animal husbandry in recent decades has deteriorated grassland ecosystems and increased greenhouse gas emissions, contributing to global climate change (Liu et al., 2021). Increasingly intense human activities have led to the degradation of the ecosystems and the continuous loss of biodiversity on the QTP, and the further decline in the supply of ecosystem services on the Plateau. The demand for ecosystem services has increased with the acceleration of urbanization. The trend of mismatches between ecosystem service supply and demand became increasingly serious (Sun et al., 2020).

2.2 Data Sources

The basic data used in this study includes the following: 1) NPP data is derived from the MODIS data of the National Aeronautics and Space Administration (NASA) with a spatial resolution of 500 m. 2) Land use data are interpreted by Landsat TM and provided by the Data Center for Resources and Environmental Sciences, Chinese Academy of Sciences (RESDC). 3) Wind direction data is obtained from the European Center for

TABLE 1 | Data type and sources.

Data category	Items	Spatial Resolution	Data sources
Remote sensing data	NPP	500 m	MODIS data of the National Aeronautics and Space Administration (NASA) (https://search.earthdata.nasa.gov/search/)
	Land use	500 m-	Data Center for Resources and Environmental Sciences, Chinese Academy of Sciences (RESDC) (http://www.resdc.cn)
Meteorological data	Wind direction	the European Center for Medium-Term Weather Forecast (https://www.ecmwf.int/)	
Socioeconomic data	Population GDP Chemical fertilizer Pesticide Plastic film Crop area Agricultural machinery Irrigated area Livestock Crop yield Meat production Electricity Heat	county-level	Statistical yearbooks of Qinghai, Sichuan, Yunnan, Tibet, Xinjiang and Gansu in 2001, 2011 and 2020; National economic and social development bulletin of some counties in 2001, 2011 and 2020

TABLE 2 | Datasets for mapping the supply and demand of carbon sequestration.

	Metrics	Unit	Data
Supply (CS)	Carbon sequestration	10^4 t C	MODIS NPP data
Demand (CD)	Carbon emission	10^4 t C	Population; Agricultural production activities; Animal husbandry; Electricity; Heat

Medium-Term Weather Forecast and is further counted to the dominant wind direction in the past 20 years according to the city scale. 4) Socioeconomic data include population of urban and rural residents, GDP, agricultural material input, crop yield, livestock production, electricity, heat, etc. The data is derived from statistical yearbooks and national economic and social development bulletins of various provinces and cities. Specific data sources are shown in **Table 1**.

2.3 Materials and Methods

2.3.1 Supply and Demand of Carbon Sequestration Service

The study referred to the evaluation of ecosystem services by Zhang et al. (2021) and Bagstad et al. (2014), using vegetation net primary productivity (NPP) to characterize the supply of carbon sequestration service, and using regional carbon emissions as the demand of carbon sequestration service, as shown in **Table 2**.

NPP can reflect not only the productivity of vegetation in the natural environment, but also the surface carbon sequestration capacity. Therefore, NPP can characterize the supply of carbon sequestration service (CS) (Jia et al., 2014). Carbon emitters are users of carbon sequestration service, so carbon emissions provide one possible measure for the demand of carbon sequestration service (CD) required to offset anthropogenic emissions (Bagstad et al., 2014). The carbon emissions calculated in this study mainly come from the production and life of residents, as shown in **Eq. 1**.

$$\mathrm{CD} = \left(C_{pop} + C_{agri} + C_{anim} + C_{elec} + C_{heat}\right) \times \frac{12}{44} \tag{1}$$

where C_{pop}, C_{agri}, C_{anim}, C_{elec}, C_{heat} refer to the carbon emission from residential breathing, agriculture, animal husbandry, electricity and heat, respectively. The specific calculation formula is as follows:

$$C_{pop} = p \times l \times 365 \tag{2}$$

where C_{pop} is calculated by the number of population p and the CO_2 emission per person per day l with the value of 0.75 kg (Zhang et al., 2021).

Agricultural production activities consume large amount of chemical fertilizers, pesticides and other products, which brings about large carbon emissions (Li M. et al., 2021). This study calculated the carbon emissions from chemical fertilizers, pesticides, agricultural plastic film, machinery, and irrigation as follows.

$$C_{agri} = N_f \times EF_f + N_P \times EF_P + N_m \times EF_m + N_e \times EF_e + N_a \times EF_a + N_{ir} \times EF_{ir} \tag{3}$$

TABLE 3 | Specific values of carbon emission factors (Xu et al., 2018).

	Carbon emission factors	Unit	Value
EF_f	Chemical fertilizers	kg/kg	0.896
EF_p	Pesticides	kg/kg	4.934
EF_m	Agricultural plastic film	kg/kg	5.18
EF_e	Crops	kg/hm^2	16.47
EF_a	Agricultural machinery	kg/kW	0.18
EF_{ir}	Irrigation	kg/hm^2	20.476

In the formula, N_f, N_P, N_m, N_e, N_a and N_{ir} represent the amount of chemical fertilizer used (kg), the amount of pesticide used (kg), the amount of agricultural plastic film used (kg), the area planted with crop (hm2), the power of agricultural machinery (kW) and the irrigated area (hm2), respectively. EF_f, EF_P, EF_m, EF_e, EF_a and EF_{ir} indicate the carbon emission factors of chemical fertilizers, pesticides, agricultural plastic film, crops, agricultural machinery, and irrigation, respectively. The specific values are listed in **Table 3**.

Animal husbandry carbon emissions are greenhouse gas emissions which are expressed in terms of equivalent carbon dioxide, including methane emissions from animal enteric fermentation and methane and nitrous oxide emissions from animal manure management (Guo et al., 2017). The formula is calculated as follows:

$$C_{anim} = \sum \left(EF_{CH_4,enteric,i} \times N_i + EF_{CH_4,manure,i} \times N_i\right) \times 28 + \sum \left(EF_{N_2O,manure,i} \times N_i\right) \times 265 \quad (4)$$

In the formula, $EF_{CH_4,enteric,i}$ and $EF_{CH_4,manure,i}$ are the methane emission factors for animal enteric fermentation and manure management, respectively, in kg/head/a. $EF_{N_2O,manure,i}$ is the nitrous oxide emission factor for animal manure management, and the unit is kg/head/a; N_i is the annual breeding amount of the i-th animal, with the unit being head/a. 28 and 265 are the global warming potential factors of methane and nitrous oxide on one-hundred-year time scale (Xu et al., 2018).

$$C_{elec} = N_{elec} \times EF_{elec} \quad (5)$$

where C_{elec} is calculated by electricity consumption N_{elec} and power emission factor EF_{elec} (Yang et al., 2019).

$$C_{heat} = N_{heat} \times EF_{heat} \quad (6)$$

where C_{heat} is calculated by the total amount of steam and hot water heating N_{heat} and emission factors EF_{heat} with value of 0.11 (Zhang et al., 2021).

To better analyze the supply-demand situation of carbon sequestration service at city scale, the difference between supply and demand of carbon sequestration (DSDC) in different cities was calculated on the Qinghai-Tibet Plateau. The formula is as follows:

$$\mathrm{DSDC}_i = CS_i - CD_i \quad (7)$$

where CS_i and CD_i are carbon sequestration service supply and demand in each city i, respectively. DSDC_i is the result of difference between the supply and demand of carbon sequestration service in each city i. When $\mathrm{DSDC}_i > 0$, it indicates that the city belongs to the ecological surplus area, where the supply of carbon sequestration service is greater than the demand. Conversely, the city belongs to the ecological deficit area if the supply is less than the demand.

2.3.2 The Network Model of Carbon Sequestration Service Flow

In the carbon sequestration service flow model of this study, we assumed that the carbon sequestration service flow connected the supply area with the demand area through the atmospheric circulation in a closed system, without considering the obstacles and resistance in the process (Schirpke et al., 2019b). The demand for carbon sequestration service in different spatial locations could be offset by the remaining supply amount in other regions. The flow path of the carbon sequestration service was mainly determined according to the dominant wind direction, and the flow source and sink was mainly determined according to the DSDC. This study used a network model to reveal the carbon sequestration service flow between different cities on the Qinghai-Tibet Plateau. The specific construction process is shown in **Figure 2**.

Step 1. Defining nodes. We set the central point of each city on the Qinghai-Tibet Plateau as the node of carbon sequestration service flow network. These central points with geographic coordinates (longitude and latitude) were extracted by ArcGIS 10.2. The weight of each node was calculated as the difference between carbon sequestration supply and demand (DSDC) in each city. If the weight was greater than 0, it meant supply could meet local demand, and therefore we defined this node as a surplus node. Otherwise, we defined it as a deficit node. Different color of nodes was utilized to indicate the surplus or deficit state. The size and shade of the nodes represented the degree of surplus or deficit.

Step 2. Defining edges. We defined carbon sequestration service flows from one location to another as edges between nodes. Referring to Wang et al. (2020), we assumed that the remaining carbon flows from node to node accumulating following the dominant wind direction, as flows satisfied the demand of each local area and moved among cities. On the contrary, if one node was in deficit and its carbon sequestration demand was still not met with supplements from other nodes, then the node would have no surplus for the adjacent node, implying that the edge was interrupted. It was worth noting that this assumption was based on accumulation, i.e., flowing until the final accumulation of carbon sequestration supply could not meet the demand. We used the black lines with arrows to represent connecting edges, indicating that there was carbon sequestration service flow on the path, and the red dashed lines represented the interrupted edges, that is, there was no service flow along the path.

Step 3. Constructing the network. Based on the definitions and assumptions above, we visualized the carbon sequestration flow network using Gephi software (https://gephi.org/) with Geo layout that accurately determined the spatial location of nodes

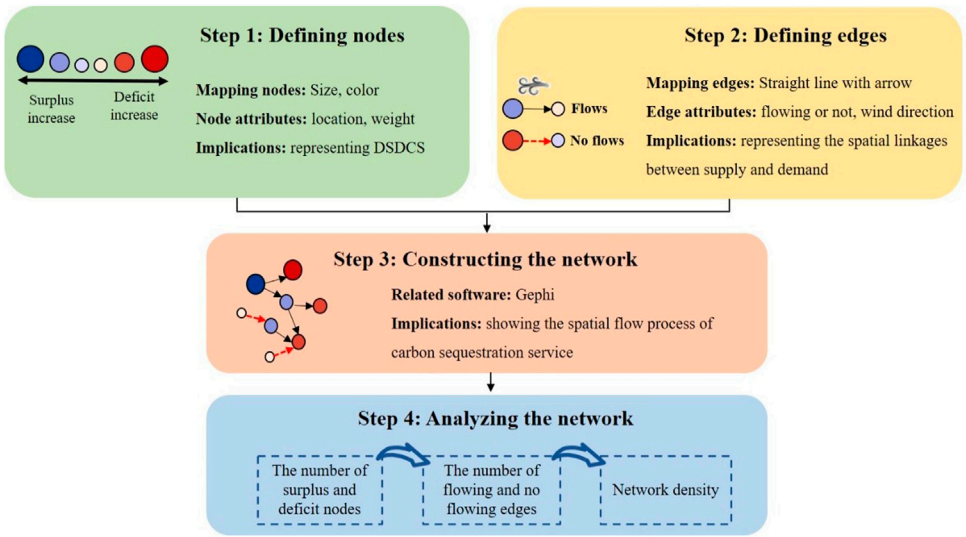

FIGURE 2 | Summary of the steps for mapping the service flow network.

TABLE 4 | Description of the driving force factors.

Variables	Data description	Unit	Cited reference
DSDC	Differences between supply and demand of carbon sequestration	10^4 t C	-
UR	Urbanization rate	%	Wang and Zhao (2018)
GDP	GDP per capita	Yuan	Kumar and Muhuri (2019)
POP	Population density	Person/km^2	Qin et al. (2019); Yang et al. (2015)
AI	Total output of crops	10^4 t	Yang et al. (2022)
GI	Total output of beef and mutton	10^4 t	Wachiye et al. (2022)
PCL	Proportion of construction land	%	Tian and Zhou (2019) Svirejeva-Hopkins and Schellnhuber (2008)

according to their geographic coordinates, making the spatial flow paths between nodes more intuitive.

Step 4. Analyzing the network. After constructing the carbon sequestration service flow network, we analyzed the network properties from three aspects. Firstly, we used the number of surplus and deficit nodes to analyze the spatial match between supply and demand of carbon sequestration services (Chen et al., 2019). Secondly, we distinguished the potential and actual supply of carbon sequestration service according to the number of flowing and no flowing edges. The carbon sequestration supply of one node may come from two parts that are the node itself and the carbon sequestration flows. Therefore, although the carbon sequestration supply of some nodes cannot meet demand under the static spatial matching, they can meet the demand because of service flows. Specifically, in the carbon sequestration service flow network, nodes starting with solid lines indicated that supply actually can meet the demand, while nodes starting with dotted lines indicated that the supply actually cannot meet the demand. Finally, we calculated network density to analyze the connectivity of the carbon sequestration service flow network. The greater the network density, the better the overall connectivity of the network.

2.3.3 The Driving Force of the Difference Between Supply and Demand of Carbon Sequestration Service

Considering data accessibility and scientific analysis, urbanization, socioeconomic conditions, demographic factors, agricultural activities, grazing intensity, and urban conditions were selected as the driving force for DSDC. Referring to previous studies, six possible indicators were used to represent these driving forces. The detailed variables are described in **Table 4**.

The geographical detector model was used to detect spatial stratified heterogeneity and reveal the main driving forces of variables (Wang and Xu, 2017). Specifically, it measures a dependent variable (Y) while also testing the coupling between Y and X (explanatory variable) and investigates the effect of the interaction between two explanatory variables on Y. There are several advantages of this method. First, the dependent and explanatory variables do not require linear assumptions. Second, the explanatory variables do not need to consider the multiple collinearity problem. Third, the method can

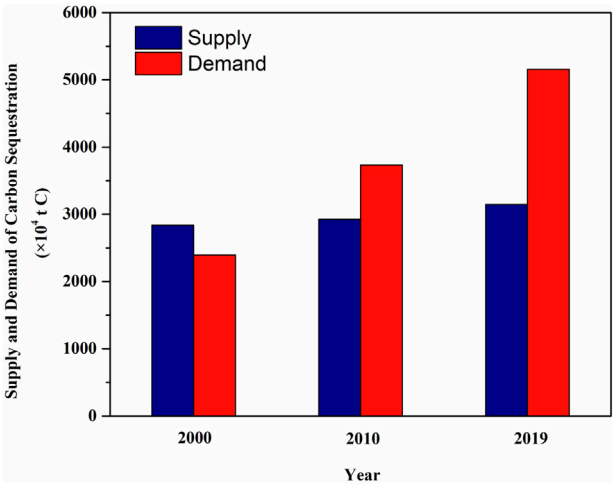

FIGURE 3 | The carbon sequestration supply and demand from 2000 to 2019.

determine how the interaction of two explanatory variables affects the dependent variable.

The module of factor detection is commonly applied to determine a specific geographical factor. Quantification of the spatial distribution difference is performed by comparing the total variance of this indicator in different regions and the entire region. The formula of q value is given below:

$$q = 1 - \frac{\sum_{h=1}^{L}\sum_{i=1}^{N_h}\left(Y_{hi} - \bar{Y}_h\right)^2}{\sum_{i-1}^{N}\left(Y_i - \bar{Y}^2\right)} = 1 - \frac{\sum_{h=1}^{L} N_h\sigma_h^2}{N\sigma^2} = 1 - \frac{SSW}{SST} \quad (8)$$

$$SST = \sum_{i}^{N}\left(Y_I - \bar{Y}\right)^2 = N\sigma^2 \quad (9)$$

$$SSW = \sum_{h=1}^{L}\sum_{i}^{N_h}\left(Y_{hi} - \bar{Y}_h\right)^2 = \sum_{h=1}^{L} N_h\sigma_h^2 \quad (10)$$

where $q \in [0, 1]$ and is the percentage of explanation for factor X to variable Y (the larger the q value, the higher the interpretation of variable Y by factor X); h = 1,. . .,L is the layer of explanatory variable X; N_h and N are the numbers of cities in layer h and the total district, respectively; Y_i and Y_{hi} denote the value of unit i in the population and layer h, respectively; σ_h^2 and σ^2 are the variance in the h layer and the region, respectively; SST is the total sum of squares; and SSW is the within sum of squares. Generally, $q \geq 0.3$ indicates that there is a comparatively strong driving force on DSDC (Chen et al., 2018). The value for q satisfies the non-central F distribution and non-centrality λ are calculated as follows:

$$F = \frac{N - L}{L - 1}\frac{q}{1 - q} \sim F(L - 1, N - L; \lambda) \quad (11)$$

$$\lambda = \frac{1}{\sigma^2}\left[\sum_{h=1}^{L}\bar{Y}_h^2 - \frac{1}{N}\left(\sum_{h=1}^{L}\sqrt{N_h Y_h}\right)^2\right] \quad (12)$$

where λ is a non-central parameter and $\bar{Y}_h$ is the mean of layer h. The significance of q can be checked by **Eq. (11) (12)** in Geodetector software

The module of interaction detection quantifies the interaction between two explanatory factors X_1 and X_2 by comparing the q value of factors X_1 and X_2 with the interaction q value ($X_1 \cap X_2$) to assess whether the factors weaken or enhance one another or are independent of each other. The module of ecological detection compares whether the effects of the two explanatory factors are significantly different by using the F-test (Wang and Xu, 2017).

3 RESULTS

3.1 The Spatio-Temporal Pattern of Carbon Sequestration Service Supply and Demand

The supply of carbon sequestration service on the Qinghai-Tibet Plateau has not changed significantly, which increased from 28.38 million tons in 2000 to 31.45 million tons in 2019. While the demand for large changes increased from 23.95 million tons in 2000 to 51.55 million tons in 2019 (**Figure 3**). It should be noted that the supply of carbon sequestration service exceeded the demand in 2000. However, the supply was less than the demand in 2010 and 2019, and the carbon deficit in 2019 exceeded by 20 million tons.

In terms of the spatial variability, the supply of carbon sequestration service gradually decreased from the southeast to the northwest (**Figure 4**). Especially, the high-supply areas were mainly concentrated on the southern parts of the Qinghai-Tibet Plateau. Compared with that in 2000 and 2010, the supply in the northwestern increased significantly in 2019. Cities with high demand for carbon sequestration service (over two million tons) increased from one in 2000 to five in 2019. Among the cities, Xining and Haidong in Qinghai province had the largest demand for carbon sequestration service, and the demand for Hotan and Kashgar in Xinjiang province has increased significantly.

Figure 5 depicted the differences between the supply and demand of carbon sequestration service in various cities on the Qinghai-Tibet Plateau in 2000, 2010 and 2019. Due to the rapid development of carbon demand, most cities have turned from carbon surpluses to deficits (such as Linxia and Chengdu), or the deficits have increased (such as Yushu and Xining), or the surpluses have weakened (such as Longnan and Shannan). However, there were still cities that have improved. For example, Ganzi and Aba in Sichuan province were in deficit in 2000 and 2010, but they had the carbon surplus in 2019. In terms of spatial distribution, we also discovered that all cities in Qinghai province were in deficit, while three cities in Yunnan province were in carbon surplus.

3.2 The Spatio-Temporal Pattern of the Carbon Sequestration Service Flow Network

According to the nodes and edges defined in Section 2.3.2, we constructed a carbon sequestration service flow network, as shown in **Figure 6**. A total of 37 nodes represented the surplus or deficit status of carbon sequestration service. The results showed that the number of carbon surplus nodes decreased from 20 in 2000 to 15 in 2010, and then increased to 18 in 2019. The number of deficit nodes increased from 17 in 2000 to 22 in 2010, and decreased to 19 in 2019 (**Table 5**).

In 2000, although there were 17 carbon deficit nodes, the transmission of atmospheric circulation through the surrounding

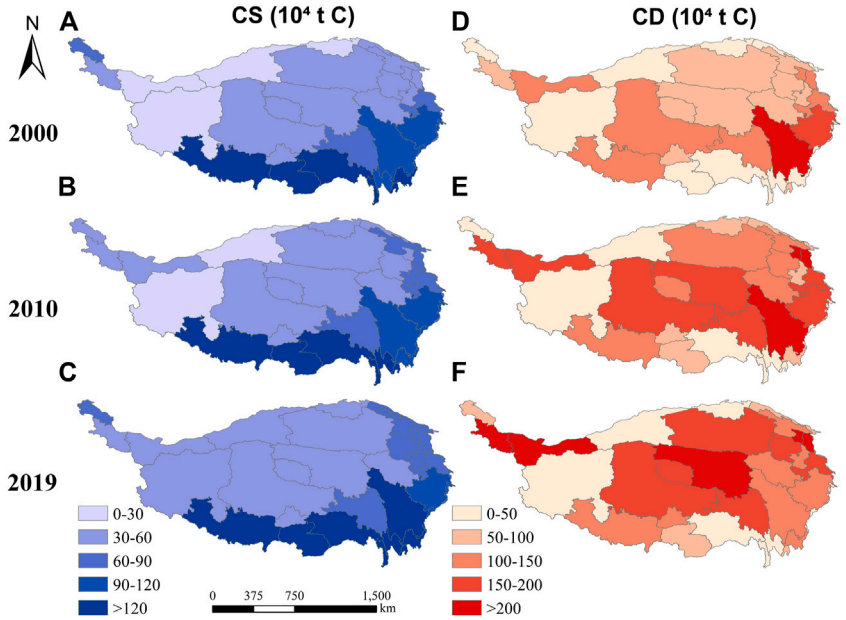

FIGURE 4 | The supply **(A,B,C)** and demand **(D,E,F)** of carbon sequestration service from 2000 to 2019 (CS: the supply of carbon sequestration service, CD: the demand of carbon sequestration service).

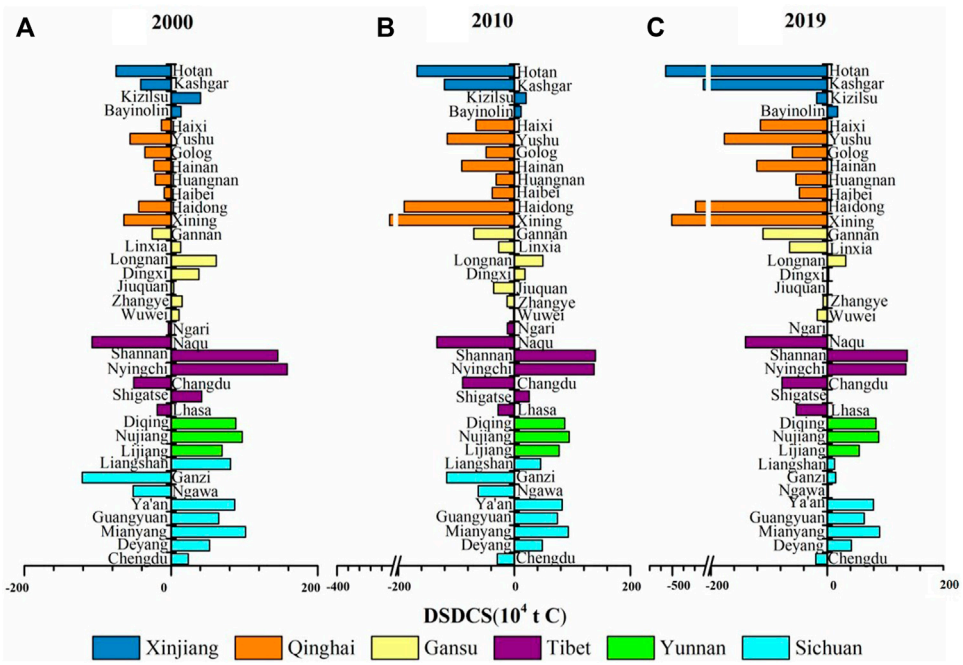

FIGURE 5 | DSDC changes in all cities in 2000 **(A)**, 2010 **(B)**, 2019 **(C)**.

areas kept the carbon sequestration service flow network intact to a certain extent. However, as there was no excess carbon surplus in the central region, a large number of interrupted edges existed in the service flow network. In 2010, the number of interrupted edges reached 14 and the severely damaged parts were concentrated in the northeast of the Qinghai-Tibet Plateau. In 2019, despite the increase in carbon surplus nodes, the number of interrupted edges still increased to 16, which showed that while the shortage of carbon sequestration service in some cities has lessened, it still has not had a positive impact on the entire region.

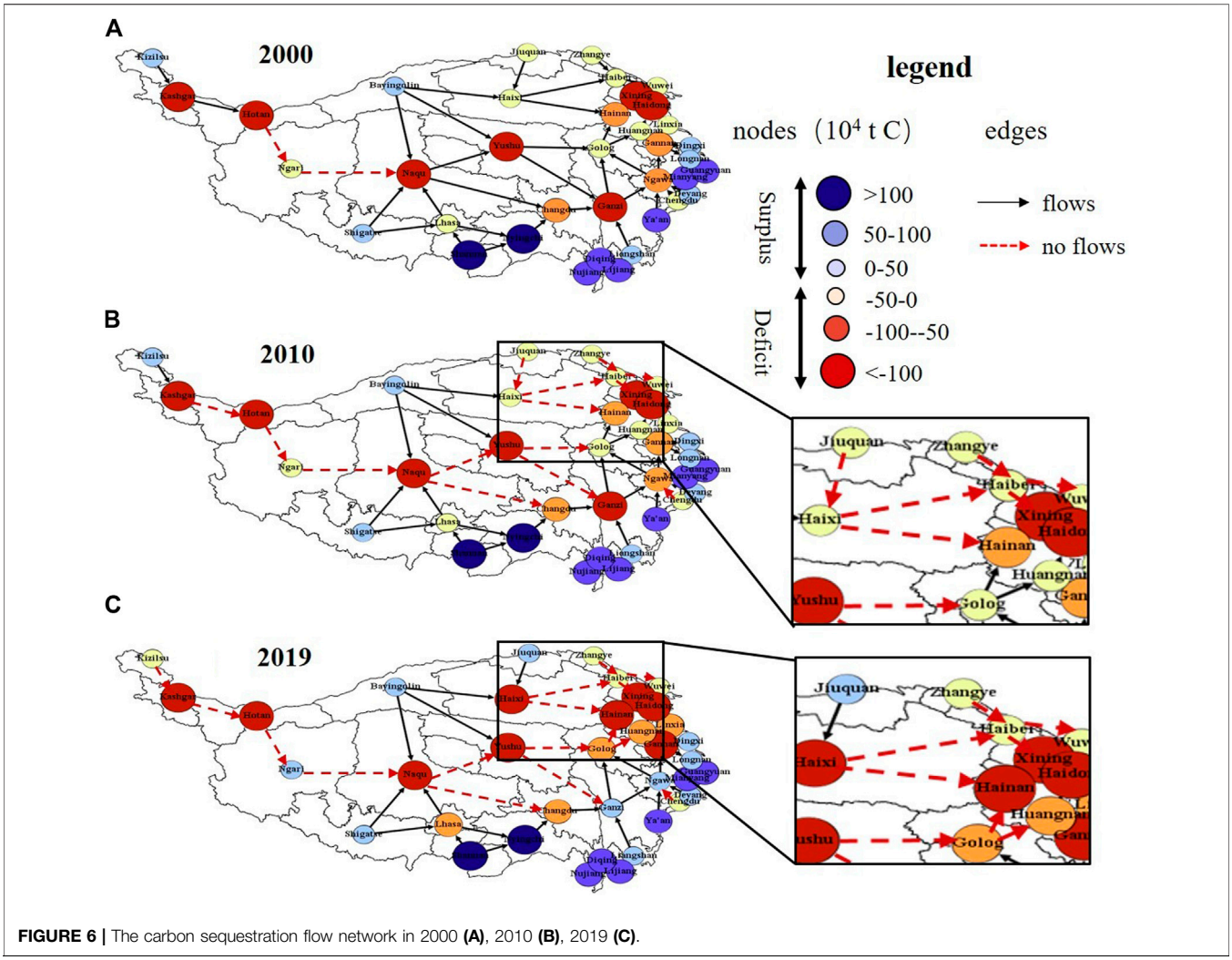

FIGURE 6 | The carbon sequestration flow network in 2000 **(A)**, 2010 **(B)**, 2019 **(C)**.

TABLE 5 | Overall characteristics of service flow network.

Year	Surplus nodes	Deficit nodes	Flow edges	No flow edges	Network density
2000	20	17	43	2	0.032
2010	15	22	31	14	0.023
2019	16	21	29	16	0.022

The network density of the service flow network dropped from 0.032 in 2000 to 0.022 in 2019. It could be seen that the shortage of carbon sequestration service on the Qinghai-Tibet Plateau was still getting worse and the connectivity of the service flow network was declining.

3.3 The Drivers of Supply-Demand Dynamics of Carbon Sequestration Service

We further analyzed the main drivers of the supply-demand dynamics of carbon sequestration service on the Qinghai-Tibet Plateau. The finding revealed that after 2000, the demand of carbon sequestration service became the primary driving force that determined the surplus and deficit of carbon sequestration service in various cities, with its influence rising from 2000 to 2015. Specifically, the percentage of explanation (q value) for carbon supply dropped from 0.536 in 2000 to 0.355 in 2019, and the percentage of explanation (q value) for carbon demand, as another explanatory variable, rose from 0.627 in 2000 to 0.926 in 2019 (**Figure 7A**). This demonstrated that the demand for carbon sequestration service in cities continued to exceed the supply.

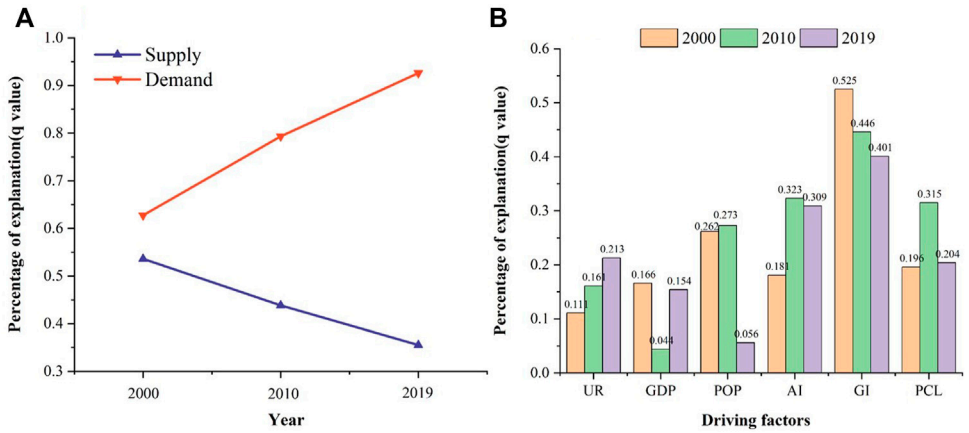

FIGURE 7 | Percentage of explanation (q value) for supply and demand of carbon sequestration service **(A)**; Percentage of explanation (q value) for each driving factor in 2000, 2010 and 2019 **(B)** (UR: urbanization rate, GDP: gross domestic product per capita, POP: population density, AI: agricultural input, GI: grazing intensity, PCL: proportion of construction land).

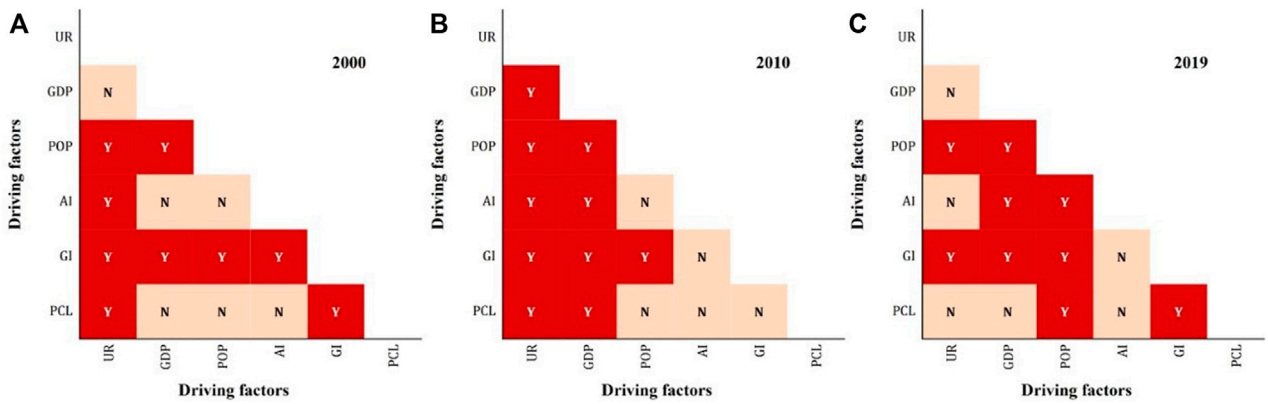

FIGURE 8 | The ecological detector results for driving factors in 2000 **(A)**, 2010 **(B)**, 2019 **(C)** (UR: urbanization rate, GDP: gross domestic product per capita, POP: population density, AI: agricultural input, GI: grazing intensity, PCL: proportion of construction land).

We then investigated the explanatory power of different driving factors for the difference between the supply and demand of carbon sequestration service, as shown in **Figure 7B**. Notably, the factors varied in their ability to explain the DSDC, with some factors having a large impact. Additionally, an ecological detector was employed to identify whether there were significant differences among the influencing factors regarding the spatial distribution of DSDC (**Figure 8**, $p < 0.05$). In 2000, Total output of beef and mutton (GI) (0.525) and Population density (POP) (0.262) had the highest explanatory power, implying that grazing intensity and population density had remarkably prominent impact on DSDC. The results from the ecological detector demonstrated that grazing intensity had a considerably different effect on DSDC than population density. In 2010, GI (0.446) exerted a significant effect on DSDC. Total output of crops (AI) (0.323) and Proportion of construction land (PCL) (0.315) also affected the DSDC. In 2019, the explanatory power of GI (0.401) has declined, but it was still the largest, followed by AI (0.309) and Urban population ratio (UR) (0.213). Furthermore, results from the ecological detector demonstrated that the effects of urbanization rate and proportion of construction land on DSDC were significantly different from those of grazing intensity. The q value of grazing intensity has been decreasing, indicating that the influence of grazing intensity on the DSDC has lessened. The result could be attributed to the high-quality development of animal husbandry in recent years. In contrast, the q values of urbanization rate and agricultural input had increasing trends, indicating that urbanization and agricultural activities had increasing impacts on DSDC. This meant that when evaluating carbon sequestration service in the future, the impact of urban and agricultural development must be taken into consideration.

Finally, we continued to analyze the explanatory power of the interaction between the factors (**Figure 9**). According to **Figure 7B**, the explanatory power of proportion of construction land and urbanization rate in factor detection were relatively low (q = 0.196 and 0.111, respectively).

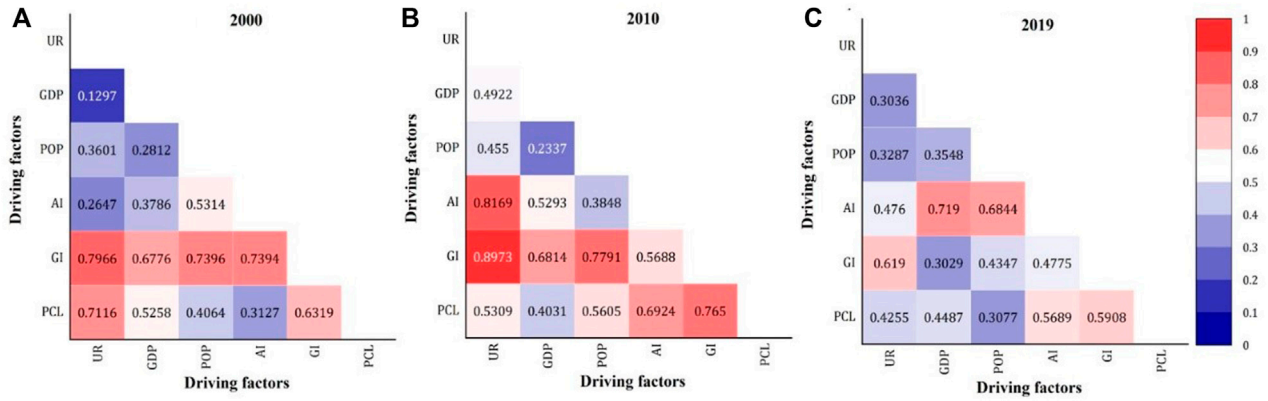

FIGURE 9 | Percentage of explanation (q value) in interaction in 2000 **(A)**, 2010 **(B)**, 2019 **(C)** (UR: urbanization rate, GDP: gross domestic product per capita, POP: population density, AI: agricultural input, GI: grazing intensity, PCL: proportion of construction land).

However, the interaction of urbanization rate with proportion of construction land had stronger explanatory power, indicating that proportion of construction land only had an important influence on DSDC when there was a sufficient level of urbanization development. The explanatory power of factor interaction in 2010 was similar to that in 2000. In 2019, AI and GDP, AI and POP, AI and PCL were found to enhance each other to jointly affect the DSDC. Agricultural input, together with economic development, population density, and the proportion of construction land, have increased the driving force for DSDC. The development of agriculture has surpassed that of animal husbandry, which had a stronger impact on carbon sequestration service and economic development.

4 DISCUSSION

4.1 The Implications for Management of Carbon Sequestration Service

Carbon sequestration service is essential for maintaining the sustainable development of humans and ecosystems (Liu et al., 2018). In this study, we quantified the supply and demand of carbon sequestration service on the Qinghai-Tibetan Plateau. Based on our results, the supply increased slowly from 2000 to 2019, but the demand changed significantly (**Figure 3**). Especially in 2019, the deficit of carbon sequestration service exceeded 20 million tons. If the supply and demand of carbon sequestration service continues to develop at this trend in the following years, we can infer that the deficit on the Qinghai-Tibetan Plateau will be more serious. Therefore, this result illustrates the necessity of strengthening management of carbon sequestration service.

For management of carbon sequestration service, we often need to identify areas with high supply or demand, as well as areas with deficit or surplus of carbon sequestration service, because it is very important for policy making and resource allocation. The supply of carbon sequestration service on the Qinghai-Tibetan Plateau gradually decreased from southeast to northwest. The regions where supply increased from 2000 to 2019 mainly included Ngari, Hotan and eastern Qinghai-Tibetan Plateau (**Figure 4**). It was not only related to the implementation of 'returning farmland to forest and grassland' policy, but also to the remarkable achievements in soil erosion control (Bi et al., 2021; Zinda et al., 2017). The regions with high demand of carbon sequestration service on the Qinghai-Tibetan Plateau were mainly characterized by intense human activities (Xiong et al., 2021; Wang et al., 2022). For example, Xining and Haidong had the largest demand of carbon sequestration service. Hotan and Kashgar in Xinjiang had significant growth in demand (**Figure 4**). Cities with more serious deficit from 2000 to 2019 were Shannan and Yushu, while the difference between supply and demand of carbon sequestration service has improved in Ganzi and Aba in Sichuan province (**Figure 5**). This was primarily due to rich ecological resources and policy conditions in northwest Sichuan to play an important role in emission reduction and carbon sequestration in recent years (Wang et al., 2017). In this study, we constructed a carbon sequestration service flow network based on the data of supply and demand of carbon sequestration service. The results showed that the connectivity of the service flow network has decreased since 2010 (**Figure 6**), especially on the northeastern part of Qinghai-Tibetan Plateau. Our results can help managers to identify the regions where carbon sequestration service can't meet the local demands, and thus develop strategies to reduce emission and allocate resources. We can also found from the results that some cities with deficits benefited from surrounding cities with surpluses. Therefore, the carbon sequestration service flow can help inform ecological compensation policy (Voghera and Giudice, 2020; Zhai et al., 2021).

The shortage of carbon sequestration service was a global problem (Ghosh et al., 2022). Our analysis showed that after 2000 the demand has been the dominant driver determining the surplus and deficit of carbon sequestration service and its influence has been increasing (**Figure 7A**). In this case, it is an effective way to reduce demand as much as possible and improve supply in key areas. These nodes connected with interruption edges should be the main areas of supply replenishment. In addition to increasing

supply, reducing consumption is another important aspect of alleviating service shortages. Our results indicated that the driving force effect of grazing intensity on the DSDC gradually weakened (**Figure 7B**). This was primarily due to the policies implemented in recent years, such as limiting and banning grazing, returning grazing to grassland, and subsidizing ecological rewards. The damage of grazing activities to grassland has been limited to a certain extent (Wang et al., 2019). However, the impact of agricultural activity has increased. In agricultural activities, the transition from traditional agriculture to organic agriculture is conducive to reducing the environmental impact of carbon emissions. However, agricultural mechanization has increased the amount of energy used, and seeding have also produced resource consumption in the process of processing and transportation, both of which has a considerable impact on carbon emissions (Jiang et al., 2020). The impact of urbanization and construction land has also increased (**Figure 7B**). The primary reason for this was that in recent years, with the support of national aid policies, the agglomeration effect of towns on the Qinghai-Tibetan Plateau has been significantly improved, and the urban infrastructure has been gradually improved, accompanied by the transformation of other land use types into construction land, which was bound to affect carbon sequestration service (van Roon, 2012; Li et al., 2021a). We also found that the explanatory power of the interaction between urbanization rate and proportion of construction land exceeded that of the single factor (**Figure 9**). The Qinghai-Tibetan Plateau had a vast territory but a small population. Although the agglomeration effect of towns has significantly increased, urbanization was still in its infancy, and the construction land was still increasing (Tian et al., 2021). Therefore, the following suggestions need to be noted. 1) In the process of future urban construction and economic development, ecological protection should be given priority and ecological security barrier construction will continue to be promoted. 2) The government should make rational plans for land use, and rationally coordinate the use of ecological land, construction land, agricultural land and other functional spaces. 3) The protection of natural forest, grassland and wetland should be strengthened in key areas where carbon sequestration service need to be improved. Meanwhile, the ecological fragile areas affected by construction activities should be restored by measures such as containment protection.

4.2 Limitations and Prospects

Our study with the methodological provided theoretical evidence and support in terms of carbon cycle optimization, planning, and protection in other regions where were also experiencing rapid urbanization. However, our study had also some limitations. To begin with, due to a lack of data, this study only used NPP to illustrate the supply of carbon sequestration service. Future research will pay more attention to the completeness and accuracy of research data. Second, the differences between and within the cities were ignored when analyzing the driving forces. The specific driving analysis should be refined to a county-level scale, accounting for the various driving effects of carbon sequestration service flows between cities. In addition, due to the limitations of the research method, this study only considered carbon sequestration service flow within the Qinghai-Tibet Plateau, and did not discuss carbon sequestration service flow between the marginal counties of the study area and outside the study area. In future research, we will focus on the service flow both inside and outside the study region, as well as a more thorough examination of spatial flow.

5 CONCLUSION

This study quantified the spatial difference between the supply and demand of carbon sequestration service on the Qinghai-Tibet Plateau, simulated the spatial flows of carbon sequestration service and revealed the driving effects of various driving factors on carbon sequestration service, which provided a new idea for the optimization of ecosystem service flow and regional carbon sequestration pattern. In the past 20 years, the demand of carbon sequestration service on the Qinghai-Tibet Plateau has greatly outpaced the supply, resulting in carbon deficits in most cities. The spatial flow was considerably affected, and the density of the carbon sequestration service flow network continued to decline. The spatial disparity between the supply and demand of carbon sequestration service was jointly influenced by a variety of human activities. With the development of urbanization, the influence of grazing has lessened, while the driving influence of agriculture and urbanization rate has gradually increased. The study of ecosystem service supply and demand is conducive to the construction of regional ecological security pattern. Reasonable simulations of ecosystem service flow can effectively alleviate the obvious spatial dislocation between the unbalanced distribution of natural resources and people's consumption needs, so as to focus on the deficit areas that require input of limited human and material resources, and realize the optimal allocation of resources.

DATA AVAILABILITY STATEMENT

Publicly available datasets were analyzed in this study. This data can be found here: https://data.cnki.net/Yearbook/Navi?type = typeandamp;code = A.

AUTHOR CONTRIBUTIONS

QW: conceptualization, writing-original draft preparation, methodology, software.SL: writing-reviewing and editing, validation. FW: writing, resources. HL: data curation, supervision. YL: writing, data curation. LY: writing, resources. JS: formal analysis, supervision. L-SPT: investigation, validation. YD: investigation, methodology.

FUNDING

This study was supported by the Second Scientific Expedition to the Qinghai-Tibet Plateau (No. 2019QZKK0405-05) and National Natural Sciences Foundation of China (No. 41571173).

REFERENCES

Abbasi, K. R., Hussain, K., Redulescu, M., and Ozturk, I. (2021). Does Natural Resources Depletion and Economic Growth Achieve the Carbon Neutrality Target of the UK? A Way Forward towards Sustainable Development. *Resour. Policy* 74, 102341. doi:10.1016/j.resourpol.2021.102341

Adams, S., Adedoyin, F., Olaniran, E., and Bekun, F. V. (2020). Energy Consumption, Economic Policy Uncertainty and Carbon Emissions; Causality Evidence from Resource Rich Economies. *Econ. Analysis Policy* 68, 179–190. doi:10.1016/j.eap.2020.09.012

Azam, K. M., and Mohsen, S. (2021). Investigating Tradeoffs between Supply, Use and Demand of Ecosystem Services and Their Effective Drivers for Sustainable Environmental Management. *J. Environ. Manag.* 289, 112534. doi:10.1016/j.jenvman.2021.112534

Bagstad, K. J., Johnson, G. W., Voigt, B., and Villa, F. (2013). Spatial Dynamics of Ecosystem Service Flows: A Comprehensive Approach to Quantifying Actual Services. *Ecosyst. Serv.* 4, 117–125. doi:10.1016/j.ecoser.2012.07.012

Bagstad, K. J., Villa, F., Batker, D., Harrison-Cox, J., Voigt, B., and Johnson, G. W. (2014). From Theoretical to Actual Ecosystem Services: Mapping Beneficiaries and Spatial Flows in Ecosystem Service Assessments. *Ecol. Soc.* 19 (2), 64. doi:10.5751/es-06523-190264

Bi, W., Wang, K., Weng, B., Yan, D., and Liu, S. (2021). Does the Returning Farmland to Forest Program Improve the Ecosystem Stability of Rhizosphere in Winter in Alpine Regions? *Appl. Soil Ecol.* 165, 104011. doi:10.1016/j.apsoil.2021.104011

Burkhard, B., Kroll, F., Nedkov, S., and Müller, F. (2012). Mapping Ecosystem Service Supply, Demand and Budgets. *Ecol. Indic.* 21, 17–29. doi:10.1016/j.ecolind.2011.06.019

Chen, G., Luo, J., Zhang, C., Jiang, L., Tian, L., and Chen, G. (2018). Characteristics and Influencing Factors of Spatial Differentiation of Urban Black and Odorous Waters in China. *Sustainability* 10, 4747. doi:10.3390/su10124747

Chen, J., Jiang, B., Bai, Y., Xu, X., and Alatalo, J. M. (2019). Quantifying Ecosystem Services Supply and Demand Shortfalls and Mismatches for Management Optimisation. *Sci. Total Environ.* 650, 1426–1439. doi:10.1016/j.scitotenv.2018.09.126

Costanza, R., d'Arge, R., de Groot, R., Farber, S., Grasso, M., Hannon, B., et al. (1997). The Value of the World's Ecosystem Services and Natural Capital. *Nature* 387, 253–260. doi:10.1038/387253a0

Daily, G. C. (1997). *Nature's Services: Societal Dependence on Natural Ecosystems*. Washington, DC: Island Press.

Dee, L. E., Allesina, S., Bonn, A., Eklöf, A., Gaines, S. D., Hines, J., et al. (2017). Operationalizing Network Theory for Ecosystem Service Assessments. *Trends Ecol. Evol.* 32, 118–130. doi:10.1016/j.tree.2016.10.011

Feurer, M., Rueff, H., Celio, E., Heinimann, A., Blaser, J., Htun, A. M., et al. (2021). Regional Scale Mapping of Ecosystem Services Supply, Demand, Flow and Mismatches in Southern Myanmar. *Ecosyst. Serv.* 52, 101363. doi:10.1016/j.ecoser.2021.101363

Field, R. D., and Parrott, L. (2017). Multi-Ecosystem Services Networks: A New Perspective for Assessing Landscape Connectivity and Resilience. *Ecol. Complex.* 32, 31–41. doi:10.1016/j.ecocom.2017.08.004

Ghosh, S., Dinda, S., Chatterjee, N. D., Dutta, S., and Bera, D. (2022). Spatial-Explicit Carbon Emission-Sequestration Balance Estimation and Evaluation of Emission Susceptible Zones in an Eastern Himalayan City Using Pressure-Sensitivity-Resilience Framework: An Approach towards Achieving Low Carbon Cities. *J. Clean. Prod.* 336, 130417. doi:10.1016/j.jclepro.2022.130417

Guo, J., Qi, D., Zhang, N., Sun, L., and Hu, R. (2017). Chinese Greenhouse Gas Emissions from Livestock:Trend and Predicted Peak Value. *J. Agro-Environ. Sci.* 36, 2106–2113. doi:10.11654/jaes.2017-0132

Holdren, J. P., and Ehrlich, P. R. (1974). Human Population and the Global Environment. *Am. Sci.* 62, 282–292.

Jia, X., Fu, B., Feng, X., Hou, G., Liu, Y., and Wang, X. (2014). The Tradeoff and Synergy between Ecosystem Services in the Grain-For-Green Areas in Northern Shaanxi, China. *Ecol. Indic.* 43, 103–113. doi:10.1016/j.ecolind.2014.02.028

Jiang, M., Hu, X., Chunga, J., Lin, Z., and Fei, R. (2020). Does the Popularization of Agricultural Mechanization Improve Energy-Environment Performance in China's Agricultural Sector? *J. Clean. Prod.* 276, 124210. doi:10.1016/j.jclepro.2020.124210

Kontogianni, A., Luck, G. W., and Skourtos, M. (2010). Valuing Ecosystem Services on the Basis of Service-Providing Units: A Potential Approach to Address the 'Endpoint Problem' and Improve Stated Preference Methods. *Ecol. Econ.* 69, 1479–1487. doi:10.1016/j.ecolecon.2010.02.019

Kremen, C., Williams, N. M., Aizen, M. A., Gemmill-Herren, B., LeBuhn, G., Minckley, R., et al. (2007). Pollination and Other Ecosystem Services Produced by Mobile Organisms: A Conceptual Framework for the Effects of Land-Use Change. *Ecol. Lett.* 10, 299–314. doi:10.1111/j.1461-0248.2007.01018.x

Kroll, F., Müller, F., Haase, D., and Fohrer, N. (2012). Rural-Urban Gradient Analysis of Ecosystem Services Supply and Demand Dynamics. *Land Use Policy* 29, 521–535. doi:10.1016/j.landusepol.2011.07.008

Kumar, S., and Muhuri, P. K. (2019). A Novel GDP Prediction Technique Based on Transfer Learning Using CO2 Emission Dataset. *Appl. Energy* 253, 113476. doi:10.1016/j.apenergy.2019.113476

Li, J., Huang, X., Chuai, X., and Yang, H. (2021a). The Impact of Land Urbanization on Carbon Dioxide Emissions in the Yangtze River Delta, China: A Multiscale Perspective. *Cities* 116, 103275. doi:10.1016/j.cities.2021.103275

Li, L., Zhang, Y., Wu, J., Li, S., Zhang, B., Zu, J., et al. (2019). Increasing Sensitivity of Alpine Grasslands to Climate Variability along an Elevational Gradient on the Qinghai-Tibet Plateau. *Sci. Total Environ.* 678, 21–29. doi:10.1016/j.scitotenv.2019.04.399

Li, M., Liu, S., Sun, Y., and Liu, Y. (2021b). Agriculture and Animal Husbandry Increased Carbon Footprint on the Qinghai-Tibet Plateau during Past Three Decades. *J. Clean. Prod.* 278, 123963. doi:10.1016/j.jclepro.2020.123963

Liu, W., Yan, Y., Wang, D., and Ma, W. (2018). Integrate Carbon Dynamics Models for Assessing the Impact of Land Use Intervention on Carbon Sequestration Ecosystem Service. *Ecol. Indic.* 91, 268–277. doi:10.1016/j.ecolind.2018.03.087

Liu, Y., Liu, S., Sun, Y., Wang, F., and Li, M. (2021). Driving Forces of Cultivated Land Evolution in Agro-Pastoral Areas on the Qinghai-Tibet Plateau Based on Ecological Niche Theory. *J. Clean. Prod.* 313, 127899. doi:10.1016/j.jclepro.2021.127899

Maass, J. M., Balvanera, P., Castillo, A., Daily, G. C., Mooney, H. A., Ehrlich, P., et al. (2005). Ecosystem Services of Tropical Dry Forests: Insights from Long-Term Ecological and Social Research on the Pacific Coast of Mexico. *Ecol. Soc.* 10, 17. doi:10.5751/es-01219-100117

Millennium Ecosystem Assessment (2005). *Ecosystems and Human Wellbeing: Synthesis*. Washington: Island Press.

Palomo, I., Martín-López, B., Potschin, M., Haines-Young, R., and Montes, C. (2013). National Parks, Buffer Zones and Surrounding Lands: Mapping Ecosystem Service Flows. *Ecosyst. Serv.* 4, 104–116. doi:10.1016/j.ecoser.2012.09.001

Qin, H., Huang, Q., Zhang, Z., Lu, Y., Li, M., Xu, L., et al. (2019). Carbon Dioxide Emission Driving Factors Analysis and Policy Implications of Chinese Cities: Combining Geographically Weighted Regression with Two-Step Cluster. *Sci. Total Environ.* 684, 413–424. doi:10.1016/j.scitotenv.2019.05.352

Reiss, J., Bridle, J. R., Montoya, J. M., and Woodward, G. (2009). Emerging Horizons in Biodiversity and Ecosystem Functioning Research. *Trends Ecol. Evol.* 24, 505–514. doi:10.1016/j.tree.2009.03.018

Reza, V., Bertanza, G., Sbaffoni, S., and Vaccari, M. (2021). Regional Industrial Symbiosis: A Review Based on Social Network Analysis. *J. Clean. Prod.* 280, 124054. doi:10.1016/j.jclepro.2020.124054

Robards, M. D., Schoon, M. L., Meek, C. L., and Engle, N. L. (2011). The Importance of Social Drivers in the Resilient Provision of Ecosystem Services. *Glob. Environ. Change* 21, 522–529. doi:10.1016/j.gloenvcha.2010.12.004

Schirpke, U., Candiago, S., Egarter Vigl, L., Jäger, H., Labadini, A., Marsoner, T., et al. (2019a). Integrating Supply, Flow and Demand to Enhance the Understanding of Interactions Among Multiple Ecosystem Services. *Sci. Total Environ.* 651, 928–941. doi:10.1016/j.scitotenv.2018.09.235

Schirpke, U., Tappeiner, U., and Tasser, E. (2019b). A Transnational Perspective of Global and Regional Ecosystem Service Flows from and to Mountain Regions. *Sci. Rep.* 9, 6678. doi:10.1038/s41598-019-43229-z

Serna-Chavez, H. M., Schulp, C. J. E., van Bodegom, P. M., Bouten, W., Verburg, P. H., and Davidson, M. D. (2014). A Quantitative Framework for Assessing Spatial Flows of Ecosystem Services. *Ecol. Indic.* 39, 24–33. doi:10.1016/j.ecolind.2013.11.024

Sun, Y., Liu, S., Shi, F., An, Y., Li, M., and Liu, Y. (2020). Spatio-Temporal Variations and Coupling of Human Activity Intensity and Ecosystem Services Based on the Four-Quadrant Model on the Qinghai-Tibet Plateau. *Sci. Total Environ.* 743, 140721. doi:10.1016/j.scitotenv.2020.140721

Svirejeva-Hopkins, A., and Schellnhuber, H.-J. (2008). Urban Expansion and its Contribution to the Regional Carbon Emissions: Using the Model Based on the Population Density Distribution. *Ecol. Model.* 216, 208–216. doi:10.1016/j.ecolmodel.2008.03.023

Tian, Y., Jiang, G., Zhou, D., and Li, G. (2021). Systematically Addressing the Heterogeneity in the Response of Ecosystem Services to Agricultural Modernization, Industrialization and Urbanization in the Qinghai-Tibetan Plateau from 2000 to 2018. *J. Clean. Prod.* 285, 125323. doi:10.1016/j.jclepro.2020.125323

Tian, Y., and Zhou, W. (2019). How Do CO2 Emissions and Efficiencies Vary in Chinese Cities? Spatial Variation and Driving Factors in 2007. *Sci. Total Environ.* 675, 439–452. doi:10.1016/j.scitotenv.2019.04.239

Turner, W. R., Brandon, K., Brooks, T. M., Gascon, C., Gibbs, H. K., Lawrence, K. S., et al. (2012). Global Biodiversity Conservation and the Alleviation of Poverty. *Bioscience* 62, 85–92. doi:10.1525/bio.2012.62.1.13

van Roon, M. R. (2012). Wetlands in The Netherlands and New Zealand: Optimising Biodiversity and Carbon Sequestration during Urbanisation. *J. Environ. Manag.* 101, 143–150. doi:10.1016/j.jenvman.2011.08.026

Voghera, A., and Giudice, B. (2020). Defining a Social-Ecological Performance to Prioritize Compensatory Actions for Environmental Regeneration. The Experimentation of the Environmental Compensation Plan. *Sustain. Cities Soc.* 61, 102357. doi:10.1016/j.scs.2020.102357

Wachiye, S., Pellikka, P., Rinne, J., Heiskanen, J., Abwanda, S., and Merbold, L. (2022). Effects of Livestock and Wildlife Grazing Intensity on Soil Carbon Dioxide Flux in the Savanna Grassland of Kenya. *Agric. Ecosyst. Environ.* 325, 107713. doi:10.1016/j.agee.2021.107713

Wang, C., Li, W., Sun, M., Wang, Y., and Wang, S. (2021). Exploring the Formulation of Ecological Management Policies by Quantifying Interregional Primary Ecosystem Service Flows in Yangtze River Delta Region, China. *J. Environ. Manag.* 284, 112042. doi:10.1016/j.jenvman.2021.112042

Wang, J., and Xu, C. (2017). Geodetector: Principle and Prospective. *Acta Geogr. Sin.* 72, 116–134. doi:10.11821/dlxb201701010

Wang, S., Fan, J., Li, Y., Wu, D., Zhang, Y., and Huang, L. (2019). Dynamic Response of Water Retention to Grazing Activity on Grassland Over the Three River Headwaters Region. *Agric. Ecosyst. Environ.* 286, 106662. doi:10.1016/j.agee.2019.106662

Wang, X., Huang, X., Zhang, X., Yan, Y., Zhou, C., Zhou, J., et al. (2022). Analysis of the Spatio-Temporal Change of Social-Ecological System Coupling: A Case Study in the Qinghai-Tibet Plateau. *Glob. Ecol. Conserv.* 33, e01973. doi:10.1016/j.gecco.2021.e01973

Wang, X., Zhou, M., Li, T., Ke, Y., and Zhu, B. (2017). Land Use Change Effects on Ecosystem Carbon Budget in the Sichuan Basin of Southwest China: Conversion of Cropland to Forest Ecosystem. *Sci. Total Environ.* 609, 556–562. doi:10.1016/j.scitotenv.2017.07.167

Wang, Y., and Zhao, T. (2018). Impacts of Urbanization-Related Factors on CO_2 Emissions: Evidence from China's Three Regions with Varied Urbanization Levels. *Atmos. Pollut. Res.* 9, 15–26. doi:10.1016/j.apr.2017.06.002

Wang, Z., Zhang, L., Li, X., Li, Y., Frans, V. F., and Yan, J. (2020). A Network Perspective for Mapping Freshwater Service Flows at the Watershed Scale. *Ecosyst. Serv.* 45, 101129. doi:10.1016/j.ecoser.2020.101129

Westman, W. E. (1977). How Much Are Nature's Services Worth? *Science* 197, 960–964. doi:10.1126/science.197.4307.960

Xiong, Q., Xiao, Y., Liang, P., Li, L., Zhang, L., Li, T., et al. (2021). Trends in Climate Change and Human Interventions Indicate Grassland Productivity on the Qinghai-Tibetan Plateau from 1980 to 2015. *Ecol. Indic.* 129, 108010. doi:10.1016/j.ecolind.2021.108010

Xu, P., Zhao, Y., Chen, H., Duan, X., Chen, F., and Wang, C. (2018). Dynamic Change of Carbon Source/Sink and Carbon Footprint of Farmland Ecosystem in Jiangsu Province. *Bull. Soil Water Conservation* 38, 238–243.

Yang, H., Wang, X., and Bin, P. (2022). Agriculture Carbon-Emission Reduction and Changing Factors Behind Agricultural Eco-Efficiency Growth in China. *J. Clean. Prod.* 334, 130193. doi:10.1016/j.jclepro.2021.130193

Yang, L., Dong, L., Zhang, L., He, B., and Zhang, Y. (2019). Quantitative Assessment of Carbon Sequestration Service Supply and Demand and Service Flows: A Case Study of the Yellow River Diversion Project South Line. *Resour. Sci.* 41, 557–571. doi:10.18402/resci.2019.03.13

Yang, L., Pan, Y., Cao, X., and Long, X. (2012). Ecosystem Services Supply and consumptionA Case in Yellow River Watershed,China. *J. Arid Land Resour. Environ.* 26, 131–138.

Yang, W., Li, T., and Cao, X. (2015). Examining the Impacts of Socio-Economic Factors, Urban Form and Transportation Development on CO2 Emissions from Transportation in China: A Panel Data Analysis of China's Provinces. *Habitat Int.* 49, 212–220. doi:10.1016/j.habitatint.2015.05.030

Yapp, G., Walker, J., and Thackway, R. (2010). Linking Vegetation Type and Condition to Ecosystem Goods and Services. *Ecol. Complex.* 7, 292–301. doi:10.1016/j.ecocom.2010.04.008

Zander, K. K., and Straton, A. (2010). An Economic Assessment of the Value of Tropical River Ecosystem Services: Heterogeneous Preferences Among Aboriginal and Non-Aboriginal Australians. *Ecol. Econ.* 69, 2417–2426. doi:10.1016/j.ecolecon.2010.07.010

Zank, B., Bagstad, K. J., Voigt, B., and Villa, F. (2016). Modeling the Effects of Urban Expansion on Natural Capital Stocks and Ecosystem Service Flows: A Case Study in the Puget Sound, Washington, USA. *Landsc. Urban Plan.* 149, 31–42. doi:10.1016/j.landurbplan.2016.01.004

Zhai, T., Zhang, D., and Zhao, C. (2021). How to Optimize Ecological Compensation to Alleviate Environmental Injustice in Different Cities in the Yellow River Basin? A Case of Integrating Ecosystem Service Supply, Demand and Flow. *Sustain. Cities Soc.* 75, 103341. doi:10.1016/j.scs.2021.103341

Zhang, X., Wang, X., Cheng, C., Liu, S., and Zhou, C. (2021). Ecosystem Service Flows in Karst Area of China Based on the Relationship between Supply and Demand. *Acta Ecol. Sin.* 41, 3368–3380. doi:10.5846/stxb202005161566

Zinda, J. A., Trac, C. J., Zhai, D., and Harrell, S. (2017). Dual-Function Forests in the Returning Farmland to Forest Program and the Flexibility of Environmental Policy in China. *Geoforum* 78, 119–132. doi:10.1016/j.geoforum.2016.03.012

Conflict of Interest: The authors declare that the research was conducted in the absence of any commercial or financial relationships that could be construed as a potential conflict of interest.

Publisher's Note: All claims expressed in this article are solely those of the authors and do not necessarily represent those of their affiliated organizations, or those of the publisher, the editors and the reviewers. Any product that may be evaluated in this article, or claim that may be made by its manufacturer, is not guaranteed or endorsed by the publisher.

frontiers | Frontiers in Environmental Science

ORIGINAL RESEARCH
published: 13 June 2022
doi: 10.3389/fenvs.2022.908057

Spatiotemporal Variation in Ecological Risk on Water Yield Service *via* Land-Use and Climate Change Simulations: A Case Study of the Ziwuling Mountainous Region, China

*Tiantian Jin, Lingling Yan, Shimei Wang and Jie Gong**

Key Laboratory of Western China's Environmental Systems (Ministry of Education), College of Earth and Environmental Sciences, Lanzhou University, Lanzhou, China

Scientists have paid attention to assessing the change in ecosystem service risk under human activities, yet few works have focused on the water yield risk induced by land-use and climate change. In this study, a framework combining water yield with ecological risk for service enhancement and human adaptation was established. The framework was applied to explore the spatiotemporal variation in water yield service and its ecological risk *via* land-use and climate change scenarios in the Ziwuling Mountainous Region (ZMR), China, using InVEST, CA–Markov, and TOPSIS models. The water yield service decreased from 69.19 mm in 1990 to 47.72 mm in 2017 in the ZMR. The water yield service in the southeast ZMR was larger than that in the northwest. The water yield service risk was high and increased first, then decreased from 1990 to 2017 in the ZMR. The high-risk and higher risk subareas were distributed in the middle and north of the ZMR. The water yield service is the highest under the EC126 scenario (48.09 mm in 2050 and 43.73 mm in 2100) and the lowest under the EP585 scenario (43.52 mm in 2050 and 40.62 mm in 2100). The water yield service risk of the EP558 scenario is the largest one, with an area ratio of the high risk of 83.95% in 2050 and 85.33% in 2100. We suggest developing water-saving agriculture and high-efficiency industrial systems, as well as ecological restoration and integrated forest social–ecological management for risk alleviation, service enhancement, and sustainable development.

Keywords: water yield, spatiotemporal change, ecological risk, scenario analysis, InVEST model, TOPSIS model

OPEN ACCESS

Edited by:
Shiliang Liu,
Beijing Normal University, China

Reviewed by:
Yanxu Liu,
Beijing Normal University, China
Tao Lu,
Chengdu Institute of Biology (CAS), China

****Correspondence:***
Jie Gong
jgong@lzu.edu.cn

Specialty section:
This article was submitted to Environmental Informatics and Remote Sensing, a section of the journal Frontiers in Environmental Science.

Received: *30 March 2022*
Accepted: *02 May 2022*
Published: *13 June 2022*

Citation:
Jin T, Yan L, Wang S and Gong J (2022) Spatiotemporal Variation in Ecological Risk on Water Yield Service via Land-Use and Climate Change Simulations: A Case Study of the Ziwuling Mountainous Region, China. Front. Environ. Sci. 10:908057. doi: 10.3389/fenvs.2022.908057

1 INTRODUCTION

Global climate change, population explosion, and the unreasonable use of natural resources have caused intense pressure and risks to the self-regulation and restoration ability of the ecosystem, which will eventually lead to the loss and degradation of ecosystem services (ESs) (Zhou and Zhao, 2013; Li et al., 2019; Gacheno and Amare, 2021). Managing and avoiding ecological risks is an essential prerequisite for achieving harmonious development between humankind and nature (Chen F. et al., 2019). Ecosystem service and ecological risk assessment have become the focus of global environmental change and sustainable development (Chen T. et al., 2019; Leal Filho et al., 2021). It is helpful to ensure regional sustainable development by evaluating ecological risk scientifically and formulating management policy to protect/restore the environmental system.

Ecosystem services (ESs) are the natural conditions and functions on which the formation of the ecosystem and ecological process, and the maintenance of human survival depend (Millennium Ecosystem Assessment, 2005; Costanza et al., 2014). As a vital component of ESs, water yield service plays an essential role in maintaining ecosystem stability and human well-being to achieve the sustainable development goals (SDGs) by the United Nations (e.g., SDG6: Clean Water and Sanitation, SDG 15: Life on Land) (UN, 2015; Bai et al., 2019; Wang et al., 2019; Dai and Wang, 2020). On the one hand, water yield service directly affects human well-being by providing adequate water for production and living and plays a key role in its entertainment and esthetic values (Sánchez-Canales et al., 2012). On the other hand, the water yield service can indirectly affect the welfare of human beings and the SDGs through the trade-off and synergistic relationship with other services (UN, 2015; Ajaz et al., 2017). It is of great significance to explore the spatiotemporal change of water yield services and its influencing factors for rational water resource use and sustainable development of the ecosystem. The methods widely used for water yield service evaluation include the InVEST (Integrated Valuation of Ecosystem Services and Trade-offs Tools) model, the SCS (Soil Conservation Service) model, and the SWAT (Soil and Water Assessment Tool) model (Lv et al., 2015; Yang et al., 2020). All these methods have their own advantages and disadvantages. For example, the SCS model has a simple structure, requires fewer parameters, and takes a long time to apply (Liu et al., 2010; Zhang et al., 2021). However, it has only one parameter and does not consider the time variable, and the model accuracy is greatly affected by time variation. The SWAT model has great computing capability and can simulate continuously and efficiently (Choudhary and Athira, 2021). Still, it has high requirements on input parameters and has great uncertainty of parameters, and it is difficult to obtain long time-series data with low accuracy (Choudhary and Athira, 2021; Aragaw and Mishra, 2022). The InVEST model was widely used due to its advantages of few parameters needed, low data required, and a wide application range (Redhead et al., 2016; Yang et al., 2020). Moreover, the input and output data are spatial raster forms, which can show the spatial visualization of ESs (Liu Y. X. et al., 2021). Furthermore, the results are precise and can directly serve for natural resource protection and ecological management. For example, Guerry et al. (2012) found that the InVEST model is a useful tool to assess (i.e., map, model, and value) multiple services provided by marine ecosystems. Benra et al. (2021) found that the InVEST Seasonal Water Yield Model (SWYM) performed well on the annual scale rather than the monthly scale in southern Chile with a potential for water ES assessments. Terrado et al. (2014) found that the InVEST model could provide a more general picture of ESs with easy accessibility to nonexperts and in a spatially explicit manner in a humanized Lobregat River basin in NE Spain. Ding et al. (2022) found that the InVEST model worked well on water yield evaluation in the Qinghai Lake Basin, China, with the simulation results close to the real situation. Dai and Wang (2020) and Wang et al. (2020) simulated the spatial distribution of water yield *via* the InVEST model and conducted quantitative attribution analysis for various geomorphologic and climatic zones in the Hengduan Mountain Region *via* the geodetector method. All these studies showed that the InVEST model was an easy and a spatially explicit tool with high reliability in evaluating water yield and spatial heterogeneity (Sharp et al., 2020).

Ecological risk assessment evaluates the possibility of adverse environmental effects that may occur or are occurring of the exposed risk receptors (Liu et al., 2020). Previous ecological risk assessment was mostly explored *via* the ecological entity characteristics, such as point source threat and regional landscape pattern change, and ignored the factors related to human well-being (Chen F. et al., 2019). Moreover, the ecological risk assessment combined with ESs mostly focuses on theoretical analysis and conceptual models. There are few studies that documented the ecological risk change *via* ES evaluation, mainly due to the lack of risk characterization methods based on ESs. More and more studies have begun to integrate ESs into ecological risk evaluation and build an ecological risk assessment framework based on ESs, which has become one of the research hotspots (Gong et al., 2021; Qian et al., 2022).

Some studies have shown that water yield service is affected by climate change and land-use/cover change (LUCC) (Pan et al., 2013; Sun et al., 2015; Xu et al., 2015, Xu X et al., 2016; Mo et al., 2021; Pei et al., 2022). Climate change can affect water yield service by changing the precipitation and evapotranspiration (i.e., solar radiation, temperature, and precipitation) (Legesse et al., 2003; Pei et al., 2022). LUCC will influence the watershed water cycle, affect the evapotranspiration, infiltration process, and water-holding capacity, then impact the water yield service (Zhao et al., 2019; Ge et al., 2020; Sharp et al., 2020). The impacts of climate change and land use on the future water yield service can be simulated *via* scenario analysis of the ecological risks on the potential water yield to put forward targeted management and control suggestions for regional sustainable development. Currently, various methods are applied to simulate trends of growth and changes in the LUCC (Ghosh et al., 2017). Several studies have used traditional models, such as cellular automaton (CA) models and logistic regressions (Xu J. et al., 2016) to simulate and predict future changes. Other studies apply integrated models such as CA–Markov models (de Freitas et al., 2018) to obtain precise and realistic results. Due to the advantage of the integration of the geospatial and remote sensing data, and biophysical and socioeconomic data for the accurate simulation (Weng, 2002; Cunha et al., 2020), the CA–Markov model is widely used to simulate land-use changes (Hyandye and Martz, 2017; Maviza and Ahmed, 2020), including Zaria in Nigeria (Koko et al., 2020), Baiyangdian Basin (Gao et al., 2021) and the Gaborone Dam Catchment (Matlhodi et al., 2021), Hainan Island (Liu Q. et al., 2021), the Majang Forest Biosphere Reserves of

Gambella, Southwestern Ethiopia (Tadese et al., 2021), and southwestern Iran (Marzieh et al., 2021). However, studies on LUCC prediction and impacts on water yield service in the Chinese Loess Plateau are still scarce and constrain its management application for water yield and human activities.

The Chinese Loess Plateau (CLP), a critical fragile ecological area with many environmental issues, has attracted much attention of scientists and governors. With the combined impacts of climate change and human socioeconomic activities, some environmental issues increasingly occurred in the CLP. For example, Zhang et al. (2022) found that the overall ecological vulnerability was moderate to high in the CLP from 2000 to 2015, and their area accounted for more than 60%. Fu et al. (2017) reported that some local soil erosion had been successfully controlled in the CLP, but the regional ecosystem remains fragile. Ensuring its water ecological security is of great significance for the sustainable development of the CLP. The Ziwuling Mountainous Region (ZMR), the only entirely preserved natural secondary forestry located in the hinterland of the CLP (Li et al., 2011), plays an essential role in soil retention, water conservation, and climate regulation. Meanwhile, intensive human activities and the fast recovery of forests and grassland have changed the local social–ecological systems in the last decades. However, there are still a few studies on the ecological risk of water yield service in the CLP. More efforts are needed to face these challenges and to pay for the harmonious development of humans and nature.

The main objective of this study was to propose and test a methodological framework for assessing the water yield service risk *via* scenario analysis of land-use and climate change. The spatial–temporal change in water yield and ecological risk and the potential trends were comprehensively analyzed using the ZMR in the CLP as an example. Specifically, we aimed to: 1) develop an ecological risk assessment framework by integrating water yield service, and land-use and climate change; 2) discern the spatial pattern and temporal change in water yield service, as well as the ecological risk; 3) simulate the potential change in the water yield service risk *via* land-use and climate change scenarios; and 4) put forward management suggestion for water yield service and human adaption to climate change.

2 METHOD AND STUDY AREA

2.1 Research Flowchart and Its Brief Introduction

Figure 1 shows the research flowchart of the method used in this study. Based on the land-use map, meteorological data, digital elevation model (DEM), and geographic vector data, the InVEST model is applied to evaluate water yield services in the ZMR. Then, the TOPSIS model is used to assess the ecological risks of water yield in the ZMR. The CA–Markov model was used here to set different land-use and climate scenarios, to compare the selected climate model data with the CMIP6 scenario model to predict the water yield services and its risk under different climate and land-use scenarios in the ZMR. Finally, we put forward some management suggestions to alleviate the water yield service risk in the future (**Figure 1**). Based on the CA–Markov module of the IDRISI Selva 17 software, this study set three different development scenarios of natural development, ecological protection, and economic construction to simulate the future land-use change. At the same time, this study applied two extreme climate scenarios, the high forcing unsustainable scenario (SSP5-8.5) and the sustainable low forcing scenario (SSP1-2.6), to obtain the possible climate change range.

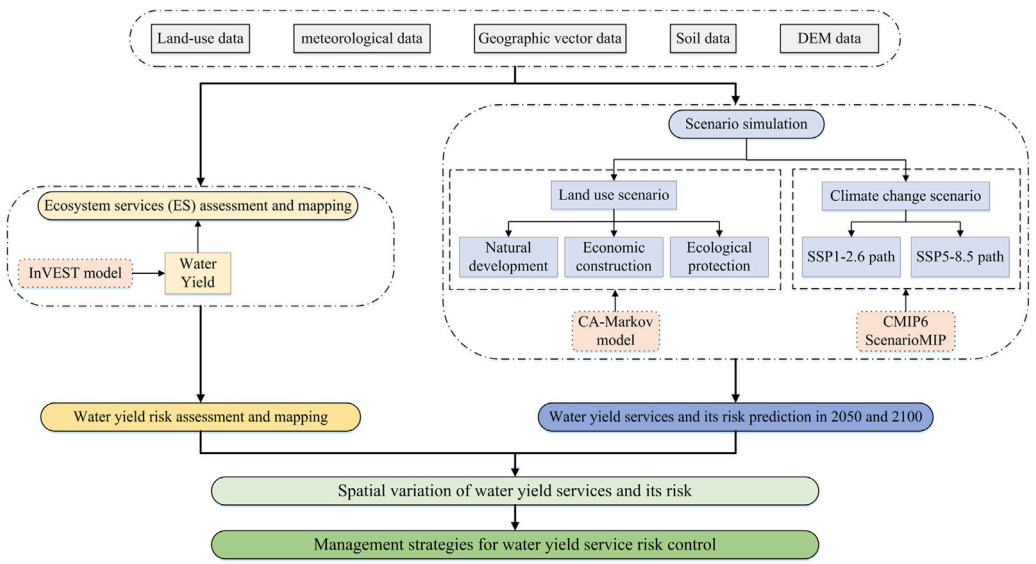

FIGURE 1 | Research flowchart.

Finally, we predict the water yield service and their risk under different climate and land-use scenarios in the future and put forward some suggestions for water yield service risk control and management (**Figure 1**).

2.2 Research Area

The Ziwuling Mountainous Region (ZMR) (34°40′–37°25′N, 107°30′–110°20′E) is referred to the Ziwuling National Nature Reserve and its surrounding areas in this study (**Figure 2**). The ZMR is located in the hinterland of the CLP (**Figure 2**), including 16 counties/districts, such as Huachi, Heshui, Ningxian, Zhengning, Wuqi, Zhidan, Ansai, Baota, Ganquan, Fuxian, Huangling, Yijun, Wangyi, Yintai, Yaozhou, and Xunyi. The ZMR belongs to a temperate continental monsoon climate with an elevation of 534–1,856 m. The annual average temperature is about 7.4°C, and the average yearly precipitation is 587 mm. The rainfall mainly occurred from July to September, and the intensive rainstorm events often lead to water and soil loss disasters.

The ZMR has a long history of human activities. Since the Ming and Qing Dynasties, the vegetation has undergone a succession of destruction, restoration, destruction, and restoration cycle. The region is rich in natural resources (such as coal, oil, and gas) and cultural tourism, with great efforts in mining and development. Meanwhile, the population and economic density keep growing, with the expansion of urban and transportation construction land. Although economic growth was promoted, it also resulted in natural disturbance and environmental pressure. As the only entirely preserved natural secondary forest in the CLP (Li et al., 2011), the forest in the ZMR plays a vital role in water conservation, climate regulation, and biodiversity (Sun, 2018). Therefore, ensuring ecological security in the ZMR is of great significance to maintaining the sustainable development of the CLP.

2.3 Data Resource and Data Processing

The land-use maps of 1990, 2000, 2010, and 2017 with a 30-m spatial resolution were downloaded from the Chinese Academy of Sciences (https://www.resdc.cn/). Land-use types included farmland, forestland, grassland, water, constructed land, and unused land according to the "Chinese Classification Criteria of Current Land Use" (GB/T21010-2017). The overall accuracies in 1990, 2000, 2010, and 2017 were all greater than 88%, which is acceptable for land-use change analysis. The digital elevation model (DEM) data with a spatial resolution of 30 m were obtained from the Geospatial Data Cloud platform (http://www.gscloud.cn/), which was used to extract the vector boundary of watershed and subwatershed and obtain topographic factors. The data of meteorological stations were obtained from the China Meteorological Data Service Center (http://data.cma.cn/) and the Chinese Academy of Sciences (https://www.resdc.cn/). To avoid the impact of extreme meteorological events on the study results, the annual average values of meteorological data from 1981 to 1990, 1991 to2000, 2001 to 2010, and 2011 to 2017 were calculated, respectively. The Anuspline, one of the professional meteorological interpolation software, was used for spatial interpolation. The processed meteorological data were used to estimate rainfall erosivity factors and evapotranspiration potential. Solar radiation data were obtained from the global meteorological database (https://worldclim.org/data/). The data are monthly grid data with a resolution of 1 km. After downscaling and averaging, the annual-scale data with a 30-m resolution were obtained to calculate the evapotranspiration

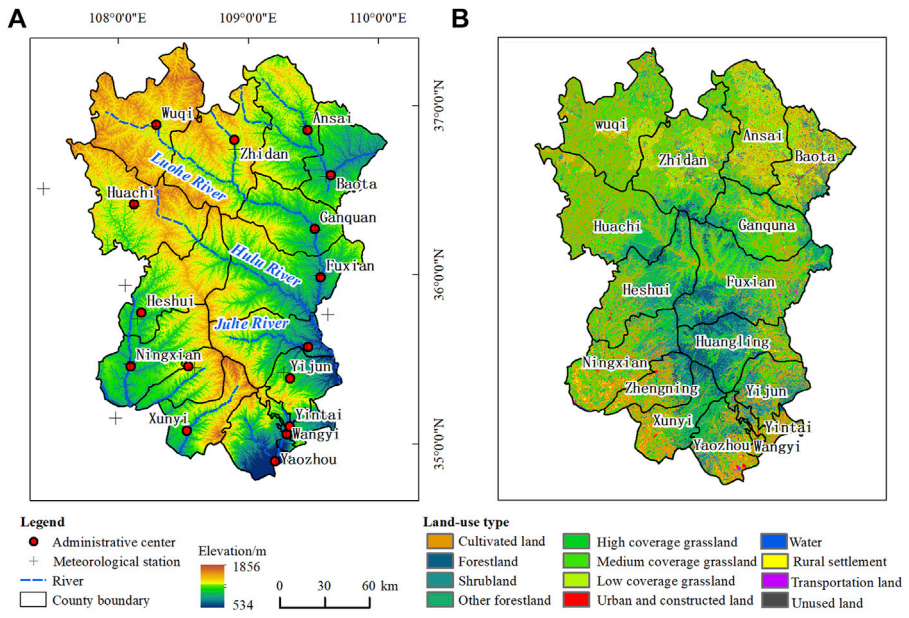

FIGURE 2 | Location of the Ziwuling Mountainous Region (ZMR) **(A)** and land-use map in 2017 **(B)**.

potential. Soil data were obtained from the Soil Information System of China (http://www.issas.ac.cn/kxcb/zgtrxxxt/) to estimate soil erodibility factor, soil depth, and maximum root restriction depth. The data of the Scenario Model Intercomparison Project (ScenarioMIP) in Coupled Model Intercomparison Project Phase 6 (CMIP6) were obtained from the website of the Earth System Grid Federation (ESGF) (https://esgf-node.llnl.gov/projects/esgf-llnl/). The prediction data were obtained from the National Climate Center (Beijing Climate Center Climate System Model version 1, BCC-CSM2-MR). More details on the data can be found in **Section 2.5.3**.

2.4 Main Methods

2.4.1 Water Yield Service

The water yield service was calculated *via* the InVEST module. The module integrates relevant parameters such as soil depth, soil permeability, and root depth in the calculation process and modifies them locally based on Budyko's hydrothermal coupling balance principle (Wu et al., 2017). The InVEST model has been widely used in water yield service studies of different scales and regions due to its minor limitations on data acquisition and strong visibility of results (Dai and Wang, 2020; Li et al., 2020; Liu J. et al., 2021; Yang et al., 2020). The calculation formulations are as follows:

$$Y_x = \left(1 - \frac{AET_x}{P_x}\right) \times P_x$$

$$\frac{AET_x}{P_x} = \frac{1 + \omega_x R_x}{1 + \omega_x R_x + {}^{1}/_{R_x}}$$

$$R_x = \frac{k_x \times ET_0}{P_x}$$

$$\omega_x = Z\frac{AWC_x}{P_x} + 1.25$$

$$AWC_x = \min\left(\text{MaxSoil Depth}_x, \text{Root Depth}_x\right) \times PAWC_x$$

where Y_x, AET_x, and P_x are the annual water yield (mm), actual annual evapotranspiration (mm), and annual precipitation (mm) at pixel x, respectively. R_x, K_x, and ET_0 are the dryness index, vegetation evapotranspiration coefficient, and evapotranspiration potential at pixel x, respectively. ω_x is a linear function (dimensionless) affected by the precipitation and soil properties. Z is the seasonal constant, which is 4 in this study. AWC_x is the available volumetric water content (mm) of plants, Max Soil Depth$_x$, Root Depth$_x$, and $PAWC_x$ are the maximum depth of soil, the maximum root depth of vegetation-covered land, and the available volumetric water content of the plants, respectively.

2.4.2 Ecological Risk Assessment Based on Ecosystem Services

The TOPSIS model (Technique for Order Preference by Similarity to an Ideal Solution) is a nonlinear evaluation method, and its evaluation value can reflect the advantages and disadvantages of the evaluation object (Yu et al., 2020). The TOPSIS model can effectively use the original data and accurately reflect the gap between the evaluated objects. As there are no special requirements for the data distribution, indicators, and sample number of evaluation indicators, the TOPSIS model is flexible and widely used, for example, in urban land resource evaluation, regional water resource assessment, and cost scheme decision-making (Dehdasht et al., 2020).

Based on the TOPSIS model, this study constructed an ecological risk assessment model based on ESs in the ZMR. The basic principles are as follows: Firstly, the sample units with the maximum and minimum ESs at grids or polygons in a certain space were selected as the positive ideal sample points and negative ideal sample points, respectively. The ES value at the positive ideal sample points was considered as the risk threshold. The Euclidean distance of the positive and negative sample points was used to represent the maximum loss of regional ESs. Then, the ecological risk index was calculated, which is the ratio between the Euclidean distance of the positive ideal sample point and the maximum loss of ESs at each unit in space. More details on the ecological risk assessment are shown below.

(1) Normalization of the ecosystem services: The maximum and minimum normalization method was used to linearly transform the original values of various ESs to eliminate the impact of data dimension and magnitude on the data.

$$r_{ij} = \frac{ES_{max\ j} - ES_{ij}}{ES_{max\ j} - ES_{min\ j}}$$

where r_{ij} is the normalized value of j ecosystem service at pixel i, ES_{ij} is the value of j ecosystem service at pixel i, and $ES_{max\ j}$ and $ES_{min\ j}$ are the maximum and the minimum pixels of j ecosystem service.

(2) Identification of the positive ideal sample points and negative ideal sample points:

$$y^+ = \begin{bmatrix} r_{max\ j-1} & r_{max\ j-2} & \cdots & r_{max\ j-n} \end{bmatrix}$$

$$y^- = \begin{bmatrix} r_{min\ j-1} & r_{min\ j-2} & \cdots & r_{min\ j-n} \end{bmatrix}$$

where y^+ is the set of positive ideal samples, which are the sample units with the normalized maximum value of various ESs; y^- is the set of negative ideal samples, which are the sample units with the normalized minimum value of various ESs; and $r_{max\ j}$ and $r_{min\ j}$ are the normalized maximum value and the normalized minimum value of j ES in the study area.

(3) Calculation of the degree of ecosystem service loss:

$$S_i^+ = \sqrt{\sum_{j=1}^{n}\left(r_{\max\ j-1} - r_{ij}\right)^2}$$

$$S_{max}^+ = \sqrt{\sum_{j=1}^{n}\left(r_{max\ j-1} - r_{min\ j-1}\right)^2}$$

where S_i^+ is the Euclidean distance between pixel i and the positive ideal sample, and the larger its value, the larger the ecological risk; and S_{max}^+ is the Euclidean distance between the positive ideal sample and the negative ideal sample, indicating the loss of ESs in a certain area.

(4) Calculation of ecological risk index:

$$ESR_i = \frac{S_i^+}{S_{\max}^+}$$

where ESR_i is the comprehensive ecological risk index at pixel i, and its value is between 0 and 1. The value 1 represents the maximum relative loss of ESs and the highest ecological risk, and the value 0 represents the minimum relative loss of ESs and the lowest ecological risk.

(5) Ecological risk grade classification: Considering the fairness of the ecological risk time-series analysis process and the consistency of risk classification standards, the equal interval classification method was applied to classify the ecological risk in different periods. The ecological risk in the study area was divided into five levels: the low risk (0–0.2), lower risk (0.2–0.4), medium risk (0.4–0.6), higher risk (0.6–0.8), and high risk (0.8–1).

2.5 Scenario Simulation of the Land-Use and Climate Change

The CA–Markov model and Scenario Model Intercomparison Project (ScenarioMIP) were used to set different scenarios on climate and land-use change to predict the ecological risk of the ZMR in 2050 and 2100, respectively.

2.5.1 Land-Use Scenario Simulation Based on the CA–Markov Model

Based on the CA–Markov module of the IDRISI Selva 17 software, this study set three different scenarios of natural development, ecological protection, and economic development (**Table 1**) to simulate future land-use change. A brief introduction of the three scenarios on land-use simulation is shown in **Table 1**.

2.5.2 Accuracy Test of Land-Use Simulation Results

The simulated and the actual land-use maps in the study area were cross-checked, and the accuracy of the simulation results was obtained. Using the CROSSTAB tool under IDRISI Selva 17 software in GIS analysis, the simulated land-use raster map and the actual land-use map in 2017 were input to test and calculate the kappa coefficients and the overall kappa of the land-use types, respectively. The kappa value is calculated using the following formula:

$$Kappa = \frac{P_o - P_c}{P_p - P_c}\left(P_o = \frac{n_1}{n}, P_c = \frac{1}{N}\right)$$

where n is the total number of land-use pixels, n_1 is the number of correct pixels for the simulation, N is the number of all land-use types, P_o is the proportion of correct pixels for the simulation, P_c is the proportion of pixels expected to be simulated correctly, and P_p is the proportion of correct pixels for the simulation under the ideal conditions. The kappa coefficient of all land-use types was greater than 0.5, and the overall simulation accuracy was high, with a Kappa coefficient of 0.937.

2.5.3 Climate Scenario Simulation Based on the CMIP6

Based on the climate model data of the Scenario Model Intercomparison Project (ScenarioMIP) in the Coupled Model Intercomparison Project Phase 6 (CMIP6), this study simulated and forecasted the future climate in the ZMR. The climate prediction scenario of the ScenarioMIP is a rectangular combination of different SSPs and the radiative forcing (representative concentration pathway, RCP) (Zhang et al., 2019). SSPs (the shared social–economic pathways) described the possible development of society in the future without the impact of climate change or climate policies, including SSP1, SSP2, SSP3, SSP4, and SSP5, which represented five different paths of sustainable development, moderate development, local development, unbalanced development, and conventional development, respectively (Fujimori et al., 2014; Weng et al.,

TABLE 1 | Brief introduction of the three scenarios on land-use simulation.

Land-use scenarios	Scenario descriptions	Scenario setting methods
Natural development	This scenario assumes that the land-use change trend remains the same as before (2010–2017)	The local landscapes continue to evolve naturally according to the previous period's development speed and spatial layout
Ecological protection	This scenario emphasizes environmental protection and limits human socioeconomic construction activities	The transfer probability of forests, grasslands, and water to urban settlement, rural settlement, and transportation lands was set as 0, and the transfer probability of other lands to forests, grasslands, and water is increased by 20%. At the same time, the shady slope and sunny slope farmlands in which the slopes are larger than 15° should be returned to forests and grasslands, respectively
Economic construction	This scenario focuses more on regional economic development, and ecological protection will pay less	The transfer probability of other lands to urban settlement, rural settlement, and transportation lands is increased by 30%, respectively, and urban payment, rural payment, and transportation lands are made into buffer zones within 300, 30, and 30 m, respectively, as a suitable development zone

2020). In CMIP5, there were four emission scenarios, including the RCP2.6, RCP4.5, RCP6.0, and RCP8.5. It meant that the radiation forcing would be stable at about 2.6 W/m^2, 4.5W/m^2, 6.0 W/m^2, and 8.5 W/m^2, respectively, by 2100. On this basis, the CMIP6 added three new RCPs, including RCP7.0, RCP3.4, and RCPs below 2.6 to fill the gap between CMIP5 RCPs. A new climate prediction scenario based on the integrated assessment model (IAM) (Chen, 2021), the SSP1-2.6 updated RCP2.6 scenario, shows the combined effects of the low radiation forcing, low vulnerability, and low mitigation pressure. This scenario predicted that by 2100, the multimode average value of global warming would be significantly lower than 2°C. By analogy, SSP2-4.5, SSP3-7.0, and SSP5-8.5, respectively, represented medium, medium to high, and high levels of development, with medium, higher, and high levels of radiation forcing and vulnerability.

In this study, two extreme climate scenarios, the high forcing unsustainable scenario (SSP5-8.5) and the sustainable low forcing scenario (SSP1-2.6), were used to obtain the possible climate change range in the ZMR, to clarify the possible impact range of climate change on ESs.

The panoply software provided by NASA's official website (http://www.giss.nasa.gov/tools/panoply) was to read file metadata information and was run in the MATLAB software to decompress and read the NC file. Finally, we obtained the required meteorological data through a series of grid calculations and correlation analysis in the ArcGIS software. As the resolution of the obtained data is only 100 km, referring to relevant studies (Martinez-Harms et al., 2017; Lv, 2019), the change values of various climate elements in the study area from 2017 to 2050 and 2017 to 2100 under the high forcing unsustainable scenarios (SSP5-8.5) and sustainable low forcing scenarios (SSP1-2.6) were calculated, respectively. Then, based on the actual meteorological data of the ZMR in 2017, the change values of climate elements in the ZMR in 2050 and 2100 were obtained (**Table 2**).

2.5.4 Land-Use and Climate Scenario Setting

Based on the CA–Markov module of the IDRISI selva17 software, this study set three scenarios of natural development, ecological protection, and economic construction to simulate the future land-use change in the ZMR. Six development scenarios were generated based on three land-use change scenarios and the two climate paths SSP1-2.6 and SSP5-8.5 of the CMIP6 ScenarioMIP to assess the ecological risks in the ZMR under different scenarios (**Table 3**).

3 RESULTS

3.1 Spatiotemporal Variation in Water Yield Service in the ZMR From 1990 to 2017

The water yield service in the ZMR decreased from 1990 to 2017 (**Figure 3**), with an average annual rate of -0.79 mm. Water yield service in the ZMR was 69.19 mm in 1990, the highest one in the study period, mainly affected by precipitation and evapotranspiration potential. The average rainfall was high (562.85 mm), and the evapotranspiration potential was the lowest (828.04 mm) in 1990. Water yield service in the ZMR was 19.98, 31.32, and 47.72 mm in 2000, 2010, and 2017, showing an increasing trend. The precipitation in 2000 was the lowest (502.34 mm), and the evapotranspiration potential was the highest (1016.25 mm), and the actual water yield service decreased in 2000. Then, the water yield service increased after 2000.

The water yield service in the southeast ZMR was larger than that in the northwest. The subareas with high value were mainly

TABLE 2 | Change values of climate elements in the ZMR under SSP1-2.6 and SSP5-8.5 scenarios in 2050 and 2100.

	Year	Precipitation (mm)	Average temperature (°C)	Average minimum temperature (°C)	Average maximum temperature (°C)
SSP1-2.6	2050	+0.920	+0.518	+0.241	+0.439
	2100	+1.554	+1.392	+0.527	+0.755
SSP5-8.5	2050	+1.604	+1.021	+0.479	+0.638
	2100	+2.349	+2.876	+1.107	+1.985

TABLE 3 | Land-use and climate scenario settings.

Comprehensive scenarios	Land-use scenarios	Climate scenarios
ND126	Natural development (ND)	SSP1-2.6
ND585	Natural development (ND)	SSP5-8.5
EP126	Ecological protection (EP)	SSP1-2.6
EP585	Ecological protection (EP)	SSP5-8.5
EC126	Economic construction (EC)	SSP1-2.6
EC585	Economic construction (EC)	SSP5-8.5

Note: ND, EP, and EC represent the natural development scenario, ecological protection scenario, and economic construction scenario of land use, respectively.

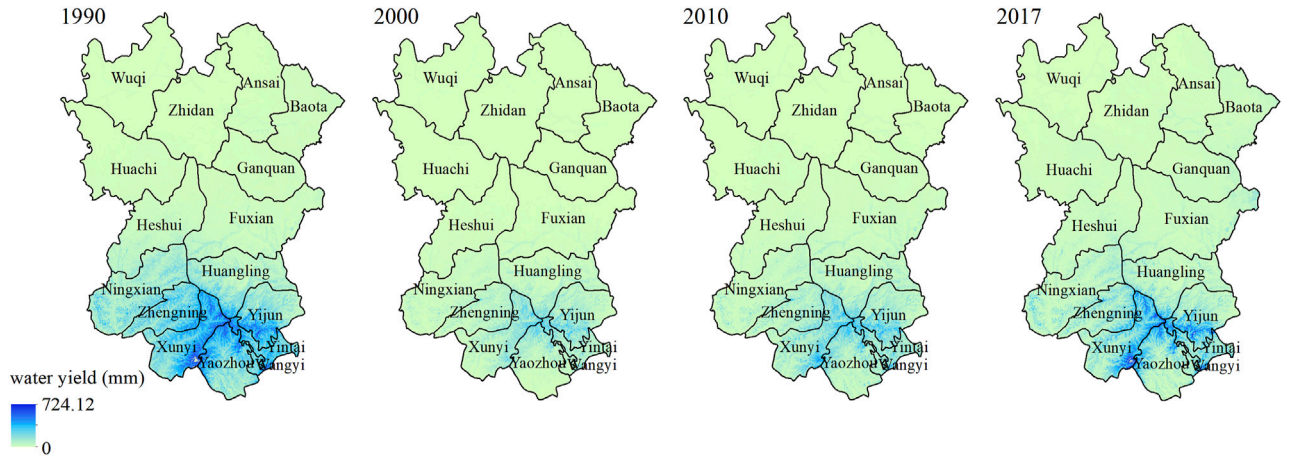

FIGURE 3 | Spatiotemporal variation in water yield service in the ZMR from 1990 to 2017.

located in the southeast ZMR, especially in Huangling, Yijun, Yintai, Wangyi, Yaozhou, Xunyi, and Zhengning, with more precipitation, lower evapotranspiration, more water surplus, and higher water yield service. The subareas with low value were mainly located in the northwest ZMR, especially in Wuqi, Zhidan, Ansai, and Huachi (**Figure 3**), with a drier climate, greater evaporation, and less water yield service.

3.2 Spatiotemporal Variation in the Water Yield Service Risk in the ZMR From 1990 to 2017

The risk level of water yield service in the ZMR first increased and then decreased from 1990 to 2017, mainly belonging to the high-risk level (**Figure 4**). The areal ratio of the high-risk subareas in the ZMR was the largest one in 1990, 2000, 2010, and 2017, accounting for 72.70%, 86.65%, 83.06%, and 83.01%, respectively (**Figure 4**). The areal ratio of the low-risk subareas was the smallest one (**Figure 4**), accounting for 2.36%, 0.27%, 0.41%, and 0.83%, respectively. The areal ratios of the lower, medium, and higher risk subareas of water yield service in the ZMR were 5.20%, 10.42%, and 9.32% in 1990. Compared with 1990, the areal ratios of the lower, medium, and higher risk subareas of water yield service in the ZMR decreased in 2000, increased in 2010, and then increased in 2017.

The spatial distribution pattern of water yield service risk in the ZMR was found to have no apparent changes during the study period (**Figure 4**). However, the subareas with high and higher risk were mainly concentrated in the middle and north ZMR, especially in Wuqi, Zhidan, Ansai, Baota, Huachi, Ganquan, Heshui, and Fuxian. The spatial distribution of the subareas of the lower and low risk was mainly located in the southern ZMR, such as Huangling, Xunyi, Yaozhou, Yintai, and Yijun. The subareas of high risk of water yield service were expanded to the south ZMR, and the subareas of low risk continued to decrease from 1990 to 2017.

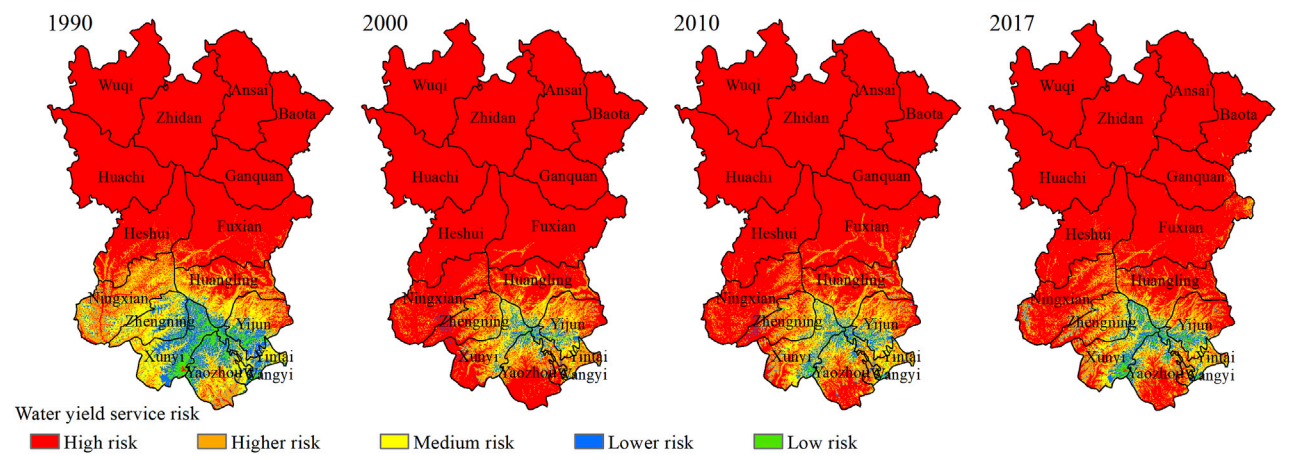

FIGURE 4 | Spatiotemporal variation in the water yield service risk in the ZMR from 1990 to 2017.

3.3 Scenario Simulations of the Water Yield Service Risk Based on Land-Use and Climate Change

3.3.1 Spatial Variation in Water Yield Service in the ZMR Under Different Scenarios in 2050 and 2100

There are apparent differences in water yield service in the ZMR under different land-use and climate scenarios (**Figure 5**). The water yield service in 2100 under different land-use and climate scenarios is lower than in 2050, with a similar overall pattern (**Figure 5**). Under the SSP1-2.6 climate scenario, the water yield service in the ZMR was 48.09 mm, 47.31 mm, and 46.46 mm under economic construction (EC), natural development (ND), and ecological protection (EP) land-use scenarios in 2050, respectively (**Figures 5A–C**), and it was 43.73 mm, 42.86 mm, and 41.91 mm under EC, ND, and EP, in 2100, respectively (**Figures 5G–I**). Under the SSP5-8.5 climate scenario, the water yield service in the ZMR was 45.11 mm (EC), 44.36 mm (ND), and 43.52 mm (EP) in 2050 (**Figures 5D–F**), and it was 42.41 mm (EC), 41.57 mm (ND), and 40.62 mm (EP) in 2100 (**Figures 5J–L**). In conclusion, the variation pattern of water yield service under different climate scenarios is the EP scenario > the ND scenario > the EC scenario. The water yield service is the highest one of the EC126 (48.09 mm in 2050 and 43.73 mm in 2100) and the lowest of the EP585 (43.52 mm in 2050 and 40.62 mm in 2100). Under the same land-use scenario, the water yield service of the SSP1-2.6 climate scenario is higher than that of SSP5-8.5.

The spatial distribution pattern of water yield service under different scenarios decreases from the southeast to the northwest in the ZMR in 2050 and 2100 (**Figure 5**). The water yield service in the ZMR is generally low except for a small part of the ZMR, with apparent spatial distribution differences. The subareas with a high value are mainly located in the southeast of the ZMR, such as Huangling, Yijun, Yintai, Wangyi, Yaozhou, Xunyi, and Zhengning. The subareas with a low value are mainly located in the northwest of the ZMR, such as Wuqi, Zhidan, Ansai, and Huachi (**Figure 5**).

3.3.2 Spatial Variation in Water Yield Service Risk in the ZMR Under Different Scenarios in 2050 and 2100

The water yield service risk in the ZMR in 2100 is larger than in 2050. Under the SSP1-2.6 climate scenario in 2050 and 2100, the areal ratio of the high-risk subareas of water yield service in the ZMR accounts for 83% and 84%, respectively, followed by the higher and medium-risk, the lower risk, and low-risk subareas (**Figure 6A–C, G–I**). Under the EP scenario, the areal ratio of the high-risk and higher risk subareas is 90.86% and 91.73% of the ZMR, respectively (**Figures 6B,H**). Under the ND scenario, the areal ratio of the high-risk and higher risk subareas is 90.77% and 91.68%, respectively (**Figures 6A,G**). Under the EC scenario, the areal ratio of the high-risk and higher risk subareas is 90.57% and 91.49%, respectively (**Figures 6C,I**). On the contrary, the areal ratio of the low-risk and lower risk subareas is the largest one, 3.74% in 2050 and 3.10% in 2100 under the EC scenario, followed by the ND scenario (3.65% in 2050 and 3.04% in 2100) and the EP scenario (3.62% in 2050 and 3.03% in 2100).

The water yield service risk of the ZMR under the SSP5-8.5 climate scenario in 2050 and 2100 is slightly higher than that under the SSP1-2.6 climate scenario (**Figure 6**). Under the EP scenario, the areal ratio of high-risk and higher risk subareas is

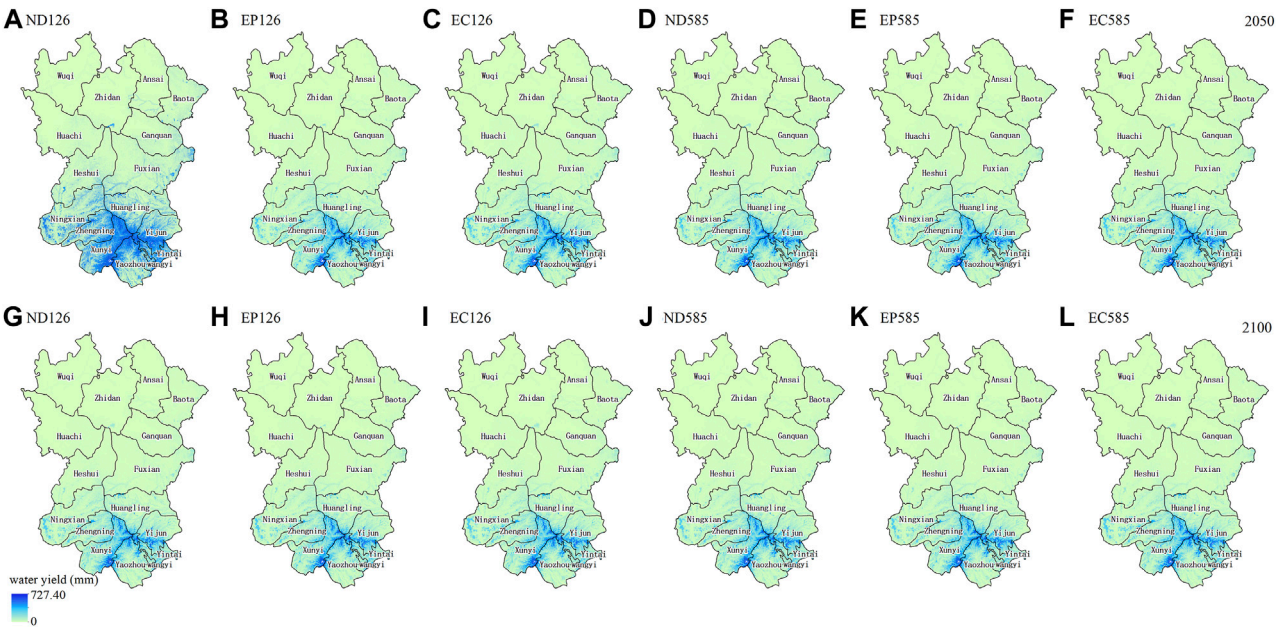

FIGURE 5 | Spatial variation in water yield service in the ZMR under different scenarios in 2050 **(A–F)** and 2100 **(G–L)**. Note: ND-the natural development scenario of land use, EP-the ecological protection scenario of land use, EC-the economic construction scenario of land use, 126-climate paths SSP1-2.6, 585-climate paths SSP5-8.5.

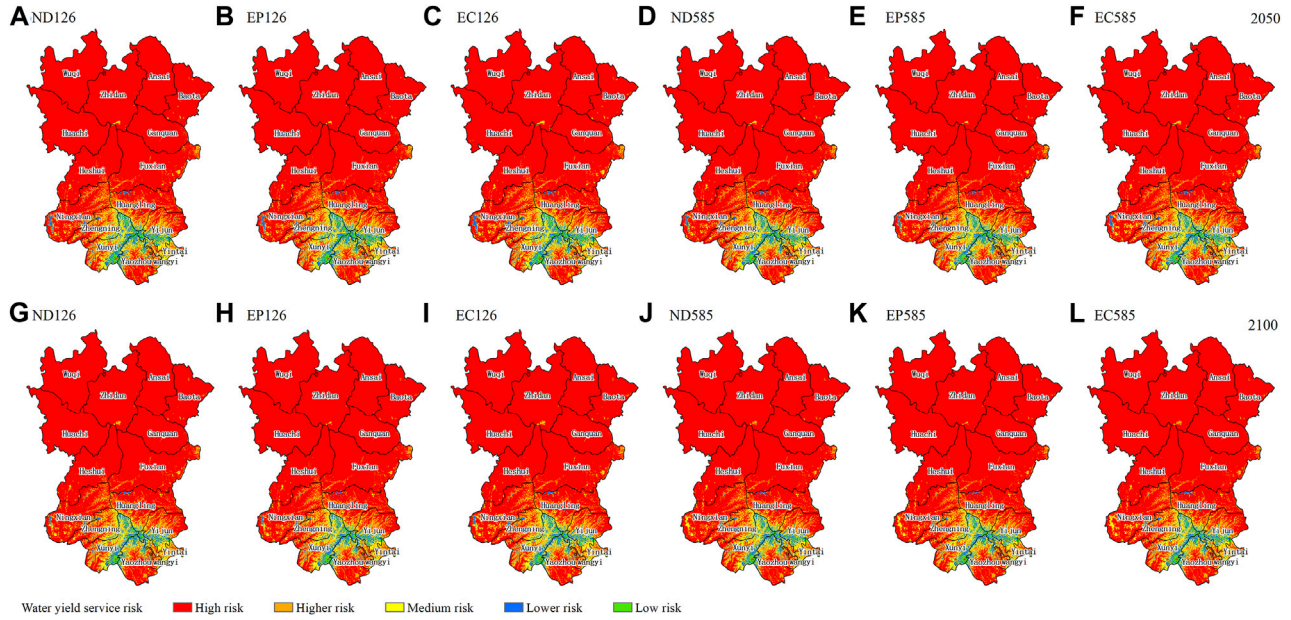

FIGURE 6 | Spatial variation in the water yield service risk in the ZMR under different scenarios in 2050 **(A–F)** and 2100 **(G–L)**. Note: ND-the natural development scenario of land use, EP-the ecological protection scenario of land use, EC-the economic construction scenario of land use, 126-climate paths SSP1-2.6, 585-climate paths SSP5-8.5.

91.48% and 92.04% of the ZMR, respectively (**Figures 6E,K**). Under the ND scenario, the areal ratio of high-risk and higher risk subareas is 91.39% and 91.99%, respectively (**Figures 6D,J**). Under the EC scenario, the water yield service risk is the lowest one, and the areal ratio of high-risk and higher risk subareas is 91.19% and 91.81%, respectively (**Figure 6F,L**). On the contrary, the areal ratio of the low-risk and lower risk subareas is the largest one (3.29% in 2050 and 2.92% in 2100) under the EC scenario, followed by the NP scenario (3.20% in 2050 and 2.88% in 2100) and the EP scenario (3.18% in 2050 and 2.87% in 2100).

The variation in the water yield service risk under the SSP5-8.5 and SSP1-2.6 climate scenarios is the same in 2050 and 2100, the EC scenario < the ND scenario < the EP scenario. The water yield service risk is the lowest of the EC126 scenario, the areal ratio of the high-risk subareas is the largest one (82.78% in 2050 and 84.22% in 2100), and the areal ratio of the low-risk and lower risk subareas is 3.74% and 3.10%, respectively. The water yield service risk is the largest of the EP558 scenario, the areal ratio of the high-risk subareas is the largest one (83.95% in 2050 and 85.33% in 2100), and the areal ratio of the low-risk and lower risk is 3.18% and 2.87%, respectively (**Figure 6**). The spatial distribution pattern of the water yield service risk in the ZMR is almost the same in 2050 and 2100 (**Figure 6**). The subareas with high-risk and higher risk are mainly located in the middle and north of the ZMR, such as Wuqi, Zhidan, Ansai, Baota, Huachi, Ganquan, Heshui, and Fuxian. The spatial distribution with the low-risk and lower risk subareas is mainly distributed in the intersection of Huangling, Xunyi, Yaozhou, Yintai, and Yijun in the south ZMR (**Figure 6**).

4 DISCUSSION

4.1 Spatiotemporal Variation in Water Yield Service in the ZMR

This study found that the water yield service in the ZMR decreased from 1990 to 2017 with a water yield of 69.19, 19.98, 31.32, and 47.72 mm, in 1990, 2000, 2010, and 2017, respectively. The results are consistent with Zhuang (2020) findings on the Loess Plateau; for example, Zhuang (2020) found that the water yield service on the Loess Plateau in 1990, 2000, 2010, and 2015 was 122.41, 68.55, 87.59, and 95.85 mm, respectively, among which the water yield service in 1990 was the highest one. Meanwhile, water yield service is affected by climate change and land-use/cover change (Pan et al., 2013; Sun et al., 2015; Xu et al., 2015, Xu X et al., 2016; Mo et al., 2021; Pei et al., 2022). Climate change can affect water yield service by changing rainfall and evapotranspiration potential (Legesse et al., 2003; Pei et al., 2022). Co-affected by the precipitation and evapotranspiration potential, the average precipitation in the ZMR was high (562.85 mm), and the evapotranspiration potential was the lowest (828.04 mm) in 1990. The precipitation was the lowest (502.34 mm), the evapotranspiration potential was the highest (1016.25 mm), and the actual water yield service decreased in 2000. Moreover, Gao et al. (2016) found that increasing constructed land will increase water yield. Constructed land expansion often increases the area of impervious water surface, changes the water balance, reduces precipitation infiltration, increases runoff, and improves the regional water yield (Lang et al., 2017; Pei et al., 2022). Furthermore, Dou et al. (2019) found that the water yield

of the constructed land and farmland is higher due to the impact of climate change and land-use/cover change, while the water yield of forests, shrubs, and grasslands is lower. The evapotranspiration of farmland is similar to that of forest and grassland, but the water infiltration is less than that of forests and grasslands, so the water yield in farmland is higher than that of forest and grassland. Forests and grasslands trap more surface runoff, increase soil infiltration and evapotranspiration, and control precipitation regulation, resulting in lower water yield (Pei et al., 2022). Thus, returning farmlands to forests and grasslands will reduce water yield service.

Our study found that the area of the building land, forest, and grassland in the ZMR increased by 181.84, 549.28, and 785.53 km^2, respectively, while farmland decreased by 1520.32 km^2 from 1990 to 2017. Meanwhile, the decrease in farmland area and the increase in forest and grassland caused the reduction in water yield service in the ZMR. The simulation of water yield service in the ZMR under different land-use and climate scenarios showed that under the SSP1-2.6 climate scenario in 2050 and 2100, the water yield service in the ZMR was 48.09 and 43.73 mm (EC), 47.31 and 42.86 mm (ND), and 46.46 and 41.91 mm (EP). Under the SSP5-8.5 climate scenario in 2050 and 2100, the water yield service in the ZMR was 45.11 and 42.41 mm (EC), 43.52 and 41.57 mm (ND), and 46.46 and 40.62 mm (EP). The variation pattern of water yield under different climate scenarios was consistent as the EC scenario > the ND scenario > the EP scenario. The water yield service was the highest under the EC126 scenario (48.09 mm in 2050 and 43.73 mm in 2100) and the lowest under the EP585 scenario (43.52 mm in 2050 and 40.62 mm in 2100). This may be due to the change in land-use types in the EP scenario; that is, compared with the ND scenario and EC scenario, the conversion probability of other lands into forests and grasslands has increased by 20%, which increases the evapotranspiration, and results in water yield service reduction in the ZMR.

4.2 Spatiotemporal Variation in the Water Yield Service Risk and Its Management Strategies for Ecological Risk Alleviation

Water yield risk in the ZMR increased first and then decreased from 1990 to 2017. The areal ratio of high-risk subareas in the ZMR was the largest. The simulation of different land-use and climate scenarios indicated that the risk of water yield service in the ZMR is higher in 2050 than that under the SSP1-2.6 climate scenarios in 2100, and they mainly belong to high-risk areas. The spatial distribution pattern of water yield service risk in the ZMR was found to have no apparent differences in 2050 and 2100. The high-risk and higher risk subareas were mainly distributed in the middle and north ZMR, especially in Wuqi, Zhidan, Ansai, Baota, Huachi, Ganquan, Heshui, and Fuxian, with oil and gas exploitation in the north ZMR. Therefore, the following methods on “open source” and “reduce expenditure” should be applied to reduce the water resource gap and develop a water-saving society in the ZMR: strengthen the protection of the water sources of the Ju River, Malian River, Silang River, Malan River, and Shichuan River in the ZMR, strictly prevent pollution and the excessive use of water sources, and prevent further degradation of water sources. Moreover, the following water-saving production methods and industrial modes are recommended to avoid unnecessary drainage and overflow to increase the recycling of the limited water resources: enhance and improve the construction of sewage treatment infrastructure. Regional environmental protection should strengthen the supervision and punishment of industrial sewage discharge and purification treatment, to promote the recycling of water resources; make reasonable planning to harvest water and regulate flood, to achieve the storage and backflow of rainwater to reduce evaporation loss, and to develop modern and high-efficient agriculture; optimize the planting structure and selection of the water-saving crops of wheat, corn, millet, beans, and buckwheat, to adopt water-saving irrigation methods such drip, sprinkler, and under-film irrigation for high water efficiency in agricultural production; carry out environmental education consistently to enhance residents’ awareness of water conservation and ecological protection. Only if these suggestions and management strategies have been well implemented, the risk of water yield would decrease and the ecological quality and ecosystem service would be enhanced and improved for the human well-being and sustainable development in the Chinese Loess Plateau and other similar mountainous areas.

4.3 Limitations and Outlook

Our work would be of value for regional ES risk control and human governance, such as the analytical framework, method and data, scenario simulation, risk management, and human adaptation. However, although major progress in ecological risk assessment, water yield valuation, and technology has been made recently, ES risk mapping and forecast, especially by using the land-use change model (i.e., CA–Markov model) and climate change models (i.e., the Scenario Model Intercomparison Project, ScenarioMIP; and the Coupled Model Intercomparison Project Phase 6, CMIP6), are still facing significant challenges due to data quality, availability, completeness, and uniformity (Yan, 2021; Gong et al., 2022), especially for the poor and fragile areas that lack basic and monitoring data. These factors will result in some errors and uncertainty. Therefore, the methods need to be further modified as experience and applications increase (Yan, 2021; Gong et al., 2022). In addition, the InVEST model is widely used for service evaluation and mapping with the advantages of few parameters, low data requirements and spatial visualization (Redhead et al., 2016; Yang et al., 2020; Liu J. et al., 2021). The results are precise and focused, and they can directly serve the local natural resource protection and ecological management. However, there are great differences in natural systems such as the temperature and precipitation, as well as human activities, due to the large north–south span of the ZMR. The water yield service risk was based on the maximum loss threshold of ESs, which may enlarge the risk level of low-value subareas of water yield service. More efforts are needed to calibrate the model parameters (i.e., the InVEST, TOPSIS, CA–Markov, and the ScenarioMIP) based on the natural ecological and socioeconomic conditions to improve the assessment accuracy. Meanwhile, this study does not consider the trade-off or synergy between water production services and

other ESs, which may improve or reduce the risk level of this service. In future research, more efforts are suggested to analyze a variety of ESs and comprehensively evaluate the ecological risk level of the study area.

5 CONCLUSIONS

Ecological risk assessment and management are of great significance for human well-being and sustainable development. In this study, we established a framework combining water yield with ecological risk for service enhancement and human adaptation. The spatiotemporal variation in water yield service and its ecological risk was explored *via* land-use and climate change simulations using InVEST, CA–Markov, and TOPSIS models. The analytical framework can comprehensively evaluate water yield service risk of land-use planning and climate change scenarios on the complex forest social–ecological systems, and services for risk control and service improvement.

The water yield service in the ZMR decreased from 1990 to 2017, with an average annual rate of -0.79 mm. Water yield service in the ZMR was 69.19, 19.98, 31.32, and 47.72 mm in 1990, 2000, 2010, and 2017, respectively. Water yield service value was the highest in 1990 and the lowest in 2000, and it differed significantly between 1990 and 2000. Water yield service in the southeast ZMR was larger than that in the northwest. Water yield service risk increased first, then decreased from 1990 to 2017 in the ZMR, mainly belonging to a high ecological risk level. The subareas of high and higher risk were mainly concentrated in the middle and north ZMR.

There are differences in water yield service under different land-use and climate scenarios in the ZMR. The water yield service in 2100 under different land-use and climate scenarios is lower than in 2050. The water yield service is the highest of the EC126 (48.09 mm in 2050 and 43.73 mm in 2100) and the lowest of the EP585 (43.52 mm in 2050 and 40.62 mm in 2100). Under the same land-use scenario, the water yield service of the SSP1-2.6 climate scenario is higher than that of the SSP5-8.5 climate scenario. Under different scenarios, the water yield service will decrease from the southeast to the northwest, and the subareas of high water yield service were mainly located in the southeast of the ZMR in 2050 and 2100. The water yield service risk in the ZMR in 2100 is larger than in 2050. The variation pattern of water yield service risk under SSP5-8.5 and SSP1-2.6 in 2050 and 2100 is the EC scenario < the ND scenario < the EP scenario. The water yield service risk of the EC126 scenario is the lowest one, and the SP558 scenario is the largest one in 2050 and 2100. The subareas of the high and higher risk are mainly located in the middle and north ZMR in 2050 and 2100. Developing water-saving agriculture and high-efficiency industrial systems, as well as ecological restoration and integrated forest landscape management, will be helpful for risk control and service enhancement, especially in mountainous areas with fragile environments and limited water resources.

DATA AVAILABILITY STATEMENT

The original contributions presented in the study are included in the article/Supplementary Material; further inquiries can be directed to the corresponding author.

AUTHOR CONTRIBUTIONS

JG conceptualized the study, acquired funding, administered the project, supervised the study, wrote the original draft, and wrote, reviewed, and edited the manuscript. TJ conceptualized the study, designed the methodology and software, performed the data curation, investigated, supervised, and visualized the study, provided resources, wrote the original draft, and wrote, reviewed, and edited the manuscript. LY conceptualized the study, performed the data curation, investigated, validated, and supervised the study, designed the methodology and software, provided resources, and performed the formal analysis. SW designed the software, performed the formal analysis, provided resources, and validated and visualized the study.

FUNDING

This work was supported by the Major Program of the National Natural Science Foundation of China (grant numbers 4179420015).

REFERENCES

Ajaz, M. A., Abd-Elrahman, A., Escobedo, F. J., Cropper, W. P., Martin, T. A., and Timilsina, N. (2017). Spatially-explicit Modeling of Multi-Scale Drivers of Aboveground Forest Biomass and Water Yield in Watersheds of the Southeastern United States. *J. Environ. Manag.* 199, 158–171. doi:10.1016/j.jenvman.2017.05.013

Aragaw, H. M., and Mishra, S. K. (2022). Multi-Site Multi-Objective Calibration of SWAT Model Using a Large Dataset for Improved Performance in Ethiopia. *Arab. J. Geosci.* 15 (4), 1–18. doi:10.1007/S12517-022-09602-5

Bai, Y., Ochuodho, T. O., and Yang, J. (2019). Impact of Land Use and Climate Change on Water-Related Ecosystem Services in Kentucky, USA, USA. *Ecol. Indic.* 102, 51–64. doi:10.1016/j.ecolind.2019.01.079

Benra, F., De Frutos, A., Gaglio, M., Álvarez-Garretón, C., Felipe-Lucia, M., and Bonn, A. (2021). Mapping Water Ecosystem Services: Evaluating InVEST Model Predictions in Data Scarce Regions. *Environ. Model. Softw.* 138, 104982. doi:10.1016/J.ENVSOFT.2021.104982

Chen, F., Li, H. B., and Zhang, A. L. (2019). Ecological Risk Assessment Based on Terrestrial Ecosystem Services in China. *Acta Geogr. Sin.* 74 (03), 432–445.

Chen, T., Bao, A. M., Guo, H., Zheng, G. X., Yuan, Y., and Yu, T. (2019). Ecological Vulnerability Assessment for a Transboundary Basin in Central Asia and its Spatiotemporal Characteristics Analysis: Taking Amu Darya River Basin as an Example. *J. Nat. Resour.* 34 (12), 2643–2657.

Chen, L. Q. (2021). *Spatiotemporal Variations and its Impact of Drought in China Based on CMIP6 Multi Model. [dissertation/master's Thesis].* [Nanjing]: Nanjing University of Information Science and Technology.

Choudhary, R., and Athira, P. (2021). Effect of Root Zone Soil Moisture on the SWAT Model Simulation of Surface and Subsurface Hydrological Fluxes. *Environ. Earth Sci.* 80, 1–16. doi:10.1007/S12665-021-09912-Z

Costanza, R., de Groot, R., Sutton, P., van der Ploeg, S., Anderson, S. J., Kubiszewski, I., et al. (2014). Changes in the Global Value of Ecosystem

Services. *Glob. Environ. Change* 26, 152–158. doi:10.1016/j.gloenvcha.2014.04.002

Cunha, E. R. d., Santos, C. A. G., Silva, R. M. d., Bacani, V. M., and Pott, A. (2021). Future Scenarios Based on a CA-Markov Land Use and Land Cover Simulation Model for a Tropical Humid Basin in the Cerrado/Atlantic Forest Ecotone of Brazil. *Land Use Policy* 101, 105141. doi:10.1016/j.landusepol.2020.105141

Dai, E. F., and Wang, Y. H. (2020). Spatial Heterogeneity and Driving Mechanisms of Water Yield Service in Hengduan Mountain Region. *Acta Geogr. Sin.* 75 (03), 607–619.

de Freitas, M. W. D., Muñoz, P., dos Santos, J. R., and Alves, D. S. (2018). Land Use and Cover Change Modelling and Scenarios in the Upper Uruguay Basin (Brazil). *Ecol. Model.* 384, 128–144. doi:10.1016/j.ecolmodel.2018.06.009

Dehdasht, G., Ferwati, M. S., Zin, R. M., and Abidin, N. Z. (2020). A Hybrid Approach Using Entropy and TOPSIS to Select Key Drivers for a Successful and Sustainable Lean Construction Implementation. *PLoS One* 15 (2), e0228746. doi:10.1371/journal.pone.0228746

Ding, J. B., Zhang, F. P., Zhang, Y., Ning, Y. Y., and Zeng, P. R. (2022). Temporal and Spatial Variations in Water Yield of the Qinghai Lake Water System under Climate and Land Use Changes. *J. Lanzhou Univ. Nat. Sci.* 58 (01), 47–56. doi:10.13885/j.issn.0455-2059.2022.01.006

Dou, P. F., Zuo, S. Z., Ren, Y., Dai, S. Q., and Yun, G. L. (2019). The Impacts of Climate and Land Use/land Cover Changes on Water Yield Service in Ningbo Region. *Acta Sci. Circumstantiae* 39 (07), 2398–2409. doi:10.13671/j.hjkxxb.2019.0122

Fu, B., Wang, S., Liu, Y., Liu, J., Liang, W., and Miao, C. (2017). Hydrogeomorphic Ecosystem Responses to Natural and Anthropogenic Changes in the Loess Plateau of China. *Annu. Rev. Earth Planet. Sci.* 45 (01), 223–243. doi:10.1146/annurev-earth-063016-020552

Fujimori, S., Kainuma, M., Masui, T., Hasegawa, T., and Dai, H. (2014). The Effectiveness of Energy Service Demand Reduction: a Scenario Analysis of Global Climate Change Mitigation. *Energy policy* 75, 379–391. doi:10.1016/j.enpol.2014.09.015

Gacheno, D., and Amare, G. (2021). Review of Impact of Climate Change on Ecosystem Services-A Review. *Ijfsa* 5 (03), 363–369. doi:10.26855/IJFSA.2021.09.004

Gao, J., Li, F., Gao, H., Zhou, C. B., and Zhang, X. L. (2016). The Impact of Land-Use Changes on Water-Related Ecosystem Services: a Study of the Guishui River Basin, Beijing, China. *J. Clean. Prod.* 163, S148–S155. doi:10.1016/j.jclepro.2016.01.049

Gao, X., Yang, L. W. Q., Li, C. X., Song, Z. Y., and Wang, J. (2021). Land Use Change and Ecosystem Service Value Measurement in Baiyangdian Basin under Simulated Multiple Scenarios. *Acta Ecol. Sin.* 41 (20), 7974–7988. doi:10.5846/stxb202012243264

Ge, J., Pitman, A. J., Guo, W., Zan, B., and Fu, C. (2020). Impact of Revegetation of the Loess Plateau of China on the Regional Growing Season Water Balance. *Hydrol. Earth Syst. Sci.* 24 (02), 515–533. doi:10.5194/hess-24-515-2020

Ghosh, P., Mukhopadhyay, A., Chanda, A., Mondal, P., Akhand, A., Mukherjee, S., et al. (2017). Application of Cellular Automata and Markov-Chain Model in Geospatial Environmental Modeling- A Review. *Remote Sens. Appl. Soc. Environ.* 5, 64–77. doi:10.1016/j.rsase.2017.01.005

Gong, J., Cao, E., Xie, Y., Xu, C., Li, H., and Yan, L. (2021). Integrating Ecosystem Services and Landscape Ecological Risk into Adaptive Management: Insights from a Western Mountain-Basin Area, China. *J. Environ. Manag.* 281, 111817. doi:10.1016/j.jenvman.2020.111817

Gong, J., Jin, T., Liu, D., Zhu, Y., and Yan, L. (2022). Are Ecosystem Service Bundles Useful for Mountainous Landscape Function Zoning and Management? A Case Study of Bailongjiang Watershed in Western China. *Ecol. Indic.* 134, 108495. doi:10.1016/J.ECOLIND.2021.108495

Guerry, A. D., Ruckelshaus, M. H., Arkema, K. K., Bernhardt, J. R., Guannel, G., Kim, C.-K., et al. (2012). Modeling Benefits from Nature: Using Ecosystem Services to Inform Coastal and Marine Spatial Planning. *Int. J. Biodivers. Sci. Ecosyst. Serv. Manag.* 8, 107–121. doi:10.1080/21513732.2011.647835

Hyandye, C., and Martz, L. W. (2017). A Markovian and Cellular Automata Land-Use Change Predictive Model of the Usangu Catchment. *Int. J. Remote. Sens.* 38 (01), 64–81. doi:10.1080/01431161.2016.1259675

Koko, A. F., Yue, W., Abubakar, G. A., Hamed, R., and Alabsi, A. A. N. (2020). Monitoring and Predicting Spatio-Temporal Land Use/land Cover Changes in Zaria City, Nigeria, through an Integrated Cellular Automata and Markov Chain Model (CA-Markov). *Sustainability* 12 (24), 10452. doi:10.3390/su122410452

Lang, Y., Song, W., and Zhang, Y. (2017). Responses of the Water-Yield Ecosystem Service to Climate and Land Use Change in Sancha River Basin, China. *Phys. Chem. Earth, Parts A/B/C* 101, 102–111. doi:10.1016/j.pce.2017.06.003

Leal Filho, W., Azeiteiro, U. M., Balogun, A.-L., Setti, A. F. F., Mucova, S. A. R., Ayal, D., et al. (2021). The Influence of Ecosystems Services Depletion to Climate Change Adaptation Efforts in Africa. *Sci. Total Environ.* 779, 146414. doi:10.1016/J.SCITOTENV.2021.146414

Legesse, D., Vallet-Coulomb, C., and Gasse, F. (2003). Hydrological Response of a Catchment to Climate and Land Use Changes in Tropical Africa: Case Study South Central Ethiopia. *J. Hydrol.* 275 (1), 67–85. doi:10.1016/S0022-1694(03)00019-2

Li, L. B., Tu, C. L., Zhao, Z. Q., Cui, L. F., and Liu, W. H. (2011). Distribution Characteristics of Soil Organic Carbon and its Isotopic Composition for Soil Profiles of Loess Plateau under Different Vegetation Condition. *S. Earth Environ.* 39 (4), 441–449. doi:10.14050/j.cnki.1672-9250.2011.04.001

Li, Z., Jiang, W., Wang, W. J., Lv, J. X., and Deng, Y. (2019). Study on the Wetland Leading Service Function of Jing-Jin-Ji Urban Agglomeration Based on the Ecosystem Services Value. *J. Nat. Resour.* 34 (08), 1654–1665. doi:10.31497/zrzyxb.20190807

Li, Y. Y., Fan, J. H., and Liao, Y. (2020). Analysis of Spatial and Temporal Differences in Water Conservation Function in Zhangjiakou Based on the InVEST Model. *Pratacultural Sci.* 37 (07), 1313–1324. doi:10.11829/j.issn.1001-0629.2020-0090

Liu, J. F., Jiang, W. G., Zhan, W. F., and Zhou, j. (2010). Processes of SCS Model for Hydrological Simulation: a Review. *Res. Soil Water Conservation* 17 (02), 120–124.

Liu, Z. H., Zhang, G. J., and Fu, F. J. (2020). Assessing Landscape Ecological Risk Based on Landscape Pattern and Services in Guangzhou during 1990-2015. *Acta Ecol. Sin.* 40 (10), 3295–3302. doi:10.5846/stxb201903060425

Liu, Y. X., Shi, X. L., and Shi, W. J. (2021). Evaluation of Water Retention Services of Forest Ecosystem in Fujian Province: Comparison between Results from the InVEST Model and Meta-Analysis. *Acta Ecol. Sin.* 41 (04), 1349–1361. doi:10.5846/stxb202003210632

Liu, Q., Yang, Z. Y., Chen, Y. Q., Lei, J. R., Chen, Z. Z., and Chen, X. H. (2021). Multi-scenario Simulation of Land Use Change and its Eco-Environmental Effect in Hainan Island Based on CA-Markov Model. *Ecol. Environ. Sci.* 30 (07), 1522–1531. doi:10.16258/j.cnki.1674-5906.2021.07.021

Liu, J., Lang, X. D., Su, J. R., Liu, W. D., Liu, H. Y., and Tian, Y. (2021). Evaluation of Water Conservation Function in the Dry-Hot Valley Area of Jinsha River Basin Based on InVEST Model. *Acta Eco Sin.* 41 (20), 8099–8111. doi:10.5846/stxb202101050035

Lv, Y. H., Hu, J., Sun, F. F., and Zhang, L. W. (2015). Water Retention and Hydrological Regulation: Harmony but Not the Same in Terrestrial Hydrological Ecosystem Services. *Acta Ecol. Sin.* 35 (15), 5191–5196.

Lv, R. F. (2019). *Spatial-temporal Associations Among Ecosystem Services and Their Driving Mechanism: A Case Study in the City Belt along the Yellow River in Ningxia [dissertation/master's Thesis]*. Lanzhou: Lanzhou University.

Martinez-Harms, M. J., Bryan, B. A., Figueroa, E., Pliscoff, P., Runting, R. K., and Wilson, K. A. (2017). Scenarios for Land Use and Ecosystem Services under Global Change. *Ecosyst. Serv.* 25, 56–68. doi:10.1016/j.ecoser.2017.03.021

Mokarram, M., Pourghasemi, H. R., Hu, M., and Zhang, H. (2021). Determining and Forecasting Drought Susceptibility in Southwestern Iran Using Multi-Criteria Decision-Making (MCDM) Coupled with CA-Markov Model. *Sci. Total Environ.* 781, 146703. doi:10.1016/J.SCITOTENV.2021.146703

Matlhodi, B., Kenabatho, P. K., Parida, B. P., and Maphanyane, J. G. (2021). Analysis of the Future Land Use Land Cover Changes in the Gaborone Dam Catchment Using CA-Markov Model: Implications on Water Resources. *Remote Sens.* 13 (13), 2427. doi:10.3390/rs13132427

Maviza, A., and Ahmed, F. (2020). Analysis of Past and Future Multi-Temporal Land Use and Land Cover Changes in the Semi-arid Upper-Mzingwane Sub-catchment in the Matabeleland South Province of Zimbabwe. *Int. J. Remote Sens.* 41 (14), 5206–5227. doi:10.1080/01431161.2020.1731001

Millennium Ecosystem Assessment (MA) (2005). *Millennium Ecosystem Assessment Synthesis Report*. Washington, D.C: Island Press.

Mo, W., Zhao, Y., Yang, N., Xu, Z., Zhao, W., and Li, F. (2021). Effects of Climate and Land Use/Land Cover Changes on Water Yield Services in the Dongjiang Lake Basin. *ISPRS Int. J. Geo-Inf.* 10 (07), 466. doi:10.3390/ijgi10070466

Pan, T., Wu, S. H., Dai, E. F., and Liu, Y. J. (2013). Spatiotemporal Variation of Water Source Supply Service in Three Rivers Source Area of China Based on InVEST Model. *Ying Yong Sheng Tai Xue Bao* 24 (01), 183–189. doi:10.13287/j.1001-9332.2013.0140

Pei, H. W., Liu, M. Z., Shen, Y. J., Xu, K., Zhang, H. J., Li, Y. L., et al. (2022). Quantifying Impacts of Climate Dynamics and Land-Use Changes on Water Yield Service in the Agro-Pastoral Ecotone of Northern China. *Sci. Total Environ.* 809, 151153. doi:10.1016/J.SCITOTENV.2021.151153

Qian, Y., Dong, Z., Yan, Y., and Tang, L. (2022). Ecological Risk Assessment Models for Simulating Impacts of Land Use and Landscape Pattern on Ecosystem Services. *Sci. Total Environ.* 833, 155218. doi:10.1016/j.scitotenv.2022.155218

Redhead, J. W., Stratford, C., Sharps, K., Jones, L., Ziv, G., Clarke, D., et al. (2016). Empirical Validation of the InVEST Water Yield Ecosystem Service Model at a National Scale. *Sci. Total Environ.* 569-570, 1418–1426. doi:10.1016/j.scitotenv.2016.06.227

Sánchez-Canales, M., López Benito, A., Passuello, A., Terrado, G., Acuña, V., Schuhmacher, M., et al. (2012). Sensitivity Analysis of Ecosystem Service Valuation in a Mediterranean Watershed. *Sci. Total Environ.* 440 (1), 140–153. doi:10.1016/j.scitotenv.2012.07.071

Sharp, R., Douglass, J., Wolny, S., Arkema, K., Bernhardt, J., Bierbower, W., et al. (2020). *InVEST 3.8.7 User's Guide*. The Natural Capital Project, Stanford University, University of Minnesota, The Nature Conservancy, and World Wildlife Fund.

Sun, S. L., Ge, S., Caldwell, P., McNulty, S., Cohen, E., Xiao, J. F., et al. (2015). Drought Impacts on Ecosystem Functions of the U.S. National Forests and Grasslands: Part II Assessment Results and Management Implications. *For. Ecol. Manage* 353, 269. doi:10.1016/j.foreco.2015.04.002

Sun, L. P. (2018). *Effect Processes and Mechanisms of Natural Restoration Process of the* Quercus Liaotungensis *Communities on Soil Characteristics in the Ziwuling Area. [dissertation/master's Thesis]*. Yangling: Northwest A & F University.

Tadese, S., Soromessa, T., Bekele, T., and Abbas, S. (2021). Analysis of the Current and Future Prediction of Land Use/land Cover Change Using Remote Sensing and the CA-Markov Model in Majang Forest Biosphere Reserves of Gambella, Southwestern Ethiopia. *Sci. World J.* 2021, 6685045. doi:10.1155/2021/6685045

Terrado, M., Acuña, V., Ennaanay, D., Tallis, H., and Sabater, S. (2014). Impact of Climate Extremes on Hydrological Ecosystem Services in a Heavily Humanized Mediterranean Basin. *Ecol. Indic.* 37, 199–209. doi:10.1016/j.ecolind.2013.01.016

UN (United Nations) (2015). Transforming Our World: the 2030 Agenda for Sustainable Development United Nations Sustainable Knowledge Platform, Sustainable Development Goals. Available at: https://sustainabledevelopment.un.org/post2015/transformingourworld.

Wang, Y., Zhao, J., Fu, J., and Wei, W. (2019). Effects of the Grain for Green Program on the Water Ecosystem Services in an Arid Area of China-Using the Shiyang River Basin as an Example. *Ecol. Indic.* 104, 659–668. doi:10.1016/j.ecolind.2019.05.045

Wang, Y. H., Dai, E. F., Ma, L., and Y, L. (2020). Spatiotemporal and Influencing Factors Analysis of Water Yield in the Hengduan Mountain Region. *J. Nat. Resour.* 35 (02), 371–386.

Weng, Y. W., Cai, W. J., and Wang, C. (2020). The Application and Future Directions of Shared Socioeconomic Pathways (SSPs). *Clim. Change Res.* 16 (02), 215–222.

Weng, Q. (2002). Land Use Change Analysis in the Zhujiang Delta of China Using Satellite Remote Sensing, GIS and Stochastic Modelling. *J. Environ. Manage.* 64 (03), 273–284. doi:10.1006/jema.2001.0509

Wu, R., Liu, G. H., and Wen, Y. H. (2017). Spatiotemporal Variations of Water Yield and Water Quality Purification Service Functions in Guanting Reservoir Basin Based on InVEST Model. *Res. Environ. Sci.* 30 (03), 406–414. doi:10.13198/j.issn.1001-6929.2017.01.73

Xu, J., Xiao, Y., Li, N., and Wang, H. (2015). Spatial and Temporal Patterns of Supply and Demand Balance of Water Supply Services in the Dongjiang Lake Basin and its Beneficiary Areas. *J. Resour. Ecol.* 6 (06), 386–396.

Xu, X., Du, Z., and Zhang, H. (2016). Integrating the System Dynamic and Cellular Automata Models to Predict Land Use and Land Cover Change. *Int. J. Appl. Earth Observation Geoinformation* 52, 568–579. doi:10.1016/j.jag.2016.07.022

Xu, J., Xiao, Y., Xie, G. D., Wang, S., and Zhu, W. B. (2016). Spatiotemporal Analysis of Water Supply Service in Dongjiang Lake Basin. *Acta Ecol. Sin.* 58 (15), 4892–4906.

Yan, L. L. (2021). *Spatiotemporal Variation of Ecological Risks and its Management Strategies Based on Ecosystem Services of the Tableland in Loess Plateau: A Case Study of Ziwuling Area. [dissertation/master's Thesis]*. [Lanzhou]: Lanzhou University.

Yang, J., Xie, B. P., and Zhang, D. G. (2020). Spatio-temporal Variation of Water Yield and its Response to Precipitation and Land Use Change in the Yellow River Basin Based on InVEST Model. *Ying Yong Sheng Tai Xue Bao* 31 (08), 2731–2739. doi:10.13287/j.1001-9332.202008.015

Yu, L. P., Song, X. Y., and Wang, Z. G. (2020). Study on the Influence of Evaluation Standardization and Evaluation Methods on Academic Evaluation: Taking TOPSIS Evaluation Method as an Example. *Inf. Stud. Theory & Appl.* 43 (02), 15–20+54. doi:10.16353/j.cnki.1000-7490.2020.02.003

Zhang, L. X., Chen, X. L., and Xin, X. G. (2019). Short Commentary on CMIP6 Scenario Model Intercomparison Project (ScenarioMIP). *Clim. Change Res.* 15 (05), 519–525.

Zhang, T., Zi, L., Yang, W. F., and Wang, J. H. (2021). Applicability of SCS Model in Flash Flood Forecasting and Early Warning. *J. Yangtze River Sci. Res. Inst.* 38 (09), 71–76. doi:10.11988/ckyyb.20200721

Zhang, L. X., Fan, J. W., Zhang, H. Y., and Zhou, D. C. (2022). Spatial-temporal Variations and Their Driving Factors of the Ecological Vulnerability in the Loess Plateau. *Environ. Sci.*, 1–18. In press. doi:10.13227/j.hjkx.202110220

Zhao, Y. R., Zhou, J. J., Lei, L., Xiang, J., Huang, M. H., Feng, W., et al. (2019). Identification of Drivers for Water Yield in the Upstream of Shiyang River Based on InVEST Model. *Chin. J. Ecol.* 38 (12), 3789–3799. doi:10.13292/j.1000-4890.201912.017

Zhou, N. Q., and Zhao, S. (2013). Urbanization Process and Induced Environmental Geological Hazards in China. *Nat. Hazards* 67 (2), 797–810. doi:10.1007/s11069-013-0606-1

Zhuang, S. H. (2020). *Study on the Response Relationship of Ecosystem Service Function of Loess Plateau to Vegetation Restoration. [dissertation/master's Thesis]*. Xi'an: Xi'an University of Technology.

Conflict of Interest: The authors declare that the research was conducted in the absence of any commercial or financial relationships that could be construed as a potential conflict of interest.

frontiers | Frontiers in Ecology and Evolution

ORIGINAL RESEARCH
published: 14 June 2022
doi: 10.3389/fevo.2022.935250

Estimation of the Surface Net Radiation Under Clear-Sky Conditions in Areas With Complex Terrain: A Case Study in Haihe River Basin

Xingran Liu[1,2], Jing Zhang[3], Haiming Yan[2] and Huicai Yang[2]*

[1] International Science and Technology Cooperation Base of Hebei Province, Hebei International Joint Research Center for Remote Sensing of Agricultural Drought Monitoring, Hebei GEO University, Shijiazhuang, China, [2] Natural Resource Asset Capital Research Center, Hebei GEO University, Shijiazhuang, China, [3] Hebei Provincial Climate Centre, Hebei Province Meteorological and Ecological Environment Laboratory, Shijiazhuang, China

OPEN ACCESS

Edited by:
Jinyan Zhan,
Beijing Normal University, China

Reviewed by:
Chunhong Zhao,
Northeast Normal University, China
Shaohua Zhao,
Ministry of Ecology and Environment Center for Satellite Application on Ecology and Environment, China

***Correspondence:**
Haiming Yan
haiming.yan@hgu.edu.cn

Specialty section:
This article was submitted to Environmental Informatics and Remote Sensing, a section of the journal Frontiers in Ecology and Evolution

Received: *04 May 2022*
Accepted: *23 May 2022*
Published: *14 June 2022*

Citation:
Liu X, Zhang J, Yan H and Yang H (2022) Estimation of the Surface Net Radiation Under Clear-Sky Conditions in Areas With Complex Terrain: A Case Study in Haihe River Basin. Front. Ecol. Evol. 10:935250. doi: 10.3389/fevo.2022.935250

The surface net radiation as an important component of the surface radiation budget has attracted wide attention; however, it is still an enormous challenge to carry out an accurate estimation of the surface net radiation in areas with complex terrain due to the scarcity of radiation observation sites and high-spatial heterogeneity of the influencing factors of the surface net radiation. Taking the Haihe River Basin as the study area, this study estimated the surface net radiation under clear-sky conditions from 2001∼2019 based on an improved algorithm of the net long-wave radiation, and the solar short-wave radiation in terms of direct radiation, diffuse sky radiation, and reflected radiation from the surrounding terrain. In this study, the regional meteorological factors were inverted based on remote sensing data to make up for the deficiency of meteorological factor interpolation. The solar short-wave radiation was corrected by considering the comprehensive influence of the atmosphere, underlying surface, and terrain, and the net long-wave radiation was optimized by localizing the algorithm coefficients. The results showed the correlation coefficient between the estimated and observed surface net radiation reached approximately 0.9, indicating the accuracy of this improved method is acceptable. Besides, the results suggested the surface net radiation was significantly influenced by the terrain, the highest value of which occurred on the south slope, followed by that on the southwest slope, west or southeast slopes, and the lowest value occurred on the north slope. In addition, there was the highest surface net radiation in summer, and there was the lowest and most frequently negative surface net radiation in winter. This study makes up for the shortcomings of the traditional spatial interpolation of meteorological factors and previous empirical formulas, and can therefore provide an important methodological foundation for the research on the surface radiation, climate, and hydrology in the areas with complex terrain.

Keywords: complex terrain, net radiation, solar radiation, remote sensing, Haihe River Basin

INTRODUCTION

The surface net radiation as an important component of the surface radiation balance serves as an important driver of regional and even global climate change (Gui et al., 2010; Gharekhan et al., 2022). The climate change in recent decades has inevitably affected the structure and function of ecosystems on the earth, leading to a series of ecological problems, such as the ecosystem imbalance, increased droughts, decreased plant productivity, and species population reduction (Li et al., 2022). The surface net radiation plays an important role in maintaining the surface water–heat balance, which is of great importance to understanding the evolution, structure, and spatial distribution of ecosystems, and it has raised considerable attention in the fields of ecology, agriculture, and water conservation (Jia et al., 2018). A series of surface radiation observation networks and sites have been globally established since the 1950s, but still failed to meet the need for relevant research in the fields of climate, hydrology, and ecology due to the uneven distribution of surface radiation observation sites, especially in complex terrain areas (Gui, 2010). The development of remote sensing technology since the 1960s has provided an innovative approach for the estimation of regional net surface radiation (Hallikainen and Kirimoto, 2008). The remote sensing technology can obtain the large-area and continuous observation data, which can effectively overcome the difficulty of assimilating data from sparse ground stations to a large spatial area (Zhang et al., 2019). There have been a variety of global surface radiation budget products based on remote sensing data (Pinker et al., 2003; Zhang et al., 2004; Tang et al., 2019), which are generally based on the atmospheric radiative transfer models that are not easy to implement and have higher uncertainties resulting from the requirement of more parameters. More importantly, there is generally low spatial resolution of the existing products based on the remote sensing inversion, which cannot reflect the spatial heterogeneity of areas with complex terrain and cannot meet the strict requirements of regional climatic and hydrological studies.

The remote sensing inversion of the net surface radiation on the regional scale, which mainly involves the estimation of solar incident radiation and net long-wave radiation, generally relies on the meteorological data from ground-based observations (Guo and Shen, 2015; Liu et al., 2017; Wu et al., 2017). Specifically, there are many commonly used inversion models of the solar incident radiation, e.g., the Zuo-Dakang Equation, Tong-Hong-Liang Equation, FAO56 Equation, Weng-Du-Ming Equation, YIN Equation, and Yang Equation (Allen et al., 1998; Yang et al., 2006; Yin et al., 2008; Cao et al., 2014). The inversion of the net long-wave radiation is generally carried out with multiple methods such as the Penman method, Brunt method, and Deng Genyun method, and the net long-wave radiation algorithm recommended by the FAO, which have the same structure but different empirical coefficients (Allen et al., 1998; Ren et al., 2006). However, the applicability of these various methods varies greatly in different regions, it is, therefore, necessary to carry out localization and verification of these methods according to the specific conditions, and to take into account the influence of the complex terrain in order to improve the applicability of these methods (Matsui and Osawa, 2015).

A number of scholars have tried to explore solar radiation in complex terrain with the help of the digital elevation model (DEM), geographic information system (GIS), and other technologies (Dozier and Frew, 1990; Dubayah and Rich, 1995; Sultan et al., 2014; Zhang et al., 2020, 2022). These previous studies suggested that the solar zenith angle, altitude, atmospheric transmittance, and surface albedo have a significant influence on the solar incident radiation in complex terrain, and the combination of the remote sensing technology and DEM can more accurately reveal the spatial distribution of solar incident radiation in complex terrain (Chen et al., 2012). However, in these relevant studies based on the remote sensing data and DEM data, scholars have generally focused more on the influence of either the atmosphere or the underlying surface, and they are more concentrated on the study of instantaneous radiation with a short-time series due to the limitation of remote sensing data (Roupioz et al., 2016; Zhang and Zhao, 2016; Hao et al., 2019). Additionally, there are scarcely meteorological stations in mountainous areas, which cannot meet the requirements of the large-scale estimation of the surface net radiation, and scholars generally have to obtain the spatial explicit information of the regional meteorological factors with spatial interpolation, which inevitably leads to some errors in the estimation of the surface net radiation (Long et al., 2010; Wu et al., 2017). Moreover, some previous studies have considered the influence of elevation (Long et al., 2010; Guo and Shen, 2015; Liu et al., 2017), but it is still difficult to distinguish the difference between shaded and sunny slopes and to accurately reflect the influence of the terrain.

The Haihe River Basin is one of the most important national grain production bases in China, where the average annual temperature has increased significantly in recent decades, and the relevant ecological issues under the background of global warming have received increasing attention from scholars. This region is located in a temperate continental monsoon climate zone, with very limited water resources, accounting for less than 1.3% of the national total water resource amount, but this region also accounted for 11% of the national arable land area, and therefore there is an outstanding contradiction between water supply and demand under climate change (Guo and Shen, 2015). More importantly, the water resources are very unevenly distributed in time and space, and the mountainous areas as the main water-producing areas are very sensitive to the changes in the surface radiation budget caused by climate change (Lei et al., 2014). It is therefore of great significance to explore the net surface radiation variation to the relevant research on agricultural, ecological, and hydrological problems of the Haihe River Basin. However, the scarcity of observation data on mountainous areas with complex terrain greatly limits the accurate acquisition of the regional net surface radiation in the Haihe River Basin. This study inverted the meteorological factors based on the remote sensing data to make up for the shortage of traditional spatial interpolation of meteorological factors, taking into account the impacts of the atmosphere,

underlying surface, and complex terrain. This study further improved the key parameters of the algorithm to achieve a more accurate inversion of the net surface radiation under clear-sky conditions in the Haihe River Basin from 2001∼2019, aiming to provide a methodological reference for the estimation of net surface radiation in areas with complex terrain and relevant research in the fields of climate, agriculture, ecology, hydrology, and so on.

MATERIALS AND METHODS

The daily net surface radiation was calculated as the difference between the incoming daily short-wave net radiation and the outgoing daily long-wave net radiation. This study first estimated the direct radiation, diffuse sky radiation, and reflected radiation from the surrounding terrain in the Haihe River Basin based on the remote sensing data and elevation data. Then, this study estimated the clear-sky solar incident radiation on the surface. Thereafter, the daily short-wave net radiation was estimated based on the surface reflectance from the remote sensing inversion. Finally, the net daily long-wave radiation of the Haihe River Basin was corrected based on the meteorological data from the remote sensing inversion, with the coefficients algorithm recommended by the FAO (**Figure 1**).

The data used in the study included the remote sensing data, elevation data, and meteorological data used to optimize the parameters and validate the results. Specifically, the remote sensing data included the MODIS surface reflectance product MOD09GA and the MODIS atmospheric precipitable water product MOD05L2 from 2001∼2019, which were downloaded at https://search.earthdata.nasa.gov/and https://ladsweb.modaps.eosdis.nasa.gov/. The meteorological data of multiple meteorological stations included the relative humidity, daily maximum temperature, and daily minimum temperature from 2001∼2019 in the daily meteorological dataset of basic meteorological elements of China National Surface Weather Station, and the daily global and net radiation in the daily radiation dataset of China, which were downloaded from the China Meteorological Data Network[1] (**Figure 2**). The elevation data were SRTM DEM data with a spatial resolution of 90 m, which were downloaded from the Geospatial Data Cloud[2]. All the data were finally processed into the spatial resolution of 0.01 degree in view of the difference in the resolution between the remote sensing and DEM data.

Estimation of Solar Incident Radiation

The solar incident radiation under complex terrain conditions consists of direct radiation, diffuse sky radiation, and reflected radiation from the surrounding terrain, as shown in Equation (1). This study estimated the instantaneous solar incident radiation amount and then extended it to the daily solar incident radiation amount by accumulating it over the sunrise and sunset time angles since the solar incident radiation varies with time during the day.

$$R_{\mathrm{s}} = R_{\mathrm{dir}} + R_{\mathrm{dif}} + R_{\mathrm{ref}} \tag{1}$$

where R_s is the solar incident radiation, R_{dir} is the direct radiation, R_{dif} is the diffuse sky radiation, and R_{ref} is the reflected radiation from the surrounding terrain.

Estimation of Direct Radiation

Direct radiation is affected by the incidence angle on slope I (i.e., the angle between the solar ray and the normal slope surface). Under the condition of $I \geq 90°$, R_{dir} is 0 as the target point is completely in shadow; under the condition of $0° \leq I < 90°$, the algorithm of R_{dir} is as follows (Wang, 2011):

$$R_{\mathrm{dir}} = V_s \times \tau \times G_{\mathrm{sc}} \times \left(\frac{r_0}{r}\right)^2 \times \cos I \tag{2}$$

where V_s is the shading coefficient, τ is the direct radiation transmissivity, G_{sc} is the solar constant (1367 $\mathrm{W{\cdot}m^{-2}}$), $\left(\frac{r_0}{r}\right)^2$ is the correction coefficient of the Earth-Sun distance, and $\cos I$ represents the influence of the incident angle on the slope surface.

The shading coefficient V_s is the area proportion of solar radiation received by the target point, and the value of 1 indicates there is no shading of the surrounding terrain, and the value of 0 indicates the target point is completely shaded. This coefficient was calculated with the algorithm of the Hillshade function using the ArcGIS software as follows:

$$V_{\mathrm{s}} = \cos z \times \cos s + \sin z \times \sin s \times \cos(\alpha - \gamma) \tag{3}$$

where z is the solar zenith angle (radians); s is the slope gradient (radians); α is the solar azimuth angle (radians), with 0 (2π), π, $\pi/2$, and $3\pi/2$ representing the due east, due west, due north, and due south, respectively; γ is the slope direction (radians), with the range of [0–2π]. Specifically, s and γ were calculated with the methods in the algorithm of the Hillshade function using the ArcGIS software; z and α were calculated with the algorithms of Wang (1999) and Allen et al. (2007) as follows:

$$\cos(z) = \sin\delta \times \sin\phi + \cos\delta \times \cos\phi \times \cos\omega \tag{4}$$

$$\alpha = \mathrm{acos}\left[\frac{\sin h \times \sin\phi - \sin\delta}{\cos h \times \cos\phi}\right] \tag{5}$$

$$\delta = 0.409 \times \sin\left(2\pi \times \frac{DOY}{365} - 1.39\right) \tag{6}$$

$$\omega = \pi \times (t - 12)/12 \tag{7}$$

where δ is the solar declination (radians); φ is the geographical latitude (radians); ω is the solar time angle (radians); h is the solar altitude (radians), which is reciprocal with z; DOY is the annual cumulative day; and t is the local time. Notably, the value of α obtained with this method is 0 (2π) for the due south, $\pi/2$ for the due west, π for the due north, and $3\pi/2$ for the due east, so these directions should be converted when they are substituted into Equation (3).

[1] http://data.cma.cn/

[2] http://www.gscloud.cn/

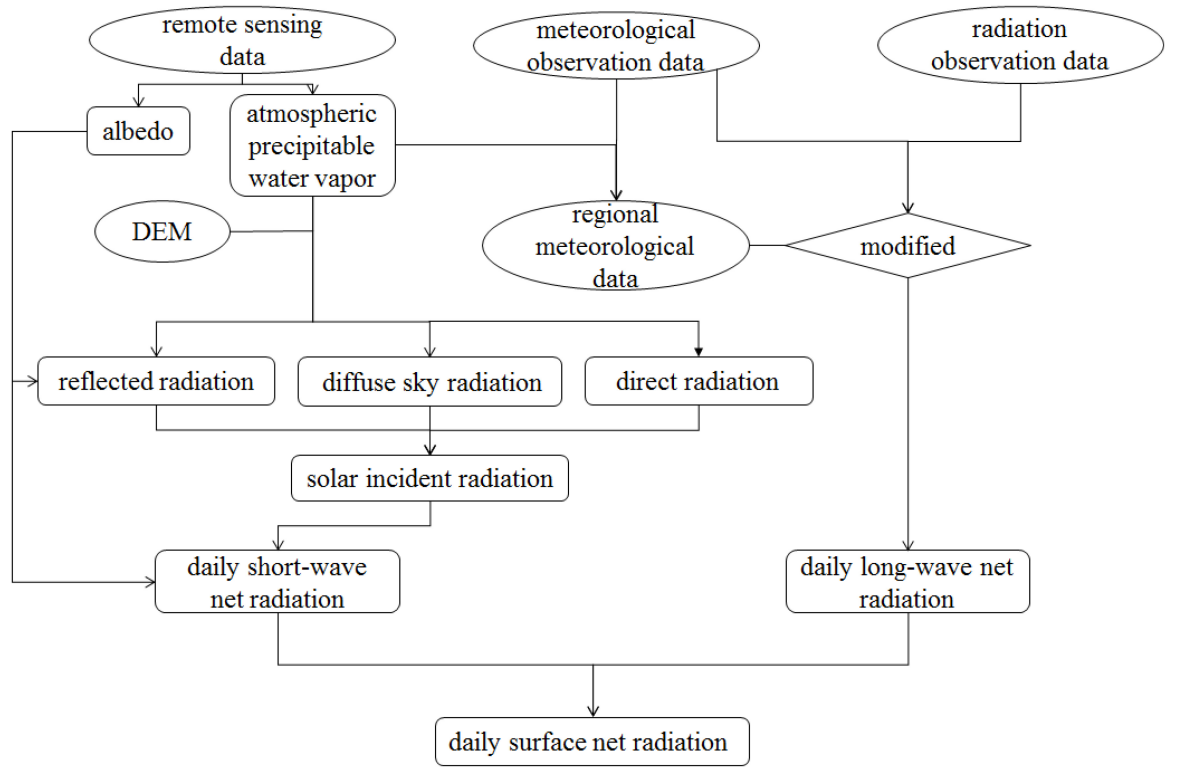

FIGURE 1 | Flow diagram of the estimation of the surface net radiation under clear-sky conditions in this study.

The clear-sky direct radiation transmissivity was estimated with the empirical equation proposed by Kreith and Kreider (1978) for calculating the atmospheric transparency coefficient as follows (Kreith and Kreider, 1978):

$$\tau = 0.56(e^{-0.56M_h} + e^{-0.095M_h}) \tag{8}$$

$$M_h = M_0 \times \frac{P_h}{P_0} \tag{9}$$

where M_h is the atmospheric volume below a certain elevation. M_0 is the atmospheric volume at the sea level, and $\frac{P_h}{P_0}$ is the atmospheric pressure correction factor, which were calculated as follows (Kreith and Kreider, 1978; List, 1984):

$$M_0 = [1229 + (614\sin h)^2]^{1/2} - 614\sin h \tag{10}$$

$$\frac{P_h}{P_0} = \left[\frac{288 - 0.0065dem}{288}\right]^{5.256} \tag{11}$$

where *dem* is the altitude (m).

Additionally, this study corrected τ during November and February into $k\tau$ since τ is affected by the season (Chen et al., 2009), and k was set to be 1.8198 according to the previous research (Liu et al., 2021).

The correction coefficient of the Earth–Sun distance was calculated with the algorithm of Wang (1999) as follows:

$$\left(\frac{r_0}{r}\right)^2 = 1/\left(\frac{r}{r_0}\right)^2 = 1/(1.000423 + 0.032359\sin\varepsilon + 0.000086\sin 2\varepsilon - 0.008349\cos\varepsilon + 0.000115\cos 2\varepsilon) \tag{12}$$

$$\varepsilon = 2\pi \times (DOY - N_0)/365.2422 \tag{13}$$

$$N_0 = 79.6764 + 0.2422 \times (Year - 1985) - INT[(Year - 1985)/4] \tag{14}$$

where *Year* is the concerned year, and INT denotes the integer function.

The influence of the incident angle on the slope surface was calculated as follows (Duffie and Beckman, 1991):

$$\cos I = \sin\delta\sin\phi\cos s - \sin\delta\cos\phi\cos\gamma\sin s + \cos\delta\cos\phi\cos s\cos\omega + \cos\delta\sin\phi\sin s\cos\gamma\cos\omega + \cos\delta\sin\gamma\sin s\sin\omega \tag{15}$$

where the slope direction γ ranges between [−π, π] and 0, −π/2, π/2, and ± π, which represent the south, east, west, and north directions, respectively.

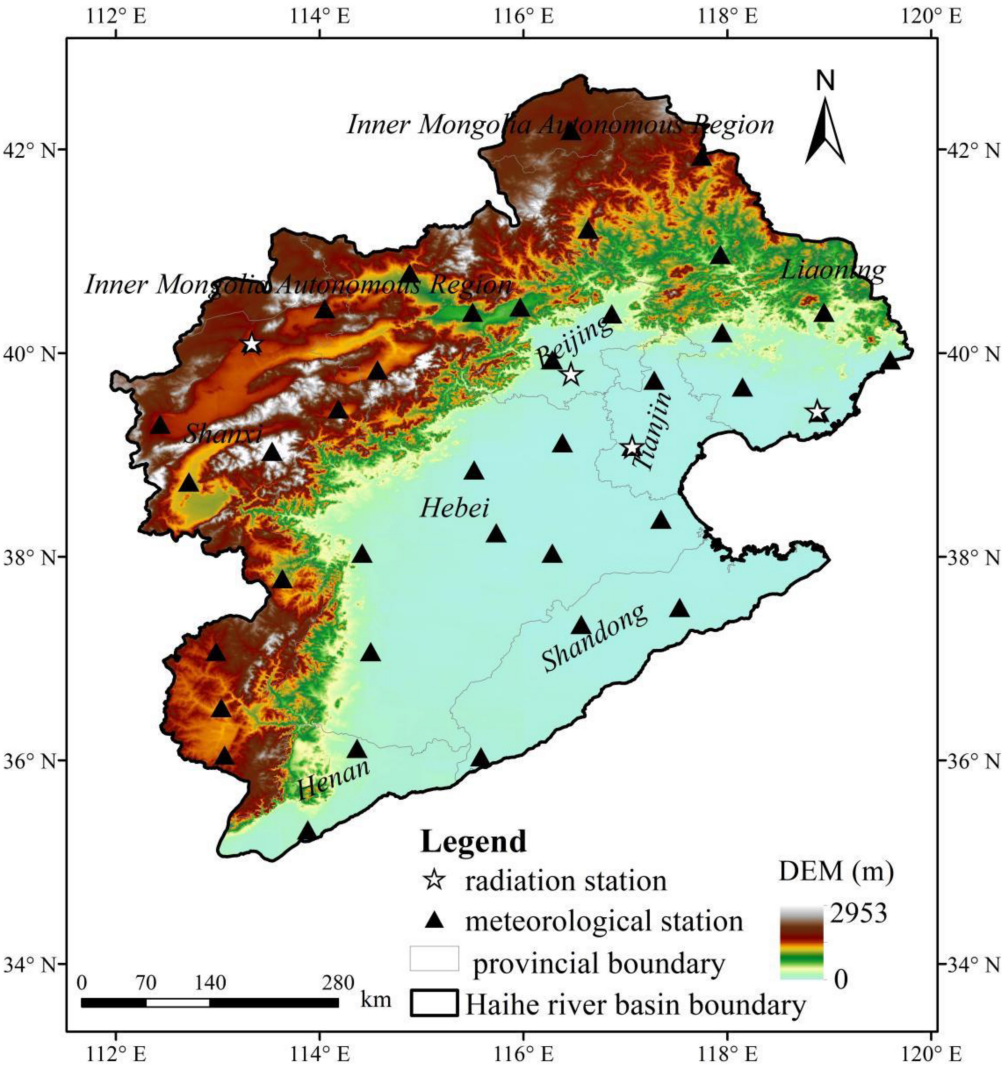

FIGURE 2 | Location of the meteorological and radiation stations in the Haihe River Basin.

Estimation of the Diffuse Sky Radiation

The surface cannot receive all the diffuse radiation from the space hemisphere under the influence of the terrain under conditions of arbitrary terrain, and this study introduced the sky view factor to determine the sky range where the diffuse radiation can be received based on the algorithm of Allen et al. (2006) as follows:

$$R_{dif} = KD \times G_{sc} \times \left(\frac{r_0}{r}\right)^2 \times \cos z \times f_i \tag{16}$$

$$f_i = 0.75 + 0.25\cos(s) - \frac{0.5s}{\pi} \tag{17}$$

where f_i is the sky view factor under conditions of isotropic scattering; KD is the transmissivity coefficient of scattered radiation, which is related to the broad-band atmospheric transmissivity KB (Asce-Ewri, 2005; Allen et al., 2010), when $KB \geq 0.15$, $KD = 0.35{-}0.36 \times KB$, and when $KB < 0.15$, $KD = 0.18 + 0.82 \times KB$.

$$KB = 0.98 \times \exp\left[\frac{-0.00146P_{\text{air}}}{K_t \cos z} - 0.075\left(\frac{pre}{\cos z}\right)^{0.4}\right] \tag{18}$$

where K_t is the atmospheric turbidity coefficient, the value of which is 1 under clear-sky conditions; pre is the atmospheric precipitable water vapor (mm); P_{air} is atmospheric pressure (kPa).

Estimation of the Reflected Radiation From the Surrounding Terrain

The land surface receives solar radiation reflected from the surrounding terrain under conditions of arbitrary terrain, especially in complex terrain areas. The reflected radiation from the surrounding terrain is influenced by the surface albedo of the surrounding terrain, slope direction, and the sky view factor, and

it can be calculated as follows (Allen et al., 2010):

$$R_{ref} = (KB + KD) \times G_{SC} \times \left(\frac{r_0}{r}\right)^2 \times \cos z \times albedo \times (1 - f_i) \quad (19)$$

where *albedo* is the ground albedo of the adjacent pixel corresponding to the slope direction of the target point.

Estimation of the Net Surface Radiation

According to the algorithm of daily net radiation recommended in FAO56 (Allen et al., 1998), the daily net radiation is calculated as the difference between the daily short-wave net radiation and daily long-wave net radiation as follows:

$$R_{\mathrm{n}} = R_{\mathrm{ns}} - R_{\mathrm{nl}} \quad (20)$$

where R_n, R_{ns}, and R_{nl} are the net daily radiation, net daily short-wave radiation, and net daily long-wave radiation ($\mathrm{MJ{\cdot}m^{-2}{\cdot}day^{-1}}$), respectively.

$$R_{\mathrm{ns}} = (1 - albedo)R_{\mathrm{s}} \quad (21)$$

where R_s is the solar incident radiation ($\mathrm{MJ{\cdot}m^{-2}{\cdot}day^{-1}}$) and *albedo* is the surface albedo, which can be extracted from the 7-band reflectance of the MOD09GA product as follows (Tasumi et al., 2008):

$$albedo = 0.215\alpha_1 + 0.215\alpha_2 + 0.242\alpha_3 + 0.129\alpha_4 + 0.101\alpha_5 + 0.062\alpha_6 + 0.036\alpha_7 \quad (22)$$

where α_i is the 7-band reflectance of the MOD09GA product, and $i = 1, 2,., 7$.

R_{nl} was corrected based on the algorithm recommended by the FAO as follows:

$$R_{\mathrm{nl}} = \sigma\left[\frac{T_{\max}^4 + T_{\min}^4}{2}\right](b - k\sqrt{e_{\mathrm{a}}})\left[1.35\frac{R_{\mathrm{s}}}{R_{\mathrm{so}}} - 0.35\right] \quad (23)$$

where σ is the Stefan–Boltzmann constant, which is 4.903×10^{-9} $\mathrm{MJ{\cdot}K^{-4}{\cdot}m^{-2}{\cdot}day^{-1}}$; T_{max}, T_{min}, and e_a are the maximum temperature, minimum temperature (K), and the actual water vapor pressure (kPa), respectively, which were inversed from the MOD05L2 product. R_{so} is the clear-sky solar short-wave radiation ($\mathrm{MJ{\cdot}m^{-2}{\cdot}day^{-1}}$). $\frac{R_s}{R_{so}}$ is 1 under clear-sky conditions; k and b are coefficients obtained by fitting the station observations.

Correction of the Daily Solar Long-Wave Net Radiation Coefficient

According to the surface net radiation calculation [Equations (20)–(23)], the relationship among the radiation, air temperature, and air–water vapor pressure under clear-sky conditions is as follows:

$$\frac{(1 - albedo)R_{\mathrm{s}} - R_{\mathrm{n}}}{\sigma[\frac{T_{\max}^4 + T_{\min}^4}{2}]} = -k\sqrt{e_a} + b \quad (24)$$

assuming $y = \frac{(1-albedo)R_{\mathrm{s}} - R_{\mathrm{n}}}{\sigma[\frac{T_{\max}^4 + T_{\min}^4}{2}]}$, $x = \sqrt{e_a}$, then $y = -kx + b$, where e_a was estimated with the algorithm in the FAO56. The linear relationship between y and x was then fitted with the albedo data inverted from the MOD09GA product, the daily solar incident radiation and daily net radiation data observed at radiation stations on clear-sky days, and the maximum temperature, minimum temperature, and relative humidity data observed at meteorological stations at corresponding locations, based on which the values of k and b were thereafter determined.

Remote Sensing Inversion of the Meteorological Factors

The atmospheric precipitable water vapor data at the corresponding locations of meteorological stations in the Haihe River Basin were extracted from the MOD05L2 product. Then the mathematical relationships among the maximum temperature, minimum temperatures, and the atmospheric precipitable water were established separately for the spring (March–May), summer (June–August), autumn (September–November), and winter (December–February) [Equations (25) and (26)]. Thereafter, the spatially explicit regional meteorological data can be inferred according to the atmospheric precipitable water vapor data based on these mathematical relationships.

$$T_{\min} = f_1(pre) \quad (25)$$

$$T_{\max} = f_2(pre) \quad (26)$$

where T_{min} and T_{max} are the daily minimum temperature and maximum temperature (°C), respectively, and *pre* is the atmospheric precipitable water vapor (cm).

There is generally a close mathematical relationship between the actual water vapor pressure and atmospheric precipitable water, and it is feasible to establish the functional relationship between the actual water vapor pressure observation data at meteorological stations and the atmospheric precipitable water data in the MOD05L2 product, based on which the spatially explicit regional water vapor pressure can be inverted. In this study, the actual water vapor pressure data at meteorological stations in the Haihe River Basin from 2001∼2019 were estimated with the data of relative humidity, maximum temperature, and minimum temperature available at meteorological stations as follows:

$$e_a = \frac{RH}{100}\left[\frac{e^{\circ}(T_{\max}) + e^{\circ}(T_{\min})}{2}\right] \quad (27)$$

$$\mathrm{e}^{\circ}(T) = 0.6108\exp\left[\frac{17.27T}{T + 237.3}\right] \quad (28)$$

where e_a is the actual water vapor pressure (kPa), *RH* is the relative humidity (%); T, T_{min}, and T_{max} are the temperature, minimum temperature, and maximum temperature (°C), respectively.

Evaluation of the Estimation Accuracy

This study evaluated the estimation accuracy by comparing the estimated results with the observation data from radiation

stations in the Haihe River Basin. Specifically, the correlation coefficient and the root mean square error were used to represent the estimation accuracy of the daily incident solar radiation and daily net radiation under clear-sky conditions from 2001∼2019 as follows:

$$R = \frac{\sum_{i=1}^{n}(x_i - \overline{x})(y_i - \overline{y})}{\sqrt{\sum_{i=1}^{n}(x_i - \overline{x})^2 \sum_{i=1}^{n}(y_i - \overline{y})^2}} \quad (29)$$

$$RMSE = \sqrt{\frac{\sum_{i=1}^{n}(x_i - y_i)^2}{n}} \quad (30)$$

where R is the correlation coefficient, $RMSE$ is the root mean square error, n is the total number of estimated radiation data to be verified, x_i is the site observation value, y_i is the estimated value, $\bar{x}_i$ is the mean of the site observation values, and $\bar{y}_i$ is the mean of the estimated values.

RESULTS AND DISCUSSION

Relationship Between the Meteorological Factors and the Remote Sensing Data

Figure 3 suggests that there was a remarkable seasonal variation of the atmospheric precipitable water vapor and temperature in the Haihe River Basin, which showed a significant correlation. Specifically, there was a very significant seasonal variation of the atmospheric precipitable water, which reached the maximum value above 8 cm in summer, the minimum value generally below 1 cm in winter, and the medium value below 4 cm in spring or autumn. The magnitude of temperature variation with atmospheric precipitation varied significantly in different seasons, specifically, the temperature variation was stronger when the atmospheric precipitable water was very low, but it gradually tended to level off when the atmospheric precipitable water exceeded 1 cm.

It is more accurate to reveal the mathematical relationship between temperature and atmospheric precipitable water vapor by fitting them by season, and the fitting results based on the atmospheric precipitable water vapor data and the MOD05L2 product at the location of meteorological stations in the Haihe River Basin from 2001∼2019 suggested that there was an obvious logarithmic relationship between the air temperature and atmospheric precipitable water vapor as shown in Equations (31) and (32). In particular, the significant correlation between air temperature and atmospheric precipitable water vapor varied with seasons. Specifically, the correlation between the air temperature and atmospheric precipitable water vapor was high in spring and autumn and low in summer and winter, with the correlation coefficient between 0.7 and 0.8 and 0.3 and 0.6, respectively.

$$T_{\min} = a_1 \ln(pre) + b_1 \quad (31)$$

$$T_{\max} = a_2 \ln(pre) + b_2 \quad (32)$$

where a_1, b_1, a_2, and b_2 are the fitted coefficients. Specifically, in spring, $a_1 = 9.2323$, $b_1 = 8.3757$, $a_2 = 8.6755$, and $b_2 = 24.621$; in summer, $a_1 = 5.2267$, $b_1 = 12.69$, $a_2 = 2.6939$, and $b_2 = 28.898$; in autumn, $a_1 = 9.5585$, $b_1 = 5.0577$, $a_2 = 10.484$, and $b_2 = 19.757$; and in winter, $a_1 = 6.448$, $b_1 = -2.1371$, $a_2 = 6.4342$, and $b_2 = 11.406$.

The relationship between the actual water vapor pressure and atmospheric precipitable data is shown in Equation (33) and **Figure 4**, which was revealed on the basis of the actual water vapor pressure data and the atmospheric precipitable data extracted from the MOD05L2 product at the location of meteorological stations from 2001∼2019.

$$e_a = 0.6215pre + 0.2017 \quad (33)$$

Verification of the Solar Radiation Inversion

Correction Coefficients of the Daily Long-Wave Net Radiation

The correction coefficients k and b in the daily long-wave net radiation algorithm were obtained by fitting the meteorological data and radiation data observed at the stations and the albedo data extracted from the remote sensing data. The results shown in **Figure 5** suggested k and b were 0.1042 and 0.3821, respectively. The long-wave net radiation algorithm recommended by the FAO was localized with the correction coefficients k and b, making it more applicable to the Haihe River Basin.

Verification of the Estimated Solar Radiation

There are four radiation observation stations in the Haihe River Basin (**Figure 2**), i.e., Beijing station (39.48°N, 116.28°E, altitude 31.3 m), Datong station (40.06°N, 113.2°E, altitude 1,067.2 m), Laoting station (39.26°N, 118.53°E, altitude 10.5 m), and Tianjin station (39.05°N, 117.04°E, altitude 2.5 m). Specifically, Beijing, Laoting, and Tianjin stations provided both the daily solar radiation and net radiation observation data, while Datong station provided only the daily solar radiation observation data. Meanwhile, the Beijing station provided more comprehensive observation available for the full period of 2001∼2019, while the other three stations only provided observation data available from 2001 to 2010.

The estimated results of the solar incident radiation and daily net radiation under clear-sky conditions from 2001∼2019 were verified with the available observation data of these radiation stations (**Figures 6**, **7**). The correlation coefficients between the estimated and observed daily solar incident radiation at Beijing, Datong, Laoting, and Tianjin stations reached 0.90, 0.91, 0.91, and 0.90, respectively, with the root mean square errors of 3.39 MJ/(m^2·day), 3.55 MJ/(m^2·day), 3.18 MJ/(m^2·day), and 3.38 MJ/(m^2·day), respectively. The correlation coefficients between the estimated and observed daily net radiation at Beijing, Laoting, and Tianjin stations were 0.90, 0.90, and 0.89, respectively, with the root mean square errors of 2.80 MJ/(m^2·day), 3.08 MJ/(m^2·day), and MJ/(m^2·day), respectively. Overall, the estimated incident solar radiation and

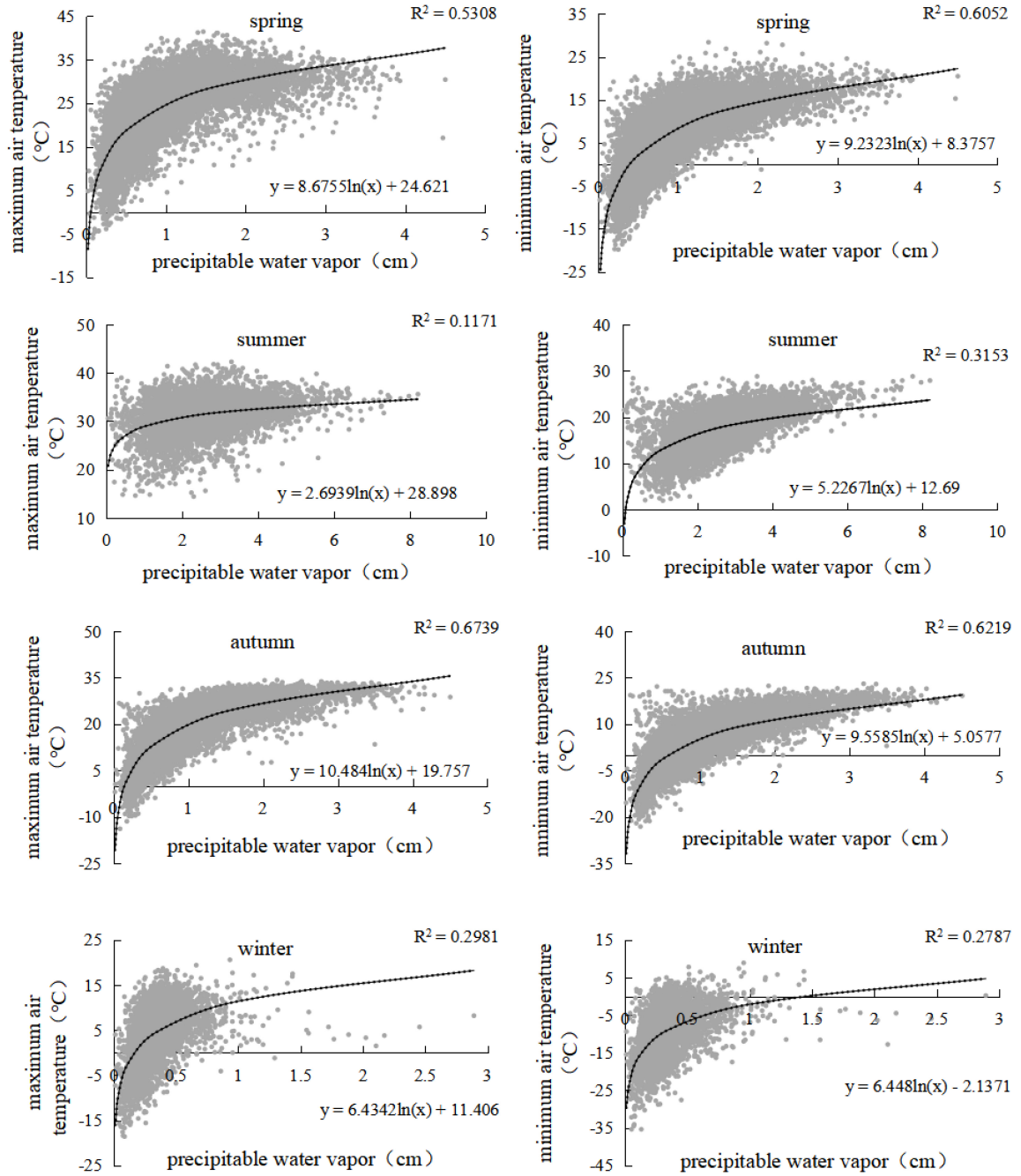

FIGURE 3 | Relationship between the temperature and atmospheric precipitable water by season in Haihe River Basin.

net daily radiations were highly consistent with the observed ones, with the estimation accuracy within the acceptable range.

Spatiotemporal Variation of Solar Radiation in the Haihe River Basin

Temporal Variation of Solar Radiation

The average solar radiation of the Haihe River Basin showed no significant inter-annual changing trends but remarkable intra-annual fluctuation during 2001∼2019 (**Figure 8**). Specifically, the annual average values of the daily solar incident radiation, daily long-wave net radiation, and daily net radiation under clear-sky conditions in the Haihe River Basin from 2001∼2019 ranged between 16.6 and 20.9 MJ/(m^2·day), 9.1 and 9.5 MJ/(m^2·day), 4.8 and 8.2 MJ/(m^2·day), respectively. Overall, the solar incident radiation and net radiation under clear-sky conditions showed significant inter-annual variation, but their annual average values showed no obvious changing

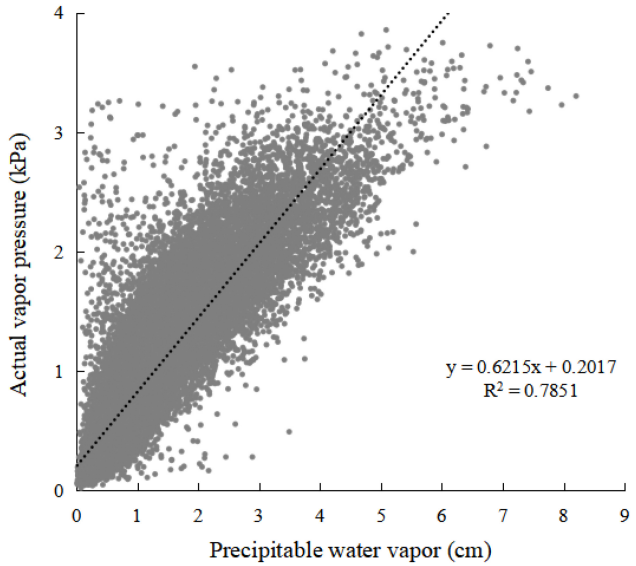

FIGURE 4 | Relationship between the actual vapor pressure and atmospheric precipitable water in Haihe River Basin.

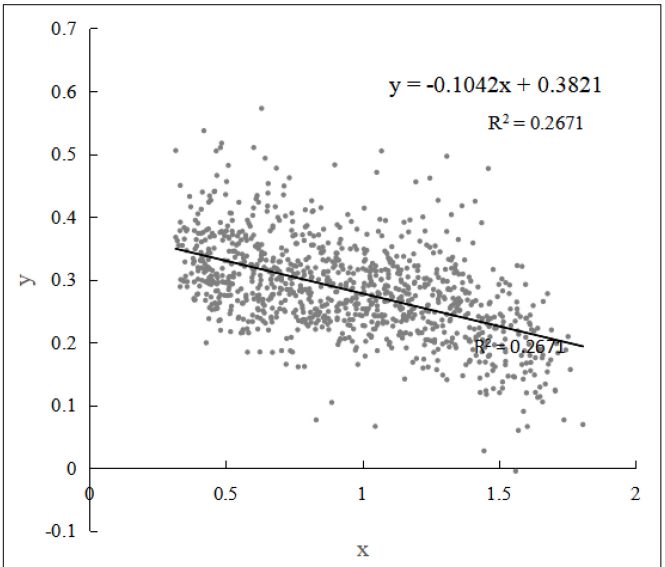

FIGURE 5 | Fitting curve of the correction coefficients *k* and *b* in the daily long-wave net radiation algorithm.

trends, which only increased slightly, with the variation slopes of 0.08 and 0.07, respectively.

There was a very significant seasonal variation in the solar radiation of the Haihe River Basin, and the average daily solar incident radiation and daily net radiation under clear-sky conditions were the highest in summer and the lowest in winter, basically showing a single-peak pattern. Specifically, the seasonal average values of daily solar incident radiation, daily net radiation, and daily long-wave net radiation ranged between 7.5 and 30.8 MJ/(m^2·day), −3.8 and 16.9 MJ/(m^2·day), and 7.5 and 10.6 MJ/(m^2·day), respectively. More specifically, the average values of daily solar incident radiation, daily net long-wave radiation, and daily net radiation in spring from 2001∼2019 ranged between 20.4 and 25.4 MJ/(m^2·day), 9.6 and 9.8 MJ/(m^2·day), and 7.4 and 11.5 MJ/(m^2·day), respectively. In summer, the solar incident radiation and daily net radiation increased to some extent, with the daily average value ranging between 26.6 and 30.3 MJ/(m^2·day) and 13.1 and 16.0 MJ/(m^2·day), respectively, while the daily long-wave net radiation decreased to some extent, with the average value ranging between 8.8 and 9.8 MJ/(m^2·day). In contrast, in autumn, the solar incident radiation and daily net radiation were relatively lower, with average daily values fluctuating between 12.1 and 16.0 MJ/(m^2·day) and 1.2 and 4.7 MJ/(m^2·day), respectively, while the daily long-wave net radiation fluctuates between 9.1 and 9.3 MJ/(m^2·day). The lowest values of solar incident radiation, net daily longwave radiation, and net daily radiation all occurred in winter, with the average daily values ranging between 8.0 and 16.5 MJ/(m^2·day), 8.1 and 8.4 MJ/(m^2·day), and −1.5 and 5.7 MJ/(m^2·day), respectively. Moreover, the seasonal solar radiation showed no significant changing trends during the study period, and the solar incident radiation in spring and the net daily radiation in summer and winter increased most remarkably, but with the slopes of growth reaching only 0.05 and 0.03, respectively.

Spatial Heterogeneity of Solar Radiation in the Haihe River Basin

The solar incident radiation at the surface differed greatly among regions in the Haihe River Basin, and the net surface radiation in the Haihe River Basin showed complex spatial heterogeneity under the influence of multiple factors such as location and terrain (**Figure 9**). Taking the solar radiation under clear-sky conditions in different seasons of 2017 as an example (**Figure 9**), this study suggested there was an obvious difference in solar incident radiation and net surface radiation in mountainous areas, where the difference between the highest and lowest solar incident radiation exceeded 11 MJ/(m^2·day) and the difference between the highest and lowest net surface radiation even exceeded 16 MJ/(m^2·day). On the one hand, the solar incident radiation is closely related to the latitude. In general, the lower the latitude is, the larger the solar altitude angle is, and the more the solar radiation reaching the ground is, and vice versa, and this study also suggested the solar incident radiation in the Haihe River Basin showed an overall decreasing trend from south to north (**Figure 9**). On the other hand, the daily outgoing long-wave net radiation is positively correlated with the temperature, which is also closely related to the latitude. Generally, the lower the latitude is, the higher the temperature is, and vice versa, which can offset the influence of solar incident radiation on the net surface radiation in latitudinal zones to a certain extent. As a result, this study suggested the spatial difference in the net surface radiation between latitudinal zones from south to north was not as significant as that of the solar incident radiation in the Haihe River Basin (**Figure 9**).

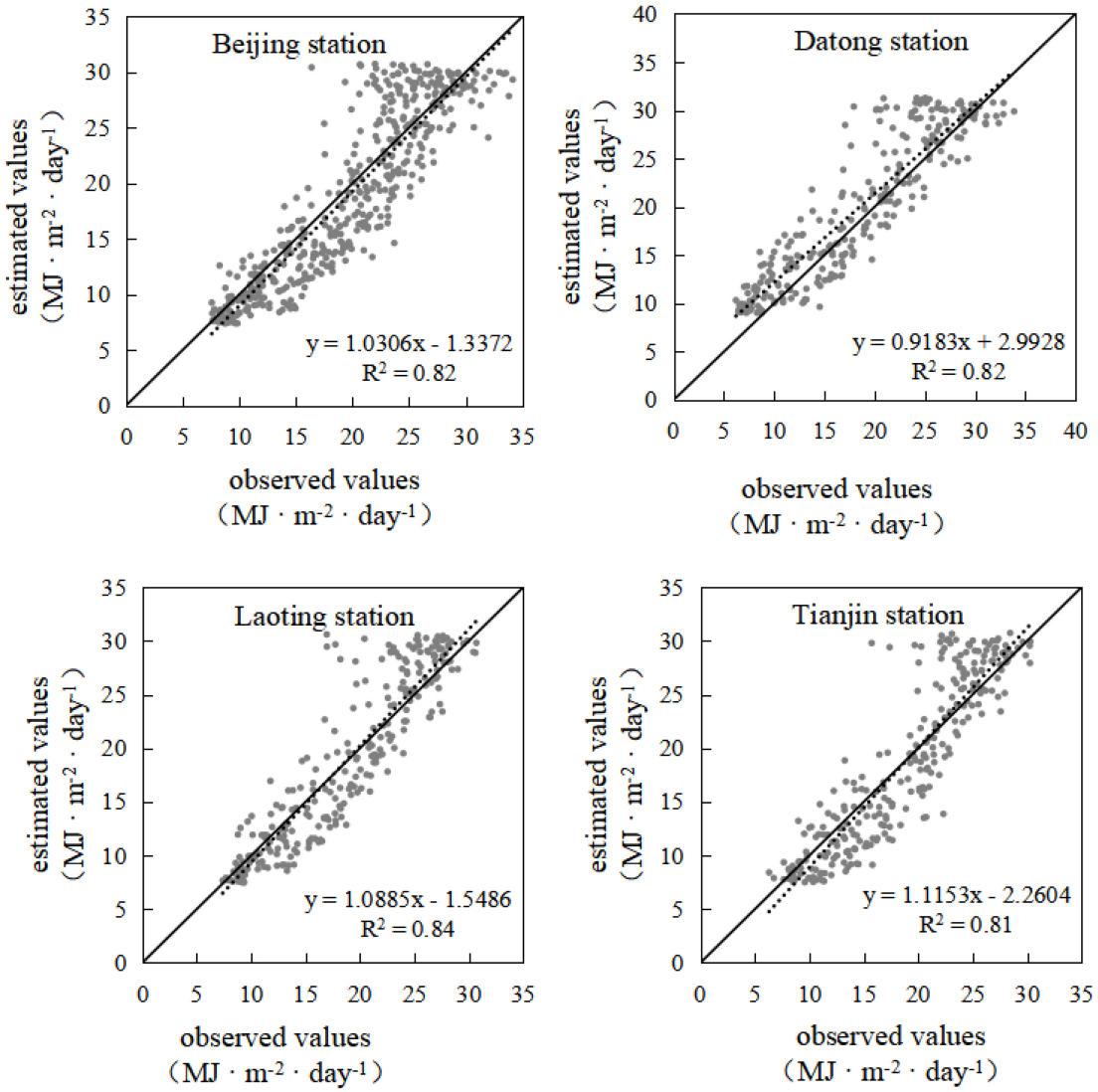

FIGURE 6 | Comparison of the estimated and observed daily solar incident radiation of the Haihe River Basin.

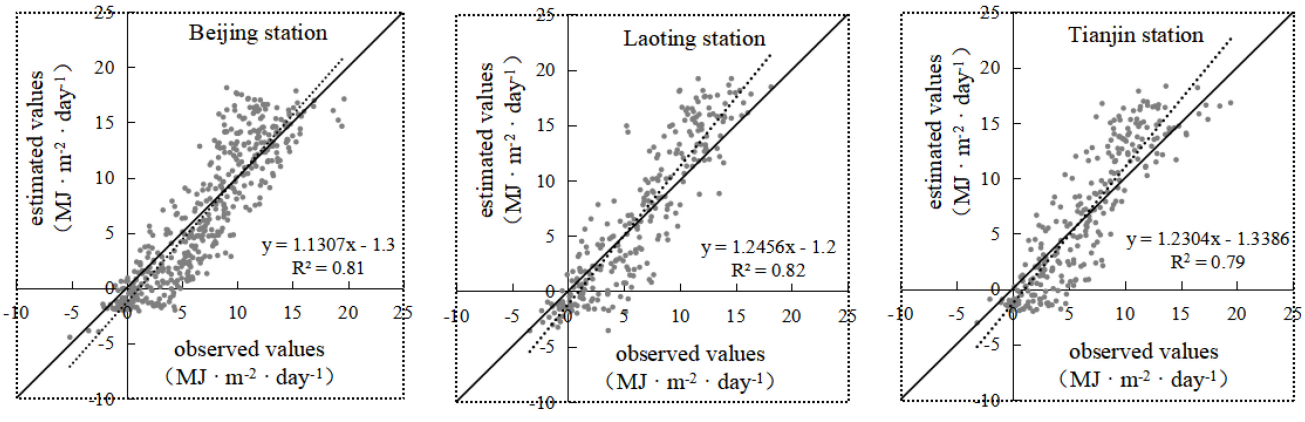

FIGURE 7 | Comparison of estimated and observed daily net radiation of the Haihe River Basin.

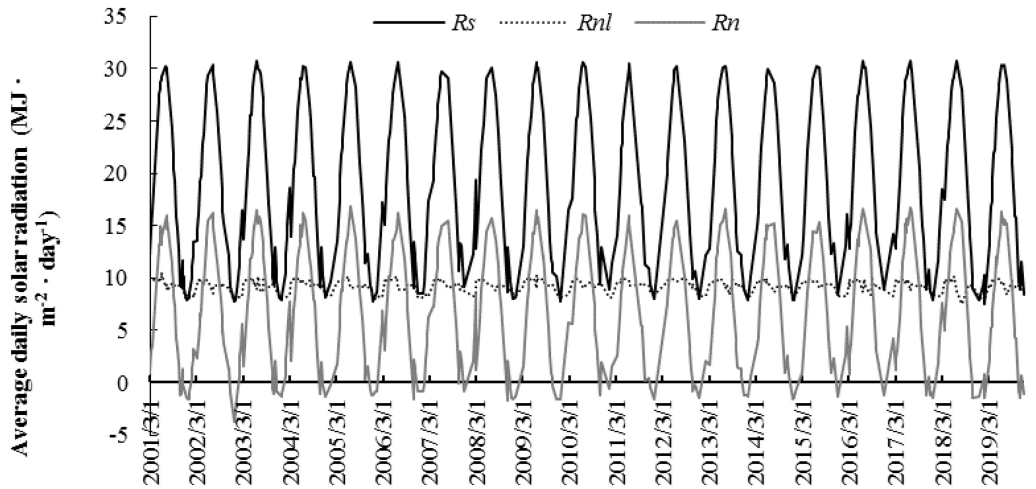

FIGURE 8 | The average values of daily solar incident radiation (*Rs*), daily long-wave net radiation (*Rnl*), and daily net radiation (*Rn*) under clear-sky conditions from 2001∼2019 in the Haihe River Basin.

There is very significant spatial heterogeneity of terrain in the Haihe River Basin, which had a very important influence on the solar radiation. Specifically, there are mainly plains with low elevation in the eastern and southern parts of the Haihe River Basin, where the simple terrain has very limited influence on both the solar incident radiation and net surface radiation. By contrast, there are the Yanshan-Taihang Mountains in the western and northern part of the Haihe River Basin, with a high altitude and very complex terrain variation, and the lowest and highest values of solar incident radiation both occurred in these mountainous areas under the influence of terrain shading and slope direction. On the one hand, there is a limited weakening effect of the atmosphere on the solar incident radiation in these mountainous areas with the high altitude, long sunshine hours, and thin air, and therefore the solar incident radiation in mountainous areas is slightly higher than that in plain areas at the same latitude. On the other hand, the sunshine hours and intensity of received solar radiation varied greatly among different slope gradients and directions. The closer to 90° the solar altitude angle on the slope is, the more the solar incident radiation is. The less the influence of the terrain shading on different slopes is, the longer the sunshine hour is, and the more solar incident radiation is. The variation of solar incident radiation is therefore much more significant in areas with strong terrain variation in these mountainous areas than the plain areas. Additionally, the daily net long-wave radiation is affected by both the temperature and water vapor pressure. In mountainous areas with high altitudes, the temperature is relatively lower and the actual water vapor pressure is also lower due to the lower water vapor content under clear-sky conditions, which jointly lead to a higher daily net long-wave radiation and slightly lower daily net radiation in the mountainous areas with little terrain variation than the plain areas. Nevertheless, the solar incident radiation on the sunny slopes of areas with strong terrain variation in mountainous areas is still much higher than that on the plains, and the highest daily surface net radiation still occurred on these sunny slopes of areas with strong terrain variation in mountainous areas.

Variation of Daily Solar Radiation on Different Slope Directions

There is a remarkable difference in the solar incident radiation received by the ground surface on different slopes in the Haihe River Basin under the influence of terrain. There is a more remarkable difference in the sunshine hour and the percentage of solar incident radiation received on a unit area on different slopes under the influence of terrain shading. This study generated the slope direction map of Haihe River Basin with the slope direction tool in the ARCGIS software to clarify the surface radiation budget of different slope directions, according to which the study area was divided into eight directions, i.e., N (0-π/8, 15π/8-2π), NE (π/8-3π/8), E (3π/8-5π/8), SE (5π/8), and SE (5π/8). 8), SE (5π/8-7π/8), S (7π/8-9π/8), SW (9π/8-11π/8), W (11π/8-13π/8), and NW (13π/8-15π/8), and thereafter this study extracted the solar radiation under the clear-sky condition on different slope directions.

The results based on the average daily solar radiation under clear-sky conditions from 2001∼2019 suggested that there was a similar descending rank order of the solar incident radiation and the surface net radiation on different slope directions, i.e., south, southwest, west or southeast, northwest, east, northeast, and north (**Figure 10**). Specifically, the south slope received the highest solar radiation, followed by the southwest slope, but the difference between them was very slight, reaching only about 0.03 MJ/(m^2·day). There was similar solar incident radiation on the west and southeast slopes, which was about 0.13 MJ/(m^2·day) lower than that on the north slope. The solar incident radiation on the northwest slope was about 0.1–0.2 MJ/(m^2·day) higher than that on the east slope and about 0.1 MJ/(m^2·day) lower than that on the southeast slope. The solar incident radiation on the northeast slope was about 0.6–0.7 MJ/(m^2·day) lower than that on the south slope, but it was about 0.3MJ/(m^2·day) higher than

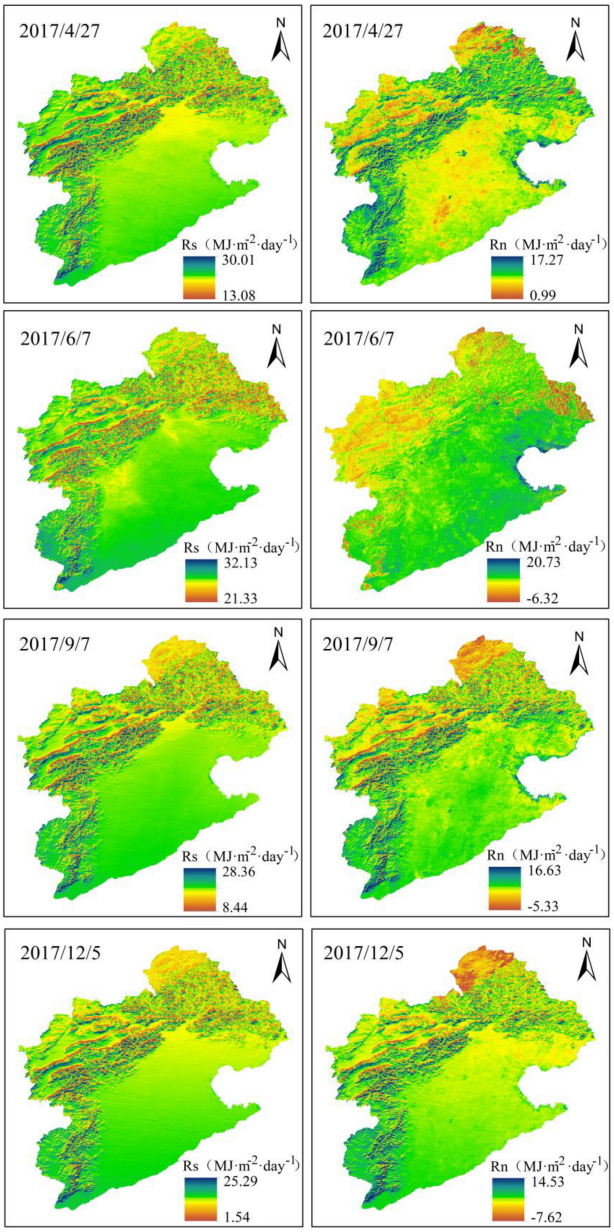

FIGURE 9 | Spatial heterogeneity of the daily solar incident radiation (Rs) and the surface net radiation (Rn) in Haihe River Basin.

that on the east slope. The north slope received the least solar incident radiation, which was about 1 MJ/(m^2·day) lower than that on the south slope.

Notably, the difference in the average surface net radiation under clear-sky conditions on different slopes varied remarkably from year to year due to the variation in the total number of clear-sky days and their distribution in different seasons in different years. Specifically, the difference between the surface net radiation in the north and south directions was about 0.8–1.1 MJ/(m^2·day) in different years. While the differences in net surface radiation on the southwest, west or southeast, northwest, east, and northeast slopes compared to the south slope reached about 0.02–0.03 MJ/(m^2·day), 0.07–0.11 MJ/(m^2·day), 0.16–0.21 MJ/(m^2·day), 0.24–0.34 MJ/(m^2·day), and 0.43–0.59 MJ/(m^2·day), respectively. Additionally, **Figure 10** shows that the annual average solar incident radiation and the surface net radiation under clear-sky conditions were higher in 2009, 2010, 2016, and 2017 and lower in 2002, 2008, and 2011. Specifically, the annual average solar radiation was the highest in 2010 and the lowest in 2002, and the difference between the solar incident radiation and the surface net radiation on different slopes reached about 4.2–4.4 MJ/(m^2·day) and 3.4–3.5 MJ/(m^2·day), respectively. This is mainly due to the fact that the sunny days in 2010 were mainly concentrated in May–October, while the sunny days in 2002 were mostly concentrated in January–May and September–December.

Discussion

The method used in this study can more accurately reveal the spatial heterogeneity of solar radiation under complex terrain conditions than the methods in previous studies. The regional meteorological data in previous studies were mostly obtained with the spatial interpolation methods, and some scholars took into account the influence of the elevation but generally failed to reflect the influence of the shaded slope. In contrast, this study improved the estimation accuracy of the meteorological factors in the Haihe River Basin by inverting the maximum and minimum temperatures and the actual water vapor pressure based on the remote sensing data, the MOD05L2 product, which can better reflect the spatial distribution of these meteorological factors. Compared with the traditional spatial interpolation method of meteorological factors used by previous scholars and even the GIDW method, which is optimized by considering the elevation factor, the method used in this study can better reflect the influence of terrain variation on the meteorological factors in areas with complex terrain, especially the meteorological difference between shaded and sunny slopes resulting from the complex terrain. Besides, this study significantly improves the estimation accuracy of the solar incident radiation in complex terrain areas by fully considering the solar incident radiation from three aspects, i.e., direct radiation, diffuse sky radiation, and reflected radiation from the surrounding terrain, amending the influence of the cosine value of the incident angle on the slope based on multiple factors, e.g., the slope gradient, slope direction and latitude, and introducing the shading coefficients to amend the influence of shading caused by the shadow of the surrounding terrain. In addition, this study has localized some key parameter values in the daily net long-wave radiation algorithm recommended by the FAO, which further improves the estimation accuracy. More importantly, this study has carried out the verification of the estimated solar radiation with the long time series observation data, which is more convincing than previous studies with the short time data.

There are still some uncertainties in this study due to the data limitation, etc. First, there is a limited number of meteorological stations available for the model verification, especially in the mountainous areas with complex terrain. Besides, there are some uncertainties resulting from the inherent error of the remote

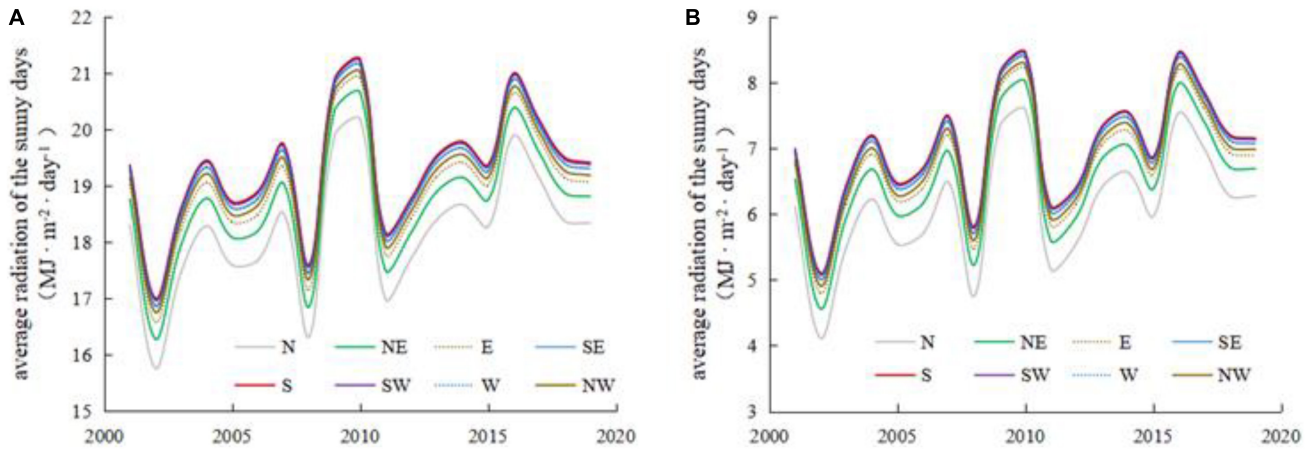

FIGURE 10 | Average daily solar radiation under clear-sky conditions on different slopes from 2001∼2019 in the Haihe River Basin. **(A)** Solar incident radiation; **(B)** Surface net radiation.

sensing data and the problems of mixed pixels due to the limited spatial resolution of the remote sensing data. In particular, there may be a remarkable difference in the quality of the remote sensing data under clear-sky conditions. In addition, the method used in this study is only applicable to the clear-sky conditions due to the limitation of the remote sensing data availability and the transmittance coefficient algorithm, and it is necessary to carry out further research for the cloudy and overcast conditions. It is therefore the next agenda of this study to explore how to extend the daily-scale surface radiation data to monthly and annual scales. Nevertheless, the results of this study can still provide important methodological support for the estimation of the surface radiation budget and relevant studies of agriculture, ecology, hydrology, and meteorology in mountainous areas with complex terrain.

CONCLUSION

This study estimated the surface net radiation under clear-sky conditions in the Haihe River Basin as an area with complex terrain from 2001∼2019 based on the topographic data, the remote sensing data, and the temperature and water vapor pressure data inverted with the remote sensing data. The main conclusions are as follows: (1) This study effectively improved the estimation accuracy of the surface net radiation algorithm by comprehensively considering the impacts of complex terrain, underlying surface and atmosphere on the surface net radiation, and localizing the parameter values in the algorithm of net long-wave radiation recommended by the FAO, with the correlation coefficient between the estimated surface net radiation and the observed value reaching approximately 0.9 and the root mean square error reaching about 3 MJ/(m^2·day). (2) The average daily solar incident radiation and daily net radiation under clear-sky conditions in the Haihe basin were the highest in summer and the lowest in winter, showing an overall single-peak pattern, and the annual average solar radiation was the highest in 2010 and the lowest in 2002. (3) The solar incident radiation and net surface radiation in the Haihe River Basin showed complex spatial heterogeneity. On the one hand, the lowest and highest values of solar incident radiation both occurred in the mountainous areas in the western and northern part of the Haihe River Basin. On the other hand, the solar radiation varied significantly on different slopes, and there was a similar descending rank order of the solar incident radiation and the surface net radiation on different slope directions in the Haihe River Basin, i.e., south, southwest, west or southeast, northwest, east, northeast, and north. (4) The method used in this study is only applicable to the clear-sky conditions due to the limitation of the remote sensing data availability and the transmittance coefficient algorithm, and it is the next agenda of this study to carry out further research for the cloudy and overcast conditions and explore how to extend the daily-scale surface radiation data to monthly and annual scales. Overall, it is necessary to further improve the algorithm used in this study, but this study can still provide important methodological support for the estimation of solar radiation in areas with complex terrain in the relevant fields.

DATA AVAILABILITY STATEMENT

The original contributions presented in this study are included in the article/supplementary material, further inquiries can be directed to the corresponding author/s.

AUTHOR CONTRIBUTIONS

XL and HaY: conceptualization, data curation, investigation, resources, funding acquisition, project administration, and supervision. XL and JZ: methodology, software, validation, visualization, and writing—original draft. JZ and HuY: writing—review and editing and formal analysis. All authors contributed to the article and approved the submitted version.

FUNDING

This research was funded by the National Natural Science Foundation of China (42101040 and 51909052); the Natural Science Foundation of Hebei Province (D2019403022); the Science and Technology Project of Hebei Education Department (BJ2019045); and the Scientific and Technological Innovation Team Project of Hebei GEO University in 2021 (KJCXTD-2021-10).

REFERENCES

Allen, R. G., Pereira, L. S., Raes, D., and Smith, M. (1998). *FAO Irrigation and drainage paper No.56*. Rome: Food and Agriculture Organization of the United Nations.

Allen, R. G., Tasumi, M., and Trezza, R. (2007). Satellite-based energy balance for mapping evapotranspiration with internalized calibration (METRIC)-Model. *J. Irrig. Drain. Eng.* 133, 380–394. doi: 10.1061/(ASCE)0733-9437(2007)133:4(380)

Allen, R. G., Tasumi, M., Trezza, R., and Kjaersgaard, J. (2010). *METRICtm: Mapping Evapotranspiration at High Resolution–Applications Manual*. Kimberly: University of Idaho.

Allen, R. G., Trezza, R., and Tasumi, M. (2006). Analytical integrated functions for daily solar radiation on slopes. *Agr. Forest Meteorol.* 139, 55–73. doi: 10.1016/j.agrformet.2006.05.012

Asce-Ewri (2005). *The ASCE Standardized Reference Evapotranspiration Equation*. ASCE Reston, VA: ASCE-EWRI Task Committee Report.

Cao, W., Xu, Y., and Duan, C. F. (2014). Research on Applicability of Solar Radiation Parametric Model in Anhui Province. *Chin. Agric. Sci. Bull.* 30, 207–212.

Chen, L., Yan, G., Wang, T., Ren, H., Calbó, J., Zhao, J., et al. (2012). Estimation of surface short-wave radiation components under all sky conditions: modeling and sensitivity analysis. *Remote Sens. Environ.* 123, 457–469. doi: 10.1016/j.rse.2012.04.006

Chen, Y. Y., Qiu, X. F., Gao, Y. H., You, Y. S., and Liao, Q. L. (2009). A study on calculation of direct solar radiation transmission rate. *Chinese J. Agrometeorol.* 30, 492–495.

Dozier, J., and Frew, J. (1990). Rapid calculation of terrain parameters for radiation modeling from digital elevation data. *IEEE T. Geosci. Remote* 28, 963–969. doi: 10.1109/36.58986

Dubayah, R., and Rich, P. M. (1995). Topographic solar radiation models for GIS. *Int. J. Geogr. Inf. Sci.* 9, 405–419. doi: 10.1080/02693799508902046

Duffie, J. A., and Beckman, W. A. (1991). *Solar Engineering of Thermal Processes*. New York: Wiley.

Gharekhan, D., Nigam, R., Bhattacharya, B. K., Desai, D., and Patel, P. (2022). Estimating regional-scale daytime net surface radiation in cloudless skies from GEO-LEO satellite observations using data fusion approach. *J. Earth. Syst. Sci.* 131:73. doi: 10.1007/s12040-021-01806-9

Gui, S. (2010). *Satellite Remote Sensing of Surface Net Radiation*. Ph.D.thesis. Wuhan, China: Wuhan University.

Gui, S., Liang, S. L., Wang, K. C., Li, L., and Zhang, X. T. (2010). Assessment of Three Satellite-Estimated Land Surface Downwelling Shortwave Irradiance Data Sets. *IEEE Geosci. Remote. S.* 7, 776–780. doi: 10.1109/LGRS.2010.2048196

Guo, Y., and Shen, Y. J. (2015). Quantifying water and energy budgets and the impacts of climatic and human factors in the Haihe River Basin, China: 1. Model and validation. *J. Hydrol.* 528, 206–216. doi: 10.1016/j.jhydrol.2015.06.039

Hallikainen, M., and Kirimoto, T. (2008). *Microwave Radiometry for Remote Sensing of the Earth Surfaces*. Chofu, Japan: SICE Annual Conference, 20–22. doi: 10.1109/SICE.2008.4654601

Hao, D. L., Wen, J. G., Xiao, Q., Wu, S. B., Lin, X. W., You, D. Q., et al. (2019). Impacts of DEM geolocation bias on downward surface shortwave radiation estimation over clear-sky rugged terrain: a case study in Dayekou Basin. China. *IEEE Geosci. Remote S.* 16, 10–14. doi: 10.1109/LGRS.2018.2868563

Jia, A. L., Liang, S. L., Jiang, B., Zhang, X. T., and Wang, G. X. (2018). Comprehensive Assessment of Global Surface Net Radiation Products and Uncertainty Analysis. *J. Geophys. Res.* 123, 1970–1989. doi: 10.1002/2017JD027903

Kreith, F., and Kreider, J. F. (1978). *Principles of Solar Engineering*. New York: Taylor & Francis Inc.

Lei, H. M., Yang, D. W., and Huang, M. Y. (2014). Impacts of climate change and vegetation dynamics on runoff in the mountainous region of the Haihe River basin in the past five decades. *J. Hydrol.* 511, 786–799. doi: 10.1016/j.jhydrol.2014.02.029

Li, Y. Q., Chen, Y., Cao, W. J., Wang, X. Y., and Niu, Y. Y. (2022). Theoretical basis of ecology for the influence of global change on resources, environment, and eco-systems. *J. Appl. Ecol.* 33, 603–612. doi: 10.13287/j.1001-9332.202203.019

List, R. J. (1984). *Smithsonian Meteorological Tables (6th reversion)*. Washington: Smithsonian Institution press.

Liu, X. R., Shen, Y. J., Li, H. J., Guo, Y., Pei, H. W., and Dong, W. (2017). Estimation of land surface evapotranspiration over complex terrain based on multi-spectral remote sensing data. *Hydrol. Process.* 31, 446–461. doi: 10.1002/hyp.11042

Liu, X. R., Zhang, H. Y., Yan, H. M., and Luo, J. M. (2021). Estimation of regional solar radiation over complex terrain. *Acta Energ. Sol. Sin.* doi: 10.19912/j.0254-0096.tynxb.2021-0127

Long, D., Gao, Y. C., and Singh, V. P. (2010). Estimation of daily average net radiation from MODIS data and DEM over the Baiyangdian watershed in North China for clear sky days. *J. Hydrol.* 388, 217–233. doi: 10.1016/j.jhydrol.2010.04.042

Matsui, H., and Osawa, K. (2015). Calibration effects of the net longwave radiation equation in Penman-type methods at Tateno, Japan. *Hydrol. Res. Lett.* 9, 113–117. doi: 10.3178/hrl.9.113

Pinker, R. T., Dan Tarpley, J., Laszlo, I., Mitchell, K. E., Houser, P. R., Wood, E. F., et al. (2003). Surface radiation budgets in support of the GEWEX Continental-Scale International Project (GCIP) and the GEWEX Americas Prediction Project (GAPP), including the North American Land Data Assimilation System (NLDAS) project. *J. Geophys. Res.* 108:8844. doi: 10.1029/2002JD003301

Ren, H. R., Luo, Y., and Xie, X. Q. (2006). Evaluation of application of several net radiation calculation methods in Huanghuaihai Plain. *Trans. Chin. Soc. Agric. Eng.* 22, 140–146.

Roupioz, L., Jia, L., Nerry, F., and Menenti, M. (2016). Estimation of daily solar radiation budget at kilometer resolution over the Tibetan Plateau by integrating MODIS data products and a DEM. *Remote Sens.* 8:504. doi: 10.3390/rs8060504

Sultan, S., Wu, R. G., Ahmad, I., and Ahmad, M. F. (2014). Modeling of diffuse solar radiation and impact of complex terrain over Pakistan using RS/GIS. *J. Geogr. Inf. Syst.* 6, 404–413. doi: 10.4236/jgis.2014.64035

Tang, W. J., Yang, K., Qin, J., Li, X., and Niu, X. L. (2019). A 16-year dataset (2000–2015) of high-resolution (3 h, 10 km) global surface solar radiation. *Earth Syst. Sci. Data* 11, 1905–1915. doi: 10.5194/essd-11-1905-2019

Tasumi, M., Allen, R. G., and Trezza, R. (2008). At-surface reflectance and albedo from satellite for operational calculation of land surface energy balance. *J. Hydrol. Eng.* 13, 51–63. doi: 10.1061/(ASCE)1084-0699(2008)13:2(51)

Wang, B. Z. (1999). Lecture of solar radiation calculation: part1. The calculation of astronomical parameters in solar energy. *Sol. Energy* 2, 8–10.

Wang, W. T. (2011). *Research on Regional Land Surface Evapotranspiration Estimation based on Remote Sensing Technology-a Case of Yiluo River Basin*. Ph.D.thesis. Kaifeng, China: Henan University.

Wu, B. F., Liu, S. F., Zhu, W. W., Yan, N. N., Xing, Q., and Tan, S. (2017). An improved approach for estimating daily net radiation over the Heihe River Basin. *Sensors* 17:86. doi: 10.3390/s17010086

Yang, K., Koike, T., and Ye, B. S. (2006). Improving estimation of hourly, daily, and monthly solar radiation by importing global data sets. *Agr. Forest Meteorol.* 137, 43–55. doi: 10.1016/j.agrformet.2006.02.001

Yin, Y. H., Wu, S. H., Du, Z., and Yang, Q. Y. (2008). Radiation calibration of FAO56 Penman-Monteith model to estimate reference crop evapotranspiration in China. *Agr. Water Manage.* 95, 77–84. doi: 10.1016/j.agwat.2007.09.002

Zhang, C. H., Guo, Y. B., He, Z. W., He, L., and Xu, H. X. (2022). Analysis of influence mechanism of spatial distribution of incoming solar radiation

based on DEM. *Earth Sci. Inform.* 15, 635–648. doi: 10.1007/s12145-021-00740-0

Zhang, S. H., Li, X. G., She, J. F., and Peng, X. M. (2019). Assimilating remote sensing data into GIS-based all sky solar radiation modeling for mountain terrain. *Remote Sens. Environ.* 231:111239. doi: 10.1016/j.rse.2019.111239

Zhang, Y. C., Rossow, W. B., Lacis, A. A., Oinas, V., and Mishchenko, M. I. (2004). Calculation of radiative fluxes from the surface to top of atmosphere based on ISCCP and other global data sets: Refinements of the radiative transfer model and the input data. *J. Geophys. Res.* 109:D19105. doi: 10.1029/2003JD004457

Zhang, Y. L., and Zhao, J. (2016). *Sensitivity Analysis of Estimating Shortwave Solar Radiation to the DEM Spatial Scale*. Beijing, China: IEEE International Geoscience and Remote Sensing Symposium, 10–15. doi: 10.1109/IGARSS.2016.7730140

Zhang, Y. L., Qin, X., Li, X., and Zhao, J. (2020). Estimation of shortwave solar radiation on clear-sky days for a valley glacier with Sentinel-2 time series. *Remote Sens.* 12:927. doi: 10.3390/rs12060927

Conflict of Interest: The authors declare that the research was conducted in the absence of any commercial or financial relationships that could be construed as a potential conflict of interest.

frontiers | Frontiers in Ecology and Evolution

ORIGINAL RESEARCH
published: 16 June 2022
doi: 10.3389/fevo.2022.907162

Ecological Water Requirement Accounting of the Main Stream of the Yellow River From the Perspective of Habitat Conservation

Fen Zhao[1,2], Chunhui Li[1]*, Wenxiu Shang[3], Xiaokang Zheng[3], Xuan Wang[1], Qiang Liu[1] and Jiuhe Bu[1]*

[1] Key Laboratory of Water and Sediment Science of Ministry of Education, School of Environment, Beijing Normal University, Beijing, China, [2] School of Resources and Environmental Engineering, Ludong University, Yantai, China, [3] Yellow River Engineering Consulting Co., Ltd., Zhengzhou, China

OPEN ACCESS

Edited by:
Fan Zhang, Institute of Geographic Sciences and Natural Resources Research (CAS), China

Reviewed by:
Wencong Yue, Dongguan University of Technology, China
Yufeng Wang, Northwest A&F University, China
Meng Xu, Zhejiang University of Finance and Economics, China

***Correspondence:**
Fen Zhao
zhaof@ldu.edu.cn
Chunhui Li
Chunhuili@bnu.edu.cn

Specialty section:
This article was submitted to Conservation and Restoration Ecology, a section of the journal Frontiers in Ecology and Evolution

Received: *29 March 2022*
Accepted: *29 April 2022*
Published: *16 June 2022*

Citation:
Zhao F, Li C, Shang W, Zheng X, Wang X, Liu Q and Bu J (2022) Ecological Water Requirement Accounting of the Main Stream of the Yellow River From the Perspective of Habitat Conservation. Front. Ecol. Evol. 10:907162. doi: 10.3389/fevo.2022.907162

The Yellow River Basin is of great significance to China's economic and social development and ecological security. The Yellow River Basin is not only an important ecological barrier but also an important economic zone. In this article, natural hydrological conditions were taken as a reference, a habitat simulation model of the key sections of the Yellow River was constructed based on the MIKE 21 model, and an ecological water requirement assessment method for river ecological integrity combined with habitat simulation and features of the hydrological reference group was established, which took account of the survival and reproduction of indicator species. The suitable flow rates for the spawning period (i.e., April to June) of *Silurus lanzhouensis* in Lanzhou (LZ) and *Cyprinus carpio* in Longmen (LM) were 350–720 and 260–400 m^3/s, respectively. Therefore, high pulse flow with a low flow peak should be guaranteed in mid- to late April. The peak flow should be at least approximately 1,000 m^3/s to ensure that fish receive spawning signals, with a high pulse flow process occurring 1–2 times in May to June. The annual ecological water requirement of the Lanzhou and Longmen section was 9.1×10^9–11×10^9 and 4.7×10^9–11.3×10^9 m^3. The model quantitatively simulated the changes in ecological water requirement of indicator fishes in key sections of the Yellow River, and an effective and realistic tool for ecological water requirement accounting of the Yellow River was provided.

Keywords: ecological water requirement (EWR), habitat simulation, MIKE 21 model, ecological water requirement process, the main stream of the Yellow River

KEY POINTS

- A new assessment method of ecological water requirement process was proposed to maintain the ecological integrity of the Yellow River.
- The ecological water requirement process and pulse flow process were determined based on the ecological flow elements.
- The changes of ecological water requirement of the Yellow River in different periods have been simulated quantitatively and effectively.

INTRODUCTION

With the continuous improvement in human understanding of river ecosystems, ecological problems caused by human activities, such as the construction of water conservancy structures, have become increasingly serious. Thus, the concept of "river health" has begun to emerge and has been accepted throughout the world in order to solve the problems of river pollution and the deterioration of water ecosystems, which have attracted wide attention from various countries (Richter, 1997; Norris and Thoms, 1999; Norris and Hawkins, 2000; Wu and Chen, 2018; Virkki et al., 2021). The ecological water requirement of a river is one of the important indicators of its health status (Thame, 2003; Rolls and Bond, 2017). With the emergence of flood disasters, river outages, and water pollution, research on ecological water requirement has generally been carried out for river ecosystems, mainly focusing on minimum and optimal flow according to the physical requirements of the river (e.g., the characteristics of fish) (Bartschi, 1976; Tennant, 1976; Bovee, 1996; Bunn and Arthington, 2002). In recent years, relevant studies have begun to consider the vertical connection of river flows, the integrity of river ecosystems has been paid attention to, the adaptability of river ecosystems has been analyzed from the perspective of flow changes, the limitations of river ecosystem types in related research have been overcome, and comprehensive analysis of different ecosystem types has gradually expanded (Hughes, 1999, 2001; Yang et al., 2020; Liu et al., 2022). A large number of studies on ecological water requirement have been carried out based on the preferences of species for certain habitats, and a habitat simulation method considering the direct relationships between runoff and organisms was established to evaluate ecological water requirement. The physical mechanism was clear, and it can provide the ecological water requirement process with dry and wet changes rather than a fixed minimum ecological water requirement (Nikghalb et al., 2016; Poff, 2018), which has been widely used in ecological water requirement assessments (Hao and Shang, 2008; Cai et al., 2010; Sun et al., 2013; Theodoropoulos et al., 2018; Wang et al., 2018; Shang et al., 2020). However, habitat simulation has mainly focused on the flow conditions in order to shape the biological habitat, and the life rhythm signals that trigger key life activities have been ignored, such as high flow pulses. Despite decades of research, the process of maintaining the ecological water requirement of the indigenous aquatic communities of rivers has not been effectively solved (Edwards and Twomey, 1982; Baumgartner et al., 2014; Brown and Williams, 2016; Arthington et al., 2018).

The Yellow River Basin is very important for China's economic and social development and ecological security. The basin is not only an important ecological barrier but also an important economic zone in China. However, water supply to ecological environment along the Yellow River has been occupied by industrial or agricultural activities through the process of urbanization in recent years, and the amount of water in the main channel of the Yellow River cannot maintain the health of the channel. Earlier studies on the ecological water requirement of the Yellow River were focused on discussing the ecological water requirement "quantity," which did not involve analysis of the specific flow process, duration, and frequency and other river hydrological conditions, and the connection and response relationship between the river ecological water requirement process and runoff elements have not been established (Zhang et al., 2008; Zhao et al., 2011; Wang et al., 2020). Research on the ecological requirements of the middle and upper reaches of the main stream of the Yellow River has mainly focused on ecosystem protection, and research on the downstream area has mainly focused on sediment water transport (Huang et al., 2004; Hao et al., 2006; Ma et al., 2007; Liu, 2009; Wang et al., 2009). Furthermore, subsequent research was based on the actual status of the ecological environment and ecological protection goals of the Yellow River, improving the accuracy of ecological water requirement models. However, the relationship between the ecological hydrological process of the river and the response of the ecosystem has not been fully clarified (Lian et al., 2011; Zhao et al., 2011; Ma et al., 2014; Huang et al., 2016).

This research aims to maintain the integrity of the indigenous communities in the Yellow River. Habitat simulation was performed, and the natural hydrological conditions were taken as a reference. The characteristic values of the natural hydrology were extracted to supplement and modify the habitat simulation results. Specifically, the MIKE 21 model was used to construct a habitat simulation model, and the changes in the water level and flow rate of the important section of the main stream of the Yellow River were analyzed and simulated. The features of the hydrological reference group were extracted according to the natural runoff conditions, and an ecological water requirement assessment method for river ecological integrity was established by supplementing and modifying the habitat simulation results with the features of the hydrological reference group. The new method proposed in this article was helpful for quantitatively simulating the changes in the ecological water requirement of indicator fish in key sections of the Yellow River, and an effective tool was provided for the actual calculation of ecological water requirement.

STUDY AREA

The Yellow River is the second longest river in China, with a length of 5,464 km and a drainage area of 752,000 km^2. It originates from the Qinghai-Tibet Plateau (northwest) and flows to the Bohai Sea (east) (**Figure 1**). The average annual precipitation in the entire Yellow River Basin is approximately 466 mm, showing a decreasing trend from southeast to northwest. The source of the Yellow River to Hekou town in Inner Mongolia is the upper reaches of the Yellow River, with a channel length of approximately 3,472 km and a watershed area of approximately 428,000 km^2. The length from Hekou town to Taohuayu in Zhengzhou encompasses the middle reaches of the Yellow River, with a channel length of approximately 1,206 km and a drainage area of approximately 344,000 km^2. The middle reaches are the main sources of floods and sediments in the Yellow River. Below Taohuayu in Zhengzhou is the lower Yellow River, with a channel length of approximately 786 km and a watershed area of approximately 23,000 km^2.

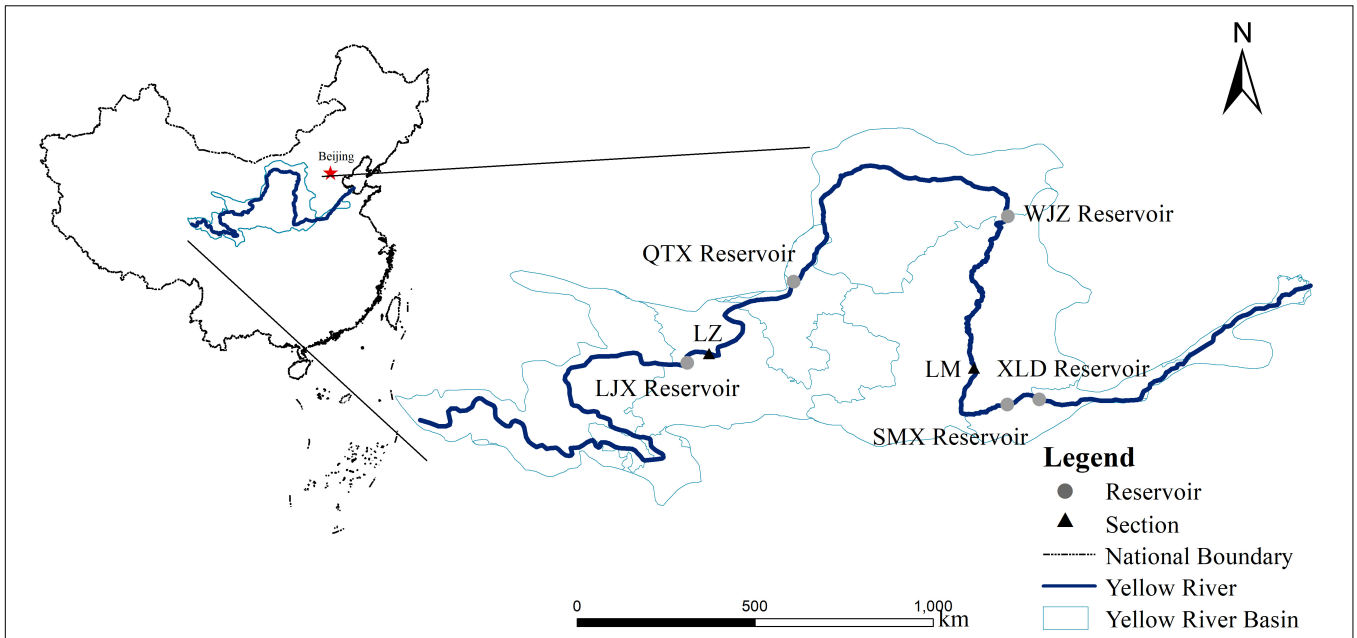

FIGURE 1 | The main stations of the Yellow River Basin (YRB). LZ, Lanzhou; LM, Longmen; H LJX reservoir, Liujiaxia reservoir; QTX reservoir, Qingtongxia reservoir; WJZ reservoir, Wanjiazhai reservoir; SMX reservoir, Sanmenxia reservoir; XLD reservoir, Xiaolangdi reservoir.

In the past 30 years, the features of fish species in the Yellow River have changed significantly due to the dramatic impact of human activities (Feng, 2010). There are few species in the upper reaches of the Yellow River, and the community is relatively simple (Ru et al., 2010; Wang et al., 2020). The species in the middle and lower reaches are more abundant than the ones in the upper reaches. The number of species gradually increases from the upper reaches to the lower reaches (Wu et al., 2006; Huang et al., 2016; Wang et al., 2017).

MATERIALS AND METHODS

The ecological water requirement in the upper reaches of the Yellow River were analyzed by selecting the LZ section in the upper reaches, the LM section in the middle reaches. Moreover, *Silurus lanzhouensis* (the Lanzhou Amur catfish) was selected as the indicator species of the LZ and XHY sections, while *Cyprinus carpio* (the Yellow River carp) was selected as the indicator species of the TDG, LM, and HYK sections.

The approach for ecological water requirement accounting of the key sections of main stream of the Yellow River is shown in **Figure 2**. The MIKE 21 model, regarded as one of professional engineering software for simulating the current, wave, sediment and environment of rivers (Dhi, 2011) was used to construct a habitat simulation (Dai et al., 2010; Xu, 2010; Doummar et al., 2012; Zhang et al., 2016). The changes in the water level and flow rate in the important sections of the main stream of the Yellow River were analyzed and simulated based on the MIKE 21 model. The features of the hydrological reference group were extracted according to the natural runoff conditions. An ecological water requirement assessment method for river ecological integrity was established by supplementing and modifying the habitat simulation results with the features of the hydrological reference group.

Process for Determining Ecological Water Requirement

The process for ecological water requirement included the ecological base flow, the ecological flow during the fish spawning period, and the flood pulse maintaining the stability of the river channel during the flood season (Poff et al., 1997; Nikghalb et al., 2016; Wang, 2017; Poff, 2018; Wang et al., 2018). River ecological base flow aims to maintain the vertical connectivity of the river, provide nutrients to the wetland, maintain an appropriate water surface width of the river fish habitat, and ensure the smallest living water area available for fish. A certain flow rate is required during the fishes spawning period in order to provide guidance, and the flow pulse surge is required to ensure that fish are stimulated by the flow required for spawning at an appropriate time. The flood process in the flood season mainly scoured the riverbed sediment, stabilized the river channel structure, and provided a migration channel for fish.

Assessment of the Ecological Water Requirement Process of Indicator Species

Combined with the basic hydrological and meteorological data of the river and the life habits in different life cycles (Morrison et al., 1992; Jiang et al., 2005; Liu et al., 2008; Dudgeon, 2010; Jiang and Wang, 2012; Shang et al., 2020), the MIKE 21 model was used to simulate the changes in the river hydrological process, the changes in the habitat of the indicator species under different flows were analyzed, and the ecological water

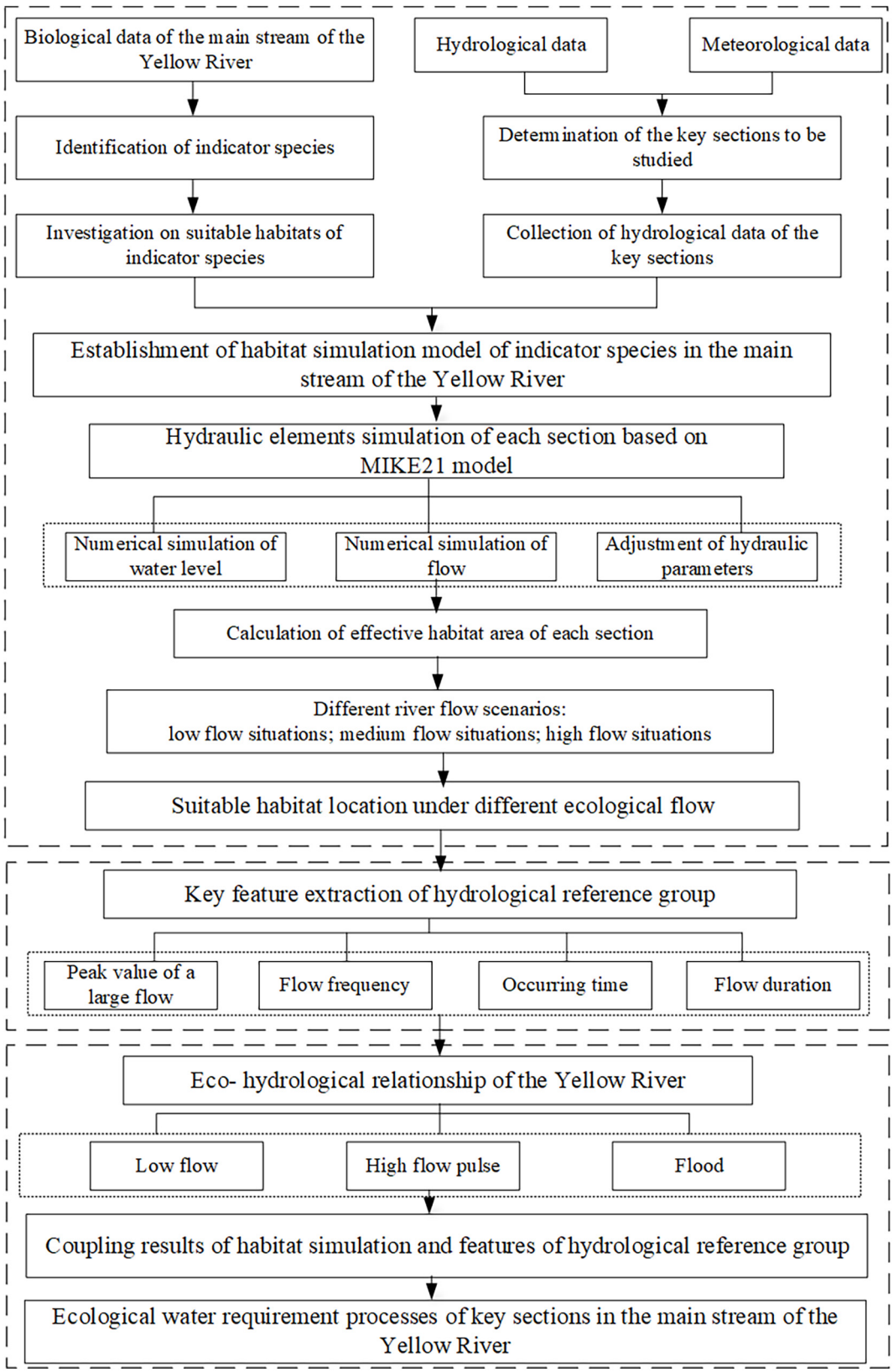

FIGURE 2 | The framework for ecological water requirement accounting from the perspective of habitat conservation.

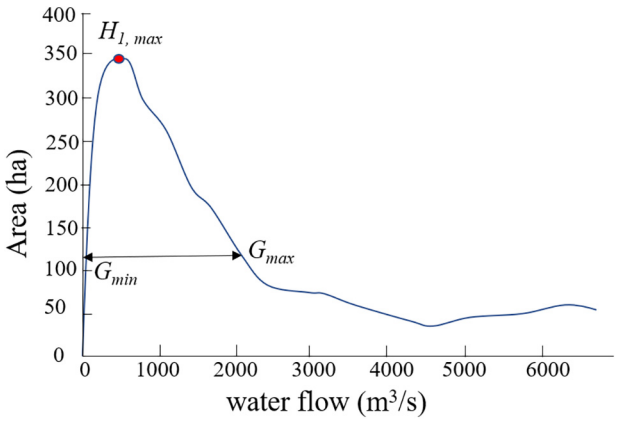

FIGURE 3 | The flow – habitat area curve of the indicator species in growing period.

requirement process of the indicator species were evaluated through habitat simulation. The peak value of the habitat area during the growth period of the indicator species was $H_{1,\ max}$. In this article, we specified that when the area of the habitat (i.e., H_{max}) was 1/3, the minimum flow range suitable for the survival and development of the indicator species was $G_{min}G_{max}$ (**Figure 3**; Wang et al., 2020). Meanwhile, the peak value of the habitat area of the indicator species in the overwintering period was $H_{2,\ max}$, the minimum flow range suitable for winter was $W_{min}W_{max}$, the peak value of habitat area in the spawning period was $H_{3,\ max}$, and the minimum flow range was $S_{min}S_{max}$.

Extraction of Key Features of the Hydrological Reference Group

When the reservoir had not been built upstream of the hydrological station, the measured hydrological conditions were used as a proxy for the natural hydrological conditions, and the measured daily runoff series during this period was used as the hydrological reference group (Ma et al., 2014). The characteristic values of the hydrological reference group mainly focused on the minimum flow and the high flow pulse.

The minimum value of natural flow N_{min} was considered to be the lower limit of flow that all indigenous aquatic organisms could tolerate. The minimum flows in the growth, overwintering and spawning periods were $N_{G,\ min}$, $N_{W,\ min}$, and $N_{S,\ min}$, respectively. Statistics of the characteristics of high-flow pulses under natural conditions were used to evaluate the high-flow pulses among the ecological water requirement. To calculate the variation range of the high flow pulse duration, peak flow, rise rate, and fall rate under natural conditions, the interval from the 1/3 quantile to the 2/3 quantile was taken as the suitable range of the ecological water requirement of high flow pulse duration (P_d), peak flow rate (P_{max}), rising rate ($P_{rate,r}$), and falling rate ($P_{rate,f}$). The average flow rate of high-flow pulses under natural conditions was taken as the appropriate value of the average flow of the ecological water requirement of high-flow pulses (P_{mean}).

Determination of Ecological Water Requirement by Coupling Results of the Habitat Simulation and Features of the Hydrological Reference Group

Ecological base flow was provided throughout the year, and the overlapping range of the flow range suitable for the indicator species and the natural flow range was taken as the base flow variation range $E_{b,\ min}E_{b,\ max}$, as shown in equations 1, 2.

$$E_{G,min} = \max\left(G_{min},\ N_{G,min}\right) \tag{1}$$

$$E_{G,max} = \min\left(G_{max},\ N_{G,max}\right) \tag{2}$$

A high flow pulse process based on the hydrological reference group was focused on. The overlapping range of the flow range suitable for spawning of the indicator species and the range of low flow changes in the flooding period under natural conditions were used to estimated the reproduction flow $E_{s,\ min}E_{s,\ max}$, as shown in equations 3, 4.

$$E_{s,min} = \max\left(S_{min},\ N_{s,min}\right) \tag{3}$$

$$E_{s,max} = \min\left(S_{max},\ N_{s,max}\right) \tag{4}$$

To maintain the safety of life and properties in the floodplain area, only non-floods are considered in this study. Based on the flow-habitation area curve, a high-flow range suitable for indicating the habitat of adult and larval species was selected.

Establishment of a Habitat Simulation Model

Determination of Model Parameters

Solution Format

This study aimed to simulate water flow changes. The low-order spatially discrete format could meet the accuracy required for the simulation results and saved program run time. Therefore, the low-order numerical calculation method was selected. The minimum and maximum number of time step sets in this model were 0.005 and 6000, respectively.

Wet and Dry Water Depths

In terms of dry and wet areas, it was necessary to set the dry water depth, wet water depth, and submerged depth to avoid or reduce the instability of the model. In this article, the recommended values of dry water depth h_{dry}, submerged water depth h_{flood}, and wet water depth h_{wet} are 0.005, 0.05, and 0.1 m, respectively.

Vortex Viscosity Coefficient

In the model, the concept of "vortex viscosity" was used to describe the integral of the fluid particles. In this article, the form of the eddy viscosity coefficient was set as a constant in the simulation area, and the default value of the program was 0.28.

Roughness of the Bed Bottom

Roughness was one of the main parameters of the hydrodynamic model. Whether its value was appropriate or not directly affected the accuracy of the model and played a vital role in the hydrodynamic model. Therefore, in this study, the change

in water depth was an important process, and the Manning coefficient should be selected as the bed bottom roughness. The land use map was used to refer to the roughness table to extract the most suitable Manning coefficient map.

Establishment of a MIKE 21 Hydrodynamic Model of the Yellow River

The main steps for constructing the MIKE 21 hydrodynamic model include splitting the terrain grid, creating boundary conditions, calibrating sensitive parameters, and verifying model results. The terrain grid file (*. mesh), time series file (*. dfs0), result file (*. dfsu), and control file (*. m21) were all indispensable files for building the model.

The quality of terrain meshing directly affects the accuracy of the simulation results. MIKE Zero's Mesh Generator was applied for meshing terrain. The grid generator generates an ASCII file that includes the geographic coordinates of each grid point, elevation data, and the topological relationship between the grid cells. The grid division needs to first determine the simulation area of the model and the resolution of the terrain grid, and then, the land boundary and the open boundary were defined. After the grid division, the existing elevation data were used for terrain interpolation.

Calibration and Verification of the Model

The model is calibrated using the flow velocity measured in 2015 to determine the simulated flow velocity and water depth. The simulation time step was 600 s, the roughness coefficient and Manning coefficient of the water area adopt the default value of the model, and the roughness coefficient and Manning coefficient of the reed area assigned according to the relevant research results. The calibration period and the verification periods were shown in **Table 1**, the calibration period was from 01/04/2015 to 01/05/2015, and the verification was divided into the following two periods: the fish spawning period (15/07/2015 to 14/08/2015) and flood period (01/09/2015 to 01/10/2015). The calibration parameters were shown in **Table 2**. In this study, the fitting coefficient R^2, Nash Sutcliffe (ENS) and the relative error (RE) between the measured value and the simulated value have been used to evaluate the simulation accuracy of the model. The value of ENS was between $-\infty$ and 1. When it closer to 1, the reliability of the model was higher; when it was much less than 0, the model result was not credible. The magnitude of R^2 determined the close correlation between measured and simulated values. When R^2 was closer to 1, it means that the simulated value was closer to the measured value, and the error between them was small.

By comparing the simulated flow with the measured flow, it was found that the fitting coefficient R^2 was 0.83–0.96, the ENS was 0.82–0.95, and the RE was less than ±5% (**Table 3**).

TABLE 1 | Calibration and verification of MIKE 21 model.

Start time	End time	Days	Target
01/04/2015	01/05/2015	31	Calibration
15/07/2015	14/08/2015	31	Verification
01/09/2015	01/10/2015	31	Verification

TABLE 2 | Parameters setting of MIKE 21 model.

Parameters	Value	Parameters	Value
Simulation time	01/04/2015–01/05/2015	Dry and wet water depth	Dry water depth 0.005 m, wet water depth 0.1 m
Step	600 s	Roughness coefficient and Manning coefficient	Spatial variation
Simulation time steps	4,320	Initial flow velocity and water depth	380 m; initial flow velocity was 0

TABLE 3 | Calibration and verification results of the MIKE 21 model.

Sections	Periods	R^2	E_{NS}	RE (%)
Lanzhou (LZ)	Calibration (14/04/2015)	0.95	0.86	4.7
	Verification (03/08/2015)	0.96	0.95	3.0
	Verification (25/09/2015)	0.85	0.83	3.0
Longmen (LM)	Calibration (14/04/2015)	0.89	0.83	4.9
	Verification (03/08/2015)	0.93	0.91	3.4
	Verification (25/09/2015)	0.83	0.82	3.4

The verification results are shown in **Figure 4**. The above results were generally reasonable. The established calculation model was consistent with the characteristics of the basin's flood evolution, and the model's calibration parameters could meet the requirements. The model can be used to evaluate the ecological water requirement.

Data Source

Meteorological Data

The precipitation, evaporation and wind speed data were obtained from the China Meteorological Data website,[1] specifically, the n/)poration and wind speed data were obtained from the China Meteorological DatV3.0)," which contained the daily values pressure, temperature, precipitation, evaporation, relative humidity, wind direction, wind speed, sunshine hours and 0 cm ground temperature elements of the 166 stations in China since January 1951.

Land Use Data

The land use data were obtained based on the actual land use maps already available for the Yellow River Basin.[2] The land use maps included categories such as dry land, rural settlements, sandy land, forested land, marshland, lakes, and other land use types.

The Manning coefficient was a very important parameter in the hydrodynamic model, and the rationality of its value directly affected the accuracy of the model simulation results. To make the results of the model more realistic, it was usually necessary to select different Manning coefficients as objects of simulation to determine the appropriate Manning coefficient. In the HD module of the MIKE 21 hydrodynamic model, a suitable

[1] http://data.cma.cn/

[2] http://www.resdc.cn/

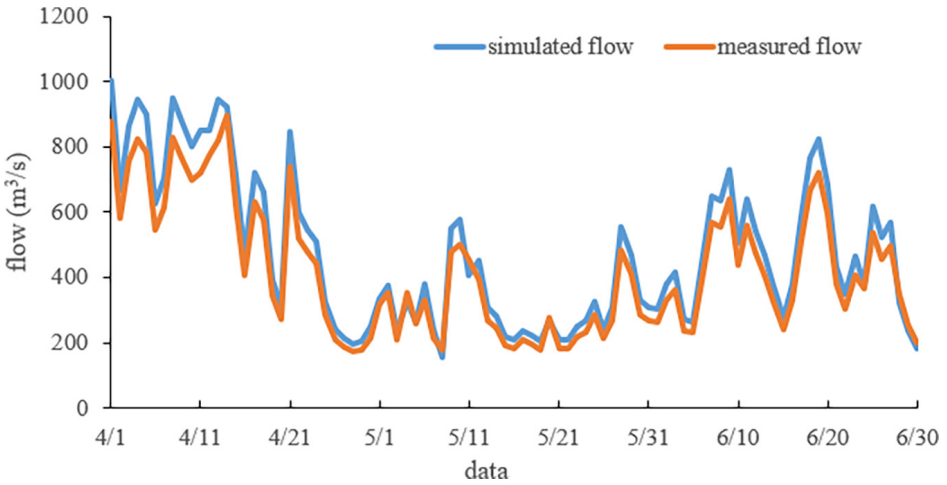

FIGURE 4 | The verification results of the LM section.

Manning coefficient map was extracted from the land use map to refer to the roughness table.

DEM Data

The DEM data of the study area were extracted from the existing DEM database (Geospatial Data Cloud[3]). The DEM used in this article had a resolution of 30 m × 30 m.

Hydrological Data and Aquatic Biological Data

The hydrological data (1946–1956) of the study area were collected from the Yellow River Water Conservancy Commission.[4] The aquatic biological data of the study area were extracted from the data published in Wu et al. (2006), Huang et al. (2016), and Wang (2017).

RESULTS AND DISCUSSION

The ecological water requirement in the upper reaches of the Yellow River was analyzed by selecting the LZ section in the upper reaches, the LM section in the middle reaches. The runoff of the QTX reservoir before construction (before 1958) and WJZ reservoir before construction (before 1994) was regarded as approximately natural runoff, and the measured daily runoff characteristics of the section from 1946 to 1956 were counted. Moreover, *S. lanzhouensis* was selected as the indicator species of the LZ section (**Figure 5A**), and *C. carpio* was selected as the indicator species of the LM section (**Figure 5B**) to simulate the process of the ecological water requirement in different periods.

The Habitat Distribution of the Main Stream of the Yellow River

A habitat simulation model was established by the MIKE 21 model to simulate the habitat distribution of *S. lanzhouensis* in different stages under different ecological flows (**Figure 6**). The ecological water requirement process was obtained based on the results of habitat simulation and features of the hydrological reference group.

A habitat simulation model was established by using the MIKE 21 model to simulate the habitat

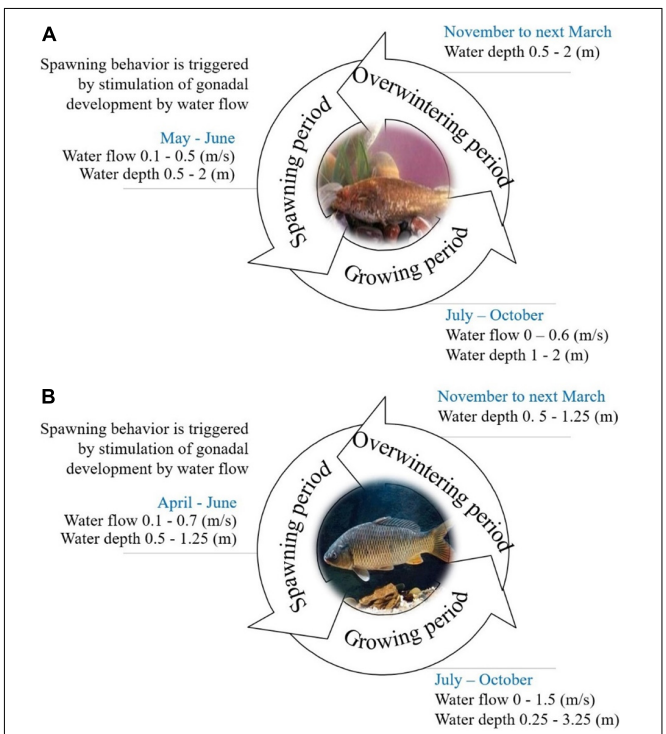

FIGURE 5 | Environmental factors of fish habitat in the Yellow River (Wu et al., 2006; Huang et al., 2016; Wang, 2017). **(A)** The environmental factors of *Silurus lanzhouensis* habitat in the Yellow River. **(B)** The environmental factors of *Cyprinus carpio* habitat in the Yellow River.

[3]http://www.gscloud.cn/

[4]http://www.yrcc.gov.cn/

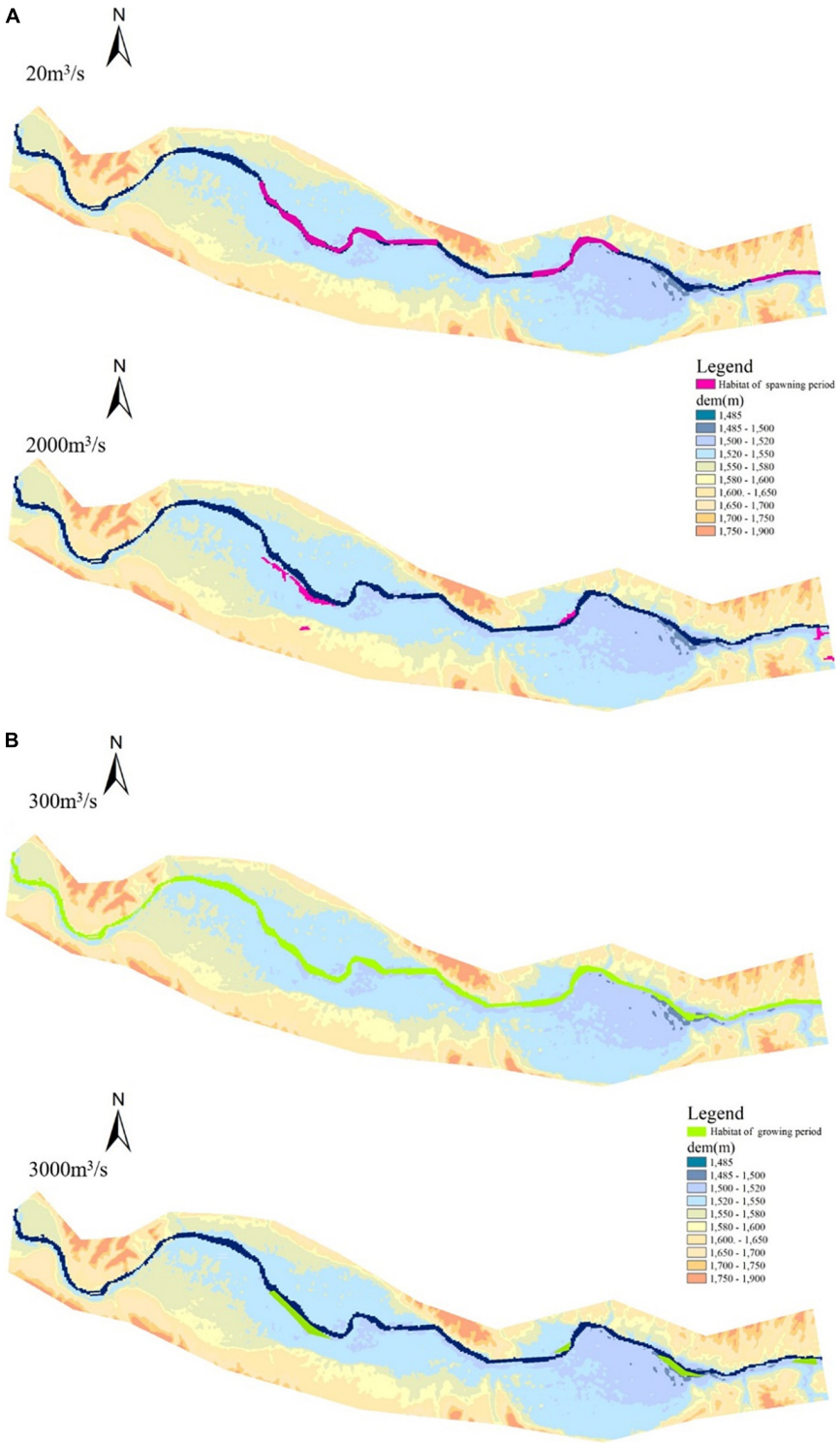

FIGURE 6 | The habitat distribution of *Silurus lanzhouensis* at different flow rates of LZ. **(A)** Habitat distribution in spawning period. **(B)** Habitat distribution in growing period.

distribution of *C. carpio* at different stages under different flows (**Figure 7**). An ecological water requirement assessment method that coupled the results of habitat simulation and features of the hydrological reference group was used to obtain the ecological water requirement process.

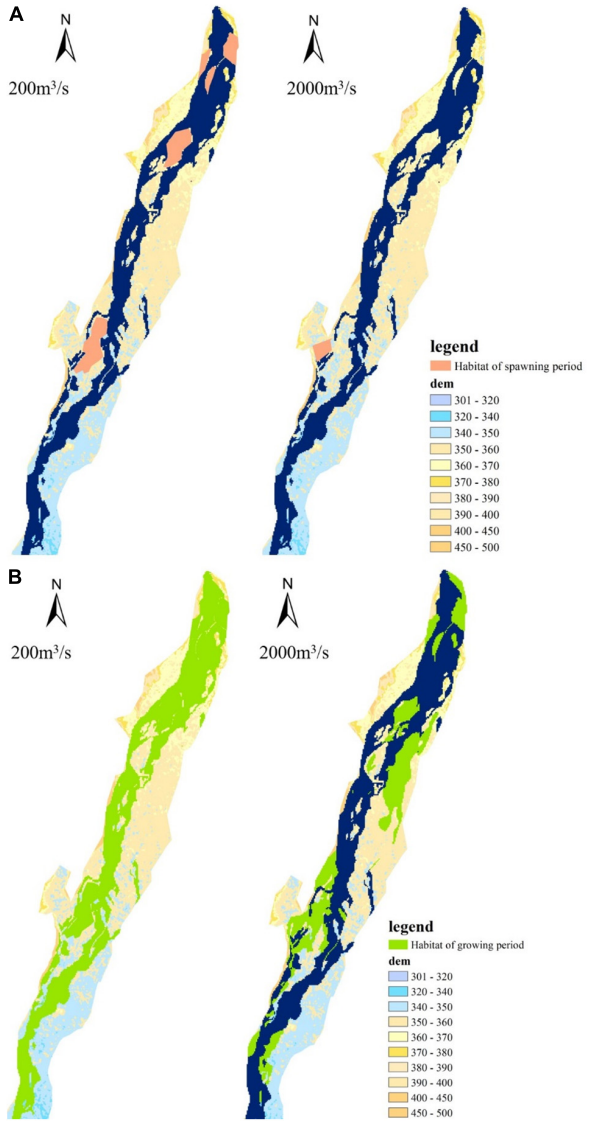

FIGURE 7 | The habitat distribution of *Cyprinus carpio* at different stages under different flows of LM. **(A)** Habitat distribution in spawning period. **(B)** Habitat distribution in growing period.

The Key Features of the Hydrological Reference Group

The river runoff before the construction of the LJX reservoir (before 1958), the QTX reservoir (before 1958), the WJZ reservoir (before 1994) and the SMX reservoir (before 1957) was approximated as the natural river runoff, and the measured daily runoff characteristics of the Lanzhou section from 1946 to 1956 were obtained. The characteristic values of the hydrological reference group mainly focused on the minimum flow and the high flow pulse.

For the LZ section, under natural conditions, the minimum flow during the growing period of *S. lanzhouensis* (July to October) was 614 m^3/s, the minimum flow during the overwintering period (November-next March) was 206 m^3/s, and the minimum flow during the spawning period (April to June) was 296 m^3/s.

The rising period of the main stream of the Yellow River was from April to June. The daily average flow process of the Lanzhou section from 1946 to 1956 showed that the high-flow pulses were mainly concentrated in April and early to mid-June. Flow events with a flow rate exceeding 1,180 m^3/s (flow rate with a cumulative frequency of 25% during the flood period in the natural period) and a duration of more than 3 days are regarded as high flow pulses. The occurrence of high flow pulses in the LZ and LM section is shown in **Tables 4**, **5**.

The Ecological Water Requirement Process of the Main Stream of the Yellow River

The ecological water requirement process of the key sections of the main stream of the Yellow River was obtained by coupling the results of habitat simulation and the features of the hydrological reference group (**Figure 8**).

Lanzhou Section

The habitat spread throughout the main trough when the flow was small, the habitat area gradually decreased as the flow increased, and the habitat mainly spread in the caves or aquatic plants on the edge of the water or in the middle of the river with a suitable flow rate of 300–3,000 m^3/s. The spawning season was from late May to early July, and the suitable flow was 350–720 m^3/s during the spawning season. During the period from November to the next March, the river mainly provides a winter habitat for fish, and a flow of 120–200 m^3/s could be fully satisfied.

Longmen Section

The habitat spread throughout the main trough when the flow was small, the habitat area gradually decreased with the increase in flow, and the habitat gradually concentrated on the edge of the water area. The back-beach area of the floodplain formed a suitable habitat, and the suitable flow range was 200–1,800 m^3/s. For the spawning ground, the habitat area increased significantly when the flow was 300 m^3/s during the spawning period (April–June), which indicated that the river section was suitable for the spawning of the *C. carpio*, for which the flow should reach 300 m^3/s. During the period from November until the next March, the river mainly provides a winter habitat for fish, and a flow of 120–260 m^3/s could be fully satisfied. In addition, considering the actual conditions of the Yellow River water volume and the demand for fish survival, the minimum flow condition for meeting the water requirement of *C. carpio* in the LM section was approximately 200 m^3/s.

The Yellow River is famous for having a small amount of water and a large amount of sand, and the amount of sediment transport is an important part of its ecological water requirement. As shown in **Table 6**, the suitable flow rates in the growing period in the LZ and LM section were 300–3,000 and 200–1,800 m^3/s; the suitable flow rates in the spawning period in the LZ and LM section were 350–720 and 260–400 m^3/s; the suitable flow rates in the overwintering period in the LZ and LM section were

TABLE 4 | Characteristic values of the high flow pulse of Lanzhou during flood period before 1957.

Index	Number	Peak flow/(m^3/s)	Average flow/(m^3/s)	Duration/days	Ascent rate/[m^3/(SD)]	Decline rate/[m^3/(SD)]
Mean	3	2,050	1,493	31	54	71
Max	0	1,250	1,200	4	20	28
Min	1.2	2,225	1,193	9	172	90
1/3 quantile	1	2,295	1,720	7	275	157
2/3 quantile	2	2,350	1,563	14	240	145

TABLE 5 | Characteristic values of the high flow pulse of Longmen during flood period before 1957.

Index	Number	Peak flow/(m^3/s)	Average flow/(m^3/s)	Duration/days	Ascent rate/[m^3/(SD)]	Decline rate/[m^3/(SD)]
Mean	2.2	2,060	1,114	11	193	165
Max	5	3,070	1,143	22	407	440
Min	0	1,120	980	4	150	150
1/3 quantile	1	1,220	1,046	7	70	70
2/3 quantile	2	2,070	1,193	12	200	180

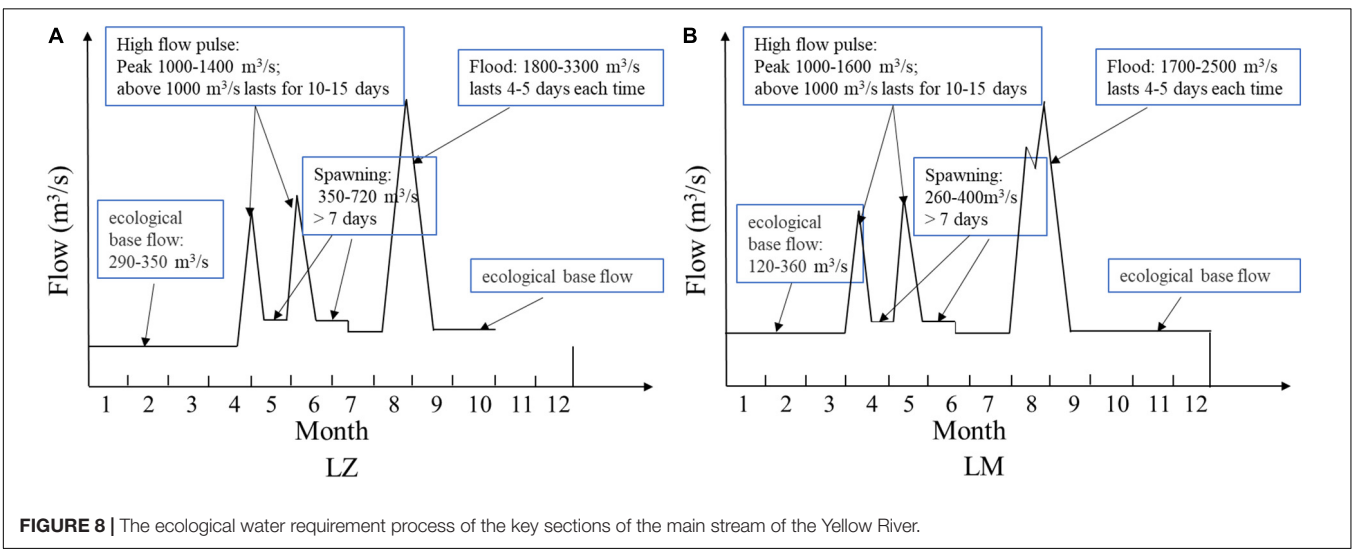

FIGURE 8 | The ecological water requirement process of the key sections of the main stream of the Yellow River.

TABLE 6 | The ecological water requirement for main sections of the main stream of the Yellow River.

Sections	Ecological flow (m^3/s)	Ecological flow in sensitive period (m^3/s)	Ecological water requirement (m^3/y)
LZ	290–350	May–June: 350–720 (the spawning pulse: 1,000–1,400); July–October: flood pulse (1,800–3,300)	9.1×10^9–11×10^9 m^3
LM	120–360	April–June: 260–400 (the spawning pulse: 1,000–1,600); July–October: flood pulse (1,700–2,500)	4.7×10^9–11.3×10^9 m^3

The flow during the breeding period should be maintained more than 5 days, the spawning pulse >10 days, and the flood pulse lasts 4–5 days.

120–200 and 120–260 m^3/s, and the annual ecological water requirement of the LZ and LM section was 9.1–11 $\times$ 10^9 and 4.7–11.3 $\times$ 10^9 m^3, respectively.

According to the comprehensive planning of the Yellow River Basin approved by the State Council points out that the minimum ecological water requirement of Longmen section from April to June was 180 m^3/s, and the suitable ecological water requirement was 240 m^3/s (Yellow River Water Resources Commission, 2013). In addition, it is proposed that the early warning flow of Longmen section was 100 m^3/s, and the minimum ecological flow of each period obtained in this study was higher than the early warning flow, and the results of ecological water requirement were reasonable.

CONCLUSION

To maintain the ecological integrity of the river, a new assessment method of ecological water requirement was proposed by coupling the results of habitat simulation with the features of the hydrological reference group, which was helpful for quantitatively simulating the changes in the ecological water

requirement of indicator fish in key sections of the Yellow River, and it was effective for identifying the variations of the ecological water requirement.

An ecological hydrological model of the main stream of the Yellow River was constructed. Five cross-sections of the Yellow River were selected to construct the eco-hydrological horizontal pattern of the main stream of the Yellow River according to the hydrological characteristics of different sections. The effective habitat area of indicator fish under different characteristic flows was simulated.

A method for the calculation of ecological water requirement was proposed, combining habitat simulation results, hydrological characteristics and the flood pulse. The ecological water requirement process of indicator fish in the main stream of the Yellow River was evaluated. The pulse flow process during the spawning period from April to June was determined based on the ecological flow elements from the simulation of daily runoff processes in the LZ and LM sections from 1946 to 1956. For LZ section, a high pulse flow process with a low flow peak should be guaranteed in mid- to late May, and the peak flow should be at least approximately 1,000 m^3/s to provide spawning signals for fish; the peak flow (i.e., from 1,200 to 1,600 m^3/s) was 1 to 2 time during the high pulse flow process in May to June. For LM section, a high pulse flow process with a low flow peak should be guaranteed in mid- to late April, and the peak flow should be at least approximately 1,000 m^3/s to provide spawning signals for fish; the peak flow (i.e., from 1,000 to 1,600 m^3/s) was 1 to 2 time during the high pulse flow process in May to June.

According to comprehensive habitat simulation of indicator fish and the ecological water requirement process based on the features of the hydrological reference group, the recommended plans for meeting the ecological water requirement process of the key sections of the main stream of the Yellow River have been determined, including the flow peak, distribution time and duration. The suitable flow rates in the growing period in LZ and LM were 300–3,000 and 200–1,800 m^3/s, respectively. The suitable flow rates in the spawning period in LZ and LM were 350–720 and 260–400 m^3/s, respectively. The suitable flow rates in the overwintering period in LZ and LM were 120–200 and 120–260 m^3/s, respectively. The annual ecological water requirement of the LZ, and LM section was 9.1×10^9–11×10^9 and 7.9×10^9–15.4×10^9 m^3, respectively.

The approach quantitatively simulated the changes in the ecological water requirement of indicator fish in key sections of the Yellow River. The approach was proven to be an effective and realistic tool for the ecological water requirement accounting in the Yellow River. Habitat simulation required a large amount of basic river data and quantitative biological data, which limited the application of this approach to a certain extent. It is recommended that the simulation results should be compared with actual measurement results to verify the reliability and accuracy of the approach.

DATA AVAILABILITY STATEMENT

The original contributions presented in the study are included in the article/supplementary material, further inquiries can be directed to the corresponding author.

AUTHOR CONTRIBUTIONS

FZ, CL, and WS conceived and designed the manuscript. FZ and XZ analyzed the data. XW, QL, and JB contributed reagents, materials, and analysis tools. FZ wrote the manuscript. All authors contributed to the article and approved the submitted version.

FUNDING

This study was supported by the Key Laboratory of Water and Sediment Science, Ministry of Education fund (SS202102) and the National Key Research and Development Program (2017YFC0404401 and 2018YFC0407403).

ACKNOWLEDGMENTS

We would like to thank the editor and reviewers for all their detailed comments and valuable suggestions in greatly improving the quality of this manuscript.

REFERENCES

Arthington, A. H., Bhaduri, A., Bunn, S. E., Jackson, S. E., Tharme, R. E., Tickner, D., et al. (2018). The Brisbane declaration and global action agenda on environmental flows (2018). *Front. Env. Sci.* 6:45. doi: 10.3389/fenvs.2018.00045

Bartschi, D. K. (1976). *A habitat-discharge method of determining instream flows for aquatic habitat. In Symposium on Instream Flow Needs*. Bethseda: American Fisheries Society, 285–294.

Baumgartner, L. J., Conallin, J., Wooden, I., Campbell, B., Gee, R., Robinson, W. A., et al. (2014). Using flow guilds of freshwater fish in an adaptive management framework to simplify environmental flow delivery for semi−arid riverine systems. *Fish Fish.* 15, 410–427. doi: 10.1111/faf.12023

Bovee, K. D. (1996). *A comprehensive overview of the instream flow incremental methodology*. Virginia: National Biological Service, Fort Collins, Corporation.

Brown, E. D., and Williams, B. K. (2016). Ecological integrity assessment as a metric of biodiversity: Are we measuring what we say we are? *Biodiv. Conserv.* 25, 1011–1035. doi: 10.1007/s10531-016-1111-0

Bunn, S. E., and Arthington, A. H. (2002). Basic principles and ecological consequences of altered flow regimes for aquatic biodiversity. *Environ. Manag.* 30, 492–507. doi: 10.1007/s00267-002-2737-0

Cai, Y. P., Wan, L., Yang, Y., Zhang, X. M., and Li, Y. J. (2010). Analysis on the environmental flow requirements for natural reproduction of Chinese Sturgeon based on habitat simulation methods. *J. Hydroecol.* 3, 1–6. doi: 10.5194/hess-14-1033-2010

Dai, Z., Li, C., Trettin, C., Sun, G., Amatya, D., and Li, H. (2010). Bi-criteria evaluation of the MIKE SHE model for a forested watershed on the South Carolina coastal plain. *Hydrology and Earth System Sciences* 14, 1033–1046. doi: 10.5194/hess-14-1033-2010

Dhi, M. B. (2011). *Mike 21 Flow Model Fm. Hydrodynamic Module User Guide*, Vol. 2002. 2001–2003.

Doummar, J., Sauter, M., and Geyer, T. (2012). Simulation of flow processes in a large-scale karst system with an integrated catchment model (Mike She)–Identification of relevant parameters influencing spring discharge. *J. Hydrol.* 426, 112–123. doi: 10.1016/j.jhydrol.2012.01.021

Dudgeon, D. (2010). Prospects for sustaining freshwater biodiversity in the 21st century: linking ecosystem structure and function. *Curr. Opin. Env. Sust.* 2, 422–430. doi: 10.1016/j.cosust.2010.09.001

Edwards, E. A., and Twomey, K. (1982). *Habitat suitability index models: common carp*. Boston, MA: Western Energy and Land Use Team, Office of Biological Services, Fish and Wildlife Service, US Department of the Interior.

Feng, H. J. (2010). *Community diversity and growth characteristic of fish between Ningxia and Inner Mongolia in the main stream of Yellow River*. Kirkland, WA: Northwest university. doi: 10.7666/d.y1679009

Hao, F. Q., Huang, J. H., Gao, C. D., Wang, X. G., and Zhang, J. J. (2006). Overview on study of eco-environmental water demand for main stream of Yellow River. (in Chinese) *Water Resour. Hydrop. Eng.* 37, 60–63. doi: 10.3969/j.issn.1000-0860.2006.02.013

Hao, Z. C., and Shang, S. H. (2008). Multi-objective assessment method based on physical habitat simulation for calculating ecological river flow demand. *J. Hydraul. Eng.* 39, 557–561. doi: 10.3321/j.issn:0559-9350.2008.05.007

Huang, J. H., Hao, F. Q., Gao, C. D., Wang, X. G., and Zhang, J. J. (2004). Preliminary Approach to Water Demand of Ecological Environment of the Yellow River. (in Chinese) *Yellow River* 26, 26–27. doi: 10.3969/j.issn.1000-1379.2004.04.012

Huang, J. H., Wang, R. L., and Ge, L. (2016). *Study on the functional continuous flow index of the important reaches of the main and tributaries of the Yellow River (in Chinese)*. Zhengzhou: Yellow River Water Conservancy Press.

Hughes, D. A. (1999). Towards the incorporation of magnitude-frequency concepts into the building block methodology used for quantifying ecological flow requirements of south African rivers. *Water South Afr.* 5, 279–284.

Hughes, D. A. (2001). Providing hydrological information and data analysis tools for the determination of ecological instream flow requirements for south African rivers. *Hydrology* 241, 140–151. doi: 10.1016/S0022-1694(00)00378-4

Jiang, X., Liu, X., Zhang, S., and Cai, Q. (2005). Distinguishing Key Species of Aquatic Ecosystem of the Main Yellow River. (in Chinese) *Yellow River* 27, 1–3.

Jiang, X. H., and Wang, H. Z. (2012). Change of structural characteristics and health assessment of aquatic ecosystems along the mainstream of the Yellow River. *J. Hydraul. Eng.* 43, 991–998.

Lian, Y., Wang, X. G., Wang, R. L., and Ge, L. (2011). *Study on the protection target and ecological water requirements of the Yellow River Ecosystem (in Chinese)*. Zhengzhou: Yellow River Water Conservancy Press.

Liu, C., Wang, Z. Y., and Sui, J. Y. (2008). Variation of flow and sediment of the Yellow River and their influential factors. *Advances in Science and Technology of Water resources* 28, 1–7.

Liu, W., Zhan, J. Y., Zhao, F., Wang, C., Zhang, F., Teng, Y. M., et al. (2022). Spatio-temporal variations of ecosystem services and their drivers in the Pearl River Delta, China. *J. Clean. Prod.* 2022:130466. doi: 10.1016/j.jclepro.2022.130466

Liu, X. Y. (2009). *Environmental Flows of the Yellow River*. Zhengzhou: Yellow River Water Conservancy Press, 5–8. doi: 10.1142/9789814280969_0002

Ma, G. H., Xia, Z. Q., Guo, L. D., Li, J., and Guo, Z. (2007). Ecological runoff for different cross-sections of the main stream of Yellow River (in Chinese). *J. Hohai Univ.* 35, 496–500.

Ma, Z. Z., Wang, Z. J., Xia, T., Gippel, C. J., and Speed, R. (2014). Hydrograph-Based Hydrologic Alteration Assessment and Its Application to the Yellow River. *J. Env. Inform.* 23:1. doi: 10.3808/jei.201400252

Morrison, M. L., Marcot, B. G., and Mannan, R. W. (1992). *Wildlife–Habitat Relationships. Concepts and Applications*. Madison, WI: The University of Wisconsin press.

Nikghalb, S., Shokoohi, A., Singh, V. P., and Yu, R. (2016). Ecological regime versus minimum environmental flow: comparison of results for a river in a semi-Mediterranean region. *Water Resour. Manag.* 30, 4969–4984. doi: 10.1007/s11269-016-1488-2

Norris, R. H., and Hawkins, C. P. (2000). Monitoring River health. *Hydrobiology* 435, 5–17. doi: 10.1023/A:1004176507184

Norris, R. H., and Thoms, M. C. (1999). What is river health? *Freshw. Biol.* 41, 197–209. doi: 10.1046/j.1365-2427.1999.00425.x

Poff, N. L. (2018). Beyond the natural flow regime? Broadening the hydro−ecological foundation to meet environmental flows challenges in a non−stationary world. *Freshw. Biol.* 63, 1011–1021. doi: 10.1111/fwb.13038

Poff, N. L., Allan, J. D., Bain, M. B., Karr, J. R., Pres-tegaard, K. L., Richter, B. D., et al. (1997). The natural flow regime: a paradigm for river con-servation and restoration. *BioScience* 47, 769–784. doi: 10.2307/1313099

Richter, B. D. (1997). How much water does a river need? *Freshw. Biol.* 32, 231–2496. doi: 10.1046/j.1365-2427.1997.00153.x

Rolls, R. J., and Bond, N. R. (2017). *Environmental and ecological effects of flow alteration in surface water ecosystems. Water for the Environment*. Cambridge, MA: Academic Press, 65–82. doi: 10.1016/B978-0-12-803907-6.00004-8

Ru, H. J., Wang, H. J., Zhao, W. H., Shen, Y. Q., Wang, Y., and Zhang, X. K. (2010). Fishes in the mainstream of the Yellow River: assemblage characteristics and historical changes (in Chinese). *Biodiv. Sci.* 18, 169–174. doi: 10.3724/SP.J.1003.2010.179

Shang, W. X., Peng, S. M., Wang, Y., Zheng, X. K., and Liu, B. J. (2020). Research on the ecological integrity-oriented environmental flow regime of the Lower Yellow River. *J. Hydraul. Eng.* 51, 367–370. doi: 10.1016/j.scitotenv.2022.153205

Sun, J.N., Zhang, S. Q., Zhu D.Z., and Fu J.J. (2013). Simulative evaluation of fish habitat of backwater tributary of Baihetan Reservoir. *Water Resourc. Hydropower Eng.* 44, 17–22. doi: 10.3969/j.issn.1000-0860.2013.10.004

Tennant, D. L. (1976). Instream flow regimens for fish, wildlife, recreation and related environmental resources. *Fisheries* 1, 359–373. doi: 10.1577/1548-8446(1976)001<0006:IFRFFW>2.0.CO;2

Thame, R. (2003). A global perspective on environmental flow assessment: emerging trends in the development and application of environmental flow methodologies. *River Res. Appl.* 19, 397–441. doi: 10.1002/rra.736

Theodoropoulos, C., Skoulikidis, N., Rutschmann, P., and Stamou, A. (2018). Ecosystem−based environmental flow assessment in a Greek regulated river with the use of 2D hydrodynamic habitat modelling. *River Res. Appl.* 34, 538–547. doi: 10.1002/rra.3284

Virkki, V., Alanärä, E., Porkka, M., Ahopelto, L., Gleeson, T., and Mohan, C. (2021). Environmental flow envelopes: quantifying global, ecosystem–threatening streamflow alterations. *Hydrol. Earth Syst. Sci. Dis.* 2021, 1–31. doi: 10.5194/hess-2021-260

Wang, G. X., Chen, M. J., Feng, H. L., Wang, L. Q., and Huang, C. S. (2009). Ecological flow regime in middle and lower reaches of the Yellow River. *J. Sun Yat-sen Univ.* 48, 125–130.

Wang, H., Wang, H., Hao, Z. C., Wang, X., Liu, M., and Wang, Y. L. (2018). Multi-objective assessment of the ecological flow requirement in the upper Yangtze national nature reserve in China using PHABSIM. *Water* 10:326. doi: 10.3390/w10030326

Wang, P. F., Shen, Y. X., Wang, C. T., Hou, J., Qian, J., Yu, Y., et al. (2017). An improved habitat model to evaluate the impact of water conservancy projects on Chinese sturgeon (Acipenser sinensis) spawning sites in the Yangtze River, China. *Ecolog. Eng.* 104, 165–176. doi: 10.1016/j.ecoleng.2017.03.021

Wang, R. L., Huang, J. H., Ge, L., Feng, H. J., Li, R. N., and Shen, H. B. (2020). Study of ecological flow based on the relationship between cyprinusy carpio habitat hydrological and ecological response in the lower Yellow River. *J. Hydraul. Eng.* 51, 1175–1187. doi: 10.13243/j.cnki.slxb.20200184

Wang, Y. (2017). *Polymorphism of SSR and analysis with growth traits in Silurus Lanzhouensis*. Yinchuan: Ningxia University.

Wu, M., and Chen, A. (2018). Practice on ecological flow and adaptive management of hydropower engineering projects in China from 2001 to 2015. *Water Pol.* 20, 336–354. doi: 10.2166/wp.2017.138

Wu, X. D., Zhang, Q., Zhao, H. X., Hou, Y., and Zhang, W. (2006). A new species of catfish in Ningxia-Silurus Lanzhouensis and its intensive morphological description. *Freshw. Fish.* 36, 26–29.

Xu, T. (2010). Calculation Principle and Application Example of a Two-dimensi onal Flow Model-MIKE21 HD. *Water Conserv. Sci. Technol. Econ.* 16, 867–869.

Yang, W., Zhao, Y. W., Liu, Q., and Sun, T. (2020). A systematic literature review and perspective on water-demand for ecology of Lake Baiyangdian. *J. Lake Sci.* 32, 294–308. doi: 10.18307/2020.0202

Yellow River Water Resources Commission (2013). *Comprehensive Planning of the Yellow River Basin (2012–2030)*. Jinan: Yellow River Water Resources Commission.

Zhang, W. G., Huang, Q., and Jiang, X. H. (2008). Study on instream ecological flow based on physical habitat simulation. *Adv. Water Sci.* 19, 192–197.

Zhang, Z., Huang, Y., Xu, C. Y., Chen, X., Moss, E. M., Jin, Q., et al. (2016). Analysis of Poyang Lake water balance and its indication of river–lake interaction. *Spring. Plus* 5, 1–15. doi: 10.1186/s40064-016-3239-5

Zhao, M. H., Zhang, X. H., and Zhang, X. H. (2011). Analysis of eco-environmental water demand in the Yellow River Channel (in Chinese). *Yellow River* 33, 58–60. doi: 10.3969/j.issn.1000-1379.2011.11.022

Conflict of Interest: WS and XZ were employed by Yellow River Engineering Consulting Co., Ltd.

The remaining authors declare that the research was conducted in the absence of any commercial or financial relationships that could be construed as a potential conflict of interest.

frontiers | Frontiers in Environmental Science

ORIGINAL RESEARCH
published: 12 July 2022
doi: 10.3389/fenvs.2022.941887

Spatiotemporal Changes in Land Use and Ecosystem Service Values Under the Influence of Glacier Retreat in a High-Andean Environment

Santiago Madrigal-Martínez[1]†, Rodrigo J. Puga-Calderón[1†], Victor Bustínza Urviola[2] and Óscar Vilca Gómez[2]*

[1]Dirección de Información y Gestión Del Conocimiento, Instituto Nacional de Investigación en Glaciares y Ecosistemas de Montaña, Huaraz, Perú, [2]Oficina Desconcentrada Macro Región Sur, Instituto Nacional de Investigación en Glaciares y Ecosistemas de Montaña, Cusco, Perú

OPEN ACCESS

Edited by:
Jinyan Zhan,
Beijing Normal University, China

Reviewed by:
Cigdem Coskun Hepcan,
Ege University, Turkey
Renato Farias Valle Junior,
Science Technology of the Triângulo Mineiro, Brazil

***Correspondence:**
Santiago Madrigal-Martínez
smadrigal@inaigem.gob.pe

†These authors have contributed equally to this work and share first authorship

Specialty section:
This article was submitted to Land Use Dynamics, a section of the journal Frontiers in Environmental Science

Received: *11 May 2022*
Accepted: *07 June 2022*
Published: *12 July 2022*

Citation:
Madrigal-Martínez S, Puga-Calderón RJ, Bustínza Urviola V and Vilca Gómez Ó (2022) Spatiotemporal Changes in Land Use and Ecosystem Service Values Under the Influence of Glacier Retreat in a High-Andean Environment. Front. Environ. Sci. 10:941887. doi: 10.3389/fenvs.2022.941887

Glaciers supply multiple ecosystem services that are threatened by climate change. The retreat and disappearance of tropical glaciers is an important dynamic that affects ecosystems and local communities. The knowledge of the impacts of this land-change dynamics on the supply of ecosystem services is lacking. In that sense, the assessment developed can provide evidence about the costs and benefits of promoting conservation and human well-being at the same time. Then, the main objective of this research is to determine the spatial–temporal changes and their effects on the economic value of ecosystem services in a glacial retreat environment. We selected the Marangani district as a study area. It comprises the La Raya Mountain range in the Andes. The assessments were carried out across two scales of observation: the municipality and the watershed level. Here, we process spectral information from Landsat Sensor using the Random Forest algorithm in the Google Earth Engine platform to classify 10 biomes. It was carried out over more than 30 years (from 1986 to 2019). After that, ecosystem services provided by the biomes were valued using the transfer method. This research shows that at the municipality level, almost all the LULCs faced variations over time, and the glaciers had the highest change, accumulating a ratio of –85.51%, whereas at the watershed level, a higher tendency of land changes is observed in the areas without glaciers, and those with glacier areas count on permanent larger bofedales. At the municipality level, the economic value of ecosystems shows that bofedales and water surfaces are the LULCs that supply the highest ecosystem services (~33,000 USD ha^{-1} yr^{-1} each). In addition, without the inflation adjustment, the total ESV is on a trajectory of losing ESV (–\$9.67 × 10^6). In the watersheds with glacier retreat, significant quantity of bofedales and natural grasslands controls the fluctuations of ESV. These high-mountain watersheds play an essential role in providing benefits and value to local communities. In general, the municipality level indicates the trajectory of changes in the district, whereas the watershed scale shows the urgency for implementing spatial conservation actions.

Keywords: glacier retreat, ecosystem service (ES) values, tropical mountain, high-Andean, land-use and land cover change, spatial scale, bofedal

1 INTRODUCTION

Glaciers are retreating and disappearing worldwide (Marzeion et al., 2014; Zemp et al., 2015), and these processes have been accelerated globally in the early 21st century (Hugonnet et al., 2021). The causes are attributed to a combination of several factors related to anthropogenic and biophysical dynamics (Marzeion et al., 2014; Veettil and Kamp, 2019). Concretely, in the case of mountain glaciers, albedo reduction, increasing temperatures, and changing precipitation are drivers that may have a significant relation to glacier retreat and mass balance changes (Crossman et al., 2013; Tang et al., 2013; Zhang et al., 2021). However, the glacier recession pattern is more complex at higher elevations of the Andes because it is likely to be related to other components of the energy balance as net radiation and ground heat fluxes (Juřicová and Fratianni, 2018). These causes may have produced a fast retreating of Andean glaciers (Dussaillant et al., 2019; Hock et al., 2019). The mountain range of La Raya (the study area), situated northwest of the Peruvian high plateau, shows an ice area decrease from 11.27 km^2 estimated from aerial photos of 1962 (Hidrandina, 1989) to 1.90 km^2 assessed from Sentinel images of 2016 (INAIGEM, 2018).

Glaciers supply multiple ecosystem services (ESS), mostly related to the provision, regulation, and maintenance of water (Cook et al., 2021). Then, the disappearance of glaciers will alter hydrological regimes in downstream systems (Milner et al., 2017), which will have consequences on water management, food and energy security, and environmental management (Rasul and Molden, 2019). However, rapid melting of glaciers has a temporary rise in streamflow (Mark and Mckenzie, 2007; Mark et al., 2009), which added to the increase in precipitation can hide the impact downstream. Moreover, concerning biodiversity, responses of ecosystems are diverse and depend on internal species attributes, local environment, and external drivers of change (Cauvy-Fraunié and Dangles, 2019). In that sense, glaciers in the high-Andean mountain ranges can be associated with sensitive ecosystems such as bofedales (peat bogs and wetlands). The studies of the effects of glacier retreats on bofedales indicate a positive relation (Dangles et al., 2017; Polk et al., 2017), but the knowledge of impacts on the ESS is limited. Then, the prolonged disappearance of glaciers is a land-cover change that already has uncertain costs for ecosystem function and services to human well-being.

Land cover and land use (LULC) change has gained prominence as the main cause of degradation and change in ecosystems worldwide (Brandt and Townsend, 2006; Yin et al., 2011; Ektvedt et al., 2012; Kuemmerle et al., 2016; Quintero-Gallego et al., 2018; Madrigal-Martínez and Miralles i García, 2019b). LULC changes are the results of a combination of socio-economic, environmental, and political factors (Lambin et al., 2003). In the mountain environments, these changes are often caused by biophysical factors, land abandonment, deforestation, agricultural expansion, and urbanization to a lesser extent (Madrigal-Martínez and Miralles i García, 2019a; Msofe et al., 2019; Jiménez-Olivencia et al., 2021). Then, mapping the spatiotemporal transitions of LULC is fundamental to identifying landscape patterns for planning sustainable ESS (Luck et al., 2012; Chaudhary et al., 2017; Egarter Vigl et al., 2017; Madrigal-Martínez and Miralles i García, 2019a).

Mapping the spatiotemporal changes of LULC has been undertaken in several studies using different methodological approaches, but with the growing use of remote sensing and geographic information system (GIS) tools (Lu et al., 2004). In the same way, different types of multisource satellite images and classification methods have been used, but among all, Random Forest (RF) is a supervised classifier algorithm broadly used that performs well (Gislason et al., 2006). These change detection techniques provide a flexible environment for rapidly developing image classification and analyzing for changes, maintaining a satisfactory level of accuracy over the area being classified. In this context, LULC maps can provide a high capacity for identifying and explaining the supply of individual ecosystem services (Burkhard et al., 2009; Koschke et al., 2012).

Knowing the value of ESS is recognized as an essential pathway to sustainability (Abson et al., 2014). Per se, a suitable assessment is needed to improve policy and decision-making linked to management of the territory (Ling et al., 2018; Dang et al., 2021; Selivanov and Hlaváčková, 2021). Thus, such assessments can provide evidence about the costs and benefits of promoting conservation and human well-being at the same time (de Groot et al., 2010). The monetary value of ecosystem services (ESV) from a global to local scale is being established to accomplish this goal (Costanza et al., 1997; Groot et al., 2010; Costanza et al., 2014; de Groot et al., 2020; Foundation for Sustainable Development, 2021). The benefit transfer method has the highest worldwide usage frequency for determining the ESV (Schägner et al., 2013). Its main improvement is that it offers a relatively quick and low-cost estimation. However, to our knowledge, studies on spatiotemporal changes of ESV related to tropical glacier retreat environments have not been conducted.

Therefore, our study maps and evaluates the LULC change and associated ESV across the Marangani district for more than 3 decades (1987–2019). We performed the assessments across two scales of observation: the municipality and the watershed level, considering at least two spatial scales which should assure robustness (Scholes et al., 2013; Felipe-Lucia et al., 2014; Madrigal-Martínez and García, 2020). Based on spectral information from Landsat Sensor using the RF algorithm, we select this district of the higher elevations of the Andes because it is part of the mountain range of La Raya–an environment where glaciers are shrinking rapidly (INAIGEM, 2018). The results of this study provide answers to the following questions: 1) which spatiotemporal changes on LULC in a territory are under the influence of glacier retreat? 2) which spatiotemporal changes and relationships between glaciers and bofedales are at the watershed level? 3) how do these changes affect the monetary value of ecosystem services? Then, we discuss the reasons for the main spatiotemporal and ESV changes and their implications for the socio-ecosystem.

2 MATERIALS AND METHODS

2.1 Study Area

The selected area is the district of Marangani (Canchis, Cusco), comprised within the Raya Mountain range (**Figure 1**). It is the third most populated district of Canchis, and the population at the end of 2017 was 10,554 (National Institute of Statistics and

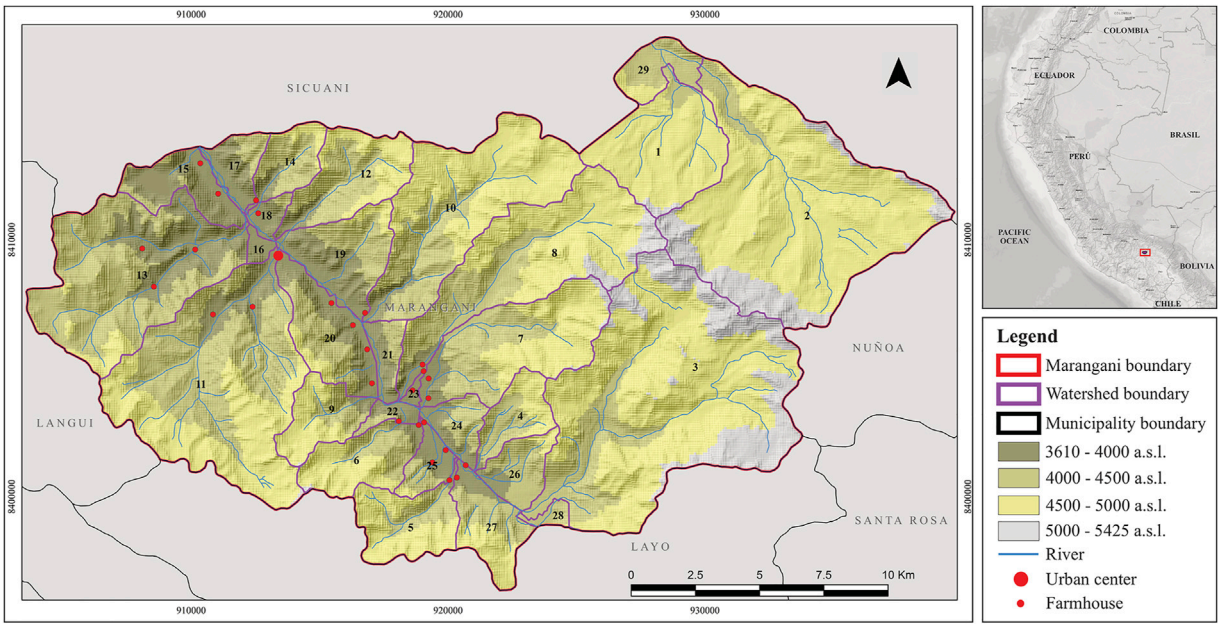

FIGURE 1 | Study area with elevation and watershed distribution (left), Peru with ESRI′ Standard map (top right). Watersheds: 1. Tañihua stream; 2. Aucara river; 3. Cantacanta river; 4. Chuabamba stream; 5. Tadiohuayco stream; 6. Llallahui stream; 7. Quiscamayo stream; 8. Quecjra river; 9. Lorocachi stream; 10. Cuyo stream; 11. Casuira river; 12. Cayco stream; 13. Comayacu stream; 14. Ccatunhuasi stream; 15. Intercuenca 1; 16. Inter-watershed 2; 17. Inter-watershed 3; 18. Inter-watershed 4; 19. Inter-watershed 5; 20. Inter-watershed 6; 21. Inter-watershed 7; 22. Inter-watershed 8; 23. Inter-watershed 9; 24. Inter-watershed 10; 25. Inter-watershed 11; 26. Inter-watershed 12; 27. Inter-watershed 13; 28. Inter-watershed 14; 29. Inter-watershed 15.

TABLE 1 | Landsat series Surface Reflectance data in each year.

Data	Acquisition year	Band	Resolution (meter)
Landsat 5 (TM)	1986	Multispectral	30
Landsat 5 (TM)	1995	Multispectral	30
Landsat 5 (TM)	2007	Multispectral	30
Landsat 8 (OLI/TIRS)	2019	Multispectral	30

Informatics, 2022). It covers an area of 440.32 km^2, comprising 29 watersheds that range from 70 to 0.5 km^2 with an average of 15 km^2. This landscape is dominated by an expansion of livestock breeding in the upper lands and farming in the fertile lowlands. It is typical of many mountain agroecosystems across the world. In that sense, Marangani has natural grasslands, sparsely vegetated areas, glaciers upstream, bofedales in the mid-stream, and agricultural land in the downstream reaches. The most important river is Vilcanota. The district has a semi-frigid rainy season with a dry winter climate (58%). Almost 47.63% of the population mainly works in the agricultural sector (National Institute of Statistics and Informatics, 2022), characterized by annual crops such as alfalfa, bean, potato, and wheat (National Institute of Statistics and Informatics, 2012). The natural pastures present in the territory make an optimal fodder for camelids, sheep, and cattle.

2.2 Spatiotemporal Analysis

2.2.1 Data Sources

This research used two types of data and information (primary and secondary information). The primary datasets are free and available on the Google Earth Engine (GEE) platform. The data acquisition was conducted during the dry season (July and August). It allowed cloud-free images. The selected years of the study were based on the period that evidenced the reduction of glaciers in Cordillera La Raya, around a decade, and in low-rainfall months. Four specific images from two Landsat Series were used (**Table 1**).

We used sort filtering functions about cloud cover for the select years in GEE. This function allows acquiring smooth continuous coverage of the scene without clouds. In our study case, the software gets the first (least cloudy) scene during the month in the dry season and nearby dates.

The primary dataset used was the atmospherically corrected Tier 1 TOA reflectance Landsat imagery. Landsat 5 was used for the first 3 years, while Landsat 8 in 2019. Operating at a spatial resolution of 30 m from both, we used 11 bands (six bands referring to the satellite, three bands made from the indices, and two topographic information bands).

The secondary data for this research were gathered from the Peru official flora cover map from 2013 (Ministry of Environment, 2015a) and its report (Ministry of Environment, 2015b). This map was used and referred together in training and testing samples with the primary data. The shape files of the study area were obtained publicly from the online server of the Ministry of Environment.

2.2.2 Land Use/Land Cover Classification

LULC units were delimited using the RF classifier within the GEE platform. We used 100 trees in the ensemble to improve the accuracy of the pixel-based supervised classification. For generating reference data (based on GEE, and Peru official

TABLE 2 | Description of LULC classes used in the study.

LULC Class	Description
Continuous urban fabric	Urban area
Agricultural areas	Andean agriculture with mainly seasonal crops
Forest plantation	Mainly *Eucalyptus* species
Natural grassland	Herbaceous vegetation consisting mainly of grasses, scrublands, and some scattered shrubby associations
Shrublands	Woody and shrubby vegetation of variable composition and structure
Sparsely vegetated areas	Low and dispersed vegetation
Glaciers	Ice masses that accumulate in the highest floors of the mountain ranges
Peat bogs and high-Andean wetlands	Hydrophilic herbaceous vegetation, permanently flooded or saturated with running water. Also known with the Spanish term bofedal
Water courses	River
Water bodies	Lagoons and lakes

flora cover map), a sampling of training and testing points—between 7 and 76—were selected of the composite images to identify the ten LULC classes (**Table 2**) for 1986, 1995, 2007, and 2019 as feature collection using the geometry tools and import. To obtain acceptable visual and statistical results, the script was repeatedly run. Also, the input images were divided into ten homogenous regions or segments (10 km × 10 km) and then classified using them. Ten GEE Code Editor scripts were used for each image to avoid confusion and assist in processing time (the links to access the script are presented in **Supplementary Table S1**). This methodology allows improving the calculation of RF in each grid and facilitates the analysis of the coverage generated. However, some biases may exist since the selection was completed manually based on the available references. The typology of the LULC classes was adopted from the Peruvian standardized nomenclature of the Corine Land Cover (CLC).

Different spectral indices were derived and added as the input parameters for training. The Normalized Difference Vegetation Index (NDVI) was used as an indicator of vegetation greenness. Then, the Modified Normalized Difference Water Index (MNDWI), a modified version of the Normalized Difference Water Index, facilitated the recognition of open water bodies by removing various noises of built-up areas, soil, and vegetation. The third index, the Normalized Difference Built-up Index (NDBI), was used to detect built-up areas.

Topographic information such as slope and elevation, derived from the SRTM (Farr et al., 2007), was also used in the classification.

Confusion matrices were used for accuracy assessment. The producer accuracy (PA), user accuracy (UA), overall accuracy (OA), and Kappa statistics (Kappa) were calculated using the previously collected samples that were scripted to be randomly segregated by 70:30 percent for training and testing, respectively. The four indexes were obtained from the confusion matrix (**Supplementary Table S2**). The UA showed the highest accuracy (100%) for glaciers during the 4 years, whereas the lowest values (50% in some grids) were for the urban class between 1986 and 1995. Forest plantations and river courses showed low accuracy (50 and 56%, respectively) in 2007 and 2019 in some grids. Similarly, PA revealed 96% for the glacier class, and 20% and 43% (in some grids) for built-up areas. Also, a similar performance can be seen in the forest plantations and the river courses classes for the years 2007 and 2019, respectively. It is due to the small area of these classes that results in rarer training and testing samples. On the contrary, the three larger extent classes (natural grasslands, sparsely vegetated areas, and wetlands) obtained values of UA and PA that averaged above 80% over the 4 years. The Kappa coefficients (0.87–0.89) were considered almost in perfect agreement. The OA indicated that 89–91% of data were correctly classified.

2.2.3 Land Use/Land Cover Change

Land-use change analyses were conducted at the municipality and watershed levels. We used the Watershed tool to delimitate watershed boundaries (Arc Map, 2022). The study calculated the LULC changes over 33 years (1986–2019) through a transition matrix obtained after using ArcGIS 10.5 (ESRI, 2019). The matrices were established for three-time periods (including 1986–1995, 1995–2007, and 2007–2019). Each transition matrix gathered the quantity of land converted from each LULC unit to any other in the study periods. Land-use changes of interest for this research were related to bofedales and glaciers as fragile ecosystems. These variations were further calculated, obtaining the intensity as the proportion of area increased and decreased at the watershed level. This index gave a relative measure of the land-use change. It was ranked in five equal intervals representing the intensity of expansion/contraction of each chosen class at the watershed level. Complementarily, the land of bofedales and glaciers remaining in each period was classified with Jenks's natural breaks. Furthermore, we performed Pearson's correlation (r) to assess the pairwise relations (land decreasing, increasing, and remaining) among the two classes for the three periods, using R (R Development Core Team, 2016).

2.3 Assessment of the Economic Value of Ecosystem Services

To estimate the ESV, we used the benefit transfer method, transferring available data from previous studies in various

TABLE 3 | Different LULC types and ESV coefficient (USD ha^{-1} yr^{-1}) adjusted by using the CPI in the Marangani district.

LULC Class	Equivalent biome	1986	1995	2007	2019
Continuous urban fabric	Urban	6,441	6,245	6,503	6,672
Agricultural areas	Cultivated areas	3,093	2,992	3,124	3,204
Forest plantations	Forest	4,928	4,778	4,976	5,105
Natural grasslands	Grass/Rangelands	6,186	5,944	6,248	6,383
Shrublands	Woodland and shrubland	5,202	4,855	5,302	5,412
Sparsely vegetated areas	Inland Un- or Sparsely Vegetated	321	307	325	333
Glaciers	Ice/Rock	4,972	4,565	5,087	5,182
Peat bogs and high-Andean wetlands	Wetlands	38,856	37,670	39,229	40,247
Water courses	Lakes/Rivers	29,688	28,624	30,015	30,770
Water bodies	Lakes/Rivers	38,112	36,358	38,632	39,548

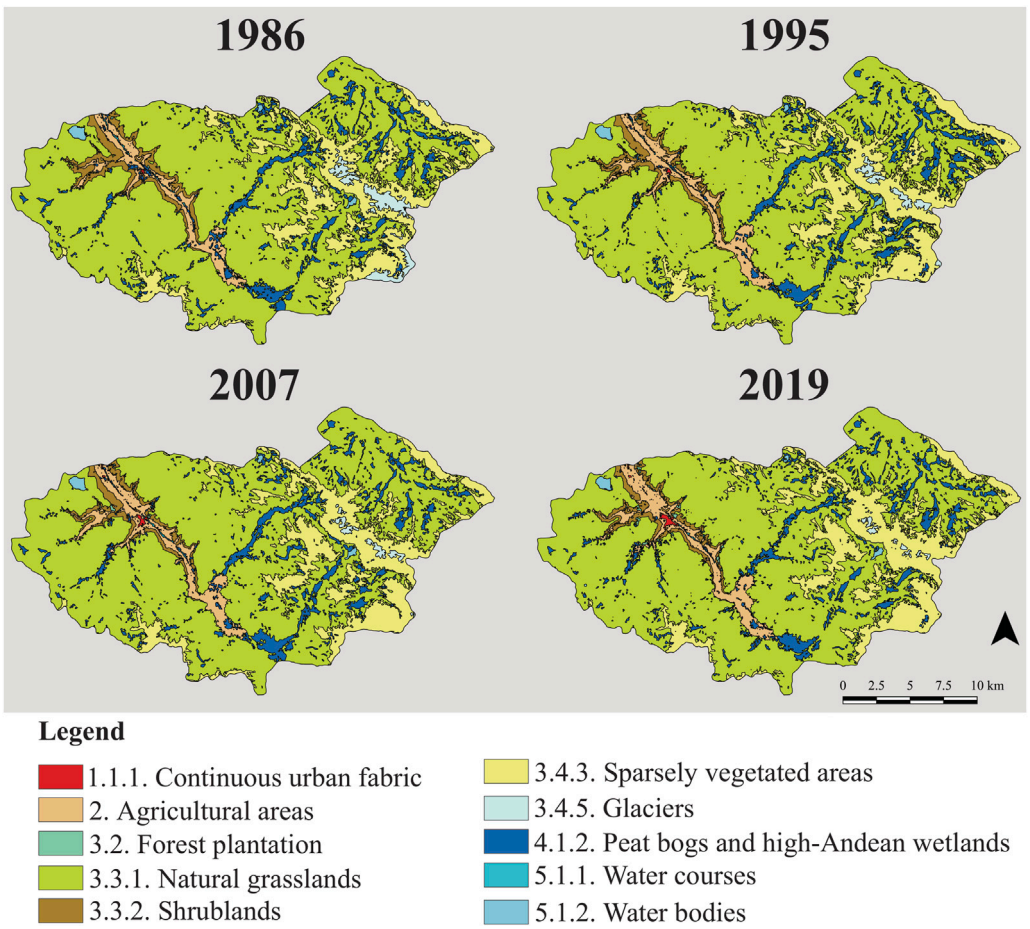

FIGURE 2 | Maps of the spatial distribution of LULC for Marangani municipality over the 4 years.

locations and from different ecosystems globally that have similitudes with the biomes of the study area. The search was carried out on the ESV database (Foundation for Sustainable Development, 2021) and published research (Costanza et al., 2014; Xie et al., 2017; de Groot et al., 2020) for 38 ecosystem services and ten biomes. After the search, only values for 23 ecosystem services were found. According to Costanza et al., (1997), the ESV coefficient (unit values in USD ha^{-1} yr^{-1}) of a given LULC was counted as all the ESV for that LULC. To achieve the total ecosystem service value of each LULC at the municipality and the watershed level, we multiply the area of each LULC type at the corresponding level by the ESV coefficient. Finally, the ESV coefficients were adjusted using the Consumer Price Index (CPI) obtained from the website of the World Bank (2022) and applying the inflation rate formula (**Table 3**).

TABLE 4 | Area of the different LULC classes for the 4 years.

	1986		1995		2007		2019	
LULC class	ha	%	ha	%	ha	%	ha	%
Continuous urban fabric	21	0.05	24	0.1	49	0.1	71	0.2
Agricultural areas	1,481	3.4	1772	4.0	1860	4.2	1851	4.2
Forest plantation	6	0.01	28	0.1	36	0.1	164	0.4
Natural grassland	29,872	67.8	29,352	66.7	30,054	68.3	30,152	68.5
Shrublands	1,402	3.2	1,145	2.6	1,013	2.3	1,069	2.4
Sparsely vegetated areas	6,691	15.2	7,451	16.9	7,033	16.0	7,155	16.2
Glaciers	897	2.0	353	0.8	246	0.6	130	0.3
Peat bogs and high-Andean wetlands	3,419	7.8	3,656	8.3	3,521	8.0	3,242	7.4
Water courses	87	0.2	72	0.2	65	0.1	41	0.1
Water bodies	157	0.4	179	0.4	154	0.3	157	0.4

3 RESULTS

3.1 Quantification of Land Cover and Land Use Changes Over Time

The spatiotemporal distribution of LULC of the Marangani district among the study years revealed some variations (**Figure 2**). The precise area of each LULC is shown in **Table 4**. Natural grasslands coincided with being the most abundant class each year, spatially dispersed covering more than 65% of the landscape. Sparsely vegetated areas delimited more than 15% of the landscape over time. This LULC is spatially associated with glaciers in the highland. The third LULC type was peat bogs and high-Andean wetlands (bofedales) with an average of 8%, mainly located in the upland depressions. Agricultural areas (>4%) were evident in the lowland valley around the main river (Vilcanota river) related to the urban center, the farmhouses, and even topography. However, shrublands mainly drew a transitional zone in the lowland that separated agriculture from the natural grassland. Last, built-up areas, forest plantations, and water surfaces enclosed less than 1% of the territory.

The details of LULC changes for 1986–1995, 1995–2007, and 2007–2019 are presented in the transition matrices (**Supplementary Tables S3–S5**). In terms of the total area, 4,217 ha (9.6%), 3,999 ha (9.1%), and 3,914 ha (9%) were transformed in each period, respectively. Two transitions (>2,900 ha) involved the deterioration and the recovery of natural grasslands and bofedales during each period. A third important transition was related to glacier retreat, being more intense during the first period (543 ha). Another significant land-use change over time (strongest during the first period, >300 ha) refers to agricultural expansion, which implicated the conversion of natural grasslands, bofedales, and shrublands. Last, the farming land abandonment represented an increase in shrublands, mainly shown during the third period (>200 ha).

3.1.1 Landscape Analysis of the Overall Trajectories of Changes

The LULC changes over time (**Table 4**) demonstrated some trajectories at the municipality level. Two classes (natural grasslands and water bodies) show low variability that indicates almost no disturbances, whereas water courses display no clear variations. Four LULC uncovers consistent patterns of increase influenced by humans at works dynamics (agriculture, urbanization, and afforestation) and glacier retreat (sparsely vegetated areas). In contrast, three classes (among them the fragile ecosystems like the bofedal and the glacier) have decreased due to the conversion into grazing and farming lands (for shrublands and bofedales) and the effects of climate change (for glaciers).

3.1.2 Watershed-Level Analysis of Changes in the Fragile Land Cover and Land Use

The intensity of glacier retreat at the watershed level is evidenced in each period (**Figure 3A**). No glacier advances are observable. During the first period, a high average decrease intensity is registered (60.65%), whereas it is moderate (average of 12.43%) for the others.

Figure 3B illustrates the intensity of land increase and decrease for bofedales in each period. The spatial distribution shows a higher tendency of land changes at the watersheds without glaciers. It may be possible because the glaciers provide a water flow that stabilizes the fluctuations (appearance balance) of the bofedales. In that sense, the watersheds with glacier areas count on permanent larger bofedales (**Supplementary Figure S1**).

At the watershed level, the relationships among the two fragile LULC changed over time (**Supplementary Table S6**). In terms of both the type of relationship and its strength, glaciers' decrease over time is negatively related to bofedales decreasing, whereas bofedal increase showed a positive correlation (for the first period) and negative during the other periods, but nonsignificant for all the relationships. Bofedal increase showed a consistent and significant negative relationship with bofedal decrease in the first period but varied from a significant positive correlation coefficient of 0.51 in the second period to a nonsignificant coefficient of 0.21 in the final period. The relationship among the areas of both classes remaining over time is significant and positive.

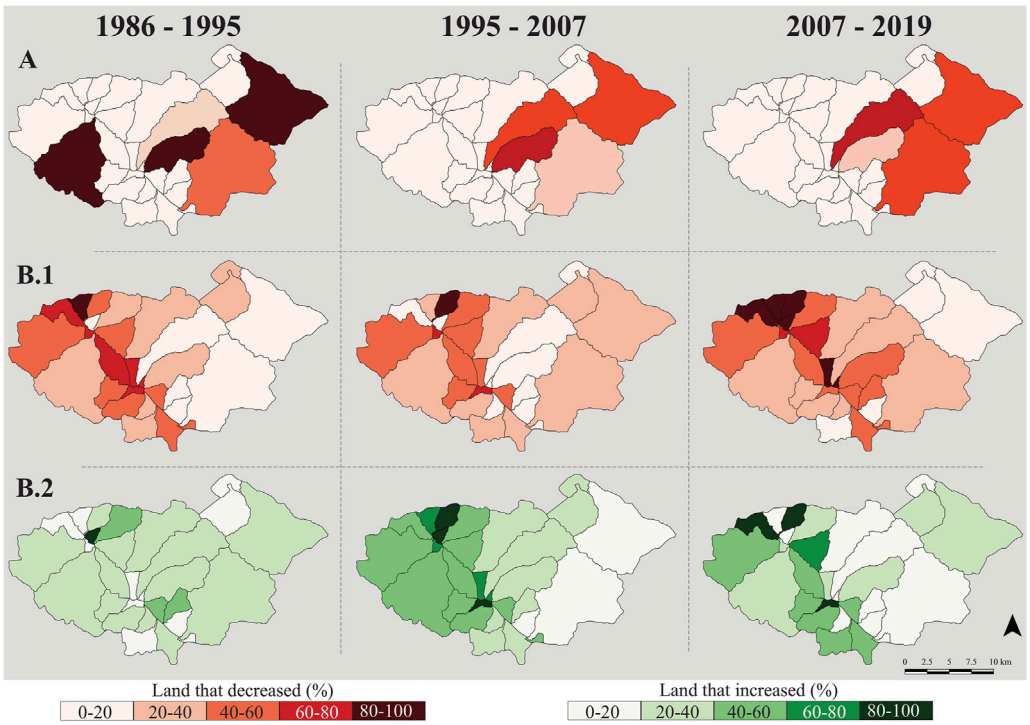

FIGURE 3 | Land decrease intensity of the glaciers **(A)** and the land decrease/increase intensity of the bofedales **(B.1,B.2)** at the watershed level in the Marangani district over the three periods.

3.2 Valuation of Ecosystem Services of the Marangani District

The search of 38 ecosystem service values for the ten study area biomes resulted in 23 ESVs found (**Supplementary Table S7**). The values (**Supplementary Table S8**) focused on provisioning (5), regulating (12), and cultural services (6) that are classified in the MEA (Millennium Ecosystem Assessment, 2005). This last group of services provides the highest total economic value (74,260.98 USD $ha^{-1}\,yr^{-1}$), mainly due to the value of recreation (57,248.23 USD $ha^{-1}\,yr^{-1}$), while regulating and provisioning afford lower values (35,356.34 and 33,124.41 USD $ha^{-1}\,yr^{-1}$), being the value of regulation of extreme events and the provision of habitat for wildlife species (9,634.75 and 18,444.80 USD $ha^{-1}\,yr^{-1}$) those who contribute most in each category. Bofedales and water surfaces are the LULCs that supply the highest ESV (~33,000 USD $ha^{-1}\,yr^{-1}$ each), mainly because of the value of the habitat for wildlife species, erosion prevention, regulation of extreme events, and recreation. However, human-related areas retain values that range between 3,211.69 and 6,687.02 USD $ha^{-1}\,yr^{-1}$ due to the provision of food production, recreation, and air quality regulation.

3.2.1 Ecosystem Service Values at the Municipality Level

The total ESV at the municipality level shifted from $\$344.85 \times 10^6$ in 1986 to $\$346.51 \times 10^6$ in 2019 (**Table 5**). Practically, there is a slightly positive change ($+\$1.66 \times 10^6$), but it is observed that without the inflation adjustment, the district is on a trajectory of losing ESV ($-\$9.67 \times 10^6$). It is mainly due to the decrease in the area of glaciers and bofedales. The bofedal is one of the main classes supplying ESV (from $\$132.85 \times 10^6$ in 1986 to $\$125.97 \times 10^6$ in 2019), although the value of glaciers is lower ($\$4.46 \times 10^6$ in 1986), and its conversion to bared areas signifies a substantial decrease of $\$3.67 \times 10^6$ in 2019. However, the highest supply of ESV corresponds to natural grasslands (attributed to its high extension), although its value is rather constant, resulting only in an increase of 1% ($+\$1.73 \times 10^6$) during the study period. Furthermore, agricultural areas and forest plantations increased the ESV from 4.58×10^6 to 5.72×10^6 and 0.03×10^6 to 0.81×10^6, respectively. These escalations are not enough to achieve a positive overall rate at the municipality level.

3.2.2 Ecosystem Service Values at the Watershed Level

The supply of ESV changed (decreased and increased) during the study period at the watershed level (**Figure 4**). The extreme changes in the economic value of the ecosystem services of the watersheds in the study area are mainly caused by considerable increase or decrease of the bofedales. For example, between 1986 and 1995, a severe ESV reduction in watersheds 16, 23, and 28 was observed. It is mainly due to the conversion of bofedales into agricultural areas. Similarly, it occurs in the comparison of the period 2007–2019. On the contrary, land abandonment facilitates the increase of bofedales between 1995 and 2007, showing better valuation. The watersheds with glaciers (numbers 2, 3, 7, and 8) did not experience a severe

TABLE 5 | ESV of each LULC at the municipality level between 1986 and 2019 and the overall trajectory of change. The values in parentheses represent the adjustment by the inflation. Top arrow for the increase and down arrow for decrease. NC = no change. Trajectories in parentheses include values from inflation adjustment.

LULC Class	ESV ($10^6$$)							Trajectory of change
	1986	1995		2007		2019		
Continuous Urban Fabric	0.14	0.15	(0.15)	0.32	(0.32)	0.46	(0.47)	↑ (↑)
Agricultural areas	4.58	5.48	(5.30)	5.75	(5.81)	5.72	(5.93)	↑ (↑)
Forest plantations	0.03	0.14	(0.13)	0.18	(0.18)	0.81	(0.84)	↑ (↑)
Natural grasslands	184.79	181.57	(174.46)	185.92	(187.79)	186.52	(192.48)	NC (↑)
Shrublands	7.29	5.96	(5.56)	5.27	(5.37)	5.56	(5.79)	↓ (NC)
Sparsely vegetated areas	2.15	2.39	(2.29)	2.25	(2.28)	2.29	(2.38)	NC (NC)
Glaciers	4.46	1.76	(1.61)	1.22	(1.25)	0.65	(0.67)	↓ (↓)
Peat bogs and high-Andean wetlands	132.85	142.06	(137.72)	136.81	(138.12)	125.97	(130.48)	↓ (↓)
Water courses	2.58	2.14	(2.06)	1.93	(1.95)	1.22	(1.26)	↓ (↓)
Water bodies	5.98	6.82	(6.51)	5.87	(5.95)	5.98	(6.21)	NC (NC)
Total	344.85	348.46	(335.80)	345.52	(349.03)	335.18	(346.51)	↓ (NC)

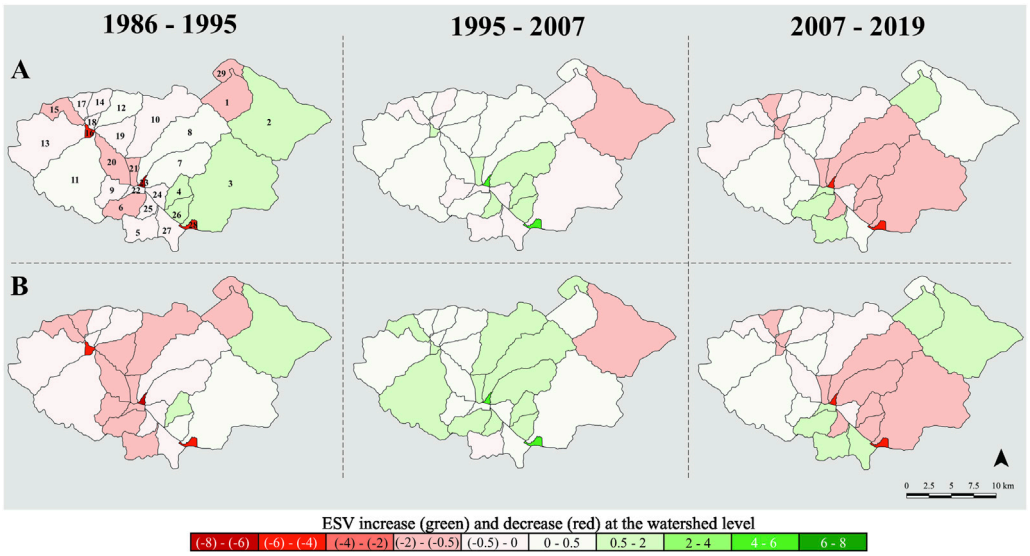

FIGURE 4 | Spatial distribution of ESV increase and decrease **(A)** and adjusted by the inflation **(B)** at the watershed level in the Marangani district over the three periods (ESV units in $10^3$$).

change in ESV. Although the glacial retreat is probed, the loss of ESV is neutralized by the considerable proportions of bofedales and high Andean grasslands. The slight variation of these biophysical structures produces a low ESV variability through the years.

4 DISCUSSION

4.1 Land Cover and Land Use Changes During More Than Three Decades has Diverse Implications on the Landscape

At the municipality level, almost all the LULCs faced variations over the study period of 33 years (**Table 4**). It should be noted that glaciers—as fragile ecosystems perturbed by climate change—had the highest change (accumulated ratio of −85.51%), which agreed with studies in the Himalayas (e.g., −23.8% and −35%, Rai et al., 2018; Shrestha et al., 2019). However, Andean glaciers seem to be under critical conditions that accelerate their disappearance (Juřicová and Fratianni, 2018; Vicente-Serrano et al., 2018). In the Marangani district, this situation reached its peak between the first period (1986–1995, ratio of −60.65%). It can be explained by the very strong ENSO warm events between 1987 and 1992 (Gergis and Fowler, 2009), which are related to the annual glacier mass balance (Wagnon et al., 2001). Consequently, the current ice loss in the study area signifies a variability of water availability on downstream socio-ecosystems that may impact agricultural irrigation of permanent crops and human-domestic use. In that sense, the cropland and the bofedales have shown a moderate increasing trend over the first period that may be driven by the increase of the population (National Institute of Statistics

and Informatics) and the water supply from glaciers, respectively, while for the second and third periods, agricultural frontier expansion showed a deceleration influenced by a decrease in the population. This decline overlaps with the displacement by domestic terrorism in the second period (Transfer Commission, 2014) and internal migration by work opportunities in the third (Bergmann et al., 2021). However, existing farmland abandonment is very low, but if this land-change dynamic continues, it can lead to risks associated with land degradation (Narendra Raj and Teiji, 2006). Furthermore, during the last two periods, the bofedales faced a reduction coexisting with a decline of the melting of glaciers, causing augmentation of natural grassland, sparsely vegetated areas, and the conversion by humans at work activities as agricultural land and forest plantation.

At the watershed level, the study observes a higher tendency of land changes in the territory without glaciers, and those with glacier areas count on permanent larger bofedales. Then, glaciers provide a water flow that stabilizes the fluctuations (appearance balance) of the bofedales. This biome is considered sensitive to changes in extreme rainfall and glacial meltwater supply (Dangles et al., 2017). The main reason is that perennial bofedales are connected to the hydrological cycle through runoff generated by melting glaciers, while temporal wetlands depend directly on precipitation (Otto et al., 2011). It suggests that the total disappearance of the glaciers in the study area would cause the main water supply contribution by snow melting and rainfall. In this case, the mountain depositional landforms—glacial rocks immersed in the biome of the sparsely vegetated area—will constitute effective water distribution and storage. This function has an operation in the short and intermediate-term (Reato et al., 2021). It may cause a predominance of temporal bofedales. This condition could have a possible variation in the benefits provided by ecosystem services in the same biome for the different compositions of species. In general, temporal bofedales (mainly species of the Poaceae family) provide food for raising animals and wildlife during the flood season, whereas perennial bofedales (mainly cushion-forming species) accumulate organic soil, forage, and water storage also in the dry season (Cooper et al., 2010; Ruthsatz, 2012). In this last service, the hydrological importance enables change in the water flow paths and discharge velocity (Otto et al., 2011). In addition, perennial wetlands provide vital habitats for wildlife and extensive grazing of camelids (Loza Herrera et al., 2015; Dangles et al., 2017).

4.2 The Economic Value of Ecosystem Services in an Environment of Glaciers Retreat Is in Decline

For the first time, the results presented here (**Table 5**) calculated the spatiotemporal changes of ESV in an environment of tropical glacier retreat. Concretely, the territory is on a trajectory of losing ESV appreciated in the scenario without inflation adjustment. This degradation is mainly due to reduction of provisioning and regulating services provided by the bofedales and the glaciers. The disappearance of these services not only has implications for a direct economic loss but also, in the case of the reduction of the flood protection provided by the glaciers, can pose the risk of dangerous glacial outburst floods on downstream communities that may lead to catastrophic economic damages (Chen et al., 2022). At the same time, the disappearance of bofedales endangers the regulation of extreme events that can increase these impacts. Likewise, the augmentation of water erosion, induced by the decline of bofedales, may affect negatively food security and natural resource management practices, principally in the poorest societies (Sartori et al., 2019), such as the study area. In the same way, the drop in water supply amplified by the reduction of both fragile ecosystems may affect livestock production, irrigated agriculture, availability and quality of water for human consumption, and generation of hydroelectricity (Carey et al., 2016), increasing the economic losses in the territory. Biophysical processes and human activities are the highest threats and causes of this situation. The ESV supplied by the human-related classes is in a crescendo, whereas the natural and semi-natural classes are losing their capital. This may result in a critical situation since the growth of provisioning services provided by agricultural development is at the expense of regulating services like water flow regulation and erosion prevention. This trajectory of ecosystem services is characteristic in mountain environments (Locatelli et al., 2017; Madrigal-Martínez and Miralles i García, 2019a).

At the watershed level, the variation of ESV is mainly influenced by the changes of bofedales into farming and grasslands. These changes harm the value of regulation services. However, the value of provisioning services like habitat for wildlife species, genetic libraries, livestock production, and raw materials increased due to expansion of pastures. In general, the economic value of these provisioning services could be underestimated by the global sources researched by Costanza et al. (2014) because the principal cattle in the study area are llamas, alpacas, and vicuñas (National Institute of Statistics and Informatics, 2012). These two last species are considered of great interest for their finest fibers worldwide and are used for luxury costumes (Vilá and Arzamendia, 2020; Zarrin et al., 2020). In the same way, the production of meat from llamas and alpacas has interesting value for their use as a principal protein source for Andean rural communities (Pérez et al., 2000); and their healthy characteristics (low in fat and cholesterol) make them attractive for local and international markets, signifying an important income for small- and medium-scale local producers (Mamani-Linares and Gallo, 2014). Moreover, llamas have smaller and simpler nanobodies beneficial for human immunology and therapeutic applications (Wesolowski et al., 2009). Furthermore, although the density of alpacas in the study area is high (123 alpacas km^{-2}), according to the levels established in other locations (Muñoz et al., 2015), biodiversity conservation is guaranteed with appropriate management practices (Alkemade et al., 2013).

In the watersheds with glacier retreat, the significant quantity of bofedales and natural grasslands controls the fluctuations of ESV. It is a consequence of the extension of grasslands that varies between 48 and 72.2% and the bofedales between 5.5 and 12%. Then, these watersheds still have an advantage from the water

flow of glaciers and supply multiple provisioning and regulating services such as water yield, habitat for wildlife species, food production, carbon sequestration, erosion control, soil fertility, and regulation of extreme events. Therefore, these high-mountain watersheds play an essential role as hotspots of ecosystem services, giving benefits and value to local communities. The identification of ES hotspots guides the prioritization of areas for conservation (Li et al., 2017). In that sense, ES hotspot maps have potential benefits that can be transmitted to stakeholders to improve management planning (Hauck et al., 2013). Also, the implication of knowing this information provides a scientific basis for making relevant decisions in a territory (Li et al., 2022). Consequently, these ES hotspot watersheds should get the priority of being strategically managed for maintaining their essential ecosystems. So, understanding the relationship between nature and people in mountain socio-ecological systems is significant for planning sustainable development strategies (Madrigal-Martínez and Miralles i García, 2019b; Payne et al., 2020), including conservation strategies at different spatial levels, such as prioritizing the small wetlands of these watersheds, according to Otto and Gibbons (2017).

4.3 Methodological Limitations of the Study

In this study, the analyses presented should be understood as using the best existing data of acceptable quality to admit robust evidence. Even so, the procedures used in processing satellite images may have a situation of some biome coverage. It is mainly related to four factors: 1) the definition of biome classes, 2) reliability of Landsat images with their limitations of the sensor used, 3) auxiliary variables in the classification, and 4) validated data and no clarity of training (Calderón-Loor et al., 2021). The selection of the training points was based on the national vegetation coverage map (Ministry of Environment, 2015b). Also, to best interpret the satellite image, the authors made an expert judgment. In that sense, subjectivity at the decision point regarding the pixel classification could cause statistical noise in the training and validation data. However, this noise in the final categorization could have a low effect on the final product (Zhu et al., 2016). In addition, the research applied the transfer method of benefits for valuation ecosystem services. Despite the benefits, it has several limitations that imply transfer errors from generalization (Schmidt et al., 2016). However, it has been taken into account that the extrapolation of the valuation is in similar geographies.

5 CONCLUSION

This research develops for the first time a study about the land-use changes and their implications on the economic value of ecosystem services under the influence of glacier retreat in a tropical mountain environment. Also, our research has provided a procedure using satellite images that obtains a robust classification as a base for the estimation of ESV, which can be applied to other areas and contexts. The research utilizes two scales of observation, the municipality and the watershed level, for 33 years. In that sense, the analysis uncovered consistent differences that define the results depending on the scale. In general, the municipality level indicates the trajectory of changes in the district, while the watershed scale shows the urgency for implementing 1) measures to moderate the severe impacts on the landscape or 2) management actions for improving the spatial conservation of ecosystems. At the municipality level, the territory suffers trade-offs mainly in the supply of regulating services, declining the total monetary value. At the watershed level, the trade-offs are more evident in the areas without glaciers, and an economic balance over time is maintained in the landscapes with glaciers.

Bofedales and glaciers are fragile ecosystems that play an essential role in supplying regulating and provisioning services benefiting the socio-ecosystem. However, these ecosystems are being impacted over time, gathering a loss of ESV. Biophysical dynamics are diminishing glaciers and, in a lesser measurement, the bofedales, while for the latter, the increase of human activity is also a threat, mostly causing the trade-off between provisioning services and regulating services such as water flow regulation and erosion prevention. It is worth noting that during the study period, the glaciers were continuously shrinking, and their spatial–temporal changes had direct implications on the increase of bare land. However, they still have positive effects on downstream ecosystems such as bofedales but negative on the total economic value due to the reduction of their capability to supply water-related services. In addition, future studies should focus on a much more exhaustive LULC classification to improve the results reached in this research. It means including perennial and temporary bofedales and open and close natural grasslands. Likewise, knowing how spatiotemporal changes affect the quality and amount of ESS in this type of environment is an important issue. Last, the relationship between the trajectories of glaciers, bofedales, and ESV needs to be researched deeply, incorporating similar scenarios to find more robust spatial–temporal patterns.

DATA AVAILABILITY STATEMENT

The original contributions presented in the study are included in the article/**Supplementary Material**; further inquiries can be directed to the corresponding author.

AUTHOR CONTRIBUTIONS

Conceptualization, SM-M and RP-C; methodology, SM-M and RP-C; software, RP-C; validation, SM-M, VB and OV; formal analysis, SM-M; investigation, SM-M; resources, SM-M; data curation, SM-M; writing—original draft preparation, SM-M and RP-C; writing—review and editing, SM-M and RP-C; visualization, SM-M; supervision, SM-M, VB; funding acquisition, VB and OV. All authors have read and agreed to the published version of the manuscript.

FUNDING

This research was funded by Instituto Nacional de Investigación en Glaciares y Ecosistemas de Montaña (INAIGEM).

SUPPLEMENTARY MATERIAL

The Supplementary Material for this article can be found online at: https://www.frontiersin.org/articles/10.3389/fenvs.2022.941887/full#supplementary-material

REFERENCES

Abson, D. J., von Wehrden, H., Baumgärtner, S., Fischer, J., Hanspach, J., Härdtle, W., et al. (2014). Ecosystem Services as a Boundary Object for Sustainability. *Ecol. Econ.* 103, 29–37. doi:10.1016/j.ecolecon.2014.04.012

Alkemade, R., Reid, R. S., van den Berg, M., de Leeuw, J., and Jeuken, M. (2013). Assessing the Impacts of Livestock Production on Biodiversity in Rangeland Ecosystems. *Proc. Natl. Acad. Sci. U.S.A.* 110, 20900–20905. doi:10.1073/PNAS.1011013108

ArcMap (2022). ArcMap 10.8 How Watershed Works. Documentation. Available at: https://desktop.arcgis.com/en/arcmap/latest/tools/spatial-analyst-toolbox/how-watershed-works.htm (Accessed February 24, 2022).

Bergmann, J., Vinke, K., Fernández Palomino, C. A., Gornott, C., Gleixner, S., Laudien, R., et al. (2021). *Assessing the Evidence: Climate Change and Migration in Peru*. Potsdam Institute for Climate Impact Research (PIK) and International Organization for Migration (IOM): Geneva.

Brandt, J. S., and Townsend, P. A. (2006). Land Use - Land Cover Conversion, Regeneration and Degradation in the High Elevation Bolivian Andes. *Landsc. Ecol.* 21, 607–623. doi:10.1007/s10980-005-4120-z

Burkhard, B., Kroll, F., Müller, F., and Windhorst, W. (2009). Landscapes' Capacities to Provide Ecosystem Services - A Concept for Land-Cover Based Assessments. *Landsc. Online* 15, 1–22. doi:10.3097/LO.200915

Calderón-Loor, M., Hadjikakou, M., and Bryan, B. A. (2021). High-resolution Wall-To-Wall Land-Cover Mapping and Land Change Assessment for Australia from 1985 to 2015. *Remote Sens. Environ.* 252, 112148. doi:10.1016/j.rse.2020.112148

Carey, M., Molden, O. C., Rasmussen, M. B., Jackson, M., Nolin, A. W., and Mark, B. G. (2016). Impacts of Glacier Recession and Declining Meltwater on Mountain Societies. *Ann. Am. Assoc. Geogr.* 107, 350–359. doi:10.1080/24694452.2016.1243039

Cauvy-Fraunié, S., and Dangles, O. (2019). A Global Synthesis of Biodiversity Responses to Glacier Retreat. *Nat. Ecol. Evol.* 3, 1675–1685. doi:10.1038/s41559-019-1042-8

Chaudhary, S., Tshering, D., Phuntsho, T., Uddin, K., Shakya, B., and Chettri, N. (2017). Impact of Land Cover Change on a Mountain Ecosystem and its Services: Case Study from the Phobjikha Valley, Bhutan. *Ecosyst. Health Sustain.* 3, 1393314. doi:10.1080/20964129.2017.1393314

Chen, H., Zhao, J., Liang, Q., Maharjan, S. B., and Joshi, S. P. (2022). Assessing the Potential Impact of Glacial Lake Outburst Floods on Individual Objects Using a High-Performance Hydrodynamic Model and Open-Source Data. *Sci. Total Environ.* 806, 151289. doi:10.1016/J.SCITOTENV.2021.151289

Cook, D., Malinauskaite, L., Davíðsdóttir, B., and Ögmundardóttir, H. (2021). Co-production Processes Underpinning the Ecosystem Services of Glaciers and Adaptive Management in the Era of Climate Change. *Ecosyst. Serv.* 50, 101342. doi:10.1016/j.ecoser.2021.101342

Cooper, D. J., Wolf, E. C., Colson, C., Vering, W., Granda, A., and Meyer, M. (2010). Alpine Peatlands of the Andes, Cajamarca, Peru. *Arct. Antarct. Alp. Res.* 42, 19–33. doi:10.1657/1938-4246-42.1.19

Costanza, R., d'Arge, R., de Groot, R., Farber, S., Grasso, M., Hannon, B., et al. (1997). The Value of the World's Ecosystem Services and Natural Capital. *nature* 387, 253–260. doi:10.1038/387253a0

Costanza, R., de Groot, R., Sutton, P., van der Ploeg, S., Anderson, S. J., Kubiszewski, I., et al. (2014). Changes in the Global Value of Ecosystem Services. *Glob. Environ. Change* 26, 152–158. doi:10.1016/J.GLOENVCHA.2014.04.002

Crossman, J., Futter, M. N., and Whitehead, P. G. (2013). The Significance of Shifts in Precipitation Patterns: Modelling the Impacts of Climate Change and Glacier Retreat on Extreme Flood Events in Denali National Park, Alaska. *PLOS ONE* 8, e74054. doi:10.1371/JOURNAL.PONE.0074054

Dang, A. N., Jackson, B. M., Benavidez, R., and Tomscha, S. A. (2021). Review of Ecosystem Service Assessments: Pathways for Policy Integration in Southeast Asia. *Ecosyst. Serv.* 49, 101266. doi:10.1016/J.ECOSER.2021.101266

Dangles, O., Rabatel, A., Kraemer, M., Zeballos, G., Soruco, A., Jacobsen, D., et al. (2017). Ecosystem Sentinels for Climate Change? Evidence of Wetland Cover Changes over the Last 30 Years in the Tropical Andes. *PLoS ONE* 12, e0175814. doi:10.1371/journal.pone.0175814

de Groot, R. S., Alkemade, R., Braat, L., Hein, L., and Willemen, L. (2010). Challenges in Integrating the Concept of Ecosystem Services and Values in Landscape Planning, Management and Decision Making. *Ecol. Complex.* 7, 260–272. doi:10.1016/j.ecocom.2009.10.006

de Groot, R., Brander, L., Solomonides, S., McVittie, A., Eppink, F., Sposato, M., et al. (2020). Ecosystem Services Valuation Database (ESVD) Update of Global Ecosystem Service Valuation Data. Available at: https://www.es-partnership.org/wp-content/uploads/2020/08/ESVD_Global-Update-FINAL-Report-June-2020.pdf (Accessed March 8, 2022).

Dussaillant, I., Berthier, E., Brun, F., Masiokas, M., Hugonnet, R., Favier, V., et al. (2019). Two Decades of Glacier Mass Loss along the Andes. *Nat. Geosci.* 12, 802–808. doi:10.1038/s41561-019-0432-5

Egarter Vigl, L., Tasser, E., Schirpke, U., and Tappeiner, U. (2017). Using Land Use/land Cover Trajectories to Uncover Ecosystem Service Patterns across the Alps. *Reg. Environ. Change* 17, 2237–2250. doi:10.1007/s10113-017-1132-6

Ektvedt, T. M., Vetaas, O. R., and Lundberg, A. (2012). Land-cover Changes during the Past 50 Years in the Semi-arid Tropical Forest Region of Northern peru. *Erdkunde* 66, 57–75. doi:10.3112/erdkunde.2012.01.05

ESRI (2019). *ArcGIS Desktop: Release 10.5*. Redlands CA: Environmental Systems Research Institute. doi:10.1209/epl/i2001-00551-4

Farr, T. G., Rosen, P. A., Caro, E., Crippen, R., Duren, R., Hensley, S., et al. (2007). The Shuttle Radar Topography Mission. *Rev. Geophys.* 45, 2004. doi:10.1029/2005RG000183

Felipe-Lucia, M. R., Comín, F. A., and Bennett, E. M. (2014). Interactions Among Ecosystem Services across Land Uses in a Floodplain Agroecosystem. *Ecol. Soc.* 19, art20. doi:10.5751/ES-06249-190120

Foundation for Sustainable Development (2021). ESVD Version 1.0. Available at: https://www.esvd.net/esvd (Accessed April 10, 2022).

Gergis, J. L., and Fowler, A. M. (2009). A History of ENSO Events since A.D. 1525: Implications for Future Climate Change. *Clim. Change* 92, 343–387. doi:10.1007/s10584-008-9476-z

Gislason, P. O., Benediktsson, J. A., and Sveinsson, J. R. (2006). Random Forests for Land Cover Classification. *Pattern Recognit. Lett.* 27, 294–300. doi:10.1016/j.patrec.2005.08.011

Groot, R. d., Fisher, B., Christie, M., Aronson, J., Braat, L., Gowdy, J., et al. (2010). Chapter 1 Integrating the Ecological and Economic Dimensions in Biodiversity and Ecosystem Service Valuation. TEEB. Available at: http://doc.teebweb.org/wp-content/uploads/Study and Reports/Reports/Ecological and Economic Foundations/TEEB Ecological and Economic Foundations report/TEEB Foundations.pdf (Accessed August 22, 2017).

Hauck, J., Görg, C., Varjopuro, R., Ratamäki, O., Maes, J., Wittmer, H., et al. (2013). "Maps Have an Air of Authority": Potential Benefits and Challenges of Ecosystem Service Maps at Different Levels of Decision Making. *Ecosyst. Serv.* 4, 25–32. doi:10.1016/j.ecoser.2012.11.003

Hidrandina (1989). *Inventario de Glaciares del Perú*. 2da Parte. Huaraz: CONCYTEC.

Hock, R., Rasul, G., Adler, C., Cáceres, B., Gruber, S., Hirabayashi, Y., et al. (2019). "High Mountain Areas," in *The Ocean and Cryosphere in a Changing Climate*. Editor H. O. Pörtner (Cambridge: Cambridge University Press), 131–202. doi:10.1017/9781009157964.004

Hugonnet, R., McNabb, R., Berthier, E., Menounos, B., Nuth, C., Girod, L., et al. (2021). Accelerated Global Glacier Mass Loss in the Early Twenty-First Century. *Nature* 592, 726–731. doi:10.1038/s41586-021-03436-z

INAIGEM (2018). *Inventario nacional de glaciares. Las cordilleras glaciares del Perú*. Huaraz: Insituto Nacional de Investigación en Glaciares y Ecosistemas de Montaña Huaraz.

Jiménez-Olivencia, Y., Ibáñez-Jiménez, Á., Porcel-Rodríguez, L., and Zimmerer, K. (2021). Land Use Change Dynamics in Euro-Mediterranean Mountain Regions: Driving Forces and Consequences for the Landscape. *Land Use Policy* 109, 105721. doi:10.1016/J.LANDUSEPOL.2021.105721

Juřicová, A., and Fratianni, S. (2018). Climate Change and its Relation to the Fluctuation in Glacier Mass Balance in the Cordillera Blanca, Peru: A Review. *Acta Univ. Carol. Geogr.* 53, 106–118. doi:10.14712/23361980.2018.10

Koschke, L., Fürst, C., Frank, S., and Makeschin, F. (2012). A Multi-Criteria Approach for an Integrated Land-Cover-Based Assessment of Ecosystem Services Provision to Support Landscape Planning. *Ecol. Indic.* 21, 54–66. doi:10.1016/j.ecolind.2011.12.010

Kuemmerle, T., Levers, C., Erb, K., Estel, S., Jepsen, M. R., Müller, D., et al. (2016). Hotspots of Land Use Change in Europe. *Environ. Res. Lett.* 11, 064020. doi:10.1088/1748-9326/11/6/064020

Lambin, E. F., Geist, H. J., and Lepers, E. (2003). Dynamics of Land-Use and Land-Cover Change in Tropical Regions. *Annu. Rev. Environ. Resour.* 28, 205–241. doi:10.1146/annurev.energy.28.050302.105459

Li, Y., Zhang, L., Yan, J., Wang, P., Hu, N., Cheng, W., et al. (2017). Mapping the Hotspots and Coldspots of Ecosystem Services in Conservation Priority Setting. *J. Geogr. Sci.* 27, 681–696. doi:10.1007/s11442-017-1400-x

Li, G., Chen, W., Zhang, X., Yang, Z., Bi, P., and Wang, Z. (2022). Ecosystem Service Values in the Dongting Lake Eco-Economic Zone and the Synergistic Impact of its Driving Factors. *Int. J. Environ. Res. Public Health* 19, 3121. doi:10.3390/ijerph19053121

Ling, M. A., King, S., Mapendembe, A., and Brown, C. (2018). A Review of Ecosystem Service Valuation Progress and Approaches by the Member States of the European Union. Cambridge, UK. Available at: www.unep-wcmc.org (Accessed April 8, 2022).

Locatelli, B., Lavorel, S., Sloan, S., Tappeiner, U., and Geneletti, D. (2017). Characteristic Trajectories of Ecosystem Services in Mountains. *Front. Ecol. Environ.* 15, 150–159. doi:10.1002/fee.1470

Loza Herrera, S., Meneses, R. I., and Anthelme, F. (2015). Comunidades vegetales de los bofedales de la Cordillera Real (Bolivia) bajo el calentamiento global. *Ecol. Boliv.* 50, 39–56.

Lu, D., Mausel, P., Brondízio, E., and Moran, E. (2004). Change Detection Techniques. *Int. J. Remote Sens.* 25, 2365–2401. doi:10.1080/0143116031000139863

Luck, G. W., Chan, K. M., and Klien, C. J. (2012). Identifying Spatial Priorities for Protecting Ecosystem Services. *F1000Res* 1, 17. doi:10.12688/f1000research.1-17.v1

Madrigal-Martínez, S., and Miralles i García, J. L. (2019a). Land-change Dynamics and Ecosystem Service Trends across the Central High-Andean Puna. *Sci. Rep.* 9, 9688. doi:10.1038/s41598-019-46205-9

Madrigal-Martínez, S., and Miralles i García, J. L. (2019b). Understanding Land Use Changes in the Central High-Andean Moist Puna. *WIT Trans. Ecol. Environ.* 238, 175–186. doi:10.2495/SC190161

Madrigal-Martínez, S., and Miralles i García, J. L. (2020). Assessment Method and Scale of Observation Influence Ecosystem Service Bundles. *Land* 9, 392. doi:10.3390/land9100392

Mamani-Linares, L. W., and Gallo, C. B. (2014). Meat Quality, Proximate Composition and Muscle Fatty Acid Profile of Young Llamas (*Lama Glama*) Supplemented with Hay or Concentrate during the Dry Season. *Meat Sci.* 96, 394–399. doi:10.1016/J.MEATSCI.2013.07.028

Mark, B. G., and Mckenzie, J. M. (2007). Tracing Increasing Tropical Andean Glacier Melt with Stable Isotopes in Water. *Environ. Sci. Technol.* 41, 6955–6960. doi:10.1021/ES071099D

Mark, B. G., McKenzie, J. M., and Gómez, J. (2009). Hydrochemical evaluation of changing glacier meltwater contribution to stream discharge: Callejon de Huaylas, Peru/Evaluation hydrochimique de la contribution évolutive de la fonte glaciaire à l'écoulement fluvial: Callejon de Huaylas, Pérou. *Hydrological Sciences Journal* 50 (6), 987. doi:10.1623/HYSJ.2005.50.6.975

Marzeion, B., Cogley, J. G., Richter, K., and Parkes, D. (2014). Attribution of Global Glacier Mass Loss to Anthropogenic and Natural Causes. *Science* 345, 919–921. doi:10.1126/SCIENCE.1254702

Millennium Ecosystem Assessment (2005). Ecosystems and Human Well-Being: Synthesis. Available at: https://www.millenniumassessment.org/en/Synthesis.html (Accessed November 21, 2019).

Milner, A. M., Khamis, K., Battin, T. J., Brittain, J. E., Barrand, N. E., Füreder, L., et al. (2017). Glacier Shrinkage Driving Global Changes in Downstream Systems. *Proc. Natl. Acad. Sci. U.S.A.* 114, 9770–9778. doi:10.1073/PNAS.1619807114

Ministry of Environment (2015a). Mapa nacional de cobertura vegetal. *Directorate-General for the Evaluation, Valuation and Financing of Natural Heritage and the Directorate-General for Territorial Planning*. Available at: https://geoservidor.minam.gob.pe/recursos/intercambio-de-datos/ (Accessed March 17, 2022).

Ministry of Environment (2015b). *Mapa nacional de cobertura vegetal. Memoria descriptiva*. Lima, Peru. Available at: http://www.minam.gob.pe/patrimonio-natural/wp-content/uploads/sites/6/2013/10/MAPA-NACIONAL-DE-COBERTURA-VEGETAL-FINAL.compressed.pdf (Accessed November 17, 2018).

Msofe, N., Sheng, L., and Lyimo, J. (2019). Land Use Change Trends and Their Driving Forces in the Kilombero Valley Floodplain, Southeastern Tanzania. *Sustainability* 11, 505. doi:10.3390/su11020505

Muñoz, M. A., Faz, A., Acosta, J. A., Martínez-Martínez, S., and Zornoza, R. (2015). Effect of South American Grazing Camelids on Soil Fertility and Vegetation at the Bolivian Andean Grasslands. *Agric. Ecosyst. Environ.* 207, 203–210. doi:10.1016/J.AGEE.2015.04.005

Narendra Raj, K., and Teiji, W. (2006). Abandonment of Agricultural Land and its Consequences. *Mt. Res. Dev.* 26, 32–40. doi:10.1659/0276-4741(2006)026[0032:AOALAI]2.0.CO;2

National Institute of Statistics and Informatics (2012). IV Censo Nacional Agropecuario. Available at: http://censos.inei.gob.pe/Cenagro/redatam/ (Accessed April 13, 2022).

National Institute of Statistics and Informatics (2022). National Institute of Statistics and Informatics National Census. Available at: https://www.inei.gob.pe/estadisticas/censos/ (Accessed April 13, 2022).

Otto, M., and Gibbons, R. E. (2017). Potential Effects of Projected Decrease in Annual Rainfall on Spatial Distribution of High Andean Wetlands in Southern Peru. *Wetlands* 37, 647–659. doi:10.1007/s13157-017-0896-2

Otto, M., Scherer, D., and Richters, J. (2011). Hydrological Differentiation and Spatial Distribution of High Altitude Wetlands in a Semi-arid Andean Region Derived from Satellite Data. *Hydrol. Earth Syst. Sci.* 15, 1713–1727. doi:10.5194/hess-15-1713-2011

Payne, D., Snethlage, M., Geschke, J., Spehn, E. M., and Fischer, M. (2020). Nature and People in the Andes, East African Mountains, European Alps, and Hindu Kush Himalaya: Current Research and Future Directions. *Mt. Res. Dev.* 40, A1–A14. doi:10.1659/MRD-JOURNAL-D-19-00075.1

Pérez, P., Maino, M., Guzmán, R., Vaquero, A., Köbrich, C., and Pokniak, J. (2000). Carcass Characteristics of Llamas (*Lama Glama*) Reared in Central Chile. *Small Ruminant Res.* 37, 93–97. doi:10.1016/S0921-4488(99)00127-3

Polk, M. H., Young, K. R., Baraer, M., Mark, B. G., McKenzie, J. M., Bury, J., et al. (2017). Exploring Hydrologic Connections between Tropical Mountain Wetlands and Glacier Recession in Peru's Cordillera Blanca. *Appl. Geogr.* 78, 94–103. doi:10.1016/J.APGEOG.2016.11.004

Quintero-Gallego, M. E., Quintero-Angel, M., and Vila-Ortega, J. J. (2018). Exploring Land Use/land Cover Change and Drivers in Andean Mountains in Colombia: A Case in Rural Quindío. *Sci. Total Environ.* 634, 1288–1299. doi:10.1016/j.scitotenv.2018.03.359

R Development Core Team (2016). *R: A Language and Environment for Statistical Computing*, 1. Vienna: R Foundation for Statistical Computing, 409. doi:10.1007/978-3-540-74686-7

Rai, R., Zhang, Y., Paudel, B., Acharya, B., and Basnet, L. (2018). Land Use and Land Cover Dynamics and Assessing the Ecosystem Service Values in the Trans-boundary Gandaki River Basin, Central Himalayas. *Sustainability* 10, 3052. doi:10.3390/su10093052

Rasul, G., and Molden, D. (2019). The Global Social and Economic Consequences of Mountain Cryospheric Change. *Front. Environ. Sci.* 7, 91. doi:10.3389/FENVS.2019.00091/BIBTEX

Reato, A., Silvina Carol, E., Cottescu, A., and Alfredo Martínez, O. (2021). Hydrological Significance of Rock Glaciers and Other Periglacial Landforms as Sustenance of Wet Meadows in the Patagonian Andes. *J. S. Am. Earth Sci.* 111, 103471. doi:10.1016/j.jsames.2021.103471

Ruthsatz, B. (2012). Vegetación y ecología de los bofedales altoandinos de Bolivia. *Phytocoenologia* 42, 133–179. doi:10.1127/0340-269X/2012/0042-0535

Sartori, M., Philippidis, G., Ferrari, E., Borrelli, P., Lugato, E., Montanarella, L., et al. (2019). A Linkage between the Biophysical and the Economic: Assessing

the Global Market Impacts of Soil Erosion. *Land Use Policy* 86, 299–312. doi:10.1016/J.LANDUSEPOL.2019.05.014

Schägner, J. P., Brander, L., Maes, J., and Hartje, V. (2013). Mapping Ecosystem Services' Values: Current Practice and Future Prospects. *Ecosyst. Serv.* 4, 33–46. doi:10.1016/J.ECOSER.2013.02.003

Schmidt, S., Manceur, A. M., and Seppelt, R. (2016). Uncertainty of Monetary Valued Ecosystem Services - Value Transfer Functions for Global Mapping. *PLOS ONE* 11, e0148524. doi:10.1371/JOURNAL.PONE.0148524

Scholes, R., Reyers, B., Biggs, R., Spierenburg, M., and Duriappah, A. (2013). Multi-scale and Cross-Scale Assessments of Social-Ecological Systems and Their Ecosystem Services. *Curr. Opin. Environ. Sustain.* 5, 16–25. doi:10.1016/j.cosust.2013.01.004

Selivanov, E., and Hlaváčková, P. (2021). Methods for Monetary Valuation of Ecosystem Services: A Scoping Review. *J. For. Sci.* 67 (2021), 499–511. doi:10.17221/96/2021-JFS

Shrestha, B., Ye, Q., and Khadka, N. (2019). Assessment of Ecosystem Services Value Based on Land Use and Land Cover Changes in the Transboundary Karnali River Basin, Central Himalayas. *Sustainability* 11, 3183. doi:10.3390/su11113183

Tang, X.-l., Lv, X., and He, Y. (2013). Features of Climate Change and Their Effects on Glacier Snow Melting in Xinjiang, China. *Comptes Rendus Geosci.* 345, 93–100. doi:10.1016/J.CRTE.2013.01.005

Transfer Commission (2014). *Hatun Willakuy: Abbreviated Version of the Final Report of the Truth and Reconciliation Commission*. Joint collaboration of the Center for Civil and Human Rights of the University of Notre Dame, the Instituto de Democracia y Derechos Humanos de la Pontificia Universidad Católica del Perú, and the International Center for Transitional Justice. Lima.

Veettil, B. K., and Kamp, U. (2019). Global Disappearance of Tropical Mountain Glaciers: Observations, Causes, and Challenges. *Geosciences* 9, 196. doi:10.3390/GEOSCIENCES9050196

Vicente-Serrano, S. M., López-Moreno, J. I., Correa, K., Avalos, G., Bazo, J., Azorin-Molina, C., et al. (2018). Recent Changes in Monthly Surface Air Temperature over Peru, 1964-2014. *Int. J. Climatol.* 38, 283–306. doi:10.1002/joc.5176

Vilá, B., and Arzamendia, Y. (2020). South American Camelids: Their Values and Contributions to People. *Sustain Sci.* 17, 707–724. doi:10.1007/S11625-020-00874-Y/TABLES/5

Wagnon, P., Ribstein, P., Francou, B., and Sicart, J. E. (2001). Anomalous Heat and Mass Budget of Glaciar Zongo, Bolivia, during the 1997/98 El Niño Year. *J. Glaciol.* 47, 21–28. doi:10.3189/172756501781832593

Wesolowski, J., Alzogaray, V., Reyelt, J., Unger, M., Juarez, K., Urrutia, M., et al. (2009). Single Domain Antibodies: Promising Experimental and Therapeutic Tools in Infection and Immunity. *Med. Microbiol. Immunol.* 198, 157–174. doi:10.1007/S00430-009-0116-7

World Bank (2022). Inflación, Precios Al Consumidor (% Anual). Data. Available at: https://datos.bancomundial.org/indicator/FP.CPI.TOTL.ZG (Accessed March 9, 2022).

Xie, G., Zhang, C., Zhen, L., and Zhang, L. (2017). Dynamic Changes in the Value of China's Ecosystem Services. *Ecosyst. Serv.* 26, 146–154. doi:10.1016/J.ECOSER.2017.06.010

Yin, J., Yin, Z., Zhong, H., Xu, S., Hu, X., Wang, J., et al. (2011). Monitoring Urban Expansion and Land Use/land Cover Changes of Shanghai Metropolitan Area during the Transitional Economy (1979-2009) in China. *Environ. Monit. Assess.* 177, 609–621. doi:10.1007/s10661-010-1660-8

Zarrin, M., Riveros, J. L., Ahmadpour, A., de Almeida, A. M., Konuspayeva, G., Vargas-Bello-Pérez, E., et al. (2020). Camelids: New Players in the International Animal Production Context. *Trop. Anim. Health Prod.* 52, 903–913. doi:10.1007/S11250-019-02197-2

Zemp, M., Frey, H., Gärtner-Roer, I., Nussbaumer, S. U., Hoelzle, M., Paul, F., et al. (2015). Historically Unprecedented Global Glacier Decline in the Early 21st Century. *J. Glaciol.* 61, 745–762. doi:10.3189/2015JOG15J017

Zhang, Y., Gao, T., Kang, S., Shangguan, D., and Luo, X. (2021). Albedo Reduction as an Important Driver for Glacier Melting in Tibetan Plateau and its Surrounding Areas. *Earth-Science Rev.* 220, 103735. doi:10.1016/J.EARSCIREV.2021.103735

Zhu, Z., Gallant, A. L., Woodcock, C. E., Jin, S., Yangl, L., Auch, R. F., et al. (2016). Optimizing Selection of Training and Auxiliary Data for Operational Land Cover Classification for the LCMAP Initiative. *ISPRS J. Photogrammetry Remote Sens.* 122, 206–221. doi:10.1016/j.isprsjprs.2016.11.004

Conflict of Interest: The authors declare that the research was conducted in the absence of any commercial or financial relationships that could be construed as a potential conflict of interest.

Publisher's Note: All claims expressed in this article are solely those of the authors and do not necessarily represent those of their affiliated organizations, or those of the publisher, the editors, and the reviewers. Any product that may be evaluated in this article, or claim that may be made by its manufacturer, is not guaranteed or endorsed by the publisher.

frontiers | Frontiers in Environmental Science

ORIGINAL RESEARCH
published: 15 July 2022
doi: 10.3389/fenvs.2022.935713

Spatiotemporal Variations of Ecosystem Service Indicators and the Driving Factors Under Climate Change in the Qinghai–Tibet Highway Corridor

Siqi Yang[1,2], *Gaoru Zhu*[1]*, *Lixiao Zhang*[2], *Honglei Xu*[1] and *Jinxiang Cheng*[1]

[1]Transport Planning and Research Institute, Ministry of Transport, Beijing, China, [2]State Key Joint Laboratory of Environmental Simulation and Pollution Control, School of Environment, Beijing Normal University, Beijing, China

In recent decades, the influence of climate change and human activities on the ecosystem services (ES) in the Qinghai–Tibet Plateau (QTP) has been extensively investigated. However, few studies focus on linear traffic corridor area, which is heavily affected by human activities. Taking the Golmud–Lhasa national highway corridor as a case, this study investigated the land-use and land-cover change (LUCC) and spatiotemporal variations of ES indicators using ecosystem indices of fractional vegetation cover (FVC), leaf area index (LAI), evapotranspiration (ET), and net primary productivity (NPP) from 2000 to 2020. The results indicated that LUCC was faster in the last decade, mostly characterized by the conversion from grassland to unused land. In buffer within 3000 m, the proportions of productive areas represented the increased trends with distance. In terms of ES variations, the improved areas outweighed the degraded areas in terms of FVC, LAI, and NPP from 2000 to 2020, mostly positioned in the Qinghai Province. In addition, FVC, LAI, and NPP peaked at approximately 6000 m over time. With regard to influencing factors, precipitation (20.54%) and temperature (14.19%) both positively influenced the spatiotemporal variation of FVC. Nearly 60% of the area exhibited an increased NPP over time, especially in the Qinghai Province, which could be attributed to the temperature increase over the last two decades. In addition, the distance effects of climatic factors on ES indicators exhibited that the coincident effects almost showed an opposite trend, while the reverse effects showed a similar trend. The findings of this study could provide a reference for the ecological recovery of traffic corridors in alpine fragile areas.

Keywords: ecosystem service indicators, buffer distance, climate change, traffic corridor, Qinghai-Tibet Plateau

OPEN ACCESS

Edited by:
Fan Zhang,
Institute of Geographic Sciences and Natural Resources Research (CAS), China

Reviewed by:
Wei Liu,
Shandong Normal University, China
Gui Jin,
China University of Geosciences, China

***Correspondence:**
Gaoru Zhu
zhugr@tpri.org.cn

Specialty section:
This article was submitted to Land-Use Dynamics, a section of the journal Frontiers in Environmental Science

Received: *04 May 2022*
Accepted: *01 June 2022*
Published: *15 July 2022*

Citation:
Yang S, Zhu G, Zhang L, Xu H and Cheng J (2022) Spatiotemporal Variations of Ecosystem Service Indicators and the Driving Factors Under Climate Change in the Qinghai–Tibet Highway Corridor. Front. Environ. Sci. 10:935713. doi: 10.3389/fenvs.2022.935713

1 INTRODUCTION

Human activities have significantly influenced the ecological environment and undermined the delivery of ecosystem services (ES), which further impacts human well-being and sustainable development (Tilman and Lehman, 2001; Millennium Ecosystem Assessment (MA), 2005; Yang et al., 2020). Traffic transportation is one of the major human activities, which greatly influence the ecosystem integrity, vegetation dynamics, animal activities, biodiversity maintenance, and ES (Forman, 2000; Laurance et al., 2014; Ibisch et al., 2016). Growing evidences showed that the traffic corridors cross various ecosystem types, resulting in land-use and land-cover change (LUCC), habitat degradation, and landscape fragmentation (Freitas et al., 2010; Liu et al., 2016; Fischer et al.,

2021). Compared with LUCC and landscape pattern change, ES changes are more important and helpful for ecological management (Liu et al., 2019). Under the influences of climate change and human activities, the vegetation and soil-related ecosystem indices can be the ES indicators as they are connected to energy exchange, hydrological cycle, and biogeochemical cycle (Sitch et al., 2003; Perrings et al., 2011; Sun et al., 2017). In addition, the ecosystem indices could reflect the yearly variation trends, which release the restriction of periodic land-use changes.

Over the last decades, remotely sensed data have become the most important data source for monitoring ecosystem dynamics at large scales and can be used to evaluate multiple ES (Zhang et al., 2011; Ying Liu et al., 2018). Previous studies mainly adopted indicators, such as normalized difference vegetation index (NDVI), fractional vegetation cover (FVC), and leaf area index (LAI), to describe the vegetation characteristics (Wu et al., 2014; Querin et al., 2016). On the contrary, other critical indices of ecosystem function, such as evapotranspiration (ET) and net primary productivity (NPP), are rarely considered in combination. ET is a dominant part of hydrological cycling, which reflects on the status of water use, and is tightly coupled with NPP at multiple scales (Chapin et al., 2002; Waring and Running, 2010). NPP plays an important role in carbon cycling and reflects on the quality of the terrestrial ecosystem (Field et al., 1998; Zhu et al., 2007). In practice, FVC and NPP are regarded as the indicators of carbon sequestration services as they represent the vegetation dynamics and productivity (Sha et al., 2020; Mu et al., 2021); in contrast, LAI and ET can be used as indicators of water provision service as they affect the hydraulic processes of ET, infiltration, aquifer recharge, and streamflow (Taugourdeau et al., 2014; Chang et al., 2017). As aforementioned, FVC, LAI, ET, and NPP are the key indicators in linking ecosystem functioning and climate feedbacks. Therefore, the use of remote sensing data could be an effective method for analyzing ES using multiple ecosystem indices.

The Qinghai–Tibet Plateau (QTP), known as "the Third Pole of the World" and "the Asian Water Tower," is a global hotspot for biodiversity and alpine ecological fragile area (Favre et al., 2015). The geographical conditions of the QTP are complex, and the ecological environment is extremely fragile (Saito et al., 2009) and thus sparsely populated. The G109, G219, and G318 national highways are the main traffic routes accessing to Lhasa (the capital of Tibet), which has significantly promoted local socioeconomic development. Established studies focused on the effects of traffic activities on the landscape pattern, vegetation cover, and soil heavy metal contents in the QTP (Ding et al., 2006; Hua Zhang et al., 2015; Song et al., 2018); however, less attention has been paid to ES changes. Under the dual impacts of climate change and human activities, the vegetation and ecosystem in linear traffic corridors have significantly changed, which poses great threats to regional ecological security (Zhang et al., 2019). How to evaluate the changes in the ecosystem pattern and ES of traffic corridors and identify the influence mechanisms in the alpine fragile region has become a vital issue to be solved.

At present, the long-term ES variation trends in human-induced linear traffic area are still inadequate. Therefore, the objectives of this study were 1) to describe the land-use dynamic characteristics in corridor areas, 2) to analyze the spatiotemporal trends of ES indicators and distance differences during the 2000–2020 period, and 3) to show the effects of LUCC and the climatic factors on ES indicator variations. This research could provide the theoretical guidance for the coordinated development of transportation and ecological environment in ecologically vulnerable areas.

2 MATERIALS AND METHODS

2.1 Study Area

The Qinghai–Tibet Highway (National Highway 109) opened to traffic in 1954; at that time, it was a gravel road. It was improved into an asphalt road in 1985 and then fully upgraded in 2010. The available traffic volume data started in 2003, with the average daily equivalent of 3904 in 2003, which then increased to 9390 in 2020. The Golmud–Lhasa highway section is the most critical section of National Highway 109. The total length of the Golmud–Lhasa highway corridor (GLHC) is 1131 km, covering 10-km buffer zones on each side of the highway; thus, the total area is 22270 km^2 and the elevation range is 2755–6210 m (**Figure 1A**, 29.55–36.49°N, 90.43–95.03°E). There are various ecosystem types distributed in the GLHC, including shrubland, grassland, steppe, and meadow. The regional climate of QTP is complex, including tropical humid, temperate semi-humid plateau monsoon, and cold temperate semi-arid plateau climates; therefore, the climatic condition of the study area is diverse. The precipitation in QTP is affected by the climate and mountains, with significant spatial differences (Renhe Zhang et al., 2015). Furthermore, the temperature in QTP is negatively correlated with latitude and altitude, the diurnal temperature range is wide, and the interannual variation is narrow (Yang et al., 2021). Based on the traffic volume monitoring and policy intervention of the Grain for Green Project (GGP), there are more human activities after 2000; thus, we selected the time intervals of 2000, 2010, and 2020 to achieve our objectives. According to the data preprocessing results, the annual average precipitation in the 2000–2020 period was 33.6–539.1 mm, decreasing from southwest to northeast. Moreover, in the 2000–2020 period, the annual average temperature was −16.7–8.5°C, decreasing from both ends to the middle. In addition, the precipitation and temperature trends in recent decades showed obvious spatial characteristics (**Figure 1B**).

2.2 Data Preparation

The prepared dataset in this study included the LUCC map, road map, remote sensing products of vegetation and ecosystem indices, and climate data. We listed the detailed information in **Table 1**.

GlobeLand30 is a global land-use dataset with medium resolution. In this study, we selected seven land types from Google Earth Engine, which included cropland, forest,

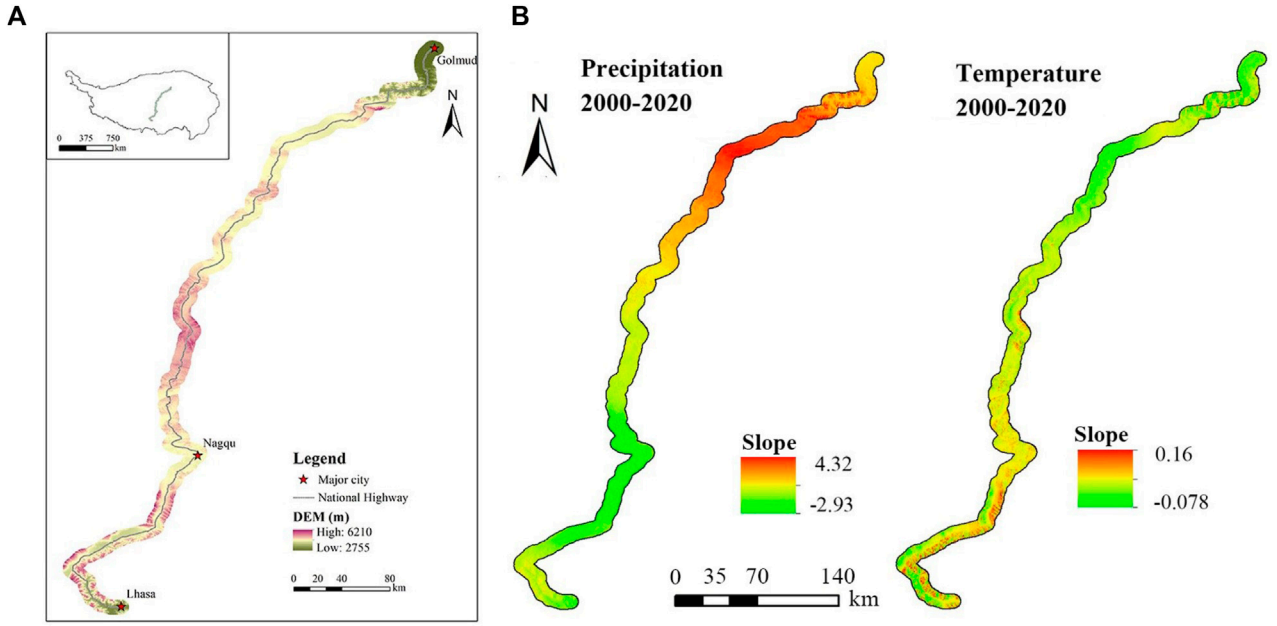

FIGURE 1 | Location of the Golmud—Lhasa national highway corridor **(A)** and climate change from 2000 to 2020 (**(B)**, the slope was calculated using the Theil—Sen estimator).

TABLE 1 | Data introduction and sources.

Variable	Source	Period	Resolution	Website
LUCC map	GlobeLand30	2000/2010/2020	30 m	www.globallandcover.com
Road map	Navigation map	2020	—	www.navinfo.com
NDVI	MOD13Q1 v006	2000–2020	250 m	https://lpdaac.usgs.gov/
LAI	MOD15A2H v006	2000–2020	500 m	https://lpdaac.usgs.gov/
ET	MOD16A2 v006	2001–2020	500 m	https://lpdaac.usgs.gov/
NPP	MOD17A3HGF v006	2001–2020	500 m	https://lpdaac.usgs.gov/
Precipitation	CRU and WorldClim	2000–2020	1 km	http://poles.tpdc.ac.cn/
Temperature	CRU and WorldClim	2000–2020	1 km	http://poles.tpdc.ac.cn/

shrubland, grassland, water body, construction land, and unused land. The road data only included the national highway, considering the long-term existence and more human activities than in railway and expressway. FVC corresponds to the fraction of ground covered by green vegetation. It describes the vegetation proportion by scaling NDVI according to NDVI maximum and NDVI minimum (**Eq. 1**).

$$\frac{NDVI - NDVI_{min}}{NDVI_{max} - NDVI_{min}} \quad (1)$$

LAI is an indicator of vegetation greenness, and the satellite-derived value corresponds to the total green LAI of all the canopy layers; thus, it can quantify the thickness of the vegetation cover. ET is a key process indicator of terrestrial ecosystems and also a proxy for vegetation condition monitoring. NPP is an indicator of ecosystem productivity, which is equal to the difference between gross primary productivity and respiration. All the ES indicator data were used on a yearly scale.

In this study, the yearly NDVI and LAI datasets were aggregated by using the maximum-value composite method, which could reduce the effects of atmospheric interference and cloud issues on values (Van Leeuwen et al., 1999), whereas ET and NPP were aggregated by sum calculation. Considering data availability, FVC and LAI were derived from 2000 to 2020, whereas ET and NPP were derived from 2001 to 2020. These datasets were resampled at 500 m × 500 m according to the resolution of most remote sensing indices and the distance intervals.

2.3 Statistical Analysis

2.3.1 Land-Use and Land-Cover Change Analysis

To describe land-use change, we first compared the areas of each land-use type in 3 years and calculated the change rate over time. Then, we used the land-use transfer matrix method to reflect the main area transitions between land-use types in two periods. To distinctly show the transferred pairs and magnitude, a chord

graph was applied. In addition to the whole variation, we employed buffer analysis to calculate the variation trend of the area proportion of each land-use type with the gradient buffer distances of 500–10,000 m in different years.

2.3.2 Spatiotemporal Trend Analysis

The interannual trends of FVC, LAI, ET, and NPP from 2000 to 2020 were determined through the nonparametric Mann–Kendall (MK) statistical test. The MK test is a rank-based method that is useful for detecting nonlinear trends (Kendall, 1975), and it has been widely applied to detect the trends of hydrological and meteorological variables in time-series analysis (Hamed, 2008). In this study, we set the significant confidence interval to 95% ($p < 0.05$).

The MK statistical test for monotone trend is defined in **Eqs. 2–4**.

$$T = \sum_{j<i} sgn\left(Z_i - Z_j\right) \tag{2}$$

$$sgn(x) = \begin{cases} 1, & if\ x > 0 \\ 0, & if\ x = 0 \\ -1, & if\ x < 0 \end{cases} \tag{3}$$

$$Var(T) = \left\{ n(n-1)(2n+5) - \sum_{j=1}^{p} + t_j\left(t_j - 1\right)\left(2t_j + 5\right) \right\} \Big/ 18 \tag{4}$$

where *sgn* is the sign function, Z_i to Z_j is the dataset of the time-series data, p is the number of tied groups in the dataset, and t_j is the number of data points in the *jth* tied group. Furthermore, if n is large, T is approximately normal.

The significance of trends can be tested by comparing the standardized variable U in **Eq. 5** with the standard normal variate at the significance level α (Kendall, 1975).

$$U = \begin{cases} \dfrac{(T-1)}{\sqrt{Var(T)}} & T > 0 \\ 0 & T = 0 \\ \dfrac{(T-1)}{\sqrt{Var(T)}} & T < 0 \end{cases} \tag{5}$$

where $U > 0$ indicates an upward trend, whereas $U < 0$ denotes a downward trend.

The Theil–Sen estimator is a robust model of a fitted line in nonparametric statistics by choosing the median of the slopes of all lines through pairs of points (Akritas et al., 1995). We used the Theil–Sen estimator to quantify the variation trend of ecosystem indices and reflected the change magnitude in specific periods. The positive estimated value indicates an upward trend, whereas the negative value represents a downward trend (**Eq. 6**).

$$\beta = Median\left(\frac{z_i - z_j}{i - j}\right) \tag{6}$$

where $1 < j < i < n$; if $\beta > 0$, it indicated an upward trend, otherwise, it indicated a downward trend.

The above time-series analysis revealed the spatial pattern of temporal variation in ES indicator dynamics. To describe the distance trend, we calculated the mean values of each ES indicator in 500–10000-m buffers and then used the heatmap graph to distinctly represent the temporal and distance trends.

2.3.3 Impact Analysis

The variations of the ES indicators were impacted by land use and climate change. Considering land-use type as a categorical variable, overlay analysis is more feasible to detect the qualitative effect on the different levels of ecosystem indices. Corresponding to static LUCC maps, the ES indicators in 2000/2001, 2010, and 2020 were reclassified using the natural breakpoint method in ArcGIS 10.8, and the classified criteria were consistent in different years for each ES indicator. Then, the Tabulate Area tool was used to conduct the mean-value raster overlay analysis to qualitatively reflect the distribution of high–low ES indicator values in each land-use type.

In pixel-level time-series analysis, multivariate regression was used to determine the impact of long-term climate change on the variations of the ES indicator. Using the annual precipitation and average annual temperature as the explanatory variables as well as ES indicators as the dependent variables, multiple linear regression equations were constructed and tested. Statistical significance was calculated using p-values at a 95% ($p < 0.05$) confidence interval.

$$y_i = \beta_0 + \beta_1 x_1 + \beta_2 x_2 + \epsilon \tag{7}$$

where y_i is the ES indicator, x_1 is the annual precipitation, x_2 is the average annual temperature, β_1 and β_2 are the slope coefficients for each explanatory variable, β_0 is the constant term of the y-intercept, and ϵ is the error term. We summarized the positive and negative areas to reflect the influence strengths.

After determining the individual influence roles of precipitation and temperature by partial regression coefficients, we used ordinary least squares regression and quadratic polynomial regression to describe the direction and strength change of climatic controls with the buffer distance increased.

3 RESULTS

3.1 Land-Use Dynamic Characteristics

During the study period, the change rates of most land-use types were stronger in 2010–2020 than in 2000–2010 (**Figure 2A**). According to the different temporal variations of each land-use type, forest, shrubland, and grassland showed relatively slight rate variations over time, although the quantity variation of grassland in 2010–2020 was obvious. In contrast, cropland, construction land, unused land, and water body showed obvious rate and quantity variations, at least in one period. Due to the small total area of cropland, the change proportions were larger than others in the same period. Construction land and unused land significantly increased from 2010 to 2020.

From the perspective of land-use transition, we used the chord graph to visualize traditional land-use transition matrix

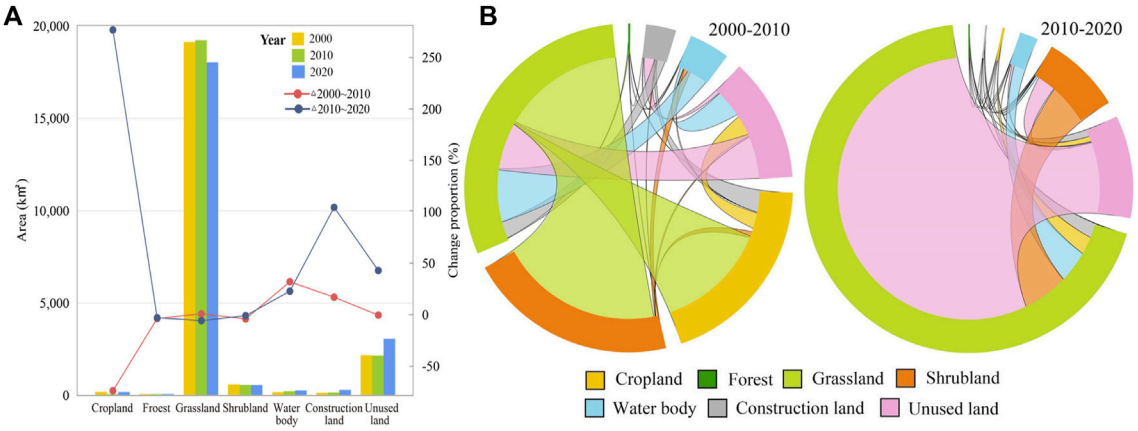

FIGURE 2 | Land-use change and land-use transition in the Qinghai–Tibet Highway corridor. The chord graph intuitively represents the transitions between different land-use types, the width of the land-use section represents the area of land use **(A,B)**, and the transparent colors represent the finally gained land use after the mutual transitions between two land-use types.

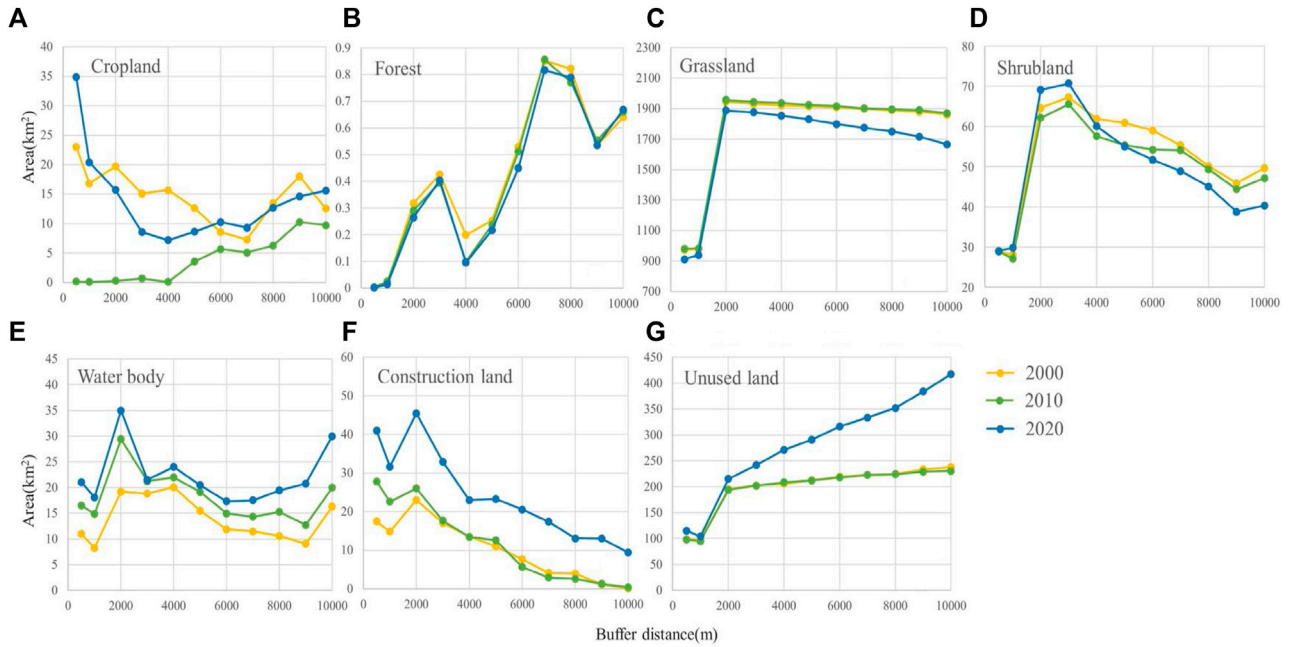

FIGURE 3 | (A) Cropland; **(B)** Forest; **(C)** Grassland; **(D)** Shrubland; **(E)** Water body; **(F)** Construction land; **(G)** Unused land.

(**Figure 2B**). From 2000 to 2010, the large areas of grassland transformed into unused land, construction land, and water body, whereas more than half of the grassland replenishment were derived from shrubland and cropland. In addition, the construction land replenishment was derived from grassland and unused land. From 2010 to 2020, the large proportion of grassland transformed into the other land-use types, especially for unused land and shrubland.

The proportions of each land-use type varied with the buffer distance in 3 years (**Figure 3**). There were obvious temporal variations of cropland proportion with the buffer distances, which showed an overall descending trend in 2000 and 2020 and an overall upward trend in 2010 (**Figure 3A**). Forest, grassland, and shrubland showed an overall upward trend, with the slightest temporal variations (**Figures 3C,D**), and grassland, shrubland, water body, and unused land attained the maximum value in the 2000–3000-m distance (**Figures 3C,E,F**). Unused land mainly showed a continuous upward trend, especially in the buffer distance of 1000 to 2000 m. In addition, the increased rate was stronger in 2020 than the other years (**Figure 3G**). In general, only

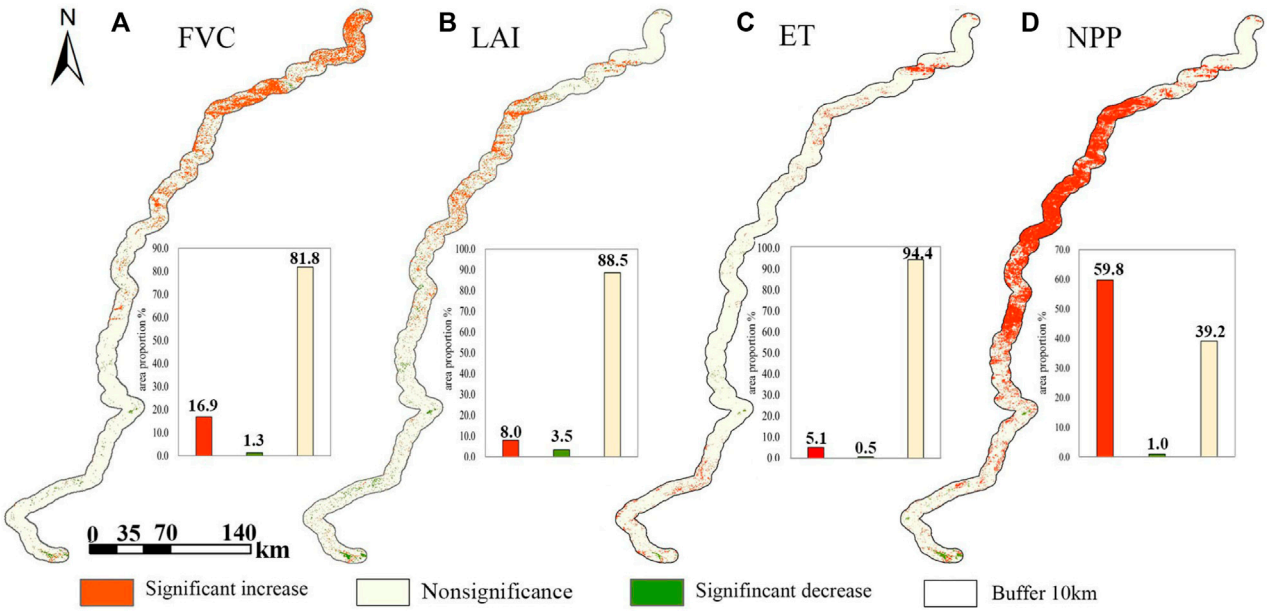

FIGURE 4 | Variation trends of ecosystem service indicators and significance tests in the study period. (**(A)** FVC; **(B)** LAI; **(C)** ET; **(D)** NPP).

cropland showed obvious differences each year. Among the land-use types with a declining quantity from 2010 to 2020, the area far from the road has a faster decreasing trend, i.e., grassland and shrubland.

3.2 The Dynamic Trends of Ecosystem Service Indicators During 2000–2020

Using the long-term time-series moderate resolution imaging spectroradiometer remote sensing products, we calculated the pixel-level temporal trend of each ES indicator. Through the analyses of Sen's slope and MK test, the results showed a distinct spatial differentiation of the FVC trend during 2000–2020, which was represented as the increased area (16.9%) mainly in the northeast and the decreased area (1.3%) mainly in the southwest and other scattered areas (**Figure 4A**). Compared with FVC, the significantly changed area was reduced in the LAI trend, especially in the northeast, which was represented by the increased area (8.0%) mainly in the central to the northwest and the decreased area (3.5%) mainly in the central to the southwest (**Figure 4B**). ET showed the least-obvious trend, in which the increased area (5.1%) was mainly in the northeast and southwest and the decreased area (0.5%) mainly in the southwest (**Figure 4C**). NPP had the most significant spatial differentiation, which was represented as the increased area (59.8%) mainly in the central and northeast and the decreased area (1.0%) mainly in the southwest (**Figure 4D**).

Each ES indicator showed obvious temporal and distance variations (**Figure 5**). From the perspective of temporal variation, FVC showed an overall upward trend; in particular, it attained the maximum value in 2018 and the minimum value in 2015, and there were fluctuations between different periods. The situation of LAI was similar to that of FVC; in particular, it attained the maximum value in 2020 and the minimum value in 2007 and 2015. ET showed no obvious variation trend and attained the maximum value in 2011. NPP showed an upward trend after 2016; in particular, it attained the maximum value in 2020 and the minimum value in 2007 and 2008. From the perspective of distance variation, FVC in different years showed a similar trend, that was the maximum ranged between 3000 and 6000 m with infinitesimal inter-annual differences. LAI also had relatively consistent temporal characteristics, which attained the maximum value in 6000 m, especially in 2015–2020. ET showed a similar trend in different years, contrary to FVC and LAI; the maximum value was attained at approximately 2000 m, which then decreased with the increasing distance. NPP was similar to FVC, and the maximum range occurred in 2000–6000 m with an infinitesimal difference. In summary, ET had the most distinctive trend, and FVC and NPP had the most similar trends of temporal and distance variations.

3.3 Effects of Land-Use and Land-Cover Change and Climatic Factors on Temporal Variation of Ecosystem Service Indicators

Figure 6 presents the variations of relative area proportions between the hierarchical levels of indices from 2000 to 2020. In the study area, the area of grassland was dominant, whereas forest was rare. The high-value ES indicators of cropland were mainly decreased over time. For FVC, there were more moderate to high values in grassland and more high values in shrubland with little temporal variation, whereas in unused land, the domination of low value decreased with time; especially in 2020, the high-value area demonstrated an obvious increase (**Figure 6A**). For LAI, the low- and high-value proportions of grassland was decreased over time, the low- and high-

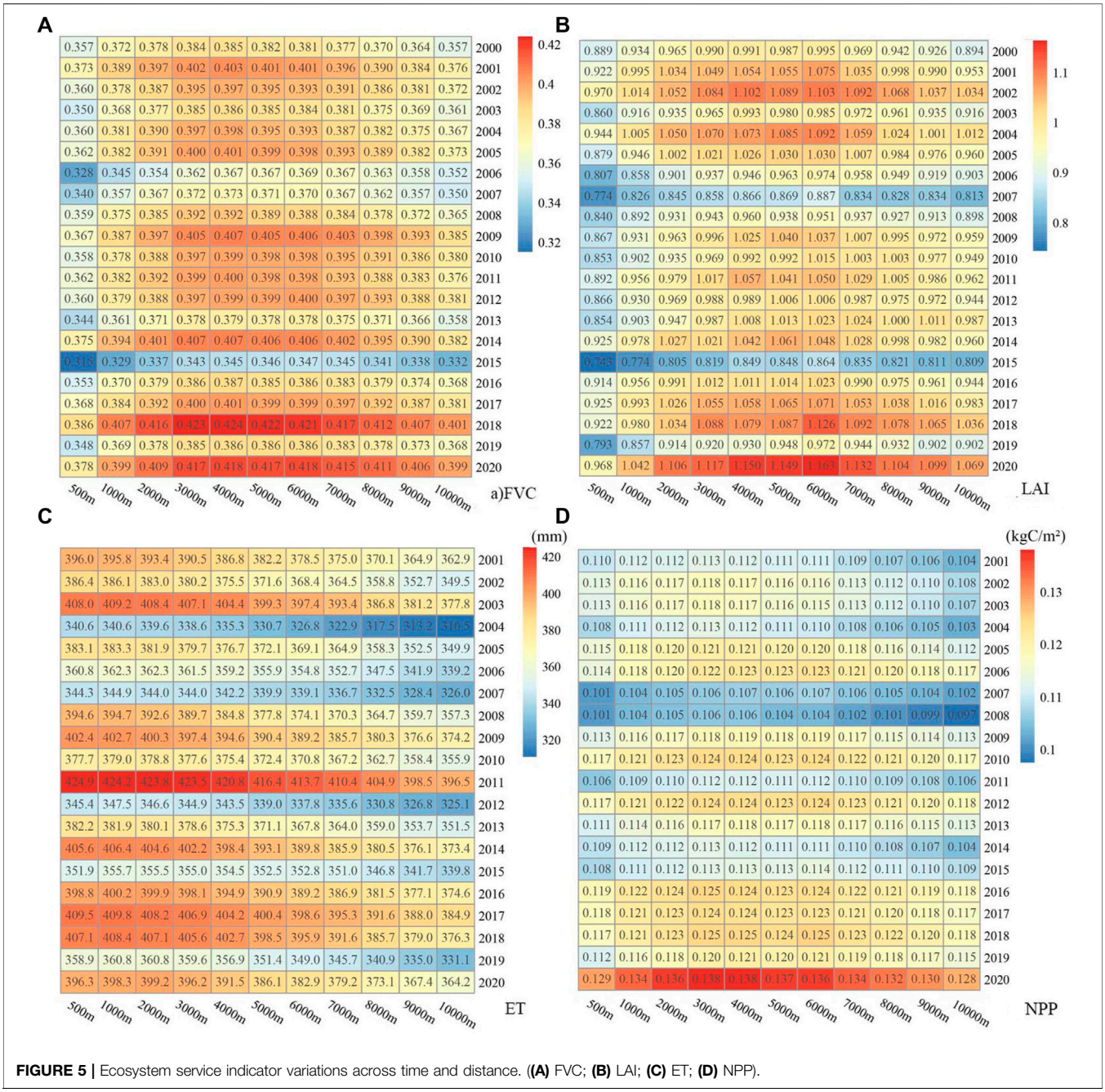

FIGURE 5 | Ecosystem service indicator variations across time and distance. (**(A)** FVC; **(B)** LAI; **(C)** ET; **(D)** NPP).

value proportions of unused land was increased over time, whereas other land-use types changed negligibly (**Figure 6B**). For ET, the high value of grassland was obviously decreased over time, whereas the high values of shrubland and unused land were obviously increased over time (**Figure 6C**). For NPP, the high value of grassland was increased over time, whereas the high value of shrubland was decreased over time; all levels of unused land were increased over time (**Figure 6D**).

Using multiple spatial regression methods, we identified the climatic controls on the temporal–spatial variations of the ES indicators (**Figure 7**). The results showed that precipitation explained more positive influences in FVC (20.54%) and LAI (3.52%), ET (18.71%) than temperature, while explained more negative influence in NPP (12.03%). With regard to temperature, it explained more negative influences in FVC (7.03%), LAI (2.23%), and ET (4.42%) and a more positive influence in NPP (13.95%). From the spatial perspective, the effects of precipitation and temperature on FVC and LAI were relatively consistent, except for the southwest part, whereas in the middle and southwest parts, ET and NPP showed opposite effects of precipitation and temperature. The results of decision coefficient (R^2) showed that the model performances of ET and NPP were better, whereas the performance of LAI was relatively poor.

FIGURE 6 | Influence of land-use types on multiple ecosystem service indicators during 2000–2020.

We calculated the variation trends of the regression coefficients with the buffer distances. By using linear and polynomial models, eight models were significant to reflect the influencing strengths and directions along with the distance gradient (**Figure 8**). From the influences of precipitation on the ES indicators, there were overall downward trends on FVC and ET and partial downward trends with the turning point of 7000 m on LAI and NPP. Regarding temperature, the ES indicators increased with the increasing distance, except for ET, and there existed the turning point of 3000 m in ET. In general, the distance trends of precipitation and temperature in FVC and ET showed nearly opposite directions, whereas in LAI and NPP, they showed similar strength change with contrasting influence directions (negative or positive).

4 DISCUSSION

4.1 The Relationship Between Land-Use Change and Distance from Road

The land-use change was more obvious in 2010–2020, which reflects the increasing human activities and climate change (Cui and Graf, 2009). As for the relative stability in 2000–2010, this is due to little human interference and mild climate change. The phenomenon that a large proportion of grassland is transformed into unused land may be due to overgrazing, which not only directly eliminates the biomass of grassland but also results in soil compaction and trait deterioration, thus hindering the growth of grass (Niu et al., 2019; Yang and Sun, 2021). As to cropland change, it showed an obvious decrease in 2010 and an obvious increase in 2020;

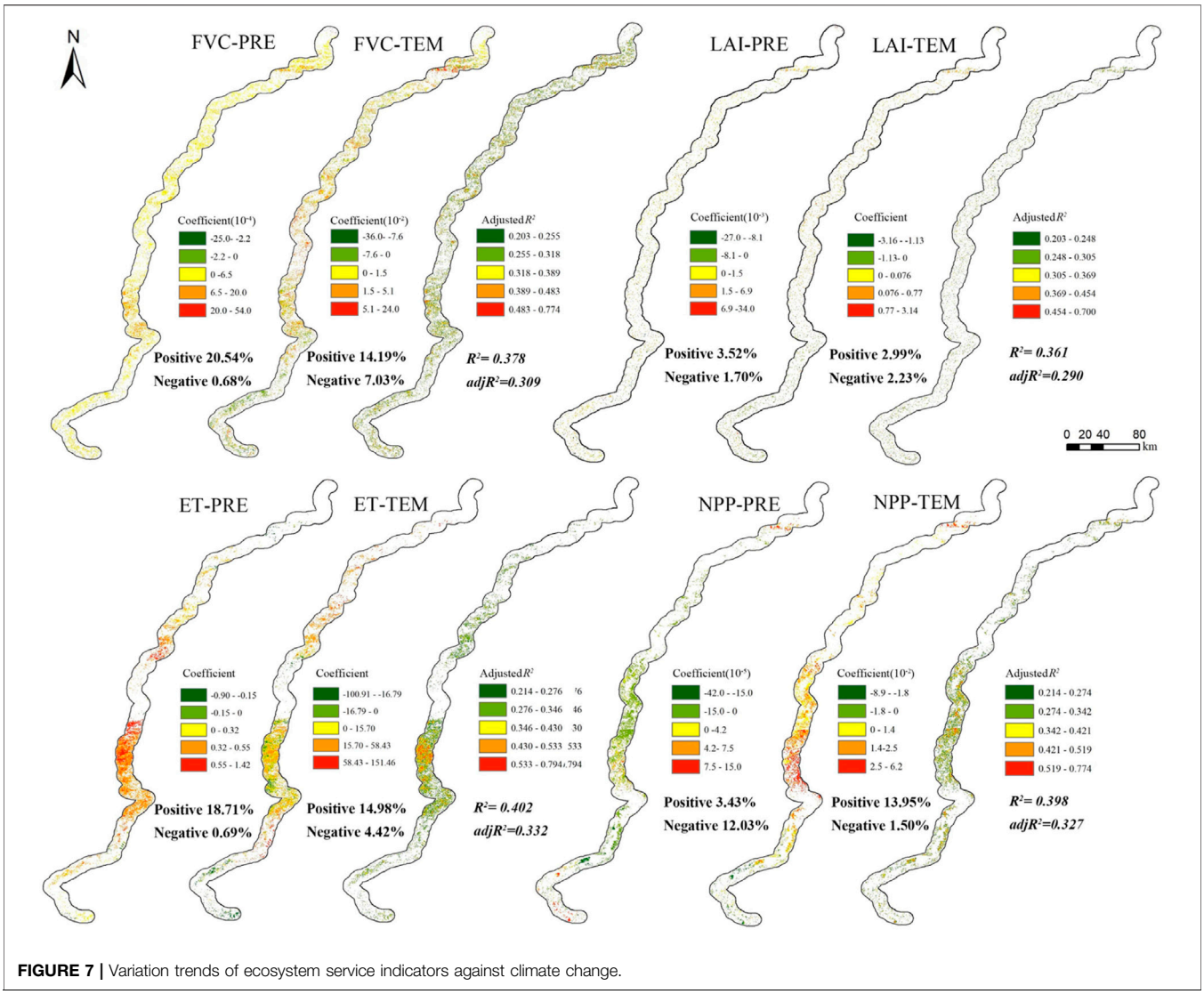

FIGURE 7 | Variation trends of ecosystem service indicators against climate change.

this could be related to the policy of the GFGP since 2002 (Xin, 2008). The reason for the cropland increase may be attributed to the growing orchard plants (which is one of the cropland types in the GlobeLand 30 data) or land reclamation in the high-altitude region (Wu et al., 2021). Among the land-use types, only the cropland proportion showed the significantly inter-decadal distance trends (**Figure 3A**). After the GFGP implementation, the previous indistinct variation of cropland turned into an upward trend with a distance increase, especially after 4000 m in 2010 and 2020. It has a finding similar to Zheng et al. (2021), who also identified 4000 m as a turning point and found that the increasing rate is slower after 4000 m; however, in this study, only in 2020, the finding exists. The descending turning point of shrubland was 3000 m with a minor inter-decadal difference, which reflected the few human activities on shrubland. For construction land, the downward trend was slower in 2020 than in previous years, which indicated the increasing human activities over time.

4.2 The Spatiotemporal Variations and Distance Characteristic of Ecosystem Service Indicators

Vegetation dynamic analysis revealed that the middle to the northeast part of FVC and the northcentral part of LAI were increased during 2000–2020 (**Figures 4A,B**). LAI is mainly used to describe vegetation structure characteristics; in general, the LAI of cropland and forest is higher than that of grassland. Thus, the northeast part of LAI not showing a significant increase might be due to the large proportion of grassland and unused land. Many studies found that LAI and NDVI exist in multiple functional relationships for different vegetation types (De Peppo et al., 2019; Rees et al., 2020). However, the LAI decreased area of the southwest part was larger than FVC decreased area (**Figures 4A,B**), which is partly due to the reduced cropland proportion in 2000–2010. The inconsistent spatial distribution for the FVC and LAI variations is probably because of the grass species difference, land-use transformation of

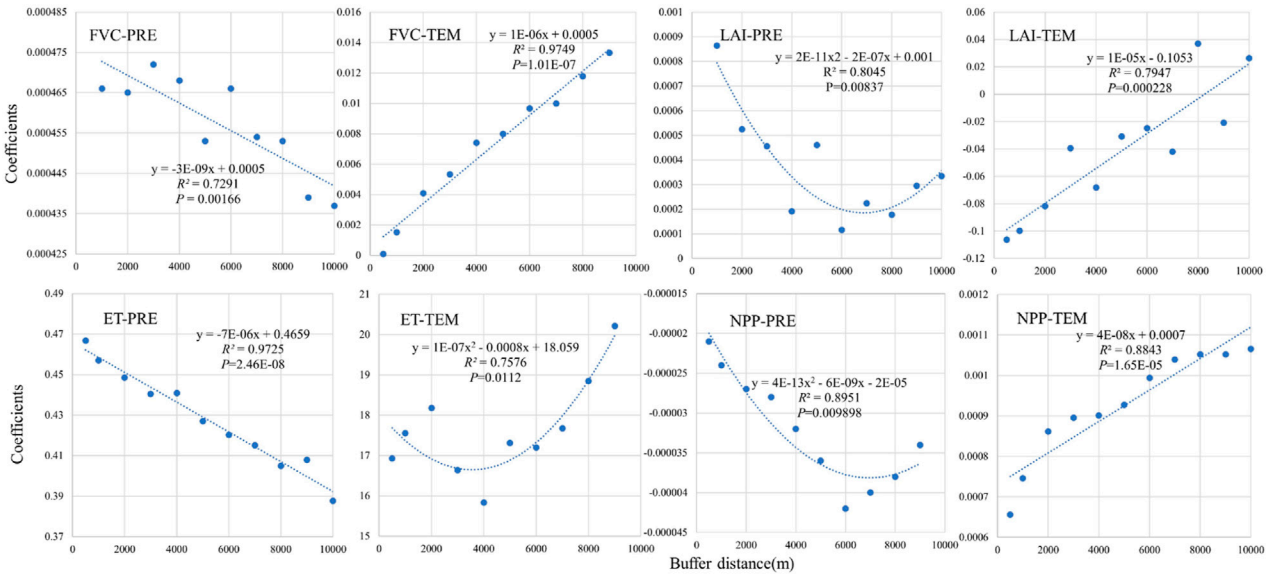

FIGURE 8 | Regression coefficients of ecosystem service indicators against climate change in buffer distances. The outliers were removed to derive the better trends.

GFGP, and environmental pressure on the carbon sequestration process (Zhang W. et al., 2021).

As for ET, a previous work demonstrated that it was increased overall during 1982–2016 in QTP, with a decreased spatial pattern from southeast to northwest (Ma and Zhang, 2022). In this study, the mainly increasing area was in the northeast and southwest (**Figure 4C**), which is also the high-temperature area. In the northeast, the significantly increased precipitation and the high solar–thermal status induced the increased ET, whereas in the southwest, precipitation was not increased, but the high solar–thermal status and land use of shrubland resulted in increased ET. NPP is closely linked to ET, in which the carbon cycle through vegetation canopy stomata impacts ecosystem productivity (Kang et al., 2016). Over a half area in this study showed a significantly increasing trend (**Figure 4D**), which is consistent with the overall increasing trend of NPP in QTP (Han et al., 2018; Yang et al., 2019; Zhang W. et al., 2021). In general, NPP and NDVI have positive correlations (Liu et al., 2021); the inconsistency between NPP and FVC indicates that the climate and vegetation species significantly differed in the long-distance linear region, therefore the relationship between NPP and FVC was not obvious. The consistent areas among the significantly increased area of ET and NPP indicated the positive relationships between the actual ET and terrestrial productivity (Ma and Zhang, 2022).

By comprehensively analyzing each ES indicator variation with the increasing time and buffer distance, several similar findings were obtained, such as the distance turning points of FVC, LAI, and NPP (**Figure 5**). Overall, the maximum value of these ES indicators was approximately 6000 m, whereas the maximum value of ET was within 2000 m. The downward shift of the ET maximum could be explained by the distribution of the water body, which is mainly positioned near the highway; in general, the ET of water body is large (Liu et al., 2020). The lower values of each index in 2015 are partly due to the reduced precipitation and temperature in this year. Comparing the ES indicators in 500 m and in 500–1000 m, the former was significantly inferior to the latter in terms of FVC, LAI, and NPP, which indicates that the intense impact on the ecosystem is within 500 m in QTP, and the ecosystem status gradually recovered as the distance increased. In addition, the 500-m distance is constrained by the data resolution; thus, it may be less by using finer data. In areas near the highway, lots of abandoned waste, materials, and gases are generated by asphalt mixture during road paving. This increases traffic volume and causes soil contamination and compaction, thus inhibiting the growth of vegetation (Jaworska and Lemanowicz, 2019; Gao et al., 2020). After 500 m, the disturbance was decreased, and vegetation gradually recovered under climate change. In addition, wind transportation may contribute to Nitrogen added topsoil and plant seed dispersal (Cheng and Chen, 2002); thus, areas located within 6000 m showed upward trends.

4.3 The Influence Factors on the Variations of Ecosystem Service Indicators

LUCC is one of the dominant factors that influence vegetation and ecosystem function (Mu et al., 2013). Through the overlay analysis of LUCC and ES indicators, the qualitative relationships between them were derived (**Figure 6**). The distinct time variations of FVC and LAI in grassland and unused land reflect the enhanced canopy cover of grass and desert plants and the increased growth rate of cropland, which is primarily due to the increasing role of the increased temperature and anthropogenic cultivation. In ET and NPP, except for forest, the other land-use types showed obvious differences. The increased area of unused land was mainly distributed in the

low-value ET area, which indicates that the position of the gained unused land is relatively far from the national highway according to the previous results. For NPP, the high-value area of cropland and shrubland was decreased, whereas that of grassland and unused land was increased, indicating the larger contributions of grassland and unused land to increasing NPP over time. Previous works confirmed the dual effects of human activities and climate change on increasing NPP, especially after 2000; however, it is still necessary to pay more attention to the ecological balance between species (Wang et al., 2013; Chen et al., 2014).

Precipitation and temperature are fundamental driving forces for ecosystem process change and vegetation distribution as well as productivity in QTP (Huang et al., 2016; Liu et al., 2021; yin Zhang et al., 2021). To analyze the climatic controls on each ES indicator, spatial multiple regression analysis is a better choice than spatial correlation analysis owing to the former's causal explanatory power. The less climatic influences on the ES indicators in the northeast part are partly due to the offset effects by human activities. This area belongs to Golmud, which is the largest logistics distribution center, where the different types of human activities could generate. In the middle part, FVC and ET were positively influenced by meteorological factors, and the positive influence of precipitation was higher than that of temperature. The FVC result is consistent with that obtained by Mu et al. (2021), because precipitation is the main constraining factor of vegetation distribution in the semi-arid region of QTP. In the NPP significantly changed area, temperature was the dominant factor, which showed a more positive influence in the middle part. The NPP result is consistent with that obtained by Gao et al. (2013), who demonstrated that temperature temporal change accounts for 80% of the interannual change in vegetation NPP during 2001–2008 in QTP. It could also be explained by the changed ecosystem structure. Huiying Liu et al. (2018) found the long-term climate warming from 1983 to 2014 in QTP, which resulted in high grass abundance. In the southwest part, precipitation was explained by more NPP change, with an almost contrasting trend to temperature due to the relative water shortage (Yang et al., 2019).

According to the distance trends of climatic influences, it is noted that the increased control of temperature with distances occurred in FVC, LAI, and NPP (**Figure 8**). This phenomenon conformed well to the distance trends of temperature, which indicated that temperature plays an important role in different zones of the buffer. Regarding precipitation, the U-type trend occurred in LAI and NPP with a 7000-m threshold, which showed the increased negative effects of precipitation on NPP within 7000 m. This is probably because the higher soil water content in the freezing-thawing area near traffic infrastructure (Wu et al., 2003); therefore, when the precipitation increased with the road distance (calculated by data), the soil water content decreased more than the precipitation increased, resulting in the decrease of NPP. This study speculates that with the increasing distance far from the road, NPP and precipitation will gradually show a positive correlation (Xu et al., 2006; Yang et al., 2019).

4.4 Implications for Ecological Protection

In GLHC, the natural environment in the middle part is relatively harsh, and the socioeconomic level is relatively low (Danggula Mountains Town and Amdo County). In the two end parts of the GLHC (Golmud City and Lhasa City), human activities increased, and few areas showed improved ES indicators. Overall, except for Golmud City, the section of the Qinghai Province showed better vegetation restoration dynamics and productivity-improved status, which can increase regional carbon sequestration service. There were few areas of increased ET and LAI; thus, the change in water provision service is dominated by precipitation. In Tibet Autonomous Region, the increasing human activities and the construction of the Nagqu–Lhasa expressway section (since 2017) might become the key factors restricting vegetation restoration. Regarding this, evidence showed the negative effect of standoff distance between roads and railways on animal activities in QTP (Wang et al., 2021). The impact of landscape fragments on vegetation dynamics has a time lag effect. It can be speculated that three parallel linear traffic infrastructures (national highway, railway, and expressway) might form a local microclimate, which will cause the cumulative weakening effects.

From the buffer analysis, the vegetation recovered well at approximately 3000–6000 m from the national highway, which can provide more carbon storage in this region. There are typical desert and grassland ecosystems along the highway. According to the established vegetation restoration on both sides of the highway, the natural restoration method is more feasible and effective than the artificial method. To achieve the multiple ES, such as water conservation, carbon sequestration, and soil retention, in this case, human intervention is needed to eliminate invasive sedge species or reseed superior local grass species to balance natural ecosystems (Chen et al., 2014). Moreover, the recovery of roadside vegetation is partly due to the water collection and ventilative soil conditions on the sides of the road. Because the survival rate of artificial grass is lower in roadside areas, adopting stripped turf is prioritized to restore the bare land surface. For the bare surface with better hydrothermal conditions, artificial seeding of grass seeds can be appropriately adopted to increase the soil retention ability.

In previous decades, to ensure that the QTP national highway is operating well, the Chinese government spent huge investments to renovate the highway four times. However, due to the negative influences of the abandoned soil mound and types of wastes on both sides of the highway, the soil is contaminated by heavy metals, vegetation undergoes degradation, and landscape aesthetics is lost. Therefore, government monitoring and recovery efforts should be duly strengthened.

4.5 Limitations and Future Perspective

This study analyzed the influences of buffer distance on land-use change, ES indicator variations, and their climatic influences, which provide the scientific support for vegetation recovery and ecological management along with the traffic infrastructures. However, there are several limitations as follows. First, the spatial resolutions of data are different, which may mask the fine changes by coarse data, and the distance variations of climatic

influences may be weakened within 1 km due to the resampling process. Second, the impact of sensors should be considered. A previous study has identified the issue of sensor degradation and overcorrection of the algorithm, which interfered with the accuracy of vegetation indices inversion, further resulting in the possible spatial errors (Tian et al., 2015). It can be more accurate by using multiple data resources and conducting the consistency analysis. Third, some environmental factors, such as radiation, elevation, and landscape pattern, are not taken into consideration. Further studies are encouraged to detect the interaction effects between various types of impact factors. Fourth, this study focused on the differences in first-level LUCC classification, which are not consider the differentiation characteristics of vegetation types, further studies could pay attention to discriminating the contributions. Last but not least, other ES, such as soil conservation, biodiversity maintenance, and aesthetic value, should be further determined (Jin et al., 2021) to fully understand the change in comprehensive ES.

5 CONCLUSION

This study aimed to investigate the ES indicator variations and the driving factors in the alpine linear traffic corridor area. On one hand, it fills the gap of ES topic in the linear area dominated by traffic activities; on the other hand, it discriminates the driving mechanism by climatic factors and distance effect in such a long-span linear region with different natural and socioeconomic conditions. It was found that LUCC was faster in the last decade, most likely due to the conversion from grassland to unused land. In buffer within 3000 m, the productive areas represented increasing trends with distance. Among the ES indicators, the increased FVC area was positively influenced by the enhanced precipitation and temperature in the Qinghai Province. NPP significantly increased, especially in the Qinghai Province, which could be attributed to the temperature increase over the last two decades. Nearly 60% of the area exhibited an increase in NPP over time, whereas a degraded status was observed in Lhasa and Nagqu, which is partly due to the expressway construction (Nagqu–Lhasa Expressway). Temperature was the main driving factor of NPP in the middle part, and the impact degree tended to increase with increasing distance. The control of precipitation on NPP exhibited a U-type negative trend with increasing distance. This is probably due to larger soil water content near the highway caused by the freezing–thawing process, which offsets the effect of increased precipitation with increasing distance. Further studies should be directed to the relevant topics to instruct the ecological recovery in linear traffic corridor areas of QTP. Overall, this study could provide practical information to guide various preservation efforts for the linear traffic construction in alpine fragile areas.

DATA AVAILABILITY STATEMENT

The raw data supporting the conclusion of this article will be made available by the authors, without undue reservation.

AUTHOR CONTRIBUTIONS

SY: Data curation, Methodology, Visualization, Writing—original draft. GZ: Supervision, Writing—review and editing. LZ: Writing—review and editing. HX: Writing—review and editing. JC: Writing—review and editing.

FUNDING

This research is financially supported by the Natural Science Foundation of China (Nos. 41601105 and 42071288); Key Science and Technology Project of Transportation Industry (Nos. 2018-MS5-127 and 2020-MS4-113).

REFERENCES

Akritas, M. G., Murphy, S. A., and Lavalley, M. P. (1995). The Theil-Sen Estimator with Doubly Censored Data and Applications to Astronomy. *J. Am. Stat. Assoc.* 90, 170–177. doi:10.1080/01621459.1995.10476499

Chang, X., Zhao, W., Liu, B., Liu, H., He, Z., and Du, J. (2017). Can Forest Water Yields Be Increased with Increased Precipitation in a Qinghai Spruce Forest in Arid Northwestern China? *Agric. For. Meteorol.* 247, 139–150. doi:10.1016/j.agrformet.2017.07.019

Chapin, F. S., Matson, P. A., Mooney, H. A., and Vitousek, P. M. (2002). *Principles of Terrestrial Ecosystem Ecology*.

Chen, B., Zhang, X., Tao, J., Wu, J., Wang, J., Shi, P., et al. (2014). The Impact of Climate Change and Anthropogenic Activities on Alpine Grassland over the Qinghai-Tibet Plateau. *Agric. For. Meteorol.* 189-190, 11–18. doi:10.1016/j.agrformet.2014.01.002

Cheng, H., and Chen, Z. (2002). The Feasibility of Natural Vegetation Restoration along Qinghai-Tibet Railway Desert Area. *China Railw.* (11), 52–54. (in Chinese). doi:10.19549/j.issn.1001-683x.2002.11.016

Cui, X., and Graf, H. F. (2009). Recent Land Cover Changes on the Tibetan Plateau: a Review. *Clim. Change* 94, 47–61. doi:10.1007/s10584-009-9556-8

De Peppo, M., Dragoni, F., Volpi, I., Mantino, A., Giannini, V., Filipponi, F., et al. (2019). "Modelling the Ground-LAI to Satellite-NDVI (Sentinel-2) Relationship Considering Variability Sources Due to Crop Type (Triticum Durum L., Zea mays L., and Medicago Sativa L.) and Farm Management," in Proceeding of the Remote Sensing for Agriculture, Ecosystems, and Hydrology XXI, October 2019 (SPIE-SOC Photo-Optical Instrumentation Engineers), 111490I.

Ding, M., Zhang, Y., Shen, Z., Liu, L., Zhang, W., Wang, Z., et al. (2006). Land Cover Change along the Qinghai-Tibet Highway and Railway from 1981 to 2001. *J. Geogr. Sci.* 16, 387–395. doi:10.1007/s11442-006-0401-y

Favre, A., Päckert, M., Pauls, S. U., Jähnig, S. C., Uhl, D., Michalak, I., et al. (2015). The Role of the Uplift of the Qinghai-Tibetan Plateau for the Evolution of Tibetan Biotas. *Biol. Rev.* 90, 236–253. doi:10.1111/brv.12107

Field, C. B., Behrenfeld, M. J., Randerson, J. T., and Falkowski, P. (1998). Primary Production of the Biosphere: Integrating Terrestrial and Oceanic Components. *science* 281, 237–240. doi:10.1126/science.281.5374.237

Fischer, R., Taubert, F., Müller, M. S., Groeneveld, J., Lehmann, S., Wiegand, T., et al. (2021). Accelerated Forest Fragmentation Leads to Critical Increase in Tropical Forest Edge Area. *Sci. Adv.* 7, eabg7012. doi:10.1126/sciadv.abg7012

Forman, R. T. T. (2000). Estimate of the Area Affected Ecologically by the Road System in the United States. *Conserv. Biol.* 14, 31–35. doi:10.1046/j.1523-1739.2000.99299.x

Freitas, S. R., Hawbaker, T. J., and Metzger, J. P. (2010). Effects of Roads, Topography, and Land Use on Forest Cover Dynamics in the Brazilian Atlantic Forest. *For. Ecol. Manag.* 259, 410–417. doi:10.1016/j.foreco.2009.10.036

Gao, Y., Zhou, X., Wang, Q., Wang, C., Zhan, Z., Chen, L., et al. (2013). Vegetation Net Primary Productivity and its Response to Climate Change during 2001-2008 in the Tibetan Plateau. *Sci. Total Environ.* 444, 356–362. doi:10.1016/j.scitotenv.2012.12.014

Gao, J., Zhang, M., Hu, Z., and Shan, W. (2020). Influence of Expressway Construction on the Ecological Environment and the Corresponding Treatment Measures: a Case Study of Changyu (Changchun-Fuyu Lalin River) Expressway, China. *Nat. Environ. Pollut. Technol.* 19, 1195–1201. doi:10.46488/nept.2020.v19i03.033

Hamed, K. H. (2008). Trend Detection in Hydrologic Data: The Mann-Kendall Trend Test under the Scaling Hypothesis. *J. Hydrology* 349, 350–363. doi:10.1016/j.jhydrol.2007.11.009

Han, Z., Song, W., Deng, X., and Xu, X. (2018). Grassland Ecosystem Responses to Climate Change and Human Activities Within the Three-River Headwaters Region of China. *Sci. Rep.* 8 (1), 1–13. doi:10.1038/s41598-018-27150-5

Hua Zhang, H., Wang, Z., Zhang, Y., Ding, M., and Li, L. (2015). Identification of Traffic-Related Metals and the Effects of Different Environments on Their Enrichment in Roadside Soils along the Qinghai-Tibet Highway. *Sci. Total Environ.* 521-522, 160–172. doi:10.1016/j.scitotenv.2015.03.054

Huang, K., Zhang, Y., Zhu, J., Liu, Y., Zu, J., and Zhang, J. (2016). The Influences of Climate Change and Human Activities on Vegetation Dynamics in the Qinghai-Tibet Plateau. *Remote Sens.* 8, 876. doi:10.3390/rs8100876

Huiying Liu, H., Mi, Z., Lin, L., Wang, Y., Zhang, Z., Zhang, F., et al. (2018). Shifting Plant Species Composition in Response to Climate Change Stabilizes Grassland Primary Production. *Proc. Natl. Acad. Sci. U.S.A.* 115, 4051–4056. doi:10.1073/pnas.1700299114

Ibisch, P. L., Hoffmann, M. T., Kreft, S., Pe'er, G., Kati, V., Biber-Freudenberger, L., et al. (2016). A Global Map of Roadless Areas and Their Conservation Status. *Science* 354, 1423–1427. doi:10.1126/science.aaf7166

Jaworska, H., and Lemanowicz, J. (2019). Heavy Metal Contents and Enzymatic Activity in Soils Exposed to the Impact of Road Traffic. *Sci. Rep.* 9, 19981. doi:10.1038/s41598-019-56418-7

Jin, G., Chen, K., Liao, T., Zhang, L., and Najmuddin, O. (2021). Measuring Ecosystem Services Based on Government Intentions for Future Land Use in Hubei Province: Implications for Sustainable Landscape Management. *Landsc. Ecol.* 36, 2025–2042. doi:10.1007/s10980-020-01116-3

Kang, X., Hao, Y., Cui, X., Chen, H., Huang, S., Du, Y., et al. (2016). Variability and Changes in Climate, Phenology, and Gross Primary Production of an Alpine Wetland Ecosystem. *Remote Sens.* 8, 391. doi:10.3390/rs8050391

Kendall, M. (1975). *Rank Correlation Methods (4th edn.) Charles Griffin*. San Franc. CA 8, 875.

Laurance, W. F., Clements, G. R., Sloan, S., O'Connell, C. S., Mueller, N. D., Goosem, M., et al. (2014). A Global Strategy for Road Building. *Nature* 513, 229–232. doi:10.1038/nature13717

Liu, X., Li, T., Zhang, S., Jia, Y., Li, Y., and Xu, X. (2016). The Role of Land Use, Construction and Road on Terrestrial Carbon Stocks in a Newly Urbanized Area of Western Chengdu, China. *Landsc. Urban Plan.* 147, 88–95. doi:10.1016/j.landurbplan.2015.12.001

Liu, W., Zhan, J., Zhao, F., Yan, H., Zhang, F., and Wei, X. (2019). Impacts of Urbanization-Induced Land-Use Changes on Ecosystem Services: A Case Study of the Pearl River Delta Metropolitan Region, China. *Ecol. Indic.* 98, 228–238. doi:10.1016/j.ecolind.2018.10.054

Liu, M., Hu, D., Yu, C., and Wang, S. (2020). Temporal and Spatial Change Characteristics of Growing Season Evapotranspiration and its Cause Analysis in Liaohe River Delta Wetland. *Acta Ecol. Sin.* 40, 701–710. (in Chinese). doi:10.5846/stxb201901180149

Liu, Y., Liu, S., Sun, Y., Li, M., An, Y., and Shi, F. (2021). Spatial Differentiation of the NPP and NDVI and its Influencing Factors Vary with Grassland Type on the Qinghai-Tibet Plateau. *Environ. Monit. Assess.* 193, 1–21. doi:10.1007/s10661-020-08824-y

Millennium Ecosystem Assessment (MA) (2005). Ecosystems and Human Wellbeing. Washington, DC: Island Press

Ma, N., and Zhang, Y. (2022). Increasing Tibetan Plateau Terrestrial Evapotranspiration Primarily Driven by Precipitation. *Agric. For. Meteorol.* 317, 108887. doi:10.1016/j.agrformet.2022.108887

Mu, S., Zhou, S., Chen, Y., Li, J., Ju, W., and Odeh, I. O. A. (2013). Assessing the Impact of Restoration-Induced Land Conversion and Management Alternatives on Net Primary Productivity in Inner Mongolian Grassland, China. *Glob. Planet. Change* 108, 29–41. doi:10.1016/j.gloplacha.2013.06.007

Mu, B., Zhao, X., Wu, D., Wang, X., Zhao, J., Wang, H., et al. (2021). Vegetation Cover Change and its Attribution in China from 2001 to 2018. *Remote Sens.* 13, 496. doi:10.3390/rs13030496

Niu, Y., Zhu, H., Yang, S., Ma, S., Zhou, J., Chu, B., et al. (2019). Overgrazing Leads to Soil Cracking that Later Triggers the Severe Degradation of Alpine Meadows on the Tibetan Plateau. *Land Degrad. Dev.* 30, 1243–1257. doi:10.1002/ldr.3312

Perrings, C., Duraiappah, A., Larigauderie, A., and Mooney, H. (2011). The Biodiversity and Ecosystem Services Science-Policy Interface. *Science* 331, 1139–1140. doi:10.1126/science.1202400

Querino, C. A. S., Beneditti, C. A., Machado, N. G., da Silva, M. J. G., da Silva Querino, J. K. A., dos Santos Neto, L. A., et al. (2016). Spatiotemporal NDVI, LAI, Albedo, and Surface Temperature Dynamics in the Southwest of the Brazilian Amazon Forest. *J. Appl. Remote Sens.* 10, 026007. doi:10.1117/1.jrs.10.026007

Rees, W. G., Golubeva, E. I., Tutubalina, O. V., Zimin, M. V., and Derkacheva, A. A. (2020). Relation between Leaf Area Index and NDVI for Subarctic Deciduous Vegetation. *Int. J. Remote Sens.* 41, 8573–8589. doi:10.1080/01431161.2020.1782505

Renhe Zhang, R., Su, F., Jiang, Z., and Gao, X. (2015). An Overview of Projected Climate and Environmental Changes across the Tibetan Plateau in the 21st Century. *Chin. Sci. Bull.* 60, 3036–3047. (in Chinese). doi:10.1360/N972014-01296

Saito, M., Kato, T., and Tang, Y. (2009). Temperature Controls Ecosystem CO2exchange of an Alpine Meadow on the Northeastern Tibetan Plateau. *Glob. Change Biol.* 15, 221–228. doi:10.1111/j.1365-2486.2008.01713.x

Sha, Z., Bai, Y., Lan, H., Liu, X., Li, R., and Xie, Y. (2020). Can More Carbon Be Captured by Grasslands? A Case Study of Inner Mongolia, China. *Sci. Total Environ.* 723, 138085. doi:10.1016/j.scitotenv.2020.138085

Sitch, S., Smith, B., Prentice, I. C., Arneth, A., Bondeau, A., Cramer, W., et al. (2003). Evaluation of Ecosystem Dynamics, Plant Geography and Terrestrial Carbon Cycling in the LPJ Dynamic Global Vegetation Model. *Glob. Change Biol.* 9, 161–185. doi:10.1046/j.1365-2486.2003.00569.x

Song, Y., Jin, L., and Wang, H. (2018). Vegetation Changes along the Qinghai-Tibet Plateau Engineering Corridor since 2000 Induced by Climate Change and Human Activities. *Remote Sens.* 10, 95. doi:10.3390/rs10010095

Sun, G., Hallema, D., and Asbjornsen, H. (2017). Ecohydrological Processes and Ecosystem Services in the Anthropocene: a Review. *Ecol. Process.* 6, 1–9. doi:10.1186/s13717-017-0104-6

Taugourdeau, S., Le Maire, G., Avelino, J., Jones, J. R., Ramirez, L. G., Jara Quesada, M., et al. (2014). Leaf Area Index as an Indicator of Ecosystem Services and Management Practices: An Application for Coffee Agroforestry. *Agric. Ecosyst. Environ.* 192, 19–37. doi:10.1016/j.agee.2014.03.042

Tian, F., Fensholt, R., Verbesselt, J., Grogan, K., Horion, S., and Wang, Y. (2015). Evaluating Temporal Consistency of Long-Term Global NDVI Datasets for Trend Analysis. *Remote Sens. Environ.* 163, 326–340. doi:10.1016/j.rse.2015.03.031

Tilman, D., and Lehman, C. (2001). Human-caused Environmental Change: Impacts on Plant Diversity and Evolution. *Proc. Natl. Acad. Sci. U.S.A.* 98, 5433–5440. doi:10.1073/pnas.091093198

Van Leeuwen, W. J. D., Huete, A. R., and Laing, T. W. (1999). MODIS Vegetation Index Compositing Approach. *Remote Sens. Environ.* 69, 264–280. doi:10.1016/s0034-4257(99)00022-x

Wang, J., Zhang, X., Chen, B., Shi, P., Shen, Z., Tao, J., et al. (2013). Causes and Restoration of Degraded Alpine Grassland in Northern Tibet. *J. Resour. Ecol.* 4, 43–49. doi:10.5814/j.issn.1674-764x.2013.01.006

Wang, Y., Guan, L., Du, L., and Qu, J. (2021). Overlapping Barrier and Avoidance Effects of the Qinghai-Tibet Highway and Railway on Four Typical Ungulates

on the Tibetan Plateau. *Chin. J. Ecol.* 40, 1091–1097. (in Chinese). doi:10.13292/j.1000-4890.202104.015

Waring, R. H., and Running, S. W. (2010). *Forest Ecosystems: Analysis at Multiple Scales*. Elsevier.

Wu, Q., Shen, Y., and Shi, B. (2003). Relationship between Frozen Soil Together with its Water-Heat Process and Ecological Environment in the Tibetan Plateau. *J. Glaciol. Geocryol.* 25, 250–255. (in Chinese).

Wu, D., Wu, H., Zhao, X., Zhou, T., Tang, B., Zhao, W., et al. (2014). Evaluation of Spatiotemporal Variations of Global Fractional Vegetation Cover Based on GIMMS NDVI Data from 1982 to 2011. *Remote Sens.* 6, 4217–4239. doi:10.3390/rs6054217

Wu, S., Yan, J., Yang, L., Cheng, X., and Wu, Y. (2021). Farmers and Herders Reclaim Cropland to Adapt to Climate Change in the Eastern Tibetan Plateau: a Case Study in Zamtang County, China. *Clim. Change* 165, 1–23. doi:10.1007/s10584-021-03098-w

Xin, H. (2008). A Green Fervor Sweeps the Qinghai-Tibetan Plateau. *Science* 321, 633–635. doi:10.1126/science.321.5889.633

Xu, X., Zhang, K., Kong, Y., Chen, J., and Yu, B. (2006). Effectiveness of Erosion Control Measures along the Qinghai-Tibet Highway, Tibetan Plateau, China. *Transp. Res. Part D Transp. Environ.* 11, 302–309. doi:10.1016/j.trd.2006.06.001

Yang, C., and Sun, J. (2021). Impact of Soil Degradation on Plant Communities in an Overgrazed Tibetan Alpine Meadow. *J. Arid Environ.* 193, 104586. doi:10.1016/j.jaridenv.2021.104586

Yang, X., Guo, B., and Han, B. (2019). Analysis of the Spatial-Temporal Evolution Patterns of NPP and its Driving Mechanisms in the Qinghai-Tibet Plateau. *Resour. Environ. Yangtze Basin* 28, 3038–3050. (in Chinese).

Yang, S., Zhao, W., Liu, Y., Cherubini, F., Fu, B., and Pereira, P. (2020). Prioritizing Sustainable Development Goals and Linking Them to Ecosystem Services: A Global Expert's Knowledge Evaluation. *Geogr. Sustain.* 1, 321–330. doi:10.1016/j.geosus.2020.09.004

Yang, D., Yi, G., Zhang, Y., and Li, J. (2021). Spatiotemporal Variation and Driving Factors of Growing Season NDVI in the Tibetan Plateau, China. *Chin. J. Appl. Ecol.* 32, 1361–1372. (in Chinese). doi:10.13287/j.1001-9332.202104.014

Yin Zhang, Y., Hu, Q., and Zou, F. (2021). Spatio-temporal Changes of Vegetation Net Primary Productivity and its Driving Factors on the Qinghai-Tibetan Plateau from 2001 to 2017. *Remote Sens.* 13, 1566. doi:10.3390/rs13081566

Ying Liu, Y., Feng, Q., Wang, C., and Tang, Z. (2018). A Risk-Based Model for Grassland Management Using MODIS Data: The Case of Gannan Region, China. *Land Use Policy* 72, 461–469. doi:10.1016/j.landusepol.2018.01.015

Zhang, T., Zeng, S., Gao, Y., Ouyang, Z., Li, B., Fang, C., et al. (2011). Using Hyperspectral Vegetation Indices as a Proxy to Monitor Soil Salinity. *Ecol. Indic.* 11, 1552–1562. doi:10.1016/j.ecolind.2011.03.025

Zhang, W., Jin, H., Li, A., Shao, H., Xie, X., Lei, G., et al. (2021). Comprehensive Assessment of Performances of Long Time-Series LAI, FVC and GPP Products over Mountainous Areas: A Case Study in the Three-River Source Region, China. *Remote Sens.* 14, 61. doi:10.3390/rs14010061

Zhang, Y., Liu, L., Wang, Z., and Bai, W. (2019). Spatial and Temporal Characteristics of Land Use and Cover Changes in the Tibetan Plateau. *Chin. Sci. Bull.* 64, 2865–2875. (in Chinese). doi:10.1360/tb-2019-0267

Zheng, F., Huang, J., Feng, Z., and Xiao, C. (2021). Impact of the Kunming-Bangkok Highway on Land Use Changes along the Route between Laos and Thailand. *Land* 10, 991. doi:10.3390/land10090991

Zhu, W., Pan, Y., and Zhang, J. (2007). Estimation of Net Primary Productivity of Chinese Terrestrial Vegetation Based on Remote Sensing. *J. Plant Ecol.* 31, 413–424. (in Chinese). doi:10.17521/cjpe.2007.0050

Conflict of Interest: The authors declare that the research was conducted in the absence of any commercial or financial relationships that could be construed as a potential conflict of interest.

frontiers | Frontiers in Ecology and Evolution

TYPE Original Research
PUBLISHED 02 August 2022
DOI 10.3389/fevo.2022.959329

OPEN ACCESS

EDITED BY
Fan Zhang,
Institute of Geographic Sciences and Natural Resources Research (CAS), China

REVIEWED BY
Wang Zhenshuang,
Dongbei University of Finance and Economics, China
Shuyao Wu,
Shandong University, China
Zhe Zhao,
Liaoning University, China

*CORRESPONDENCE
Jing Wang
wangj@cau.edu.cn

SPECIALTY SECTION
This article was submitted to Conservation and Restoration Ecology, a section of the journal Frontiers in Ecology and Evolution

RECEIVED 01 June 2022
ACCEPTED 11 July 2022
PUBLISHED 02 August 2022

CITATION
Zhang J, Song Y and Wang J (2022) Spatiotemporal patterns of gross ecosystem product across China's cropland ecosystems over the past two decades.
Front. Ecol. Evol. 10:959329.
doi: 10.3389/fevo.2022.959329

Spatiotemporal patterns of gross ecosystem product across China's cropland ecosystems over the past two decades

Jiaying Zhang, Yang Song and Jing Wang*

College of Resources and Environmental Sciences, China Agricultural University, Beijing, China

As the largest artificial ecosystem on Earth, croplands not only secure the basic living materials for people but also provide ecological service values for human society. For croplands, ecosystem services have proven to be of great value and are closely linked to human activities and climate change. However, spatiotemporal patterns of cropland ecosystem services and their drivers still need to be further assessed quantitatively. In this study, we provided a comprehensive evaluation of ecosystem services across China's cropland ecosystems over the past two decades using gross ecosystem product (GEP) as a single metric of the monetary evaluation of final ecosystem services. The values of material services, regulating services, and cultural services were calculated to summarize the GEP value of cropland ecosystems in China. Our results showed that the multiyear mean value of GEP was 4.35×10^7 million CNY. The value of regulating services reached 3.86×10^7 million CNY, followed by material services of 4.76×10^6 million CNY and cultural services of 1.16×10^5 million CNY. GEP value was different among provinces, leading to a heterogeneous spatial pattern associated with population and cultivated area. Moreover, we analyzed the trends in the GEP value at the provincial and national scales. The results showed that the GEP value of China's cropland ecosystems has increased over the period. The values of the material, regulating, and cultural services have increased at a rate of $(0.35 \pm 0.01) \times 10^6$ million CNY a^{-1}, $(1.12 \pm 0.10) \times 10^6$ million CNY a^{-1}, and $(0.002 \pm 0.0002) \times 10^6$ million CNY a^{-1}, respectively ($P < 0.05$). The majority of provinces had an increasing trend in GEP, yet some developed provinces, e.g., Beijing and Shanghai, showed a decreasing trend. Furthermore, we evaluated the impacts of social-economic and natural factors on changes in GEP. We found that rising prices for agricultural products and services boosted an increase in GEP. Meanwhile, the spatiotemporal patterns of GEP were also associated with the adjustments of planting area in each province. Overall, our findings highlight the importance of assessing spatiotemporal patterns of cropland ecosystem services for decision-makers.

KEYWORDS

gross ecosystem product, ecosystem service, cropland, driving factor, spatial distribution

Introduction

China's economy has maintained a rapid growth rate over the past two decades (World Bank, 2020), yet the ensuing environmental problems are becoming one of the most serious threats to ecological sustainability and security (Intergovernmental Panel on Climate Change (IPCC), 2018; Feng et al., 2021). The balance between social and natural values plays an essential role in achieving sustainable development for every country (Polasky et al., 2019; Jiang et al., 2021). Economic development will inevitably cause changes in the internal structure of natural capital (Li et al., 2021). In recent years, the Chinese government has recognized the importance of addressing the goal of sustainable development by protecting and restoring ecosystems (Naustdalslid, 2014), as President Xi Jinping's theory that "lucid waters and lush mountains are invaluable assets." More paths such as the development of ecological civilization are needed to harmonize the apparent contradiction between economic development and environmental protection (Ma and Wei, 2021; Ma et al., 2021). The Seventeenth Congress of the Communist Party of China pointed out the construction of an ecological civilization with Chinese characteristics. In the cropland ecosystem, it has faced the problems of soil erosion and land degradation by natural forces and human pollution such as excessive application of chemical fertilizers and burning of straw. One of the aims of ecological civilization is to solve these issues for realizing the sustainable development of agriculture (Fan, 2011; Zhang, 2012).

As the world's largest artificial ecosystem, the agro-ecosystem covers nearly 40% of the global terrestrial area (Food Agriculture Organization of the United Nations, 2020). As a country with a large population, China has to consider the relationships between food production, environmental degradation, and economic development in cropland ecosystems (van Vliet et al., 2017; Zheng et al., 2019). Resolving the conflict between social-economic development and the conservation of highly productive farmland is significant and has an impact on food security (Lambin and Meyfroidt, 2011). Numerous policies for cropland conservation have been implemented all over the world, such as the Farmland Protection Program (USA) and the Basic Law of Agriculture (Japan). Since the late 1990s, China has adopted a series of policies to protect croplands in order to ensure national food security (Yang and Li, 2000; Skinner et al., 2001). The cropland area is essential to ensure food security in China. In recent years, China's food production has been increasing, but it is still facing the challenge of multiple difficulties in stabilizing the quantity, improving the quality, and preserving the ecology of cropland (Ministry of Agriculture Rural Affairs, 2021). To ensure food security, the actual cropland area in the country is maintained at 129 million hectares under the red line policy of 120 million hectares, which is about 12.7% of the national territory and ranks fourth in the world (Food Agriculture Organization of the United Nations, 2020). Therefore, valuing natural capital in China's cropland ecosystems is of importance for decision-makers, especially under the current national strategy (Song and Pijanowski, 2014; Jiang et al., 2016).

Ecosystem services mean the direct and indirect contributions of ecosystems to human society, representing part of the total economic value of the planet, including material services, regulating services, and cultural services (Costanza et al., 1997; Ouyang et al., 2016). The term "ecosystem services" is always used to assess natural resources and potential ecological benefits for human beings to survive and develop (Xu et al., 2021). For cropland ecosystems, the most important functions for human wellbeing and sustainable development are material product supply, climate regulation, soil retention, air purification, and carbon sequestration (Rodriguez-Entrena et al., 2014; Divinsky et al., 2017; Granado-Diaz et al., 2020). The values of these ecosystem services in croplands are enormous and often underappreciated (Power, 2010). Cropland ecosystems are facing the dual challenge of increasing food production while continuing to provide much-needed environmental goods and services (Cao et al., 2020). China's massive croplands make its ecosystems even more important for maintaining ecological balance, improving the environment, and protecting the basic conditions for human survival (Diaz et al., 2018; Losacco et al., 2021). Considering China's greater dependence on grain production, there will be a greater need for decision-makers to clarify changes in the provision and delivery of cropland ecosystem services to ensure self-sufficient agriculture production and sustainable cropland management (Fan et al., 2012).

There is a growing interest in the assessment and valuation of ecosystem services (Carpenter et al., 2006; Jackson et al., 2016; Gomez-Baggethun et al., 2019). The approaches from the perspective of social-ecological systems are used to analyze, assess, and quantify ecosystem services (Torres et al., 2021). For instance, the Millennium Ecosystem Assessment introduced a wide-disseminated framework for managing ecosystem services, showing the possibility of using economic valuation to value natural capital in ecosystems (Millennium Ecosystem Assessment., 2005). Previous studies used the economic valuation methods to better understand how ecosystems provide value to people and how to protect that value (Ranganathan, 2011). On this basis, more studies applied ecological-economic models to estimate the value of ecosystem services from forests, wetlands, and croplands at local and national levels (Dong et al., 2007; Guo et al., 2008; Nelson et al., 2009; Goldstein et al., 2012; Li et al., 2015; Ouyang et al., 2020). However, these approaches that translate ecosystems' contributions to the economy into monetary terms could be inconsistent, leading to their results that may not be comparable with each other.

To achieve a uniform measurement of ecosystem services, Ouyang et al. (2020) developed gross ecosystem product (GEP)

to summarize the value of the contributions of nature to economic activity in a single monetary metric. Analogous to gross domestic product (GDP), GEP uses market prices and surrogates to calculate the value of ecosystem services and then aggregate them into a measure of the ecosystems to human society. Their results demonstrated that it is feasible to produce an estimate of GEP with currently available data and methods, and GEP can provide decision-makers with a clear understanding of the monetary value of ecosystem services (Wang et al., 2019a; Liang et al., 2021). In recent years, the ministry of ecology and environment of the People's Republic of China has published the technical guideline on gross ecosystem product which allowed to assess China's GEP with finite data and methods (Chinese Academy of Environmental Planning Research Center for Eco-Environmental Sciences, 2020).

The GEP has been assessed in various studies, but it is still difficult to compare the results, especially in agriculture. On the one hand, there is a shortage of unified assessment methods. On the other hand, the range of estimation and indicators is not consistent. Relevant studies show that the assessment of GEP mostly focuses on ecosystems such as forests and wetlands, and there are few specific studies on croplands, let alone a nationwide assessment of cropland ecosystem services and differentiation of human and natural impacts. In this study, we conducted a comprehensive analysis using GEP as a metric of the monetary evaluation of the final ecosystem services to assess the stock of the ecosystem and the flow of value in China's cropland ecosystems and their drivers from 2001 to 2019. The GEP of material services, regulating services, and cultural services was calculated to account for food production, water retention, soil retention, carbon sequestration, air purification, climate control, biodiversity, and agricultural tourism. The biophysical quantities were estimated using the statistical survey method, precipitation storage method, RUSLE model, carbon sequestration mechanism model, pollutant purification model, and evapotranspiration model following the recommended approaches by the Technical Guideline on Gross Ecosystem Product. The market value method, travel cost method, shadow project method, replacement cost method, and conservation value method were used to calculate the monetary value. Moreover, we analyzed spatial and temporal patterns of GEP across China's cropland ecosystems over the past two decades. Furthermore, we further set up seven experimental scenarios and used the linear least square regression method with an *F*-test to evaluate the effects of natural factors (including precipitation, high-temperature days, and evapotranspiration) and social-economic factors (including acreage and prices) on inter-annual changes in GEP. The aims of our study are as follows: (1) to evaluate the spatial pattern of GEP across China's cropland ecosystems; (2) to analyze the temporal pattern of GEP in China at the provincial scale during 2001–2019; and (3) to assess the impacts of natural factors and social-economic factors on GEP variation between years.

Materials and methods

Data

In our research, there were mainly three types of data, namely, crop data, meteorological data, and geographic information, obtained from the government departments, the industry standards, and the literature. Data from the government departments included the planting areas, prices, DEM, and climate factors. They were selected mainly from the National Bureau of Statistics, the Ministry of Agriculture and Rural Affairs, the Shuttle Radar Topography Mission, the Chinese National Metrological Information Center, and so on (Supplementary Figure 1 and Supplementary Tables 1, 2). To better assess the GEP in China's cropland, two industry standards containing the Technical Guideline on Gross Ecosystem Product and Guidelines for measurement and estimation of soil erosion in production and construction projects (SL 773-2018) were used. Moreover, other data, such as parameters, were collected from reviewing the literature (Supplementary Table 3). More detailed data descriptions are provided in the Supplementary material.

The technical framework of China's cropland ecosystem assessment

Ecological assessment systems of China's GEP in cropland have considered the individual characteristics, structure, and ecological services. The accounting index of GEP was divided into three major services and six smaller classes. We chose the ecological services described above because previous studies have shown their importance to cropland ecosystems, and we had available data and methods to evaluate their value according to the Technical Guideline on Gross Ecosystem Product (Yuan et al., 2011; Li et al., 2016; Tzilivakis et al., 2019; Cai et al., 2020). Material services, regulating services, and cultural services are accounted for in Eq. (1). Furthermore, water retention, soil retention, carbon sequestration, air purification, climate control, and biodiversity are accounted for in Eq. (2), relative to data availability:

$$\mathbf{GEP} = \mathbf{EPV} + \mathbf{ERV} + \mathbf{ECV} \quad (1)$$

$$\mathbf{ERV} = \mathbf{WR} + \mathbf{SR} + \mathbf{CS} + \mathbf{AP} + \mathbf{CC} + \mathbf{BI} \quad (2)$$

where GEP is the value of the cropland gross ecosystem product; EPV is the value of cropland ecosystem products; ERV is the value of regulating services; ECV is the value of cultural services; WR, SR, CS, AP, CC, and BI represent the value of water retention, soil retention, carbon sequestration, air purification,

TABLE 1 Description of the evaluation methods of different types of ecosystem services.

Type	Description	Methods		Indexes used for evaluation	
		Biophysical	Monetary	Biophysical	Monetary
EPV	Products that humans can obtain from croplands	Statistical survey method	Market value method	Agricultural products	The output value of agricultural products
ECV	Provision of spiritual sensations and artistic experiences	Statistical survey method	Travel cost method	Number of tourists and level of consumption	Tourism income
WR	Interception and storage precipitation, enhancement of soil infiltration, and accumulation	Precipitation storage method	Shadow project method	Precipitation storage	Costs of constructing water storage and conservation facilities
SR	Protection of soil and reduction of water erosion	RUSLE model	Replacement cost method	Estimated average soil loss	Costs of reservoir dredging project and pollution treatment
CS	Absorption of CO_2 from the atmosphere to synthesize organic biomass and fix carbon in plants or soil	Carbon sequestration mechanism model	Market value method	Soil, fertilizer, and straw carbon sequestration	Trading prices in the Chinese major carbon market during 2018-2019
AP	Absorption and purifier air pollutants	Pollutant purification model	Replacement cost method	Absorption of sulfur dioxide, nitrogen oxides, particulates	Costs of purifying air pollutants according to the Environmental Protection Tax Law
CC	Reducing air temperature and increasing humidity	Evapotranspiration model	Replacement cost method	The total energy consumed by evapotranspiration	The electricity consumption price required for human adjustment of corresponding temperature and humidity
BI	Providing habitats for species	Statistical survey method	Conservation value method	Area of the nature reserve	Costs per unit area of the nature reserve

climate control, and biodiversity, respectively. All the variables were defined in Table 1.

The technical framework for the GEP of cropland contained two steps. First, the biophysical value of products and services was calculated by obtaining the output and quantity in China's cropland. To calculate the GEP, the biophysical value is measured followed by the monetary value. Second, we collected different prices to assess the monetary value. More detailed assessment methods are provided in Table 1 and Supplementary material.

Estimation of different influences of natural and social-economic factors on ecosystem services value

Experimental scenario design

To reveal the relationship between climate change, human activities, and GEP, we set up separate scenarios where the normal scenario allowed all the variables to change with time, and in the other scenarios, we kept one of all the variables at the 2001 level while allowing the other variables to change over time. These experimental scenarios considered both natural and social-economic influences on the biophysical and monetary value and also referred to the literature on driving factors of ecosystem services (Schroter et al., 2005; Haberl et al., 2007; Wang et al., 2016). To be specific, S_0, S_P, S_H, S_E, S_N, S_A, S_C, and S_S represent the scenarios of normal, no variation in precipitation, high-temperature days, evapotranspiration, all three natural factors, planting area, product prices, and two social-economic factors, respectively. Owing to some prices set by the government nationwide, therefore, we chose other drivers to compare in order to represent variation between provinces.

Analysis methods

The trends in material services, regulating services, cultural services, GEP, and all the scenarios in China's croplands were estimated using the linear least square regression method with an *F*-test. Moreover, we analyzed the correlation between the trend of GEP and natural factors (including precipitation, high-temperature days, and evapotranspiration) and social-economic factors (including planting area and prices) over the whole study area. To be specific, the dominant factor is chosen by selecting the maximum difference between the trend of S_0 and the trend of S_i (i is the kind of scenario).

Results

Spatial pattern of GEP across China's cropland ecosystems

To evaluate the spatial pattern of GEP across China's cropland ecosystems from 2001 to 2019, we accounted for the values of the material, regulating, and cultural services and then aggregated them into GEP at the provincial and national scales (Figure 1 and Supplementary Table 4). The multiyear mean values of material services, regulating services, and cultural services of China's cropland ecosystems were 4.76×10^6 million CNY, 3.86×10^7 million CNY, and 1.16×10^5 million CNY, respectively. The multiyear mean value of GEP was 4.35×10^7 million CNY. However, our results showed that the values of the material, regulating, and cultural services were different among provinces, leading to a heterogeneous spatial pattern of GEP across China's cropland ecosystems. Specifically, the values of material and regulating services in the southern provinces were higher than those in the northern provinces, and the values of cultural services were high in the provinces of the North China Plain and Guangdong Province. The spatial pattern of GEP was similar to that of regulating services across China's cropland ecosystems, implying that cropland ecosystems contributed more to regulating services in the southern provinces. Moreover, we found that one-quarter of the provinces (including Sichuan, Henan, Hunan, Hubei, Yunnan, Guangdong, and Guangxi) contributed to over 50% of the total values of GEP across China's cropland ecosystems. Unlike natural ecosystems, cropland ecosystems were associated with human activities. Most of those provinces with high GEP were located on the east side of the Heihe-Tengchong line. Therefore, the spatial pattern of GEP was influenced by the population and cultivated area of each province according to the GEP accounting method.

Temporal pattern of GEP across China's cropland ecosystems

To examine the temporal pattern of GEP across China's cropland ecosystems from 2001 to 2019, we analyzed the trends in the values of the material, regulating, cultural services, and GEP at the provincial and national scales (Figure 2 and Supplementary Table 4). The values of the material, regulating, and cultural services have increased at a rate of $(0.35 \pm 0.01) \times 10^6$ million CNY a^{-1}, $(1.12 \pm 0.10) \times 10^6$ million CNY a^{-1}, and $(0.002 \pm 0.0002) \times 10^6$ million CNY a^{-1}, respectively ($P < 0.05$). Over this period, GEP associated with China's cropland ecosystems has increased at a rate of $(1.47 \pm 0.11) \times 10^6$ million CNY a^{-1} ($P < 0.05$). Our results showed that the increase in the value of regulating services accounted for the majority of the increase in GEP over the past two decades. Specifically, the values of soil retention, climate control, water retention, carbon sequestration, air purification, and biodiversity have increased at a rate of $(0.86 \pm 0.08) \times 10^6$ million CNY a^{-1}, $(0.11 \pm 0.02) \times 10^6$ million CNY a^{-1}, $(0.10 \pm 0.01) \times 10^6$ million CNY a^{-1}, $(0.04 \pm 0.003) \times 10^6$ million CNY a^{-1}, $(0.004 \pm 0.001) \times 10^6$ million CNY a^{-1}, and $(0.004 \pm 0.0004) \times 10^6$ million CNY a^{-1}, respectively ($P < 0.05$). Moreover, our results showed that the changes in the values of the material, regulating, and cultural services were different among provinces, leading to a heterogeneous temporal pattern of GEP across China's cropland ecosystems. The provinces with a high multiyear mean GEP (including Sichuan, Henan, Hunan, Hubei, Yunnan, Guangdong, and Guangxi) have a large increase in GEP due to the fast rise of the value of regulating services. However, not all provinces showed an increase in GEP, e.g.,

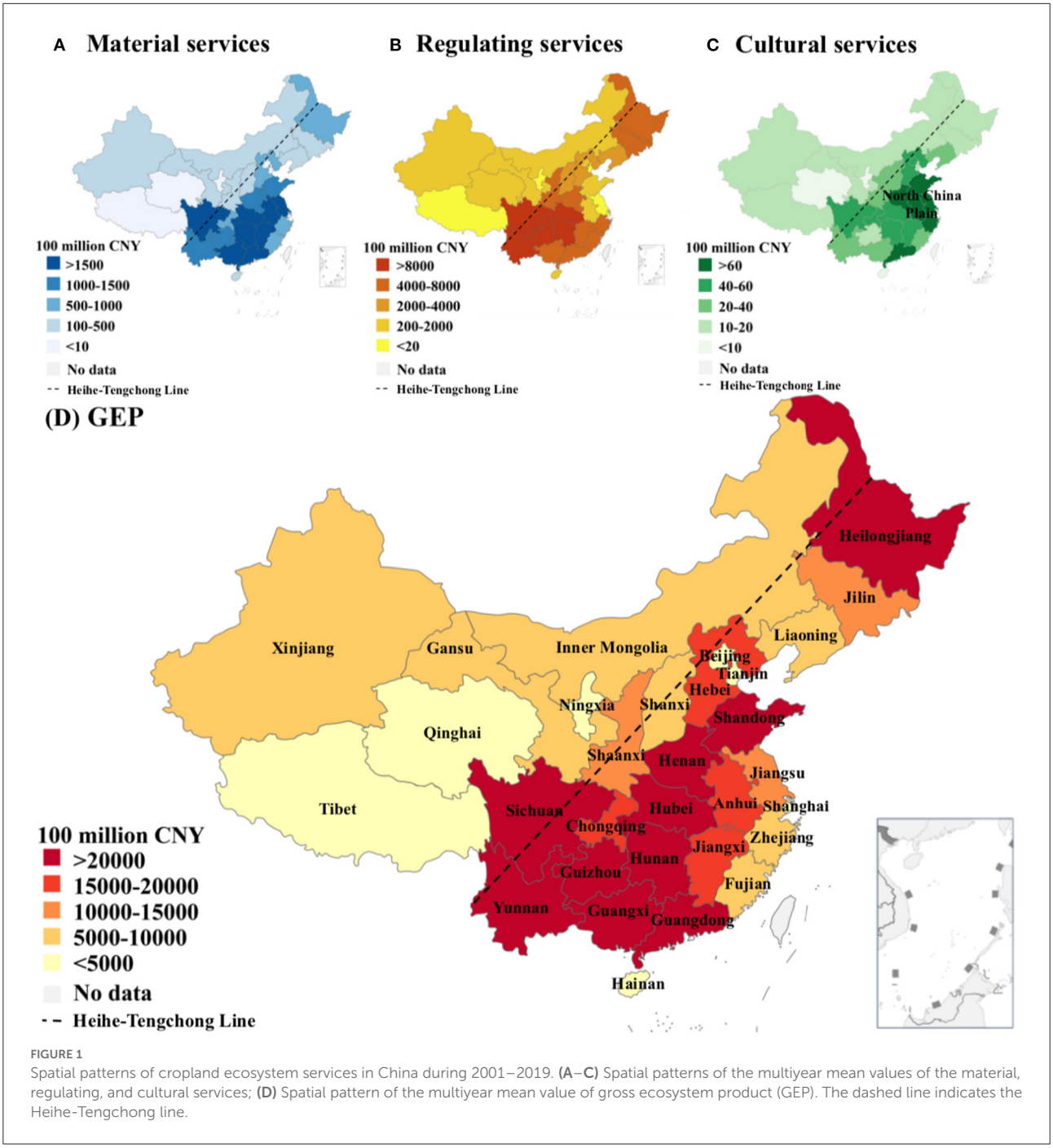

FIGURE 1
Spatial patterns of cropland ecosystem services in China during 2001–2019. **(A–C)** Spatial patterns of the multiyear mean values of the material, regulating, and cultural services; **(D)** Spatial pattern of the multiyear mean value of gross ecosystem product (GEP). The dashed line indicates the Heihe-Tengchong line.

Beijing and Shanghai. Similar to the spatial patterns of cropland ecosystem services in China, the temporal patterns showed an important role in regulating services in boosting the total GEP of cropland ecosystems in China, especially in the southern provinces. In addition, we found a rapid increase in GEP in Xinjiang and Inner Mongolia. With shifting the centers of population and economy, GEP growth may no longer be limited by the Heihe-Tengchong line.

Effects of natural and social-economic drivers on GEP

In this study, we performed several types of experimental scenarios to separate the effects of natural (i.e., precipitation, high-temperature days, and evapotranspiration) and social-economic (i.e., planting area and product prices) drivers on GEP during 2001–2019 (Figure 3 and Supplementary Table 5).

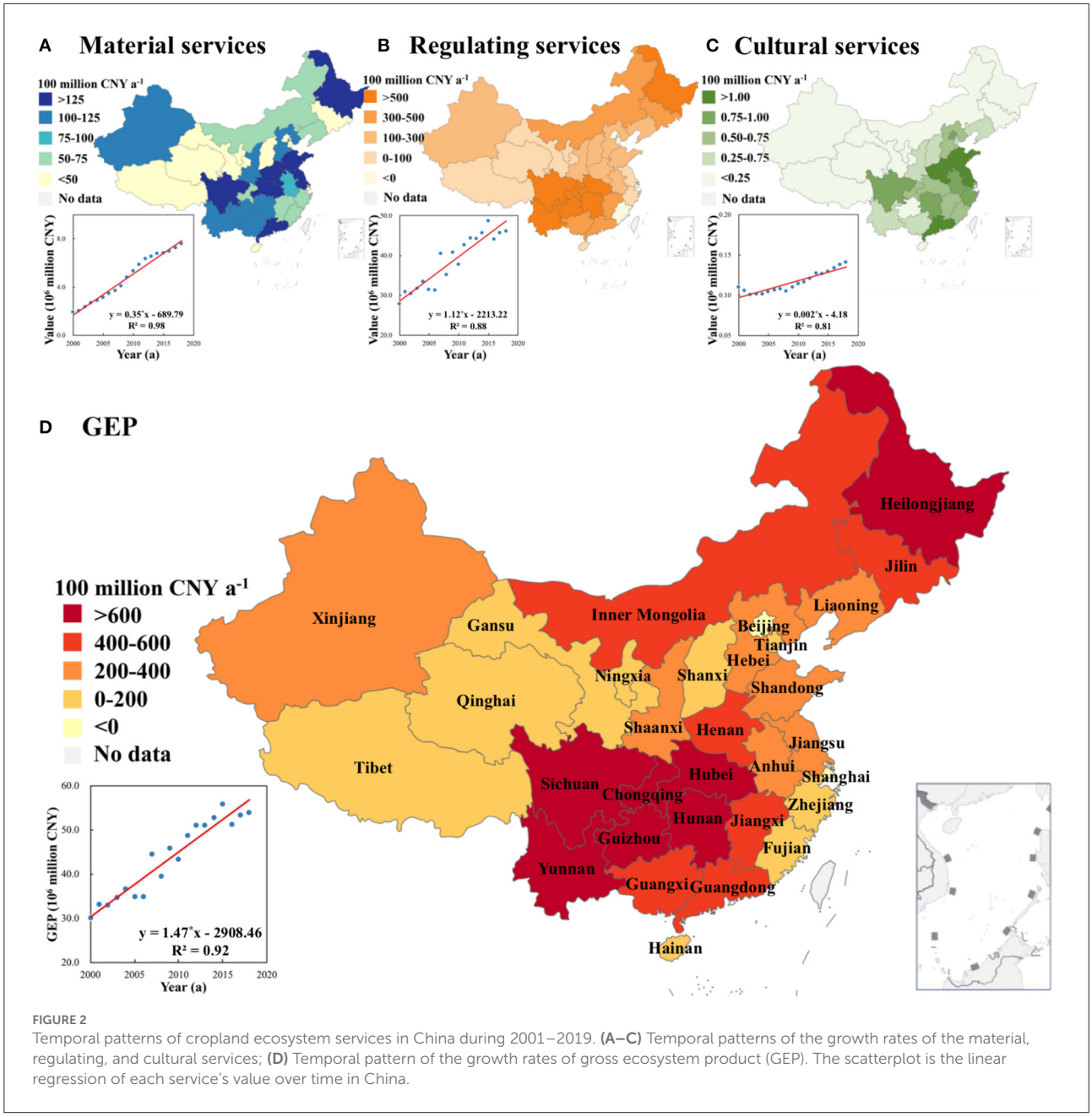

FIGURE 2
Temporal patterns of cropland ecosystem services in China during 2001–2019. **(A–C)** Temporal patterns of the growth rates of the material, regulating, and cultural services; **(D)** Temporal pattern of the growth rates of gross ecosystem product (GEP). The scatterplot is the linear regression of each service's value over time in China.

The normal scenario (S_0) allowed all the variables to change with time, showing a GEP trend at a rate of (1.47 ± 0.11) × 10^6 million CNY a^{-1} ($P < 0.05$). For the other scenarios, we held one of all the variables constant at its 2001 level, while allowing the other variables to change with time. Our results showed that the natural effects of precipitation, high-temperature days, and evapotranspiration on GEP were (1.10 ± 0.07) × 10^6 million CNY a^{-1}, (1.47 ± 0.11) × 10^6 million CNY a^{-1}, and (1.39 ± 0.10) × 10^6 million CNY a^{-1}, respectively. The effect of precipitation contributed to a significant increase in GEP during 2001–2019, accounting for (0.37 ± 0.09) × 10^6 million CNY a^{-1}. The total effect of natural drivers on GEP was (1.02 ± 0.06) × 10^6 million CNY a^{-1}. Moreover, the social-economic effects of planting area and prices on GEP were (1.19 ± 0.09) × 10^6 million CNY a^{-1} and (0.44 ± 0.06) × 10^6 million CNY a^{-1}, respectively. The effect of product prices contributed to a significant increase in GEP during 2001–2019, accounting for (1.03 ± 0.06) × 10^6 million CNY a^{-1}. The total effect of social-economic drivers on GEP was (0.23 ± 0.05) × 10^6 million CNY a^{-1}. Overall, we found that social-economic factors had a greater impact on GEP than natural factors, driving the increase

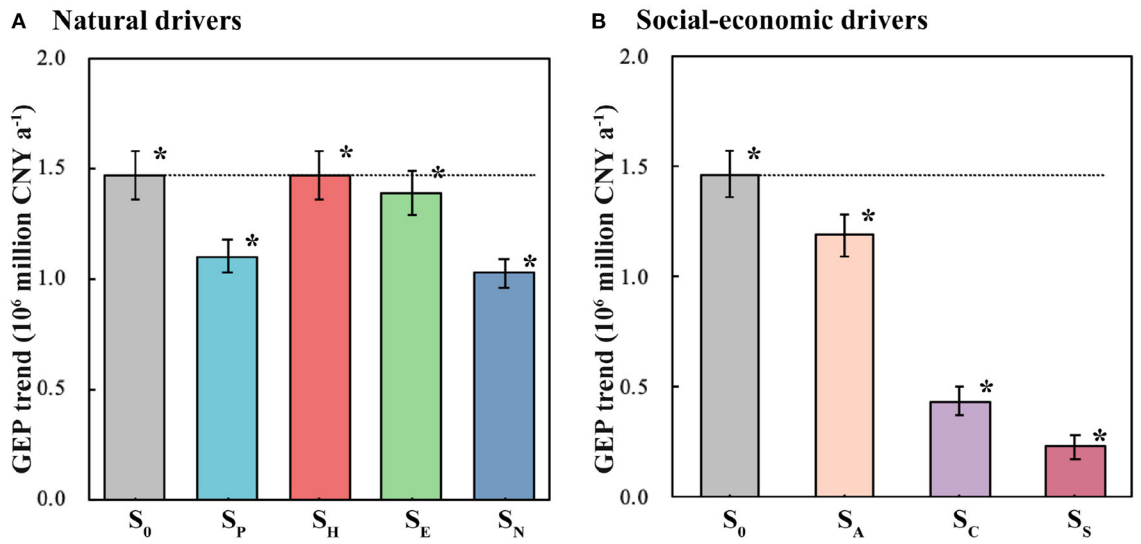

FIGURE 3
Effects of **(A)** natural and **(B)** social-economic drivers on GEP. S_0, S_P, S_H, S_E, S_N, S_A, S_C, and S_S represent the scenarios of normal, no variation in precipitation, high-temperature days, evapotranspiration, all three natural factors, planting area, product prices, and two social-economic factors, respectively. The dotted lines indicate the value of S_0. * indicates significance at the 0.05 level.

in ecosystem services in China's croplands over the past two decades.

Furthermore, we evaluated the effects of natural and social-economic drivers on GEP for each province during 2001–2019 (Figure 4 and Supplementary Table 6). Considering the uniformity of prices across 31 provinces in China, we only separated the effects of the other variables (i.e., precipitation, high-temperature days, evapotranspiration, and planting area) on GEP at the provincial scale. Our results showed that the trends in GEP were dominated by the changes in planting area in 20 of the 31 provinces over the past two decades. Specifically, the increases in planting area led to the growth of GEP in most provinces, such as Hunan, Yunnan, and Guizhou. However, for the provinces with faster economic development, such as Guangdong, Fujian, Hebei, Zhejiang, Hainan, Shanghai, Tianjin, and Beijing, the decreases in planting area resulted in slow growth and even a decrease in GEP. In addition, the changes in precipitation dominated the growth of GEP by affecting 8 of the 31 provinces, including Sichuan, Hubei, Jiangxi, and so on. Meanwhile, the changes in evapotranspiration dominated the growth of GEP affecting 3 of the 31 provinces, including Guangxi, Shandong, and Tibet. As we mentioned above, the changes in GEP were more relevant to social-economic factors rather than natural factors at both the provincial and national scales. China's social-economic policies (e.g., land-use change, ecological redline policy, and macro-economic control) exhibited a significant role in cropland ecosystem services over the past two decades.

Discussion

As the foundation of social development, agriculture has consistently played an irreplaceable role in the national economy (Swinton et al., 2007; Power, 2010; Schipanski et al., 2014). The assessment of products and services within croplands helps to better understand the current state of agricultural development (Duguma et al., 2019; Balzan et al., 2020). However, many ecosystem services have indirect market-based prices in the current assessment system, and each service has different price accounting methods, making the assessment results more dependent on choices of distinct methods and consequently less comparable (Polasky et al., 2015). Therefore, a valuation was carried out for the cropland ecosystem services in China during 2001–2019 for 31 provinces (autonomous regions and municipalities) in our study, aiming to address the uncertainty of existing assessment strategies for the selection of indicators and inter-annual variables for each province. For example, Xie et al. (2015) calculated the value of the ecological services equivalent factor for rice, wheat, and maize. The factor was only defined as the value of the natural production of croplands with a national average yield of 3406.5 CNY·hm^{-2}. After adding ecological services of croplands, the value has increased to 12919.2 CNY·hm^{-2} (Huang et al., 2022). Compared with previous studies, our estimated GEP is slightly larger than their findings (Chen et al., 2020; Yang et al., 2020; Jia et al., 2021). The major reason could be due to the selection of ecosystem indicators, inconsistent pricing methods for products and services, and inter-annual variations in model parameters. Some previous

10.3389/fevo.2022.959329

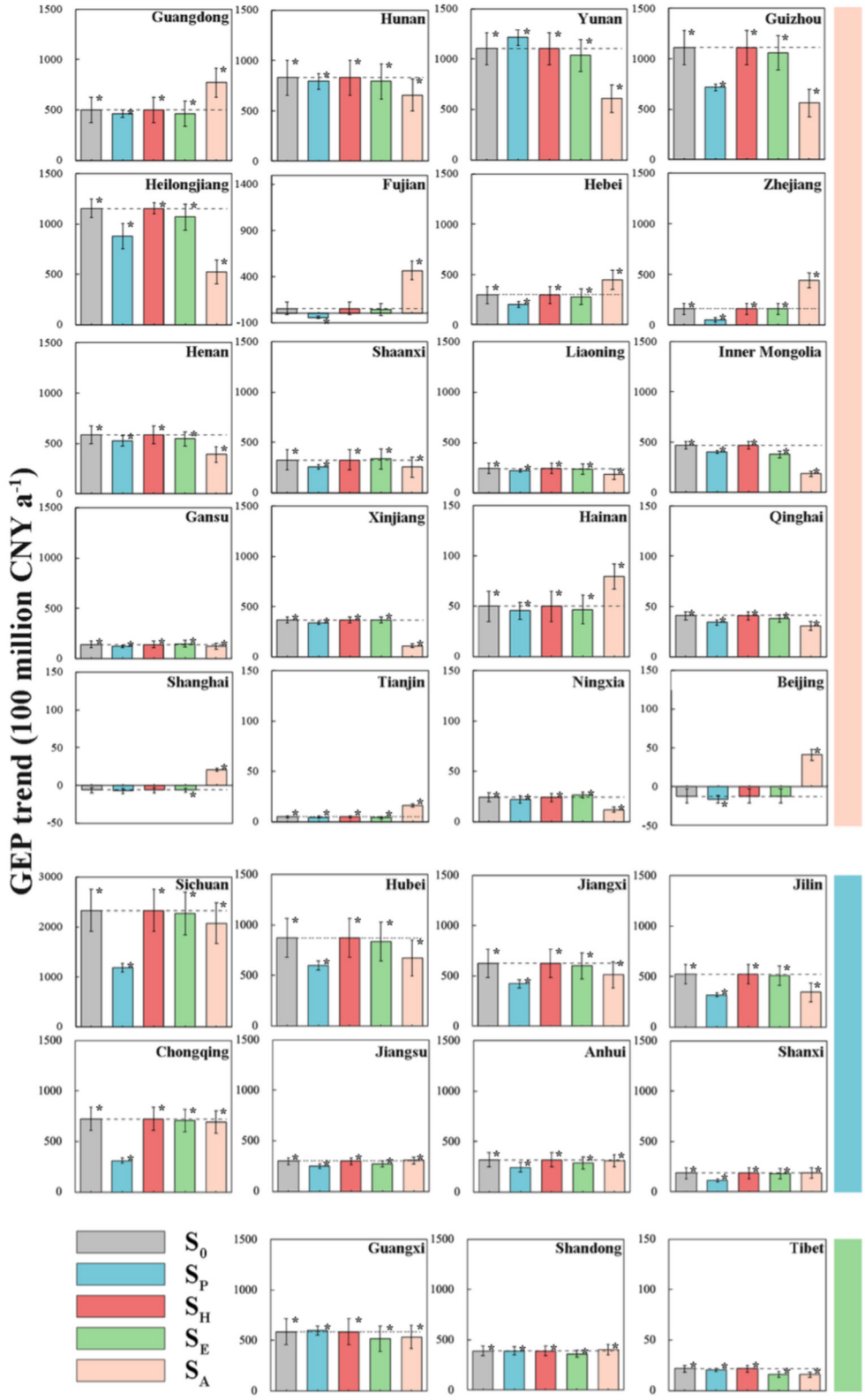

FIGURE 4
Effects of natural and social-economic drivers on GEP for 31 provinces in China. S_0, S_P, S_H, S_E, S_N, S_A, S_C, and S_S represent the scenarios of normal, no variation in precipitation, high-temperature days, evapotranspiration, all three natural factors, planting area, product prices, and two social-economic factors, respectively. The dotted lines indicate the value of S_0. * indicates significance at the 0.05 level. The colors of the rectangle on the right side indicate the dominant driver.

studies have concluded that material services were the dominant services of cropland ecosystem, which is mainly attributed to the fact that the material produced in the previous studies contained the additional products of cropland. For example, Yin et al. (2022) considered the value of straw, which was included in the carbon sequestration of regulating services in our study. In addition, compared with previous studies, we integrated more regulating services subsets to further expand its value (Bai et al., 2010; Marinidou et al., 2019; Cai et al., 2020). Therefore, it is recommended to strengthen the standardization of essential aspects such as ecological product assessment framework, index system, methods, and key parameters in the research of GEP, so as to achieve the systematic, repeatability, and horizontal comparability of results.

In our study, we found that the values of the southern provinces were generally higher than those of the northern provinces. More than half of China's croplands were in Hebei, Shandong, Henan, Shanxi, Heilongjiang, Jilin, Liaoning, and Sichuan (Song and Deng, 2017). However, China's precipitation resources were abundant but unbalanced, leading to a spatially heterogeneous distribution of GEP (Wang et al., 2016). Moreover, the provinces with high GEP were located on the east side of the Heihe-Tengchong line, which indicates a positive correlation between agriculture, population density, and topography (Wang et al., 2019b). Our results also showed that the major reasons why GEP was increasing in most of China's provinces were the effects of variation in price, planting area, and precipitation. Similarly, the findings on population, social-economic level, and industry scale for spatial heterogeneity have been proved in other studies (Gordeev et al., 2021; Wang et al., 2021, 2022; Zeng and Wang, 2022). In China, the effects of population growth and urbanization were significant. The decrease in food supplies has made structural inflation inevitable (Durevall et al., 2013). China's government has implemented a policy of agricultural subsidies to encourage cultivation, which was aiming at maintaining planting areas and safeguarding production (Huang and Yang, 2017). However, due to economic development accelerating the process of urbanization and reducing planting area, the two provinces where GEP was decreasing were Beijing and Shanghai. Due to the responses exhibited in both areas, specific ecological protection policies should be adopted. Besides, the provinces that were influenced by precipitation were mostly distributed along the Yangtze River. The phenomenon may be caused by the significant effects of meteorological factors on the extreme precipitation of the Yangtze River (Zou et al., 2021).

At present, the assessment of GEP in croplands is still in a developing stage, there are many imperfections. The effort in this study represents a start toward accounting of GEP in croplands, but much work remains. First, data limitations lead to an inaccurate estimation of assessment. Therefore, it is important to improve the scale, resolution, and frequency of data collection to examine a comprehensive and accurate accounting. Second, the growth periods of different plants should be considered in the calculation and using meteorological data at different stages. Maybe we estimated the contribution of croplands slightly higher than it actually was by using annual data. Third, although we have considered the influence of three natural factors and two social-economic factors and set up seven different scenarios based on each ecosystem service assessment process and referring to previous literature, the drivers of cropland ecosystems are still complex and various. We need to measure more comprehensively the drivers of cropland ecosystems, such as the population density and the transfer of GEP in croplands among provinces after policy regulation. This is an issue that needs to be considered in the future.

Conclusion

This study uses GEP as a metric of the monetary evaluation of final ecosystem services to estimate the stock of the ecosystem and the flow of value in China's cropland ecosystems and their drivers from 2001 to 2019 based on crop data, meteorological data, and geographic information. The study presents the following conclusions: (1) The average of China's GEP in croplands over the past two decades was 4.35×10^7 million CNY. From the perspective of different ecosystem services, the value of regulating services reached 3.86×10^7 million CNY and accounted for 88.78% of the gross ecosystem products. This was followed by material services 4.76×10^6 million CNY and cultural services 1.16×10^5 million CNY. Specifically, the values in the southern provinces were higher than those in the northern provinces. (2) In general, the temporal pattern of GEP across China's cropland ecosystems showed a positive trend during 2001–2019. GEP associated with China's cropland ecosystems has increased at a rate of $(1.47 \pm 0.11) \times 10^6$ million CNY a^{-1} ($P < 0.05$). The values of the material, regulating, and cultural services have increased at a rate of $(0.35 \pm 0.01) \times 10^6$ million CNY a^{-1}, $(1.12 \pm 0.10) \times 10^6$ million CNY a^{-1}, and $(0.002 \pm 0.0002) \times 10^6$ million CNY a^{-1}, respectively ($P < 0.05$). Within the regulating services, the value of soil retention increased most rapidly, followed by climate control, water retention, and carbon sequestration, and the slowest was in the values of air purification and biodiversity. However, not all provinces showed an increase in GEP, e.g., Beijing and Shanghai. (3) In addition, social-economic factors have contributed more to cropland GEP than natural factors. In particular, inflation has significantly improved GEP over the past two decades. Furthermore, except for economic factors, the planting area influenced most provinces. It is expected that the results of our study will provide a novel insight for the future ecological assessments of cropland. This information will assist stakeholders in the scientific management of agriculture in China and draw greater attention to the utility of its resources.

Data availability statement

The original contributions presented in the study are included in the article/Supplementary material, further inquiries can be directed to the corresponding author/s.

Author contributions

JZ collected and calculated the data and wrote the manuscript. YS helped design the structure of the manuscript and revised it. JW was involved in the study design and critically revised the manuscript. All authors have contributed to the article and approved the submitted version.

Funding

This research was supported by the National Key Research and Development Program of China (2021YFD1901104) and the 2115 Talent Development Program of China Agricultural University (00109016).

Acknowledgments

We would like to acknowledge the Chinese Academy of Environment Planning and Research Center for Eco-Environmental Sciences (CAS) for proposing the method of GEP assessment. We acknowledge all the producers of the datasets used in this study. We thank the editors and three reviewers for their constructive comments to further improve the quality of this manuscript.

Conflict of interest

The authors declare that the research was conducted in the absence of any commercial or financial relationships that could be construed as a potential conflict of interest.

Publisher's note

All claims expressed in this article are solely those of the authors and do not necessarily represent those of their affiliated organizations, or those of the publisher, the editors and the reviewers. Any product that may be evaluated in this article, or claim that may be made by its manufacturer, is not guaranteed or endorsed by the publisher.

Supplementary material

The Supplementary Material for this article can be found online at: https://www.frontiersin.org/articles/10.3389/fevo.2022.959329/full#supplementary-material

References

Bai, Y., Ouyang, Z. Y., and Zheng, H. (2010). Environmental benefit-loss analysis of agro-ecosystem in Haihe River basin, China. *Chin. J. Appl. Ecol.* 21, 2938–2945. doi: 10.13287/j.1001-9332.2010.0409

Balzan, M. V., Sadula, R., and Scalvenzi, L. (2020). Assessing ecosystem services supplied by agroecosystems in Mediterranean Europe: a literature review. *Land-Basel* 9, 245–266. doi: 10.3390/land9080245

Cai, S. Z., Zhang, X. L., Cao, Y. H., Zhang, Z. H., and Wang, W. (2020). Values of the farmland ecosystem services of Qingdao City, China, and their changes. *J. Resour. Ecol.* 11, 443–453. doi: 10.5814/j.issn.1674-764x.2020.05.002

Cao, Y., Li, G. Y., Tian, Y. H., Fang, X. Q., Li, Y., and Tan, Y. Z. (2020). Linking ecosystem services trade-offs, bundles and hotspot identification with cropland management in the coastal Hangzhou Bay area of China. *Land Use Policy* 97, 104689. doi: 10.1016/j.landusepol.2020.104689

Carpenter, S. R., DeFries, R., Dietz, T., Mooney, H. A., Polasky, S., Reid, W. V., et al. (2006). Millennium ecosystem assessment: research needs. *Science* 314, 257–258. doi: 10.1126/science.1131946

Chen, J., Yu, L. X., Yan, F. Q., and Zhang, S. W. (2020). Ecosystem service loss in response to agricultural expansion in the small Sanjiang Plain, Northeast China: process, driver and management. *Sustainability* 12, 2430–2445. doi: 10.3390/su12062430

Chinese Academy of Environmental Planning and Research Center for Eco-Environmental Sciences. (2020). *The Technical Guideline on Gross Ecosystem Product (GEP) (1.0 Version)*. Accessed online at: http://www.caep.org.cn/zclm/sthjyjjhszx/zxdt_21932/202010/W020201029488841168291.pdf (accessed September 30, 2020).

Costanza, R., dArge, R., deGroot, R., Farber, S., Grasso, M., Hannon, B., et al. (1997). The value of the world's ecosystem services and natural capital. *Nature* 387, 253–260.

Diaz, S., Pascual, U., Stenseke, M., Martin-Lopez, B., Watson, R. T., Molnar, Z., et al. (2018). Assessing nature's contributions to people. *Science* 359, 270–272. doi: 10.1126/science.aap8826

Divinsky, I., Becker, N., and Bar, P. (2017). Ecosystem service tradeoff between grazing intensity and other services: a case study in Karei-Deshe experimental cattle range in northern Israel. *Ecosyst. Serv.* 24, 16–27. doi: 10.1016/j.ecoser.2017.01.002

Dong, X. B., Gao, W. S., Chen, Y. Q., and Liang, W. L. (2007). Valuation of fragile agro-ecosystem services in the Loess region: a case study of Ansai county in China. *Outlook Agr.* 36, 247–253. doi: 10.5367/000000007783418561

Duguma, M. S., Feyssa, D. H., and Biber-Freudenberger, L. (2019). Agricultural biodiversity and ecosystem services of major farming systems: a case study in Yayo coffee forest biosphere reserve, Southwestern Ethiopia. *Agriculture* 9, 48–74. doi: 10.3390/agriculture9030048

Durevall, D., Loening, J. L., and Birru, Y. A. (2013). Inflation dynamics and food prices in Ethiopia. *J. Dev. Econ.* 104, 89–106. doi: 10.1016/j.jdeveco.2013.05.002

Fan, M. S., Shen, J. B., Yuan, L. X., Jiang, R. F., Chen, X. P., Davies, W. J., et al. (2012). Improving crop productivity and resource use efficiency to ensure food security and environmental quality in China. *J. Exp. Bot.* 63, 13–24. doi: 10.1093/jxb/err248

Fan, Y. (2011). *Study on Ecological Civilization Construction with Characteristic of China* (Doctoral thesis). Wuhan: Wuhan University.

Feng, Y. X., He, S. W., and Li, G. D. (2021). Interaction between urbanization and the eco-environment in the Pan-Third Pole region. *Sci. Total Environ*. 789, 140811. doi: 10.1016/j.scitotenv.2021.148011

Food and Agriculture Organization of the United Nations. (2020). *FAO Statistics*. Available online at: https://www.fao.org/faostat (accessed September 1, 2021).

Goldstein, J. H., Caldarone, G., Duarte, T. K., Ennaanay, D., Hannahs, N., Mendoza, G., et al. (2012). Integrating ecosystem-service tradeoffs into land-use decisions. *Proc. Natl. Acad. Sci. U. S. A*. 109, 7565–7570. doi: 10.1073/pnas.1201040109

Gomez-Baggethun, E., Tudor, M., Doroftei, M., Covaliov, S., Nastase, A., Onara, D. F., et al. (2019). Changes in ecosystem services from wetland loss and restoration: an ecosystem assessment of the Danube Delta (1960–2010). *Ecosyst. Serv*. 39, 100965. doi: 10.1016/j.ecoser.2019.100965

Gordeev, R. V., Pyzhev, A. I., and Yagolnitser, M. A. (2021). Drivers of spatial heterogeneity in the Russian forest sector: a multiple factor analysis. *Forests*. 12, 1635. doi: 10.3390/f12121635

Granado-Diaz, R., Gomez-Limon, J. A., Rodriguez-Entrena, M., and Villanueva, A. J. (2020). Spatial analysis of demand for sparsely located ecosystem services using alternative index approaches. *Eur. Rev. Agric. Econ*. 47, 752–784. doi: 10.1093/erae/jbz036

Guo, H., Wang, B., Ma, X. Q., Zhao, G. D., and Li, S. N. (2008). Evaluation of ecosystem services of Chinese pine forests in China. *Sci. China Ser. C*. 51, 662–670. doi: 10.1007/s11427-008-0083-z

Haberl, H., Erb, K. H., Krausmann, F., Gaube, V., Bondeau, A., Plutzar, C., et al. (2007). Quantifying and mapping the human appropriation of net primary production in earth's terrestrial ecosystems. *Proc. Natl. Acad. Sci. U. S. A*. 104, 12942–12945. doi: 10.1073/pnas.0704243104

Huang, H. C., Lei, M., Kong, X. B., and Wen, L. Y. (2022). Spatial pattern change of cultivated land and response of ecosystem service value in China. *Res. Soil Water Conserv*. 29, 339–348.

Huang, J. K., and Yang, G. L. (2017). Understanding recent challenges and new food policy in China. *Glob Food Secur. Agric*. 12, 119–126. doi: 10.1016/j.gfs.2016.10.002

Intergovernmental Panel on Climate Change (IPCC). (2018). *Global Warming of 1.5°C: An IPCC Special Report on the Impacts of Global Warming of 1.5°C Above Pre-Industrial Levels and Related Global Greenhouse Gas Emission Pathways, in the Context of Strengthening the Global Response to the Threat of Climate Change, Sustainable Development, and Efforts to Eradicate Poverty*. Geneva: World Meteorological Organization.

Jackson, S. T., Duke, C. S., Hampton, S. E., Jacobs, K. L., Joppa, L. N., Kassam, K. A. S., et al. (2016). Toward a national, sustained US ecosystem assessment. *Science* 354, 838–839. doi: 10.1126/science.aah5750

Jia, Y., Liu, Y., and Zhang, S. (2021). Evaluation of agricultural ecosystem service value in arid and semiarid regions of northwest China based on the equivalent factor method. *Environ. Process*. 8, 713–727. doi: 10.1007/s40710-021-00514-2

Jiang, H. Q., Wu, W. J., Wang, J. N., Yang, W. S., Gao, Y. M., Duan, Y., et al. (2021). Mapping global value of terrestrial ecosystem services by countries. *Ecosyst. Serv*. 52, 101361. doi: 10.1016/j.ecoser.2021.101361

Jiang, M., Xin, L. J., Li, X. B., and Tan, M. H. (2016). Spatiotemporal variation of China's state-owned construction land supply from 2003 to 2014. *Sustainability* 8, 1137. doi: 10.3390/su8111137

Lambin, E. F., and Meyfroidt, P. (2011). Global land use change, economic globalization, and the looming land scarcity. *Proc. Natl. Acad. Sci. U. S. A*. 108, 3465–3472. doi: 10.1073/pnas.1100480108

Li, S. N., Zhang, J. J., Chen, J., and Zhao, Y. H. (2016). Review on farmland ecosystem services and its valuation. *J. Hebei Agric. Sci*. 20, 87–94. doi: 10.16318/j.cnki.hbnykx.2016.03.023

Li, Y. L., Deng, H. B., and Dong, R. C. (2015). Prioritizing protection measures through ecosystem services valuation for the Napahai Wetland, Shangri-La County, Yunnan Province, China. *Int. J. Sust. Dev. World* 22, 142–150. doi: 10.1080/13504509.2014.926298

Li, Z. H., Wang, J., Kong, X. S., Zhang, B. E., Liu, J. J., Ding, S., et al. (2021). Effects of ecosystems preservation on economic growth in China's coastal region: Multilevel modeling and exploration. *Ecol. Indic*. 132, 108224. doi: 10.1016/j.ecolind.2021.108224

Liang, L. N., Siu, W. S., Wang, M. X., and Zhou, G. J. (2021). Measuring gross ecosystem product of nine cities within the Pearl River Delta of China. *Environ. Chall*. 4, 100105. doi: 10.1016/j.envc.2021.100105

Losacco, D., Ancona, V., De Paola, D., Tumolo, M., Massarelli, C., Gatto, A., et al. (2021). Development of ecological strategies for the recovery of the main nitrogen agricultural pollutants: a review on environmental sustainability in agroecosystems. *Sustainability* 13, 7163–7180. doi: 10.3390/su13137163

Ma, K. P., and Wei, F. W. (2021). Ecological civilization: a revived perspective on the relationship between humanity and nature. *Natl. Sci. Rev*. 8, 112. doi: 10.1093/nsr/nwab112

Ma, T. X., Hu, Y. S., Wang, M., Yu, L. J., and Wei, F. W. (2021). Unity of nature and man: a new vision and conceptual framework for the post-2020 global biodiversity framework. *Natl. Sci. Rev*. 8, 265. doi: 10.1093/nsr/nwaa265

Marinidou, E., Jimenez-Ferrer, G., Soto-Pinto, L., Ferguson, B. G., and Saldivar-Moreno, A. (2019). Agro-ecosystem services assessment of silvopastoral experiences in Chiapas, Mexico: towards a methodological proposal. *Exp. Agric*. 55, 21–37. doi: 10.1017/S0014479717000539

Millennium Ecosystem Assessment. (2005). *Ecosystems and Human Well-Being: Synthesis*. Washington, DC: Island Press

Ministry of Agriculture and Rural Affairs. (2021). *14th Five-Year National Agriculture Green Development Plan*. Available online at: http://www.moa.gov.cn/nybgb/2021/202109/202112/t20211207_6384020.htm (accessed March 23, 2022).

Naustdalslid, J. (2014). Circular economy in China: the environmental dimension of the harmonious society. *Int. J. Sust. Dev. World* 21, 303–313. doi: 10.1080/13504509.2014.914599

Nelson, E., Mendoza, G., Regetz, J., Polasky, S., Tallis, H., Cameron, D. R., et al. (2009). Modeling multiple ecosystem services, biodiversity conservation, commodity production, and tradeoffs at landscape scales. *Front. Ecol. Environ*. 7, 4–11. doi: 10.1890/080023

Ouyang, Z., Zheng, H., Xiao, Y., Polasky, S., Liu, J., Xu, W., et al. (2016). Improvements in ecosystem services from investments in natural capital. *Science* 352, 1455–1459. doi: 10.1126/science.aaf2295

Ouyang, Z. Y., Song, C. S., Zheng, H., Polasky, S., Xiao, Y., Bateman, I. J., et al. (2020). Using gross ecosystem product (GEP) to value nature in decision making. *Proc. Natl. Acad. Sci. U. S. A*. 117, 14593–14601. doi: 10.1073/pnas.1911439117

Polasky, S., Kling, C. L., Levin, S. A., Carpenter, S. R., Daily, G. C., Ehrlich, P. R., et al. (2019). Role of economics in analyzing the environment and sustainable development. *Proc. Natl. Acad. Sci. U. S. A*. 116, 5233–5238. doi: 10.1073/pnas.1901616116

Polasky, S., Tallis, H., and Reyers, B. (2015). Setting the bar: standards for ecosystem services. *Proc. Natl. Acad. Sci. U. S. A*. 112, 7356–7361. doi: 10.1073/pnas.1406490112

Power, A. G. (2010). Ecosystem services and agriculture: tradeoffs and synergies. *Philos. Trans. R. Soc. B*. 365, 2959–2971. doi: 10.1098/rstb.2010.0143

Ranganathan, J. (2011). *Natural Capital: Theory and Practice of Mapping Ecosystem Services*. New York, NY: Oxford University Press.

Rodriguez-Entrena, M., Espinosa-Goded, M., and Barreiro-Hurle, J. (2014). The role of ancillary benefits on the value of agricultural soils carbon sequestration programmes: evidence from a latent class approach to Andalusian olive groves. *Ecol. Econ*. 99, 63–73. doi: 10.1016/j.ecolecon.2014.01.006

Schipanski, M. E., Barbercheck, M., Douglas, M. R., Finney, D. M., Haider, K., Kaye, J. P., et al. (2014). A framework for evaluating ecosystem services provided by cover crops in agroecosystems. *Agric. Syst*. 125, 12–22. doi: 10.1016/j.agsy.2013.11.004

Schroter, D., Cramer, W., Leemans, R., Prentice, I. C., Araujo, M. B., Arnell, N. W., et al. (2005). Ecosystem service supply and vulnerability to global change in Europe. *Science* 310, 1333–1337. doi: 10.1126/science.1115233

Skinner, M. W., Kuhn, R. G., and Joseph, A. E. (2001). Agricultural land protection in China: a case study of local governance in Zhejiang Province. *Land Use Policy* 18, 329–340. doi: 10.1016/S0264-8377(01)00026-6

Song, W., and Deng, X. Z. (2017). Land-use/land-cover change and ecosystem service provision in China. *Sci. Total Environ*. 576, 705–719. doi: 10.1016/j.scitotenv.2016.07.078

Song, W., and Pijanowski, B. C. (2014). The effects of China's cultivated land balance program on potential land productivity at a national scale. *Appl. Geogr*. 46, 158–170. doi: 10.1016/j.apgeog.2013.11.009

Swinton, S. M., Lupi, F., Robertson, G. P., and Hamilton, S. K. (2007). Ecosystem services and agriculture: cultivating agricultural ecosystems for diverse benefits. *Ecol. Econ*. 64, 245–252. doi: 10.1016/j.ecolecon.2007.09.020

Torres, A. V., Tiwari, C., and Atkinson, S. F. (2021). Progress in ecosystem services research: a guide for scholars and practitioners. *Ecosyst. Serv*. 49, 101267. doi: 10.1016/j.ecoser.2021.101267

Tzilivakis, J., Warner, D. J., and Holland, J. M. (2019). Developing practical techniques for quantitative assessment of ecosystem services on farmland. *Ecol. Indic*. 106, 105514. doi: 10.1016/j.ecolind.2019.105514

van Vliet, J., Eitelberg, D. A., and Verburg, P. H. (2017). A global analysis of land take in cropland areas and production displacement from urbanization. *Glob. Environ. Change* 43, 107–115. doi: 10.1016/j.gloenvcha.2017.02.001

Wang, F., Zhang, S. L., Hou, H. P., Yang, Y. J., and Gong, Y. L. (2019a). Assessing the changes of ecosystem services in the Nansi lake wetland, China. *Water* 11, 788. doi: 10.3390/w11040788

Wang, H., Zhou, S. L., Li, X. B., Liu, H. H., Chi, D. K., and Xu, K. K. (2016). The influence of climate change and human activities on ecosystem service value. *Ecol. Eng.* 87, 224–239. doi: 10.1016/j.ecoleng.2015.11.027

Wang, H. Z., Pan, X. M., and Zhang, S. B. (2021). Spatial autocorrelation, influencing factors and temporal distribution of the construction and demolition waste disposal industry. *Waste Manage.* 127, 158–167. doi: 10.1016/j.wasman.2021.04.025

Wang, Z., Xia, H. B., Tian, Y., Wang, K., Hua, H., Geng, W. J., et al. (2019b). A big-data analysis of HU Line existence in the ecology view and new economic geographical understanding based on population distribution. *Acta Ecol. Sin.* 39, 5166–5177. doi: 10.5846/stxb201812212776

Wang, Z. S., Zhang, Z. S., and Liu, J. K. (2022). Exploring spatial heterogeneity and factors influencing construction and demolition waste in China. *Environ. Sci. Pollut. R.* doi: 10.1007/s11356-022-19554-8

World Bank, GDP statistics. (2020). Available online at: https://data.worldbank.org.cn/country/china. (accessed July 1, 2021).

Xie, G. D., Zhang, C. X., Zhang, L. M., Chen, W. H., Li, S. M., et al. (2015). Improvement of the evaluation method for ecosystem service value based on per unit area. *J. Nat. Resour.* 30, 1243–1254. doi: 10.11849/zrzyxb.2015.08.001

Xu, Y. N., Wei, J. N., Li, Z. J., Zhao, Y. X., Lei, X. Y., Sui, P., et al. (2021). Linking ecosystem services and economic development for optimizing land use change in the poverty areas. *Ecosyst. Health Sust.* 7, 325–336. doi: 10.1080/20964129.2021.1877571

Yang, H., and Li, X. B. (2000). Cultivated land and food supply in China. *Land Use Policy* 17, 73–88. doi: 10.1016/S0264-8377(00)00008-9

Yang, Y. J., Wang, K., Liu, D., Zhao, X. Q., and Fan, J. W. (2020). Effects of land-use conversions on the ecosystem services in the agro-pastoral ecotone of northern China. *J. Clean Prod.* 249, 119360. doi: 10.1016/j.jclepro.2019.119360

Yin, Y., Xi, F. M., Bing, L. F., and Wang, J. Y. (2022). A quantitative study on cultivated land compensation based on ecological value accounting——Taking Shenyang city as an example. *Nat. Resour. Econ. China*. doi: 10.19676/j.cnki.1672-6995.000750

Yuan, Y., Liu, J. T., and Jin, Z. D. (2011). An integrated assessment of positive and negative effects of high-yielding cropland ecosystem services in Luancheng County, Hebei Province of North China. *Chin. J. Ecol.* 30, 2809–2814. doi: 10.13292/j.1000-4890.2011.0412

Zeng, J. H., and Wang, C. (2022). Temporal characteristics and spatial heterogeneity of air quality changes due to the COVID-19 lockdown in China. *Resour. Conserv. Recy.* 181, 106223. doi: 10.1016/j.resconrec.2022.106223

Zhang, M. Y. (2012). Research on soil and water environmental problems in the construction of agro-ecological civilization: a case study of Henan Province. *Adv. Mater. Res. Switz.* 347–353, 2749–2753. doi: 10.4028/www.scientific.net/AMR.550-553.2749

Zheng, W. W., Ke, X. L., Zhong, T., and Yang, B. H. (2019). Trade-offs between cropland quality and ecosystem services of marginal compensated cropland: a case study in Wuhan, China. *Ecol. Indic.* 105, 613–620. doi: 10.1016/j.ecolind.2018.05.089

Zou, L., Xia, J., and Zhang, Y. (2021). Spatial-temporal characteristics of extreme precipitation in the middle and lower reaches of the Yangtze River. *Resour. Environ. Yangtze Basin*. 30, 1264–1274. doi: 10.11870/cjlyzyyhj202105023

frontiers | Frontiers in Environmental Science

ORIGINAL RESEARCH
published: 12 August 2022
doi: 10.3389/fenvs.2022.931937

Carbon Neutrality, International Trade, and Agricultural Carbon Emission Performance in China

Gaoya Li[1], *Cuiping Hou*[1] *and Xijun Zhou*[2]*

[1]Department of Accounting, Xinzhou Teachers University, Xinzhou, China, [2]Economics and Management Department, Xinzhou Teachers University, Xinzhou, China

International trade and agricultural development play important roles in carbon neutrality. This study uses the Malmquist index to quantify agricultural carbon emission performance and the panel data regression model to analyze the relationship between international trade and agricultural carbon emission performance. Data from 2005 to 2020 were used. The results show that the agricultural carbon emission of China has increased slowly since 2005. There is still an improvement space for low-carbon agricultural productivity. As for the relationship between agricultural international trade and carbon emission performance, the coefficient of the total trade in agricultural products is 0.0444. Suggestions on agricultural international trade and the development of low-carbon agricultural production are put forward, which will provide technical support for carbon neutrality.

Keywords: carbon neutral, international trade, agricultural carbon emission, spatial pattern, Malmquist index

OPEN ACCESS

Edited by:
Fan Zhang,
Institute of Geographic Sciences and Natural Resources Research (CAS), China

Reviewed by:
Wang MeiTu,
Shanxi Agricultural University, China
Maolin Liao,
Chinese Academy of Social Sciences (CASS), China

***Correspondence:**
Xijun Zhou
zxj19820511@126.com

Specialty section:
This article was submitted to Land Use Dynamics, a section of the journal Frontiers in Environmental Science

Received: *29 April 2022*
Accepted: *03 June 2022*
Published: *12 August 2022*

Citation:
Li G, Hou C and Zhou X (2022) Carbon Neutrality, International Trade, and Agricultural Carbon Emission Performance in China. Front. Environ. Sci. 10:931937. doi: 10.3389/fenvs.2022.931937

1 INTRODUCTION

Carbon reduction has become the inevitable choice and optimal path to dealing with climate change (Chang and Dong, 2016). The balance between agricultural carbon emissions and economic benefits resulting from trade liberalization and economic development has become an important development indicator (Yang, 2019a). The effects of trade liberalization on agricultural carbon emissions need to be quantified.

The development of China's agricultural trade has encountered major obstacles. After two consecutive years of decline (Bu et al., 2018), China's agricultural imports and trade deficit increased again in 2020. The total import and export of agricultural products exceeded US $200 billion, reaching record highs. The trade deficit, which had been shrinking in the past few years, has grown again, driven by rapid import growth (Wang et al., 2018; Sohlberg and Yvon, 2019). In the process of rapid economic growth, environmental pollution has become increasingly prominent, and global climate change caused by anthropogenic greenhouse gas emissions has become a global concern (Yu and Chen, 2017; Wu et al., 2018). On the relationship between environmental degradation and economic growth, various hypotheses, such as the Porter hypothesis, the pollution haven hypothesis, the resource curse, and the environmental Kuznets curve, have been proposed (Fu et al., 2018). The relationship between economic growth and carbon emissions is becoming a hot research topic in academia (Li, 2013; Yang, 2019b). Compared with the transportation and energy sectors, the agricultural sector contributes less to global emissions (Li, 2012). The rural revitalization strategy of China aims to realize sustainable development of rural areas, which contains requirements for environmental protection, such as establishment of environmental governance systems and improvement of living environments (Balsalobre-Lorente et al., 2019). The agricultural carbon budget of China benefits from trade surplus in major agricultural products, while these benefits have

been offset recently because of rapid increases in imports of grains, edible oilseeds, and other agricultural products (Pendrill et al., 2019). Therefore, finding low-carbon pathways to develop China's agricultural sector has become an important priority.

Carbon emissions have attracted the attention of different scholars since the 1990s, and many scholars have begun to explore the relationship between carbon emissions and the economy and trade, especially for the effect of carbon emissions caused environmental problems on economic development (Li and Cui, 2017). Generally, in the early stage of industrial development, the leading industries in the economic structure are mainly agriculture. With economic development and the rapid increase in fossil energy use, carbon emissions will also rapidly increase. In the later stages of industrial development, the economy gradually shifted to the secondary and tertiary industries, the emission structure will be gradually improved by efficient energy use, environmental quality will be further improved, and the evolution of the industry process and the environment Kuznets curve will be fully consistent. In the study of urban air quality, Grossman and Kruger (1991) explored the empirical relationship between environmental quality and per capita income and found that when per capita income reaches $4,000–$5,000, there will be a willingness and tendency to reduce environmental pollution, which proves that the relationship between economic growth and environmental carbon emissions is not entirely conflicted.

Because of strict environmental systems, pollution emissions will slow down at every stage of economic growth below emission levels without institutional impacts. Besides, the inflection point of environmental emissions will occur ahead of time, and the environmental Kuznets curve will become relatively stable, and the curve will be lower. With economic growth, environmental problems will be improved, and in this sense, pollution control is not more important than promoting economic growth. Specifically in terms of carbon emissions, the study points out that the relationship between carbon emissions and GDP per capita is structurally stable, and the relationship between carbon emissions and GDP per capita is upwardly skewed, but economic growth is not sufficient to reduce carbon emissions; thus, all countries should strive to reduce carbon emissions.

2 THEORETICAL FRAMEWORK

Study on the impact of trade on carbon emissions can be divided into three categories **Figure 1**. First, research can be based on the assumption that international trade is conducive to carbon emission reduction (Tian et al., 2016) and that Chinese enterprises will borrow or improve technology (Chen et al., 2019) to meet strict sustainability standards imposed by international clients. Second, some studies are based on the assumption that international trade hinders the reduction of carbon emissions (Cui and Li, 2017); they assume that the pursuit of greater economic benefits in a highly competitive world promotes the adoption of cheaper modes of production at the expense of the environment (Xia, 2014). Third, some studies are based on the assumption that education level, laws, regulations, and other aspects of the country of production jointly determine or influence the national capacity to absorb technology and reduce carbon emissions (Yang and Martinez-Zarzoso, 2014); therefore, these studies assume that the effect of international trade on carbon emissions is ambiguous.

2.1 Capital Formation Resulting From Trade

Agricultural carbon emissions performance is influenced by capital, technology, knowledge, management, and other elements of international trade applied to the national technological level and industrial structure adjustment (Diao et al., 2012). Therefore, in order to understand agricultural trade and mechanisms that influence agricultural carbon emissions performance, it is necessary to first identify spillover effects on the national capital. Existing studies show that the agricultural production of a country is equivalent to that involved in agricultural trade through technology spillovers and industrial connection (Chen and He, 2017). However, this depends on the quantity and quality of the products being exported. If imported products are high in quality or low in cost, they may crowd out the domestic market, while the opposite may happen if imported products are lacking or play a guiding role in the domestic market (Fojtíková, 2018).

2.2 Technology Transfer Resulting From Trade

Technological progress has become an important driving force for industrial development (You and Wu, 2014); especially in modern times, taking advantage of technological progress has become the goal of many governments in the world. The agricultural production of China is impacted by technology transfer from trade, especially when production reaches a certain scale (Cheng et al., 2019). However, extensive agriculture can only meet domestic demands; without an increased focus on pure industrial capital, further development of the agricultural industry would be difficult. Agricultural trade can promote the upgrading of industrial technology through technical assistance and technology licensing and sales, thereby promoting reductions in agricultural carbon emissions (Zhang and Tian, 2019).

2.3 Technology Spillover Resulting From Trade

Technology transfer resulting from trade can lead to agricultural carbon emission reductions across the country. The demonstration and imitation effect and the market competition effect are some of the technology spillover effects of agricultural trade (Jiang et al., 2015; Li et al., 2015). With the development of trade, Chinese enterprises learn from, imitate, and absorb the experience of more technologically advanced countries (Qin, 2013). Therefore, their production and efficiency can be continuously improved, and carbon emissions can be reduced. This demonstration and imitation effect is dependent on the learning capacity of the local production team, as well as the mastery and management of

TABLE 1 | Input and output indicators of agricultural production efficiency index system.

	Variables	Indicators	Units
Input indicators	Labor input	The number of employees in the primary industry	10,000 people
	Land input	Crop planting area	Thousands of hectares
	Fertilizer input	The scalar quantity of agricultural fertilizer	10,000 tons of
	Pesticide input	Pesticide use	Tons of
	Agriculture film input	Agriculture film use	Tons of
	agricultural machinery input	Total power of agricultural machinery	Million kilowatt-hour
Output indicators	Agricultural, forestry, livestock, and fishery output value		100 million yuan
	Agricultural carbon emission		10,000 tons of

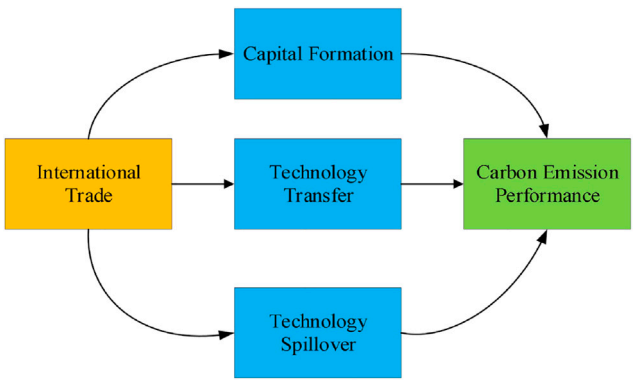

FIGURE 1 | Theoretical framework between international trade and carbon emission performance.

advanced technology (Tian et al., 2014). The market competition effect is an indirect effect, which can be positive or negative. The positive effect leads to more efficient allocation of domestic resources and improvement of national welfare (Rozelle, 2017). Availability of advanced technology from foreign countries intensifies competition among domestic companies, which promotes improved company management, and creates a virtuous circle for the reduction of carbon emissions.

In this study, the mechanism of trade influencing agricultural carbon emission performance is systematically analyzed, the crowding-in and crowding-out effects caused by trade is researched, which can ultimately lead to emission reductions (Zhang et al., 2017). In addition, the structural effect of resource consumption brought about by exports when the country has a dominant market position is examined, which otherwise brings about the imitation of technology and emission reductions.

3 DATA AND METHODS

3.1 Data

On the basis of existing studies, a logical, science-based index system that can evaluate agricultural production efficiency is constructed. It provides a basis for the objective evaluation of agricultural carbon emission performance. Following existing definitions of agricultural production efficiency and similar index systems proposed in other studies and considering data accessibility, purpose, and other factors, the input and output indicators for the index system are identified (**Table 1**). The decision-making unit includes 31 provinces, municipalities, and autonomous regions in China.

Three main categories are included in input indicators: labor, land, and agricultural resources. For each province, municipality, or autonomous region, the number of persons employed in the primary agricultural industry (unit: 10,000 people) is used as the labor indicator. Land indicators include proportions of different crops, proportions of fallow, and abandoned land in different regions. Agriculture consumes resources that mainly include chemical fertilizers, pesticides, agricultural film, farm machinery, and water. The main agricultural resources indicators include quantities of agricultural fertilizer, pesticide, and agricultural film used; total agricultural machinery power (unit: kilowatts); quantity of water used for irrigation; and the surface area of the provincial effective irrigation area.

This study focuses on two output variables: total output of agriculture, forestry, husbandry, and fishery and agricultural carbon emissions.

The data derives from China Statistical Yearbooks from 2000 to 2016, provincial statistical yearbooks in the same period, a collection of agricultural statistical data spanning the last 30 years of reform and opening-up, and a collection of statistical data spanning the 60 years since the establishment of the People's Republic of China. Data availability on use of chemical fertilizers, pesticides, agricultural film, sown area, total power of agricultural machinery, effective irrigation area, and working population involved in the primary agricultural industry varies between years. The total value of agricultural output (gross value of agricultural, forestry, livestock, and fishery output) is calculated using the agricultural producer price index. Constrained by data availability, the study is limited to the provincial level.

3.2 Malmquist Productivity Index

Intertemporal dynamics and the geometric mean of the Malmquist productivity index are utilized to account for the undesired output of carbon emissions. The agricultural carbon emission performance index (ACPTFP) is defined as a slack-based measure of efficiency based on directional distance functions:

$$ACPTFP(x_k^{t+1}, y_k^{t+1}, b_k^{t+1}; x_k^t, y_k^t, b_k^t) = \left[\frac{\overrightarrow{S_c^t}(x_k^{t+1}, y_k^{t+1}, b_k^{t+1})}{\overrightarrow{S_c^t}(x_k^t, y_k^t, b_k^t)} \times \frac{\overrightarrow{S_c^{t+1}}(x_k^{t+1}, y_k^{t+1}, b_k^{t+1})}{\overrightarrow{S_c^{t+1}}(x_k^t, y_k^t, b_k^t)} \right]^{\frac{1}{2}}$$
$$= \frac{\overrightarrow{S_c^{t+1}}(x_k^{t+1}, y_k^{t+1}, b_k^{t+1})}{\overrightarrow{S_c^t}(x_k^t, y_k^t, b_k^t)} \times \left[\frac{\overrightarrow{S_c^t}(x_k^{t+1}, y_k^{t+1}, b_k^{t+1})}{\overrightarrow{S_c^{t+1}}(x_k^{t+1}, y_k^{t+1}, b_k^{t+1})} \times \frac{\overrightarrow{S_c^t}(x_k^t, y_k^t, b_k^t)}{\overrightarrow{S_c^t}(x_k^t, y_k^t, b_k^t)} \right]^{\frac{1}{2}}$$
$$= EC(x_k^{t+1}, y_k^{t+1}, b_k^{t+1}; x_k^t, y_k^t, b_k^t) \times TC(x_k^{t+1}, y_k^{t+1}, b_k^{t+1}; x_k^t, y_k^t, b_k^t) \quad (1)$$

where ACPTFP between time period t and $t+1$ is calculated by multiplication, division, and referencing to adjacent time periods and can be decomposed into the technology efficiency change index (EC) and the technology progress index (TC). An ACPTFP value greater than 1 indicates an increase in carbon emission performance; otherwise, it indicates a decrease in performance. An EC value greater than 1 indicates improvement in technical efficiency; otherwise, it indicates deterioration of technical efficiency. A TC value greater than 1 indicates advance of the agricultural production technology frontier; otherwise, it indicates a retreat.

3.3 Panel Data Regression Model

Agricultural trade and carbon emissions performance involve technology spillovers and effects that are similar to those of foreign direct investment. Therefore, the international direct investment model of Coe and Helpman (1995) is also used, which has been widely adopted and has become a classic international technology spillover model:

$$LnTFP_i = \alpha_i^0 + \alpha_i^d \ln S_i^d + \alpha_i^f \ln S_i^f \quad (2)$$

where, i represents the region, $LnTFP$ represents the agricultural carbon emission performance, $\ln S_i^d$ represents the spillover stock of domestic research and development (R&D) investment, and $\ln S_i^d$ represents the spillover stock of foreign R&D investment obtained from agricultural trade. According to this model, national productivity depends on its own R&D investment and knowledge spillover from foreign R&D. Based on an econometric model, the carbon emission performance index (ACPTFP) is defined as follows:

$$ACPTFP = \alpha_0 + \alpha_1 TRADE_{it} + \alpha_2 RDG + \mu_i + \varepsilon_{it} \quad (3)$$

where i and t represent the different provinces and time, respectively; ACPTFP represents the agricultural carbon emission performance; TRADE represents the agricultural product; RDG represents the domestic R&D investment; μ_i is the unobservable regional effects; and ε_{it} is the random disturbance terms. Studies have indicated that human capital can influence technological innovation and the capacity and speed at which foreign technologies can be absorbed. Besides, financial development is able to bring about sufficient capital to satisfy demand and can also provide credit funds to support innovations in production and environmental protection technologies. As more innovations are supported, there is a higher chance that at least some will succeed, guaranteeing carbon emission reductions. Environmental regulation is an important variable and affects agricultural carbon emissions in two ways. On the one hand, regulations can add compliance costs, raising production costs and forcing companies that are unable to bear these new costs to be crowded out of the market. On the other hand, companies that adopt new technology to follow higher environmental standards may become more competitive and be compensated by being chosen by more consumers. Besides, different industrial structures will also have an impact on agricultural carbon emissions. Therefore, human capital, financial development, environmental regulation, and industrial structure are included into the empirical model for agricultural carbon emissions performance:

$$ACPTFP = \alpha_0 + \alpha_1 TRADE_{it} + \alpha_2 RDG_{it} + \alpha_3 HUM_{it} + \alpha_4 FIN_{it} + \alpha_5 REG_{it} + \alpha_6 IND_{it} + \mu_i + \varepsilon_{it} \quad (4)$$

where HUN_{it} represents the human capital, FIN_{it} represents the financial development, REG_{it} represents the environmental regulation, IND_{it} represents the industrial structure, and ε_{it} represents the random disturbance term.

Studies show that agricultural trade and financial development have effects on agricultural carbon emissions. Reduction in carbon emissions can lead to more sustainable and competitive products, which, in turn, impact economic growth and trade. Besides, economic growth can also increase demands for financial and other products. Therefore, the empirical model for agricultural carbon emissions performance is further modified. A first-order lag term of agricultural carbon emission performance is introduced to address possible endogeneity issues and time series data gaps:

$$ACPTFP_{it} = \beta_0 + \beta_1 ACPTFP_{i,t-1} + \beta_2 TRADE_{it} + \beta_3 RDG_{it} + \beta_4 HUM_{it} + \beta_5 FIN_{it} + \beta_6 REG_{it} + \beta_7 IND_{it} + \mu_i + \varepsilon_{it} \quad (5)$$

where $ACPTFP_{i,t-1}$ represents the first-order lag term of agricultural carbon emission performance. To ensure the consistency of coefficient and standard error estimates without having to determine the form of conditional variance functions, the ordinary least squares (OLS) regression is performed, and heteroscedasticity-robust standard errors of coefficients are calculated.

4 RESULTS AND DISCUSSION

4.1 Agricultural Carbon Emission Performance

The ACPTFP is calculated on the basis of relative efficiency. Therefore, interpretation and analysis of ACPTFP values are a form of dynamic analysis that takes into account relative effects.

Low-carbon agricultural productivity has increased slowly since 2005 (**Table 2**). The average annual contribution of technical efficiency (EFF) to productivity is only 0.04%. The average annual contribution of scale efficiency (SECH) to productivity has been increasing slightly, by 0.10% annually, while that of pure technical efficiency (PECH) has been

TABLE 2 | Agricultural carbon emission performance, 2005–2020.

Time Period	ACPTFP	EC	TC
2005–2006	1.0290	0.9880	1.0427
2006–2007	1.0202	1.0338	0.9955
2007–2008	1.0561	1.0156	1.0480
2008–2009	1.0879	1.0196	1.0725
2009–2010	1.0825	1.0122	1.0737
2010–2011	1.0831	1.0063	1.0805
2011–2012	1.0946	1.0067	1.0911
2012–2013	1.1031	1.0081	1.0974
2013–2014	1.1029	1.0088	1.0962
2014–2015	1.1073	1.0085	1.1006
2015–2016	1.1142	1.0071	1.1089
2016–2017	1.1138	1.0065	1.1089
2017–2018	1.1115	1.0064	1.1065
2018–2019	1.1080	1.0055	1.1039
2019–2020	1.1036	1.0053	1.0996

decreasing by 0.06% annually. There is still an improvement space for low-carbon agricultural productivity.

4.2 Impact of Agricultural Trade on Agricultural Carbon Emission Performance

To identify the most appropriate model for the data, the F test and the Hausman (H) test are utilized. The null hypothesis of the F test is that the mixed regression model is superior, and it is rejected because of the p value of 0.00 (**Table 3**). The null hypothesis of the H test is that the random-effects model is superior, and it is rejected because of the p value of 0.00. Therefore, the fixed effect model is chosen.

To measure the impact of agricultural trade on carbon emission performance, the OLS and the generalized method of moments (GMM) are used to estimate parameters in the model and calculate heteroscedasticity-robust standard errors of the coefficients. In order to minimize errors and effects of missing variables, all variables are entered into the model to determine the role of agricultural trade. Then, to estimate model parameters, other control variables were added in order, so that the effect of each control variable could be identified. Models (1)–(3) are calculated using the OLS and robust standard errors (**Table 4**). Only the impacts of trade and human capital on emission performance are included in Model (1). Some variables of industrial development and environmental regulation are included in Model (2), and more variables are included in Model (3). All variables are statistically significant in both models. For Model (4), the Wald test is statistically significant at the 1% level. The Sargan test fails to reject the null hypothesis; therefore, all instruments are valid. The AR (1) and AR (2) tests fail to reject the null hypotheses; therefore, there is no first- or second-order autocorrelation. These test results prove the robust dynamic panel model and reliable estimates of parameters. In addition, the coefficient of the first-order lag term of agricultural carbon emission performance is positive and large, indicating that emission performance is affected by the variables in the model and is also negatively affected by emission performance of the previous period.

Columns 2–4 show results from the OLS regression; numbers in brackets are t-values of the standard error of the variable. Column 5 shows results from the GMM; numbers in brackets are Z-values of the variable or p-values of the Wald, AR (1), AR (2), and Sargan tests.

Model (4) is examined more closely to explore its economic significance. The coefficient of total agricultural trade is 0.0444, which is statistically significant at the 5% level, indicating that agricultural trade significantly promotes emission performance. The results are consistent with findings reported in other studies, the agricultural sector of China is at the stage of learning and adopting advanced technology from foreign countries; its production systems are being upgraded in the process.

Trade has led to a large number of foreign products entering the Chinese market, meeting the needs of Chinese people. It has also brought advanced technology and management standards to China. Although these technologies are less advanced compared with those of foreign countries, they have considerably increased average domestic production. Therefore, trade has had a strong effect on the increase in agricultural carbon emission performance, validating the hypothesis of technology spillover. In addition, some agricultural enterprises will move into the agricultural service sector to help other companies to upgrade their technologies. Through the demonstration and imitation effect, domestic agricultural production will be transformed, and competition in the domestic market will be accelerated.

Through comparative analysis among different regions, it can be found that from the perspective of regional heterogeneity, the proportion of the tertiary industry to the performance of agricultural carbon emissions has a difference in the eastern region, the central region, the western region, and the northeast region. Besides, in the eastern and northeast regions, the proportion of the first industry to the performance of agricultural carbon emissions shows a negative effect, while in the central and western regions, the proportion of the first industry to the performance of agricultural carbon emissions shows a positive effect, which is due to the development of the region. From a national perspective, the performance of agricultural carbon emissions showed a downward trend with the increase of the proportion of the agricultural output value, indicating that the development of agriculture needs to achieve green transformation and high-quality development, rather than the current high-emission, high-energy consumption. It is

TABLE 3 | F and Hausman (H) tests of fixed effects and random effects.

Inspection Method	Null Hypothesis	Statistics	Value of *P*
F test	Mixed regression model is better	3.46	0.0000
H test	The random-effects model is better	201.16	0.0000

TABLE 4 | Results of multiple regression models.

Variable	OLS Regression			System GMM
	(1)	(2)	(3)	(4)
ACPTFP (−1)				−2.5393***
				(−7.16)
ATD (−1)	0.0027*	−0.0033*	−0.0046**	0.0444**
	(1.02)	(−1.76)	(−2.03)	(3.86)
HUM	1.26**	1.7225***	1.7031***	4.2143***
	(2.54)	(2.89)	2.86	(3.14)
IND		2.7446***	2.7475***	0.08178
		(5.38)	(5.39)	(0.55)
IND (−1)		−2.5198***	−2.5148***	−0.0034**
		−5.63	(−5.62)	(−2.94)
REG			0.0658	0.3613
			(1.05)	(1.21)
F	3.34	10.15	8.34	
Wald				59.23*** (0.000)
AR (1)				−1.04 (0.30)
AR (2)				−1.33 (0.18)
Sargan				14.77 (0.32)

*Note: *, **, and *** represent statistical significance at the 10, 5, and 1% levels, respectively.*

necessary to turn to more energy-saving and low-consumption links; at the same time, the central and western regions of fertilizer, pesticides, and other agricultural carbon emissions performance is the main reason for the low.

At the regional level, the ratio of agricultural exports to the total value of primary industry is negatively related to agricultural carbon emission performance, which shows that the main role of agricultural exports in agricultural carbon emission performance is the increase of agricultural carbon emissions. Although the size of the role is different among regions, the central region has the greatest role and the negative effect at the national level.

The ratio of agricultural imports to the first industry has a positive effect on the performance of agricultural carbon emissions at the regional level, where the central region exerts the greatest role, which is linked to the regional geographical location and characteristics. Besides, agricultural imports can bring advanced management and technical experience to the region, thus further improving the performance of agricultural carbon emissions.

The proportion of agricultural labor force to the national labor force has a negative effect on the performance of agricultural carbon emissions, except for the western region. It is closely related to the large area of local land and sparsely populated area, and the increase of agricultural labor force in the western region will strengthen the existing labor force's efforts in agriculture, thereby reducing agricultural carbon emissions and improving agricultural carbon emission performance.

The urbanization rate has a negative effect on the performance of agricultural carbon emissions, except for the western region. It is due to the increase of agricultural production demand in the process of urbanization, resulting in the blind expansion of regional production, thus reducing the performance of agricultural carbon emissions. For the western region, the level of agricultural carbon emission performance still needs to be further improved, and for this reason, the expanded agricultural production demand will drive the performance of agricultural carbon emissions in the western region.

5 CONCLUSION AND DISCUSSION

In this study, carbon emission performance is calculated, and the effect of international trade on carbon emission performance is assessed. agricultural carbon emission performance has increased slowly since 2005. The average annual contribution of EFF to productivity is only 0.04%. The average annual contribution of SECH to productivity has been increasing slightly, by 0.10% annually, while that of PECH has been decreasing by 0.06% annually. There is still an improvement space for low-carbon agricultural productivity. In the econometric model of agricultural carbon emission performance, the coefficient of total trade in agricultural products is 0.0444, which is statistically significant at the 5% level, indicating that agricultural trade significantly promotes emission performance. The results are consistent with findings reported in other studies. The agricultural sector of China is at the stage of learning and adopting advanced technology from foreign countries; its production systems are being upgraded in the process. The results disclose the relationship among carbon neutrality, international trade, and carbon emission performance, which is of vital importance to future carbon neutrality. The countryside is the main area of the ecological environment, and the ecology is the biggest development advantage of the countryside. Rural industries should be greener. We must really make good use of the "two mountains" concept; continuously improve the "value" of green waters and green mountains; explore the "value" of Jinshan Yinshan; accelerate the development of forest and grassland tourism, river and lake wetland tourism, and other emerging industries; actively develop tourism agriculture, green health, ecological education, and other services; and walk out of a sustainable rural development path of ecological beauty, industrial prosperity, and people's prosperity. Agricultural emission reduction does not mean not to apply fertilizer, not to spray medicine, or not to raise pigs but to work the reduction cycle and turn waste into treasure. It is necessary to continue promoting the reduction of chemical fertilizers and pesticides, the replacement of chemical fertilizers with organic fertilizers for fruit and vegetable tea, and green prevention and control products and technologies. It is necessary to promote the resource utilization of agricultural waste, so that livestock and poultry manure can be turned into biogas power generation, biogas slurry and biogas residue can be used as organic fertilizer, and straw can be used as biomass fuel.

DATA AVAILABILITY STATEMENT

The raw data supporting the conclusions of this article will be made available by the authors, without undue reservation.

AUTHOR CONTRIBUTIONS

GL and XZ conceived the study and wrote the paper. GL and CH analyzed data for figures and tables. All authors contributed to manuscript development and edited the final version.

FUNDING

This study was supported by funding from the Program of Humanities and Social Sciences in Shanxi University of China (Grant No. 2019W144) and the Soft Science Project of Shanxi Province, China (Grant No. 2019041005-1).

REFERENCES

Balsalobre-Lorente, D., Driha, O. M., Bekun, F. V., and Osundina, O. A. (2019). Do agricultural Activities Induce Carbon Emissions? the BRICS Experience. *Environ. Sci. Pollut. Res.* 26, 25218–25234. doi:10.1007/s11356-019-05737-3

Bu, X., Dong, S., Li, F., and Li, Y. (2018). Agricultural Trade Pattern and Potential in China and Russia. *IOP Conf. Ser. Earth Environ. Sci.* 190, 012046. doi:10.1088/1755-1315/190/1/012046

Chang, Y., and Dong, S. (2016). Study on Evaluation Model of International Trade in Agricultural Products Based on Unascertained Measure. *Chem. Eng. Trans.* 51, 673–678. doi:10.3303/CET1651113

Chen, L., and He, F. (2017). Measurements and Factors of Carbon Emission Efficiency. *Pol. J. Environ. Stud.* 26, 1963–1973. doi:10.15244/pjoes/69939

Chen, Q., Löschel, A., Pei, J., Peters, G. P., Xue, J., and Zhao, Z. (2019). Processing Trade, Foreign Outsourcing and Carbon Emissions in China. *Struct. Change Econ. Dyn.* 49, 1–12. doi:10.1016/j.strueco.2019.03.004

Cheng, Y., Lv, K., Wang, J., and Xu, H. (2019). Energy Efficiency, Carbon Dioxide Emission Efficiency, and Related Abatement Costs in Regional China: a Synthesis of Input-Output Analysis and DEA. *Energy Effic.* 12, 863–877. doi:10.1007/s12053-018-9695-8

Cui, Q., and Li, Y. (2017). Will Airline Efficiency Be Affected by "Carbon Neutral Growth from 2020" Strategy? Evidences from 29 International Airlines. *J. Clean. Prod.* 164, 1289–1300. doi:10.1016/j.jclepro.2017.07.059

Diao, W. Y., Tian, B. P., Ma, P., and Wang, X. E. (2012). Trade Ecological Footprint Analysis of China's Agricultural. *Adv. Mater. Res.* 524-527, 2340–2343. doi:10.4028/www.scientific.net/AMR.524-527.2340

Fojtíková, L. (2018). China's Trade Competitiveness in the Area of Agricultural Products after the Implementation of the World Trade Organization Commitments. *Agric. Econ. - Czech* 64, 379–388. doi:10.17221/163/2017-AGRICECON

Fu, Y., Zhao, J., Wang, C., Peng, W., Wang, Q., and Zhang, C. (2018). The Virtual Water Flow of Crops between Intraregional and Interregional in Mainland China. *Agric. Water Manag.* 208, 204–213. doi:10.1016/j.agwat.2018.06.023

Jiang, Y., Cai, W., Wan, L., and Wang, C. (2015). An Index Decomposition Analysis of China's Interregional Embodied Carbon Flows. *J. Clean. Prod.* 88, 289–296. doi:10.1016/j.jclepro.2014.04.075

Li, A., Zhang, Z., and Zhang, A. (2015). Why Are There Large Differences in Performances when the Same Carbon Emission Reductions Are Achieved in Different Countries? *J. Clean. Prod.* 103, 309–318. doi:10.1016/j.jclepro.2014.08.022

Li, P. (2013). "Influential Factors and Area Differentiation of Carbon Emissions for Agriculture in China," in Proceeding of the 2013 "Suzhou-Silicon Valley-Beijing" International Innovation Conference: Technology Innovation and Diasporas in a Global Era, 292–296. doi:10.1109/SIIC.2013.6624203

Li, X. (2012). Technology, Factor Endowments, and China's Agricultural Foreign Trade: A Neoclassical Approach. *China Agric. Econ. Rev.* 4, 105–123. doi:10.1108/17561371211196801

Li, Y., and Cui, Q. (2017). Carbon Neutral Growth from 2020 Strategy and Airline Environmental Inefficiency: A Network Range Adjusted Environmental Data Envelopment Analysis. *Appl. Energy* 199, 13–24. doi:10.1016/j.apenergy.2017.04.072

Pendrill, F., Persson, U. M., Godar, J., Kastner, T., Moran, D., Schmidt, S., et al. (2019). Agricultural and Forestry Trade Drives Large Share of Tropical Deforestation Emissions. *Glob. Environ. Change* 56, 1–10. doi:10.1016/j.gloenvcha.2019.03.002

Qin, S. (2013). "Study on International Trade of China's Agricultural Products," in *Lecture Notes in Electrical Engineering* (Berlin,Germany: Springer Nature), 467–473. doi:10.1007/978-3-642-35440-3_61

Rozelle, S. D. (2017). *Agricultural Trade and Policy in China*. England: Routledge. doi:10.4324/9781315199658

Sohlberg, M., and Yvon, A. (2019). China - Domestic Support for Agricultural Producers (China-Agricultural Producers), DS511. *World Trade Rev.* 18, 531–532. doi:10.1017/s1474745619000302

Tian, J., Yang, H., Xiang, P., Liu, D., and Li, L. (2016). Drivers of Agricultural Carbon Emissions in Hunan Province, China. *Environ. Earth Sci.* 75, 1–17. doi:10.1007/s12665-015-4777-9

Tian, Y., Zhang, J.-b., and He, Y.-y. (2014). Research on Spatial-Temporal Characteristics and Driving Factor of Agricultural Carbon Emissions in China. *J. Integr. Agric.* 13, 1393–1403. doi:10.1016/S2095-3119(13)60624-3

Wang, X., Li, Y., and Hu, J. (2018). Analysis on the Agricultural Trade between China and Countries along "One Belt, One Road". *Me* 09, 1977–1986. doi:10.4236/me.2018.912123

Wu, X., Zhang, J., and You, L. (2018). Marginal Abatement Cost of Agricultural Carbon Emissions in China: 1993-2015. *Caer* 10, 558–571. doi:10.1108/CAER-04-2017-0063

Xia, Y. (2014). Carbon Emissions Embodied in the International Trade of China: A Hypothesised-Country-Based Study. *Ijogct* 7, 203–228. doi:10.1504/IJOGCT.2014.059276

Yang, J. (2019b). Does International Agricultural Trade Matter for Carbon Emissions: A Case Study of the Area Along "the Belt and Road Initiative". *IOP Conf. Ser. Earth Environ. Sci.* 310, 052072. doi:10.1088/1755-1315/310/5/052072

Yang, J. (2019a). Study on the Impact of Carbon Emissions on International Agricultural Trade of Countries Along "The Belt and Road Initiative" with China. *IOP Conf. Ser. Mat. Sci. Eng.* 592, 012188. doi:10.1088/1757-899X/592/1/012188

Yang, S., and Martinez-Zarzoso, I. (2014). A Panel Data Analysis of Trade Creation and Trade Diversion Effects: The Case of ASEAN-China Free Trade Area. *China Econ. Rev.* 29, 138–151. doi:10.1016/j.chieco.2014.04.002

You, H., and Wu, C. (2014). Analysis of Carbon Emission Efficiency and Optimization of Low Carbon for Agricultural Land Intensive Use. *Nongye Gongcheng Xuebao/Transactions Chin. Soc. Agric. Eng.* 30, 224–234. doi:10.3969/j.issn.1002-6819.2014.02.030

Yu, Y., and Chen, F. (2017). Research on Carbon Emissions Embodied in Trade between China and South Korea. *Atmos. Pollut. Res.* 8, 56–63. doi:10.1016/j.apr.2016.07.007

Zhang, B., and Tian, X. (2019). Economic Transition under Carbon Emission Constraints in China: An Evaluation at the City Level. *Emerg. Mark. Finance Trade* 55, 1280–1293. doi:10.1080/1540496X.2018.1523056

Zhang, Y., Zhang, J., Wang, C., Cao, J., Liu, Z., and Wang, L. (2017). China and Trans-Pacific Partnership Agreement Countries: Estimation of the Virtual Water Trade of Agricultural Products. *J. Clean. Prod.* 140, 1493–1503. doi:10.1016/j.jclepro.2016.10.001

Conflict of Interest: The authors declare that the research was conducted in the absence of any commercial or financial relationships that could be construed as a potential conflict of interest.

Publisher's Note: All claims expressed in this article are solely those of the authors and do not necessarily represent those of their affiliated organizations or those of the publisher, the editors, and the reviewers. Any product that may be evaluated in this article, or claim that may be made by its manufacturer, is not guaranteed or endorsed by the publisher.

Frontiers in Environmental Science

Explores the anthropogenic impact on our natural world

An innovative journal that advances knowledge of the natural world and its intersections with human society. It supports the formulation of policies that lead to a more inhabitable and sustainable world.

Discover the latest Research Topics

See more →

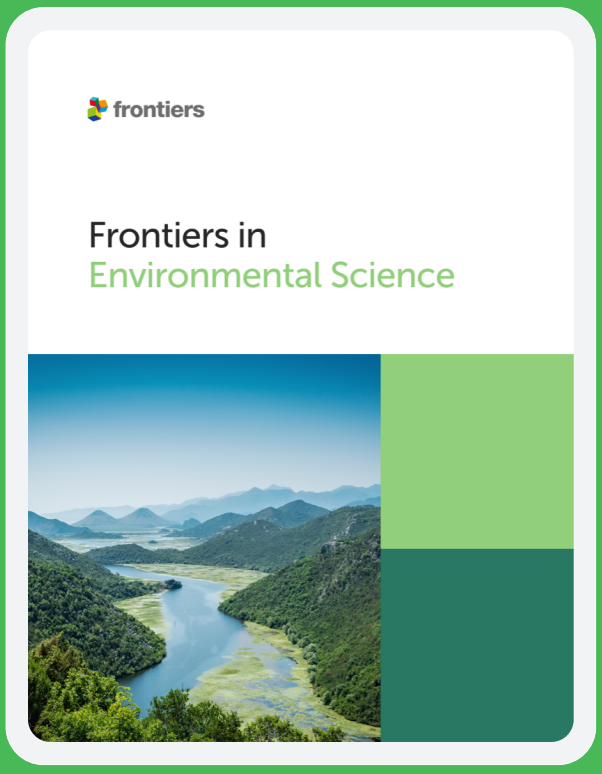

Frontiers

Avenue du Tribunal-Fédéral 34
1005 Lausanne, Swizerland
frontiersin.org

Contact us

+41 (0)21 510 17 00
frontiersin.org/about/contact